Sjoerd Harder *Editor*

Alkaline-Earth Metal Compounds

Oddities and Applications

Springer

45
Topics in Organometallic Chemistry

Topics in Organometallic Chemistry
Recently Published Volumes

Alkaline-Earth Metal Compounds

Oddities and Applications

Volume Editor: Sjoerd Harder

With Contributions by

J.-F. Carpentier · M.R. Crimmin · R. Fischer · H. Görls ·
M.S. Hill · C. Jones · M. Köhler · S. Kobayashi · S. Krieck ·
J. Langer · R.E. Mulvey · S.D. Robertson · K. Ruhlandt-Senge ·
Y. Sarazin · A. Stasch · A. Torvisco · T. Tsubogo ·
M. Westerhausen · Y. Yamashita

Editor
Sjoerd Harder
Inorganic and Analytical Chemistry
University of Erlangen
Egerlandstr. 1
91058 Erlangen
Germany

Printed on acid-free paper

Sjoerd Harder

Inorganic and Analytical Chemistry
University of Erlangen
Egerlandstr. 1
91058 Erlangen
Germany
sjoerd.harder@chemie.uni-erlangen.de

Editorial Board

Topics in Organometallic Chemistry
Also Available Electronically

Topics in Organometallic Chemistry is included in Springer's eBook package *Chemistry and Materials Science*. If a library does not opt for the whole package the book series may be bought on a subscription basis. Also, all back volumes are available electronically.

For all customers who have a standing order to the print version of *Topics in Organometallic Chemistry*, we offer free access to the electronic volumes of the Series published in the current year via SpringerLink.

If you do not have access, you can still view the table of contents of each volume and the abstract of each article by going to the SpringerLink homepage, clicking on "Chemistry and Materials Science," under Subject Collection, then "Book Series," under Content Type and finally by selecting *Topics in Organometallic Chemistry*.

You will find information about the

– Editorial Board
– Aims and Scope
– Instructions for Authors
– Sample Contribution

at springer.com using the search function by typing in *Topics in Organometallic Chemistry*.
Color figures are published in full color in the electronic version on SpringerLink.

Aims and Scope

The series *Topics in Organometallic Chemistry* presents critical overviews of research results in organometallic chemistry. As our understanding of organometallic structures, properties and mechanisms grows, new paths are opened for the design of organometallic compounds and reactions tailored to the needs of such diverse areas as organic synthesis, medical research, biology and materials science. Thus the scope of coverage includes a broad range of topics of pure and applied organometallic chemistry, where new breakthroughs are being made that are of significance to a larger scientific audience.

The individual volumes of *Topics in Organometallic Chemistry* are thematic. Review articles are generally invited by the volume editors.

In references *Topics in Organometallic Chemistry* is abbreviated Top Organomet Chem and is cited as a journal. From volume 29 onwards this series is listed with ISI/Web of Knowledge and in coming years it will acquire an impact factor.

Preface

Group 2 alkaline-earth metals like magnesium and calcium make up several rock forming minerals and are among the most abundant metals in the earth's crust. Inorganic salts like lime have been used since prehistoric times and the Great Wall of China certainly owes it durability to the fact that lime hardens with age. Even though group 2 elements like beryllium, strontium, and barium are rare, their unique properties have generated many important niche applications.

This book, however, does not deal with inorganic chemistry but covers selected advances in the organometallic chemistry of the alkaline-earth metals. The group 2 metal magnesium had an early start in the field: in 1912, Victor Grignard was awarded the Nobel Prize in chemistry for his organomagnesium complexes that "greatly advanced the progress of organic chemistry." These so-called Grignard reagents are, after more than a century, still indispensable in modern organic synthesis and likely the first organometallic compound prepared by chemistry students at the start of their career.

Although organomagnesium chemistry is the topic of several specialized chemistry books, the volume in your hands is most likely the first that covers special aspects over the whole series of the alkaline-earth metals. Despite magnesium's early start in organometallic chemistry, all other elements were largely neglected and only occasional research reports can be found scattered in the literature. Whereas beryllium has the unpopular reputation as the most poisonous nonradioactive element, the chemistry of the heavier congener calcium (and to a lesser extent that of strontium and barium) is now rapidly starting to develop. This sudden growth, which started a century after the invention of the Grignard reagents, is mainly driven by applications (polymerization chemistry, catalysis, organic synthesis), thus nicknaming dormant calcium as a "sleeping beauty." Apart from developments in the chemistry of the heavier group 2 metals, magnesium chemistry is also currently witnessing strongly revived interests in the form of TURBO-Grignard reagents, catalysis, or low-valent Mg(I) chemistry. Therefore, publication of this book could have hardly been more timely.

One reason for the delayed development of organocalcium chemistry is the fact that these compounds can not merely be made through Grignard-type synthetic

routes but need special synthetic methods that are described in the first chapter "Heavy Alkaline-Earth Metal Organometallic and Metal Organic Chemistry: Synthetic Methods and Properties" by Ana Torvisco and Karin Ruhlandt-Senge. The second chapter "Heavier Group 2 *Grignard* Reagents of the Type Aryl-Ae(L)$_n$-X (Post-*Grignard* Reagents)", by Matthias Westerhausen, Jens Langer, Sven Krieck, Reinald Fischer, Helmar Görls, and Mathias Köhler, shows that in certain cases and under special conditions, "heavy" calcium-Grignards indeed can be prepared and isolated. Their high reactivity likely could be exploited in synthesis.

"Stable Molecular Magnesium(I) Dimers: A Fundamentally Appealing yet Synthetically Versatile Compound Class", by Cameron Jones and Andreas Stasch, is breaking the dogma that organomagnesium chemistry is exclusively based on Mg^{2+}. First low-valent Mg(I) compounds are not just oddities but have been successfully applied as specialist reducing reagents. "Modern Developments in Magnesium Reagent Chemistry for Synthesis", by Robert E. Mulvey and Stuart D. Robertson, describes the advent of engineered Grignard reagents in which classical organomagnesium reagents are activated by reactivity boosting additives. Not only high reactivity but also selectivity and functional group tolerance are among their substantial benefits.

The next three chapters deal with applications in catalysis. Catalysis is typically the domain of the transition metals. The availability of *d*-orbitals allows for fast and reversible changes in the metal's oxidation states (a prerequisite in many catalytic cycles) and activation of a large variety of strong bonds like H–H, C=O, C=C, and C≡C. However, *d*-orbital participation is not a requirement for catalysis. Rather than by redox processes and/or orbital overlap, group 2 metal catalysts function similar to d^0-organolanthanide catalysts and assist chemical conversion simply by their combination of Lewis acidity (the metal cation) and nucleophilicity (the organic rest). "Alkaline-Earth Metal Complexes in Homogeneous Polymerization Catalysis", by Jean-François Carpentier and Yann Sarazin, starts with applications in polymerization catalysis. The biocompatible nature of a metal like calcium makes it especially attractive as a catalyst for biodegradable polymers or for materials with medicinal applications. "Homogeneous Catalysis with Organometallic Complexes of Group 2", by Mark R. Crimmin and Michael S. Hill, describes the numerous possibilities of catalytic functionalization of alkenes and alkynes and deals with the organometallic aspects of group 2 metal catalysis. "Chiral Ca-, Sr-, and Ba-catalyzed asymmetric direct-type aldol, Michael, Mannich, and related reactions", by Tetsu Tsubogo, Yasuhiro Yamashita, and Shū Kobayashi, on the other hand, is written from an organic chemist's point of view mainly referring to catalytic functionality based on Brønsted basicity (ligands) and mild Lewis acidity (metal). The impressive progress in stereoselective catalysis promises a bright future of these benign catalysts in the pharmaceutical industry.

The goal of this volume is not only to inform the broader chemistry community of latest developments in the area of alkaline-earth organometallic chemistry. It should especially arouse interest in this long neglected group of metals and stimulate its further development in a large variety of fields.

November 2012, Erlangen, Germany   Prof. Dr. Sjoerd Harder

Contents

Heavy Alkaline-Earth Metal Organometallic and Metal Organic Chemistry: Synthetic Methods and Properties

Ana Torvisco and Karin Ruhlandt-Senge

Abstract Despite the growing utility of heavy alkaline-earth metal organometallics, their high reactivity resulted in limited accessibility. Over the last decade, synthetic strategies have been developed to overcome challenges, resulting in unprecedented growth of this chemistry. The synthetic accessibility is going hand in hand with exciting and ever expanding utilities of the compounds in applications as diverse as catalysis or materials chemistry. This article provides a comprehensive overview of the various synthetic methodologies along with considerations on their structure–property relationships.

Keywords Alkaline-earth metals · Metal activation · Redox transmetallation · Salt metathesis · Synthetic methodologies

Contents

A. Torvisco and K. Ruhlandt-Senge (✉)
Department of Chemistry, Syracuse University, 1-014 CST, Syracuse, NY 13244, USA
e-mail: kruhland@syr.edu

Abbreviations

C_6H_5	Aryl
C_6F_5	Pentafluoroaryl
CPh_3	Triphenylmethanide
Dipp	2,6-Diisopropylphenyl
DME	Dimethoxyethane
Et_2O	Ditheylether
HMPA	Hexamethylphosphoric triamide
Odpp	2,6-Diphenylphenoxide
2,6-OMe	2,6-Dimethoxybenzene
Mes	2,4,6-Trimethylphenyl
Ph_2pz	Diphenylpyrazolate
RTLE	Redox transmetallation/ligand exchange
THF	Tetrahydrofuran
TMEDA	N,N,N',N'-tetramethyl-1,2-ethylenediamine
pTol	4-Methylphenyl
2,6-Tol	2,6-Dimethylphenyl

1 Introduction

Over the last decade, the organometallic and metal organic chemistry of the heavy alkaline-earth metals has changed from obscurity to an exciting, rapidly developing area of chemistry. Among the newer developments is the use of the compounds in catalysis, or in organic transformations, indicating applications not thought possible just 10 years ago. With these developments, organoalkaline-earth metal compounds are emerging as a recognized branch of chemistry, with significant potential in a wide array of applications including synthesis and catalysis [1–9], polymer chemistry [10–24], and materials applications [25–28].

Key to the emergence of alkaline-earth metal organometallic and metal organic chemistry is the examination and development of synthetic protocols that allow the preparation and isolation of target compounds that can then be employed in a variety of applications. As such, the detailed examination of established synthetic methodologies and the exploration of novel reaction routes have been critical to the growth of alkaline-earth metal chemistry. Difficulties encountered are based on the high reactivity of the resulting compounds, which has led to severe restrictions of viable synthetic methodologies.

The lighter metals beryllium and magnesium, with their small radii, display relatively high charge/size ratios, coinciding with the capacity for bond polarization and the induction of bond covalency. As such, among the alkaline-earth metals, these elements display metal–carbon bonds with increased covalent character affording relatively stable species. Due to the toxicity of beryllium and its compounds [29], little work has been done, but magnesium containing compounds have been most

intensely studied as evidenced by the established use of Grignard and diorgano-magnesium reagents in synthetic applications [29–31]. In contrast, the larger radius, strongly negative redox potential, combined with high hydro- and oxophilicity, high electropositive character, and the lack of energetically accessible and empty d-orbitals are responsible for the difficulties encountered when working with the heavy alkaline-earth metals and their compounds. The metals react easily with oxygen or water under formation of oxides or hydroxides; the resulting compounds are very sensitive to hydrolysis. Furthermore, the metal–ligand bond is typically quite weak, resulting in significant lability due to large differences in electronegativity; metal–ligand bonds are largely electrostatic, further contributing to the lability of the target compounds. Their large ionic radii (CN = 6, Ca^{2+} = 1.00; Sr^{2+} = 1.18; Ba^{2+} = 1.35 Å [32]) do not only promote metal ligand bonds but are also responsible for low solubility, as the metals' steric saturation is often achieved by aggregation requiring the use of polar co-solvents to break up the aggregates. Exacerbating the solubility problem, many organoalkaline-earth metal compounds readily react with ethereal solvents under ether scission chemistry, further limiting synthetic variables. This problem can often be overcome by reducing the temperature; thus many reactions are conducted at or below −40 °C.

As shown in this article, the in-depth exploration of established synthetic avenues and the development of new methodologies give rise to exciting chemistry with many opportunities. Classical methods involving magnesium have been modified to extend towards the heavier congeners, and the chemistry of other metal systems has been examined to offer new strategies. For example, the close charge/size ratio for Ca^{2+} (1.00 Å) with Yb^{2+} (1.02 Å) and Sr^{2+} (1.18 Å) with Eu^{2+} (1.17 Å) and Sm^{2+} (1.22 Å) makes the parallel exploration of their chemistry exciting [32]. Despite displaying structural similarities, the more negative redox potentials for the alkaline-earth metals ($E° = -2.87$ V(Ca^{2+}); $E° = -2.89$ V(Sr^{2+}); $E° = -2.90$ V(Ba^{2+})) make them more reactive than their lanthanide counterparts ($E° = -2.22$ V(Yb^{2+}); $E° = -2.30$ V (Sm^{2+}); $E° = -1.99$ V(Eu^{2+})) [33].

This article will describe synthetic advances that have resulted in the preparation of many of the recent heavy organoalkaline-earth compounds, along with selected examples. In addition, the impact of synthetic variables including solvent choice, reaction temperature, or presence of co-ligands and their effect on the chemistry of the heavy alkaline-earth metals will be discussed. The advances in synthetic methodologies have been shown to offer competitive product purity and yields, employ environmentally friendly reagents, and provide the basis for the further exciting growth of heavy alkaline-earth metal chemistry.

2   Grignard Reagents

The groundbreaking discovery of the preparation of organomagnesium halides by treatment of magnesium metal with an organic halide in the presence of diethyl ether [Eq. (1)] by Victor Grignard in 1900 provided a groundbreaking facile synthetic access. Due to the versatility and applicability of the reagents in a wide

range of synthetic applications, magnesium-based Grignard reagents are among the most extensively studied main group organometallic species. Several excellent review articles are available on the topic [29, 34–43]. Furthermore, a detailed review article on heavy alkaline-earth "Grignard" analogs is included in this book; so this account is kept very brief.

$$Mg_{(act)} + RX \rightarrow RMgX \tag{1}$$

where act = activated; X = F, Cl, Br, I; R = alkyl, aryl.

Analogous chemistry involving the heavier metal congeners [Eq. (2)] has been met with limited success until quite recently. The increased reactivity of the target compounds is rendering their preparation more challenging than the magnesium derivatives as the combination of relatively unreactive metal with the highly reactive target compounds poses a unique synthetic challenge. Further complications involve the high tendency of the reagents towards ether cleavage, limiting reaction conditions significantly.

The first heavy alkaline-earth metal Grignard reagent, EtCaI, was reported by Beckmann; however, detailed ana1ytical data have not been available. Current work indicates that Beckmann's species was in fact $CaI_2 \cdot thf_n$ [36]. Attempts by Gilman resulted in similar findings [44]. Likewise, several others reported similar results [11, 12, 38, 44–65], but only recently, heavy alkaline-earth-based Grignard reagents have become available that are fully characterized [66–78].

Similarly to the magnesium Grignard preparation [29, 34–43], the synthesis of the calcium and more recently that of strontium and barium analogs are highly dependent on the purity of the source metal which can be achieved by distillation of the metals [55]. Distillation also removes the oxide layer, thus providing a significant means of metal activation. However, distillation does not result in the increase of metal surface area, a major factor in shortening reaction time [69, 79–81]. Effective activation methods include reduction of the alkaline-earth metal iodides with potassium metal or lithium napthalide [82], the preparation of surface-enhancing amalgams by addition of mercury, co-condensation methods, [49, 68, 69, 71, 83–87], and solvation of the metals in anhydrous, liquid [88–93] or gaseous [49, 88, 90, 93] ammonia. Most commonly, the alkaline-earth metal is dissolved in ammonia, with quick removal of solvent in order to avoid formation of the amide $(M(NH_2)_2)$, resulting in highly reactive metal powder [67]. As the tendency towards amide formation increases with metal radius, this methodology has been used most successfully for calcium; however, for strontium and barium, $M(NH_2)_2$ formation is difficult to avoid [94–97]. Additionally, the presence of glass beads in the flask can increase the overall surface area of the activated metal [71]. This method has been used successfully for calcium [67, 71]. As a result, several aryl calcium derivatives have been reported (Fig. 1) [66–76], while only one barium [77] and one strontium [78] species have been identified.

$$M_{(act)} + RX \rightarrow RMX \tag{2}$$
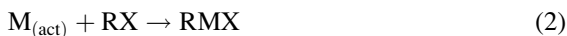
where M = Ca, Sr, Ba; R = aryl; X = Cl, Br, I.
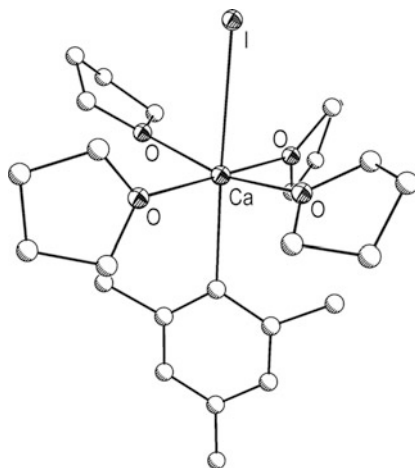
Fig. 1 Crystal structure of MesCaI(thf)$_4$ [68] (Mes or 2,4,6-trimethylphenyl). Hydrogen atoms have been omitted for clarity. All non-carbon atoms are shown as *shaded ellipsoids*
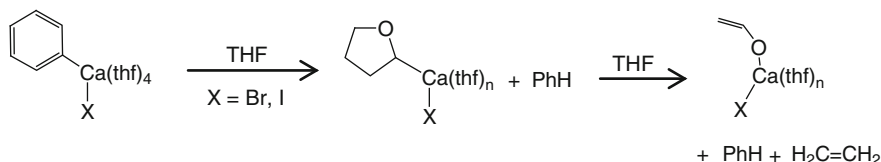
Scheme 1 A generalized decomposition route for aryl calcium halide complexes. The acidic proton from the THF co-ligand is abstracted, yielding benzene, followed by liberation of ethene and formation of an aryl calcium ethenolate. The above mechanism is proposed based on observations from NMR experiments [71] and is in agreement with other established ether cleavage decomposition routes [99, 100]

In accordance with the high reactivity of the aryl calcium halides, ether cleavage reactions are prevalent [66, 71, 74, 77, 98]. In analogy with the magnesium-based Grignard reagents, a strong solvent dependency exists, with best results obtained in THF (tetrahydrofuran), and longer reaction times in diethyl ether. No reaction occurs in aliphatic and aromatic hydrocarbons. Ether cleavage reactions are typically suppressed by short reaction times and maintain reaction temperatures at or below −40 °C. However, ether cleavage occurs readily according to the common mechanism shown in Scheme 1 [71, 98].

A significant difference in reactivity exists for aryl and alkyl halides with the iodides being most reactive. As a result, the use of iodoarenes has been most successful. A slight increase in temperature makes available the bromo derivatives; however, fluoro- and chloroarenes do not show reactivity [71].

In analogy to magnesium Grignard reagents, the corresponding calcium derivatives also exhibit temperature- and solvent-dependent Schlenk equilibria where both the diaryl and dihalide calcium derivatives can be identified [69]. Despite increasing success in the preparation of calcium Grignard analogs, the compounds

Fig. 2 Crystal structure of
Mes$_2$Ca(thf)$_3$ synthesized via
use of heavy Grignards in
THF [70]. Hydrogen atoms
have been omitted for clarity.
All non-carbon atoms are
shown as *shaded ellipsoids*
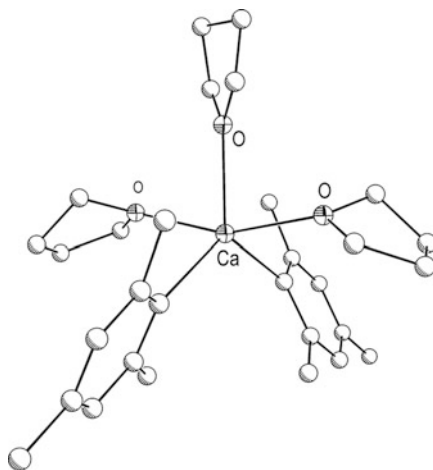
remain highly reactive and require strictest control of starting material quality along
with the most stringent exclusion of oxygen and moisture. However, the high
reactivity of the compounds also makes them attractive in synthetic applications,
specifically due to the high pKa of the benzene derivatives (pKa ~ 43) [101]. This
route has been utilized to synthesize cyclopentadienides [102], phosphides [102],
naphthyls [103], and a low valent calcium species [104].

As shown impressively by Westerhausen et al., the stability of the calcium
Grignard reagents critically depends on the metals' coordination number. Substitution
of three donors in the six-coordinate PhCaI(thf)$_4$ by two DME (dimethoxyethane)
co-ligands affords the seven-coordinate PhCaI(dme)$_2$ which results in an 30 °C
increase in compound stability [67, 69, 98]. In addition, stability of target organome-
tallic compounds can also be increased by increasing the steric demand of
the aryl ligands by employing substituted aryl halides (MesBr, pTolBr,
2,6-dimethoxyphenylBr, 2,6-pTolBr, naphthylBr) as shown for Mes$_2$Ca(thf)$_3$
(Fig. 2) [65, 67, 70–72, 75]. However, substitution in the *ortho* position may result
in rearrangements and in some cases Wurtz-type coupling [66].

3 Hydrocarbon Elimination or Organoelimination

Organoelimination has been the workhorse for the preparation of a wide array
of magnesium-based species due to the commercial availability or easy access
to the diorganomagnesium reagent [Eq. (3)]. Specifically, the commercial Bu$_2$Mg
(a statistical mixture between the secondary and n-butyl species) provides easy
access towards benzylates [105], cyclopentadienides [86, 106–108], indenides
[109, 110], acetylides [111], amides [112, 113], alkoxides [114], aryloxides
[115–122], fluoroalkoxides [123], siloxides [114], thiolates [124–128], phosphanides
[129, 130], selenolates [124, 131], tellurolates [131, 132], and arsenides [129, 133]
in both high yield and purity. The significant difference in acidity between the
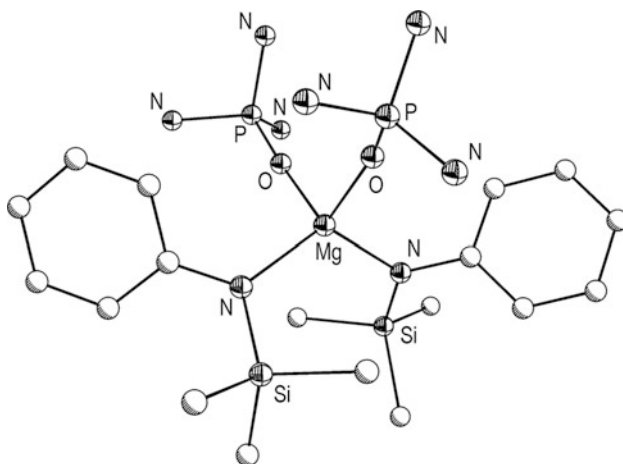
Fig. 3 Crystal structure of Mg[N(SiMe$_3$)(Mes)]$_2$(hmpa)$_2$ (HMPA or hexamethylphosphoric triamide) synthesized via organoelimination in hexane [134]. Hydrogen atoms and methyl groups from HMPA have been omitted for clarity. All non-carbon atoms are shown as *shaded ellipsoids*
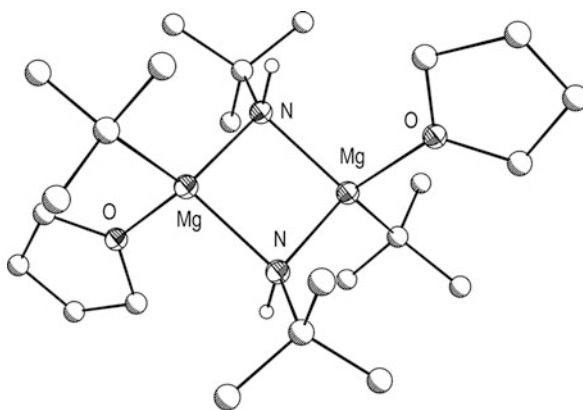
Fig. 4 Structure of the heteroleptic [(*t*-Bu)Mg(thf)]$_2$ synthesized via organoelimination in THF [137]. Hydrogen atoms from all the methyl groups have been omitted for clarity. All non-carbon atoms are shown as *shaded ellipsoids*

resulting *n/sec*BuH (p*K*a ~ 53) and most ligands drives the reaction, while the volatile nature of the butane by-product provides a facile work-up. Donor adducts are easily obtained by addition of co-ligand preferably after the reaction took place (Fig. 3) [135, 136].

$$n/\sec Bu_2Mg + 2RH \xrightarrow{\text{Hexane}} MgR_2 + 2BuH(g) \qquad (3)$$

where RH = benzene, cyclopentadiene, indene, acetylene, amine, alcohol, phenol, fluoroalcohol, siloxane, thiol, phosphane, selenol, tellurol, arsane.

Fig. 5 Structure of Mg[N
(SiMe$_3$)(Dipp)]$_2$ (Dipp or 2,6-
diisopropylphenyl)
synthesized via
organoelimination in hexane
[135]. Mg$\cdots$C(π) interactions
shown as *dashed lines*.
Hydrogen atoms have been
omitted for clarity. All non-
carbon atoms are shown as
shaded ellipsoids
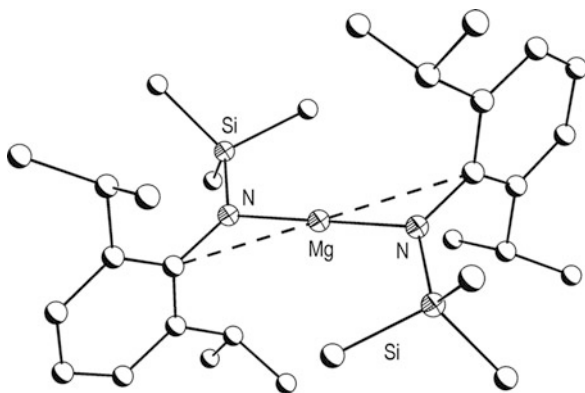
Fig. 6 Crystal structure of
Ca(PhCH$_2$)$_2$(thf)$_4$
synthesized via salt
metathesis in THF [149].
Non-benzylic hydrogen
atoms have been omitted for
clarity. All non-carbon atoms
are shown as *shaded
ellipsoids*
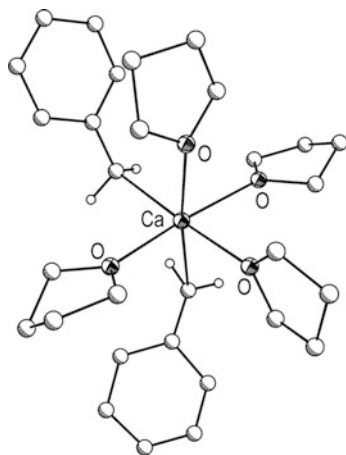
Organoelimination has been shown to be solvent and ligand dependent, with the
presence of polar solvents frequently leading to incomplete reactions with retention
of one of the two alkyl moieties resulting in heteroleptic species (Fig. 4) [135–141].
As a result, reactions are preferentially conducted in nonpolar solvents such as hexane
or toluene. However, use of non-donating solvents typically results in aggregation
under formation of dimers or higher aggregates for less sterically demanding ligand
systems, while monomeric, donor-free compounds can be obtained for sterically
more demanding ligands (Fig. 5) [135, 142, 143]. In case of very sterically demanding
ligands, overnight reflux is required for product formation [134–136, 142].

While providing facile access for the magnesium species, this route is less
straightforward for the heavier alkaline-earth metals due to limitations of
suitable dialkyl or aryl reagents. However, the recent preparation of dibenzyl
reagents of the heavy alkaline-earth metals M(PhCH$_2$)$_2$ (M = Ca–Ba) [144–148]
(Alexander, Ruhlandt-Senge, Unpublished results) (Fig. 6) and their reaction with
acidic ligands under liberation of toluene have provided a powerful synthetic
strategy [Eq. (4)].
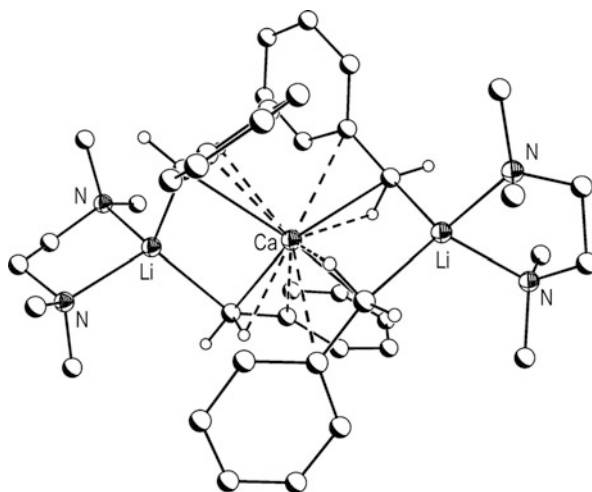
Fig. 7 Crystal structure of (tmeda)$_2$Li$_2$Ca(PhCH$_2$)$_4$ [146]. Ca···C(π) and Ca···H–C agostic interactions are shown as *dashed lines*. Non-benzylic hydrogen atoms have been omitted for clarity. All non-carbon atoms are shown as *shaded ellipsoids*

Ca(PhCH$_2$)$_2$(thf)$_4$ + 2 Li(PhCH$_2$)tmeda   Ca[N(SiMe$_3$)$_2$]$_2$(thf)$_2$ + 2 Li(PhCH$_2$)tmeda

Toluene, RT   Toluene, RT

(tmeda)$_2$Li$_2$Ca(PhCH$_2$)$_4$·PhMe

Scheme 2 Reaction pathways towards (tmeda)$_2$Li$_2$Ca(PhCH$_2$)$_4$ [146]

$$(PhCH_2)_2M + 2RH \xrightarrow[-78\,°C]{THF} MR_2 + 2PhCH_3 (1) \tag{4}$$
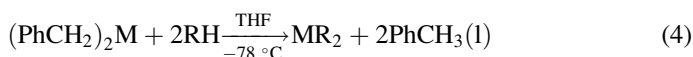
where M = Ca, Sr, Ba; RH = di- and triphenylmethane, acetylene, cyclopentadiene, amine.

Since the p*K*a of toluene is quite high (p*K*a ~ 41), the dibenzyl reagents allow for the metallation of many ligand systems [101]. In addition, the formation of toluene as a side product facilitates work-up and thus the isolation of target molecules. Limitations of the route pertain to the low solubility of the dibenzyl reagents in hydrocarbons requiring the use of THF to achieve homogeneous reaction conditions. However, the dibenzyl compounds' highly reactive nature results in ether cleavage if temperatures are not kept below −40 °C [31, 150].

Synthetic access to the dibenzyl reagents is provided by several reaction routes, historically concerning redox transmetallation involving the reaction of a barium mirror with dibenzylmercury [149, 151–156]. A more convenient route involves the reaction of the easily accessible M[N(SiMe$_3$)$_2$]$_2$(thf)$_2$ (M = Sr–Ba [157]) with the metal exchange reagent Li(PhCH$_2$)tmeda (TMEDA, *N,N,N′,N′*-tetramethyl-1,2-ethylenediamine) [144–148] (Alexander, Ruhlandt-Senge, Unpublished results).

Fig. 8 Crystal structure of
Ba(Ph₂CH)₂(18-crown-6)
synthesized *via*
organoelimination in THF
[147]. Ba···C(π) interactions
are shown as *dashed lines*.
Non-benzylic hydrogen
atoms have been omitted for
clarity. All non-carbon atoms
are shown as *shaded
ellipsoids*
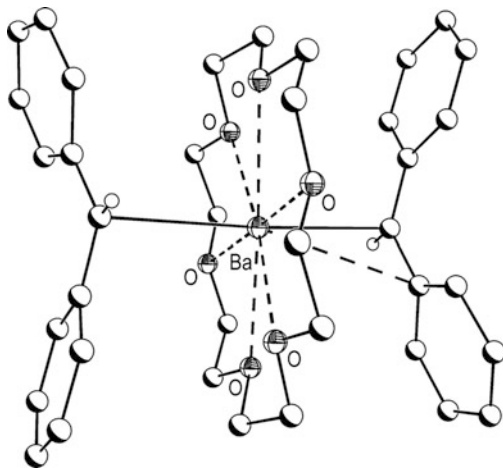
These reactions can be conducted in Et₂O [144]; however, cleaner reaction products
are obtained when the reaction is performed in toluene [146].

However, similar chemistry for the calcium analog remains difficult, as shown
with the isolation of the heterobimetallic benzyl calciate obtained by the treatment
of benzyllithium with Ca[N(SiMe₃)₂]₂(thf)₂ in the presence of TMEDA (Fig. 7).
The calciate can also be obtained by treatment of Ca(PhCH₂)₂(thf)₄ with two
equivalents of Li(PhCH₂)tmeda (Scheme 2) [146]. A comparison of reactivity
between the homometallic Ca(PhCH₂)₂(thf)₄ and the calciate shows significantly
increased reactivity for the heterobimetallic calciate species, a result in agreement
with reactivity trends of other alkaline-earth organometallic "ate" complexes
[158–177].

Toluene elimination has been used to afford a family of highly reactive alkaline-
earth di- and triphenylmethanide complexes (Fig. 8), displaying a range of ion associ-
ation modes depending on co-ligands [31, 99, 100, 145, 147, 149, 150, 178]. Other
examples include acetylides [179], cyclopentadienides [180], and amides [112, 181].

4 Transamination

The development of the heavy alkaline-earth metal bis(bis(trimethylsilyl)amides,
M[N(SiMe₃)₂]₂(thf)₂, has been instrumental in the use of the transamination
route as a viable and dependable synthetic route towards the preparation of
alkaline-earth metal compounds. The amides, M[N(SiMe₃)₂]₂(thf)₂, can be
prepared *via* salt metathesis involving treatment of the metal halides with alkali
metal amide (Ca–Ba) [182, 183]. The heavier metal (Sr, Ba) amides can also
be obtained by direct metallation in liquid, anhydrous ammonia (Sr and Ba)
[83, 90, 91, 184–187].

Recently, the redox transmetallation/ligand exchange (RTLE) route in the pres-
ence of Ph₃Bi as the transmetallation reagent has provided the heavy alkaline-earth

Fig. 9 Crystal structure of $Sr[OC(CF_3)_3]_2(thf)_4$ synthesized via transamination in THF [123]. Hydrogen atoms have been omitted for clarity. All non-carbon atoms are shown as *shaded ellipsoids*


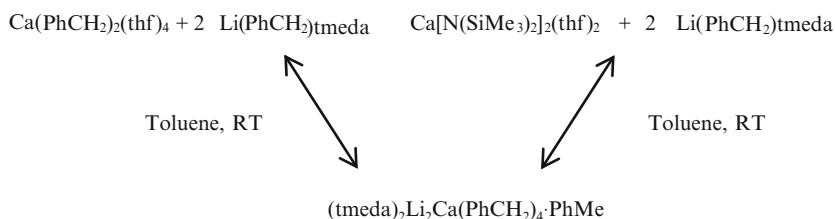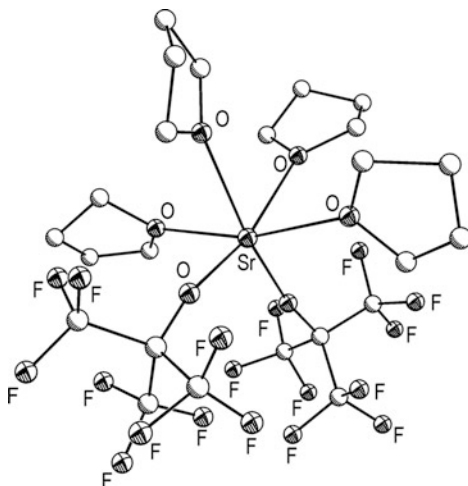metal amides in high yield and purity from the metal in a convenient one-pot reaction [157], a reaction that will be discussed in more detail below. In addition to the ease of preparation of the bis(bis(trimethylsilyl)amides, their stability and solubility in a wide range of both polar and nonpolar solvents make them very attractive starting materials.

Transamination involves the reaction of the bis(bis(trimethylsilyl)amides with an acidic substrate (pKa < 30) [Eq. (5)] under liberation of free amine, HN (SiMe$_3$)$_2$ (pKa ~ 30) [31, 188]. The low boiling point of the resulting amine allows for its easy removal under vacuum, and thus facile work-up. As shown in [Eq. (5)], the reaction is based on an equilibrium; as such, product yields can be increased by quick removal of the liberated amine.

$$M[N(SiMe_3)_2]_2(thf)_2 + 2RH \rightleftarrows MR_2(thf)_2 + 2HN(SiMe_3)_2 \qquad (5)$$
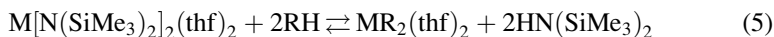
where M = Mg, Ca, Sr, Ba; RH = benzene, di- and triphenylmethane, cyclopentadiene, acetylene, pyrazole, amine, guanidine, alcohol, fluoroalcohol, thiol, phosphane, selenol, tellurol, arsane.

However, the main limitation for transamination reactions is the pKa of hexamethyldisilazane (pKa ~ 30) [188], as only substrates with a lower pKa than that of the HN(SiMe$_3$)$_2$ can be utilized. Representative examples of products obtained include benzylates [178], di- and triphenylmethanides [178], cyclopentadienides [189, 190], acetylides [179, 191, 192], pyrazolates [112], amides [112, 113], guanidinates [15, 193, 194], alkoxides [116, 119, 195], fluoroalkoxides (Fig. 9) [123], thiolates [124, 128, 196, 197], phosphanides [130, 198–202], selenolates [124, 131], tellurolates [131, 132], and arsenides [133, 203–205].

On the other hand, highly acidic ligands may promote N–Si bond cleavage in the trimethylsilyl moiety, resulting in the formation of primary amine [Eq. (6)]; this reaction is especially prevalent in the presence of excess acid. A second protonation affords NH$_3$. N–Si bond scission can be suppressed by slow and dilute addition of acidic ligand [206].

$$HN(SiMe_3)_2 + 2RH \rightarrow Me_3SiR + 2H_2NSiMe_3 \qquad (6)$$

$$H_2NSiMe_3 + RH \rightarrow Me_3SiR + NH_3$$
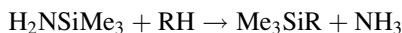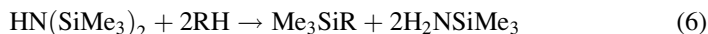
where RH = alkane, arene, silane.

Additionally, the alkaline-earth metal bis(bis(trimethylsilyl)amides) have been reported to initiate ether scission chemistry, as shown with the ring opening of crown ethers or THF [100, 207].

5 Salt Metathesis

Salt metathesis [Eq. (7)] is a well-established route in the synthesis of a variety of alkaline-earth metal alkyls [186, 208–210], allyls [211–214], benzylates [149, 178], cyclopentadienides [17, 108, 215–219], pentadienyls [220], fluorenyls [17, 221], indenyls [222], amides [112, 113, 223], β-diketiminates [112], guanidinates [15, 194], alkoxides [224], aryloxides [224], silanides [210, 225–228], thiolates [229], phosphanides [230, 231], selenolates [229], and germanides [232, 233]. However, the route has been rarely used for the synthesis of more reactive alkyl and aryl metal complexes, largely due to issues pertaining to ether cleavage chemistry as metathesis typically requires the presence of an ethereal solvent.

Salt metathesis is a two-step procedure; the initial step involves metallation of the ligand. Different metallating agents are available; conveniently, alkali metal hydrides may be used, as they cleanly liberate hydrogen gas under quantitative formation of the alkali metal derivatives. As the hydrides exhibit limited solubility, even in THF, alternative frequently used metallating agents are alkali metal bis(trimethylsilyl)amides. Most frequently, potassium derivatives are utilized (see below); as such, the following narrative below focuses specifically on those. The formation of the potassium derivatives is followed by its in situ addition to the sparingly soluble alkaline-earth metal halides in THF. Amongst the halides, the fluorides are the least soluble, whilst the iodides display the highest solubility. For the heavier metals, homogeneous reaction conditions can only be achieved if the iodides along with THF as the solvent are employed. Furthermore, the reaction is critically dependent on high-quality halides.

$$AH + RH \xrightarrow[-0\,°C]{THF} AR + H_2(g)$$

$$2AR + MX_2RH \xrightarrow[THF/Hexane]{} MR_2 + 2AX(s) \qquad (7)$$
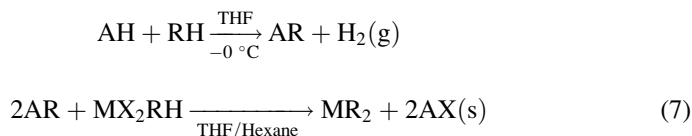
where M = Be–Ba; A = Li–K; X = Cl, Br, I; RH = alkane, allene, benzene, cyclopentadiene, pentadiene, fluorene, indene, amine, β-diketimine, guanidine, alcohol, phenol, silane, thiol, phosphane, selenol, germane.

Fig. 10 Crystal structure of Ca(C(SiMe$_3$)$_3$)$_2$ synthesized via salt metathesis in benzene [186]. Ca···C(π) interactions are shown as *dashed lines*. Hydrogen atoms have been omitted for clarity. All non-carbon atoms are shown as *shaded ellipsoids*
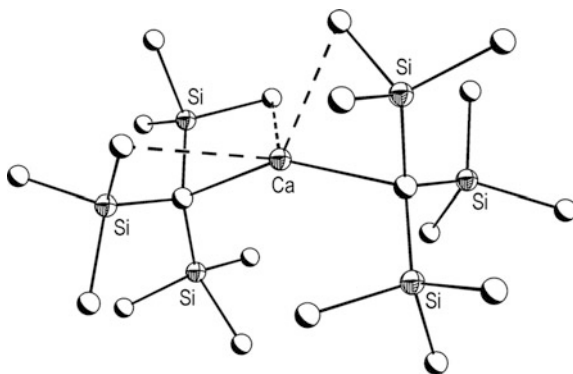
The reaction is driven by the precipitation of the alkali metal halide. In THF, it has been shown that KI typically precipitates cleanly providing the best results. Thus, the combination of potassium reagents (see above) with the iodides has been widely employed in this route. Limitations of this reaction route include the limited solubility of the alkaline-earth metal iodides and potassium derivatives, requiring the need for ethereal solutions. This need for polar solvents may result in ether cleavage reactions.

While salt elimination has been employed for the preparation of the metallocenes, it remains a challenging route towards other groups of organometallics due to the need for preparation of highly reactive potassium precursors [234]. As mentioned above, salt metathesis is typically conducted in THF due to increased solubility of the starting material. Eaborn *et al.* nicely demonstrate the problems associated with salt metathesis in the synthesis of Ca[C(SiMe$_3$)$_3$]$_2$ [186] (Fig. 10). Exposure of this compound to diethyl ether leads to immediate ether scission under formation of Ca(OEt)$_2$. As a result, the salt metathesis reaction was performed in benzene. Due to solubility limitations, the reaction time was extended to 48 h resulting in higher yields [186]. Examples of organometallic compounds prepared by salt metathesis in THF include M[C(SiMe$_3$)$_3$]$_2$(thf)$_n$ (M = Ca, n = 2; M = Sr, Ba, n = 3) [209], Ca(CH$_2$Ph)$_2$(thf)$_4$ (Fig. 6) [149] and more recently Ca[C(SiHMe$_2$)$_3$]$_2$(thf)$_2$ [210].

6 Direct Metallation

The preparation of heavy alkaline-earth metal organometallics involving the reaction of the metal with an acidic ligand substrate remains a very straightforward synthetic strategy, generally requiring an oxide-free metal surface. For highly acidic ligand systems, reflux conditions are sufficient [235, 236]. Direct metallation can also be employed for magnesium as evidenced by the preparation of magnesium anthracene derivatives in the presence of THF; however, finely dispersed metal powder is required [237–240].

Less acidic systems, however, benefit from metal activation. This can be accomplished through various avenues, including the use of highly pure metal

and/or a variety of activation methods including reduction of the alkaline-earth metal iodides with potassium metal or lithium napthalide [82], preparation of surface-enhancing amalgams by addition of mercury, as well as co-condensation methods, [49, 68, 69, 71, 83–87, 187] Extensively explored were also reactions of the metals in anhydrous, liquid [88–93] or gaseous [49, 88, 90, 93] ammonia as discussed in detail below.

Recently, mild solid-state chemistry, involving the treatment of the metals in the presence of the ligand and a flux agent in the absence of a solvent, has been highly successful towards the preparation of various heavy alkaline-earth metal aryloxides, including the heterobimetallic species [AM(ODpp)$_3$] (ODpp or 2,6-diphenylphenoxide) (A = Na, K; M = Ca–Ba) [241] or [Li$_2$Ba(ODpp)$_4$] [164].

6.1 Direct Metallation via Anhydrous NH$_3$(l) Activation

The ready solubility of the heavy alkaline-earth metals in anhydrous, liquid ammonia, under formation of solvated electrons, provides convenient access to a highly reactive form of the metals [Eq. (8)]. As the reactivity of the metals increases as descending the group, reactions involving barium occur more rapidly, while reflux conditions for strontium and calcium (bp NH$_3$ = −33 °C) are required. Coinciding with increased reactivity, the propensity of forming the insoluble M(NH$_2$)$_2$ is much more prevalent for strontium and barium [94–97, 223]. M(NH$_2$)$_2$ may react with acidic substrates under NH$_3$ formation.

The dissolved metals are treated with two equivalents of acidic ligand resulting in hydrogen elimination, under clean isolation of target compounds [242]. The presence of polar co-ligand promotes the reaction [242], as demonstrated by the synthesis of the bis(bis(trimethylsilyl)amides, where presence of THF promotes increased yields [243]. Setbacks of the route include work with condensed gases (bp of NH$_3$ = −33 °C) and the purification of ammonia (condensation over sodium), as commercial gaseous NH$_3$ is not anhydrous.

$$M_{(act)} + 2RH \xrightarrow[-78\ °C,\ NH_3(l)]{THF/Toluene} MR_2 + H_2(g) \qquad (8)$$
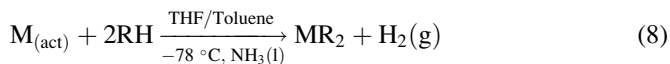
where M = Ca, Sr, Ba; RH = cyclopentadiene, fluorene, amine, pyrazole, anthracene, alcohol, phenol, fluoroalcohol, thiol, silane, siloxane, selenol.

Direct metallation via anhydrous ammonia activation has been used to successfully prepare cyclopentadienides [244–246], fluorenyls [247], amides [112, 113, 223], pyrazolates (Fig. 11) [112], anthracenides [249], alkoxides [250], aryloxides [251–254], fluoroalkoxides [123], thiolates [196, 255–257], silanides [258], siloxides [250], selenolates [255, 256], and a rare methanide, Ba[(PhCH (C$_5$H$_3$N-2))]$_2$(diglyme)(thf) [259]. Sparsely soluble ammonia adducts of the
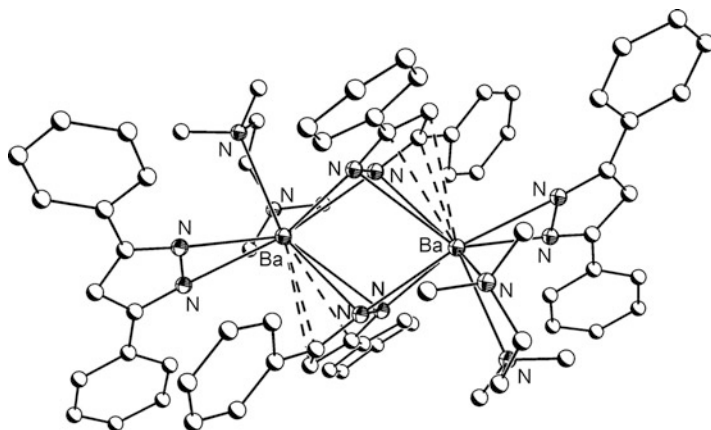
Fig. 11 Crystal structure of $[\{Ba(Ph_2pz)_2(tmeda)\}_2]\cdot TMEDA$ synthesized via direct metallation through ammonia activation in toluene [248]. $Ba\cdots C(\pi)$ interactions are shown as *dashed lines*. Hydrogen atoms have been omitted for clarity. All non-carbon atoms are shown as *shaded ellipsoids*

metal complexes are frequently observed, but removal of ammonia can be achieved by heating to form the target complex.

6.2 Direct Metallation under Mild Solid-State Conditions

Direct metallation using mild solid-state conditions prevents possible ether cleavage chemistry by circumventing the exposure of heavy alkaline-earth metal derivatives to ethereal solvents. Combination of pure metal samples with acidic ligands often in the presence of a flux agent under mild (≤ 250 °C) reaction conditions in evacuated and sealed Carius (thick walled glass) tubes allows the preparation of the alkaline-earth derivatives in high yields and purity [Eq. (9)] [164, 241, 251, 260–264]. Absence of co-ligands and polar solvents results in facile preparation and crystallization of co-ligand-free compounds (Fig. 12). These reactions can be easily monitored by the evolution of dihydrogen gas from the metal surface.

$$M(s) + 2RH \xrightarrow{\leq 250\,^\circ C} MR_2 + H_2(g) \tag{9}$$
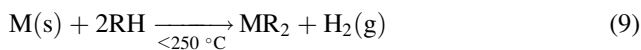
where M = Ca, Sr, Ba; RH = pyrazole, phenol.

Addition of mercury can facilitate product formation for calcium and the less reactive lanthanides through formation of metal amalgams, but it is generally not needed for the heavier alkaline-earth metals, consistent with their more negative
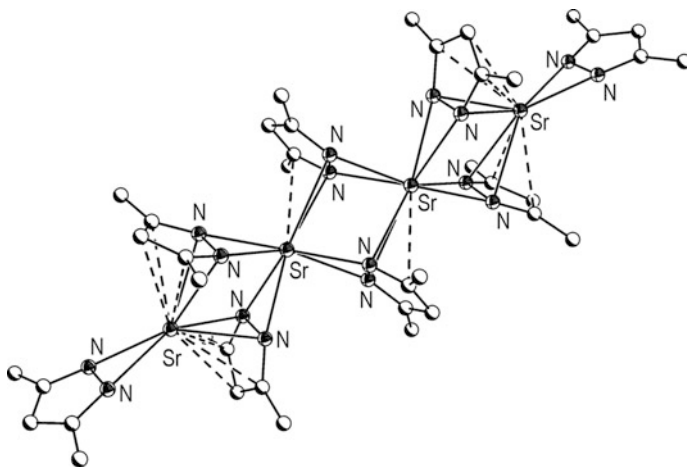
Fig. 12 Structure of $[Sr_4(^tBu_2pz)_8]$ synthesized via direct metallation under solvent-free conditions [264]. $Sr\cdots C(\pi)$ interactions are shown as *dashed lines*. Methyl groups on the *tert*-butyl substituent's and hydrogen atoms have been omitted for clarity. All non-carbon atoms are shown as *shaded ellipsoids*

redox potentials. In some instances, the presence of an inert reaction medium or flux agent which has a low melting point is necessary, especially if the ligand will not melt at the reaction temperatures. An example of an effective flux agent is 1,2,4,5-tetramethylbenzene [264] or 1,2,5-tri-*tert*-butylbenzene (Mes*H) [164, 241, 262, 264, 265]. In some cases, the ligand itself proves to be a suitable reaction medium [251, 260, 261, 263, 266].

Slow cooling of reaction mixtures frequently affords X-ray quality crystals of homoleptic co-ligand-free compounds. Isolation of target compounds is straightforward: washing the reaction mixtures with hexane will remove unreacted ligand and flux agent. Extraction of crude products in polar solvents or in the presence of co-ligands affords the respective co-ligand containing products. This reaction route has been successful in preparing several alkaline-earth pyrazolate species [112] as well as alkaline-earth metal aryloxides [251, 262, 263]. Importantly, the techniques have been successful in the preparation of heterobimetallic alkali–alkaline [164, 241], alkaline–lanthanide [262], and alkaline–alkaline [262] compounds that in the presence of a donor solvent decompose into the homometallic parent compounds. Due to the absence of Lewis bases, the co-ligand-free target compounds exhibit different structural motifs than the co-ligand containing counterparts. The co-ligand-free compounds are especially attractive for the investigation of weak, non-covalent interactions including $M\cdots C(\pi)$ and agostic interactions which frequently provide steric saturation for the large alkaline-earth metal centers (Fig. 13).

While metal activation under mild solid-state conditions provides a straightforward reaction route, some limitations and safety concerns should be addressed. The acidity and ultimately the thermal stability of the ligands present the main concern to this reaction route. Since temperatures above 150 °C are needed for a
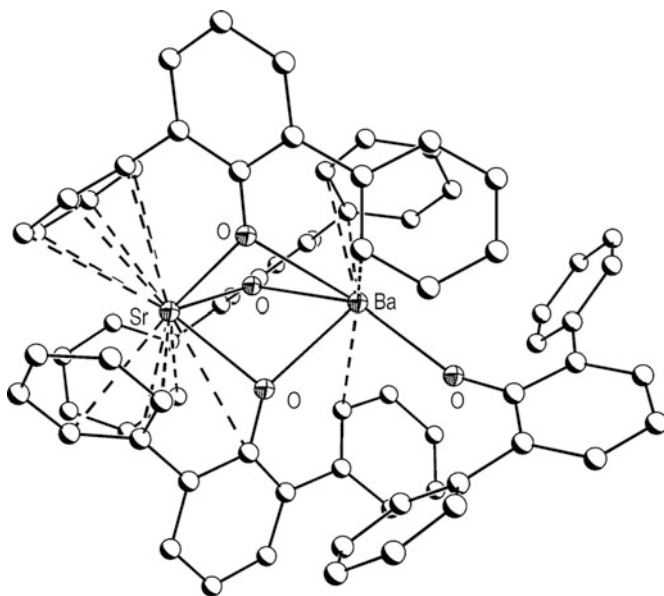
Fig. 13 Crystal structure of [BaSr(Odpp)$_4$] synthesized via direct metallation under solvent-free conditions [262]. M···C(π) interactions are shown as *dashed lines*. Note the decreased number of M···C(π) interactions on the larger barium due to the presence of a terminal aryloxide ligand. Hydrogen atoms have been omitted for clarity. All non-carbon atoms are shown as *shaded ellipsoids*

smooth reaction, partial decomposition of the ligand typically is a concern. In addition, careful control of reaction scale is critical as gases are being generated in a closed system.

7 Redox Transmetallation

Redox transmetallation is the classic route to prepare organometallic alkaline-earth compounds [29]. This route takes advantage of the electropositive nature of the alkaline-earth metals by reacting them with sacrificial mercury, tin, or thallium organometallic complexes [Eq. (10)]. This method provides good product yields in either polar solvents, but acceptable yields are also observed in aromatic or hydrocarbon solvents [267], while providing for straightforward product purification involving removal of unreacted reagent and metal product by filtration, followed by crystallization of target compound from a suitable solvent.

$$M(s) + M'R_2 \rightarrow MR_2 + M'(s) \tag{10}$$
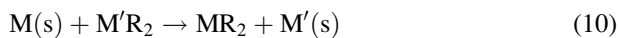
where M = Ca, Sr, Ba; M$'$ = Hg, Sn; R = bis(trimethylsilyl)amide; M$'$ = Tl; R = pyrazolate.

To this effect, organomercurials have been used extensively as transmetallating agents to afford pure co-ligand-free organoberyllium and magnesium compounds [29, 268]. The mercurials have also been used for the preparation of bis(bis(trimethylsilyl)amides [207]. More recently, tin-based transmetallation chemistry allowed the preparation of the amides [267], while thallium pyrazolates were employed in the synthesis of the corresponding alkaline-earth derivatives [Ca(Ph$_2$pz)$_2$(thf)$_4$] and [Sr(Ph$_2$pz)$_2$(dme)$_2$] (Ph$_2$pz or diphenylpyrazolate) [260]. Limiting this route is the inherent toxicity of the redox transmetallation agents.

7.1 Redox Transmetallation/Ligand Exchange

Redox transmetallation/ligand exchange (RTLE) provides a variant to redox transmetallation. This route typically utilizes alkaline-earth metal pieces or filings and an aryl (C$_6$H$_5$) or less frequently pentafluoroaryl (C$_6$F$_5$) mercurial as the transmetallating agent with the in situ formation of a reactive alkaline-earth organometallic intermediate. This intermediate is not stable under the reaction conditions and is immediately followed by ligand exchange involving a protic substrate under formation of the target compound and liberation of benzene or pentafluorobenzene [Eq. (11)]. Reactions of this nature are typically performed as a one-pot reaction in the presence of a polar solvent. This methodology is very well established in lanthanoid chemistry (using mercurials as redoxtransmetallating agent) and has been used for the preparation of a variety of alkaline-earth organometallic compounds including cyclopentadienides [269], pyrazolates [112, 270], formamidinates [271, 272], and aryloxides [251, 273].

$$M(s) + HgR'_2 \rightarrow MR'_2 + Hg(s) \qquad (11)$$

$$MR'_2 + 2RH \rightarrow MR_2 + 2R'H$$
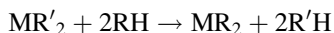
where M = Ca, Sr, Ba; R′ = C$_6$F$_5$, C$_6$H$_5$; R = cyclopentadienide, pyrazolate, formamidinate, aryloxide.

Inherently crucial to the reaction is the presence of a ligand with a lower pKa than the resulting benzene (pKa ~ 43) or pentafluorobenzene (pKa ~ 26). In addition, reaction times are metal size dependent as a consequence of more negative redox potentials upon descending the group of alkaline-earth metals [274].

Recent advances to this synthetic strategy have been made by replacing the toxic organomercurial by the transmetallation agent Ph$_3$Bi [Eq. (12)] [157]. In addition to being less toxic than the classic organomercurial [LD$_{50}$ Ph$_3$Bi: 180 g kg^{-1} (dog, oral); LD$_{50}$ Ph$_2$Hg : 50–400 mg kg^{-1} (rat, oral)] [275], Ph$_3$Bi offers several advantages: it is commercially available, inexpensive, and air and moisture stable, and allows an easy work-up of the target compounds while providing good product yields. As the reaction depends on the difference in redox potentials between the two

Fig. 14 Crystal structure of $Ba[N(Mes)(SiMe_3)]_2(thf)_3$ synthesized via redox transmetallation/ligand exchange (RTLE) [157]. $Ba\cdots C(\pi)$ interactions shown as *dashed lines*. Hydrogen atoms have been omitted for clarity. All non-carbon atoms are shown as *shaded ellipsoids*
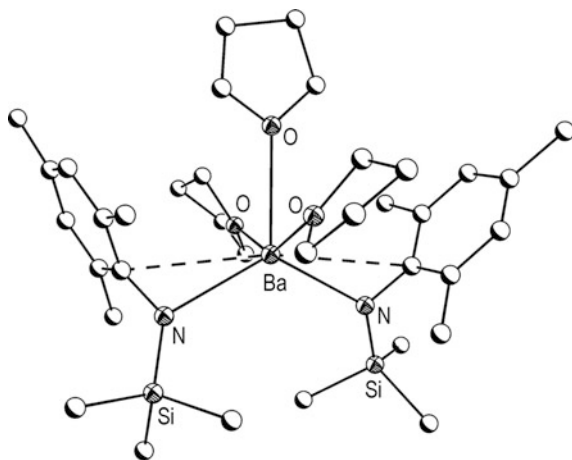
metals, mercury, with its positive redox potential, works very well ($E^o = 0.851$ V (Hg)) [274]. Replacing mercury with the less positive bismuth ($E^o = 0.308$ V(Bi)) [274] thus limits the reaction route to the metals with the most negative redox potentials, such as heavy alkaline-earth metals ($E^o = -2.87$ V(Ca^{2+}); $E^o = -2.89$ V(Sr^{2+}); $E^o = -2.90$ V(Ba^{2+})) [33]. The rare earth metals with their less negative redox potentials ($E^o = -2.22$ V(Yb^{2+}); $E^o = -2.30$ V(Sm^{2+}); $E^o = -1.99$ V(Eu^{2+})) [33] do not perform well with Ph_3Bi.

$$3M(s) + 2Ph_3Bi \rightarrow 3MPh_2 + 2Bi(s) \qquad (12)$$

$$MPh_2 + 2RH \rightarrow MR_2 + 2PhH(l)$$
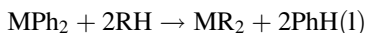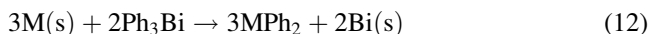
where M = Ca, Sr, Ba; RH = cyclopentadiene, amine, pyrazole, phenol.

Analogous to redox transmetallation ligand exchange in the presence of organomercurials, ligands with lower pKa than the resulting benzene (pKa ~ 43) are necessary. Reaction times are metal size dependent, reactions involving barium occurring at faster times than the lighter metals. Optimization of reaction conditions including use of metal filings and sonication has allowed for the preparation of several heavy alkaline-earth metal amides [157] (Fig. 14), cyclopentadienides [246], and aryloxides [251].

8 Metal Exchange

Metal exchange reactions have been used in the preparation of heavy alkali organometallics by reaction of alkali metal alkoxide or aryloxide with an organolithium reagent under precipitation of lithium alkoxide/aryloxide. For these reactions, careful ligand choice enables the separation of the two solid reaction products. Two variants of this reaction for alkaline-earth metal organometallics

Fig. 15 Crystal structure of
$[Ca(N(SiMe_3)_2)(18\text{-crown-}6)][CPh_3]$ (CPh_3 or
triphenylmethanide) [145].
Hydrogen atoms have been
omitted for clarity. All
non-carbon atoms are shown
as *shaded ellipsoids*
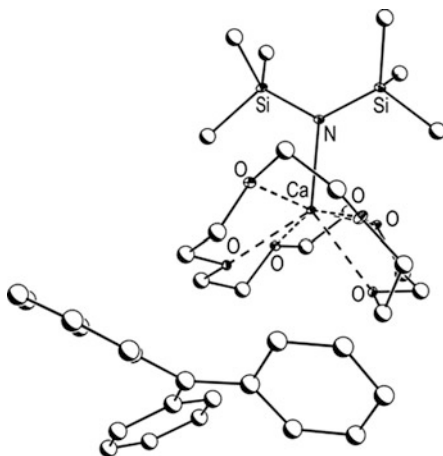
have been reported: reaction of heavy alkaline-earth alkoxide with benzyllithium
[144] [Eq. (13)] and treatment of the alkaline-earth bis(bis(trimethylsilyl)amides
with a lithium reagent [144–147] [Eq. (14)].

$$M(OR)_2 + 2PhCH_2Li \rightarrow (PhCH_2)_2M + 2LiOR \tag{13}$$

where M $=$ Ba; R $=$ 2,4,6-tri-*tert*butylphenyl.

$$M[N(SiMe_3)_2]_2(thf)_2 + 2LiR \rightarrow MR_2 + 2LiN(SiMe_3)_2 \tag{14}$$
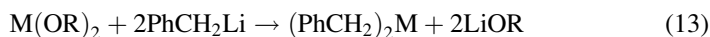
where M $=$ Ca, Sr, Ba; R $=$ benzyl, di-, triphenylmethanide.

As seen for alkali metals, separation of the two solid reaction products is the
major setback to this route. In addition, alkaline-earth metal *tert*-butoxides are
difficult to prepare in a pure form [276], as ether cleavage reactions frequently
initiate oxide or hydroxide containing products (Westerhausen, Private Communi-
cation). Alternatively, the corresponding easily accessible amides can be used.
These will also aid in the isolation of products. Due to the soluble nature of the
resulting lithium amide, separation of products is more facile, as the products
typically precipitate. Use of the alkaline-earth bis(bis(trimethylsilyl)amides in
conjunction with benzylic lithium reagents has afforded a pathway to the prepara-
tion in high yields of alkaline-earth organometallics in the form of benzylates
[144, 146, 147] which are the starting materials necessary for organoelimination
reactions leading to di- and triphenylmethanides (see above) (Fig. 15) [145].

9 Conclusions

The rapid development of alkaline-earth organometallic and metal organic
chemistry has been made possible by the examination and often modifications
of established synthetic strategies, in addition to the exploration of alternative

methodologies. The understanding of the impact of reaction variables including reaction temperature and solvent choice has been instrumental in the synthesis of novel alkaline-earth metal species. These developments will continue to progress the chemistry of alkaline-earth metals and provide the necessary tools towards preparation of compounds with synthetic and material applications.

References

1. Crimmin MR, Barrett AGM, Hill MS, Hitchcock PB, Procopiou PA (2008) Organometallics 27:497
2. Crimmin MR, Casely IJ, Hill MS (2005) J Am Chem Soc 127:2042
3. He X, Hurley E, Noll BC, Henderson KW (2008) Organometallics 27:3094
4. Datta S, Roesky PW, Blechert S (2007) Organometallics 26:4392
5. Datta S, Gamer MT, Roesky PW (2008) Organometallics 27:1207
6. Crimmin MR, Barrett AGM, Hill MS, Hitchcock PB, Procopiou PA (2007) Organometallics 26:2953
7. Buch F, Brettar J, Harder S (2006) Angew Chem Int Ed 45:2741
8. Orzechowski L, Harder S (2007) Organometallics 26:2144
9. Crimmin MR, Barrett AGM, Hill MS, Procopiou PA (2006) Org Lett 9:331
10. Harder S, Feil F, Weeber A (2001) Organometallics 20:1044
11. Lindsell WE, Robertson FC, Soutar I (1983) Eur Polym J 19:115
12. Lindsell WE, Robertson FC, Soutar I, Richards DH (1981) Eur Polym J 17:107
13. Schumann H, Steffens A, Hummert M (2009) Z Anorg Allg Chem 635:1041
14. Sarazin Y, Howard RH, Hughes DL, Humphrey SM, Bochmann M (2006) Dalton Trans:340
15. Feil F, Harder S (2005) Eur J Inorg Chem 2005:4438
16. Weeber A, Harder S, Brintzinger HH, Knoll K (2000) Organometallics 19:1325
17. Feil F, Harder S (2003) Eur J Inorg Chem 2003:3401
18. Harder S, Feil F, Knoll K (2001) Angew Chem Int Ed 40:4261
19. Chisholm MH, Gallucci JC, Phomphrai K (2004) Inorg Chem 43:6717
20. Chisholm MH, Gallucci JC, Phomphrai K (2003) Chem Commun:48
21. Piao L, Deng M, Chen X, Jiang L, Jing X (2003) Polymer 44:2331
22. Zhong Z, Schneiderbauer S, Dijkstra PJ, Westerhausen M, Feijen J (2003) Polym Bull 51:175
23. Zhong Z, Schneiderbauer S, Dijkstra PJ, Westerhausen M, Feijen J (2001) J Polym Environ 9:31
24. Westerhausen M, Schneiderbauer S, Kneifel Alexander N, Söltl Y, Mayer P, Nöth H, Zhong Z, Dijkstra Pieter J, Feijen J (2003) Eur J Inorg Chem 2003:3432
25. Hampden-Smith MJ, Kodas TT, Ludviksson A (1998) Chem Adv Mater:143
26. Jones AC (1998) Chem Vap Deposition 4:169
27. Jones AC (2002) J Mater Chem 12:2576
28. Wojtczak WA, Fleig PF, Hampden-Smith MJ (1996) Adv Organomet Chem 40:215
29. Elschenbroich C (2006) Organometallics. Wiley-VCH Verlag GmnH & Co. KGaA, Weinheim
30. Smith JD (1999) Adv Organomet Chem 43:267
31. Alexander JS, Zuniga MF, Guino-o MA, Hahn RC, Ruhlandt-Senge K (2006) The organometallic chemistry of the alkaline earth metals, vol 1, The Encyclopedia of inorganic chemistry. Wiley, New York, NY, p 116
32. Shannon RD (1976) Acta Crystallogr Sect A A32:751

33. Miessler GL, Tarr DA (2004) Inorganic chemistry. Prentice Hall, NJ
34. Grignard V (1990) C R Hebd Seances Acad Sci 130:1322
35. Grignard V (1901) Annal Chim Phys 24:433
36. Beckmann E, Beck K, Schlegel H (1905) Ber Dtsch Chem Ges 38:904
37. Lindsell WE (1982) In: Wilkinson G, Stone FGA, Abel EW (eds) Comprehensive organo-metallic chemistry, vol 1. Pergamon Press, Oxford, p 155
38. Markies PR, Akkerman OS, Bickelhaupt F, Smeets WJJ, Spek AL (1991) X-ray structural analyses of organomagnesium compounds. In: Stone FGA, Robert W (eds) Adv Organomet Chem, vol 32. Academic, New York, NY, p 147
39. Bickelhaupt F (1994) J Organomet Chem 475:1
40. Wakefield BJ (1995) Organomagnesium methods in organic synthesis. Academic, London
41. Richey HG (2000) Grignard reagents new developments. Wiley, Chichester
42. Ackermann L, Althammer A (2009) Chem unserer Zeit 43:74
43. Seyferth D (2009) Organometallics 28:1598
44. Gilman H, Schulze F (1926) J Am Chem Soc 48:2463
45. Glacet C (1938) Bull Soc Chim Fr 5:895
46. Masthoff R, Krieg G (1966) Z Chem 6:433
47. Ioffe ST, Nesmeyanov AN (1967) The organo compounds of magnesium, beryllium, calcium,. strontium and barium. North Holland Publishing Company, Amsterdam
48. Masthoff R, Schüler H, Krieg G (1968) J Organomet Chem 13:37
49. Gowenlock BG, Lindsell WE, Singh B (1978) J Chem Soc Dalton Trans:657
50. Eisch JJ, King RB (1981) In: Press A (ed) Organometallic synthesis, vol 2. Academic, New York, NY, p 101
51. Hanusa TP (1993) Chem Rev 93:1023
52. Hanusa TP (2000) Coord Chem Rev 210:329
53. Masthoff R, Vieroth C (1968) J Prakt Chem:182
54. Bryce-Smith D, Skinner A (1963) J Chem Soc A:577
55. Kawabata N, Matsumura A, Yamashita S (1973) Tetrahedron 28:1069
56. Kawabata N, Matsumura A, Yamashita S (1973) J Org Chem 38:4268
57. Mochida K, Yamanishi T (1987) J Organomet Chem 332:247
58. Zemlyanichenko MA, Sheverdina NI, Chernoplekova VA, Kocheshkov KA (1972) Zh Obshch Khim 42:841
59. Paleeva IE, Sheverdina NI, Zemlyanichenko MA, Kocheshkov KA (1973) Dokl Akad Nauk SSSR 210:1134
60. Paleeva IE, Sheverdina NI, Kocheshkov KA (1974) Zh Obshch Khim 44:1135–1137
61. Gowenlock BG, Lindsell WE (1977) J Organomet Chem:1
62. Hanusa TP (1990) Polyhedron 9:1345
63. Westerhausen M (2001) Ang Chem Int Ed 40:2975
64. Alexander JS, Ruhlandt-Senge K (2002) Eur J Inorg Chem 11:2761
65. Langer J, Krieck S, Görls H, Westerhausen M (2009) Angew Chem Int Ed 48:5741
66. Fischer R, Görls H, Westerhausen M (2005) Inorg Chem Commun 8:1159
67. Fischer R, Gärtner M, Görls H, Westerhausen M (2006) Organometallics 25:3496
68. Fischer R, Gärtner M, Görls H, Westerhausen M (2006) Angew Chem Int Ed 45:609
69. Westerhausen M, Gärtner M, Fischer R, Langer J, Yu L, Reiher M (2007) Chem Eur J 13:6292
70. Fischer R, Gärtner M, Görls H, Yu L, Reiher M, Westerhausen M (2007) Angew Chem Int Ed 46:1618
71. Gärtner M, Görls H, Westerhausen M (2007) Synthesis:725
72. Langer J, Görls H, Westerhausen M (2007) Inorg Chem Commun 10:853
73. Westerhausen M (2008) Coord Chem Rev 252:1516
74. Krieck S, Görls H, Westerhausen M (2009) J Organomet Chem 694:2204
75. Krieck S, Goörls H, Westerhausen M (2010) J Am Chem Soc 132:12492

76. Langer J, Krieck S, Fischer R, Görls H, Westerhausen M (2010) Z Anorg Allg Chem 636:1190
77. Langer J, Gärtner M, Fischer R, Görls H, Westerhausen M (2007) Inorg Chem Commun 10:1001
78. Langer J, Görls H, Westerhausen M (2010) Organometallics 29:2034
79. Johnson WC, Stubbs MF, Sidwell AE, Pechukas A (1939) J Am Chem Soc 61:318
80. McCreary WJ (1958) J Met 10:615
81. Evers J, Weiss A, Kaldis E, Muheim J (1973) J Less Common Metals 30:83
82. McCormick MJ, Moon KB, Jones SP, Hanusa TP (1990) J Chem Soc Chem Comm:778
83. Cloke FGN, Hitchcock PB, Lappert MF, Lawless GA, Royo B (1991) J Chem Soc Chem Comm:724
84. Hutchings DS, Junk PC, Patalinghug WC, Raston CL, White AH (1989) J Chem Soc Chem Commun:973
85. Mochida K, Hiraga Y, Takeuchi H, Ogawa H (1987) Organometallics 6:2293
86. Gardiner MG, Raston CL, Kennard CHL (1991) Organometallics 10:3680
87. Klabunde KJ (1975) Acc Chem Res 8:393
88. Jutzi P, Leffers W, Mueller G, Huber B (1989) Chem Ber 122:879
89. Drake SR, Otway DJ (1992) Polyhedron 11:745
90. Drake SR, Otway DJ (1991) J Chem Soc Chem Commun:517
91. Drake SR, Otway DJ, Perlepes SP (1991) Main Group Met Chem 14:243
92. Thompson JC (1976) Monographs on the physics and chemistry of materials: electrons in liquid ammonia. Oxford University Press, London
93. Drake SR, Otway DJ (1991) J Chem Soc Chem Commun:1060
94. Juza R, Schumacher H (1963) Z Anorg Allg Chem 324:278
95. Juza R (1964) Angew Chem 76:290
96. Mammano N, Sienko MJ (1970) J Solid State Chem 1:534
97. Biltz W, Hüttig GF (1920) Z Anorg Allg Chem 114:241
98. Westerhausen M (2009) Z Anorg Allg Chem 635:13
99. Alexander JS, Ruhlandt-Senge K (2001) Angew Chem Int Ed 40:2658
100. Alexander JS, Ruhlandt-Senge K, Hope H (2003) Organometallics 22:4933
101. Ripin D, Evans D. http://daecr1.harvard.edu/pKa/pKa.html
102. Gärtner M, Görls H, Westerhausen M (2007) Organometallics 26:1077
103. Gärtner M, Görls H, Westerhausen M (2008) J Organomet Chem 693:221
104. Krieck S, Goörls H, Yu L, Reiher M, Westerhausen M (2009) J Am Chem Soc 131:2977
105. Nagel U, Nedden HG (1997) Chem Ber 130:535
106. Schumann H, Gottfriedsen J, Glanz M, Dechert S, Demtschuk J (2001) J Organomet Chem 617:588
107. Vollet J, Baum E, Schnöckel H (2003) Organometallics 22:2525
108. Weber F, Sitzmann H, Schultz M, Sofield CD, Andersen RA (2002) Organometallics 21:3139
109. Sanchez R (1986) Organomet Synth 3:391
110. Jaenschke A, Olbrich F, Behrens U (2009) Z Anorg Allg Chem 635:2550
111. Guino-o MA, Baker E, Ruhlandt-Senge K (2007) J Coord Chem 61:125
112. Torvisco A, O'Brien AY, Ruhlandt-Senge K (2011) Coord Chem Rev 255:1268
113. Lappert MF, Protchenko AV, Power PP (2009) In: Lappert MF (ed) Metal amide chemistry. Wiley, Chichester
114. Zechmann CA, Boyle TJ, Rodriguez MA, Kemp RA (2001) Inorg Chim Acta 319:137
115. Calabrese J, Cushing MA, Ittel SD (1988) Inorg Chem 27:867
116. Boyle TJ, Coker EN, Zechmann CA, Voigt JA, Rodriguez MA, Kemp RA, Mallen MZ (2002) Chem Mater 15:309
117. Teng W, Guino-o M, Hitzbleck J, Englich U, Ruhlandt-Senge K (2006) Inorg Chem 45:9531
118. Zechmann CA, Boyle TJ, Rodriguez MA, Kemp RA (2000) Polyhedron 19:2557
119. Henderson KW, Honeyman GW, Kennedy AR, Mulvey RE, Parkinson JA, Sherrington DC (2003) Dalton Trans:1365

120. Yu T-L, Wu C-C, Chen C-C, Huang B-H, Wu J, Lin C-C (2005) Polymer 46:5909
121. Shueh M-L, Wang Y-S, Huang B-H, Kuo C-Y, Lin C-C (2004) Macromolecules:37
122. Zuniga MF, Kreutzer J, Ruhlandt-Senge K (2007) Inorg Chem 46:10400
123. Buchanan WD, Guino-o MA, Ruhlandt-Senge K (2010) Inorg Chem 49:7144
124. Ruhlandt-Senge K (1995) Inorg Chem 34:3499
125. Niemeyer M, Power PP (1997) Inorg Chim Acta 263:201
126. Sousa Pedrares A, Teng W, Ruhlandt-Senge K (2003) Chem Eur J 9:2019
127. Chadwick S, Englich U, Senge MO, Noll BC, Ruhlandt-Senge K (1998) Organometallics 17:3077
128. Chadwick S, Englich U, Ruhlandt-Senge K (1999) Inorg Chem 38:6289
129. Westerhausen M, Pfitzner A (1995) J Organomet Chem 487:187
130. Westerhausen M, Schwarz W (1993) J Organomet Chem 463:51
131. Gindelberger DE, Arnold J (1994) Inorg Chem 33:6293
132. Gindelberger DE, Arnold J (1992) J Am Chem Soc 114:6242
133. Westerhausen M, Makropoulos N, Piotrowski H, Warchhold M, Nöth H (2000) J Organomet Chem 614–615:70
134. Torvisco A, Ruhlandt-Senge K (2011) Organometallics 30:986
135. Vargas W, Englich U, Ruhlandt-Senge K (2002) Inorg Chem 41:5602
136. Gillett-Kunnath M, Teng W, Vargas W, Ruhlandt-Senge K (2005) Inorg Chem 44:4862
137. Olmstead MM, Grigsby WJ, Chacon DR, Hascall T, Power PP (1996) Inorg Chim Acta 251:273
138. Engelhardt LM, Jolly BS, Junk PC, Raston CL, Skelton BW, White AH (1986) Aust J Chem 39:1337
139. Yang K-C, Chang C-C, Huang J-Y, Lin C-C, Lee G-H, Wang Y, Chiang MY (2002) J Organomet Chem 648:176
140. Conway B, Hevia E, Kennedy AR, Mulvey RE, Weatherstone S (2005) J Chem Soc Dalton Trans:1532
141. Westerhausen M, Bollwein T, Makropoulous N, Piotrowski H (2005) Inorg Chem 44:6439
142. Tang Y, Zakharov LN, Rheingold AL, Kemp RA (2005) Organometallics 24:836
143. Bartlett RA, Olmstead MM, Power PP (1994) Inorg Chem 33:4800
144. Harder S, Brintzinger HH, Weeber A (2000) Organometallics 19:1325
145. Guino-o MA, Torvisco A, Teng W, Ruhlandt-Senge K (2012) Inorg Chim Acta 389:122–130
146. Guino-o MA, Campana CF, Ruhlandt-Senge K (2007) Chem Commun:1692
147. Alexander JS, Ruhlandt-Senge K (2004) Chem Eur J 10:1274
148. Alexander JS (2003) Doctoral Dissertation, Chemistry, Syracuse University, Syracuse
149. Harder S, Müller S, Hübner E (2004) Organometallics 23:178
150. Alexander JS, Ruhlandt-Senge K (2002) Eur J Inorg Chem:2761
151. West P, Woodville MC (1973) United States Patent. In: Patent US (ed) United States Patent 3,718,703
152. De Groof B, Van Beylen M, Szwarc M (1975) Macromolecules 8:396
153. De Groof B, Mortier W, Van Beylen M, Swarc M (1977) Macromolecules 10:598
154. Arest-Yakubich AA (1981) Russ Chem Rev 50:601
155. Nakhmanovich BI, Arest-Yakubovich AA (1976) Dokl Phys Chem 228:426
156. Takahashi K, Kondo Y, Asami R (1978) JCS Perkin II:577
157. Gillett-Kunnath M, MacLellan JG, Forsyth CM, Andrews PC, Deacon GB, Ruhlandt-Senge K (2008) Chem Commun 37:4490
158. Weiss E (1993) Angew Chem Int Ed 32:1501
159. Mulvey RE (2001) Chem Commun:1049
160. Hitchcock PB, Huang Q, Lappert MF, Wei X-H, Zhou M (2006) Dalton Trans:2991
161. Davies RP (2000) Inorg Chem Commun 3:13
162. Kennedy AR, Mulvey RE, Rowlings RB (2002) J Organomet Chem 648:288
163. He X, Noll BC, Beatty A, Mulvey RE, Henderson KW (2004) J Am Chem Soc 126:7444
164. Zuniga MF, Deacon GB, Ruhlandt-Senge K (2007) Chem Eur J 13:1921

165. Maudez W, Häussinger D, Fromm KM (2006) Z Anorg Allg Chem 632:2295
166. Coan PS, Streib WE, Caulton KG (1991) Inorg Chem 30:5019
167. Bock H, Hauck T, Näther C, Rösch N, Staufer M, Häberlen OD (1995) Angew Chem Int Ed 34:1353
168. Fromm KM, Gueneau ED, Goesmann H (2000) Chem Commun:2187
169. Fromm KM (2006) Dalton Trans:5103
170. Frankland AD, Lappert MF (1996) J Chem Soc Dalton Trans:4151
171. Hitchcock PB, Khvostov AV, Lappert MF (2002) J Organomet Chem 663:263
172. Kinsley SA, Streitwieser A Jr, Zalkin A (1985) Organometallics 4:52
173. Fischer R, Görls H, Westerhausen M (2007) Organometallics 26:3269
174. Hevia E, Henderson KW, Kennedy AR, Mulvey RE (2006) Organometallics 25:1778
175. Westerhausen M, Gückel C, Habereder T, Vogt M, Warchold M, Nöth H (2001) Organometallics 20:893
176. Knapp V, Müller G (2001) Angew Chem Int Ed 40:183
177. Schubert B, Weiss E (1984) Chem Ber 117:366
178. Torvisco A, Ruhlandt-Senge K (2011) Inorg Chem 50:12223
179. Guino-o MA, Alexander JS, McKee ML, Hope H, Englich U, Ruhlandt-Senge K (2009) Chem Eur J 15:11842
180. Orzechowski L, Piesik DFJ, Ruspic C, Harder S (2008) Dalton Trans:4742
181. Gärtner M, Görls H, Westerhausen M (2007) Inorg Chem 46:7678
182. Boncella JM, Coston CJ, Cammack JK (1991) Polyhedron 10:769
183. Tanner PS, Burkey DJ, Hanusa TP (1995) Polyhedron 14:331
184. Kuhlman RL, Vaartstra BA, Caulton KG (1997) Inorg Synth 31:8
185. Bartsch R, Drost C, Klingebiel U (1996) In: Herrmann WA, Auner N, Klingebiel U (eds) Synthetic methods of organometallic and inorganic chemistry, vol 2. Herrmannr/Brauer, Thieme, Stuttgart, p 62
186. Eaborn C, Hawkes S, Hitchcock PB, Smith JD (1997) Chem Commun:1961
187. Hitchcock PB, Lappert MF, Lawless GA, Royo B (1990) J Chem Soc Chem Commun:1141
188. Fraser RR, Mansour TS, Savard S (1985) J Org Chem 50:3232
189. Tanner PS, Hanusa TP (1994) Polyhedron 13:2417
190. Hays ML, Hanusa TP, Nile TA (1996) J Organomet Chem 514:73
191. Green DC, Englich U, Ruhlandt-Senge K (1999) Angew Chem Int Ed 38:354
192. Green DC, Englich U, Ruhlandt-Senge K (1999) Angew Chem 111:365
193. Lachs JR, Barrett AGM, Crimmin MR, Kociok-Köhn G, Hill MS, Mahon MF, Procopiou PA (2008) Eur J Inorg Chem 2008:4173
194. Cameron TM, Xu C, Dipasquale AG, Rheingold AL (2008) Organometallics 27:1596
195. Borup B, Samuels JA, Streib WE, Caulton KG (1994) Inorg Chem 33:994
196. Chadwick S, Englich U, Noll B, Ruhlandt-Senge K (1998) Inorg Chem 37:4718
197. Teng W, Englich U, Ruhlandt-Senge K (2000) Inorg Chem 39:3875
198. Crimmin MR, Barrett AGM, Hill MS, Hitchcock PB, Procopiou PA (2007) Inorg Chem 46:10410
199. Westerhausen M, Löw R, Schwarz W (1996) J Organomet Chem 513:213
200. Matthias W (1994) J Organomet Chem 479:141
201. Westerhausen M, Birg C, Krofta M, Mayer P, Seifert T, Nöth H, Pfitzner A, Nilges T, Deiseroth H-J (2000) Z Anorg Allg Chem 626:1073
202. Westerhausen M, Digeser MH, Nöth H, Knizek J (1998) Z Anorg Allg Chem 624:215
203. Westerhausen M, Digeser MH, Knizek J, Schwarz W (1998) Inorg Chem 37:619
204. Westerhausen M, Birg C, Piotrowski H, Habereder T, Suter M, Nöth H (2001) Z Anorg Allg Chem 627:882
205. Westerhausen M, Birg C, Piotrowski H (2000) Eur J Inorg Chem 2000:2173
206. Chadwick S, Englich U, Ruhlandt-Senge K (1998) Angew Chem Int Ed 37:3007
207. Bradley DC, Hursthouse MB, Ibrahim AA, Abdul Malik KM, Motevalli M, Moseler R, Powell H, Runnacles JD, Sullivan AC (1990) Polyhedron 9:2959

208. Izod K, Liddle ST, Clegg W (2003) J Am Chem Soc 125:7534
209. Crimmin MR, Barrett AGM, Hill MS, MacDougall DJ, Mahon MF, Procopiou PA (2008) Chem Eur J 14:11292
210. Yan K, Upton BM, Ellern A, Sadow AD (2009) J Am Chem Soc 131:15110
211. Quisenberry KT, White RE, Hanusa TP, Brennessel WW (2010) New J Chem 34:1579
212. Chmely SC, Carlson CN, Hanusa TP, Rheingold AL (2009) J Am Chem Soc 131:6344
213. Jochmann P, Dols TS, Spaniol TP, Perrin L, Maron L, Okuda J (2009) Angew Chem Int Ed 48:5715
214. Harvey MH, Hanusa TP, Young VGJ (1999) Ang Chem Int Ed 38:217
215. McCormick MJ, Williams RA, Levine LJ, Hanusa TP (1988) Polyhedron 7:725
216. Williams RA, Tesh KF, Hanusa TP (1991) J Am Chem Soc 113:4843
217. Harvey MJ, Quisenberry KT, Hanusa TP, Young VG Jr (2003) Eur J Inorg Chem 2003:3383
218. Burkey DJ, Williams RA, Hanusa TP (1993) Organometallics 12:1331
219. Burkey DJ, Hanusa TP, Huffman JC (1994) Adv Mater Opt Electron 4:1
220. Overby JS, Hanusa TP (1994) Angew Chem Int Ed 33:2191
221. Feil F, Müller C, Harder S (2003) J Organomet Chem 683:56
222. Overby JS, Hanusa TP (1996) Organometallics 15:2205
223. Westerhausen M (1998) Coord Chem Rev 176:157
224. Tesh KF, Hanusa TP, Huffman JC, Huffman CJ (1992) Inorg Chem 31:5572
225. Teng W, Ruhlandt-Senge K (2004) Organometallics 23:2694
226. Gaderbauer W, Zirngast M, Baumgartner J, Marschner C, Tilley TD (2006) Organometallics 25:2599
227. Farwell JD, Lappert MF, Marschner C, Strissel C, Tilley TD (2000) J Organomet Chem 603:185
228. Lerner H-W, Scholz S, Bolte M, Wiberg N, Nöth H, Krossing I (2003) Eur J Inorg Chem 2003:666
229. Ruhlandt-Senge K, Davis K, Dalal S, Englich U, Senge MO (1995) Inorg Chem 34:2587
230. Langer J, Al-Shboul TMA, Younis FM, Görls H, Westerhausen M (2011) Eur J Inorg Chem 2011:3002
231. Gärtner M, Görls H, Westerhausen M (2007) Z Anorg Allg Chem 633:2025
232. Lee VY, Takanashi K, Ichinohe M, Sekiguchi A (2004) Angew Chem Int Ed 43:6703
233. Teng W, Ruhlandt-Senge K (2004) Organometallics 23:952
234. Torvisco A, Decker K, Uhlig F, Ruhlandt-Senge K (2009) Inorg Chem 48:11459
235. Purdy AP, Berry AD, Holm RT, Fatemi M, Gaskill DK (1989) Inorg Chem 28:2799
236. Purdy AP, George CF, Callahan JH (1991) Inorg Chem 30:2812
237. Bogdanovic B, Janke N, Kruger C, Mynott R, Schlichte K, Westeppe U (1985) Ang Chem Int Ed 24:960
238. Engelhardt LM, Harvey S, Raston CL, White AH (1988) J Organomet Chem 341:39
239. Lehmkuhl H, Shakoor A, Mehler K, Kruger C, Angermund Y, Tsay H (1985) Chem Ber 118:4239
240. Ramsden HE (1976) US patent 3344190
241. Zuniga MF, Deacon GB, Ruhlandt-Senge K (2008) Inorg Chem 47:4669
242. Vaarstra BA, Huffman JC, Streib WE, Caulton KG (1991) Inorg Chem 30:121
243. Vargas W, Ruhlandt-Senge K (2003) Eur J Inorg Chem 2003:3472
244. Sitzmann H, Dezember T, Ruck M (1998) Angew Chem 110:3293
245. Hammel A, Schwarz W, Weidlein J (1989) J Organomet Chem 378:347
246. Takahashi Y, O'Brien A, Torvisco A, Wolf M, Deacon GB, Ruhlandt-Senge K (in preparation)
247. Mösges G, Hampel F, Kaupp M, Schleyer PR (1992) J Am Chem Soc 114:10880
248. O'Brien AY, Hitzbleck J, Torvisco A, Deacon GB, Ruhlandt-Senge K (2008) Eur J Inorg Chem 172
249. Boennemann H, Bogdanovic B, Brinkmann R, Egeler N, Benn R, Topalovic I, Seevogel K (1990) Main Group Met Chem 13:341

250. Drake SR, Streib WE, Folting K, Chisholm MH, Caulton KG (1992) Inorg Chem 31:3205
251. Deacon GB, Junk PC, Moxey GJ, Guino-o M, Ruhlandt-Senge K (2009) Dalton Trans:4878
252. Cole ML, Deacon GB, Forsyth CM, Junk PC, Proctor KM, Scott JL, Strauss CR (2007) Polyhedron 26:244
253. Drake SR, Otway DJ, Hursthouse MB, Malik KMA (1992) Polyhedron 11:1995
254. Miele P, Foulon J-D, Hovnanian N, Cot L (1993) Polyhedron 12:267
255. Ruhlandt-Senge K, Englich U (2000) Chem Eur J 6:4063
256. Englich U, Ruhlandt-Senge K (2001) Z Anorg Allg Chem 627:851
257. Chadwick S, Englich U, Ruhlandt-Senge K (1998) Chem Commun:2149
258. Teng W, Englich U, Ruhlandt-Senge K (2003) Angew Chem Int Ed 42:3661
259. Gardiner MG, Raston CL, Viebrock H (1996) Chem Commun:1795
260. Hitzbleck J, O′Brien AY, Forsyth CM, Deacon GB, Ruhlandt-Senge K (2004) Chem Eur J 10:3315
261. O′Brien AY, Hitzbleck J, Torvisco A, Deacon GB, Ruhlandt-Senge K (2008) Eur J Inorg Chem 1:172
262. Deacon GB, Junk PC, Moxey GJ, Ruhlandt-Senge K, St Prix C, Zuniga MF (2009) Chem Eur J 15:5503
263. Deacon GB, Forsyth CM, Junk PC (2000) J Organomet Chem 607:112
264. Hitzbleck J, Deacon GB, Ruhlandt-Senge K (2004) Angew Chem Int Ed 43:5218
265. Deacon GB, Junk PC, Moxey GJ (2009) Chem Asian J 4:1309
266. Deacon GB, Forsyth CM, Junk PC, Skelton BW, White AH (1999) Chem Eur J 5:1452
267. Westerhausen M (1991) Inorg Chem 30:96
268. Claggett AR, Ilsley WH, Anderson TJ, Glick MD, Oliver JP (1977) J Am Chem Soc 99:1797
269. Deacon GB, Forsyth CM, Jaroschik F, Junk PC, Kay DL, Maschmeyer T, Masters AF, Wang J, Field LD (2008) Organometallics 27:4772
270. Deacon GB, Junk PC, Urbatsch A (2011) Dalton Trans 40:1601
271. Hauber S-O, Lissner F, Deacon GB, Niemeyer M (2005) Angew Chem Int Ed 44:5871
272. Cole ML, Deacon GB, Forsyth CM, Konstas K, Junk PC (2006) Dalton Trans:3360
273. Deacon GB, Junk PC, Moxey GJ (2010) New J Chem 34:1731
274. Cotton FA, Wilkinson G, Murillo CA, Bochmann M (1999) Adv Inorg Chem, 6th edn. Wiley-Interscience, New York, NY
275. Suzuki H, Matano Y (2001) Organobismuth chemistry. Elsevier, Amsterdam
276. Caulton KG, Chisholm MH, Drake SR, Folting K (1990) J Chem Soc Chem Commun:1349

Heavier Group 2 *Grignard* Reagents of the Type Aryl-Ae(L)*n*-X (Post-*Grignard* Reagents)

Matthias Westerhausen, Jens Langer, Sven Krieck, Reinald Fischer, Helmar Görls, and Mathias Köhler

Abstract Whereas hitherto no general procedure has been developed for the synthesis of alkylcalcium halides, arylcalcium halides were found to be easily accessible post-*Grignard* reagents. The large discrepancy between the inertness of metallic calcium and the organocalcium derivatives requires an activation of the metal prior to use. The arylcalcium compounds can be obtained in large yields from iodoarenes and in smaller yields from bromoarenes. Chloro- and fluoroarenes represent no suitable substrates for the direct synthesis with calcium. Diverse substituents and functional groups are tolerated in *para* and *meta* position, whereas in *ortho* position the tolerance of functional groups is reduced. Only the *para*-phenyl substituted arylcalcium derivatives are destabilized and instantaneously undergo degradation reactions. These arylcalcium complexes commonly crystallize with six-coordinate calcium centers in distorted octahedral environments. Bulky substituents allow the preparation of organometallics with smaller coordination numbers whereas the use of multidentate ethers with small bites (intraligand O⋯O distance) leads to compounds with seven- or eight-coordinate calcium atoms. The arylcalcium halides show spectroscopic properties and reactivities more similar to organolithium compounds than to classic *Grignard* reagents. Reduction of iodoarenes is also possible with strontium and barium, but these homologous reagents are more reactive than the calcium derivatives enhancing the tendency to cleave solvent molecules. The objective of this review includes the credo that arylcalcium halides and pseudohalides are valuable synthons in organometallic chemistry which can be at least as valuable as organolithium reagents due to their ease of preparation and manageability on the one hand and their high and tunable reactivity on the other.

Keywords Arylcalcium · Calcium · Diarylcalcium · Ether degradation · Organylcalcium · Post-grignard reagents

M. Westerhausen (✉), J. Langer, S. Krieck, R. Fischer, H. Görls and M. Köhler
Institute of Inorganic and Analytical Chemistry, Friedrich Schiller University of Jena, Humboldtstrasse 8, D-07743 Jena, Germany
e-mail: m.we@uni-jena.de

Contents

List of Abbreviations

Ae	Alkaline-earth metal
Ar	Aryl
Bu	Butyl
18-crown-6	1,4,7,10,13,16,-Hexaoxacyclooctadecane
Cp	Cyclopentadienyl
Diglyme	Diethylene glycol dimethyl ether
Diox	1,4-Dioxane
DME	1,2-Dimethoxyethane
e^-	Electron
Et	Ethyl
HMTETA	*N,N,N′,N″,N‴,N‴*-Hexamethyltriethylenetetramine
L	Ligand
M	Metal
Me	Methyl
Mes	2,4,6-Trimetylphenyl
Naph	Naphthyl
Ph	Phenyl
Pr	Propyl
R	Substituent
Solv	Solvent
THF	Tetrahydrofuran
THP	Tetrahydropyran
Tipp	2,4,6-Tri-isopropylphenyl
TMEDA	*N,N,N′,N′*-Tetramethylethylenediamine
Tol	4-Methylphenyl
TMTN	*N,N′,N″*-Trimethyl-1,4,7-triazacyclononane

1   Introduction: *Grignard* Reagents

The common *Grignard* reaction, discovered by *Victor Grignard* in 1900, involves the insertion of magnesium atoms into a carbon–halogen bond of alkyl and aryl halides in diethyl ether or tetrahydrofuran (thf) yielding organomagnesium halides. In 1912 *Grignard* was awarded with the Nobel Prize in chemistry because the *Grignard* compounds are easy to prepare which ensured that these valuable reagents were used widely and exhaustively in organic and organometallic chemistry [1, 2]. Despite the enormous success of the *Grignard* reagents the mechanism of their formation still is controversial [3–8].

Many factors influence the applicability and yields of the *Grignard* reaction such as the strengths of the carbon–halogen bonds, particle size and purity of the magnesium metal, bulkiness of the organyl group, hybridization of the carbon atom, nature and dryness of the solvents, and absence of oxygen. The reaction of magnesium turnings with organic halides often requires an induction period before the reaction proceeds exothermically (Scheme 1). In order to start the *Grignard* reaction the magnesium turnings can be activated with, e.g., a few crystals of iodine, a few drops of methyl iodide, 1,2-dibromoethane, or *Grignard* and MgX$_2$ solutions as well as with mercury or mercury halide. Other activation procedures involve reduction of magnesium dihalide with potassium (*Rieke* magnesium) or the degradation of the tetrahydrofuran complex of anthracene-magnesium in hot toluene (*Bogdanović* magnesium). Ultrasound treatment also can enhance the reactivity of the magnesium turnings. With respect to the enormous interest, this chemistry is summarized in several text books [9–12].

In ether solutions a dynamic equilibrium, the *Schlenk* equilibrium, is operative for the *Grignard* reagents which is dependent on donor strength and polarity of the solvent. The basic *Schlenk* equilibrium interchanges RMgX derivatives into the homoleptic compounds MgR$_2$ and MgX$_2$ (Scheme 2) [13] with solvent bases saturating the coordination spheres of the magnesium centers. However, oligonuclear intermediates such as molecular RMg(μ-X)$_2$MgR, R$_2$Mg(μ-X)$_2$ Mg, and RMg(μ-R)(μ-X)MgX as well as ionic [RMg]$^+$X$^-$ and other species are discussed [14, 15]. The complexity of the solution behavior shows an enormous importance on the understanding of the properties of *Grignard* reagents. In general stronger *Lewis* bases shift the *Schlenk* equilibrium toward the homoleptic derivatives whereas in less *Lewis* basic solvents heteroleptic RMgX is favored [16] because MgR$_2$ are stronger *Lewis* acids than RMgX. However, bulky groups R can stabilize heteroleptic RMgX in order to reduce inter-ligand repulsion [14]. This *Schlenk* equilibrium is significantly influenced by the nature of the halide. Due to the fact that MgX$_2$ forms an insoluble coordination polymer with 1,4-dioxane which precipitates from the *Grignard* solutions the equilibrium can be shifted nearly quantitatively toward homoleptic MgR$_2$.

The ionicity of the Mg–C bond lies between Li–C and Zn–C bonds based on the *Allred–Rochow* electronegativities of the metals lithium, magnesium, and zinc of 0.97, 1.23, and 1.66, respectively. Despite the fact that the nucleophilicity of the

$$\text{R-X} + \text{Mg} \longrightarrow \text{R-X}^{\cdot-} + \text{Mg}^{\cdot+} \longrightarrow \text{R}^{\cdot} + \text{X}^{-} + \text{Mg}^{\cdot+} \longrightarrow \text{R-Mg-X}$$
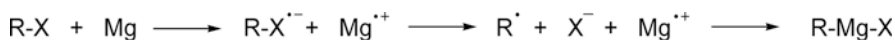
Scheme 1 Direct synthesis of *Grignard* reagents via insertion of magnesium into a carbon–halogen bond yielding organomagnesium halides
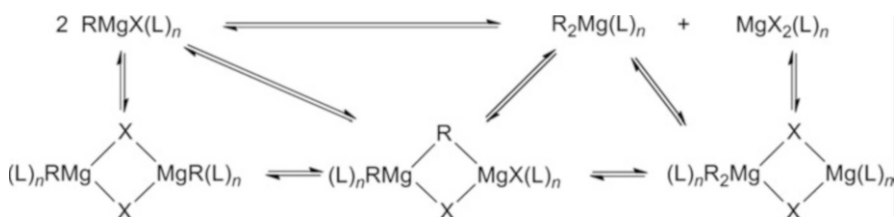
Scheme 2 *Schlenk* equilibrium of *Grignard* reagents interchanging heteroleptic RMgX into homoleptic MgR$_2$ and MgX$_2$
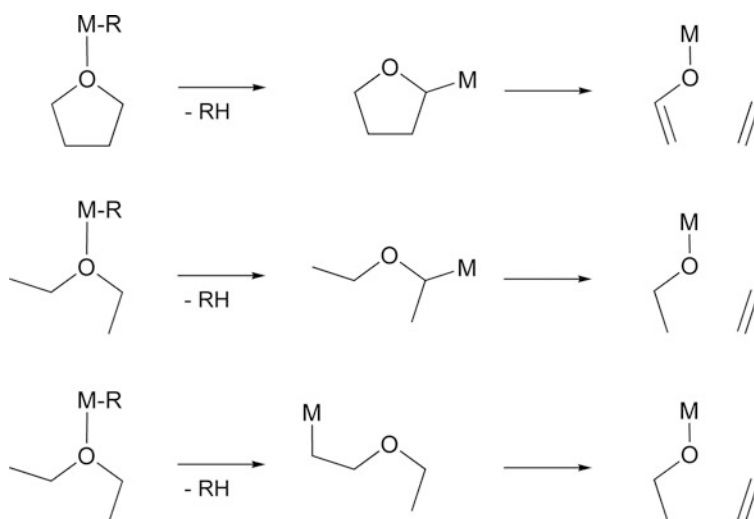
Scheme 3 Ether degradation of tetrahydrofuran (*top*) and diethyl ether (*middle* and *bottom*) after initial deprotonation in α- or β-position

Grignard reagents is lower than of lithium-based organometallics, ether degradation (Scheme 3) and side reactions such as *Wurtz*-type C–C coupling and β-hydrogen abstraction can occur. A detailed study of the reduction of 1-bromo-2,2,3,3-tetramethylcyclopropane with magnesium in diethyl ether showed the formation of the desired *Grignard* complex RMgBr with a yield of 28 % but also significant amounts of RH (68 %) and traces of R–R (2 %) [17]. In addition large amounts of 2,3-diethoxybutane were formed as a consequence of diethyl ether degradation supporting the presence of radical species in solution. The presence of dissolved MgBr$_2$ has a large influence on the reactivity of the metal (and the amount of

by-products) and also led to the finding that no induction period is apparent [17]. A detailed study of the direct synthesis of arylmagnesium halides in ethereal solvents verified that products of ionic and radical degradation pathways were formed [18].

Due to the enormous importance of the *Grignard* reagents and the complexity of the *Grignard* solutions, substantial studies were addressed to the structures of organomagnesium compounds [19–22]. In *Grignard* complexes of the type RMgX the magnesium atoms prefer distorted tetrahedral coordination spheres as in monomeric [(Et$_2$O)$_2$Mg(Ph)Br] [23] and [(thf)$_2$Mg(Ph)Br] [24]. Larger coordination numbers of five were observed for the methyl derivatives [(thf)$_3$ Mg(Me)Br] [25] and [(thf)(tmeda)Mg(Me)Br] [26]. Distorted octahedral compounds were isolated if bidentate bases with rather small intramolecular O···O distances (bites) were bound at magnesium as, e.g., in [(dme)$_2$ Mg(tol)Br] [27] (tol = *p*-tolyl).

Oligonuclear derivatives such as (thf)$_6$Mg$_4$R$_2$Cl$_6$ [28, 29] and RMg(μ-Br)$_3$Mg (thf)$_3$ [30] support the diversity of magnesium-containing molecules present in *Grignard* solutions. Also solvent-separated ionic species such as [(thf)$_3$ Mg (μ-Cl)$_3$ Mg(thf)$_3$]$^+$ [(thf)Mg(R)Cl$_2$]$^-$ [29] (magnesium magnesiates) could be crystallized. Dinuclear anions of the type [Ph$_2$Mg(μ-Cl)$_2$MgPh$_2$]$^{2-}$ [29] also contain tetracoordinate metal atoms. The coordination number of diarylmagnesium depends on the bulkiness of the aryl groups. In [Mg(C$_6$H$_2$-2,4,6-tBu$_3$)$_2$] [31] the dicoordinate metal center has a bent structure (C-Mg-C 158.4°). Smaller aryl groups allow the formation of base adducts [32] or of the one-dimensional coordination polymer [Mg(μ-Ph)$_2$]$_\infty$ [33] as is also observed for [Mg(μ-Me)$_2$]$_\infty$ [34] and [Mg(μ-Et)$_2$]$_\infty$ [35]. Intermediate bulkiness leads to dimeric structures as in [Mg(C$_6$H$_3$-2,6-Et$_2$)$_2$]$_2$ [36]. Solvent molecules can bind to dimers yielding [(thf)$_2$Mg$_2$(tol)$_2$(μ-tol)$_2$] [33] or can lead to a breakup of oligomeric structures giving most commonly monomers of the type (L)$_2$MgR$_2$. 1,4-Dioxane is also able to build coordination polymers of the type [(μ-diox)MgR$_2$]$_\infty$ with tetracoordinate alkaline-earth metal atoms [18, 37, 38]. Larger coordination numbers are realized in diorganylmagnesium complexes with oligodentate *Lewis* bases with small bites as in, e.g., [(diglyme)Mg(C$_6$H$_4$-4-*t*Bu)$_2$] [39] and a rotaxane complex of diphenylmagnesium [40].

The diversity of molecular structures often makes it difficult to elucidate a detailed reaction mechanism for the synthesis of *Grignard* reagents as well as their reactions with substrates. Several concepts were developed to control and enhance reactivity and selectivity of organomagnesium derivatives. These strategies include the use of heterobimetallic *Grignard* reagents [41–43] and addition of metal halides [44, 45] with the reactive species being "ate" complexes. A further alteration of reactivity and selectivity can be achieved by using magnesium amides [46–49] which can be combined with other metal amides [50] or derivatized according to the concept of frustrated *Lewis* pairs [51] by addition of BF$_3$ [52]. The use of multicomponent reagents makes the reaction mechanisms much more complex and hard to predict because usually no structural information is known about these reagents and intermediates.

Reactivity and selectivity can also be altered by choosing the heavier s-block congeners, with calcium being the most appealing element. Calcium is one of the most abundant and most spread metals on earth. Lithium is a rare chemical element.

With increasing application in battery technology, its price will increase rapidly. In addition, calcium is absolutely nontoxic regardless of its concentration. Calcium is also very attractive because it combines typical s-block behavior (highly heteropolar bonds, salt-like behavior, electrostatic interactions as dominating structural principle) with the behavior of early d-block elements (*Lewis* acidity of the cation, catalytic activity, d-orbital participation in bonding).

The objective of this review includes the demonstration that preparation and handling of calcium-based post-*Grignard* reagents are comparable to the widely used organolithium complexes and first examples demonstrate that an at least as powerful reactivity and fruitful organometallic chemistry can be expected from arylcalcium complexes.

2 Synthesis of Post-*Grignard* Reagents

Arylcalcium halides were firstly mentioned by *Beckmann* in 1905 [53] prepared by the reduction of aryl halides by calcium. However, several years later *Gilman* and *Schulze* [54] had difficulties verifying these results and summarized that

– The formation of organocalcium iodides appears to be restricted to iodides.
– Only primary iodoalkanes undergo reaction with calcium with the exception of benzyl iodide.
– The post-*Grignard* reaction is quite sluggish, irregular, and not always certain.
– The yields of organocalcium iodides are far from satisfactory.
– Organocalcium iodides are generally less reactive than the corresponding organomagnesium halides.

These authors [54] concluded that organocalcium iodides can be prepared in poor yields from a limited class of iodides with the highest yields for phenylcalcium iodide and that these compounds were soluble in ether being less reactive than common *Grignard* reagents. The crucial importance of the solvent was investigated by *Bryce-Smith* and *Skinner* [55]. The necessity of ethereal media was discovered; however, THF and diethyl ether were attacked by the organocalcium derivatives leading to low yields [56]. Generally, the insertion of calcium into a carbon–halogen bond proceeded faster in THF than in diethyl ether. In addition, these authors stated that phenylcalcium iodide chemically resembles organolithium compounds more than *Grignard* reagents because comparable to RLi, PhCaI readily underwent a halogen–metal exchange reaction with 1-bromonaphthalene whereas RMgX needed much more drastic reaction conditions. This exchange reaction was employed to prepare protected 2-(phenylcalcio)-1,3-xylylene-[18]crown-5 from diphenylcalcium and 2-bromo-1,3-xylylene-[18]crown-5 [56] (Scheme 4); diphenylcalcium was prepared *via* the reduction of iodobenzene with calcium in THF at −20 °C, removal of all volatiles after 24 hours, and subsequent dissolution in diethyl ether. Also addition to conjugated ketones supports stronger similarities to organolithium compounds than to *Grignard* reagents [57]. ^{1}H NMR experiments
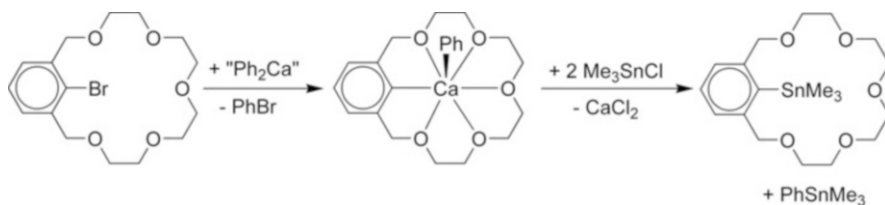
Scheme 4 Synthesis of 2-(phenylcalcio)-1,3-xylylene-[18]crown-5 via halogen–metal exchange reaction of bromoarene with diphenylcalcium

also showed that the chemical shifts of para-tolylcalcium iodide resembled much more the parameters of para-tolyllithium than those of the corresponding magnesium-based *Grignard* reagent [58].

Purity of the employed calcium metal and nature of impurities also seemed to have a tremendous impact on the post-*Grignard* reaction. Pure calcium reacted not only with iodobenzene but also with chloro- and bromobenzene; however, the yields for the lighter halogenobenzenes were significantly lower (yields of PhCaI 97 %, PhCaBr 55 %, PhCaCl 14 %) [59]. As ether degradation represents a severe side reaction, reduction of iodobenzene was also studied in toluene at high temperatures; however, the yields were as low as 3 % [60]. In addition, *Wurtz*-type coupling reactions also reduced the yields. Nevertheless, alkylcalcium halides were accessible in hydrocarbon solvents. Quantum chemical studies on solvation and stabilization of CaI$_2$ and CpCaI by THF were performed by *Harvey* and *Hanusa* [61]. This brief overview on the development of organocalcium chemistry demonstrates the challenges related to these organometallics.

2.1 Activation of the Heavier Alkaline-Earth Metals

In contrast to the highly reactive alkali metals (due to their relatively low melting points), heavier alkaline-earth metals require an activation process prior to use in order to enhance the relative inertia of these strong electropositive metals themselves. In principle, this provides a wide range of chemical and physical methods with the common goal to furnish a large reactive surface by partial overcoming of lattice and atomization energies forming smaller metal aggregates. Practicality and suitability of the activated alkaline-earth metals (marked as Ae*) as well as the yields of the desired reaction products differ depending on the respective methods:

– Usage of very pure metals [59, 60, 62] or purification by vacuum distillation of the alkaline-earth metals generating highly reactive crystalline metals, freed from halide, oxide, and nitride impurities [63, 64].
– Sonochemical activation *via* ultrasound treatment of the reaction mixture [65].

$$Ca \xrightarrow{NH_3\,(l)} \{Ca(NH_3)_x{}^{2+} + 2\ e(NH_3)_y{}^-\} \xrightarrow[-NH_3]{} [Ca(NH_3)_6] \xrightarrow[-NH_3]{} Ca^*$$
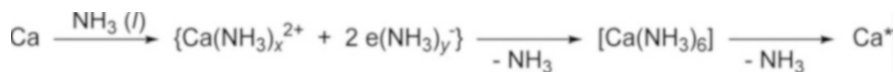
Scheme 5 Activation of calcium via dissolution in liquid ammonia and subsequent removal of ammonia from an ammonia adduct

– Enlargement of the surface by dissolving of the metals in mercury yielding the corresponding amalgam alloys [66–68].
– Cocondensation reaction of the alkaline-earth metal and the substrate (note: it is challenging to realize the correct stoichiometry [69–72]).
– Thermal decomposition of the metal hydrides, particularly calcium dihydride [73].
– Dissolution of the metals in liquid ammonia and usage of the metal-ammonia solution [74] or the ammonia-saturated organic solvents [75] leading to formation of ammonia adducts.
– Dissolution of the metals in liquid ammonia and subsequent removal of ammonia to give highly reactive metal powders [76, 77].
– Reduction of alkaline-earth metal dihalides with ethereal solutions of lithium and potassium biphenylide, respectively, according to *Rieke* [78].
– Reduction of alkaline-earth metal diiodides with elemental potassium forming highly reactive metals (*Rieke* method) [79, 80] or usage of potassium graphite as reducing agent (*Fürstner* method) [81].
– Formation of the alkaline-earth metal anthracene complexes and subsequent thermal decomposition to give activated metal powders - *Bogdanović* method [82, 83].

Westerhausen and coworkers [76, 84] established an advantageous method to activate calcium on a multi-gram scale by dissolving calcium in liquid ammonia. The general activation protocol is shown in Scheme 5.

Commercially available calcium granules were placed with glass balls (about 4 mm diameter) in a *Schlenk* flask (Fig. 1) and ammonia was condensed at −60 °C yielding an intensively blue-colored solution caused by dissociation (formal oxidation) and formation of ammonia-solvated calcium cations and electrons in ammonia cages. After complete dissolution of the metal the solvent ammonia was distilled off. During depletion of ammonia gold-colored calcium bronze was formed which can be best described as the calcium hexaamine complex $[Ca(NH_3)_6]$ with an alkaline-earth metal(0) center [85, 86]. Further evacuation of the system led to removal of weakly coordinated ammonia and after drying for several hours in vacuo activated calcium metal was formed as finely divided pyrophoric powder as well as a metal mirror on the surface of the glass balls leading to an enormous enhancement of the metal surface.

During the synthesis of arylcalcium halides *via* direct synthesis the reaction mixture was shaken continuously in order to generate a reactive surface by uninterrupted rubbing of the glass balls against each other. The immediate removal of

Fig. 1 Activation of commercially available calcium with liquid ammonia; *Top left*: Calcium granules and glass balls are placed in the *Schlenk* flask. *Top right*: Dissolution of calcium in liquid ammonia leads to a *dark blue* solution. *Bottom left*: During removal of ammonia calcium bronze forms. *Bottom right*: Activated and pyrophoric calcium powder is deposited on the surface of the glass balls after removal of all ammonia

ammonia prevents the formation of calcium amide during the activation process. In the case of the heavier homologous strontium and barium, however, this competitive reaction cannot be prevented completely yielding significant quantities of the corresponding metal amides, Ae(NH$_2$)$_2$.

Activation of calcium metal *via* dissolution in liquid ammonia.

Calcium turnings (1 g, 25 mmol) and glass balls (diameter 4 mm; 50 g) were placed in a 500 mL *Schlenk* flask and covered with liquid (anhydrous) ammonia at $-60\,^{\circ}$C resulting in a deep blue solution. In order to prevent formation of $Ca(NH_2)_2$, ammonia should be removed immediately by carefully distillation in vacuo. During this procedure the blue color disappears and a bronze-colored solution is observed. After removal of all volatile materials, the remaining calcium powder was dried in high vacuo for 4–6 hours at room temperature until a pressure of 10^{-2} mm Hg is reached. The remaining gray ammonia-free metal powder was used for subsequent procedures. CAUTION: This calcium powder can inflame spontaneously by contact with air, oxygen, or water and has to be handled and stored in an inert gas atmosphere.

2.2 Grignard *Reaction with Activated Calcium*

The first synthetic procedure of a post-*Grignard* reagent of calcium dates back to 1905. As mentioned earlier *Beckmann* reported that calcium metal reacted with iodoethane and iodobenzene in diethyl ether to form the corresponding organocalcium derivatives by insertion of the metal into the reactive halogen carbon bond [53]. It took more than a hundred years to develop a convenient high-yield synthesis on a large scale [87], even though early attempts gave Ph_3C–Ca–Cl with good yields [88]. Unlike their magnesium analogs, which found numerous applications in organic and organometallic chemistry, the organocalcium compounds were barely noticed for decades, since their synthesis was somewhat erratic and varying results were obtained under identical conditions. Only iodobenzene gave good yields of phenylcalcium iodide in solution and therefore was used in subsequent investigations by the group of *Gilman* [54].

During these early investigations, the purity of the employed calcium was found to be one of the important factors influencing its reactivity. While the presence of magnesium enhanced the formation of the organocalcium derivatives, sodium had the opposite effect. Besides purification, other strategies like amalgamation [66–68] were successfully tested later on to increase the reactivity of the bulk metal. Additionally, the enhancement of the reactive surface by different methods ranging from simple milling to more sophisticated methods like the co-condensation or even gas phase reaction of calcium vapor and substrate was tested. Although the latter strategies were found to be very effective in case of halobenzenes, leading to high product yields and making even aromatic chloro and fluoro derivatives useful substrates in *Grignard*-type reactions of calcium [69, 70], simpler methods are more appealing from a practical point of view. The dissolution of the metal in liquid ammonia and its subsequent removal leading to highly divided calcium powder are a
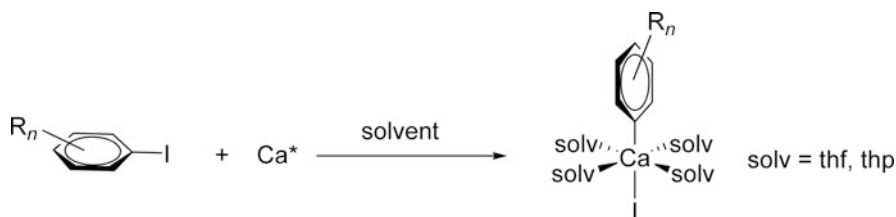
Scheme 6 Direct synthesis of solvated PhCaI (post-*Grignard* reagent). The coordination of four solvent molecules leads to a distorted octahedral environment of the calcium center with the anionic ligands in transposition

simple, economic, and yet powerful alternative to overcome the low reactivity of the bulk metal (Scheme 6).

Recent investigations using this approach finally led to isolation of well-defined arylcalcium halides which could be characterized by X-ray diffraction methods [49, 89–92]. THF is the most widely used solvent in these reactions, but less polar tetrahydropyran (THP) or diethyl ether was found to be suitable, too. The content of formed arylcalcium halides in solution was determined by acidimetric titration of a hydrolyzed aliquot and yields up to 95 % were reported for some substrates in THF (Table 1). In most cases the post-*Grignard* reagents can be isolated as colorless mononuclear solvent adducts of the type [ArCaX(solv)$_n$] from the filtered reaction mixture in THF or THP by cooling. A yield of 70 % of solid [PhCaI(thf)$_4$] was isolated under optimized conditions. The molecular structures of the diethyl ether solvates are not known as of yet.

Unsubstituted and substituted iodobenzenes gave higher yields of arylcalcium halides than their corresponding bromo counterparts, while chloro benzenes are essentially unreactive. The substitution pattern of the aromatic ring has significant influence on the yield and the stability of the formed products. Alkyl substituents in ortho position destabilize the formed calcium derivatives due to increased steric strain. Mesitylcalcium iodide, for instance, decomposes rapidly at ambient temperature in THF solutions [96]. The reaction of calcium with sterically more demanding iodo-2,4,6-tri(tert-butyl)benzene yields 2,5-dimethyl-2,5-bis(3,5-di-tert-butylphenyl) hexane as a major component *via* a multistep reaction sequence starting with the insertion of Ca into the C–I bond (Scheme 7) [91, 92]. Additionally, halogen substituents in ortho position led to unstable arylcalcium derivatives which decomposed presumably *via* an aryne mechanism [84]. Various substituents such as F, Cl, I, OMe, NMe$_2$ [84], or SiPh$_3$ [95] are tolerated in meta and para position, with phenyl substituents being the exception [95]. For instance, the reaction of 1-bromo-2,4,6-triphenylbenzene under typical conditions did not result in isolation of the desired post-*Grignard* reagent but led to the formation of a product which was interpreted as the calcium(I) compound {[(thf)$_3$Ca]$_2$(1,3,5-Ph$_3$C$_6$H$_3$)} with a structure best described as an "inverse" sandwich [100]. The instability of the phenyl modified systems was ascribed to the intermediate formation of a calcium substituted biphenyl subunit with two co-planar benzene rings. The low-lying π*-orbital of this species makes it accessible for further electron uptake from remaining calcium inducing the decomposition of the primarily formed arylcalcium halide by

Table 1 Synthesis of arylcalcium halides *via* direct synthesis from haloarene and activated calcium powder

Substrate	Solvent	Yield (%)[a]	Isolated arylcalcium derivative [isolated yield (%)]	Lit.
PhI	THF	93	[(Ph)CaI(thf)$_4$] (70[b])	[76, 84]
PhI	THP	82	[(Ph)CaI(thp)$_4$] (24)	[93]
PhI	Et$_2$O	82	–	[94]
PhBr	THF	71	[(Ph)CaBr(thf)$_4$]	[76, 84]
PhCl	THF	<5	–	[84]
p-Me-C$_6$H$_4$I	THF	60	[(*p*-Me-C$_6$H$_4$)CaI(thf)$_4$] (38)	[76, 84]
p-Me-C$_6$H$_4$I	THP	84	[(*p*-Me-C$_6$H$_4$)CaI(thp)$_4$] (40)	
m-Me-C$_6$H$_4$I	THF	60	[(*m*-Me-C$_6$H$_4$)CaI(thf)$_4$] (44)	
p-Ph-C$_6$H$_4$I	THF	–	–	[84]
p-F-C$_6$H$_4$I	THF	75	[(*p*-F-C$_6$H$_4$)CaI(thf)$_4$]	[84]
p-Cl-C$_6$H$_4$I	THF	81	[(*p*-Cl-C$_6$H$_4$)CaI(thf)$_4$]	[84]
p-I-C$_6$H$_4$I	THF	95	[(*p*-I-C$_6$H$_4$)CaI(thf)$_4$]	[84]
p-MeO-C$_6$H$_4$I	THF	89	[(*p*-MeO-C$_6$H$_4$)CaI(thf)$_4$]	[84]
p-Me$_2$N-C$_6$H$_4$I	THF	91	[(*p*-Me$_2$N-C$_6$H$_4$)CaI(thf)$_4$]	[84]
p-Ph$_3$Si-C$_6$H$_4$I	THF	85	[(*p*-Ph$_3$Si-C$_6$H$_4$)CaI(thf)$_4$]	[95]
Me$_2$Si(C$_6$H$_4$-*p*-I)$_2$	THF	56	[Me$_2$Si{C$_6$H$_4$-*p*-CaI(thf)$_4$}$_2$]	[95]
MesI	THF	86	[(Mes)CaI(thf)$_4$] (37); [(Mes)$_2$Ca(thf)$_3$] (12[c])	[96, 97]
MesBr	THF	<5	–	[84]
2,4,6-(*t*Bu)$_3$-C$_6$H$_2$I	THF	53[d]	–	
2,6-(*p*-tol)-C$_6$H$_3$I	THF	76	[{2,6-(*p*-tol)-C$_6$H$_3$CaI(thf)$_3$]	[98]
2,6-(MeO)$_2$-C$_6$H$_3$I	THF	56	[(thf)$_2$Ca{µ-2,6-(MeO)$_2$-C$_6$H$_3$}$_3$CaI(thf)]	[97]
C$_6$F$_5$I	THF	<5	–	[84]
1-iodonaphthalene	THF	68	[(1-Naph)CaI(thf)$_4$]	[84, 99]
1-bromonaphthalene	THF	52	[(1-Naph)Ca(µ-Br)(thf)$_3$]$_2$ (29)	[99]

[a]In solution; determined by acidimetric titration of a hydrolyzed aliquot
[b]Optimized conditions
[c]Corrected value
[d]Synthesis at −55 °C
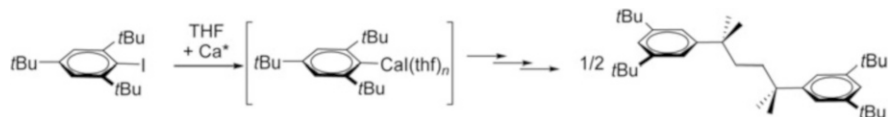
Scheme 7 Reaction of iodo-2,4,6-tri(*tert*-butyl)benzene with activated calcium in THF. After the insertion of Ca into the C–I bond and formation of post-*Grignard* reagent a degradation sequence finally yields the C–C coupling product, 2,5-dimethyl-2,5-bis(3,5-di-*tert*-butylphenyl)hexane, as a major product

subsequent reactions. This theory is supported by the formation of stable arylcalcium halides such as [(thf)$_3$Ca{2,6-(4-CH$_3$-C$_6$H$_4$)$_2$C$_6$H$_3$}I] bearing tolyl substituents in ortho position [98]. Here, the formation of a co-planar biphenyl subunit is hampered for steric reasons.

The direct synthesis of iodoarenes with calcium proceeds smoothly, but attempted double-*Grignard* formation employing 1,4-diiodobenzene yielded the monometalated derivative [(*p*-I-C$_6$H$_4$)CaI(thf)$_4$] as the main product [84]. Similar results were obtained in THP as solvent. In contrast, dimetalation of 1,4-dihalogenated benzene was reported for lithium [101] and magnesium [102, 103] under appropriate conditions. So far, the only dimetalated derivative formed by a Ca-*Grignard*-analog reaction is [Me$_2$Si{C$_6$H$_4$[–*p*-CaI(thf)$_4$]$_2$] [95], in which the metalated arene rings are separated by an SiMe$_2$ group prohibiting electronic communication between the two post-*Grignard* moieties.

The higher homologues of calcium, strontium, and barium are reactive in the direct synthesis, too, yielding arylstrontium and arylbarium halides, but due to their even higher reactivity, the primary products of those reactions resisted all efforts to be isolated as pure, well-defined compounds. Solely secondary products such as [(tmeda)Sr(I)(μ-Ph)$_2${μ-N(Me)CH$_2$CH$_2$NMe$_2$}Sr(tmeda)] (with a cleaved tmeda molecule) [104, 105] or [{Ph$_2$Ba(thf)$_2$}$_4$·BaO(thf)] (oxygen-centered Ba$_5$ square pyramid) which might stem from solvent degradation reactions [105] were isolated.

General procedure for the synthesis of arylcalcium iodides (post-*Grignard* reagents) [84].

CAUTION: These compounds are extremely sensitive towards moisture and air. Therefore they have to be prepared, handled, and manipulated in an inert atmosphere (nitrogen or argon). Solvents and reagents have to be degassed and saturated with nitrogen or argon prior to use.

A *Schlenk* flask with activated calcium and glass balls is filled with THF (20 mL per 15 mmol calcium) and cooled to 0 °C. Then, 0.8 equivalents of the aryl halide are slowly added. Thereafter, the flask is shaken at 0 °C for 1 h and for additional 6 h at ambient temperature. The obtained dark-colored suspension is filtered through a *Schlenk* frit, covered with diatomaceous earth. The conversion is determined by acidic consumption of a hydrolyzed aliquot of the filtrate. The residue on the filter is extracted with additional portions of THF (20 mL) until the extracts are free of further substantial amounts of product as controlled by acidimetric titration of a hydrolyzed aliquot. Cooling of these solutions to −78 °C leads to precipitation of the appropriate arylcalcium halide within one day. The product is collected on a cooled *Schlenk* frit and dried in vacuo. Depending on the amount of co-crystallized calcium diiodide, recrystallization of the crude product from THF can be necessary in order to isolate pure post-*Grignard* complexes of the type [(thf)$_n$Ca(Ar)I]. The amount of bound thf is determined by integration of ^{1}H NMR signals.
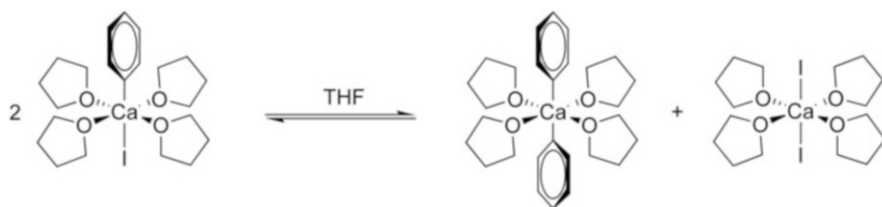
Scheme 8 *Schlenk*-type equilibrium between heteroleptic [(thf)$_4$Ca(Ph)I] and homoleptic [(thf)$_4$CaPh$_2$] and [(thf)$_4$CaI$_2$] in THF

2.3 Synthesis of Diarylcalcium

While a still-growing number of the heteroleptic derivatives [(Ar)CaX(solv)$_n$] was reported during the last decade, the chemistry of the related homoleptic diarylcalcium derivatives is still underdeveloped and only a few well-characterized examples are known. In ethereal solutions these two types of species are connected by an equilibrium resembling the *Schlenk* equilibrium of organomagnesium compounds. A simplified version is shown in Scheme 8, indicating that the diorganyl species should be accessible if the appropriate conditions are found to shift the equilibrium to the right.

While in THF and THP the heteroleptic species commonly dominate in solution at ambient temperature and can in several cases easily be isolated just by cooling of the reaction mixtures, the situation in diethyl ether seems to be different. Upon cooling, large crops of [CaI$_2$(Et$_2$O)$_4$] were observed in contrary to the magnesium derivatives where diethyl ether favors the isolation of heteroleptic species and the more polar THF shifts the *Schlenk* equilibrium towards the homoleptic products. However, the isolation of one or the other species does not necessarily tell anything about the position of the equilibrium at ambient temperature, since preferred crystallization of one species might shift the equilibrium during cooling and crystallization. So far, no reliable data concerning the position of this equilibrium in diethyl ether have been published and all attempts to isolate the desired diorganylcalcium species from diethyl ether solutions after removal of substantial amounts of CaI$_2$ failed.

However, type and polarity of the solvent are by far not the only factors influencing the *Schlenk*-type equilibrium. Besides others, the substitution pattern of the aromatic ring alters the relative solubilities of the species present and finally enabled the isolation of all three species from the equilibrium mixture in case of the mesityl derivative [96, 97]. The compound [(Mes)$_2$Ca(thf)$_3$] [97] was isolated in 12 % yield by fractionized crystallization and characterized by single crystal X-ray diffraction experiments.

More target-oriented approaches to shift the *Schlenk*-type equilibrium comparable to the well-established protocols known for the magnesium derivatives still have to be developed. While the addition of 1,4-dioxane to *Grignard* solutions leads
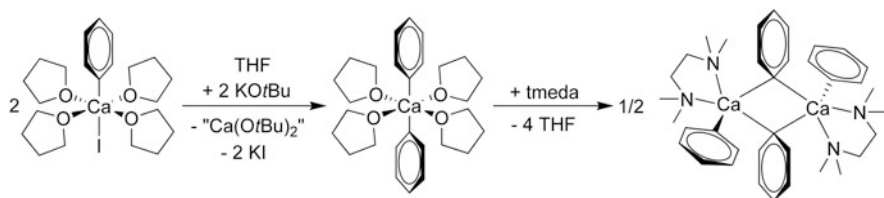
Scheme 9 Synthesis of the dimeric tmeda adduct of diphenylcalcium. After the (salt)metathesis reaction of phenylcalcium iodide with potassium *tert*-butoxide and addition of tmeda dinuclear [(Ph)Ca(μ-Ph)(tmeda)]$_2$ can be isolated

to precipitation of polymeric insoluble dioxane adducts of magnesium halides, leaving soluble diorganylmagnesium species in solution [37, 38], an adaption of this method to calcium failed so far.

The addition of KOtBu to solutions of [(Ar)CaI(thf)$_x$] in THF was found to be more promising [106]. The precipitates formed in this reaction did not only contain the expected potassium iodide but also the calcium tert-butoxide species, while the homoleptic diorganylcalcium species which formed *via* the *Schlenk*-type equilibrium stayed in solution and were isolated as thf adducts by cooling. In this way, [(1-Naph)$_2$Ca(thf)$_4$] was obtained [106]. The coordinated thf ligands in such diorganylcalcium derivatives can be replaced by other neutral donors such as tmeda and hexamethyltriethylentetraamine (hmteta) afterwards. Depending on the co-ligands added, monomeric or dimeric complexes were observed, as demonstrated in case of diphenylcalcium where [*cis*-(Ph)$_2$Ca(hmteta)] and [(Ph)Ca(μ-Ph)(tmeda)]$_2$ were isolated (Scheme 9). However, scope and limitations of this promising strategy are still under investigation.

Procedure for the synthesis of di(1-naphthyl)calcium [(1-Naph)$_2$Ca (thf)$_4$] [106].

CAUTION: Organocalcium compounds react violently with moisture and water and, therefore, strictly anaerobic conditions have to be maintained during synthesis and handling of arylcalcium compounds. All solvents have to be thoroughly dried, degassed, and saturated with an inert gas (nitrogen or argon) prior to use.

Solid KOtBu (0.13 g; 1.16 mmol) was added at ambient temperature to a solution of [(1-Naph)CaI(thf)$_4$] (0.67 g, 1.15 mmol) in THF (12 mL). The resulting suspension was stirred for 30 min, and then all solids were removed by filtration. Storage of the yellow mother liquor at −40 °C for 2 days led to precipitation of 0.23 g of yellow crystals of [(1-Naph)$_2$Ca(thf)$_4$]·THF (0.35 mmol, 61 %), which were collected by filtration and dried in vacuo till the crystals are dry and freely moveable in the flask ([(1-Naph)$_2$Ca(thf)$_4$]·THF) or till a pressure of 10^{-2} mm Hg is reached leading to removal of intercalated tetrahydrofuran and to the formation of ([(1-Naph)$_2$Ca(thf)$_4$]). Integration of a ^{1}H NMR signals is recommended to determine the thf content.
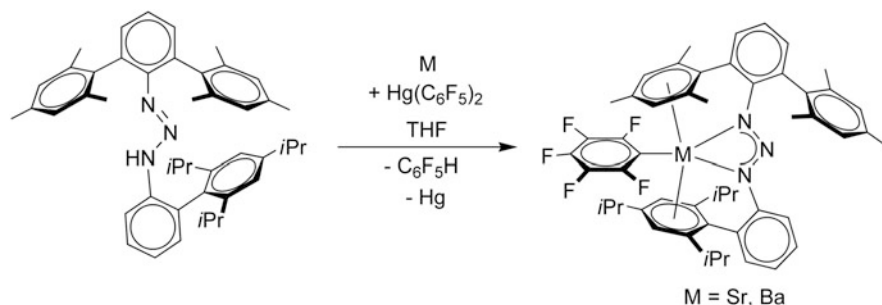
Scheme 10 Transmetalation of an organomercury compound with alkaline-earth metals yielding the corresponding pentafluorophenyl complexes

2.4 *Alternative Routes to Post*-**Grignard** *Reagents*

Due to its good practicability and the tolerance of many functional groups and substitution patterns the direct synthesis (insertion of an alkaline-earth metal into a polar carbon–halogen bond) represents the most common method for syntheses of arylcalcium compounds, in particular arylcalcium halides. To the best of our knowledge, other methodologies, *e.g.*, salt metathesis and transmetalation provide only special success from which up to now no general synthetic strategies have been derived.

Transmetalation of di(phenyl)mercury with calcium metal was described already approximately 40 years ago, but the reported organocalcium species were characterized only by derivatization or hydrolytic work-up [66, 68]. Heteroleptic heavier alkaline-earth metal organometallics were prepared by *Niemeyer* et al. [107] *via* transmetalation of bis(perfluorophenyl)mercury and the alkaline-earth metal with subsequent deprotonation of a sterically crowded triazene ligand yielding $[(C_6F_5)Ae-\eta^2-N_3\{(2,6-Mes_2Ph)(2'-TippPh)\}]$ (Ae = Ca(thf), Sr, Ba; Mes$_2$Ph = C_6H_3-2,6(2,4,6-Me$_3C_6H_2)_2$; 2'-TippPh = C_6H_5-2(2,4,6-iPrC$_6H_3$)) as shown in Scheme 10. It is noteworthy that the transmetalation and deprotonation were carried out in THF, but only the organocalcium compound crystallizes as thf donor adduct, whereas the heavier homologous strontium and barium (owing to their larger ionic radii and softness) saturate their coordination spheres exclusively by additional metal π-arene interactions with triazenide-bound aryl groups and crystallize solvent free. This concept combines an increased solubility in organic solvents by bulky peripheral ligands and the protection of the reactive metal–carbon bond by encapsulation (Ca–C 250(1), Sr–C 267.3(7), and Ba–C 280.8(5) pm) [107]. Electronic saturation (reduced nucleophilicty of the triazenide ligand by charge delocalization) and steric protection allow a kinetic stabilization of the reactive Ae–C$_i$(phenyl) bond.

Transmetalation of phenylcopper(I) with activated calcium leads to the formation of sparingly soluble $[(thf)_3Ca(\mu-Ph)_3Ca(thf)_3]^+$ [Ph-Cu-Ph]$^-$, according to Scheme 11 [108]. The solvent-separated calcium cuprate(I) compound consists of a phenyl-calcium cation and a [Ph$_2$Cu]$^-$ counter-anion. The calcium atoms in the
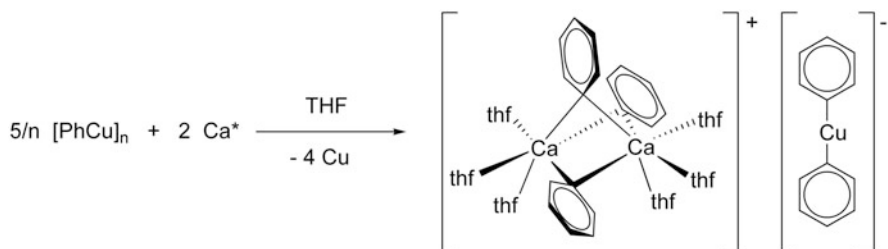
Scheme 11 Transmetalation of phenylcopper with calcium yielding the cuprate $[\{(thf)_3Ca\}_2(\mu\text{-}Ph)_3]^+$ $[Ph_2Cu]^-$
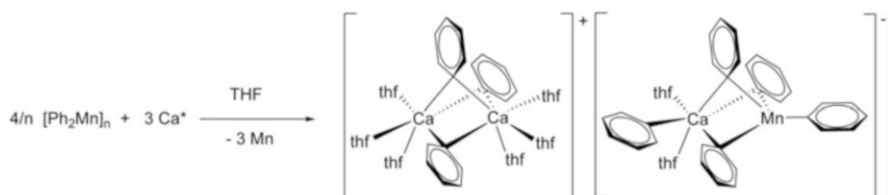
Scheme 12 Transmetalation of di(phenyl)manganese with activated calcium in THF yielding a tetranuclear solvent-separated ion pair

dinuclear complex cation are hexacoordinated with three bridging phenyl groups resulting in an octahedral coordination sphere. The cation can be considered as two calcium-centered octahedrons interconnected *via* a common face formed by three ipso carbon atoms. The di(phenyl)cuprate(I) anion is planar with a strictly linear C_i-Cu-C_i unit. This solvent-separated ion pair does not react with excess of activated calcium and, hence, di(phenyl)calcium cannot be generated from this transmetalation product.

Transmetalation of di(phenyl)manganese(II) with activated calcium powder leads to an unusual calcium calciamanganate(II), consisting of two solvent-separated dinuclear ions $[(thf)_3Ca(\mu\text{-}Ph)_3Ca(thf)_3]^+$ $[(thf)_2PhCa(\mu\text{-}Ph)_3MnPh]^-$, according to Scheme 12 [106]. The complex cation is isostructural to that of the previously mentioned calcium cuprate(I) with average Ca–C bond lengths of 260.6 pm. However, the unusual heterobimetallic complex anion consists of the strong electropositive calcium(II) ion and the less electropositive transition metal manganese(II) ion. The two metal centers are bridged by three slightly tilted phenyl groups and each metal ion binds to a terminal phenyl group. The calcium atom completes the coordination sphere by ligation of two thf donor bases. This arrangement allows a markedly shortening of the terminally bound phenyl substituents (Ca–Ci 248.6(5), av. Ca–C$_{\mu\text{-}Ph}$ 282.3 pm). The heterobimetallic anion can also be described as a contact ion pair of a phenylcalcium unit $[(thf)_2CaPh]^+$ coordinated to $[MnPh_4]^{2-}$ resulting in a calciamanganate(II) anion.

In most cases transmetalation in donor solvents (e.g., ethers) leads to solvent-separated alkaline-earth metal metallates with organyl-enriched metalate anions
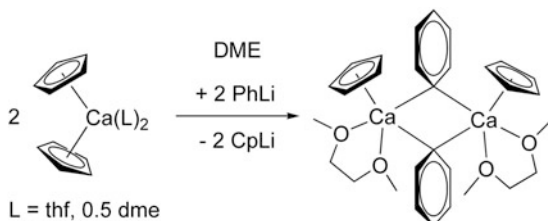
Scheme 13 (Salt-)Metathesis reaction of solvated calcocene with phenyllithium in 1,2-dimethoxyethane yielding heteroleptic $[(dme)Ca(\eta^5-C_5H_5)(\mu-C_6H_5)]_2$
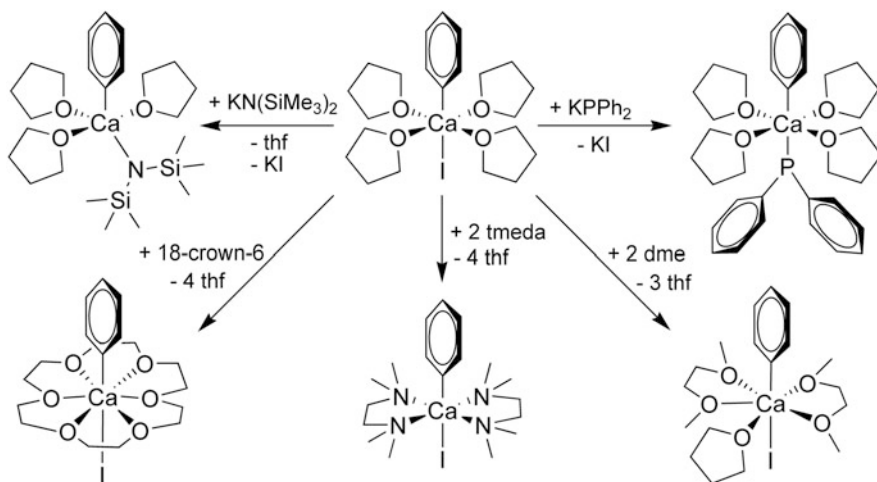
Scheme 14 Modification of phenylcalcium iodide including exchange of the iodide anion via salt metathesis reactions (*top row*) and exchange of the neutral thf coligands by other *Lewis* bases such as dme, 18-crown-6, and tmeda (*bottom row*)

being *inter alia* Al, V, and Cu [49, 87–92, 108–110]. However, a complete metal–metal exchange is hampered due to the fact that metalates are commonly sterically shielded and also because an anion has to be reduced.

Salt metathesis reactions are very well suited for the synthesis of di(benzyl) calcium compounds [111], whereas only a few examples for the synthesis of arylcalcium species *via* this method are described. *Ruspic* and *Harder* [112] reacted (2,6-dimethoxyphenyl)potassium and calcium diiodide and isolated a tetranuclear oxide-centered cage compound $[Ca_4\{2,6-(MeO)_2C_6H_3\}_6O]$. Very recently, *Westerhausen* and coworkers investigated the metathesis reaction of phenyllithium and calcocene, which can be regarded as a pseudohalide, yielding heteroleptic dinuclear $[(dme)Ca(\eta^5-C_5H_5)(\mu-C_6H_5)]_2$ with bridging phenyl moieties according to Scheme 13 [113]. The heteroleptic di(organo)calcium complex undergoes a *Schlenk*-type equilibrium depending on the concentration of the chelating 1,2-dimethoxyethane base (dme). An increasing amount of dme leads to a preference for the homoleptic compounds di(phenyl)calcium and $[(dme)Ca(\eta^5-C_5H_5)_2]$, as suggested by NMR investigations.

Ligand substitution reactions allow diverse variations of [PhCaI(thf)$_4$]. In Scheme 14 selected reactions are shown. If the post-*Grignard* reagent is dissolved in other donor solvents such as dme, tmeda, or treated with 18-crown-6, the thf ligands are substituted [76, 93, 104]. Exchange of the iodide anion can be achieved *via* (salt)metathesis reactions of [PhCaI(thf)$_4$] with potassium salts as also displayed in Scheme 14 yielding heteroleptic [PhCaX(thf)$_n$] with X being N(SiMe$_3$)$_2$ ($n = 3$) or PPh$_2$ ($n = 4$) [94].

3 Properties of Post-*Grignard* Reagents

In order to evaluate the reactivity of post-*Grignard* reagents pure isolated complexes are mandatory. Much of confusion in older literature originates from data obtained from reaction solutions and derivatization reactions because isolation of pure organocalcium complexes proved to be challenging. These compounds are extremely air and moisture sensitive and can inflame spontaneously in air. Due to their good solubility in ethereal solutions also crystallization and separation from impurities were not always straightforward. In addition, *Schlenk* equilibrium and ether degradation, both depending on the nature of the ether solvent and the temperature, complicate simple characterization strategies.

3.1 NMR Studies

Although the first NMR investigation of an arylcalcium compound, namely para-tolylcalcium iodide, dates back to the year 1968 [58] and several arylcalcium derivatives were synthesized in the decades before and thereafter [114, 115], almost no NMR data were available until 2005, when the *Westerhausen* group started the reinvestigation of arylcalcium chemistry and established reliable protocols to isolate these complexes in pure form.

In the last years, a growing number of soluble new compounds were prepared and characterized by NMR techniques, now allowing comparison of chemical shifts and elucidation of systematic trends in order to gain further insight into the solution behavior of these complexes. Deuterated THF is commonly used as the solvent of choice for this kind of investigations due to the fact that this solvent ensures an excellent solubility of most of the arylcalcium derivatives. However, it should be kept in mind that this solvent also represents a rather strong *Lewis* base and easily replaces other neutral donor ligands such as tmeda, dme, thp, or diethyl ether as a result of its superior donor ability and/or the statistical excess used. Hence, often only the NMR spectra of the corresponding thf complexes in addition to the spectrum of the liberated ligands are observed.

Scheme 15 summarizes the ^{1}H NMR and ^{13}C NMR data of the simplest representative of the arylcalcium halides, [(Ph)CaI(thf)$_4$], in [D$_8$]THF [75]. A characteristic
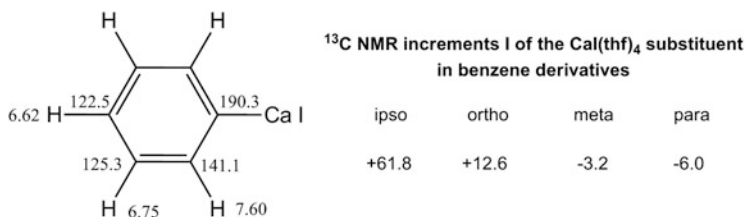
Scheme 15 ^{1}H and ^{13}C NMR parameters of phenylcalcium iodide in [D$_8$]THF. The ^{13}C NMR increments are listed in comparison to benzene

low-field shift of $\delta = 190.3$ was found for the ipso carbon atom of the terminal phenyl group, comparable with the one observed for the monomeric lithium compound [(Ph)Li(thf)$_3$] ($\delta = 196.4$) [116] but more pronounced than in case of the magnesium complex [(Ph)MgBr(Et$_2$O)$_2$] ($\delta = 164.9$). The data of [(Ph)CaI(thf)$_4$] can be used to extract the increments of the substituent CaI(thf)$_4$ (see Scheme 15), which are useful to predict and correctly assign the NMR data of hitherto unknown arylcalcium compounds on the basis of empirical increment systems for substituted benzenes [117].

Table 2 summarizes observed and calculated ^{13}C NMR shifts of a variety of substituted phenylcalcium iodides in THF. Although the additivity of such empirical increments is an oversimplification, neglecting steric and electronic substituent interactions, the calculated values show acceptable deviations from the observed chemical shifts. Larger differences were observed for the ipso carbon of sterically crowded derivatives such as [(Mes)CaI(thf)$_4$] [93] as well as for compounds where quinoid mesomeric forms might contribute to the overall structure like in case of [(p-Me$_2$N-C$_6$H$_4$)CaI(thf)$_4$] [84].

The influence of the other anionic ligand (halide, pseudohalide, aryl group) at the calcium center on the ^{13}C chemical shifts of the aryl rest is rather small, as a comparison of several phenyl and naphthyl derivatives with different anions reveals (see Table 3, entries 1–5, 8–11). Even a simultaneous change of the anion from iodide to bis(trimethylsilyl)amide and of the number of coordinated thf molecules from four to three has almost no influence on the chemical shifts of the ipso carbon atoms of coordinated aryl groups (entry 1 and 4, Table 3). The diorganyl calcium compound [(1-Naph)$_2$Ca(thf)$_4$] [106] seems to be an exception and a moderate low-field shift of the ipso carbon atom of about 3.5 ppm to $\delta = 198.9$ was observed when compared to [(1-Naph)CaI(thf)$_4$] ($\delta = 195.4$) [84]. While a related pair of magnesium compounds, [(Ph)MgBr(Et$_2$O)$_2$] ($\delta = 164.9$) and [(Ph)$_2$ Mg(thf)$_2$] ($\delta = 170.1$) [118], shows a similar low-field shift for the ipso carbon atom in the ^{13}C NMR spectrum of the diorganyl, the reported values of [(Ph)CaI(thf)$_4$] and [(Ph)$_2$Ca(thf)$_4$] are quite similar (see Table 3).

However, the diorganylcalcium compound [(Ph)$_2$Ca(thf)$_4$] shows broad signals for the phenyl group in THF at room temperature, indicating fluxional behavior in solution and only averaged signals were observed. It is well known that phenyl

Table 2 Comparison of observed and calculated ^{13}C NMR shifts of substituted arylcalcium iodides [(Aryl)CaI(thf)$_4$]

| Aryl | ^{13}C NMR | | | | |
	δ C$_{ipso}$ obs. (calc.)[a]	δ C$_{ortho}$ obs. (calc.)[a]	δ C$_{meta}$ obs. (calc.)[a]	δ C$_{para}$ obs. (calc.)[a]	Lit.
p-Tolyl	185.3 (187.2)	141.3 (141.1)	126.2 (125.9)	130.4 (131.8)	[84]
m-Tolyl	189.7 (190.3)	142.1 (141.7)	132.5 (134.6) [C]	123.5 (123.1)	
		138.0 (138.0)	125.0 (125.3) [CH]		
p-Cl-C$_6$H$_4$	187.8 (188.3)	142.5 (142.1)	125.0 (125.5)	129.0 (128.9)	[84]
m-Cl-C$_6$H$_4$	194.7 (191.3)	139.7 (141.3)	133.1 (131.7) [C]	122.4 (122.7)	
		138.6 (139.1)	126.6 (126.3) [CH]		
p-I-C$_6$H$_4$	188.9 (189.9)	143.5 (143.7)	133.9 (135.2)	89.7 (90.2)	[84]
p-MeO-C$_6$H$_4$	178.0 (182.2)	141.5 (142.0)	111.6 (110.3)	157.3 (153.8)	[84]
m-MeO-C$_6$H$_4$	192.3 (191.2)	133.5 (133.0)	157.8 (156.6) [C]	107.5 (107.5)	
		125.4 (126.1)	126.0 (126.2) [CH]		
p-Me$_2$N-C$_6$H$_4$	173.6 (178.3)	140.8 (141.8)	111.8 (109.3)	147.4 (143.5)	[84]
m,m'-Me$_2$C$_6$H$_3$	189.7 (190.3)	139.2 (138.6)	132.2 (134.6)	124.6 (123.7)	
Mesityl[b]	182.5/183.0 (188.4)	147.1/146.6 (150.4)	124.2/123.7 (123.4)	131.0/131.1 (131.8)	[96]

[a]$\delta_i = 128.5 + \Sigma I$; increments *I* were taken from [117] and from Scheme 15
[b]Two almost identical signal sets were observed at low temperatures and interpreted as mixture of [(Mes)CaI(thf)$_4$] and [Mes$_2$Ca(thf)$_3$] due to an operative *Schlenk*-type equilibrium

groups can occupy bridging positions in oxygen-centered calcium cages, dinuclear cations, and neutral compounds. As a result of the change in coordination mode from terminal to bridging, a high-field shift of the ipso carbon atom of the phenyl group was observed for the complexes [(Cp)Ca(μ-Ph)(dme)]$_2$ [113] and [(Ph)Ca (μ-Ph)(tmeda)]$_2$ [106] (Table 3, entries 6 and 7). Similarly, dimeric phenyllithium in THF containing bridging phenyl groups shows a signal for the ipso carbon atom at $\delta = 188.2$, while the monomer gave rise of a signal at $\delta = 196.4$ for the terminal phenyl ligand [116]. For [(Ph)Ca(μ-Ph)(tmeda)]$_2$ [106] this phenomenon is less pronounced, since the terminal and the bridging phenyl group rapidly exchange their positions and, hence, only one time-averaged signal set was observed. The coordination mode also influences the signals of the ortho-CH group of the phenyl ring in the ^{1}H NMR spectra. Here, a low-field shift to δ values above 8 is indicative for bridging phenyl groups ([(Ph)Ca(μ-Ph)(tmeda)]$_2$: $\delta = 8.56$ [106]; [(Cp)Ca(μ-Ph)(dme)]$_2$: $\delta = 8.26$ [113]).

Looking back to the beginnings with today's knowledge, the value $\tau = 1.755$ ($\delta = 8.24$) of the *ortho* hydrogen atoms of para-tolylcalcium iodide reported by *Fraenkel* et al. [58] rather points to an oxygen-centered calcium cage containing bridging tolyl groups. Nevertheless, the year 1968 marks the occurrence of the first valid NMR spectrum of an arylcalcium compound.

Table 3 ^{13}C NMR data of phenylcalcium and naphthylcalcium derivatives

Entry		^{13}C NMR shifts of the aryl group				
Phenyl derivatives		δC_{ipso}	δC_{ortho}	δC_{meta}	δC_{para}	Lit
1	[(Ph)CaI(thf)$_4$)]	190.3	141.1	125.3	122.5	[76]
2	[(Ph)CaBr(thf)$_4$)]	190.0	142.1	125.4^a	123.3	[76]
3	[(Ph)Ca(PPh$_2$)(thf)$_4$)]	190.1	141.6	125.7	123.2	[94]
4	[(Ph)Ca{N(SiMe$_3$)$_2$} (thf)$_3$)]	189.3	140.8	125.4	122.7	[94]
5	[(Ph)$_2$Ca(thf)$_4$)]	190.0^b	142.7^b	125.6	123.7^b	[106]
6	[(Ph)Ca(μ-Ph)(tmeda)]$_2$	186.0	141.9	126.9	125.7	[106]
7	[(Cp)Ca(μ-Ph)(dme)]$_2$	184.5	143.5	128.7	125.9	[113]
Naphthyl derivatives		δC_{ipso}		δ values of remaining aryl-C atoms		
8	[(1-Naph)CaI(thf)$_4$]	195.4	122.2, 122.9, 123.1, 124.6, 128.8, 134.1, 136.9, 138.0, 146.2			[84]
9	[(1-Naph)CaBr(thf)$_3$]$_2$	196.8	122.0, 122.7, 123.0, 124.4, 128.7, 134.0, 137.3, 138.2, 146.5			[99]
10	[(1-Naph)Ca{N(SiMe$_3$)$_2$} (thf)$_3$]	195.1	122.2, 123.1, 123.2, 124.6, 128.8, 134.1, 137.2, 137.6, 145.9			[99]
11	[(1-Naph)$_2$Ca(thf)$_4$]	198.9	122.0, 122.6, 123.0, 124.4, 128.8, 134.1, 137.7, 138.4, 146.9			[106]

^{a}Corrected value
^{b}Broad signal

3.2 Structural Characteristics

Arylcalcium complexes are commonly prepared in ethereal solutions *via* reduction of aryl halides with finely divided and highly reactive calcium powder. Because diethyl ether has a rather low boiling point these exothermic reactions are advantageously carried out in tetrahydrofuran (THF) or tetrahydropyran (THP). Due to an operative *Schlenk* equilibrium usually three species are present in solution: heteroleptic [(Ar)CaI(L)$_n$] as well as homoleptic [CaI$_2$(L)$_n$] and [(Ar)$_2$Ca(L)$_n$]. Fractionated crystallization and subsequent recrystallization are mandatory in order to remove excess of calcium, unreacted substrates, and ether degradation products.

In THF and THP complexes of the type [(Ar)CaI(L)$_4$] crystallize in a molecular structure with the anionic ligands in a trans arrangement, thus reducing electrostatic repulsion. The six-coordinate alkaline-earth metal is in a distorted octahedral environment. Due to the operative *Schlenk* equilibrium the crystalline post-*Grignard* reagents can contain varying amounts of calcium diiodide which leads to an enhanced spreading of the Ca–C bond lengths and to ellipsoids which are occasionally oriented along the Ca–C bond.

The neutral coligands can be substituted by dissolution of [(Ar)CaI(thf)$_4$] or [(Ar)CaI(thp)$_4$] in other donor solvents or by adding multidentate *Lewis* bases. The bulkiness of these coligands influences the coordination number of the calcium center. The most common situation shows a six-coordinate calcium in a distorted
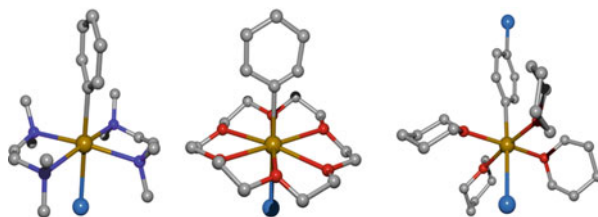
Fig. 2 Molecular structures of [(Ph)CaI(tmeda)$_2$] (*left*), [(Ph)CaI(18-crown6)] (*middle*), and [(4-I-C$_6$H$_4$)CaI(thp)$_4$] (*right*). In all molecule representations the atoms are shown with arbitrary radii and all hydrogen atoms are neglected for clarity reasons. Color code: C *gray*, Ca *gold*, halogen *blue*, N *dark blue*, O *red*

octahedral environment which is also realized for [(Ph)CaI(tmeda)$_2$] [104] (Fig. 2, left). Enhanced coordination numbers are observed if thf ligands are substituted by multidentate coligands with rather small distances between the *Lewis* donor atoms (small bite angles). Thus, coordination numbers of seven and eight are realized in the complexes [(Ph)CaI(thf)(dme)$_2$] [76] and [(Ph)CaI(18-crown-6)] [93] (Fig. 2, middle), respectively. Functional groups in *meta* and *para* positions do not alter the coordination behavior of the central alkaline-earth metal atom and similar molecular structures are observed as, e.g., for [(4-I-C$_6$H$_4$)CaI(thp)$_4$] (Fig. 2, right). Enlargement of the aryl group leads to significant distortion of the coordination sphere of the calcium center.

Smaller coordination numbers arise when the bulkiness of the anionic ligands increases. Thus, substitution of the iodide ion by a bis(trimethylsilyl)amide moiety yields [(Ph)Ca{N(SiMe$_3$)$_2$}(thf)$_3$] with a five-coordinate metal atom [94] (Fig. 3, left). Lower ether contents should lead to dimerization or even to higher aggregates. Quantum chemical studies suggest aggregation *via* bridging phenyl groups rather than bridging iodide ions [90]. Harder bromide ions, however, can very well act as bridging ligands as realized in [(1-Naph)Ca(μ-Br)(thf)$_3$]$_2$ [99] (Fig. 3, right).

Similar observations as discussed above for post-*Grignard* reagents also account for the molecular structures of diarylcalcium derivatives. As a representative example [(1-Naph)$_2$Ca(thf)$_4$] [106] is displayed in Fig. 4 (left). The aryl groups are *trans*-oriented and a distorted octahedral environment is observed for the alkaline-earth metal center. Increase of the steric demand of the aryl groups leads to smaller coordination numbers as found for [(Mes)$_2$Ca(thf)$_3$] [97] (Fig. 4, middle) with a five-coordinate calcium atom. According to the VSEPR concept [119–121] the bulkier Lewis donors are located in the equatorial plane whereas the smaller bases are bound in axial positions. This finding leads to a bent C–Ca–C fragment in this derivative. As shown in Fig. 4 (right) a *cis* arrangement of the aryl groups is realized with the tetradentate chelate base *N,N,N′,N″,N‴,N‴*-hexamethyltriethylenetetramine (hmteta) in the complex [(Ph)$_2$Ca(hmteta)]. This coligand also enforces a cis isomer of [CaI$_2$(hmteta)] [93] in the crystalline state and it seems impossible that this tetradentate base enables the formation of *trans*-di(phenyl)calcium in its complex.

Fig. 3 Molecular structures of [(Ph)Ca{N(SiMe$_3$)$_2$}(thf)$_3$] (*left*) and [(1-Naph)Ca(μ-Br)(thf)$_3$]$_2$. Color code and representation details are described in Fig. 2 (color code: Si *light blue*)
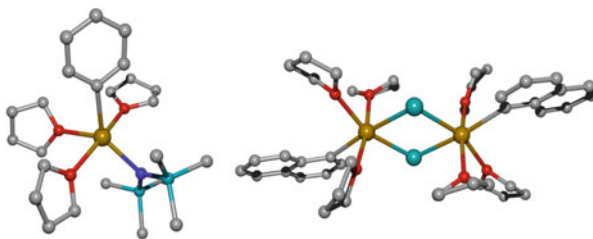
Fig. 4 Molecular structures of diarylcalcium complexes [(1-Naph)$_2$Ca(thf)$_4$] (*left*), [(Mes)$_2$Ca(thf)$_3$] (*middle*), and [(Ph)$_2$Ca(hmteta)] (*right*). Color code and representation details are described in Fig. 2
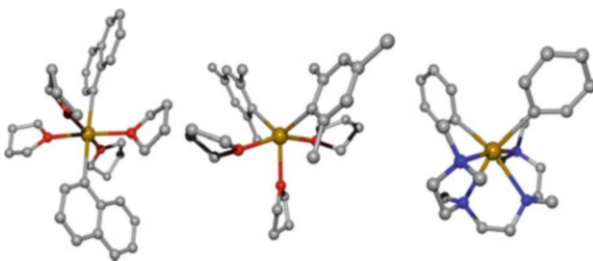
Fig. 5 Molecular structures of dimers with bridging phenyl groups, transoid [PhCa(μ-Ph)(tmeda)]$_2$ (*left*) and cisoid [CpCa(μ-Ph)(dme)]$_2$. Color code and representation details are described in Fig. 2
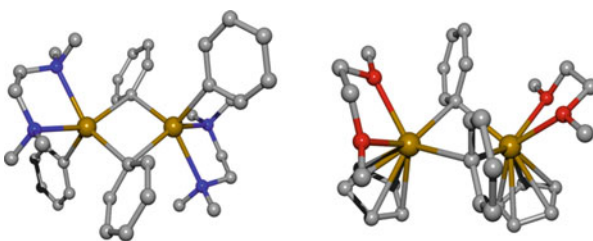
Dimerization *via* bridging phenyl groups is observed for the tmeda complex of diphenylcalcium as shown in Fig. 5 (left) for [PhCa(μ-Ph)(tmeda)]$_2$ [106]. Bridging phenyl groups are also observed in heteroleptic [CpCa(μ-Ph)(dme)]$_2$ [113] which crystallizes as a cis isomer from DME solution. The molecular structure is represented in Fig. 5 to the right. The cyclopentadienide groups can be considered as very soft pseudohalides which similar to iodide ligands avoid bridging positions between two rather hard *Lewis* acids (Fig. 6).

Organomagnesium compounds with three bridging groups are not common, but a few examples exist. The reaction of dimethylmagnesium with *N,N′,N″*-trimethyl-1,4,7-triazacyclononane (tmtn) yields solvent-separated [(tmtn)Mg(μ-Me)$_3$Mg(tmtn)]$^+_2$ [{Me$_2$Mg(μ-Me)$_2$}$_2$Mg]$^{2-}$ [122]. Heteroleptic [(Me$_3$Si)$_3$CMg(μ-Br)$_3$Mg(thf)$_3$] contains three bridging bromide ions [30]. Three bridging ligands between two metal atoms enforce rather small nonbonding M⋯M distances leading to electrostatic repulsion between the cations and also between the anionic bridging ligands. Furthermore, intramolecular steric strain leads to a breakup of at least one bridge if bulkier groups are bound. Homologous calcium forms longer bonds to the ligands than magnesium reducing electrostatic repulsive forces and steric

Fig. 6 Heterobimetallic solvent-separated complex [(thf)$_3$Ca(μ-Ph)$_3$Ca(thf)$_3$]$^+$ [(thf)$_2$CaPh(μ-Ph)$_3$MnPh]$^-$ with bridging phenyl groups between two metal centers (color code: Mn *violet*)
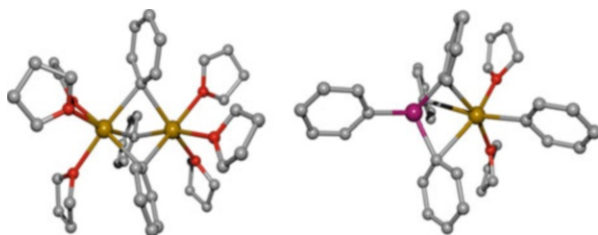
hindrance. This enables three phenyl bridges in the complex cation [(thf)$_3$Ca (μ-Ph)$_3$Ca(thf)$_3$]$^+$ and the anion [(thf)$_2$CaPh(μ-Ph)$_3$MnPh]$^-$.

Selected structural parameters of calcium-based post-*Grignard* reagents as well as homoleptic diarylcalcium complexes are summarized in Table 4. The most accurate distances in these compounds are the Ca–I bond lengths. However, the values vary within a rather large range and can be taken as a sensitive indicator for the charge on the calcium atom assuming an electrovalent Ca–I bond. This interpretation allows the deduction of the covalent and ionic contributions of the *trans*-positioned Ca–C bond. Adducts of calcium diiodide may serve as reference molecules and, hence, are included in Table 4.

The wide ranges for the Ca–C, Ca–I, and Ca–O distances are remarkable and make simple interpretations difficult. The large and soft iodide anion is highly polarizable with the consequence of a flat energy surface with respect to the variation of the Ca–I distance. Quantum chemical calculations of *Harvey* and *Hanusa* verified that a 15 pm stretch of the Ca–I bonds in [CaI$_2$(thf)$_6$] only requires 7.1 kJ·mol^{-1} [61]. The shortest Ca–I bond is realized in the cation [CaI(thf)$_5$]$^+$ with a value of 302.9 pm [109]; the largest distance is found in [(Ph)CaI(tmeda)$_2$] with a Ca–I distance of 330.2 pm [104]. Due to the softness and the polarizability of the iodide anion small effects can lead to rather large changes of the Ca–I values. In ionic calcium iodides with Ca^{2+} centers short bonds are observed. In heteroleptic arylcalcium iodides the Ca–C bond contains significant covalent contributions leading to a decreased charge on calcium and, hence, to a weaker electrostatic attraction between cation and iodide anion. A strong influence is also caused by steric repulsion of bulky coligands such as tmeda.

The donor strength (*Lewis* basicity) of suitable coligands such as ethers and amines plays a minor role and intramolecular Ca–O bond lengths often vary significantly with values in the 233–270 pm range. The largest values are observed for the crown ether adducts due to the large coordination number of the calcium atom. The fact that the coordination site of 18-crown-6 is slightly too large for Ca^{2+} might also be responsible for the variance of the Ca–O values in [(Ph)CaI(18-crown-6)].

The Ca–C bonds vary between 251 and 265 pm whereas especially these values may be hampered by an uncertainty caused by small amounts of iodine atoms substituting the phenyl groups. The crystal structure of [(Ph)CaI(18-crown-6)] was

Table 4 Selected structural data of arylcalcium compounds, calcium dihalides and related derivatives

Entry	C.N.[a]	Ca–C (pm)	Ca–L[b] (pm)	C–Ca–(I/C) (°)	Lit.
Phenylcalcium derivatives					
$[(Ph)Ca\{N(SiMe_3)_2\}(thf)_3]$	5	234.7(2)[c]	239.2(2), 241.0(2), 241.4(2)	128.7(1)[d]	[94]
$[(Ph)Ca(\mu\text{-}Ph)(tmeda)]_2$	5	250.8(3)[d]	257.1(2), 261.0(2)	–	[106]
$[(Ph)CaBr(thf)_4]$	6	288.99(8)	236.4(3), 239.4(3), 239.4(3), 239.5(3)	178.51(9)	[76]
$[(Ph)CaI(thf)_4]$	6	317.8(3)	237.0(11), 237.6(10), 237.9(12), 239.2(9)	177.4(2)	[76]
$[(Ph)CaI(thp)_4]$	6	312.1(1)	240.2(4), 241.4(4), 242.7(3), 244.7(4)	171.8(1)	[93]
$[(Ph)CaI(tmeda)_2]$	6	330.2(1)	257.5(5), 259.0(5)	177.6(2)	[104]
$[(Ph)Ca(PPh_2)(thf)_4]$	6	253.4(5)	235.5(3), 236.9(3), 238.8(3), 238.8(3)	174.1(1)	[94]
$[(Ph)_2Ca(hmteta)]$	6	256.4(3), 260.7(3)	257.9(3), 263.1(3), 263.6(3), 264.4(3)	109.7(1)	–
$[(Ph)CaI(dme)_2(thf)]$	7	319.2(1)	248.6(3), 248.7(3), 249.5(3), 249.7(3), 251.2(3)	175.35(9)	[76]
$[(Ph)CaI(18C6)]$	8	313.4(2)	261.9(6), 262.6(6), 263.3(6), 265.8(6), 269.9(6), 270.0(6)	177.5(4)	[93]
$[CpCa(\mu\text{-}Ph)(dme)]_2$	7	244.3[e]	240.7(2), 247.0(2)	–	[113]
$[(thf)_6Ca_2(\mu\text{-}Ph)_3]^+[Cu(Ph)_2]^-$	6	–	240.4(2), 241.4(2), 241.8(2)	–	[108]
$[(thf)_6Ca_2(\mu\text{-}Ph)_3]^+[(thf)_2(Ph)Ca(\mu\text{-}Ph)_3Mn(Ph)]^-$	6	248.6(5)[f]	235.9(3), 240.2(3)[f]	–	[106]
Substituted arylcalcium derivatives					
$[(Mes)_2Ca(thf)_3]$	5	252.0(3)	236.7(3), 241.1(2)	119.6(2)[g]	[97]
$[(pTol)Ca(\mu\text{-}pTol)(tmeda)]_2$	5	260.0(4)[g]	257.0(3), 259.2(3)	–	–
$[(2,6\text{-}pTol_2\text{-}C_6H_3)CaI(thf)_3]$	5	307.54(7)	234.4(3), 238.4(4), 239.0(3)	108.20(9)	[98]
$[(2,6\text{-}pTol_2\text{-}C_6H_3)Ca(HBEt_3)(thf)(dme)]$	5	293.0(5)[h]	235.7(2), 244.7(2), 247.1(2)	–	[123]
$[(Mes)CaI(thf)_4]$	6	320.84(9)	239.3(3), 240.2(3), 240.9(3), 241.9(3)	177.4(1)	[96]
$[(pTol)CaI(thf)_4]$	6	317.3(1)	237.3(4), 237.6(4), 238.0(4), 239.9(3)	174.6(1)	[76]
$[(pTol)CaI(thp)_4]$	6	315.71(9)	238.3(3), 238.4(3), 240.2(3), 243.8(3)	176.4(1)	
$[(4\text{-}MeO\text{-}C_6H_4)CaI(thp)_4]$	6	315.60(8)	239.2(3), 239.7(3), 243.5(3), 244.1(3)	176.3(1)	
$[(4\text{-}Cl\text{-}C_6H_4)CaI(thp)_4]$	6	313.6(2)	239.4(5), 240.0(6), 240.5(5), 243.7(5)	175.0(2)	
$[(4\text{-}I\text{-}C_6H_4)CaI(thp)_4]$	6	315.1(1)	238.0(3), 238.2(3), 239.1(3), 245.1(3)	176.1(1)	
$[(m\text{-}Tol)CaI(thf)_4]$	6	314.3(1)	236.5(4), 238.2(4), 239.6(4), 240.0(5)	176.9(2)	

Compound	CN[a]	Ca–X	Ca–C	Ca–L[b]	Angle	Ref.
[(3,5-Me₂-C₆H₃)CaI(thf)₄]	6	319.12(6)	254.0(3)	235.1(2), 238.2(2), 239.7(2), 241.8(2)	175.3(6)	[84]
Naphthylcalcium derivatives						
[(1-Naph)CaI(thf)₄]	6	318.7(1)	255.2(6)	231.3(8), 238.1(8)	177.7(2)[i]	[99]
[(1-Naph)Ca(μ-Br)(thf)₃]₂	6	293.41(8), 294.57(8)	252.8(4)	239.9(3), 240.6(3), 241.0(3)	—	[99]
[(1-Naph)₂Ca(thf)₄]	6	—	261.8(4), 263.9(3)	239.0(2), 239.8(2), 240.4(2), 241.6(3)	176.8(1)	[106]
[(1-Naph)Ca{N(SiMe₃)₂}](thf)₃]	5	235.0(4)[c]	251.4(6)	238.3(4), 239.5(5), 241.6(4)	116.5(2)	[99]
Adducts of calcium dihalide						
[CaBr₂(thf)₄]	6	288.46(4)	—	236.4(3), 236.9(3)	180.0	[99]
[CaBr₂(thp)₄]	6	283.87(6), 284.00(6)	—	236.6(2), 237.6(2), 237.8(2), 237.9(2)	179.27(3)	[93]
[CaBr₂(dme)₂(AcOH)]	7	283.5(3), 291.6(2)	—	239.3(8), 244.0(8), 246.3(7), 246.4(7), 250.9(8)	173.2(1)	[124]
[CaI₂(thf)₄]	6	311.25(9)	—	234.9(7), 239.5(8)	180.0	[125]
[CaI₂(thp)₄]	6	307.7(1), 307.9(1)	—	235.7(3), 236.4(3), 237.3(3), 237.5(3)	177.74(3)	[93]
[CaI₂(Et₂O)₄]	6	310.7(1), 312.2(1)	—	237.2(3), 237.3(3), 238.9(3), 240.7(4)	176.93(4)	[93]
[CaI₂(tmeda)₂]	6	313.09(4)	—	256.2(5), 257.0(5)	180.0	[93]
[CaI₂(hmteta)]	6	305.44(7), 305.97(7)	—	253.8(3), 255.4(3), 256.4(3), 256.8(3)	103.78(2)	[93]
[CaI₂(dme)₂(thf)]	7	313.42(2)	—	238.4(2), 246.2(2), 250.9(2)	179.09(2)	[126]
[CaI₂(thf)₂(diglyme)]	7	311.83(7), 312.06(7)	—	240.2(2), 244.5(3), 244.7(3), 249.7(3), 251.5(3)	175.63(3)	[93]
[CaI₂(18C6)]	8	303.43(7)	—	264.9(5)	180.0	[93]
Others						
[CaI(thf)₅]⁺ [V(Mes)₄]⁻	6	302.86(9)	—	233.7(3), 234.4(3), 234.5(3), 235.3(3), 240.1(3)	—	[109]
[Ca(thf)₆]²⁺ [{V(Mes)₄}⁻]₂	6	—	—	233.1(2), 234.4(2), 237.7(2)	—	[109]

[a] Coordination number of the calcium center
[b] L represents the neutral donor ligand and distances between Ca and O or N are listed
[c] Distance between Ca and N of the amide anion
[d] Bond lengths to bridging phenyl groups: Ca–C$_{br}$ 257.1(2), 261.8(2); angles: C$_{term}$–Ca–C$_{br}$ 104.97(7), 112.38(8); C$_{br}$–Ca–C$_{br}$ 94.94(6)
[e] Distance between the calcium atom and the center of the Cp ligand
[f] Values of the (Ph)Ca(thf)₂ subunit of the anion, containing a terminal phenyl group
[g] Bond lengths to bridging tolyl groups: Ca–C$_{br}$ 258.9(4), 259.0(4); angles: C$_{term}$–Ca–C$_{br}$ 112.0(1), 114.7(1); C$_{br}$–Ca–C$_{br}$ 92.5(1)
[h] Ca···B distance of the calcium boranate unit
[i] C–Ca–Br bond angles: 96.54(9) and 173.6(1)°

determined at a single crystal containing 15 % of [CaI$_2$(18-crown-6)] [93]. In all of these cases the main axis of the ellipsoid of the ipso carbon atom points away from the calcium center causing a feigned elongation of the Ca–C bond, and in addition, rather large e.s.d. values in comparison to the standard deviations of the Ca–O distances are occasionally obtained. Furthermore, some of the structures are also hampered due to disordering and flexibility of coligands or parts thereof. The shortest Ca–C bond lengths show values of 251 pm and are characteristic for Ca–C single bonds in arylcalcium derivatives. Comparable Ca–C distances were observed in alkylcalcium derivatives such as [Ca{C(SiMe$_3$)$_3$}$_2$] (245.9(9) pm) [127], [(thf)$_2$Ca{CH(SiMe$_3$)$_2$}$_2$] (248.3(5) pm) [128], [(diox)$_2$Ca{CH(SiMe$_3$)$_2$}$_2$] (249.3(2) pm) [71], [(thf)$_2$CaC (PPh$_2$=NDipp)$_2$] (254.8(2) pm) [129], and others.

Generally, the coordination number of calcium is determined by the bulkiness of the anionic and neutral ligands with a preference to six-coordinated alkaline-earth metal centers in distorted octahedral environments. Bond lengths for calcium depend on several factors:

– Smaller coordination numbers should lead to shorter Ca–I, Ca–C, and Ca–O/N bonds due to reduced intramolecular strain. However, small coordination numbers are achieved by introduction of bulky groups and ligands, partly counteracting this effect.
– The donor strength of the neutral *Lewis* basic coligands should influence the Ca–O/N distances. The differences of the *Lewis* basicity are rather small and other factors interfere with this effect. Alteration of the donor strength always is accompanied with a change of steric demand. Thus, THF is a stronger base than diethyl ether, but this cyclic ether is also less demanding and leads to a smaller crowding around the calcium center.
– The charge on the calcium cation should especially influence the distances between metal ions, but this effect should be less pronounced for the rather covalent Ca–C bond. Therefore, a larger positive charge on calcium leads to significantly smaller Ca–I/Br distances, but the influence on Ca–O/N and Ca–C distances is much smaller.

Generally arylcalcium halides are monomeric in the solid state and in solution. Even though there exist rare examples of bridging aryl groups and iodide anions, ethers (THF, THP, diethyl ether) and amines (TMEDA) are preferred to saturate the coordination sphere of the calcium atoms. The harder bromide anion, however, seems to be a more suitable bridging ligand as realized in crystalline [(1-Naph)Ca (μ-Br)(thf)$_3$]$_2$. As "free" aryl anions are less likely to exist, ligand exchange processes according to the *Schlenk* equilibrium should proceed through an associative mechanism with a dinuclear intermediate. As bridging aryl groups and halide anions are less favored in post-*Grignard* compounds, this type of intermediates is not easily detectable.

X-ray structure determination of extremely air and moisture sensitive compounds.

Due to the fact that elemental analysis often is not reliable due to loss of coligand during handling (besides thermal decomposition and hydrolysis) solution NMR techniques and X-ray structure analysis at single crystals represent the most powerful tools for the characterization of these post-*Grignard* reagents. Due to the fact that isolated arylcalcium complexes lose ether and decompose immediately after isolation, crystals have to be stored in a saturated atmosphere of the coligand or in their mother liquor. For X-ray structure determinations the single crystals have to be selected, isolated, and transferred to the diffractometer. In order to prevent phase transitions, collection and handling of crystals are done at the same temperature as the crystallization temperature. Therefore, the crystals were removed from the mother liquor (which is kept in an appropriate cooling bath) and immediately transferred into precooled perfluorinated oil. The crystal quality can safely be controlled under a microscope and a suitable single crystal is mounted on the diffractometer and cooled immediately to approximately $-100\,^\circ$C in order to protect the single crystal from thermal decomposition, loss of coligand, and hydrolysis. Suitable detailed procedures were published by *Stalke* and coworkers [130, 131].

4   Reactivity Investigations

Calcium-based organometallics already proved to be valuable catalyst systems in diverse reactions such hydroamination, hydrophosphanylation, hydrogenation, hydrosilylation, and polymerization reactions [91, 92, 132, 133]. In stoichiometric applications heterobimetallic organometallics are assessable *via* the addition of arylcalcium complexes to other organometallic compounds [90, 134]. Thus, cuprates [108, 110], vanadates [109], alanates [135], and others can be prepared *via* addition of arylcalcium halide to the corresponding arylmetal derivative or *via* transmetalation of the organometallic complex with calcium metal. These heterobimetallic compounds show different reactivities than the homoleptic organometallic derivatives and – depending on the relative electronegativities - calcium metalates or metal calciates are formed [134].

In addition to these applications the nucleophilicity of calcium-based organometallics can be exploited in stoichiometric reactions. The enormous reactivity toward weak acids justifies consideration of these reagents as superbases [49] with the tendency to degrade ethers as a characteristic feature. Due to the fact that two recent and excellent review articles already focus on catalytic applications [132, 133] we limit the discussion on selected stoichiometric reactivity studies.

4.1 Ether Degradation

Already in the beginning of the investigation of organocalcium compounds the deprotonation power toward ethereal solvents was noticed (see Chapter 2). Therefore, the synthesis of post-*Grignard* reagents has to be performed at ambient temperature or below and storage at low temperatures is recommended. Heating during preparation should be avoided. In addition, also calcium atoms itself are able to attack ethers and detailed investigations suggest that an oxidative addition of the O–C bond of ether to calcium yields calcium alcoholates and alkylcalcium, but insertions of calcium into C–H and C–C bonds must also occur to explain the product diversity obtained after hydrolysis [136]. Codeposition of calcium and diethyl ether and subsequent hydrolysis yielded a variety of products such as alkanes, alkenes, and alkynes including acetylene and propyne. Therefore, removal of excess of activated calcium from the post-*Grignard* solutions seems to be advantageous.

Degradation of ethereal solvent was intensively studied in organolithium chemistry and four major pathways (α-, β-, α,β'-elimination and *Wittig* rearrangement) have been proposed [137] depending on the nature of the ether molecule (cyclic or acyclic) and the position of nucleophilic attack. In general, coordination of the ether molecule at the electropositive metal cation (followed by deprotonation) is the first reaction step. Based on these investigations, THF is nearly exclusively deprotonated in α-position finally leading to ethylene and a metal vinylalcoholate, while diethyl ether is predominantly metalated in β-position and subsequent rearrangement reactions give metal ethanolate besides ethylene.

When discussing ethereal solvent degradation in *Grignard*-type reactions, one should discriminate between the preparation stage and the final product stage. During the preparation of the post-*Grignard* reagents, proceeding most likely by single electron transfer steps, side reactions typical for radical reactions should be expected. Later on, the formed post-*Grignard* reagents react as very strong bases with present solvent molecules more likely by ionic or covalent mechanisms. Although less pronounced, classic *Grignard* reagents also show ether degradation and occasionally ether degradation products are found which can best be explained by often yet unknown radical mechanisms [18] besides the products expected for ionic mechanisms. It is understandable that it is not always possible to distinguish between products formed by one or the other reaction type when the original reaction mixture is analyzed. However, the isolation of pure post-*Grignard* reagents now allows the investigation of the reactions induced by these species under well-defined conditions to deduce a more detailed picture of ether degradation.

It is expected that half-life times of organocalcium compounds, similar to related organolithium reagents, strongly depend on solvent, temperature, and nucleophilicity of the organyl group [138].

As a representative example the decomposition of *p*-tolylcalcium iodide in THF at ambient temperature was studied. In 0.05 M to 0.2 M solutions of *p*-tolylcalcium iodide, containing 0.4 mL of THF and 0.2 mL of [D$_6$]benzene, a half-life time of eight

days was determined. A concentration dependency was not found suggesting an intramolecular degradation mechanism. The products observed *via* NMR investigation, toluene, ethylene, and calcium vinylalcoholate species, point towards initial α-deprotonation of THF by the organocalcium compound, followed by its cycloreversion as the major pathway, in agreement with results observed for organolithium derivatives.

Another species present in differing concentrations, which was interpreted earlier as a calcium vinylalcoholate, is actually a calcium derivative containing bridging *p*-tolyl groups. This compound is already present at the beginning of the decomposition experiments in varying concentrations, depending on the crop of *p*-tolylcalcium iodide under investigation. Therefore, it is rather an impurity which stems from the original synthesis of the arylcalcium compound. Since during earlier efforts to prepare arylcalcium complexes oxygen-centered cage compounds such as [{(2,6-(MeO)$_2$C$_6$H$_3$)$_2$Ca}$_3$·CaO] [112], [{(thf)$_2$Ca(Ph)I}$_3$·(thf)CaO] [139], and [{(Et$_2$O)$_2$Ca(Ph)$_2$}$_4$·(Et$_2$O)CaO] [94] were isolated, the observed impurity could represent another member of this group of compounds. The source of the oxide centers in these different cages is uncertain and does not necessarily have to be the same. Solvent degradation by a radical pathway during preparation of the post-*Grignard* reagents is one possible explanation, but also adventitious traces of water or oxygen leaking in during handling and manipulation could represent oxygen sources. Extensive formation of calcium oxide species during THF degradation by *p*-tolylcalcium iodide under the applied conditions seems unlikely since already small amounts of "CaO" capture a multitude of post-*Grignard* equivalents and the NMR signals of the formed cluster species would increase rapidly and, hence, should be detectable. Further decomposition products could not be identified by NMR measurements, during calcium-mediated thf degradation in a sealed NMR tube (Fig. 7).

However, upon heating of a solution of phenylcalcium iodide in THF to reflux for several hours, the cage [(CaO)·(thf)$_3$Ca(μ-I)$_2$]$_4$ (Fig. 5, right) was obtained in good yield, showing that the reaction conditions strongly influence the outcome of the THF degradation [140].

In THP, the decomposition of *p*-tolylcalcium iodide is considerably slower than in THF. After 17 days at ambient temperature, approximately 50 % of the primary species [(tol)CaI(thp)$_4$] are still intact. During this period of time an increasing amount of species containing bridging *p*-tolyl groups was formed, indicating that the overall loss of *p*-tolylcalcium species is far less pronounced than observed for the primary species [(tol)CaI(thp)$_4$]. After 6 weeks still less than half of the arylcalcium derivatives decomposed as judged by the amount of toluene formed.

4.2 Directed ortho-Calciations

The initial deprotonation of THF and diethyl ether as initial step of ether degradation clearly demonstrates the depronative power of calcium-based post-*Grignard*
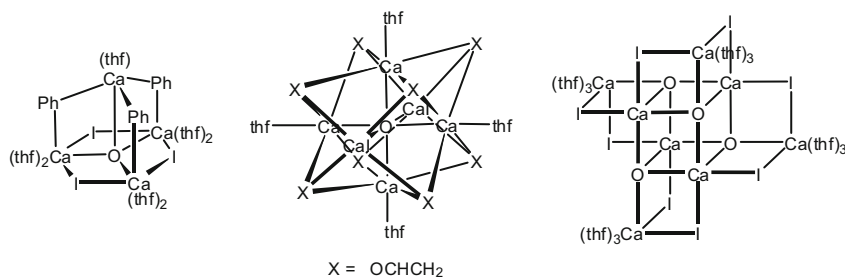
Fig. 7 Schematic drawings of ether degradation products: oxygen-centered Ca_4 tetrahedron with bridging phenyl groups and iodide anions (*left*), oxygen-centered Ca_6 octahedron with vinylate anions above the planes (*middle*), Ca_4O_4 heterocubane with CaI_2 bound at the periphery of the cubane cage. In all these cages vacant sites at calcium are occupied with thf ligands

reagents. As mentioned earlier, arylcalcium complexes can therefore be considered as superbases [49]. Selective calciation can be achieved in neighborhood to *Lewis* donor sites. Here we select two representative examples of directed ortho-calciation (DOC). Selective deprotonation in ortho position to the functionality can be realized with oxygen and nitrogen donor sites in the substituents.

The salt metathesis reaction of 2,6-bis(methoxy)phenyl potassium with calcium diiodide in THF over a period of three days yielded nearly quantitatively an oxygen-centered tetranuclear cage compound with a central Ca_4 tetrahedron, $[\{(2,6-(MeO)_2C_6H_3)_2Ca\}_3 \cdot CaO]$ [112]. The direct synthesis of 1-iodo-2,6-dimethoxybenzene with activated calcium in THF at 0 °C gave 2,6-dimethoxyphenylcalcium iodide with a yield of 56 % [97]. In contrast to these protocols directed ortho-calciation of 1,3-dimethoxybenzene with phenylcalcium iodide yielded the desired organocalcium complex with a yield of 83 % according to Scheme 16. Cooling of the concentrated reaction solution led to crystallization of dinuclear $[\{2,6-(MeO)_2C_6H_3\}_3Ca_2I(thf)_3]$ with three bridging aryl groups (Fig. 8, left) [97].

Both calcium atoms exhibit rather large coordination numbers of eight: three bridging ipso carbon atoms, three methoxy bases, and two tetrahydrofuran ligands or one tetrahydrofuran ligand and one iodide anion, respectively. Large coordination numbers of calcium, bridging positions of the aryl groups, and crowding around the metal centers lead to large Ca–C bond lengths that range substantially from 261.3(6) to 275.0(6) pm. Furthermore, the Ca–I and Ca–O distances are increased, too, and values of 330.6(1) pm as well as those of 246.9(4), 247.6(4), and 251.5(4) are observed, respectively.

The high reactivity of phenylcalcium complexes often leads to side reactions. The addition reaction of less aggressive $[(thf)_2Ca\{N(SiMe_3)_2\}_2]$ with benzonitrile and a subsequent 1,3-trimethylsilyl migration quantitatively yields bis(tetrahydrofuran) calcium-bis[N,N'-bis(trimethylsilyl)benzamidinate] [141]. Phenylcalcium iodide, however, oligomerizes and polymerizes benzonitrile. Using potassium bis[N,N'-bis(trimethylsilyl)benzamidinate] as a precursor complex, the concentration of benzonitrile is very low due to an operative equilibrium between this benzamidinate
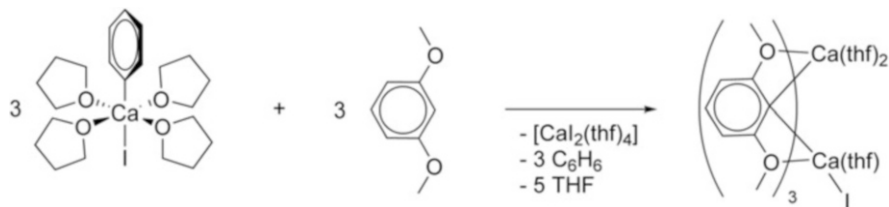
Scheme 16 Directed ortho-calciation (DOC) of 1,3-dimethoxybenzene with phenylcalcium iodide in THF yielding dinuclear [{2,6-(MeO)$_2$C$_6$H$_3$}$_3$Ca$_2$I(thf)$_3$]
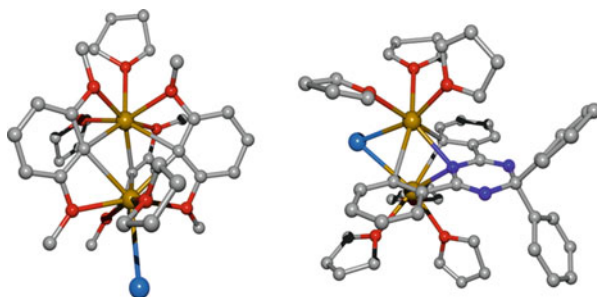
Fig. 8 Molecular structures of dinuclear [{2,6-(MeO)$_2$C$_6$H$_3$}$_3$Ca$_2$I(thf)$_3$] (*left*) and dinuclear [{4,4-Ph$_2$-2,6-(H$_4$C$_6$)$_2$C$_3$N$_3$}$_3${Ca(thf)$_3$}$_2$I] (*right*). Color codes are described in Fig. 2

on the one hand and potassium bis(trimethylsilyl)amide and benzonitrile on the other. Now a stepwise addition of phenylcalcium iodide to benzonitrile finally leads to triply calciated 2,4,4,6-tetraphenyl-1,3,5-triazacyclohexa-2,5-diene according to Scheme 17 [94]. The molecular structure of this dinuclear complex [{4,4-Ph$_2$-2,6-(H$_4$C$_6$)$_2$C$_3$N$_3$}{Ca(thf)$_3$}$_2$I] is represented in Fig. 8 (right). Here, DOC is observed as the final reaction step.

The calcium atoms show coordination numbers of seven and bind with three thf ligands, two bridging aryl groups, a bridging iodide anion, and a bridging amide. Despite the bridging position of the iodide anion, rather small Ca–I distances of 324.3 (2) and 325.8(2) pm are found whereas the Ca–C bonds are elongated (266.8(6) and 268.7(6) pm) [94].

5 Conclusion and Perspective

Arylcalcium complexes show similarities to the widely used organolithium complexes and organomagnesium halides. Whereas the reactivity and the spectro-scopic properties correspond more to the behavior of organolithium reagents, the solution behavior displays similarities to that of *Grignard* reagents. The arylcalcium iodides and the organomagnesium halides show a *Schlenk* equilibrium between heteroleptic RAeX and homoleptic AeR$_2$ and AeX$_2$. These reactive metalation reagents also have in common that they are able to degrade ethers.
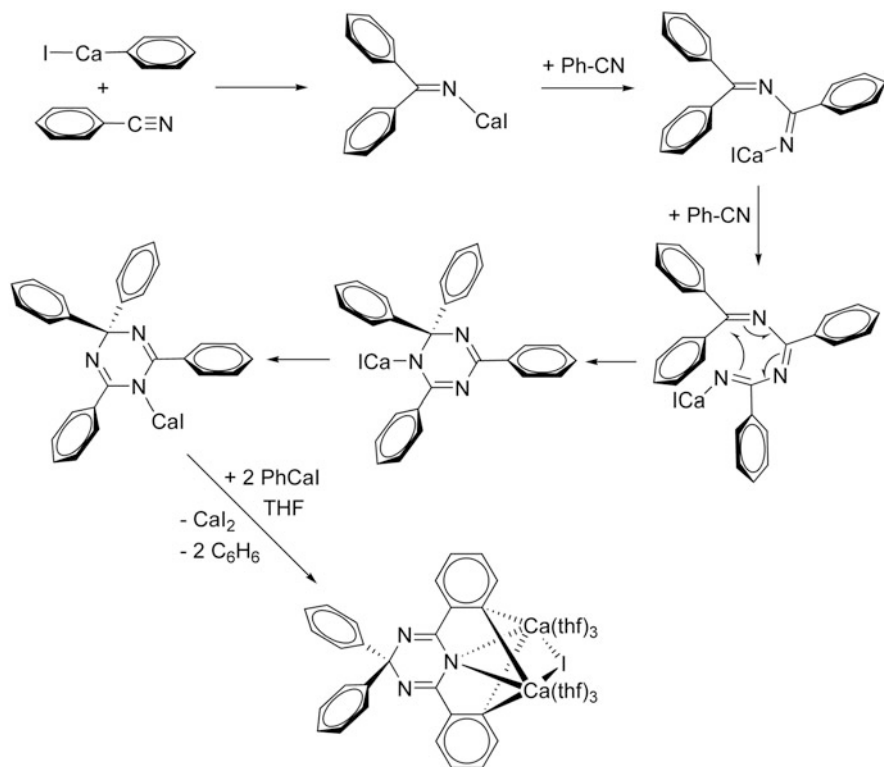
Scheme 17 Proposed mechanism of the reaction of phenylcalcium iodide (coordinated thf ligands are omitted for clarity) with benzonitrile. In order to guarantee a low concentration of PhCN this substrate is generated in a preceding equilibrium of [{Ph-C(NSiMe$_3$)$_2$}K] with KN(SiMe$_3$)$_2$ and PhCN

Arylcalcium complexes have to be prepared in ethereal solvents where they are highly soluble. In contrast to these alkaline-earth metal reagents, organolithium complexes often form aggregates such as tetrameric methyllithium or hexameric *n*-butyllithium [142–145] which are also soluble in hydrocarbons.

The arylcalcium complexes are valuable organometallics which can easily be prepared, purified, manipulated, and used for calciation reactions. They are more reactive than the homologous magnesium compounds offering an extended spectrum of application. Their reactivity is comparable to organolithium reagents in many aspects but different in others. 2,4,6-Tri(tert-butyl)phenyllithium and 2,4,6-tri (tert-butyl)phenylmagnesium halide are sterically protected organometallics; in contrast to these complexes the *ortho*-bound tert-butyl substituent is deprotonated during the reaction of 1-iodo-2,4,6-tri(tert-butyl)benzene with calcium. In addition, 2,4,6-Ph$_3$C$_6$H$_2$-Li and 2,4,6-Ph$_3$C$_6$H$_2$-MgX are stable, but arylcalcium complexes are extremely reactive and can undergo side reactions if a phenyl group is bound in *para* position. Whereas lithium represents a characteristic hard s-block element,

calcium combines properties of s-block elements and early transition metals. The discrepancy between the reactivity of arylcalcium complexes and the inertness of the alkaline-earth metal itself can be overcome by simple activation procedures. Metal and calcium-based organometallics can safely be handled and manipulated in an inert gas atmosphere consisting of nitrogen or argon. Lithium metal, however, is much more reactive forming oxides and nitrides upon contact with oxygen or nitrogen. Therefore, nitrogen cannot serve as a protecting inert gas atmosphere during direct synthesis of RLi from lithium metal and organylhalides. The common use of organyllithium reagents is mainly based on their commercial availability.

Arylcalcium halides and pseudohalides represent valuable synthons in organometallic chemistry and can be at least as valuable as organolithium reagents. This is due to their ease of preparation and manageability on the one hand and their high and tunable reactivity on the other. Several features with respect to the direct synthesis of arylcalcium reagents can be generalized:

– The synthesis of post-*Grignard* reagents has to be performed in ethereal solvents such as THF, tetrahydropyran, or diethyl ether (no reactions occur in hydrocarbons). In these ethereal solvents arylcalcium iodides are highly soluble and preferably monomeric with hexacoordinate calcium centers in distorted octahedral environments.
– Calcium metal is rather inert and should be activated prior to use. A nitrogen inert gas atmosphere is sufficient to prepare activated calcium and to handle and manipulate calcium-based organometallics.
– The highest yields are achieved when iodoarenes are employed for the direct synthesis of arylcalcium halides. Lower yields are observed for the bromoarenes whereas the homologous fluoro- and chloroarenes show no reactivity toward calcium activated with ammonia.
– Temperatures below ambient temperatures have to be maintained in order to avoid side reactions such as ether degradation. For the same reason excess of calcium metal should be removed after the preparation of post-*Grignard* reagents.
– A diversity of groups is tolerated in *para* position of phenylcalcium halide. A para-phenyl group can destabilize the product. Substituents in ortho positions tend to undergo side reactions much more easily and even tert-butyl groups do not represent suitable protecting groups.
– Characterization of arylcalcium complexes has to be performed under exclusion of air and moisture. The most meaningful tools include NMR spectroscopic investigations and X-ray structure determinations.

Organocalcium compounds already proved to be valuable reagents for the directed *ortho* metalation and other stoichiometric deprotonation reactions of H-acidic compounds such as amines or phosphanes. In addition, there exist already catalytic applications for organocalcium complexes such as hydroamination and hydrophosphanylation of alkynes as well as catalytic activity in hydrogenation and hydrosilylation reactions. Due to the fact that the organocalcium chemistry shows a vast development only in very recent years the discovery of many more

stoichiometric and catalytic applications can be expected in inorganic, organic, and organometallic chemistry. Very recently, *Ritter* agreed on the usefulness and demand of organocalcium reagents and stated that "these developments have opened the curtains and let the sun shine on [organo]calcium chemistry" [146].

The synthesis of arylstrontium and –barium complexes is much more challenging than the preparation of organocalcium derivatives for two reasons: On the one hand, the reactivity of these post-alkaline-earth metals is much higher leading to alkaline-earth metal amides during the activation procedure with liquid ammonia. On the other hand, ether cleavage or solvent attack is much more pronounced hampering the isolation of pure products. Nevertheless, the interest in these compounds also grew in the past few years expecting strong superbases for metalation reactions.

The organocalcium chemistry shows many facets and, hence, covers diverse fields of applications which should not remain unmentioned. Very recently, organoalkaline-earth metal(I) compounds of magnesium [147] and calcium [100] were prepared, but the calcium compounds remained curiosities as of yet [148–151]. Calcocenes represent the best established organocalcium reagents [152–159]. However, due to the rather small pK_a values of cyclopentadienes their calcium derivatives can be considered as pseudohalides [113]. In this category also alkynylcalcium complexes [160–162] should be mentioned with CaC_2 being well known for a long time. Whereas reliable preparative procedures for simple alkylcalcium reagents are missing till today [49], two classes of substituted alkylcalcium complexes gain on importance due to their availability. On the one hand, benzylcalcium derivatives [98, 111, 163–166] can be used for calciation reactions and as polymerization initiators. These complexes are usually prepared via (salt)metathesis reactions from benzylpotassium and calcium diiodide. On the other hand, trialkylsilyl-substituted methylcalcium reagents [71, 127, 128] are soluble in common organic solvents and the reactive Ca–C bonds are sterically protected by bulky silyl groups at the molecule periphery. Both strategies involve the reduction of the negative charge on the α-carbon atom by delocalization into the phenyl groups and by hyperconjugation to the silyl substituents. Common procedures involve metal–metal exchange reactions (usually the synthesis of the lithium derivative, conversion to the potassium complex, and finally a metathesis reaction with CaI_2 yielding the organocalcium reagent). The arylcalcium complexes are extremely appealing due to the fact that the direct synthesis is a simple, straightforward high-yield procedure. The organomagnesium chemistry experienced the breakthrough after the development of a simple protocol for the synthesis of *Grignard* reagents; a comparable progress is assumed for the calcium-based post-*Grignard* reagents.

References

1. Seyferth D (2009) The Grignard reagents. Organometallics 28:1598–1605
2. Bickelhaupt F (1994) Organomagnesium chemistry: nearly hundred years but still fascinating. J Organomet Chem 475:1–14
3. Walborsky HM (1990) Mechanism of Grignard reagent formation. The surface nature of the reaction. Acc Chem Res 23:286–293
4. Walborsky HM (1991) Wie entsteht eine Grignard-Verbindung? Chemie in unserer Zeit 25:108–116
5. Walborsky HM, Zimmermann C (1992) The surface nature of Grignard reagent formation. Cyclopropylmagnesium bromide. J Am Chem Soc 114:4996–5000
6. Garst JF (1991) Grignard reagent formation and freely diffusing radical intermediates. Acc Chem Res 24:95–97
7. Garst JF, Ungváry F (2000) Mechanisms of Grignard reagent formation. In: Richey HG Jr (ed) Grignard reagents: new developments, Chap. 7. Wiley, Chichester, pp 185–275
8. Garst JF, Soriaga MP (2004) Grignard reagent formation. Coord Chem Rev 248:623–652
9. Richey HG Jr (2000) Grignard reagents: new developments. Wiley, Chichester
10. Wakefield BJ (1995) Organomagnesium methods in organic synthesis. Academic, London
11. Rappoport Z, Marek I (2008) The chemistry of organomagnesium compounds (Patai Series: The chemistry of functional groups). Wiley, Chichester
12. Schlosser M (1973) Struktur und Reaktivität polarer Organometalle: Eine Einführung in die Chemie organischer Alkali- und Erdalkalimetall-Verbindungen. Springer, Heidelberg
13. Schlenk W, Schlenk W (1929) Über die Konstitution der Grignardschen Magnesiumverbindungen. Chem Ber 62:920–924
14. Heard PJ (2008) NMR of organomagnesium compounds. In: Rappoport Z, Marek I (eds) The chemistry of organomagnesium compounds (Patai Series: The chemistry of functional groups), Chap. 3. Wiley, Chichester, pp 131–154
15. Yamabe S, Yamazaki S (2008) Theoretical studies of the addition of RMgX to carbonyl compounds. In: Rappoport Z, Marek I (eds) The chemistry of organomagnesium compounds (Patai Series: The chemistry of functional groups), Chap. 9. Wiley, Chichester, pp 369–402
16. Liebman JF, Holm T (2008) The thermochemistry of organomagnesium compounds. In: Rappoport Z, Marek I (eds) The chemistry of organomagnesium compounds (Patai Series: The chemistry of functional groups), Chap. 2. Wiley, Chichester, pp 101–129
17. Garst JF, Lawrence KE, Batlaw R, Boone JR, Ungváry F (1994) Magnesium bromide in Grignard reagent formation. Inorg Chim Acta 222:365–375
18. Langer J, Krieck S, Fischer R, Görls H, Walther D, Westerhausen M (2009) 1,4-Dioxane adducts of bis(2,4,6-trimethylphenyl)magnesium: synthesis, ether cleavage reactions, and structural diversity of Grignard reagent/1,4-dioxane complexes. Organometallics 28:5814–5820
19. Markies PR, Akkerman OS, Bickelhaupt F, Smeets WJJ, Spek AL (1991) X-ray structural analyses of organomagnesium compounds. Adv Organomet Chem 32:147–226
20. Holloway CE, Melnik M (1994) Magnesium compounds: classification and analysis of crystallographic and structural data. J Organomet Chem 465:1–63
21. Bickelhaupt F (2000) Structures of organomagnesium compounds as revealed by X-ray diffraction studies. In: Richey HG Jr (ed) Grignard reagents: new developments, Chap. 9. Wiley, Chichester, pp 299–328

22. Jastrzebski JTBH, Boersma J, van Koten G (2008) Structural organomagnesium chemistry. In: Rappoport Z, Marek I (eds) The chemistry of organomagnesium compounds (Patai Series: The chemistry of functional groups), Chap. 1. Wiley, Chichester, pp 1–99

23. Stucky G, Rundle RE (1964) The constitution of the Grignard reagent, phenylmagnesium bromide dietherate. J Am Chem Soc 86:4825–4830

24. Schröder FA (1969) Zur Kenntnis der Grignard-Verbindung $C_6H_5MgBr(C_4H_8O)_2$ sowie über die Koordinationsverbindung $MgBr_2(C_4H_8O)_4$. Chem Ber 102:2035–2043

25. Vallino M (1969) Structure cristalline de $CH_3MgBr\cdot 3C_4H_8O$. J Organomet Chem 20:1–10

26. Yousef RI, Walfort B, Rüffer T, Wagner C, Schmidt H, Herzog R, Steinborn D (2005) Synthesis, characterization and Schlenk equilibrium studies of methylmagnesium compounds with O- and N-donor ligands—the unexpected behavior of [MgMeBr(pmdta)] (pmdta = N,N, N',N",N"-pentamethyldiethylenetriamine). J Organomet Chem 690:1178–1191

27. Vestergren M, Eriksson J, Håkansson M (2003) Absolute asymmetric synthesis of "chiral-at-metal" Grignard reagents and transfer of the chirality to carbon. Chem Eur J 9:4678–4686

28. Toney J, Stucky GD (1971) The stereochemistry of polynuclear compounds of the main group elements. $[C_2H_5Mg_2Cl_3(C_4H_8O)_3]_2$, a tetrameric Grignard reagent. J Organomet Chem 28:5–20

29. Sakamoto S, Imamoto T, Yamaguchi K (2001) Constitution of Grignard reagent RMgCl in tetrahydrofuran. Org Lett 3:1793–1795

30. Al-Juaid SS, Eaborn C, Hitchcock PB, Jaggar AJ, Smith JD (1994) The reaction of $(Me_3Si)_3CBr$ with Mg in tetrahydrofuran (THF) or diethyl ether. Crystal structure of $(Me_3Si)_3CMg(\mu\text{-}Br)_3\,Mg(THF)_3$. J Organomet Chem 469:129–133

31. Wehmschulte RJ, Power PP (1995) Synthesis and characterization of the σ-bonded, quasi-linear, metal(II) diaryls $MMes*_2$ (M = Mg, Mn, Fe; Mes* = $2,4,6\text{-}t\text{-}Bu_3C_6H_2\text{-}$). Organometallics 14:3264–3267

32. Waggoner KM, Power PP (1992) Synthesis and X-ray structural characterization of Mg $(2,4,6\text{-}C6H2)(THF)2$ (R = Me, i-Pr) and the three-coordinate magnesiate species [Li(THF) $0.6(Et_2O)0.4][Mg(2,4,6\text{-}i\text{-}Pr_3C_6H_2)_3]$. Organometallics 11:3209–3214

33. Markies PR, Schat G, Akkerman OS, Bickelhaupt F, Smeets WJJ, van der Sluis P, Spek AL (1990) The coordination modes of simple diarylmagnesium species: some representative X-ray crystal structures. J Organomet Chem 393:315–331

34. Weiss E (1964) Die Kristallstruktur des Dimethylmagnesiums. J Organomet Chem 2:314–321

35. Weiss E (1965) Die Kristallstruktur des Diäthylmagnesiums. J Organomet Chem 4:101–108

36. Wehmschulte RJ, Twamley B, Khan MA (2001) Synthesis and characterization of an unsolvated dimeric diarylmagnesium compound and ist magnesium iodide byproducts. Inorg Chem 40:6004–6008

37. Parvez M, Pajerski AD, Richey HG Jr (1988) (Dioxane)dineopentylmagnesium: a polymeric structure. Acta Cryst C44:1212–1215

38. Fischer R, Walther D, Gebhardt P, Görls H (2000) Reactive intermediates of the catalytic carbomagnesiation reaction: isolation and structures of $[Cp_2ZrEt]_2(\mu\text{-ethene})$, $[Cp_2Zr(ethene)$ (L)] (L = THF, pyridine), and [(indenyl)$_2$Zr(ethene)(THF)] and of metallacycles with norbornene. Organometallics 19:2532–2540

39. Markies PR, Akkerman OS, Bickelhaupt F, Smeets WJJ, Spek AL (1994) Complexation of bis(p-tert-butylphenyl)magnesium with xylylene crown ethers and glymes. Organometallics 13:2616–2627

40. Markies PR, Nomoto T, Akkerman OS, Bickelhaupt F (1988) X-ray structure of (1,3-xylyl-18-crown-5)diphenylmagnesium: an organometallic rotaxane. J Am Chem Soc 110:4845–4846

41. Mulvey RE (2001) s-Block metal inverse crowns: synthetic and structural synergism in mixed alkali metal-magnesium (or zinc) amide chemistry. Chem Commun:1049–1056

42. Mulvey RE, Mongin F, Uchiyama M, Kondo Y (2007) Deprotonative metalation using ate compounds: synergy, synthesis, and structure building. Angew Chem Int Ed 46:3802–3824, Angew Chem 119:3876–3899

43. Yorimitsu H, Oshima K (2008) The chemistry of organomagnesium ate complexes. In: Rappoport Z, Marek I (eds) The chemistry of organomagnesium compounds (Patai Series: The chemistry of functional groups), chap 15. Wiley, Chichester, pp 681–715

44. Knochel P, Gavryushin A, Brade K (2008) Functionalized organomagnesium compounds: Synthesis and reactivity. In: Rappoport Z, Marek I (eds) The chemistry of organomagnesium compounds (Patai Series: The chemistry of functional groups), chap 12. Wiley, Chichester, pp 511–593

45. Ackermann L, Althammer A (2009) Moderne Magnesiumorganische Chemie. Chemie in unserer Zeit 43:74–83

46. Lappert MF, Power PP, Sanger AR, Srivastava RC (1980) Metal and metalloid amides, chap 3, p 45–67. Ellis Horwood, Chichester

47. Lappert M, Protchenko A, Power PP, Seeber A (2009) Metal amide chemistry, chap 3, p 39–78. Wiley, Chichester

48. Hull KL, Henderson KW (2008) Organomagnesium-group 15- and organomagnesium-group 16-bonded complexes. In: Rappoport Z, Marek I (eds) The chemistry of organomagnesium compounds (Patai Series: The chemistry of functional groups), chap 10. Wiley, Chichester, pp 403–436

49. Westerhausen M, Langer J, Krieck S, Glock C (2011) Calcium-based organometallics and superbases – alkyl-, aryl-, and amidocalcium compounds. Rev Inorg Chem 31:143–184

50. Mulvey RE (2009) Avant-garde metalating agents: structural basis of alkali-metal-mediated metalation. Acc Chem Res 42:743–755

51. Stephan DW, Erker G (2010) Frustrated Lewis pairs: metal-free hydrogen activation and more. Angew Chem Int Ed 49:46–76, Angew Chem 122:50–81

52. Jaric M, Haag BA, Unsinn A, Karaghiosoff K, Knochel P (2010) Highly selective metalations of pyridines and related heterocycles using frustrated Lewis pairs of tmp-zinc and tmp-magnesium bases with BF$_3$·OEt$_2$. Angew Chem Int Ed 49:5451–5455, Angew Chem 122:5582–5586

53. Beckmann E (1905) Einige Anwendungen von metallischem Calcium. Ber Dtsch Chem Ges 38:904–906

54. Gilman H, Schulze F (1926) Organocalcium Iodides. J Am Chem Soc 48:2463–2467

55. Bryce-Smith D, Skinner AC (1963) Organometallic compounds of Group II. Part IV. Preparation and reactions of organocalcium halides. J Chem Soc:577–585

56. Markies PR, Nomoto T, Schat G, Akkerman OS, Bickelhaupt F (1991) Unusual Metalation and Halogen-Metal Exchange Reactions between 1,3-Xylyl Crown Ethers and Organomagnesium Reagents. X-ray Structure of 2-[(*p-tert*-Butylphenyl)magnesio]-1,3-xylylene-18-crown-5. Organometallics 10:3826–3837

57. Gilman H, Kirby RH (1941) Addition Reactions of Organometallic Compounds with Conjugated Systems. J Am Chem Soc 63:2046–2048

58. Fraenkel G, Dayagi S, Kobayashi S (1968) Nuclear Magnetic Resonance and Ultraviolet Spectroscopy of Substituted Aromatic Organometallic Compounds of Lithium, Magnesium, and Calcium. J Phys Chem 72:953–961

59. Kawabata N, Matsumura A, Yamashita S (1973) Preparation of Organocalcium Halides. Tetrahedron 29:1069–1071

60. Kawabata N, Matsumura A, Yamashita S (1973) Preparation of Organocalcium Halides in Hydrocarbon Solvents. J Org Chem 38:4268–4270

61. Harvey MJ, Hanusa TP (2000) Mono(cyclopentadienyl) Complexes of Calcium, Strontium, and Barium, {[C$_5$(SiMe$_3$)$_3$H$_2$](Ca, Sr, Ba)I(thf)$_n$}$_x$. Influence of Alkali-Metal Cations on Ligand Exchange Reactions Organometallics 19:1556–1566

62. Kawabata N, Matsumura A, Yamashita S (1973) Reactions of methylcalcium iodide. J Org Chem 38:3403–3406

63. Evers J, Weiss A, Kaldis E, Muheim J (1973) Purification of calcium and barium by reactive distillation. J Less-Common Met 30:83–95

64. Kaldis E, Muheim J, Evers J, Weiss A (1973) Purification of strontium by reactive distillation. J Less-Common Met 31:169–173

65. Suslick KS (1986) Organometallic Sonochemistry. Adv Organomet Chem 25:73–119
66. Zemlyanichenko MA, Sheverdina NI, Chernoplekova VA, Kocheshkov KA (1972) Solution of organocalcium compounds of Ar_2Ca type. Zh Obshch Khim 42:841–843
67. Paleeva IE, Sheverdina NI, Kocheshkov KA (1973) Individual organocalcium compounds of Ar_2Ca type. Dokl Akad Nauk SSSR 210:1134–1135
68. Paleeva IE, Sheverdina NI, Kocheshkov KA (1974) Aromatic, Ar_2Ca-type organocalcium compounds and their complexes. Zh Obshch Khim 44:1135–1137
69. Mochida K, Ogawa H (1983) Preparation and reactions of solvent-free arylcalcium halides ArCaX (X = F, Cl, Br). J Organomet Chem 243:131–135
70. Mochida K, Yamanishi T (1987) A new method for preparation of organocalcium halides by cocondensation of calcium vapor with solvents. J Organomet Chem 332:247–252
71. Cloke FGN, Hitchcock PB, Lappert MF, Lawless GA, Royo B (1991) Lipophilic strontium and calcium alkyls, amides and phenoxides; X-ray structures of the crystalline square-planar $[\{trans\text{-}Sr(NR'_2)_2(\mu\text{-}1,4\text{-dioxane})\}_\infty]$ and tetrahedral $[CaR_2(1,4\text{-dioxane})_2]$; $R' = SiMe_3$, $R = CH(SiMe_3)_2]$. J Chem Soc, Chem Commun:724–726
72. Klabunde KJ (1975) Organic chemistry of metal vapors. Acc Chem Res 8:393–399
73. Johnson WC, Strubbs MF, Sidwell AE, Pechukas A (1939) The rate of formation and the dissociation of calcium hydride. J Am Chem Soc 61:318–329
74. Utke AR, Sanderson RT (1964) Reactions of calcium with organonitrogen compounds and aromatic hydrocarbons. J Org Chem 29:1261–1264
75. Drake SR, Otway DJ (1991) The synthesis of metal organic compounds of calcium, strontium and barium by ammonia gas-saturated ethereal solvents. J Chem Soc, Chem Commun:517–519, Erratum: Drake SR, Otway DJ (1991) Corrigendum. J Chem Soc, Chem Commun:1060
76. Fischer R, Gärtner M, Görls H, Westerhausen M (2006) Synthesis and spectroscopic properties of arylcalcium halides. Organometallics 25:3496–3500
77. Biltz W, Hüttig GF (1920) Beiträge zur systematischen Verwandtschaftslehre. XII: Über die Verbindungen von Ammoniak mit metallischem Calcium, Strontium und Barium. Z Anorg Allg Chem 114:241–265
78. Wu T-C, Xiong H, Rieke RD (1990) Organocalcium chemistry: preparation and reactions of highly reactive calcium. J Org Chem 55:5045–5051
79. Rieke RD (1989) Preparation of organometallic compounds from highly reactive metal powders. Science 246:1260–1264
80. McCormick MJ, Moon KB, Jones SR, Hanusa TP (1990) Preparation of activated calcium, strontium, and barium powders by reduction of alkaline earth di-iodides. J Chem Soc, Chem Commun:778–779
81. Fürstner A (1993) Chemistry of and with highly reactive metals. Angew Chem Int Ed 32:164–190, Angew Chem 105:171–197
82. Bogdanović B, Liao S-T, Mynott R, Schlichte K, Westeppe U (1984) Rate of formation and characterization of magnesium anthracene. Chem Ber 117:1378–1392
83. Bogdanović B, Janke N, Kinzelmann H-G, Westeppe U (1988) Neue Magnesiumanthracen-Komplexe durch Ligandenaustausch. Chem Ber 121:33–37
84. Gärtner M, Görls H, Westerhausen M (2007) Synthesis of arylcalcium halides—general procedure, scope and limitations. Synthesis:725–730
85. Glausinger WS, White TR, von Dreele RB, Gordon DA, Marzke RF, Bowman AL, Yarnell JL (1978) Structures and molecular motions in alkaline earth hexammines. Nature 271:414–417
86. Damay P, Leclercq F, Chieux P (1990) Geometry of the ND_3 group in a metallic $Ca(ND_3)_6$ compound and in solid and liquid deuteroammonia as measured by neutron scattering. Phys Rev B 41:9676–9682
87. Westerhausen M (2001) 100 Years after Grignard: Where does the organometallic chemistry of the heavy alkaline earth metals stand today? Angew Chem Int Ed 40:2975–2977, Angew Chem 113:3063–3065

88. Masthoff R, Schüler H, Krieg G (1968) Über Organometallverbindungen der II. Hauptgruppe VI Synthese und Eigenschaften von Triphenylmethylcalcium-chlorid-Donor-Akzeptor-komplexen J Organomet Chem 13:37–43

89. Westerhausen M, Gärtner M, Fischer R, Langer J (2007) Arylcalcium compounds: Syntheses, structures, physical properties, and chemical behaviour. Angew Chem Int Ed 46:1950–1956, Angew Chem 119:1994–2001

90. Westerhausen M, Gärtner M, Fischer R, Langer J, Yu L, Reiher M (2007) Heavy Grignard reagents: challenges and possibilities of aryl alkaline earth metal compounds. Chem Eur J 13:6292–6306

91. Westerhausen M (2008) Heavy Grignard reagents—synthesis and reactivity of organocalcium compounds. Coord Chem Rev 252:1516–1531

92. Westerhausen M (2009) Recent developments in organic chemistry of calcium—an element with unlimited possibilities in organometallic chemistry? Z Anorg Allg Chem 635:13–32

93. Langer J, Krieck S, Fischer R, Görls H, Westerhausen M (2010) Post-Grignard reagents: Influence of the coligands *L* on the molecular structures of phenylcalcium iodides [(*L*)$_n$Ca(*R*)I] and calcium diiodides [(*L*)$_n$CaI$_2$]. Z Anorg Allg Chem 636:1190–1198

94. Gärtner M, Görls H, Westerhausen M (2007) Heteroleptic Phenylcalcium derivatives via metathesis reaction of PhCa(thf)$_4$I with potassium compounds. Organometallics 26:1077–1083

95. Langer J, Görls H, Westerhausen M (2007) Phenylcalcium iodides with silyl substituents in para-position. Inorg Chem Commun 10:853–855

96. Fischer R, Gärtner M, Görls H, Westerhausen M (2006) Synthesis of 2,4,6-trimethylphenylcalcium iodide and degradation in THF solution. Angew Chem Int Ed 45:609–612, Angew Chem 118:624–627

97. Fischer R, Gärtner M, Görls H, Yu L, Reiher M, Westerhausen M (2007) THF solvates of extremely soluble bis(2,4,6-trimethylphenyl)calcium and tris(2,6-dimethoxyphenyl) dicalcium iodide. Angew Chem Int Ed 46:1618–1623, Angew Chem 119:1642–1647

98. Krieck S, Görls H, Westerhausen M (2010) Mechanistic elucidation of the formation of the inverse Ca(I) sandwich complex [(thf)$_3$Ca(μ-C$_6$H$_3$-1,3,5-Ph$_3$)Ca(thf)$_3$] and stability of aryl-substituted phenylcalcium complexes. J Am Chem Soc 132:12492–12501

99. Gärtner M, Görls H, Westerhausen M (2008) Synthesis and derivatization of naphthylcalcium halides as well as degradation in THF solution. J Organomet Chem 693:221–227

100. Krieck S, Görls H, Yu L, Reiher M, Westerhausen M (2009) Stable "inverse" sandwich complex with unprecedented organocalcium(I)—crystal structures of [(thf)$_2$ Mg(Br)-C$_6$H$_2$-2,4,6-Ph$_3$] and [(thf)$_3$Ca(μ-C$_6$H$_3$-1,3,5-Ph$_3$)Ca(thf)$_3$]. J Am Chem Soc 131:2977–2985

101. Bloomfield PR (1959) Improvements in or relating to the preparation of organic lithium compounds. Brit Patent 904456

102. Rieke RD, Bales SE (1973) Activated metals. The effect of added metal salts on magnesium reactivity. J Chem Soc, Chem Commun:879–880

103. Bruhat G, Thomas V (1926) The dimagnesium derivatives of benzene. Compt rend 183:297–299

104. Langer J, Görls H, Westerhausen M (2010) Stability and reactivity of phenylstrontium compounds in solution. Organometallics 29:2034–2039

105. Langer J, Gärtner M, Fischer R, Görls H, Westerhausen M (2007) Reinvestigation of the reaction of strontium and barium with iodobenzene and molecular structure of the heavy Grignard reagent [((thf)$_2$BaPh$_2$)$_4$·(thf)BaO] with an oxygen-centered square Ba$_5$ pyramid. Inorg Chem Commun 10:1001–1004

106. Langer J, Krieck S, Görls H, Westerhausen M (2009) An efficient general synthesis of halide-free diarylcalcium. Angew Chem Int Ed 48:5741–5744, Angew Chem 121:5851–5854

107. Hauber S-O, Lissner F, Deacon GB, Niemeyer M (2005) Stabilization of aryl–calcium, –strontium, and –barium compounds by designed steric and π-bonding encapsulation. Angew Chem Int Ed 44:5871–5875, Angew Chem 117: 6021–6025

108. Fischer R, Görls H, Westerhausen M (2007) Syntheses and structure of the solvent-separated calcium cuprate [(thf)$_3$Ca(μ-Ph)$_3$Ca(thf)$_3$]$^+$ [Ph-Cu-Ph]$^-$. Organometallics 26:3269–3271

109. Langer J, Krieck S, Görls H, Kreisel G, Seidel W, Westerhausen M (2010) Organic heterobi-metallic complexes of the alkaline-earth metals (Ae = Ca, Sr, Ba) with tetrahedral metallate anions of three-valent metals (M = B, Al, Ga, and V). New J Chem 34:1667–1677

110. Krieck S, Görls H, Westerhausen M (2010) Structural diversity of calcium cuprates via addition and transmetalation reactions of mesity copper(I). Chem Asian J 5:272–277

111. Harder S, Müller S, Hübner E (2004) Syntheses and crystal structures of simple dibenzylcalcium complexes: useful reagents in the preparation of calcium compounds. Organometallics 23:178–183

112. Ruspic C, Harder S (2005) Synthesis and structure of an arylcalcium compound with an unusual calcium tetrahedron containing an encapsulated oxide. Organometallics 24:5506–5508

113. Fischer R, Langer J, Krieck S, Görls H, Westerhausen M (2011) Coordination behaviour of calcocene and its use as a synthon for heteroleptic organocalcium compounds. Organometallics 30:1359–1365

114. Gowenlock BG, Lindsell WE (1977) The organometallic chemistry of the alkaline-earth metals. J Organomet Chem Libr, Organomet Chem Rev 3:1–73

115. Lindsell WE (1982) Calcium, strontium and barium. In: Wilkinson G, Stone FGA, Abel EW (eds) Comprehensive organometallic chemistry—the synthesis, reactions and structures of organometallic compounds, vol 1. Pergamon Press, New York, NY, pp 237–252, Chap. 4.2.4

116. Reich HJ, Green DP, Medina MA, Goldenberg WS, Gudmundsson BÖ, Dykstra RR, Phillips NH (1998) Aggregation and reactivity of phenyllithium solutions. J Am Chem Soc 120:7201–7210

117. Hesse M, Meier H, Zech B (2005) Spektroskpische Methoden in der organischen Chemie. Thieme, Stuttgart

118. Gärtner M, Fischer R, Langer J, Görls H, Walther D, Westerhausen M (2007) Syntheses and structures of alkaline-earth metal bis(diphenylamides). Inorg Chem 46:5118–5124

119. Gillespie RJ, Silvi B (2002) The octet rule and hypervalence: two misunderstood concepts. Coord Chem Rev 233–234:53–62

120. Gillespie RJ (1992) The VSEPR model revisited. Chem Soc Rev 21:59–69

121. Gillespie RJ (2008) Fifty years of the VSEPR model. Coord Chem Rev 252:1315–1327, and literature cited therein

122. Viebrock H, Behrens U, Weiss E (1994) A novel organomagnesium compound consisting of two triple-decker cations [LMg(μ-Me)$_3$MgL]$^+$ and an octamethyltrimagnesate anion: [{Me$_2$Mg(μ-Me)$_2$}$_2$Mg]$^{2-}$. Angew Chem Int Ed Engl 33:1257–1259, Angew Chem 106:1364–1365

123. Krieck S, Görls H, Westerhausen M (2010) Synthesis and characterization of rare examples of stable potassium and arylcalcium triethylboranate complexes. Inorg Chem Commun 13:1466–1469

124. Dell'Amico DB, Bradicich C, Labella L, Marchetti F (2006) Complexes of calcium halides with 1,2-dimethoxyethane (DME). Inorg Chim Acta 359:1659–1665

125. Henderson KW, Rood JA, Noll BC (2005) A low-temperature investigation of *trans*-diiodo-tetrakis(tetrahydrofuran)calcium(II). Acta Cryst E61:m2006–m2007

126. Gärtner M, Görls H, Westerhausen M (2007) *trans*-Bis(1,2-dimethoxyethane-$\kappa^2 O$:O')diiodo (tetrahydrofuran-κO)calcium(II). Acta Cryst E63:m3169

127. Eaborn C, Hawkes SA, Hitchcock PB, Smith JD (1997) The first structurally characterized solvent-free σ-bonded diorganocalcium, Ca[C(SiMe$_3$)$_3$]$_2$. Chem Commun:1961–1962

128. Crimmin MR, Barrett AGM, Hill MS, MacDougall DJ, Mahon MF, Procopiou PA (2008) Bis (trimethylsilyl)methyl derivatives of calcium, strontium and barium: Potentially useful dialkyls of the heavy alkaline-earth elements. Chem Eur J 14:11292–11295

129. Orzechowski L, Harder S (2007) Isolation of an intermediate in the catalytic trimerization of isocyanates by a monomeric calcium carbine with chelating iminophosphorane substituents. Organometallics 26:2144–2148

130. Kottke T, Stalke D (1993) Crystal handling at low temperatures. J Appl Cryst 26:615–619

131. Stalke D (1998) Cryo crystal structure determination and application to intermediates. Chem Soc Rev 27:171–178
132. Harder S (2010) From Limestone to Catalysis: Application of Calcium Compounds as Homogeneous Catalysts. Chem Rev 110:3852–3876
133. Barrett AGM, Crimmin MR, Hill MS, Procopiou PA (2010) Heterofunctionalization Catalysis with Organometallic Compounds of Calcium, Strontium and Barium. Proc R Soc 466:927–963
134. Westerhausen M (2006) Recent developments in the field of organic heterobimetallic compounds of the alkaline-earth metals. Dalton Trans:4755–4768
135. Krieck S, Görls H, Westerhausen M (2008) Synthesis and properties of calcium tetraorganylalanates with [Me$_{4-n}$AlPh$_n$]$^-$ anions. Organometallics 27:5052–5057
136. Billups WE, Konarski MM, Hauge RH, Margrave JL (1980) Carbon-carbon bond formation in the reaction of calcium atoms with ethers. J Am Chem Soc 102:3649–3650
137. Maercker A (1987) Ether cleavage with organo-alkali-metal compounds and alkali metals. Angew Chem Int Ed Engl 26:972–989, Angew Chem 99:1002–1019
138. Stanetty P, Mihovilovic MD (1997) Half-lives of organolithium reagents in common etheral solvents. J Org Chem 62:1514–1515
139. Fischer R, Görls H, Westerhausen M (2005) Reinvestigation of the synthesis of phenylcalcium iodide and the first structural characterization of a heavy Grignard reagent as [((thf)$_2$CaPhI)$_3$·(thf)CaO] with a central Ca$_4$ tetrahedron. Inorg Chem Commun 8:1159–1161
140. Krieck S, Görls H, Westerhausen M (2009) Reactivity studies of phenylcalcium iodide towards THF yielding phenyl-free cage compounds—crystal structures of [{(thf)Ca(O-CH=CH$_2$)$_2$}$_4$·CaO·CaI$_2$] and [(CaO)$_4$·4(thf)$_3$CaI$_2$]. J Organomet Chem 694:2204–2209
141. Westerhausen M, Schwarz W (1992) Calcium-bis[N, N'-bis(trimethylsilyl)benzamidinat]-THF (1/2)—Synthese, specktroskopische Charakterisierung und Struktur. Z Naturforsch 47b:453–459
142. Setzer WN, Schleyer PvR (1985) X-ray structural analyses of organolithium compounds. Adv Organomet Chem 24:353–451
143. Weiss E (1993) Structures of organo alkali metal complexes and related compounds. Angew Chem Int Ed Engl 32:1501–1523, Angew Chem 105:1565–1587
144. Stey T, Stalke D (2004) Lead structures in lithium organic chemistry. In: Rappoport Z, Marek I (eds) The chemistry of organolithium compounds (Patai Series: The Chemistry of functional groups), chap 2. Wiley, Chichester, pp 47–120
145. Gessner VH, Däschlein C, Strohmann C (2009) Structure formation principles and reactivity of organolithium compounds. Chem Eur J 15:3320–3334
146. Ritter SK (2011) Calcium's awakening. Chem Eng News 89(10):49–51
147. Green SP, Jones C, Stasch A (2007) Stable magnesium(I) compounds with Mg–Mg bonds. Science 318:1754–1757
148. Stach A, Jones C (2011) Dalton Trans 40:5659–5672
149. Westerhausen M (2008) Molecular magnesium(I) compounds—from curiosity to kudos. Angew Chem Int Ed 47:2185–2187, Angew Chem 120:2215–2217
150. Krieck S, Westerhausen M (2009) Subvalenz bei elektropositiven s-Block-Metallen. Chem in unserer Z 43:384–390
151. Krieck S, Yu L, Reiher M, Westerhausen M (2010) Subvalent organometallic compounds of the alkaline-earth metals in low oxidation states. Eur J Inorg Chem:197–216
152. Jutzi P (1986) π-Bonding to main group elements. Adv Organomet Chem 26:217–295
153. Jutzi P (1990) Cyclopentadienyl complexes with main group elements as central atoms—a decade of research. J Organomet Chem 400:1–17
154. Hanusa TP (1990) New developments in the organometallic chemistry of calcium, strontium and barium. Polyhedron 9:1345–1362
155. Hanusa TP (1993) Ligand influences on structure and reactivity in organoalkaline-earth chemistry. Chem Rev 93:1023–1036

156. Burkey DJ, Hanusa TP (1995) Structural lessons from main-group metallocenes. Comments Inorg Chem 17:41–77
157. Hays ML, Hanusa TP (1996) Substituent effects as probes of structure and bonding in mononuclear metallocenes. Adv Organomet Chem 40:117–170
158. Jutzi P, Burford N (1999) Structurally diverse π-cyclopentadienyl complexes of the main group elements. Chem Rev 99:969–990
159. Hanusa TP (2002) New developments in the cyclopentadienyl chemistry of the alkaline-earth metals. Organometallics 21:2559–2571
160. Burkey DJ, Hanusa TP (1996) Synthesis and solution behavior of (tetraisopropylcyclopentadienyl)calcium acetylide complexes. Molecular structure of $\{[(C_3H_7)_4C_5H]Ca(\mu-C{\equiv}CPh)(thf)\}_2$. Organometallics 15:4971–4976
161. Green DC, Englich U, Ruhlandt-Senge K (1999) Calcium, strontium, and barium acetylides—new evidence for bending in the structures of heavy alkaline-earth metal derivatives. Angew Chem Int Ed 38:354–357, Angew Chem 111:365–367
162. Barrett AGM, Crimmin MR, Hill MS, Hitchcock PB, Lomas SL, Mahon MF, Procopiou PA, Suntharalingam K (2008) β-Diketiminato calcium acetylides: synthesis, solution dimerization, and catalytic carbon-carbon bond formation. Organometallics 27:6300–6306
163. Feil F, Harder S (2000) α, α-Bis(trimethylsilyl)-substituted benzyl complexes of potassium and calcium. Organometallics 19:5010–5015
164. Harder S, Feil F, Weeber A (2001) Structure of a benzylcalcium diastereomer: an initiator for the anionic polymerization of styrene. Organometallics 20:1044–1046
165. Feil F, Müller C, Harder S (2003) α-Methyl-benzylcalcium complexes: syntheses, structures and reactivity. J Organomet Chem 683:56–63
166. Guino-o MA, Campana CF, Ruhlandt-Senge K (2008) A unique heterobimetallic benzyl calciate - an organometallic mixed-metal species involving a heavy alkaline-earth metal. Chem Commun:1692–1694

Stable Molecular Magnesium(I) Dimers: A Fundamentally Appealing Yet Synthetically Versatile Compound Class

Cameron Jones and Andreas Stasch

Abstract The chemistry of the group 2 metals (alkaline-earth metals) is dominated by the +2 oxidation state. In 2007, we reported the first examples of magnesium(I) dimers which are stable at ambient temperature. Since that time a number of other examples have come forward and their fundamental and applied chemistry has rapidly emerged. All of these complexes feature "deformable" covalent Mg–Mg single bonds, and are kinetically stabilised towards disproportionation processes by the incorporation of sterically bulky, anionic or dianionic, chelating N-donor ligands. The high reactivity of magnesium(I) dimers has led to their use as specialist reagents in organic and organometallic/inorganic synthesis. They have proved especially useful as hydrocarbon soluble, stoichiometric, selective, and safe reducing agents in these areas. This chapter focuses on stable molecular compounds of the general type LMgMgL (L = anionic ligand), paying attention to their synthesis, structure, bonding, theoretical and spectroscopic analysis, as well as their further chemistry.

Contents

C. Jones (✉) and A. Stasch (✉)
School of Chemistry, Monash University, PO Box 23, Melbourne, VIC 3800, Australia
e-mail: cameron.jones@monash.edu; andreas.stasch@monash.edu

1 Introduction

The study of metal–metal bonded molecular complexes has fascinated scientists for many decades. Their investigations have afforded chemists a greater understanding of the nature of metal–metal bonds, which rarely mirrors the classical situation in single and multiple bonded organic compounds. This knowledge has, in turn, allowed metal–metal bonded complexes to find an array of applications in areas as varied as catalysis, materials chemistry, and bio-inorganic chemistry [1]. Much of the increased interest in metal–metal bonded complexes that we have witnessed over the past 50 years stems from Cotton's landmark preparation of $K_2[Re_2Cl_8]\cdot2H_2O$, the dianion of which contained the first recognised quadruple bond between two elements [2]. Since that report, there have been numerous breakthroughs in d-block metal–metal bonding. Two of the most spectacular recent examples are Power's Cr–Cr quintuply bonded compound, Ar*CrCrAr* (Ar* = bulky terphenyl) [3], and Carmona's zinc(I) dimer, Cp*ZnZnCp* (Cp* = C_5Me_5) [4].

Perhaps surprisingly, although crystallographically authenticated compounds containing unsupported p-block metal–metal bonds have been known for more than 50 years, it has only been relatively recently that their chemistry has flourished. This is in large part due to major advances in compounds containing multiple bonds between two group 13 or group 14 metals [5]. The most archetypal of these are the heavier group 14 alkyne analogues, REER (E = Si, Ge, Sn, or Pb; R = bulky substituent) [6, 7], first prepared by the groups of Power [8, 9], Sekiguchi [10], and Wiberg [11]. Unlike alkynes, these compounds all possess *trans*-bent structures and E–E bond orders ranging from near 3 (E = Si) to 1 (E = Pb). The development of new, and often controversial, "non-classical" bonding models has been required to describe the unusual bonding in these systems. As a result of these analyses, it is now clear that the frontier electronic configurations of such compounds can in some ways mimic those of transition metal complexes. Accordingly, there is currently a competitive drive to develop the "transition metal-like" chemistry of cheap and non-toxic low oxidation state p-block complexes in many areas of synthesis, small molecule activations and catalysis [12–14].

Although unsupported metal–metal bonds between two f-block elements are unknown in molecular complexes, rapid progress has been made over the last decade in developing the chemistry of compounds containing unsupported bonds between an f-block metal and a d- or p-block metal. Many such complexes are now known, and the area has been reviewed [15]. This fascinating field will no doubt offer many surprises in coming years, one example of which that has recently been realised is the first identification of weak Ga–U π-bonding in a molecular complex [16].

What of metal–metal bonding between two s-block elements? Until late 2007 there were no structurally authenticated examples of such compounds that were stable at anywhere near ambient temperature. That said, a number of dimeric systems, e.g. HMgMgH [17, 18] and ClMgMgCl [19], had been prepared and studied in inert gas matrices at very low temperatures (ca. 10 K, see Sect 1.1). In addition, a variety of theoretical studies suggested that while the M–M bonds in compounds of the type, RMMR (R = anionic ligand, M = group 2 metal), are not robust, they should perhaps be sufficiently strong (especially for M = Be or Mg) for such compounds to exist at ambient temperature (see Sect. 2.3), but only if considerable kinetic protection is afforded to the MM fragment by sterically bulky ligands (R) [17–46]. Moreover, given the well-known chemical similarities between magnesium and zinc, another hint that magnesium(I) dimers, in particular, might be accessible was the stability of Carmona's zinc(I) dimer, Cp*ZnZnCp* [4], and a series of subsequently reported zinc–zinc bonded systems [47, 48]. All of these facts, combined with the prior preparation of stable systems bearing unsupported bonds between magnesium and other electropositive metals, e.g. Ga [49, 50], prompted us to commence a study to investigate the preparation of the first stable magnesium(I) dimers.

This chapter will chart the development of the chemistry of magnesium(I) dimers, and related compounds, since they were first reported by us in late 2007 [27]. It will summarise the stabilisation strategies that allowed their eventual synthesis, their physical properties, structure, bonding, and their remarkable reactivity. This latter feature of magnesium(I) dimers will be given particular attention as it has rapidly emerged over the past 3 years, and highlights the significant potential these compounds have as reagents for organic and inorganic synthetic chemists. As molecular compounds bearing Mg–Mg covalent bonds must, by definition, contain the metal in the formal oxidation state of +1 or 0, a brief general overview of the sparse low oxidation state chemistry of the group 2 metals will be given at the outset of this chapter. It should be noted that aspects of the chemistry of stable magnesium(I) dimers have been covered in several recent review articles [20–22, 51, 52].

1.1 Low Oxidation State Chemistry of the Group 2 Metals: A Brief Overview

The low oxidation state chemistry of the s-block elements is the least developed of all the metals in the periodic table. This is not surprising as these elemental metals are easily oxidised, have low electronegativities, and normally form redox inert ionic compounds with the metal having a stable noble gas electronic configuration (M^+ for group 1 and M^{2+} for group 2 metals). Indeed, for all of the group 2 elements, the disproportionation of their M^+ ions to the elemental metal and M^{2+} ions is highly exothermic [53]. That said, some progress has been made towards accessing low oxidation state group 2 metal compounds and materials (other than magnesium(I) dimers) [20–22]. A brief summary is given below.

As is the case for all of the alkali metals, it has been known for some time that the heavier group 2 metals, Ca, Sr, and Ba, can be dissolved in liquid ammonia to give intensely blue-coloured solutions which contain solvated electrons [54–56]. From these, the hexa-ammine complexes of the formally zero-valent metals, $[M(NH_3)_6]$, have been isolated and the structure of the calcium complex has been determined from neutron scattering experiments [57–59]. The well-known propensity of the alkali metals to form related crystalline electrides, $[M(L)_n]^+(e^-)$, and alkalides, $[M(L)_n]^+[M']^-$ (M, M' = alkali metal) [60, 61], is not shared by the group 2 metals to any great extent. That said, inorganic electrides containing group 2 metal ions have been reported, e.g. the thermally stable and electrically conducting material, $[Ca_{24}Al_{28}O_{64}]^{4+}(4e^-)$ [62, 63].

A number of other inorganic solids can be considered as containing sub-valent group 2 metal centres. These include various sub-nitrides of the heavier group 2 elements [64], and a variety of ternary hydrides such as Mg_4IrH_5 [65] and Mg_3RuH_3 [66]. The latter have in common very short Mg–Mg interactions in the solid state, e.g. 2.754 Å for Mg_4IrH_5, and can be formulated as containing $[Mg–Mg]^{2+}$ dications, e.g. $[Mg_2]^{2+}_2[IrH_3]^{2-}[H]^-_2$ for Mg_4IrH_5. Similarly, it has been proposed that the superconducting properties of MgB_2 can be partly attributed to the formation of $[Mg_2]^{2+}$ ions in the solid state (Mg–Mg distance: 3.083 Å) [67]. For the sake of comparison, calculations on the $[Mg_2]^{2+}$ ion indicate that it should be a relatively long-lived, metastable species in the gas phase, with a singlet ground state, $^1\Sigma_g^+$, and a Mg–Mg distance of 2.89 Å [23]. This seems to be corroborated by the mass spectrometric detection of experimentally generated $[Mg_2]^{2+}$ and $[Mg_3]^{2+}$ ions in the gas phase [68].

Simple molecular compounds containing Mg–Mg bonds have been prepared and studied, but these only exist for extended periods at extremely low temperatures. For example, the parent magnesium(I) dimer, HMgMgH, has been generated from the reaction of laser-ablated magnesium atoms with dihydrogen, and trapped in solid noble gas or hydrogen matrices at temperatures of 10 K or less [17, 18]. IR spectroscopic analyses of the matrices revealed that monomeric ·MgH was also trapped during the experiments. Similarly, the products obtained from the reaction of solid MgB_2 with HCl gas at 700 K were trapped in an inert gas matrix at 10 K and found to include ClMgMgCl and ·MgCl by IR and Raman spectroscopy, in combination with DFT calculations [19]. In this study attempts were made to synthesise more stable magnesium(I) species, Cp*MgMgCp* and BrMgMgBr, which although stable to some extent in solution decomposed to Mg metal above −60 °C. In addition to matrix isolation studies, magnesium(I) radicals, ·MgX (X = halide) and ·Mg–CH_3, have been studied in the gas phase by a range of spectroscopic methods, including millimetre and submillimetre wave spectroscopy, and fluorescence spectroscopy [69]. Related radicals such as ·MgNC and possibly others, e.g. ·MgCCH and ·MgCCCN, have been detected at the extremely low temperatures and pressures that are prevalent in interstellar clouds [70].
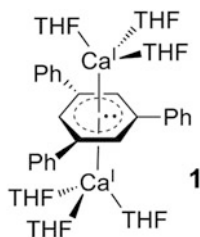
Fig. 1 The calcium(I) inverse sandwich complex, **1**

One other area where Mg–Mg bonded species have been proposed to exist is in the formation of Grignard reagents RMgX (R = monoanionic organic substituent, X = halide) [71, 72]. Despite the huge synthetic importance of these compounds, the mechanism of their formation from the reaction of elemental magnesium and organo-halides, RX, is still unknown. It has, however, been suggested that this proceeds via Mg^I intermediates, e.g. RMgMgX. Theoretical studies have provided some credence to this proposal with the conclusion that the insertion of a Mg atom into RMgX molecules is generally slightly exothermic [24–26]. In related work, Grignard-like reagents, e.g. PhMg$_4$F, have been obtained from metal vapour syntheses and were claimed to be stable in solution under ambient conditions. MALDI-TOF mass spectrometric and hydrolysis experiments were used to formulate these compounds [73–75].

Other than the magnesium(I) dimers described in the following sections, the only other well-defined alkaline-earth metal(I) species to be reported to date is the remarkable calcium(I) compound, [{(THF)$_3$Ca}$_2$C$_6$H$_3$Ph$_3$-1,3,5] **1** (Fig. 1) [76]. This black, pyrophoric, crystalline solid was prepared from the reaction of 1,3,5-triphenylbenzene with activated calcium in THF, in the presence of a catalytic amount of 1-bromo-2,4,6-triphenylbenzene. The energetic states of the extended π-system of the arene ligand lie between the first and second ionisation energy of the metal, leading to "incomplete" oxidation of the metal and its stabilisation by the reducing ligand system. Further studies implied that the mechanism of the reaction involves a salt comprising a doubly deprotonated triphenylbenzene calcium cation, and a triphenylbenzene radical anion, [{(THF)$_3$Ca}$_2${μ-C$_6$H$_2$-(C$_6$H$_4$)Ph$_2$}(μ-O-CH=CH$_2$)][C$_6$H$_3$Ph$_3$]. This compound was crystallographically characterised, and it is believed that its formation involves proton transfer from, and degradation of the reaction solvent, THF [77, 78]. It was shown by X-ray crystallography, EPR spectroscopy, and DFT calculations that **1** is paramagnetic with a triplet state, $S = 1$, with two unpaired electrons delocalised over the organic ligand. Moreover, DFT calculations highlighted significant d-orbital electronic contribution from each Ca^I centre, which is delocalised over the dianionic ligand fragment of the complex. The C–C bonds in the central ring are elongated to 1.464 Å and the bonds to the three Ph groups are shortened to 1.435 Å, while the Ca$\cdots$Ca separation in the complex is 4.28 Å.
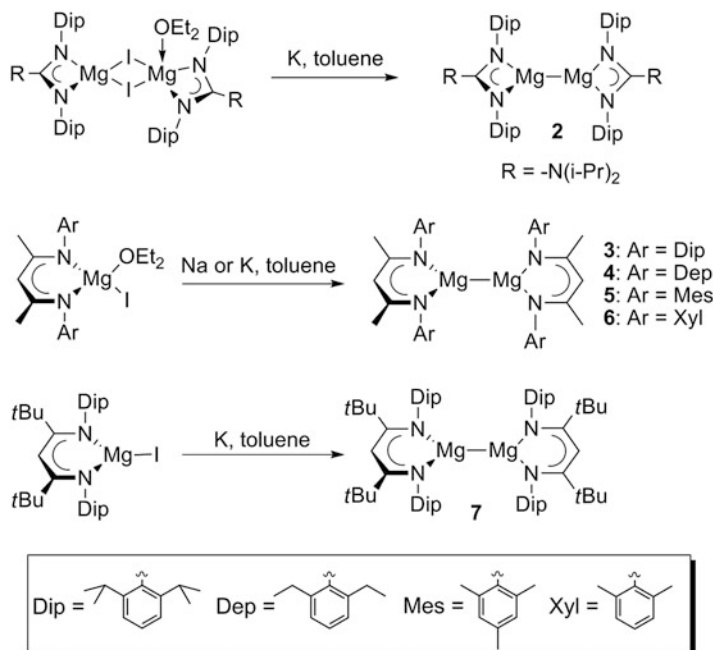
2 Stable Magnesium(I) Dimers

2.1 Synthesis, Stability and Physical Properties

A variety of quantum chemical calculations on magnesium(I) dimers (see Sect. 2.3) have predicted significant Mg–Mg bond dissociation energies (BDEs) of around 45–50 kcal/mol. This, combined with the emerging chemistry of related, kinetically stabilised zinc(I) dimers, prompted us to explore the possibility of preparing ambient stable magnesium(I) compounds for the first time. It was clear at the outset of this study that sterically bulky ligands would be required to achieve this goal. Moreover, it seemed likely that bi- or higher dentate ligands would be necessary to electronically satisfy the Mg centres in the target dimers, and to provide further stabilisation through the chelate effect. This proposal was later borne out by computational studies [19].

In our laboratories we have developed a range of extremely bulky guanidinate ligands, $[(DipN)_2CNR_2]^-$ (Dip = 2,6-diisopropylphenyl; -NR$_2$ = bulky amino group) [52], which we have utilised to kinetically stabilise a variety of highly reactive complexes with p- or d-block metal centres in the +1 oxidation state [79–87]. In addition, we have exploited the steric bulk of these guanidinates to stabilise the first square planar lanthanide(II) systems [88, 89], and several heteroleptic zinc(II) halide complexes [90]. Throughout this study the coordinating and stabilising properties of these guanidinates have been shown to more closely resemble those of bulky β-diketiminates, e.g. $[(DipNCR)_2CH]^-$ (R = alkyl) [14, 91], than less bulky guanidinate (or amidinate) ligands [92]. Given the wide application of β-diketiminates (Nacnacs) to the stabilisation of low oxidation state compounds involving metals from across the periodic table, both ligand classes were seen as ideal candidates for the preparation of stable low oxidation state magnesium complexes.

The first success in this study came with the preparation of the colourless dimeric magnesium(I) compound, $[\{(Priso)Mg\}_2]$ **2**, (Priso = $[(DipN)_2CN(i\text{-}Pr)_2]^-$) and the closely related yellow β-diketiminato coordinated system, $[\{(^{Dip}Nacnac)Mg\}_2]$ **3** ($^{Dip}Nacnac = [(DipNCMe)_2CH]^-$), in 2007 (Scheme 1) [27]. These compounds were readily accessed by the reduction of heteroleptic magnesium(II) iodide precursor complexes with an excess of potassium metal in toluene at room temperature. The guanidinato and β-diketiminato magnesium(II) iodide precursor complexes can be easily prepared by reaction of the protonated ligands (PrisoH and ^{Dip}NacnacH) with methyl magnesium iodide in diethyl ether. Similar moderately yielding reductions carried out with either sodium or potassium metal have subsequently been shown to afford a range of magnesium(I) compounds, **4–7**, incorporating β-diketiminato ligands of varying steric bulk, but always having substituted phenyl groups at their N-centres [28, 51]. In all cases, the compounds are remarkably stable towards disproportionation processes (not decomposing until >300 °C in the case of **3**), though they display varying degrees of air and moisture sensitivity, which is generally inversely proportional to the steric bulk of
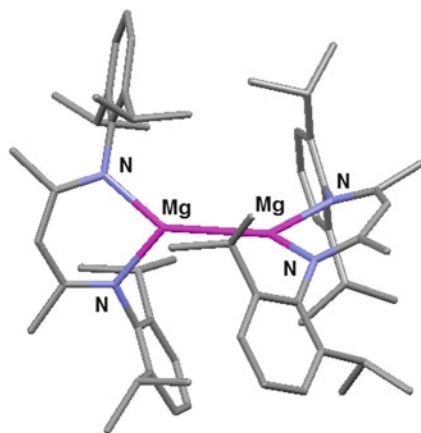
Scheme 1 Preparation of the magnesium(I) dimers, **2–7**

the Nacnac ligand involved. In contrast, reduction of the phenyl substituted β-diketiminate, [(^{Ph}Nacnac)MgI(OEt$_2$)] (^{Ph}Nacnac = [(PhNCMe)$_2$CH]$^-$), did not lead to a magnesium(I) dimer, but instead afforded the homoleptic magnesium(II) complex, [(^{Ph}Nacnac)$_2$Mg] [28]. This outcome suggests that ^{Ph}Nacnac is not of sufficient steric bulk to stabilise Mg^I centres towards disproportionation processes. It should also be noted that attempts to extend the chemistry of Mg^I dimers to the preparation of stable Be–Be and Ca–Ca bonded complexes have so far been unsuccessful. These attempts include the alkali metal reductions of [(^{Mes}Nacnac)BeI] and [(^{Dip}Nacnac)CaI(OEt$_2$)] which both yielded complex product mixtures [28].

Efforts have been made to prepare "mixed Nacnac" Mg^I dimers via the alkali metal co-reductions of 50:50 mixtures of two different Mg^{II} iodide precursor complexes. Such reactions generally led to product mixtures, and no evidence for the preparation of the target products has yet been forthcoming. On one occasion, however, the potassium reduction of [(^{Dip}Nacnac)MgI(OEt$_2$)] and [(^{Mes}Nacnac)MgI (OEt$_2$)] afforded the mixed ligand hydride/iodide bridged product, [(^{Dipp}Nacnac) Mg(μ-H)(μ-I)Mg(^{Mes}Nacnac)], in very low yield [28]. It was presumed that the hydride ligand originated from a solvent abstraction process. This result prompted us to re-examine the potassium reduction of [(^{Dip}Nacnac)MgI(OEt$_2$)], for the presence of hydride containing products. An NMR spectroscopic analysis of the total reaction mixture revealed that, in addition to the major product **3**, ca. 15 % of the mixture comprised the Mg^{II} hydride species, [{(^{Dip}Nacnac)Mg(μ-H)}$_2$], while

Scheme 2 Preparation of the magnesium(I) dimers, **8–14**

another magnesium hydride complex, presumably [(^{Dip}Nacnac)Mg(μ-H)(μ-I)Mg (^{Dip}Nacnac)], was also present [28]. This raised the question as to whether [{(^{Dip}Nacnac)Mg(μ-H)}$_2$] could lie on one reaction pathway to **3**. This was later seemingly confirmed by the direct reduction of pure [{(^{Dip}Nacnac)Mg(μ-H)}$_2$] with potassium, which gave **3**, albeit in low yield [31]. Related to this reduction is the observation by Harder et al. that heating a magnesium hydride cluster stabilised by a bis(β-diketiminate) ligand, [(para)$_3$Mg$_8$H$_{10}$] (para = [{(DipNCMe)CH (MeCN)}$_2$(μ-C$_6$H$_4$-1,6)]$^{2-}$), to 200 °C led to elimination of 5 equivalents of H$_2$ and generation of a red solid. It was suggested that this solid could be a mixed valence magnesium cluster, [(para)$_3$ Mg$_8$], though this has not been confirmed experimentally [93].

The β-diketiminato magnesium(I) dimers, **3** and **5**, have been shown to form dark orange to red adducts, **8–13**, with the Lewis bases THF, 1,4-dioxane (dioxane), 4-dimethylaminopyridine (DMAP), or 4-t-butylpyridine (tBuPy) (Scheme 2) [28, 30]. Interestingly, there is no evidence for the reduction of the pyridine ligands in **10** and **11**, and therefore all of the 4-coordinate adducts are magnesium(I) dimers in their own right. Their formation can be compared to the treatment of the zinc(I) dimer, Cp*ZnZnCp*, with DMAP, which contrastingly leads to the unsymmetrical adduct, [(η^5-Cp*)ZnZn(η^1-Cp*)(DMAP)$_2$], in which both DMAP ligands coordinate one Zn centre with concomitant "ring-slippage" of its attendant Cp* ligand [94]. While the pyridine adducts, **10** and **11**, are thermally very robust, the adducts incorporating the weaker Lewis bases, THF and dioxane, viz. **8**, **9**, and **12**, are less so. In fact, the coordination of the ether molecules can be readily reversed when crystals of the adducts are placed under vacuum, heated under a dinitrogen atmosphere, or dissolved in aromatic solvents such as benzene or toluene. It is of note that the very bulky dimer, **7**, does not form adducts with any of the Lewis bases

Fig. 2 The molecular structure of [{(^{Dip}Nacnac)Mg}$_2$] **3**

mentioned here, presumably because its sterically hindered Mg centres prevent it from doing so.

The only other ambient stable low oxidation state magnesium compound to be reported outside our group is the dianionic magnesium(I) dimer, **14**, which was prepared in "one pot" by the potassium reduction of the α-diimine, ^{MeDip}DAB (^{MeDip}DAB = (DipNCMe)$_2$), in the presence of MgCl$_2$ in THF (Scheme 2) [29]. The pink product, **14**, features a central Mg$_2$$^{2+}$ cation coordinated by two doubly reduced diazabutenediide ligands, ^{MeDip}DAB^{2-}, which have π-interactions with two [K(THF)$_3$]$^+$ counterions. Unlike the neutral dimers, **3** and **5**, the magnesium centres of compound **14** are resistant to coordination by THF.

2.2 Structural Properties

The three-coordinate magnesium(I) dimers, **2**–**7**, possess unsupported Mg–Mg bonds and essentially planar Mg coordination environments (see, for example, Fig. 2). The Mg–Mg distances in the neutral compounds range from 2.808(1) Å for **5** [28] to 2.875(1) Å for **4** [51], and there is little correlation between the bond length and the steric bulk of the Nacnac ligand involved (see Table 1). As might be expected the Mg–Mg distance in the dianionic complex, **14** 2.937(2) Å [29], is significantly greater than in the neutral species. The bond distances for the compounds are comparable with the sum of two covalent radii for magnesium (2.82 Å) [96, 97], but are significantly shorter than the Mg–Mg distances in diatomic (3.89 Å) [98] or elemental (3.20 Å) magnesium [99].

All of the guanidinate and β-diketiminate compounds exhibit significant delocalisation over their ligand backbones, though there is considerable variation in the relative orientation of the two Mg heterocycles within the series. This is most probably due to a low barrier to rotation around the Mg–Mg bonds, and probably reflects the sterics of the ligand involved and/or crystal packing forces. The two Mg

Table 1 Selected crystallographic and physical data for dimeric magnesium(I) compounds

Compound	Mg–Mg[a] distance/Å	Mg–N$_{ligand}$[a] distance/Å	Mg–X$_{donor}$[a] distance/Å	CN$_{Mg}$	M.P.[b]/C	Colour	References
[{(Priso)Mg}₂] **2**	2.8508(12)	2.0736(10)	–	3	170–173	Colourless	[27]
[{(^{Dip}Nacnac)Mg}₂] **3**	2.8457(8)	2.060	–	3	301–303	Yellow	[27]
[{(^{Dip}Nacnac)Mg}₂] **3**[c]	2.8624(15)	2.065	–	3	301–303	Yellow	[30]
[{(^{Dip}Nacnac)Mg}₂] **3**[d]	2.8456(2)	2.065	–	3	301–303	Yellow	[95]
[{(^{Dep}Nacnac)Mg}₂] **4**	2.8752(12)	2.058	–	3	121–124[e]	Yellow	[51]
[{(^{Mes}Nacnac)Mg}₂] **5**	2.808(1)	2.038	–	3	201–203	Yellow	[28]
[{(^{Mes}Nacnac)Mg}₂] **5**[f]	2.81(2)	2.043	–	3	201–203	Yellow	[28]
[{(^{Xyl}Nacnac)Mg}₂] **6**	2.8212(11)	2.042	–	3	180–181	Yellow	[51]
[{(^{tBu}Nacnac)Mg}₂] **7**	2.847(2)	2.073	–	3	278–280	Orange	[28]
[{(^{Dip}Nacnac)Mg(THF)}₂] **8**	3.0560(12)	2.159	2.1733(13)	4	68–71	Red-orange	[30]
[{(^{Dip}Nacnac)Mg(Dioxane)}₂] **9**	3.1499(18)	2.152	2.2438(18)	4	59–62	Orange	[30]
[{(^{Dip}Nacnac)Mg(DMAP)}₂] **10**	3.1962(14)	2.178	2.2353(18)	4	159–160	Red-brown	[30]
[{(^{Dip}Nacnac)Mg(tBuPy)}₂] **11**	3.1260(15)	2.162	2.2257(18)	4	248–250	Red-brown	[30]
[{(^{Mes}Nacnac)Mg(THF)}₂] **12**[g]	ca. 2.89	ca. 2.11	ca. 2.17	4	86–89	Red	[28]
[{(^{Mes}Nacnac)Mg(DMAP)}₂] **13**	2.937(1)	2.125	2.206	4	142–143	Red-brown	[28]
[{K(THF)₃}{(^{MeDip}DAB)Mg}₂] **14**	2.9370(18)	2.047	–	3	n.r.	Pink	[29]

CN coordination number, *M.P.* melting point, *n.r.* not reported

[a]Bond distance including esd in parentheses or mean value

[b]Typically denotes full decomposition

[c]Polymorph

[d]From high-resolution X-ray data at 89 K

[e]Melts without significant decomposition

[f]Neutron diffraction study

[g]Approximate distances from a low-quality crystal structure
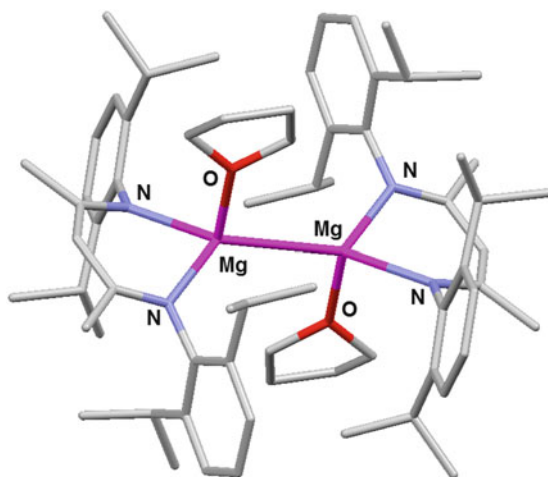
Fig. 3 The molecular structure of [{(^{Dip}Nacnac)Mg(THF)}$_2$] **8**

heterocycles in the compounds range from being essentially orthogonal to each other (**2**, **3** and **7**), to being close to co-planar (**4** and **14**). Intermediate orientations have also been encountered (**5** and **6**). It is noteworthy that, in some cases these dimeric compounds are isostructural, or even isomorphic, with related Nacnac transition metal(I) complexes. Examples here include [{(^{Dip}Nacnac)Mn}$_2$] [100], [{(^{Dip}Nacnac)Zn}$_2$] [101], and [{(^{Mes}Nacnac)Zn}$_2$] [102].

The pyridine or ether adducts of **3** and **5**, viz. **8–13**, have been crystallographically characterised, and all possess two 4-coordinate Mg centres (each coordinated by one Lewis base) and unsupported Mg–Mg bonds (see Table 1 and Fig. 3). The adducts incorporating the bulkier ^{Dip}Nacnac ligand, **8–11**, exhibit magnesium heterocycles that are distorted from planarity and are close to parallel to each other, while the magnesium heterocycles of the less bulky adducts, **12** and **13**, approach an orthogonal arrangement. What is most striking about the adducts is that their Mg–Mg bond lengths are significantly longer (by up to ca. 12 %) than their uncoordinated counterparts, even when the increase in Mg coordination number in the adducts is taken into account. This suggests that the potential energy surface about the equilibrium Mg–Mg bond distances in all the dimers is quite shallow, and that these bonds are "deformable". This proposal is backed up by theoretical [30] and experimental evidence [95] (see Sect. 2.3). That said, the unsupported Mg–Mg bonds in the three-coordinate dimers do not appear to be susceptible to facile cleavage. Evidence for this is their remarkable stability towards disproportionation, and the fact that when solutions of two dimers, e.g. **3** and **5**, in non-coordinating solvents are heated at temperatures of up to 100 °C, there is no evidence of "scrambling" of the Mg heterocycles between the dimers [28]. This indicates that there is no appreciable dimer/monomer equilibrium in solution for the compounds.

An inherent problem associated with the crystallographic characterisation of Mg^I dimers is that it is difficult to prove that the compounds are not, in fact, hydride

bridged Mg^{II} species. In the case of **5** the absence of hydride ligands has been verified by carrying out a neutron diffraction study on the compound [28]. Another way to indirectly prove the absence of hydride ligands is to make the magnesium(II) hydride counterpart of the magnesium(I) dimer and compare the physical and structural properties of the compound pairs. We have achieved this with the preparation of $[\{(^{Dip}Nacnac)Mg(\mu\text{-}H)\}_2]$ **15** [30] and $[\{(^{tBu}Nacnac)Mg(\mu\text{-}H)\}_2]$ **16** [28], viz. the hydride analogues of $[\{(^{Dip}Nacnac)Mg\}_2]$ **3** and $[\{(^{tBu}Nacnac)Mg\}_2]$ **7**, via reactions of the appropriate magnesium butyl compound, $[(Nacnac)MgBu^n]$, with phenylsilane. Moreover, the Mg^{II} hydride analogues of **3** and **5**, viz. $[\{(^{Dip}Nacnac)Mg(\mu\text{-}H)\}_2]$ **15** and $[\{(^{Mes}Nacnac)Mg(\mu\text{-}H)\}_2]$ **17,** have been prepared by hydrogenation of the corresponding magnesium(I) compound with aluminium(III) hydride reagents [31] (see Sect. 3.2). Addition of THF or DMAP to **15** and **16**, respectively, yielded the donor complexes, dimeric $[\{(^{Dip}Nacnac)Mg(THF)(\mu\text{-}H)\}_2]$ **18** and monomeric $[(^{tBu}Nacnac)MgH(DMAP)]$ **19**, the latter of which was the first structurally authenticated compound to possess a terminal Mg–H bond [28]. Although, in general, the dimeric magnesium hydride compounds have similar structural arrangements and $Mg \cdots Mg$ separations to the corresponding Mg^{I} dimers in the solid state, their physical and spectroscopic properties are very different. For example, all of the Mg^{II} hydrides are colourless whereas the Mg^{I} dimers are coloured. Furthermore, the magnesium hydride compounds typically show a resonance in their ^{1}H NMR spectra at ca. δ 4 ppm, which corresponds to their hydride ligands. This signal, of course, is absent in the ^{1}H NMR spectra of the Mg^{I} dimers.

2.3 Theoretical Analyses

A variety of studies have dealt with theoretical investigations into group 2 metal(I) dimers, LMML (L = monoanionic ligand, M = group 2 metal) [17–28, 30–46] or $[(DAB)MM(DAB)]^{2-}$ (DAB = doubly reduced diazabutadiene) [29, 103]. Neutral molecules that have been studied include those with L = H, halides, alkyl groups, aryl groups, cyclopentadienyl and related heterocyclic ligands, all metal ligands, and chelating monoanionic N-ligands. Of these, Mg–Mg bonded complexes have been most investigated and generally feature a linear LMML fragment with Mg–Mg bond lengths of ca. 2.76–2.89 Å and BDEs of ca. 45–48 kcal/mol. One example worth noting here is ClMgMgCl which has a calculated BDE of 47.1 kcal/mol. Raman spectroscopic studies, in combination with calculations, revealed a vibrational frequency of 176 cm^{-1} ($\nu_1[\Sigma_g]$) for its Mg–Mg bond [19]. Similar low-frequency stretches were found in the Raman spectra of some of the stable magnesium(I) dimers described above [27, 28, 30]. A force constant of 0.65 mdyn/Å was determined for the Mg–Mg bond in ClMgMgCl, which lies between those of the Na–Na bond in Na_2 and a typical Al–Al bond, as might be expected [19].

With respect to the other group 2 metals, theoretical studies have predicted significantly shorter and stronger Be–Be bonds in compounds of the type LBeBeL,

with Be–Be distances of ca. 2.06–2.08 Å and BDEs of ca. 70 kcal/mol for L = Cp. In contrast, calculations on LCaCaL molecules show much longer and weaker metal–metal bonds than for the lighter elements, with Ca–Ca distances of ca. 3.73–3.82 Å (i.e. almost 1 Å longer than respective Mg–Mg bonds) and BDEs of <30 kcal/mol.

The results of all computational studies on group 2 metal(I) dimers, LMML, have in common that the molecules have singlet ground states and close to linear geometries. For the magnesium dimers, the insertion of Mg atoms into L_2Mg molecules to give LMgMgL is slightly exothermic in the gas phase. However, when the much larger enthalpy of vaporisation for bulk magnesium metal is taken into account (ca. 35.2 kcal/mol) [104], the overall reaction from solid Mg metal is endothermic. Consequently, the disproportionation of LMgMgL into L_2Mg and Mg_{metal} is exothermic, and therefore LMgMgL molecules are not thermodynamically stable. The conclusion here is that they can only be kinetically protected from disproportionation reactions by using sterically demanding ligands. One study has additionally suggested that bi- or higher dentate ligands will be a necessity for the stabilisation of Mg^I dimers [19].

With respect to the nature of the bonding in neutral guanidinate or β-diketiminate chelated magnesium(I) dimers, it has been found that the Mg–Mg interaction is typically associated with the HOMO of the molecules. These single σ-bonds generally exhibit a Wiberg bond index of ca. 0.9 and have high (ca. 90 %) s-character. In contrast, theoretical investigations on a model of complex **14** revealed significant p-orbital contribution (ca. 55 %) to the Mg–Mg bonding molecular orbital (HOMO-2) [29]. Furthermore, substantial π-bonding character was found for the nearly degenerate LUMO and LUMO+1 of a model of **2** (with a HOMO–LUMO gap of ca. 93 kcal/mol) [27], the LUMO+2 and LUMO+3 of a model of **3** [30], and the LUMO+2 of **14** [29]. These data, in combination with calculated natural charges on all models, imply that the molecules are best viewed as covalently bonded dimagnesium dications, Mg_2^{2+}, stabilised by ionic interactions with bulky anionic ligands.

As mentioned in the previous section, a wide range of dihedral angles between the Mg heterocycles of Mg^I dimers have been observed experimentally. Computational studies of the model β-diketiminato magnesium(I) dimer, $[\{(^HNacnac)Mg\}_2]$ ($^HNacnac = [(HNCH)_2CH]$), have revealed a very small energy difference of ca. 0.12 kcal/mol between its D_{2d} (orthogonal ligand arrangement) and D_{2h} (co-planar ligand arrangement) forms [30]. Although the magnitude of the barrier for rotation around the Mg–Mg bond was not calculated, this is most probably a low-energy process that is dominated by the steric bulk of the ligands used in the experimental compounds, **3–7**.

To shed light on the origin of the significant elongation (by ca. 0.2 Å) of experimental Mg^I dimers upon coordination by ethers and pyridines, the potential energy surface about the equilibrium Mg–Mg bond length of $[\{(^HNacnac)Mg\}_2]$ has been calculated [30]. This was found to be very shallow in that it requires only ca. 1.2 kcal/mol or 3.5 kcal/mol to elongate the bond by 0.20 Å and 0.35 Å, respectively. Lewis base adducts of this model, $[\{(^HNacnac)Mg(L)\}_2]$ (L = THF

or 1,4-dioxane), also showed elongated Mg–Mg bonds after geometry optimisations, but only by ca. 0.08 Å. This indicates that the longer bonds in compounds **8** and **9** are further influenced by the steric bulk of the β-diketiminate ligands. Like the uncoordinated model, $[\{(^{H}Nacnac)Mg\}_2]$, the donor adducts, $[\{(^{H}Nacnac)Mg(L)\}_2]$, have very high s-character in the Mg–Mg bonds, with bond orders of close to 1 (L = THF: 0.97; L = 1,4-dioxane: 0.99). The HOMO-LUMO gaps in the adducts (ca. 70 kcal/mol) are slightly lower than that for three-coordinate $[\{(^{H}Nacnac)Mg\}_2]$ (ca. 89.5 kcal/mol) [30].

An experimental charge density (ECD) study has been carried out on $[\{(^{Dip}Nacnac)Mg\}_2]$ **3** using high-resolution single crystal X-ray diffraction data in combination with theoretical models. The results of this study largely mirror those from previous quantum chemical investigations in that **3** was found to have average charges on its Mg and N centres of +1.15 and −1.20, respectively. The study located a bond critical point almost midway along its Mg–Mg vector, which confirmed the presence of a covalent bond between the two metal atoms [95]. That said, the electron density between the two atoms is quite diffuse, which is in line with the experimentally observed "deformability" of the bond. All of these observations are consistent with the view that **3** and other neutral Mg^{I} dimers can be considered as containing a covalently bonded Mg_2^{2+} cation, stabilised by ionic interactions with bulky anionic ligands.

This view, however, may not represent the full picture with regard to Mg–Mg bonding in **3**. Further multipole modelling of the ECD data, and supporting DFT studies, subsequently revealed a non-nuclear local maximum of electron density distinct from nuclear positions (or a non-nuclear attractor, NNA), in a large region of the negative Laplacian between both Mg atoms. This feature can be thought of as each Mg atom "binding" to the NNA [105]. Accordingly, a (3, −3) critical point was found at the NNA (typically only found for atomic positions) and two less symmetrically arranged (3, −1) bond critical points were located between each Mg and the NNA. Thus, a pseudo-atomic basin of ca. 0.8 electrons was formulated in the Mg–Mg inter-atomic space. Charges of ca. +1.55 were found on the Mg centres using this revised model. It is worth noting that **3** is the first example of a stable molecular compound displaying an NNA. These have previously only been found for some elemental s-block metals and related unstable molecules such as Li_2 and Na_2.

3 Magnesium(I) Dimers as Specialist Reducing Agents in Synthesis

Once reproducible synthetic routes to room temperature stable magnesium(I) dimers were developed, the opportunity to explore the further chemistry of these reactive species presented itself. It seemed reasonable that one of the main synthetic possibilities these compounds held was as specialist reducing agents in organic and organometallic synthesis. This is especially so as magnesium(I) dimers possess a

unique combination of properties that could make them attractive alternatives to more "traditional" reducing agents (e.g. magnesium metal, alkali metals, SmI_2, etc.) that are extensively used in innumerable synthetic protocols. These properties include their moderate air and moisture sensitivity, their impressive thermal stability, and their high solubility in many coordinating and non-coordinating organic solvents. Furthermore, the dimers can be prepared in good yields on gram scales, are readily manipulated using standard Schlenk line and glove-box techniques, are of low toxicity, and do not present any significant fire hazard. No data are yet available on the reduction potentials of magnesium(I) dimers, though it seems very likely these will lie between those of samarium(II) reagents [106, 107] and alkali metals [108]. If so, magnesium(I) dimers should be categorised as moderate to strong reducing agents. It is of note that the reduction potentials for the Mg^{2+}/Mg (-2.36 V vs. NHE) and Mg^{2+}/Mg^+ (-2.05 V vs. NHE) couples have been reported [99], and it is not inconceivable that magnesium(I) dimers will be shown to be similarly reducing. Published work detailing the use of Mg^I dimers as specialist reducing agents in organic and inorganic synthesis is summarised below.

3.1 Use of Magnesium(I) Dimers in Organic Synthesis

Magnesium compounds have been utilised as reagents by synthetic organic chemists for more than 100 years. Unquestionably, the most important of these are Grignard reagents [71, 72], which although not normally thought of as reducing agents can participate in transformations which are believed to occur via a net single-electron transfer (SET) from the magnesium reagent to an organic substrate. One example of such a reaction is the pinacol coupling of ketones. Other magnesium reagents that have been employed in numerous one-electron reductions of organic (and organometallic) substrates are the Mg/MgX_2 (X = Br or I) mixtures [109]. Their reducing ability has been proposed to derive from the mixtures being in equilibrium with minute quantities of univalent magnesium compounds, $\cdot MgX$ or $XMgMgX$, in organic solutions. However, perhaps the most widely used one-electron reductant currently used in organic synthesis is not a magnesium reagent, but samarium(II) iodide, SmI_2 [106, 107]. This is commercially available and has been applied to a multitude of organic transformations. Unfortunately, the selectivity of many reactions involving SmI_2 is difficult to control. As a result, it would certainly be worthwhile to the organic chemist to have access to more selective reducing agents.

In order to ascertain if magnesium(I) dimers "fit the bill" in this respect we have examined their reactivity towards a variety of unsaturated organic substrates. Almost all work carried out in this area has involved β-diketiminato coordinated Mg^I dimers. This results from their higher yielding syntheses and greater thermal stability relative to the guanidinato coordinated complex, $[\{(Priso)Mg\}_2]$ **2**. In all of the reactions carried out so far, the magnesium(I) dimer acts as a facile two-centre/two-electron reductant towards an unsaturated substrate. Examples here include the
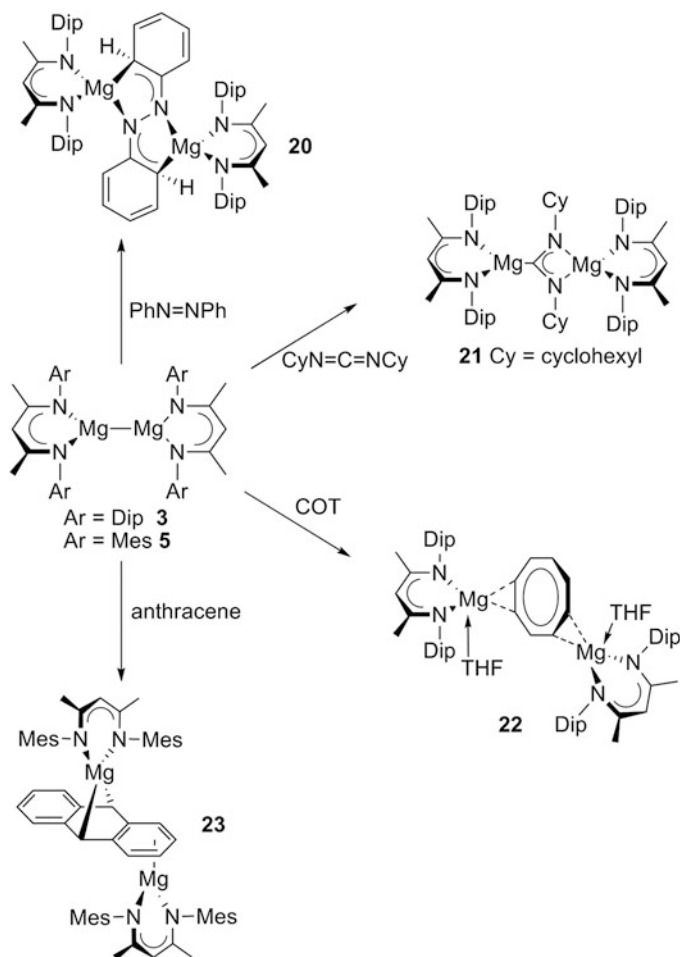
Scheme 3 Two-electron reduction of organic substrates by magnesium(I) dimers

two-electron reductions of azobenzene (PhN=NPh) [110], the carbodiimide, CyN=C=NCy [27], cyclooctatetraene (COT) [110], or anthracene [111], in which the substrate inserted into the Mg–Mg bond of Mg^I dimer, leading to the chemo-selective formation of complexes, **20–23** in high yields (Scheme 3).

The novelty of these reduction products indicates that magnesium(I) compounds may prove more widely useful as selective reducing agents in organic (and organometallic) syntheses. For example, although many complexes incorporating doubly reduced azobenzenes have been reported, the "de-aromatised" bis(κ^2-azaallylic) structural motif adopted by the [PhNNPh]$^{2-}$ ligand in **20** is unprecedented. Furthermore, complex **21** represents the first of only two reported examples of magnesium magnesioamidinate complexes. The other, [(Priso)Mg{μ-(NDip)$_2$C}Mg (Priso)], was prepared by treating [{(Priso)Mg}$_2$] **2** with DipN=C=NDip [51],
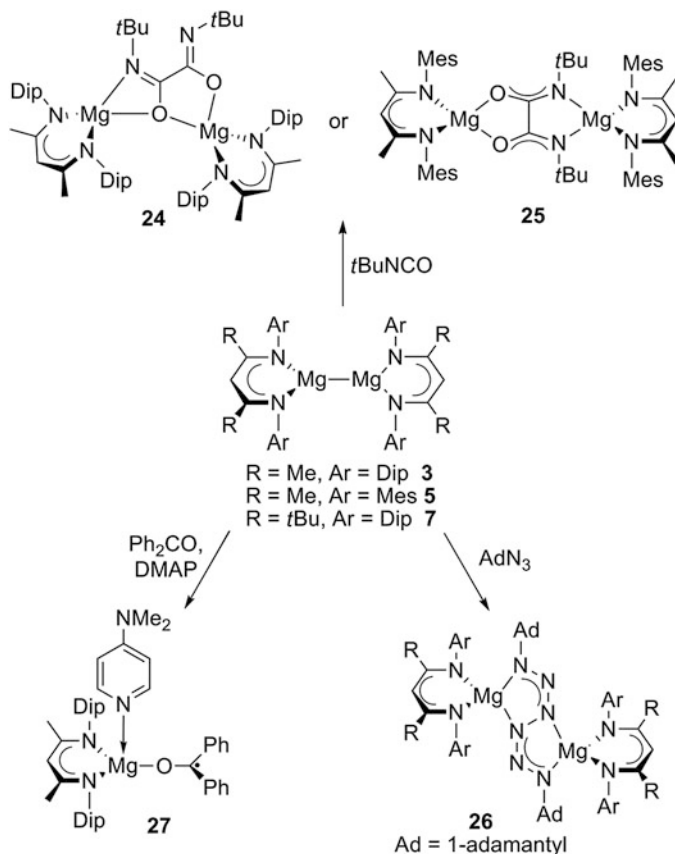
Scheme 4 Reductive coupling or one-electron reduction of organic substrates by magnesium(I) dimers

which is the only known demonstration of **2** acting as a reducing agent to date. The novelty of compound **22** is derived from the fact that it is an unprecedented example of a crystallographically characterised magnesium–COT complex, while the high solubility of **23** could lead to it finding use as a reducing agent in its own right (cf.poorly soluble [(THF)$_3$ Mg(anthracene)] [112, 113]).

Reductive C–C and N–N bond coupling reactions have also been reported for magnesium(I) compounds. Reactions of note here are those with the isocyanate, t-BuNCO, or 1-adamantyl azide (AdN$_3$), which selectively afforded the magnesium oxamide compounds, **24** and **25**, and the unusual hexazenediide complexes, **26** (Scheme 4) [28, 110]. Only one reduction of an unsaturated substrate has been reported that does not yield a dinuclear complex, i.e. the reduction of benzophenone with **3**. This gave rise to a high yield of the thermally stable, purple-blue magnesium ketyl complex, **27**, after addition of DMAP to the reaction mixture [111, 114].

The hexazenediide complexes, **26**, are exceptional in that they are formed via the first main group metal induced reductive couplings of an alkyl azide. The only other

report of organic azide reductive couplings came from Holland et al. who carried out related reactions between β-diketiminato iron(I) fragments and AdN$_3$ [115]. The remarkable stability of **26**, which contain six covalently bonded N-centres, could lend such complexes to a number of uses, for example in the synthesis of N-heterocycles, or as precursors for the preparation of high-energy materials. Furthermore, the novelty of compound **27** comes from the fact that it is the first crystallographically characterised example of a magnesium ketyl complex. The existence of such ketyls was first proposed by Gomberg and Bachmann who, in 1927, suggested the radical, [IMg(OCPh$_2$·)], as an intermediate in the pinacol coupling of benzophenone with a Mg/MgI$_2$ mixture [116]. The EPR spectrum of **27** indicates that the majority of its unpaired spin density is located on the C$_3$O fragment of the ketyl ligand.

All reduction reactions involving Mg^I dimers have been carried out in non-coordinating solvents. It is probable that those involving functionalised substrates proceed via coordination of the substrate to one or both of the Mg centres of the dimer prior to its reduction or reductive coupling. Evidence for this proposal comes from the observation that the double reduction of CyN=C=NCy with **3** to give **21** is rapid, even at −50 °C in toluene, whereas it does not proceed at ambient temperature in THF. It is believed that this difference occurs because **3** exists as the THF adduct, [{(^{Dip}Nacnac)Mg(THF)}$_2$] **8**, in solution, and therefore its coordinatively saturated Mg centres are effectively "blocked" from nucleophilic attack by the carbodiimide [30]. Further evidence comes from the fact that the unfunctionalised substrates, COT and anthracene, for which strong magnesium coordination is disfavored, are more resistant towards reduction by Mg^I dimers. Indeed, the double reduction of COT only proceeds in toluene, heated at reflux, over more than 1 h. It is also of note that the reactivity of **3**, **5** and **7** was found to be inversely proportional to the steric bulk of the β-diketiminate ligand involved. A pertinent illustration of this point is the fact that the bulkiest dimer, **7**, does not react with PhN=NPh or CyN=C=NCy at room temperature, and does not form adducts with THF or DMAP under normal conditions [28].

It is instructive to briefly draw comparisons between the reactivity of the magnesium(I) dimers, **3** and **5**, and the analogous magnesium(II) hydride species, **15** and **17**, towards unsaturated substrates. The reactions involving the latter compounds are of interest as all previously reported reductions with magnesium hydride species have involved poorly characterised compounds of the type, RMgH. These have led to varying outcomes, e.g. hydromagnesiation of the organic substrate [117], or formation of reduced paramagnetic products via SET processes [118]. In contrast, the reactions of **15** with the unsaturated systems, azobenzene, CyN=C=NCy, or 1-adamantyl azide, have been shown to yield only hydromagnesiated products [110], cf. the doubly reduced or reductively coupled products, **20**, **21**, and **26**, from the reductions of the same substrates with magnesium(I) dimers [27, 28, 110]. No similar chemistry has been reported for the less bulky magnesium hydride complex, **17**, but its high reactivity is evident from the very facile reaction of the compound with silicone polymer grease, i.e. (Me$_2$SiO)$_n$. This led to cleavage of Si–O bonds within the polymer and formation of a silanolate bridged magnesium

hydride dimer, [(^{Mes}Nacnac)Mg(μ-H){μ-OSi(H)Me$_2$}Mg(^{Mes}Nacnac)] [31]. In situ generation of β-diketiminato magnesium hydrides has furthermore been employed in the hydromagnesiation and dearomatisation of pyridines and quinolines [119, 120] and the catalytic hydroboration of pyridines [121]. It is worth noting that the reactivity of **15** towards unsaturated substrates in many cases is similar to that reported for closely related β-diketiminato calcium [122], zinc [123], or iron hydride [124] complexes.

3.2 Use of Magnesium(I) Dimers in Inorganic/Organometallic Synthesis

The chemistry of low oxidation state p-block chemistry has rapidly developed over the past decade, not only because of the considerable fundamental interest in such compounds, but also because their high reactivity is lending them to an increasing number of synthetic and other applications [12–14]. The growth of this field has been heavily reliant on the availability of a range of reducing agents to access such compounds from the reduction of "normal oxidation state" precursor complexes. The most widely utilised of these are the elemental s-block metals (normally Li, Na, K, or Mg), potassium graphite (KC$_8$), and alkali metal naphthalide solutions [108]. These reductions can be problematic, and often lead to "over-reduction" of the precursor complex, and/or other side reactions occurring. The problems associated with these reagents are mainly derived from their strongly reducing character and/or their insolubility. Both factors make it difficult to control the stoichiometry and selectivity of reduction reactions they are involved in. Furthermore, the handling of alkali metals presents a significant fire hazard in the laboratory. To overcome many of the drawbacks of traditional reducing agents, we (and others) have begun to explore the use of magnesium(I) dimers as hydrocarbon soluble, stoichiometric, selective, and safe reducing agents in inorganic/organometallic synthesis, as summarised below.

Of considerable initial interest to us was an exploration of the reactivity of Mg^I dimers towards the lightest element, hydrogen. In this respect, it seemed reasonable that if these dimers did react with dihydrogen to give the corresponding magnesium (II) hydrides, [LMg(μ-H)$_2$MgL] (L = guanidinate or β-diketiminate), they would be exploitable as soluble molecular models for the study of the hydrogenation of magnesium metal (which gives MgH$_2$). This reaction is reversible, and the Mg/MgH$_2$ couple is an important hydrogen storage system [125]. The results of one computational study suggested that the reactions of several guanidinato coordinated magnesium(I) dimers with dihydrogen should be spontaneous, as they are exothermic by as much as 25 kcal/mol [38]. In practice, however, **2** and the related β-diketiminate coordinated dimers, **3** and **5**, are unreactive towards H$_2$ at 80 °C, and under 1 or 5 atm [27, 28]. In contrast, complexes **3** and **5** do react at 80 °C under 70 atm. H$_2$, but these reactions give rise to complex product mixtures, not including
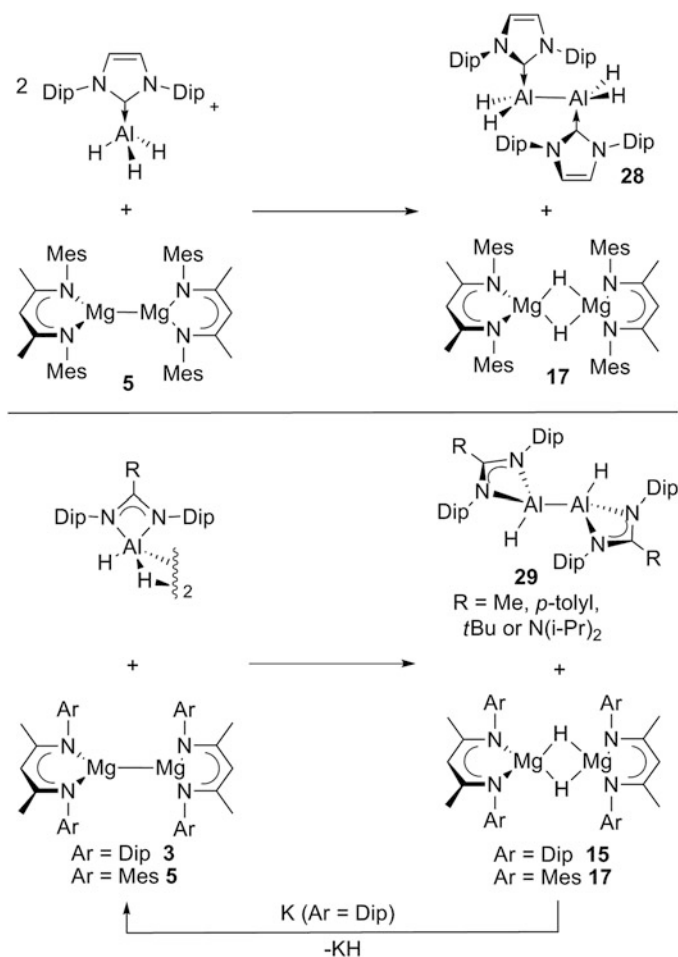
Scheme 5 Hydrogenation of magnesium(I) dimers by reaction with aluminium hydride complexes

the magnesium hydrides, **15** or **17**. The lack of reactivity of the magnesium(I) dimers towards dihydrogen under ambient conditions presumably reflects a signifi- cant kinetic barrier to their hydrogenation, as is known to be the case for the exothermic ($\Delta H = -17.9$ kcal/mol) hydrogenation of magnesium metal to give MgH_2, which only proceeds at elevated temperatures, ca. 300 °C [125].

The facile hydrogenation of **3** and **5** was eventually achieved through their reactions with a range of aluminium(III) hydride complexes, used as a source of hydrogen (Scheme 5) [31]. It is noteworthy that the by-products from these reactions, **28** and **29**, were the first reported examples of neutral aluminium(II) hydride complexes that are stable at ambient temperature. The thermal stability of compound **28** (decomp. >190 °C) is particularly significant as this is an NHC adduct of the parent dialane(4), Al_2H_4, which had only been previously observed in
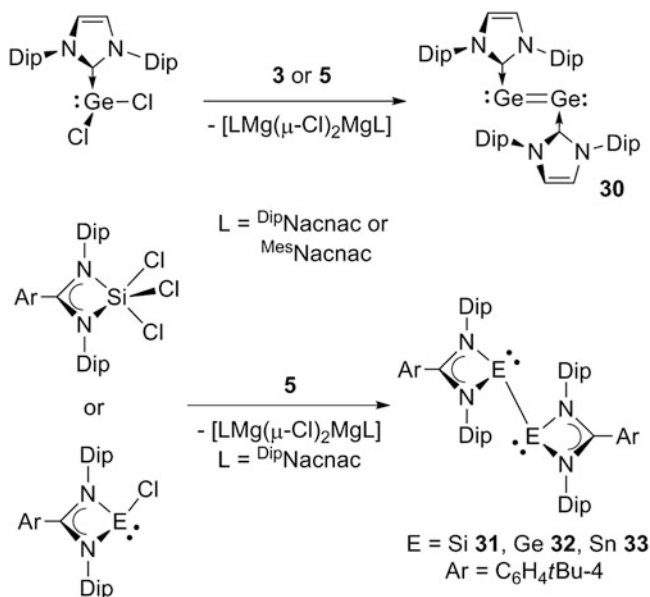
Scheme 6 Reduction of group 14 element chloride complexes with magnesium(I) dimers

solid H_2 matrices at temperatures of ca. 5 K [126]. There is little doubt that the thermal stability of **28** is derived from the steric bulk and high nucleophilicty of its NHC ligands, as is the case for closely related NHC adducts of group 13 metal(II) halide fragments [127]. Moreover, the preparation of **28** and **29** highlights the versatility of magnesium(I) dimers as selective reducing agents, as our earlier attempts to reduce group 13 metal hydride complexes with a variety of other reagents, e.g. sodium naphthalide, met with failure [128].

A DFT computational study of a model of the hydrogenation reaction that gave **17** (and **28**) revealed that at ambient temperature it is only mildly exothermic ($\Delta G = -4.0$ kcal/mol), and therefore potentially reversible. Although this has not been demonstrated in practice, the dehydrogenation of bulkier **15** (to give **3**) was achieved by its treatment with potassium metal [31]. It is worthy of note that a subsequent theoretical analysis of the hydrogenation of β-diketiminato coordinated magnesium(I) dimers with a series of group 13 trihydride complexes, $[(NHC)EH_3]$ ($NHC = :C\{N(Me)C(H)\}_2$; E = B, Al, Ga, or In), showed that these reactions become increasingly exothermic with heavier E [129]. Taken as a whole, the results of these investigations lead to the conclusion that magnesium(I) dimers may well find use as soluble molecular models for the study of the mechanisms and/or kinetics of the hydrogenation of magnesium metal, and magnesium containing alloys.

By far the most success in using magnesium(I) dimers as reducing agents in inorganic/organometallic synthesis has come from the preparation of low oxidation state group 14 complexes, as summarised in Schemes 6 and 7. The first such
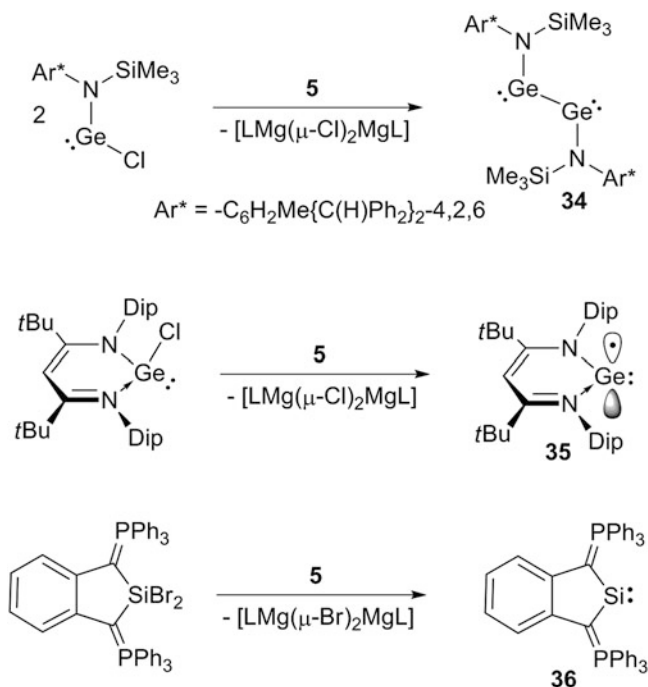
Scheme 7 Further reductions of group 14 element halide complexes with a magnesium(I) dimer

compound to be accessed was the formal germanium(0) complex, **30** [130]. Its synthesis was inspired by a previous study by Robinson et al., who prepared the silicon(0) analogue of the compound, viz. [(IPr)Si=Si(IPr)] (IPr = :C{N(Dip)C (H)}$_2$), via the KC$_8$ reduction of [SiCl$_4$(IPr)] [131]. This landmark study led to a flurry of subsequent reports from several groups (including Robinson's) on the preparation of other NHC coordinated zero (and +1) oxidation state main group element complexes [132–134]. However, our attempts to prepare **30** via the reduction of [GeCl$_2$(IPr)] with either sodium metal or KC$_8$, led only to deposition of elemental germanium and the generation of free IPr. In contrast, the corresponding reactions with 1 equivalent of the Mg^I dimers, **3** or **5**, at ambient temperature afforded **30**, albeit in low yields. Interestingly, when the reactions were carried out with half an equivalent of the magnesium(I) dimer, the suspected intermediate in the formation of **30**, viz. [(IPr)Ge^I(Cl)Ge^I(Cl)(IPr)], was not obtained and, instead, a mixture of **30** and unreacted [GeCl$_2$(IPr)] resulted. The by-products from the reactions that gave **30** are the magnesium(II) chloride complexes, [LMg (μ-Cl)$_2$MgL] (L = ^{Dip}Nacnac or ^{Mes}Nacnac), which have poor solubility in the diethyl ether reaction solvent, and were therefore easily separated from **30**. Computational studies of a model of diamagnetic **30** indicated that it is best viewed as an NHC adduct of the Ge$_2$ fragment, and as a result it has the potential to act as a soluble source of that element in further synthetic protocols, though this is yet to be realised.

Magnesium(I) dimers have also been shown to be more effective reducing agents than alkali metals in the syntheses of a series of monomeric or dimeric group 14 element(I) systems. For example, in 2006 we reported the low yield preparations of the first amidinate or guanidinate chelated germanium(I) dimers, $[\{[\kappa^2\text{-}N,N'\text{-}RC(NDip)_2]Ge\}_2]$ (R = t-Bu or $N(C_6H_{11})_2$), via the potassium metal reduction of the germanium(II) precursor complexes, $[\{\kappa^2\text{-}N,N'\text{-}RC(NDip)_2\}GeCl]$ [82]. Several years later Roesky and co-workers synthesised closely related germanium(I) and silicon(I) dimers, $[\{[\kappa^2\text{-}N,N'\text{-}PhC(Nt\text{-}Bu)_2]E\}_2]$ (E = Si or Ge), in low yields via the potassium or KC_8 reduction of $[\{\kappa^2\text{-}N,N'\text{-}PhC(Nt\text{-}Bu)_2\}SiCl_3]$ or $[\{\kappa^2\text{-}N,N'\text{-}PhC(Nt\text{-}Bu)_2\}GeCl]$ [135, 136]. All three compounds contain unsupported E–E single bonds and can be considered as intramolecularly base-stabilised examples of disilynes or digermynes, REER (R = bulky monodentate ligand) [5–7]. Importantly, Roesky's silicon(I) system has been shown to be extremely effective in the activation of a range of small molecules, the reduction of unsaturated organic substrates, etc. [14, 137]. To aid an expansion of the further chemistry of such systems, we sought to develop their high yield preparations using magnesium(I) dimers as alternatives to K or KC_8 reducing agents. This was achieved with the reductions of the amidinate coordinated precursors, $[\{\kappa^2\text{-}N,N'\text{-}(C_6H_4t\text{-}Bu\text{-}4)C(NDip)_2\}SiCl_3]$ or $[\{\kappa^2\text{-}N,N'\text{-}(C_6H_4t\text{-}Bu\text{-}4)C(NDip)_2\}ECl]$ (E = Ge or Sn), with either 1.5 or 0.5 equivalents of $[\{(^{Mes}Nacnac)Mg\}_2]$ **5** [138]. These reductions gave rise to **31** and **32** in good yields (91 % and 71 %, respectively, Scheme 6). Although the corresponding tin(I) dimer, **33**, could only be obtained in low yield (36 %), it is of note that no similar amidinate coordinated systems had previously been reported. It is also noteworthy that in this study, reductions of $[\{\kappa^2\text{-}N,N'\text{-}(C_6H_4t\text{-}Bu\text{-}4)C(NDip)_2\}SiCl_3]$ with Li metal, lithium naphthalide, or magnesium anthracene were carried out for purpose of comparison. At best, only low yields of impure **31** could be recovered from these reactions.

As an extension of this work, $[\{(^{Mes}Nacnac)Mg\}_2]$ was used as the reducing agent in the moderate yield formation of the two-coordinate dimer, **34**, which can be considered as an unprecedented example of a digermyne containing a Ge–Ge single bond, or, alternatively, as a 1,2-bis(germylene) [139]. Attempts to prepare **34** via the reduction of [LGeCl] (L = $-N(Ar^*)(SiMe_3)$ and $Ar^* = C_6H_2Me\{C(H)Ph_2\}_2\text{-}4,2,6$) with alkali metals or KC_8 led to "over-reduction" and/or very low yields of **34**. Compound **34** is extremely reactive and was shown to activate dihydrogen in either solution or the solid state at temperatures as low as $-10\,^\circ C$ to yield the mixed valence germanium hydride compound, $[LGeGe(H)_2 L]$ [139]. Considering that related multiply bonded, terphenyl-substituted digermynes are of increasing importance to the "transition metal-like" activation of small molecules, etc. [12, 13], it is likely that the Mg^I-mediated synthesis of **34** will allow its further chemistry, and the chemistry of related two-coordinate element(I) dimers, to be rapidly developed.

The reduction reactions that gave the germanium(I) dimers, **32** and **34**, from monomeric germanium(II) precursors presumably proceed via monomeric germanium(I) radical intermediates, which dimerise to give the products. As no examples of such radicals had been previously isolated, the preparation of one was attempted

by the Mg^I reduction of a very bulky β-diketiminato chelated germanium(II) precursor. This reaction was successful and led to the formation of **35** in a 38 % isolated yield (Scheme 7) [140]. The compound was characterised by EPR/ENDOR spectroscopies and X-ray crystallography, and it was subsequently shown to react with the mild chlorinating agent, C_2Cl_6, to quantitatively regenerate the germanium(II) precursor. It is of note that although the reduction of the precursor complex with alkali metals did not give **35**, its reaction with a THF solution of sodium naphthalide did afford the compound in an almost identical yield to that in which **5** was the reducing agent [140, 141]. Similarly, the only other compound reported to be prepared using an Mg^I dimer as a reducing agent, viz. the ylide-stabilised carbocyclic silylene **36** (Scheme 7), can otherwise be synthesised via the reduction of a dibromosilane precursor with 2 equivalents of KC_8 in THF [142]. That said compound **36** is not stable for extended periods in the THF solvent required for that alkali metal reduction, whereas in the reaction mixture resulting from the treatment of the dibromosilane with $[\{(^{Mes}Nacnac)Mg\}_2]$ **5** in benzene, the silylene is stable at ambient temperature for months.

4 Conclusions and Outlook

Dimeric magnesium(I) compounds with diffuse, covalent Mg–Mg single bonds can be kinetically stabilised from disproportionation processes by chelation of the Mg_2^{2+} dicationic fragment by bulky anionic N-donor ligands. Using this strategy, a variety of dimeric magnesium(I) complexes have been isolated over the past 4 years. Although these display varying degrees of air and moisture sensitivity, they are generally very thermally stable (up to 300 °C in one case). This remarkable stability has rapidly led to "bottleable" magnesium(I) dimers, especially those stabilised by sterically demanding β-diketiminate ligands, finding use as hydrocarbon soluble, stoichiometric, selective, and safe reducing agents in organic and organometallic synthesis.

   Given the rapid development of the chemistry of magnesium(I) dimers since they were first reported in 2007, it is very likely that the future will hold many significant advances for these compounds and for low oxidation state s-block chemistry in general. Magnesium(I) compounds will certainly continue to find use as specialist reducing agents in synthetic protocols, and as models for the study of the chemistry of magnesium metal itself. One exciting possibility here is the employment of magnesium(I) compounds to shed light on the mechanism of formation of Grignard reagents, which is unknown to this day. In addition, the application of magnesium(I) dimers to catalytic processes remains an elusive yet imminently achievable goal. In coming years we can expect to see other stable low oxidation state s-block complexes emerging. These may include complexes with Be–Be or Ca–Ca bonds, group 1 metal–metal bonds, and even closely related f-block metal–metal unsupported bonds. Furthermore, mixed valence group 2 "metalloid" cluster compounds (L_mM_n, $n > m$) and monomeric group 2 metal(I) radical

species, LM^{I}, are attractive, and potentially applicable, synthetic targets. Whatever the case, it is certain that now the field of stable low oxidation state s-block complexes has been initiated, many more practitioners will be attracted to it, and many more exciting results are waiting for us just around the corner.

5   Addendum

Since the submission of this chapter, several papers have appeared which further highlight the utility of Mg^{I} dimers as reducing agents in synthesis. The reduction of the bulky tin(II) halide complex, [(^{tBu}Nacnac)SnCl], with half an equivalent of [{(^{Mes}Nacnac)Mg}$_2$] afforded the tin(I) dimer, [{(^{tBu}Nacnac)Sn}$_2$]. This represents the first example of a group 14 element(I) dimer incorporating β-diketiminate ligands. Interestingly, the corresponding reduction of [(^{tBu}Nacnac)GeCl] with [{(^{Mes}Nacnac)Mg}$_2$] did not give a germanium(I) dimer, but instead led to a reductive C–N cleavage of the ^{tBu}Nacnac ligand [143]. The same Mg^{I} reagent has been used for the reduction of the bis(thiolato) silicon(IV) bromide, [Br$_2$Si(SAr$^{#}$)$_2$] (Ar$^{#}$ = C$_6$H$_3$Mes$_2$-2,6), which yielded the stable silylene, [:Si(SAr$^{#}$)$_2$] [144]. It is of note that a related boryl/amido-stabilised silylene, [:Si{N(Dip)(SiMe$_3$)} {B(^{Dip}DAB)}] (^{Dip}DAB={(Dip)N=C(H)}$_2$), was reported simultaneously [145], and both compounds represent the first examples of structurally characterised, two-coordinate, acyclic silicon(II) species. The treatment of ammonia borane H$_3$N·BH$_3$ (AB) with the bulkier Mg^{I} dimer, [{(^{Dip}Nacnac)Mg}$_2$], led to reductive dehydrogenation of AB and the formation of a moderate yield of the amido borane complex, [{(^{Dip}Nacnac)Mg(NH$_2$BH$_3$)}$_2$] [146]. The preparation of this compound by an alternate route had been previously reported [147].

References

1. Cotton FA, Murillo CA, Watson RA (2005) Multiple bonds between metal atoms, 3rd edn. Springer, New York, NY
2. Cotton FA, Curtis NF, Harris CB, Johnson BFG, Lippard SJ, Mague JT, Robinson WR, Wood JS (1964) Science 145:1305
3. Nguyen T, Sutton AD, Brynda M, Fettinger JC, Long GJ, Power PP (2005) Science 310:844
4. Resa I, Carmona E, Gutierrez-Puebla E, Monge A (2004) Science 305:1136
5. Fischer RC, Power PP (2010) Chem Rev 110:3877
6. Power PP (2007) Organometallics 26:4362
7. Rivard E, Power PP (2007) Inorg Chem 46:10047
8. Pu L, Twamley B, Power PP (2000) J Am Chem Soc 122:3524
9. Stender M, Phillips AD, Wright RJ, Power PP (2002) Angew Chem Int Ed 41:1785
10. Sekiguchi A, Kinjo K, Ichinohe M (2004) Science 305:1755
11. Wiberg N, Niedermayer W, Fischer G, Nöth H, Suter M (2002) Eur J Inorg Chem 2002:1066
12. Power PP (2010) Nature 463:171
13. Power PP (2011) Acc Chem Res 44:627

14. Asay M, Jones C, Driess M (2011) Chem Rev 111:354
15. Liddle ST, Mills DP (2009) Dalton Trans:5592
16. Liddle ST, McMaster J, Mills DP, Blake AJ, Jones C, Woodul WD (2009) Angew Chem Int Ed 48:1077
17. Wang X, Andrews L (2004) J Phys Chem A 108:11511
18. Tague TJ Jr, Andrews L (1994) J Phys Chem 98:8611
19. Köppe R, Henke P, Schnöckel H (2008) Angew Chem Int Ed 47:8740
20. Krieck S, Yu L, Reiher M, Westerhausen M (2010) Eur J Inorg Chem 2010:197
21. Krieck S, Westerhausen M (2009) Chem Unserer Zeit 43:384
22. Westerhausen M (2008) Angew Chem Int Ed 47:2185
23. Hogreve H (2004) Chem Phys Lett 394:32
24. Nemukhin AV, Topol IA, Weinhold F (1995) Inorg Chem 34:2980
25. Jasien PG, Dykstra CE (1985) J Am Chem Soc 107:1891
26. Jasien PG, Dykstra CE (1983) J Am Chem Soc 105:2089
27. Green SP, Jones C, Stasch A (2007) Science 318:1754
28. Bonyhady SJ, Jones C, Nembenna S, Stasch A, Edwards AJ, McIntyre GJ (2010) Chem Eur J 16:938
29. Liu Y, Li S, Yang X-J, Yang P, Wu B (2009) J Am Chem Soc 131:4210
30. Green SP, Jones C, Stasch A (2008) Angew Chem Int Ed 47:9079
31. Bonyhady SJ, Collis D, Frenking G, Holzmann N, Jones C, Stasch A (2010) Nat Chem 2:865
32. Kan Y-H (2009) J Mol Struct (THEOCHEM) 894:88
33. Zhang X, Li S, Li Q-S (2009) Mol Phys 107:855
34. Gong L, Wu X, Qi C, Li W, Xiong J, Guo W (2009) Mol Phys 107:197
35. Mercero JM, Piris M, Matxain JM, Lopez X, Ugalde JM (2009) J Am Chem Soc 131:6949
36. Pankewitz T, Klopper W, Henke P, Schnöckel H (2008) Eur J Inorg Chem 2008:4879
37. Velazquez A, Fernandez I, Frenking G, Merino G (2007) Organometallics 26:4731
38. Datta A (2008) J Phys Chem C 112:18727
39. Zhang Y, Xu Y, Li S, Li QS, Cui J (2007) Mol Phys 105:2951
40. Westerhausen M, Gärtner M, Fischer R, Langer J, Yu L, Reiher M (2007) Chem Eur J 13:6292
41. Liu Z-Z, Tian WQ, Feng J-K, Li W-Q, Cui Y-H (2007) J Mol Struct (THEOCHEM) 809:171
42. Dinda R, Ciobanu O, Wadepohl H, Hübner O, Acharyya R, Himmel H-J (2007) Angew Chem Int Ed 46:9110
43. Li QS, Xu Y (2006) J Chem Phys A 110:11898
44. Xie Y, Schaefer HF III, Jemmis ED (2005) Chem Phys Lett 402:414
45. Jasien PG, Dykstra CE (1984) Chem Phys Lett 106:276
46. Brites V, Guitou M, Leonard C (2011) J Chem Phys 134:054314
47. Carmona E, Galindo A (2008) Angew Chem Int Ed 47:6526
48. Grirrane A, Resa I, Rodríguez A, Carmona E (2008) Coord Chem Rev 252:1532
49. Jones C, Mills DP, Platts JA, Rose RP (2006) Inorg Chem 45:3146
50. Bonello O, Jones C, Stasch A, Woodul WD (2010) Organometallics 29:4914
51. Stasch A, Jones C (2011) Dalton Trans 40:5659
52. Jones C (2010) Coord Chem Rev 254:1273
53. Cotton FA, Wilkinson G, Murillo CA, Bochmann M (1999) Advanced inorganic chemistry, 6th edn. Wiley, New York, NY
54. Symons MCR (1976) Chem Soc Rev 5:337
55. Thompson JC (1976) Electrons in liquid ammonia. Clarendon, Oxford
56. Zurek E, Edwards PP, Hoffmann R (2009) Angew Chem Int Ed 48:8198
57. Damay P, Leclerq F, Chieux P (1990) Phys Rev B 41:9676
58. Glaunsinger WS, White TR, Von Dreele RB, Gordon DA, Marzke RF, Bowman AL, Yarnell JL (1978) Nature 271:414
59. Von Dreele RB, Glaunsinger WS, Bowman AL, Yarnell JL (1975) J Phys Chem 79:2992
60. Dye JL (2009) Acc Chem Res 42:1564

61. Dye JL (1979) Angew Chem Int Ed Engl 18:587
62. Matsuishi S, Toda Y, Miyakawa M, Hayashi K, Kamiya T, Hirano M, Tanaka I, Hosono H (2003) Science 301:626
63. Kim SW, Shimoyama T, Hosono H (2011) Science 333:71
64. Simon A (2004) In: Driess M, Noth H (eds) Molecular clusters of the main group elements. Wiley-VCH, Weinheim, p 246
65. Bonhomme F, Stetson NT, Yvon K, Fischer P, Hewat AW (1993) J Alloys Compd 200:65
66. Bonhomme F, Yvon K, Fischer P (1992) J Alloys Compd 186:309
67. King RB (2002) Polyhedron 21:2347
68. Saito Y, Ishida T, Noda T (1991) J Am Soc Mass Spectrom 2:76
69. Rubino R, Williamson JM, Miller TA (1995) J Chem Phys 103:5964
70. Petrie S (2003) Aust J Chem 56:259
71. Rappoport Z, Marek I (2008) The chemistry of organomagnesium compounds, part 1. Wiley, Chichester
72. Richey HG Jr (2000) Grignard reagents: new developments. Wiley, Chichester
73. Tjurina LA, Smirnov VV, Potapov DA, Nikolaev SA, Esipov SE, Beletskaya IP (2004) Organometallics 23:1349
74. Tyurina LA, Smirnov VV, Esipov SE, Beletskaya IP (2002) Mendeleev Commun 12:108
75. Tjurina LA, Smirnov VV, Barkovskii GB, Nikolaev EN, Esipov SE, Beletskya IP (2001) Organometallics 20:2449
76. Krieck S, Görls H, Yu L, Reiher M, Westerhausen M (2009) J Am Chem Soc 131:2977
77. Krieck S, Görls H, Westerhausen M (2010) Organometallics 29:6970
78. Krieck S, Görls H, Westerhausen M (2010) J Am Chem Soc 132:12492
79. Jin G, Jones C, Junk PC, Stasch A, Woodul WD (2008) New J Chem 32:835
80. Jones C, Junk PC, Platts JA, Stasch A (2006) J Am Chem Soc 128:2206
81. Jones C, Junk PC, Platts JA, Rathmann D, Stasch A (2005) Dalton Trans:2497
82. Green SP, Jones C, Junk PC, Lippert K-A, Stasch A (2006) Chem Commun 2006:3978
83. Green SP, Jones C, Jin G, Stasch A (2007) Inorg Chem 46:8
84. Jones C, Schulten C, Rose RP, Stasch A, Aldridge S, Woodul WD, Murray KS, Moubaraki B, Brynda M, La Macchia G, Gagliardi L (2009) Angew Chem Int Ed 48:7406
85. Jones C, Schulten C, Fohlmeister L, Stasch A, Murray KS, Moubaraki B, Kohl S, Ertem MZ, Gagliardi L, Cramer CJ (2011) Chem Eur J 17:1294
86. Rose RP, Jones C, Schulten C, Aldridge S, Stasch A (2008) Chem Eur J 14:8477
87. Jones C, Mills DP, Stasch A (2008) Dalton Trans:4799
88. Heitmann D, Jones C, Mills DP, Stasch A (2010) Dalton Trans:1877
89. Heitmann D, Jones C, Junk PC, Lippert K-A, Stasch A (2007) Dalton Trans:187
90. Jones C, Furness L, Nembenna S, Rose RP, Aldridge S, Stasch A (2010) Dalton Trans 39:8788
91. Bourget-Merle L, Lappert MF, Severn JR (2002) Chem Rev 102:3031
92. Edelmann FT (2008) Adv Organomet Chem 57:183
93. Harder S, Spielmann J, Intemann J, Bandmann H (2011) Angew Chem Int Ed 50:4156
94. Schuchmann D, Westphal U, Schulz S, Florke U, Bläser D, Boese R (2009) Angew Chem Int Ed 48:807
95. Overgaard J, Jones C, Stasch A, Iversen BB (2009) J Am Chem Soc 131:4208
96. Pyykkö P, Atsumi M (2009) Chem Eur J 15:186
97. Cordero FB, Gomez V, Platero-Prats AE, Reves M, Echeverria J, Cremades E, Barragan F, Alvarez S (2008) Dalton Trans:2832
98. Huber KP, Herzberg G (1979) Molecular spectra and molecular structure IV. Constants of diatomic molecules. Van Nostrand Reinhold, New York, NY
99. Emsley J (1995) The elements, 2nd edn. Clarendon, Oxford
100. Chai J, Zhu H, Stückl AC, Roesky HW, Magull J, Bencini A, Ganeschi A, Gatteschi D (2005) J Am Chem Soc 127:9201

101. Wang Y, Quillian B, Wei P, Wang H, Yang X-J, Xie Y, King RB, Schleyer PR, Schaefer HF III, Robinson GH (2005) J Am Chem Soc 127:11944
102. Schulz S, Schuchmann D, Westphal U, Bolte M (2009) Organometallics 28:1590
103. Li S, Yang X-J, Liu Y, Zhao Y, Li Q-S, Xie Y, Schaefer HF, Wu B (2011) Organometallics 30:3113
104. Binneweis M, Milke E (2002) Thermochemical data of elements and compounds, 2nd edn. Wiley-VCH, Weinheim
105. Platts JA, Overgaard J, Jones C, Iversen BB, Stasch A (2011) J Phys Chem A 115:194
106. Nicolaou KC, Ellery SP, Chen JS (2009) Angew Chem Int Ed 48:7140
107. Kagan HB (2003) Tetrahedron 59:10351
108. Connelly NG, Geiger WE (1996) Chem Rev 96:877
109. Rausch MD, McEwen WE, Kleinberg J (1957) Chem Rev 57:417
110. Bonyhady SJ, Green SP, Jones C, Nembenna S, Stasch A (2009) Angew Chem Int Ed 48:2973
111. Jones C, McDyre L, Murphy DM, Stasch A (2010) Chem Commun 46:1511
112. Harvey S, Junk PC, Raston CL, Salem G (1988) J Org Chem 53:3134
113. Bogdanovic B (1985) Angew Chem Int Ed Engl 24:262
114. Murphy DM, McDyre LE, Carter E, Stasch A, Jones C (2011) Magn Reson Chem 49:159
115. Cowley RE, Elhaïk J, Eckert NA, Brennessel WW, Bill E, Holland PL (2008) J Am Chem Soc 130:6074
116. Gomberg M, Bachmann WE (1927) J Am Chem Soc 49:236
117. Ashby EC, Lin JJ, Goel AB (1978) J Org Chem 43:1557
118. Goel AB, Ashby EC (1981) J Organomet Chem 214:C1
119. Hill MS, MacDougall DJ, Mahon MF (2010) Dalton Trans 39:11129
120. Hill MS, Kociok-Köhn G, MacDougall DJ, Mahon MF, Weetman C (2011) Dalton Trans 40:12500
121. Arrowsmith M, Hill MS, Hadlington T, Kociok-Köhn G, Weetman C (2011) Organometallics 30:5556
122. Spielmann J, Harder S (2007) Chem Eur J 13:8928
123. Schulz S, Eisenmann T, Schmidt S, Bläser D, Westphal U, Boese R (2010) Chem Commun 46:7226
124. Yu Y, Sadique AR, Smith JM, Dugan TR, Cowley RE, Brennessel WW, Flaschenriem CJ, Bill E, Cundari TR, Holland PL (2008) J Am Chem Soc 130:6624
125. Bogdanović B, Ritter A, Spliethoff B (1990) Angew Chem Int Ed Engl 29:223
126. Weng X, Andrews L, Tam S, DeRose ME, Fajardo ME (2003) J Am Chem Soc 125:9218
127. Baker RJ, Farley RD, Jones C, Kloth M, Murphy DM (2002) Chem Commun 2002:1196
128. Jones C, Rose RP (2007) New J Chem 31:1484
129. Holzmann N, Stasch A, Jones C, Frenking G (2011) Chem Eur J 17:13517
130. Sidiropoulos A, Jones C, Stasch A, Klein S, Frenking G (2009) Angew Chem Int Ed 48:9701
131. Wang Y, Xie Y, Wei P, King RB, Schaefer HF III, Schleyer PR, Robinson GH (2008) Science 321:1069
132. Wang Y, Robinson GH (2009) Chem Commun 2009:5201
133. Wolf R, Uhl W (2009) Angew Chem Int Ed 48:6774
134. Dyker CA, Bertrand G (2008) Science 321:1050
135. Sen SS, Jana A, Roesky HW, Schulzke C (2009) Angew Chem Int Ed 48:8536
136. Nagendran S, Sen SS, Roesky HW, Koley D, Grubmüller H, Pal A, Herbst-Irmer R (2008) Organometallics 27:5459
137. Sen SS, Khan S, Samuel PP, Roesky HW (2012) Chem Sci 3:659
138. Jones C, Bonyhady SJ, Holzmann N, Frenking G, Stasch A (2011) Inorg Chem 50:12315
139. Li J, Schenk C, Goedecke C, Frenking G, Jones C (2011) J Am Chem Soc 133:18622
140. Woodul WD, Carter E, Müller R, Richards AF, Stasch A, Kaupp M, Murphy DM, Driess M, Jones C (2011) J Am Chem Soc 133:10074
141. Woodul WD, Richards AF, Stasch A, Driess M, Jones C (2010) Organometallics 29:3655

142. Asay M, Inoue S, Driess M (2011) Angew Chem Int Ed 50:9589
143. Choong SL, Schenk C, Stasch A, Dange D, Jones C (2012) Chem Commun 48:2504
144. Rekken BD, Brown TM, Fettinger JC, Tuononen HM, Power PP (2012) J Am Chem Soc 134:6504
145. Protchenko AV, Birjkumar KH, Dange D, Schwarz AD, Vidovic D, Jones C, Kaltsoyannis N, Mountford P, Aldridge S (2012) J Am Chem 134:6500
146. Jones C, Bonyhady SJ, Nembenna S, Stasch A (2012) Eur J Inorg Chem 2012:2596
147. Spielmann J, Piesik DF-J, Harder S (2010) Chem Eur J 16:8307

Modern Developments in Magnesium Reagent Chemistry for Synthesis

Robert E. Mulvey and Stuart D. Robertson

Abstract Last year (2012) commemorated the 100th anniversary of the award of the Nobel Prize to Victor Grignard for his development of Grignard reagents (at the simplest level expressed as "RMgX", where R is an organic group and X is a halogen), one of the most widely utilised classes of synthetic reagent. A century on but only in the past decade or so has magnesium reagent chemistry entered a new and exciting phase, surpassing the limitations of what traditional Grignard reagents can do. Modern magnesium reagents have been designed to possess essentially comparable reactivity to their great rivals, organolithium reagents (traditional Grignard reagents are orders of magnitude less reactive than organolithium reagents), but at the same time to maintain the superior selectivity and broader functional group tolerance of their traditional ancestors. The key to the design of these new reagents is their multicomponent constitution with the organomagnesium engine powered by an activating alkali-metal additive, often a halide salt or another organometallic entity. This chapter outlines some of the most significant advances in this emerging field.

Keywords Alkali-metal · Deprotonation · Magnesiate · Synthesis · Turbo-Grignard Reagents

Contents

R.E. Mulvey (✉) and S.D. Robertson
Department of Pure and Applied Chemistry, WestCHEM, University of Strathclyde,
Glasgow G1 1XL, UK
e-mail: r.e.mulvey@strath.ac.uk

1   History: A Brief Glimpse

The use of magnesium reagents in organic synthetic chemistry can trace its roots back over 100 years thanks to the pioneering work of Grignard [1]. His eponymous centurion reagents [2], the development of which won this French chemist the Nobel Prize for Chemistry in 1912, have been used the world over for organic transformations. Grignard reagents are organomagnesium halides (at the simplest level of formula "RMgX") and are generally prepared by the insertion of magnesium metal into a polarised carbon–halogen bond as depicted in Fig. 1. They can consequently be used in nucleophilic addition reactions across unsaturated bonds, e.g. a carbonyl functionality, making them highly important reagents for controlled carbon–carbon bond formation.

Deprotonative metallation, the breaking of a C–H (or X–H) bond for the making of a more reactive and more synthetically useful C–M (or X–M; where X = e.g. N, O, S) bond, is typically the domain of hard alkali-metal reagents such as alkyl lithiums (R–Li) or lithium secondary amides (R_2N–Li) which have very polar, reactive metal–ligand bonds, moving towards but not quite reaching R^- carbanions or R_2N^- anions. Indeed, while Grignard's name is synonymous with organomagnesium chemistry, organolithium compounds could arguably be described as "Schlenk reagents" after their pioneer, the German chemist Wilhelm Schlenk, who, unlike Grignard, lost out on a Nobel Prize because the awarding committee did not believe organolithiums would ever be useful! [3] Schlenk's contributions in lithium chemistry have however been posthumously recognised by the Gesellschaft Deutscher Chemiker (GDCh, the German Chemists Association), who co-named a biennial award for excellence in the field of theoretical and practical lithium chemistry after him (the Arfvedson–Schlenk Award; with Johan Arfvedson, the Swedish chemist who discovered the element lithium in 1817). In organomagnesium chemistry, Schlenk is commemorated by the equilibrium reaction that disproportionates heteroleptic RMgX complexes into their homoleptic R_2Mg and MgX_2 component parts, work which was in fact carried out in conjunction with his son, Wilhelm Jr., as part of his Ph.D. studies [4].

The high reactivity of organolithium reagents can also be considered their Achilles heel since it means that they routinely have to be sedated by low
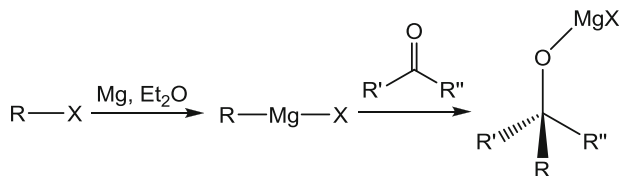
Fig. 1 Empirical preparation of a Grignard reagent and its addition across a carbonyl group
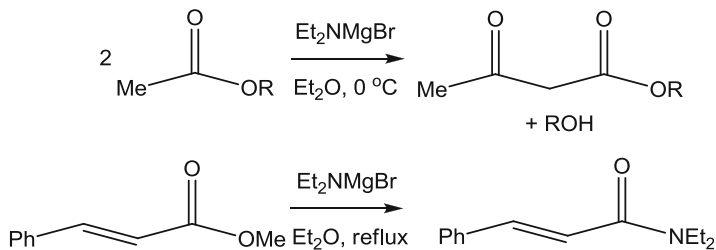
Fig. 2 Early reactions of Hauser using a secondary amido magnesium bromide reagent

temperature, they are often indiscriminate with regard to the site at which they metallate and they also display considerable intolerance towards certain synthetically important functional groups including ester, carbonyl, nitrile, halide and sulphoxide. However, organomagnesium reagents have more covalent, and hence less reactive, metal–ligand bonds meaning that they can display far superior functional group tolerance and considerably greater chemoselectivity; consequently they can generally be used at room temperature without fear of significant side reactions.

Early developments in the use of magnesium reagents for deprotonative metallation began in the late 1940s, when Hauser and co-workers made progress replacing the alkyl ligand of a Grignard reagent with a secondary amide, with the resultant products [(R$_2$N)MgX and (R$_2$N)$_2$Mg; the Hauser bases—although it should be noted that halomagnesium secondary amides were first mentioned as early as 1903 by Meunier [5], around the same time that Grignard was carrying out his own important magnesium studies] finding use in the self condensation of esters [6, 7] and in 1,2 or 1,4 nucleophilic additions to derivatives of cinnamic acid (Fig. 2) [8].

Research in this area advanced further in the 1980s and 1990s thanks largely to the innovation of Eaton and co-workers, of introducing the sterically demanding secondary amide 2,2,6,6-tetramethylpiperidide (TMP, by then a well-known amide in lithium chemistry thanks largely to the work of Olofson [9] and Lappert [10]; see Fig. 3 for its steric profile) into magnesium chemistry in the form of (TMP)MgBr which was shown to *ortho*-magnesiate carboxamides (Fig. 4) [11].

Mulzer then took this a step further, testing the chloro congener (TMP) MgCl and discovering that it was more effective than Eaton's reagent for the
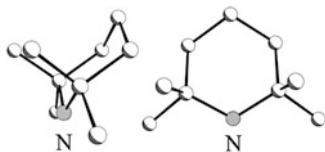
Fig. 3 Chair-form of the TMP anion (nitrogen atom shaded) emphasising the considerable steric protection of the anionic nitrogen centre by the methyl arms
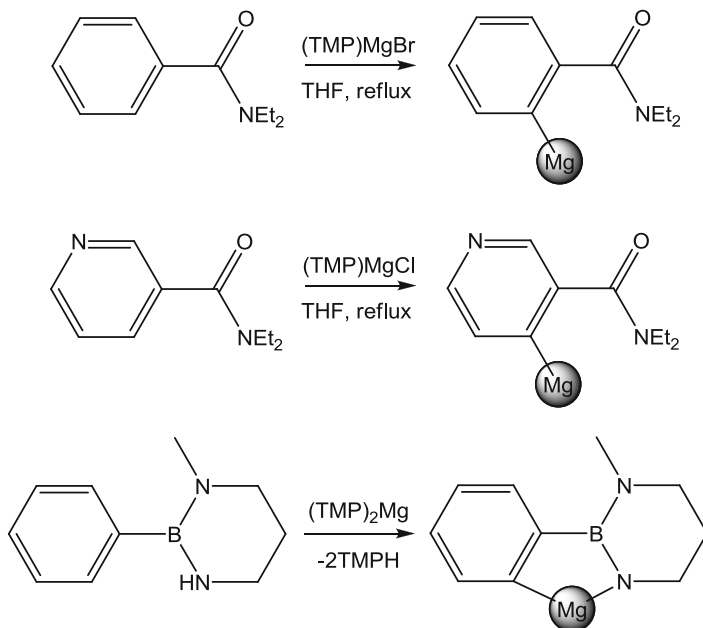
Fig. 4 Examples of TMP-magnesium reagents being used in selective deprotonation reactions

ortho-magnesiation of carbamates and pyridinecarboxamides (Fig. 4) [12]. Kondo, Sakamoto and co-workers then re-visited the diisopropylamido magnesium bases iPr_2NMgX (X = Cl, Br) and $(iPr_2N)_2Mg$, reporting their utility as selective deprotonating agents for phenylsulphonyl-substituted indoles (deprotonating exclusively at the 2-position) [13] and for heterocyclic thiophene and thiazole (again deprotonating exclusively at the 2-position) [14]. Thiazoles with substituents in 2- and 3-positions were also examined, with the 5-position being metallated. These reactions were carried out at room temperature in THF, with a twofold excess of base required; no di-metallation was ever witnessed despite this excess.

Compared to LiTMP, the bis-amido reagent $(TMP)_2Mg$ finds extremely limited use in synthetic transformations as it is a kinetically poor base. $(TMP)_2Mg$ does however have one considerable advantage, it is stable in refluxing THF and

Fig. 5 A representative example of directed *ortho* metallation
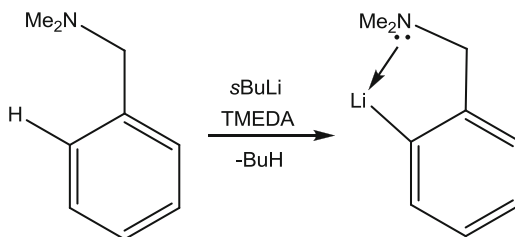
consequently can be utilised with poorly soluble/unreactive substrates. This reagent also displays tolerance of ester functionality as demonstrated by Eaton who *ortho*-magnesiated methyl benzoate at room temperature in <1 h [11]. Mulvey and co-workers deprotonated a methyl arm of lithium 1,1,1,3,3,3-hexamethyldisilazide (LiHMDS) with $(TMP)_2Mg$, resulting in a heterometallic, heteroleptic chiral complex of empirical formula $LiMg(TMP)[N(SiMe_3)(SiMe_2CH_2)]$ [15]. Also, in a recent paper by Kawachi et al., a diaminoborylbenzene was *intramolecularly ortho*-magnesiated with $(TMP)_2Mg$ (Fig. 4), with the solid-state structure revealing that the metallated intermediate is co-complexed with another molecule of $(TMP)_2Mg$ and then dimerises to give a tetramagnesiate [16], a common motif in magnesium structural chemistry.

A driving force for reactions such as these, whether by lithium or in a considerably more limited way by magnesium reagents, is the presence of an *ortho*-directing group—typically a functional group containing a Lewis basic heteroatom sometimes within a double or triple bond. In a protocol elaborated by Snieckus and Beak and known as directed *ortho* metallation (D*o*M) [17], the functional group plays a dual role in promoting the metallation reaction. This is achieved firstly through the complex induced proximity effect (CIPE), whereby the heteroatom's lone pair of electrons can act as an anchor point for the Lewis acidic metal reagent, holding it in place close to the *ortho* site to allow it to execute the deprotonation (Fig. 5). The second influence is through an inductive acidifying effect, whereby the electron withdrawing nature of the substituent increases the acidity of the nearest (*ortho*) hydrogen atom and has a stabilising influence over the resulting carbanion.

Magnesium reagents, which have less polar metal–anion bonds making them less reactive, are generally much less suited to deprotonating aromatic substrates. Furthermore, they can be poorly soluble in organic solvents, meaning that a large excess of base is required. The knock-on effect of this is that competing reactions between the excess base and any electrophile can complicate functionalisation of the metallated intermediate. Further complications involve bis-amido magnesium reagents acting as reducing agents (i.e. sources of hydride ion from organic frameworks), while the sluggish reactivity of these complexes often requires heating to induce reaction at reasonable rates. These negative points have recently started to be addressed by using a bimetallic (or more strictly a multicomponent) approach, that is, by combining the less reactive (softer) magnesium reagent with a more reactive (harder) alkali-metal reagent, with the resulting heterometallic complex seemingly displaying the beneficial properties of each of the component parts

Fig. 6 Synthetic protocols for forming Turbo-Grignard (**D**) and Turbo-Hauser reagents (**A**, **B** and **C**)

iPrCl + LiCl $\xrightarrow{\text{Mg}}$ iPrMgCl·LiCl (Turbo-**D**) $\xrightarrow{i\text{Pr}_2\text{N(H)}}$ iPr$_2$NMgCl·LiCl (Turbo-**C**)

iPrMgCl·LiCl (Turbo-**D**) $\xrightarrow{\text{TMP(H)}}$

(TMP)MgCl·LiCl (Turbo-**A**) $\xrightarrow{\text{LiTMP}}$ (TMP)$_2$Mg·2LiCl (Turbo-**B**)
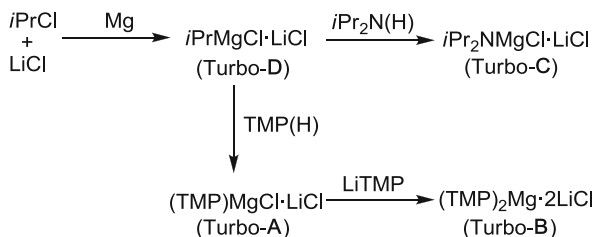
(alkali-metal reactivity; magnesium selectivity). There are currently two different general approaches by which this can be achieved, by incorporating the alkali-metal into the molecular framework either via a halide salt or alternatively via an organometallic reagent. These two distinct approaches are summarised in the following section.

2 Modern Advances Part One: The Halide Salt Method

2.1 Introduction

The first approach to modifying the reactivity of a magnesium reagent is through the addition of a stoichiometric amount of an alkali-metal halide salt. Lithium chloride (LiCl) appears often ideal for this role. Understanding the role and broad scope of application of LiCl "additives" in various aspects of s-block metal chemistry is undergoing somewhat of a renaissance recently with, for example, Collum demonstrating that addition of as little as 0.5 mol% LiCl can have a massive effect on reactivity in diverse reactions such as *ortho* lithiation of arenes directed by halogen containing directing groups [18] or nucleophilic addition of lithium diisopropylamide to unsaturated esters [19]. Within the context of alkaline-earth metal chemistry, at the most basic level the halide salt promotes solubility of the parent sterically hindered Hauser base in part due to decreasing aggregation, with the resultant heterometallic co-complex being utilised in polar THF solution. The best documented examples of such "Turbo-Hauser bases", so-called because of their increased reactivity with respect to the LiCl-free Hauser base, are the TMP containing bases (TMP)MgCl·LiCl (Turbo-**A**) and (TMP)$_2$Mg·2LiCl (Turbo-**B**). These "Turbo-Hauser" reagents, and the less sterically hindered congener (iPr$_2$N) MgCl·LiCl (Turbo-**C**), find use as selective metal-hydrogen exchange reagents and were originally designed as a follow-up to the "Turbo-Grignard reagent" iPrMgCl·LiCl (Turbo-**D**), which itself was initially prepared as a metal-halogen exchange reagent. Their synthesis is relatively facile; reagents Turbo-**A** and Turbo-**B** are prepared by treating reagent Turbo-**D** with R$_2$N(H) in THF for 24 h at room temperature, while reagent Turbo-**B** is simply prepared from Turbo-**A** and LiTMP. Turbo-**D** is initially prepared by reaction of metallic Mg with iPrCl in the presence of anhydrous LiCl (see Fig. 6 for full details).
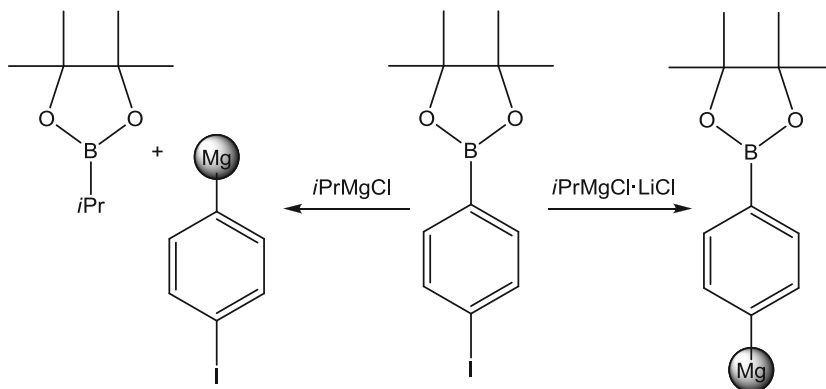
Fig. 7 Contrasting reactivity of *i*PrMgCl in the absence and presence of LiCl

2.2 Uses in Metal-Halogen Exchange Reactions

While Br/Li exchange is a relatively fast process and consequently needs to be carried out at low temperature, Br/Mg exchange is much slower, meaning heat must be applied which can induce competing side reactions with sensitive functional groups. Thus the use of Turbo-Grignard reagents in metal-bromine exchange reactions perfectly demonstrates the cooperative effects of having two different metals in one reagent, since they can be used successfully under a room temperature regime. Knochel first demonstrated this in the reaction of 4-bromoanisole with *i*PrMgCl·LiX (where X = Cl, Br, BF$_4$, ClO$_4$), also proving that LiCl is superior to other alkali-metal salt additives through systematically varying the salt component LiX [20]. The LiCl additive also modifies the selectivity, since *i*PrMgCl will react with a *para*-iodo dioxaborolane at the boronic ester functionality, yet *i*PrMgCl·LiCl will execute direct magnesiation via Mg/I exchange (Fig. 7) [21].

It is not only aromatic carbon–halogen bonds which are susceptible to metallation with a Turbo-Grignard reagent under mild conditions but also alkenyl (*sp*^{2} hybridised) carbon–halogen bonds. For example, as shown in Fig. 8, Knochel has extended the use of the reagent *i*PrMgCl·LiCl to the functionalisation of cyclic and acyclic alkenyl iodides such as 1-iodo-3-methylenecyclohex-1-ene and 1-iodo-oct-1-ene with retention of stereochemistry upon electrophilic quenching; importantly additional studies on related substrates showed that nitrile, halide and ester functionalities are all tolerated during this metallation (soft magnesiation) [22, 23].

2.3 Uses in Metal-Hydrogen Exchange Reactions

While the "Turbo-Grignard" reagents are proficient at metal-halogen exchange, the amide-based "Turbo-Hauser" reagents are more useful in selective metal-hydrogen
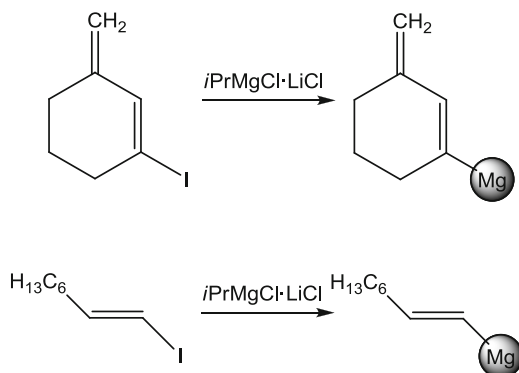
Fig. 8 Examples of metal-halogen exchange of olefinic substrates using Turbo-**D**
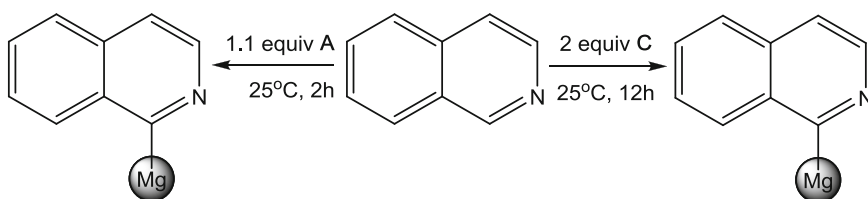
Fig. 9 Contrasting reactivity of Turbo-**A** and Turbo-**C** for direct magnesiation of isoquinoline
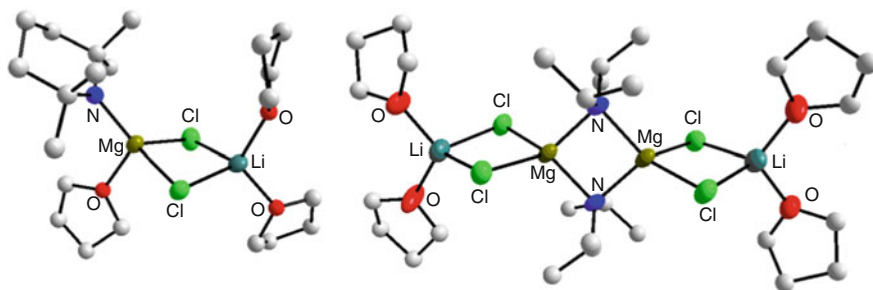
Fig. 10 Molecular structures of Turbo-**A** and Turbo-**C** with H atoms omitted for clarity

exchange, i.e. deprotonation reactions. Diisopropylamido reagent Turbo-**C** was discovered to be less reactive than its TMP counterparts Turbo-**A** or Turbo-**B** for deprotonative metallation reactions due at least in part to its lower solubility. This reactivity difference was established by the deprotonation of isoquinoline: only 2 h at room temperature are required with 1.1 molar equivalents of reagent **A**, while 12 h and 2 molar equivalents of reagent **C** are needed for comparable (>90 %) metallation efficiency (Fig. 9) [24].

This difference in solubility and reactivity can be attributed at least in part to differing aggregation states, proven by the elucidation of solid-state structures (Fig. 10) which show Turbo-**A** to exist in a dinuclear arrangement [25], while

Fig. 11 Contrasting sites
of metallation using a
homometallic or
heterometallic reagent
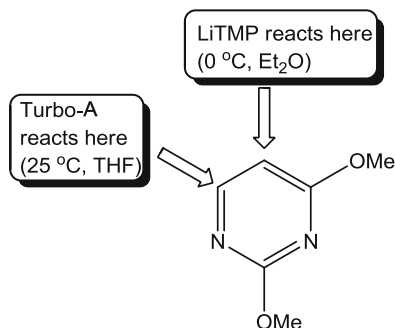
Turbo-**C** adopts a dimeric, tetranuclear motif [26]. A diffusion ordered spectros-
copy (DOSY) NMR study revealed however that these molecular constitutions are
not retained in the solution state, with the presence of solvent-separated ion pairs
(ates—believed to be $[Li(THF)_4]^+[RMgCl_2 \cdot (THF)_x]^-$) seemingly being responsible
for the observed reactivity.

Of course other factors are also partly responsible for this differing reactivity,
most obviously the steric and electronic make-up of the active base as TMP is a
more reactive base than diisopropylamide with the pK_a of TMP(H) (37.3) being
greater than that of DA(H) (35.7) [27]. However, it should be stressed that caution
must be applied when considering pK_a values of metal bases as the final value is a
function of not only the metal in question, but also of solvent, concentration and
temperature.

The principal advantages of the bases described thus far are their high kinetic
basicity, coupled with good solubility, high chemoselectivity and improved func-
tional group compatibility compared to homometallic organo-alkali-metal or mag-
nesium bases. Routinely they are utilised in the temperature range of −20 to 25 °C
which is a particularly desirable feature for the synthetic chemist and for the process
chemist. Selectivity and room temperature compatibility are clearly illustrated
by the example of the sensitive ether-functionalised heterocycle 2,4-
dimethoxypyrimidine which is metallated preferentially at the 5-position by
LiTMP in diethyl ether at 0 °C [28] but at the 6-position by Turbo-**A** at room
temperature in THF solution [29] (Fig. 11).

The applicability of Turbo-Hauser **A** towards aromatic substrates is expertly
proven by the susceptibility of the substituted aromatic ethyl 3-chlorobenzoate to
undergo four consecutive direct magnesiations/electrophilic quenches to yield a
hexasubstituted benzene derivative (Fig. 12) [30]. The second metallation requires
careful choice of solvent; in neat THF a competitive deprotonation occurs in a
90:10 ratio in favour of the desired product, which can be improved to a near
quantitative level of 98.5:1.5 ratio by employing the less polar THF/Et$_2$O (1:2)
mixture. It should also be noted that the third and fourth metallations must be
carried out at −50 °C, reflecting the greater sensitivity of the multi-functionalised
benzenes.

In the absence of electron-donating functionality on the heteroatomic ring,
electron-deficient pyridine rings are generally challenging to metallate with
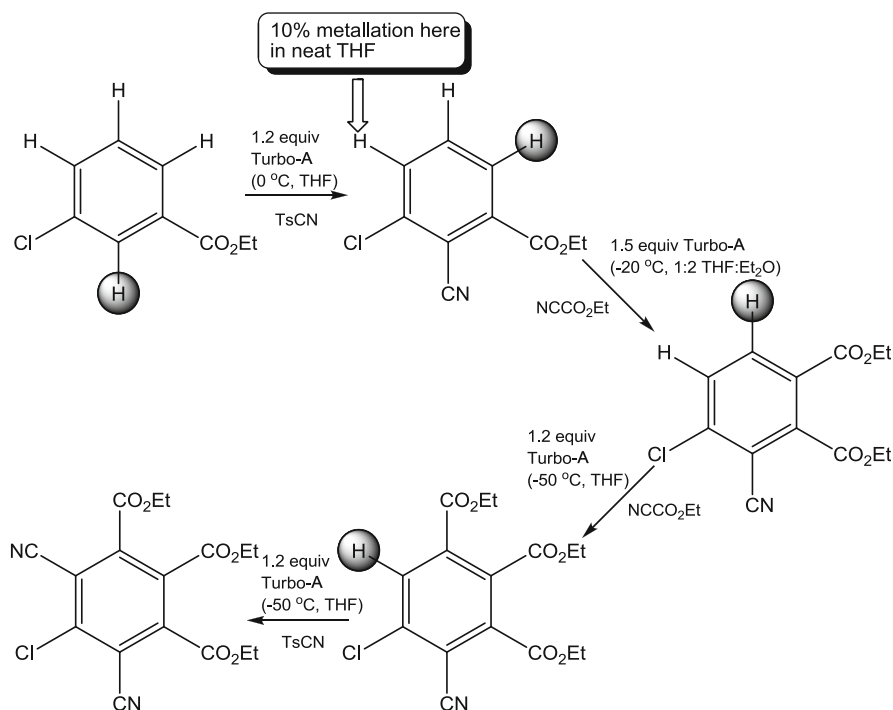
Fig. 12 Reaction sequence using Turbo-**A** multiple times to give a hexasubstituted benzene

conventional lithium containing reagents. However this challenge can be met by employing Turbo-**A** in THF solution resulting in the formation of functionalised pyridines in high yield. Non-activated pyridines can also be metallated by a slightly modified derivative of Turbo-**A**, whereby Lewis acidic BF_3 is incorporated into the base to generate the Lewis acid–Lewis base multicomponent complex TMPMgCl·BF_3·LiCl (**A**·BF_3) [31]. The presence of the Lewis acidic BF_3 clearly plays an important role through pre-complexation to the substrate as demonstrated by the reaction of heterocyclic 3-fluoropyridine. This substrate is metallated at the 2 position with Turbo-**A** on its own; however, in the additional presence of BF_3 direct magnesiation switches exclusively to the more remote 4-position (Fig. 13).

Other important direct magnesiations of aromatic substrates with Turbo-Hauser **A** carried out by Knochel and co-workers include key steps in the preparation of the NK3 receptor antagonist "talnetant" [32] and the fungicide "mepanipyrim" [33] (Fig. 14). Knochel has also expertly applied reagent **A** in direct magnesiation reactions of various thiophene containing units, an important subunit within pharmaceuticals, for example, by carrying out four consecutive magnesiations to yield a tetrasubstituted derivative [34]. The more complex thienothiophene subunit, which boasts applications in materials chemistry due to its conjugated π system, can also be magnesiated directly with Turbo-**A**, while this protocol can be applied for the preparation of linear oligomeric thienothiophene molecules (Fig. 14) [35]. Mori has also recently used Turbo-**A** as well as the bromo congeners (TMP)MgBr·LiBr
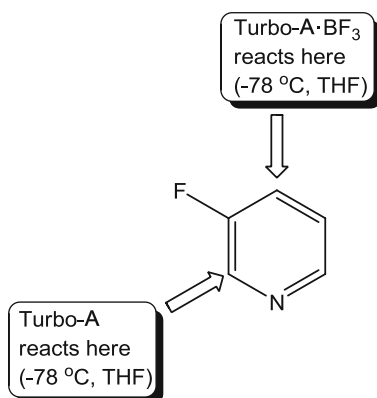
Fig. 13 Contrasting reactivity of Turbo-**A** in the presence and absence of BF$_3$
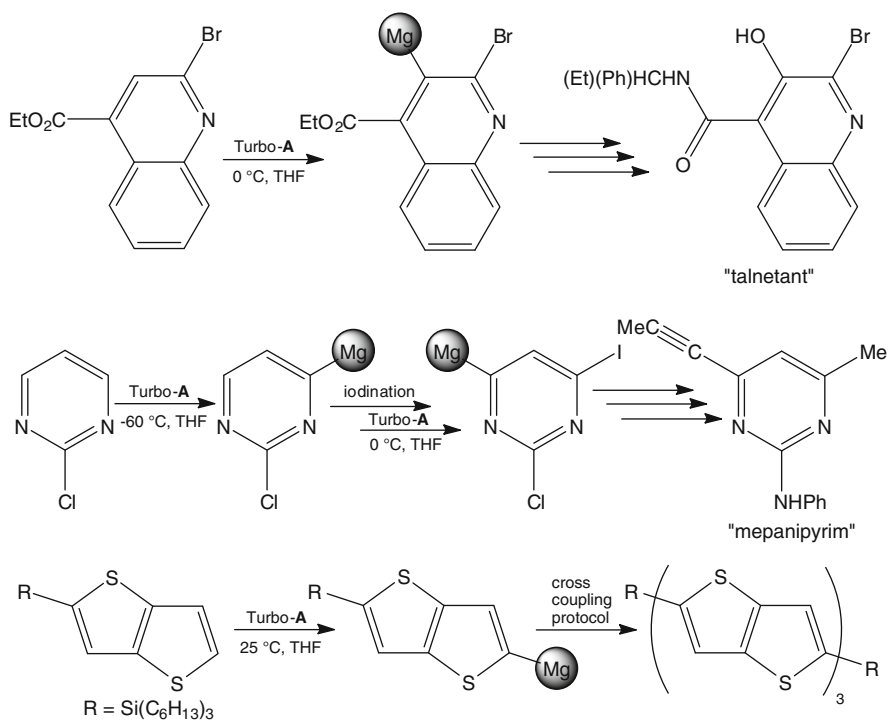
Fig. 14 Representative synthetic applications of Turbo-**A**

and (TMP)$_2$Mg·2LiBr as selective deprotonating agents with substituted thiophenes to efficiently prepare well-defined head-to-tail oligomers [36, 37].
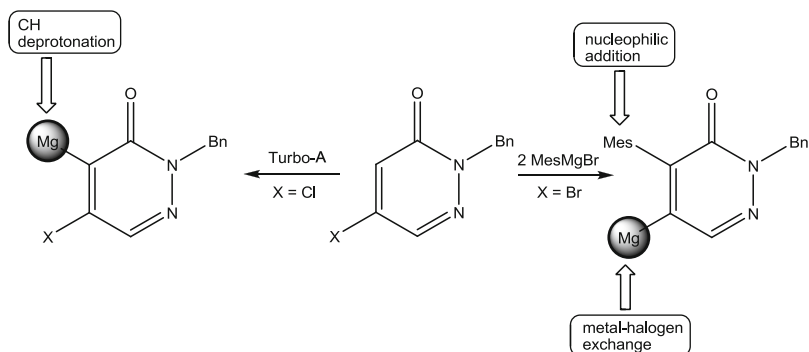
Fig. 15 Contrasting reactivity of Turbo-**A** vs. a conventional Grignard reagent
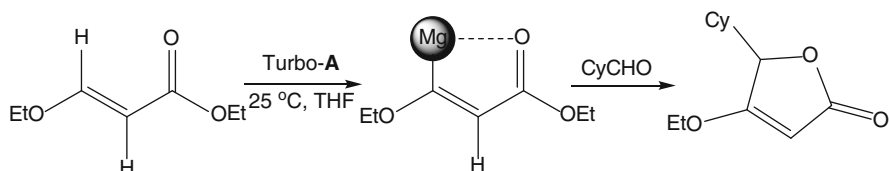
Fig. 16 Direct magnesiation of an olefinic substrate using Turbo-**A**

The synthetic utility of reagent **A** has also been exploited by Maes and co-workers, who have studied its reaction with pyridazin-3(2H)-ones (Fig. 15) [38]. Interestingly C4 deprotonation was achieved with 5- and 6-halogenated derivatives using Turbo-**A**, while in contrast nucleophilic addition and magnesium-halogen exchange (order and mechanism not specified) were witnessed with 2 molar equivalents of the classical Grignard reagent MesMgBr.

The excellent direct magnesiating properties of Turbo-Hauser reagent **A** extends beyond the confines of aromatic substrates (though these are by far the most frequently encountered substrates in such transformations). For example, the ether-functionalised ester, ethyl 2-ethoxyacrylate, can be selectively magnesiated in a reaction favoured by the stabilising effect of the adjacent carbonyl group, with work-up of the reaction mixture affording a non-aromatic cyclic lactone in an excellent yield (Fig. 16) [39].

The importance of LiCl activation is emphasised by Urabe and co-workers, who demonstrated that nucleophilic substitution of a hydride anion by CH_2Ph in a phenylsilane substrate can be achieved in a considerably greater yield using $PhCH_2MgBr$ in the presence of a stoichiometric amount of the lithium salt (Fig. 17) [40]. Interestingly, the amount of LiCl could be reduced to only 5 mol% without a decrease in conversion when compared to the stoichiometric reaction.

In cases where a stronger base than Turbo-**A** is required (generally when the organic substrate has a high pK_a value), the bis-amido Hauser reagent $(TMP)_2Mg \cdot 2LiCl$ (**B**), equipped with two active base units, can be employed. Its enhanced reactivity (higher kinetic basicity) is demonstrated indirectly by the
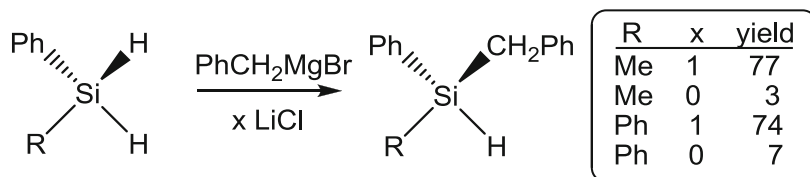
Fig. 17 Influence of LiCl on the silylation of a Grignard reagent

R	x	yield
Me	1	77
Me	0	3
Ph	1	74
Ph	0	7
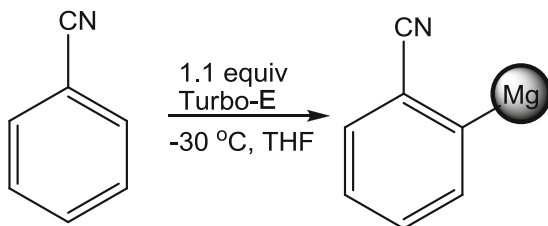
Fig. 18 Direct *ortho*-magnesiation of benzonitrile using Turbo-**E**

fact that it is only stable for 24 h at room temperature in THF solution, while beyond this time a considerable decrease in reactivity is witnessed, at least in part to ring cleavage of THF. The less sterically hindered bis-amido reagent [(*t*Bu) (*i*Pr)N]$_2$Mg·2LiCl (Turbo-**E**) does not suffer from such a reactivity decrease, maintaining its activity after 21 days in THF at 4 °C. Knochel has utilised Turbo-**B** for direct *ortho*-magnesiation in the synthesis of 6-hexylsalicylic acid, a component of the essential oil of *Pelargonium sidoides* DC [41], while Turbo-**E** will directly magnesiate benzonitrile in THF at −30 °C in only 3 h (Fig. 18) [42].

Like reagent **A**, Turbo-Hauser **B** is an effective magnesiating agent for non-aromatic, olefinic substrates. A lactone, a piperidine [39] and a camphor derivative [43] have all been smoothly magnesiated using Turbo-**B** in <30 min in the temperature range −30 °C to +25 °C with functionalisation of the magnesiated intermediate giving the final product in good to excellent yield (Fig. 19).

Knochel has recently reported a number of other heterometallic magnesium containing bases such as the heterotrimetallic co-complexes (TMP)$_2$Zn·2MgCl$_2$· 2LiCl, (TMP)$_2$M·2MgCl$_2$·4LiCl (M = Mn [44], Fe [45]) and (TMP)$_4$Zr·4MgCl$_2$· 6LiCl [46]. However, these only incorporate the alkaline-earth metal seemingly as a solubilising salt additive in the form of MgCl$_2$ while the metallation appears to be actually carried out by the TMP-bound metal and as such these complexes, the structures of which are unknown, fall beyond the scope of the present discussion. We do note here however that MgCl$_2$ has a profound role to play since its absence in, for example, (TMP)$_2$Zn·2LiCl greatly reduces the reactivity of the co-complex [47].
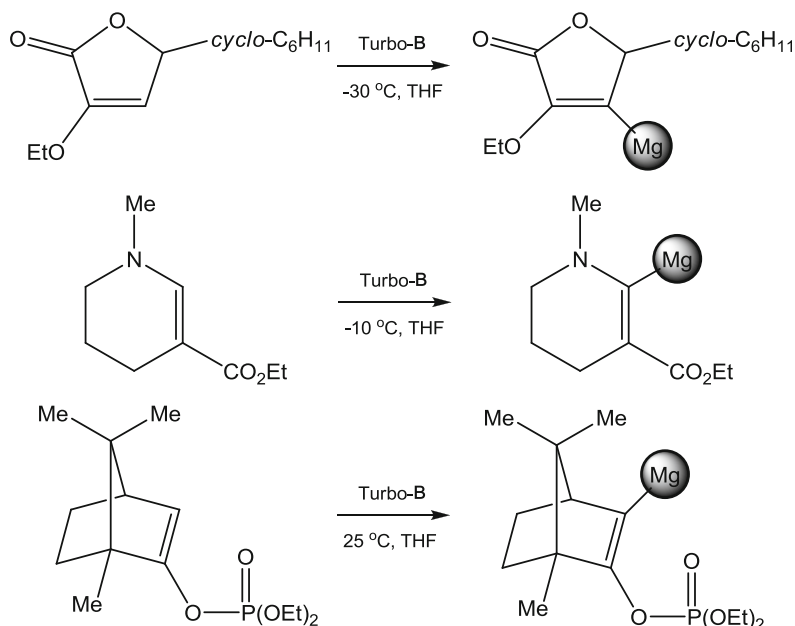
Fig. 19 Direct metallation of olefinic substrates with Turbo-**B**

3 Modern Advances Part Two: The Organic Anion Approach

3.1 Introduction

A second, complementary method for activating magnesium reagents also involves the use of an alkali-metal additive, but rather than utilising this in the form of a halide salt, an organo-alkali-metal reagent is preferred. While the application of these complexes has flourished over the past 10 or so years, they too can trace their routes back a long time (1951) when another pioneer of magnesium chemistry, Georg Wittig, reported the first lithium magnesiate, "LiMgPh₃" [48]. Incidentally, Wittig succeeded Schlenk as head of organic chemistry at the University of Tübingen. However, unlike his predecessor, Wittig became a Nobel Laureate (1979) albeit not for his contribution to s-block chemistry [49]. Wittig coined the name "ates" to distinguish these complexes from classical organomagnesium and organolithium complexes and noted the reactivity of the central metal (in this case Mg) was due to a special "anionic activation". In particular, he noted the contrasting reactivity of his ate complex LiMgPh₃ against that of its homometallic component LiPh since the former gives mainly 1,4 addition to benzalacetophenone, while the latter favours 1, 2 addition. The "ates" descriptor was reinforced by Wittig's student Tochtermann, who published the first review of ate complexes in 1966, 15 years after their initial discovery [50]. Coates and Heslop of the University of Durham
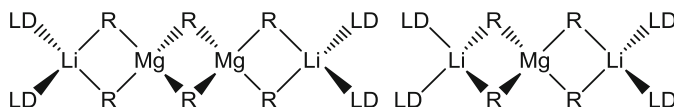
Fig. 20 Generic Weiss-motifs of lower order (*left*) and higher order (*right*) lithium magnesiates (R = alkyl anion, LD = neutral Lewis Donor)

were also among the first researchers to note cooperative effects between the different metals in ate formulations [51]. On mixing *n*BuLi with Me$_2$Mg in solution, they insightfully reasoned that the resulting species "is clearly not simply a mixture of the starting materials, as is evident from the much enhanced solubility of dimethylmagnesium in ether solutions of butyl-lithium". It was also around this time that the development of stoichiometric variant "higher order" alkali-metal magnesiates occurred (i.e. alkali-metal-rich compounds of general formula M_xMgR_{2+x}, $x > 1$). Seitz and co-workers carried out ^{1}H and ^{7}Li NMR studies to identify the higher order species present in ethereal mixtures of MeLi and Me$_2$Mg [52] since Hurd had previously identified higher order complexes in closely related alkali-metal alkyl zincates [53]. Seitz observed at least three different higher order magnesiates in solution in rapid equilibrium, with $x = 2$, 3 and 4. Since these early but crucial observations, structural studies have contributed significantly to a greater understanding of such complexes with both contacted ion and solvent-separated derivatives possible. Principal in making such distinctions was Weiss and co-workers, who identified that the contacted ion structures preferred a linear arrangement of metals connected by bridging anions, with tetrahedral strongly Lewis acidic magnesium in the central positions and the alkali-metal occupying the outer region, solvated by a neutral Lewis donor in many cases [54]. Two examples of these so-called *Weiss motifs* are depicted in Fig. 20.

It is common though not always the case that higher or lower order variations of magnesiates can be synthesised by simply varying the ratio of organomagnesium to organo-alkali-metal reagent in the reaction mixture. Alkali-metal magnesiates can be prepared in various ways. The best known general methods are co-complexation of the parent diorganomagnesium and organo alkali-metal complexes or salt metathesis of a Grignard reagent/magnesium dihalide with an organo alkali-metal reagent, as shown in Fig. 21.

The former co-complexation method is the most suitable for preparing heteroanionic magnesiates, while the latter is more suited to homoanionic magnesiates. By simply varying the stoichiometry of the chosen starting materials, either higher or lower order magnesiates can be obtained. Considering the variation possible in the identity of the organic anions (alkyl, aryl, amido, alkoxy, for example) and any neutral Lewis donors, it is clear that a vast array of possibilities and permutations exist for alkali-metal magnesiates in general.

Fig. 21 Common
preparative routes to alkali-
metal magnesiates
(M = alkali-metal)

$$R_2Mg + x \, RM \longrightarrow M_xMgR_{2+x} \quad \text{co-complexation}$$

$$RMgCl + x \, RM \longrightarrow \left. \begin{array}{c} M_{x-1}MgR_{1+x} \\ + \\ MCl \end{array} \right\}$$

$$MgCl_2 + x \, RM \longrightarrow \left. \begin{array}{c} M_{x-2}MgR_x \\ + \\ 2 \, MCl \end{array} \right\} \text{metathesis}$$
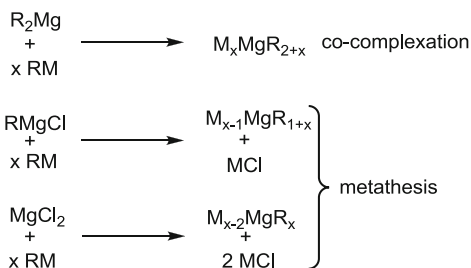
3.2 Uses in Metal-Halogen Exchange Reactions

As alluded to earlier, lower order magnesiates, where in general the alkali-metal-to-magnesium ratio is unity, have been known since Wittig first described LiMgPh$_3$ in 1951. In the intervening years a number of variations have been described and their utility in synthetic transformations studied in depth. Similar to the heterometallic halide salt magnesiates described in Sect. 2, the alkali-metal alkyl magnesiates can be efficient agents for metal-halogen exchange. Oshima and co-workers have demonstrated this utility in a variety of reactions involving homo- or heteroleptic lithium alkyl magnesiates with halo-substituted aromatics [55]. They found that the ate formed upon mixing nBuLi with nBu$_2$Mg, LiMgnBu$_3$, smoothly carries out metal-halogen exchange on aryl halides at 0 °C in high yield with tolerance of a variety of functionality including ester, amide or cyano groups. They also discovered that the heteroleptic variant LiMgiPrnBu$_2$ displays greater reactivity than the homoleptic butyl congener since the former could react even at −78 °C, while the latter could not [56]. Jain and co-workers similarly utilised LiMgiPrnBu$_2$ in metal-halogen exchange of *meta*- and *para*-halogenated phenols and ϖ-phenoxyalcohols with no evidence of *ortho*-deprotonation occurring [57].

Trisalkyl lithium magnesiates can also be utilised for selective functionalisation by carefully tuning the stoichiometry, reaction conditions or identity of the alkyl groups. For example single metal-halogen exchange of homo- or hetero-dihalogenated aryl substrates is possible (reaction occurring preferentially at the iodo functionality in hetero-dihalogenated examples: see Fig. 22a). Double metal-halogen exchange of *para*-diiodobenzene was accomplished by Oshima and co-workers using 1 molar equivalent of LiMgnBu$_3$, but single metal-halogen exchange could be achieved by using the less reactive bis-methyl modification LiMgnBuMe$_2$ (Fig. 22b). However the tris-butyl reagent LiMgnBu$_3$ can only carry out single metal-halogen exchange on *para*-dibromobenzene (Fig. 22c).

On moving to *ortho*-dibromobenzene, single metal-halogen exchange occurs; however, the resulting complex with a bromide and metal adjacent to one another is set up to form benzyne via a 1,2 elimination reaction.

Mongin and co-workers have also utilised LiMgBu$_3$ in magnesium-halogen exchange reactions with 2- , 3- and 4-bromoquinoline [58], successfully trapping the magnesiated intermediate with a variety of electrophiles in good yields and also

Fig. 22 Selected examples of the use of lithium alkyl magnesiates in metal-halogen exchange reactions with aryl halides
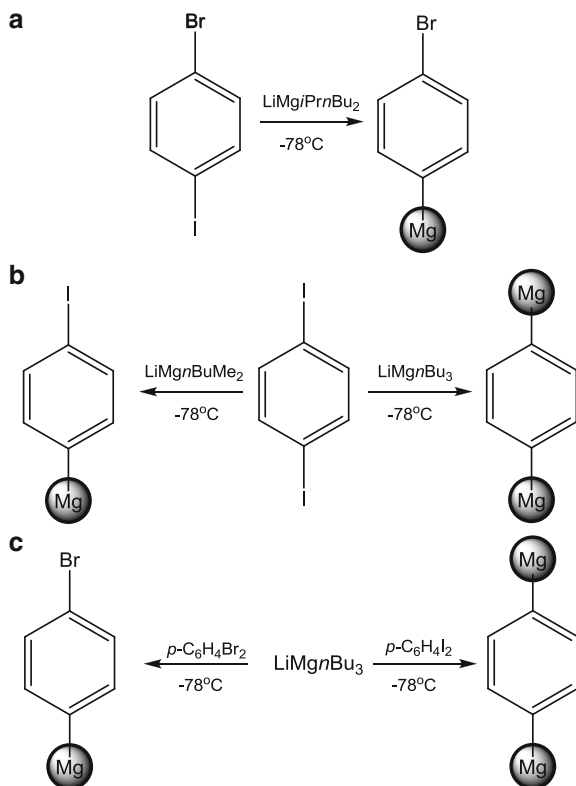
executing the first cross-couplings with lithium triarylmagnesiates to yield polyaromatic heterocyclic organic species [59, 60]. Only mild reaction conditions were typically required for such reactions (namely THF or toluene solution, $-10\,°C$, 2–3 h).

Iida and Mase have demonstrated the importance of solvent choice in their metal-halogen exchange reactions between $LiMgBu_3$ and 2,6-dibromopyridine [61]. Single magnesium-bromine exchange occurs in both THF and toluene when a 1:1 stoichiometry of metal reagent and substrate is employed. However, when an excess of reagent is utilised in THF solution double metal-halogen exchange takes place. Interestingly, on switching to toluene solution only a single exchange reaction occurs even in the presence of excess lithium magnesiate.

Gros and co-workers have recently studied the use of a lithium magnesiate reagent containing a chiral dianionic ligand for enantioselective synthesis [62,63]. In their approach both lower and higher order LiMgBu(chiral-dianion) and Li_2MgBu_2(chiral-dianion) species execute metal-halogen exchange with 2-bromopyridine as the substrate just as efficiently as homoleptic lithium butyl magnesiates. Quenching such magnesiated intermediates with a variety of aldehydes provides a route to chiral alcohols. They also found that (R,R)-TADDOL
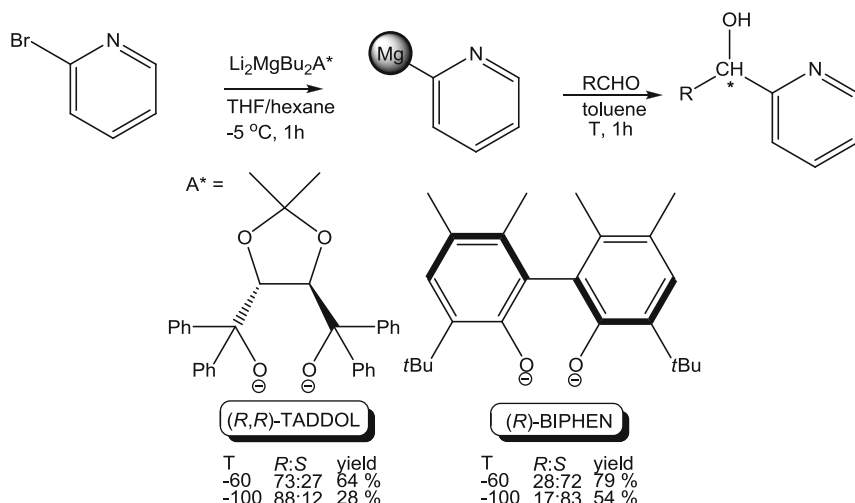
Fig. 23 The utilisation of chiral dianions in ate formulations for enantioselective synthesis

or (R)-BIPHEN were the optimum ligands for asymmetric addition (Fig. 23). Interestingly the former favours the R enantiomer (optimum enantioselectivity 88:12), while the latter favours the S enantiomer (17:83). Such optimum enantioselectivity required cryogenic conditions (-100 °C) and resulted in a diminished yield with respect to that obtained on increasing the temperature to -60 °C. While the enantioselectivity and yields are not ideal, this research represents a promising start for future development in asymmetric synthesis.

Alkali-metal alkyl magnesiates can also be effective for carrying out metal-halogen exchange of aliphatic substrates. An example is provided by Oshima who effected metal-bromine exchange of dibromomethylsilanes with $LiMgBu_3$ at low temperature (-78 °C) in THF (bottom pathway, Fig. 24) [64]. Warming the solution to room temperature resulted in (copper catalysed) alkyl migration with resulting electrophilic quenching yielding α-functionalised α-silyl pentane. A different reactivity was witnessed for the methyl homologue $LiMgMe_3$, with only the monomethylated bromo product being observed [65]. This distinction was attributed to the greater reactivity of intermediate A over $LiMgMe_3$, meaning that A preferentially abstracts a bromine atom from $R_3SiCHBr_2$ to generate the monomethylated product as demonstrated in the top pathway of Fig. 24.

The utility of these trisalkyl lithium magnesiates for metal-halogen exchange has also been exploited for the functionalisation of copolymerised bromopolystyrene beads [66].

Lithium magnesiate $LiMgBu_3$ has been used for the smooth magnesium/bromine exchange of 5-bromo-2-methoxypyridine as an entry to the biologically active 5-substituted-2-methoxypyridines at 0 °C in THF, obtaining the desired electrophilically quenched products in reasonable yield [67]. This protocol displayed
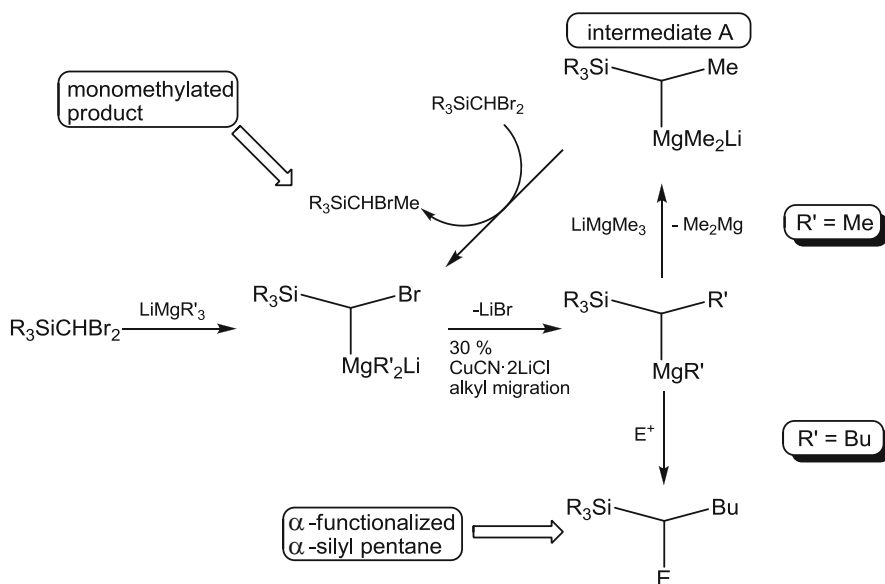
Fig. 24 Contrasting reactivity of butyl vs. methyl lithium magnesiates in metallation reactions of dibromomethylsilanes

one of the major advantages of a lithium magnesiate, namely its effective utilisation at more user-friendly temperatures, since the analogous lithium/bromine exchange with homometallic organolithium reagents typically requires a subambient temperature range in the same solvent.

While the majority of metal-halogen exchange reactions using $LiMgR_3$ are carried out in situ and then followed by electrophilic interception to provide new organic substrates, Oshima has also demonstrated the ability of the metallated intermediates to undergo $TiCl_4$ mediated homocoupling to yield bis-aryl species in good yield under mild conditions [68].

3.3 Polymerisation

An alternative use of alkali-metal alkyl magnesiates is as initiators of polymerisation. For example, in very early work Morton discovered that the sodium magnesiate $NaMgBu_3$ can be utilised for the polymerisation of styrene with predictable molecular weights and narrow polydispersity [69]. Hsieh and co-workers also found that $LiMgBu_3$ can be similarly exploited for the polymerisation of butadiene, noting too that the homometallic Bu_2Mg could not execute this effect on its own and that it was the presence of lithium which synergistically caused participation and activation of the carbon–magnesium bonds [70]. Since these initial discoveries, the scope of lithium magnesium reagents which can successfully
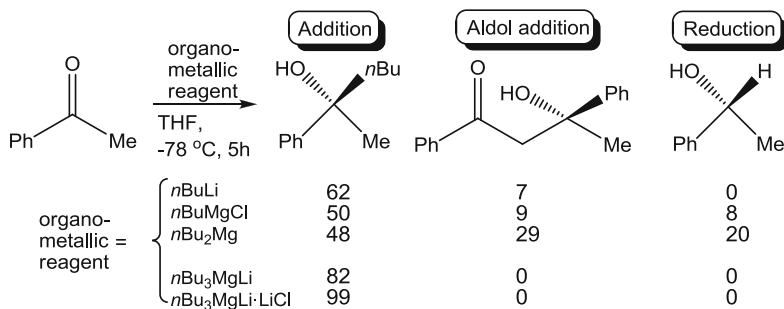
Fig. 25 Comparison of various metallic reagents in their reactions with acetophenone

initiate polymerisation has broadened with heteroleptic alkyl/alkoxide and alkyl/phenoxide both being successfully used for this purpose. The former yielded isotactic-rich polystyrene (homometallic congeners contrastingly gave syndiotactic-rich polystyrene) [71], while the latter gave isoselective polymerisation of methyl methacrylate [72]. Mulvey has also successfully applied the intriguing potassium (amido) magnesiate $[(toluene)_2K(ferrocene)_2]^+$ [Mg $(HMDS)_3]^-$ (obtained from reaction of $KMg(HMDS)_3$ with ferrocene) as an initiator for the polymerisation of methyl methacrylate. The counter-cation seemingly plays an important role here as the high syndiotacticity content (84 %) of the polymer cannot be replicated with either $KMg(HMDS)_3$ or KHMDS (44 and 31 %, respectively) [73].

3.4 Magnesiates as Nucleophile Sources

Alkali-metal alkyl magnesiates also find use as sources of nucleophilic alkyl anions. At the forefront of this research is Ishihara who demonstrated that $LiMgnBu_3$ adds to a ketone in THF at $-78\,^\circ C$ with superior yields to that obtained when using any of the homometallic reagents $nBuLi$, $nBuMgCl$ or nBu_2Mg [74]. No side products from reduction or aldol addition reactions were witnessed unlike in the case of the homometallic reagents (see comparison in Fig. 25). In a protocol similar to that discussed in Sect. 2, it was also noted that stoichiometric amounts of LiCl increased the yield further to 99 %. Heteroleptic ates (e.g. the mixed alkyl $EtMe_2MgLi$) react selectively with the ethyl group preferentially being involved in the C–C bond formation.

Nucleophilic allylation has been achieved by Sośnicki using the generic heteroleptic allyl/bis-alkyl lithium magnesiate $LiMgBu_2(allyl)$ [75]. The substrates studied contained a piperidine ring as the common central motif, with a variety of N-substituted derivatives (e.g. N-lithio, N-alkyl, N-aryl, N-allyl) being the focus of attention. Allylation typically occurs at the 6-position (Fig. 26) although the allyl group is also found on occasion at the 4-position as a result of an intramolecular Cope rearrangement which is strongly dependent on choice of reaction temperature
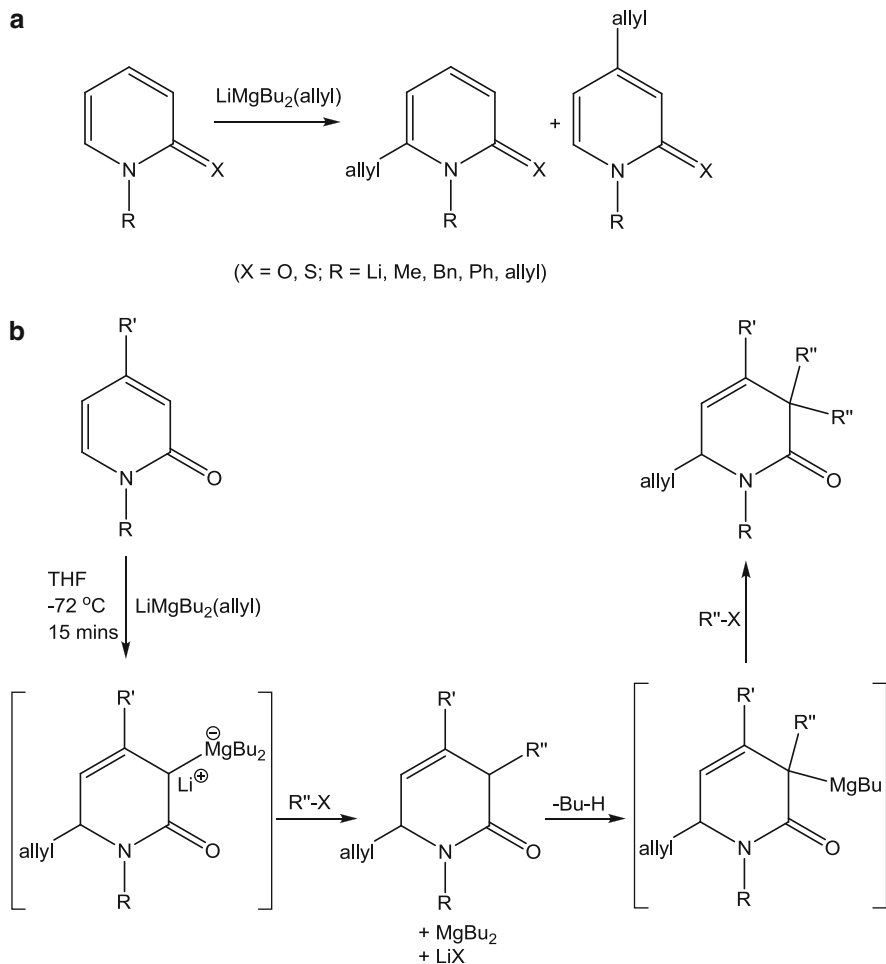
Fig. 26 Allylation reactions using a lithium magnesiate reagent

and solvent. Various stoichiometries were studied with an (allyl)MgCl, 2 BuLi combination [i.e. an "ate" formulation of $LiMgBu_2$(allyl)] proving optimum [76]. Ring closing metathesis of the 6-allylated derivative has consequently been employed as a useful synthetic route to access the important quinolizidine skeleton [77].

Sośnicki and Struk were also able to apply their allyl/alkyl lithium magnesiate base in a one-step symmetrical double alkylation of lactams at the challenging carbon site adjacent to the carbonyl group [78]. The dual alkylation was assigned to the reactivity of Bu_2Mg which was believed to be extruded after the first alkylation but is basic enough to execute a second magnesiation (Fig. 26b).

Fleming elegantly demonstrated the beneficial cooperative effects between magnesium and lithium in the reaction of a cyano containing alkylmagnesium
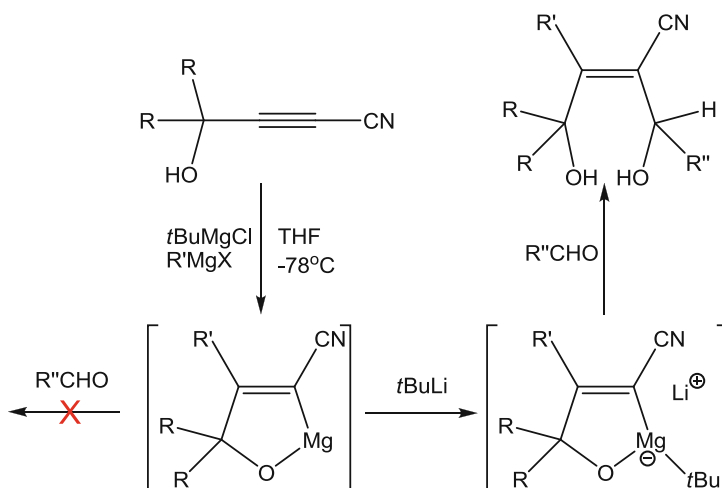
Fig. 27 Lithium promoted reaction of a magnesiated substrate with an aldehyde

x	yield
0	-
1	7
2	54
3	82
4	78
5	63
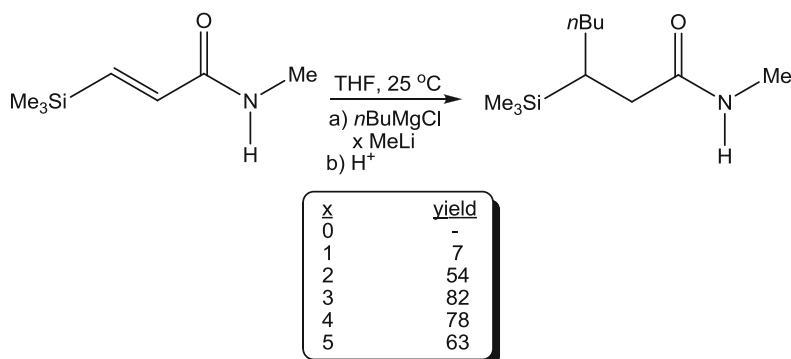
Fig. 28 Effect of Grignard/organolithium reagent ratio for a Michael addition reaction

alkoxide with an aldehyde [79]. The magnesium species was found to be inert towards alkylation with RCHO; however, when tBuLi was added prior to the aldehyde the alkylation reaction proceeded [80]. This modified reactivity was assigned to the in situ formation of an intermediate ate complex (Fig. 27).

Michael addition of Grignard reagents to α,β-unsaturated amides and carboxylic acids has been the subject of a study by Asaoka [81]. For example, no evidence of a Michael addition product between 3-(trimethylsilyl)acrylamide and nBuMgCl was forthcoming in THF at room temperature; however, activating the Grignard reagent with MeLi allowed this reaction to proceed. A variety of different Grignard reagent: MeLi ratios were studied with 1:1 giving only a modest yield (7 %). By adding a two- to fivefold excess of MeLi the yield was improved substantially, suggesting participation of an ate complex (Fig. 28).

Fig. 29 Regioselective magnesiations of 5- and 6-membered heterocycles using a trisalkyl magnesium base. Note only the position of magnesiation is indicated, not the full formula of the putative products
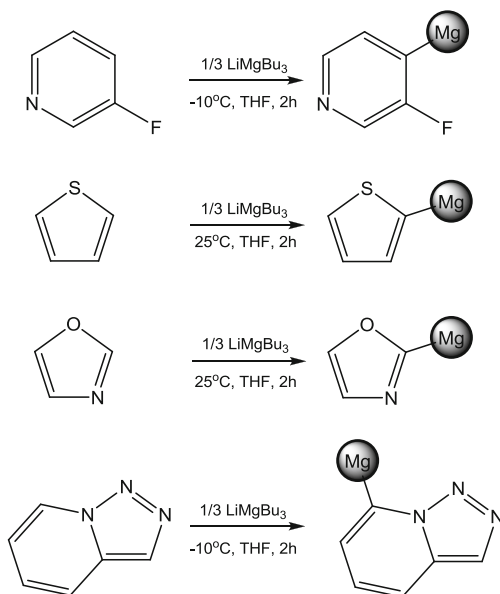
3.5 Uses in Metal-Hydrogen Exchange Reactions

One of the most useful applications of alkali-metal alkyl magnesiates is in selective deprotonative magnesiation (C–H to C–Mg exchange) of organic substrates. A major player in this research is Mongin who has studied the applicability of LiMgBu$_3$ with a variety of organic substrates. In particular, she discovered that this base can tolerate halogen functionality in, for example, 3-fluoropyridine, with magnesiation occurring at the 4-position (Fig. 29) which is in contrast to that witnessed with BuLi/Lewis donor in Et$_2$O which metallates preferentially at the 2-position (Lewis donor = TMEDA or diazabicyclo(2.2.2)octane—DABCO) [82]. The yield of electrophilically quenched product (using 3,4,5-trimethoxybenzaldehyde) was boosted from 55 to 74 % by the presence of the bidentate neutral Lewis donor TMEDA. Thiophenes [83], oxazoles [84] and [1,2,3] triazolo[1,5-*a*]pyridines [85] were likewise regioselectively deprotonated using this in situ base mixture. Interestingly, the reactivity of the thiophenes was also boosted by TMEDA involvement while that of the other two heterocyclic classes were not. Also good for atom efficiency, only 1/3 of an equivalent of LiMgBu$_3$ is required for these metallation reactions, suggesting that the base reacts through all three of its anionic alkyl arms.

Mulvey, Hevia and co-workers found a similar reactivity (i.e. reactivity via all of its butyl anions) in their C-metallation of 1-methylindole with the higher order sodium magnesiate Na$_2$MgBu$_4$·2TMEDA crystallographically characterising the product of a 4:1 stoichiometric reaction as the Weiss motif Na$_2$Mg(indol-2-yl)$_4$·2TMEDA [86].
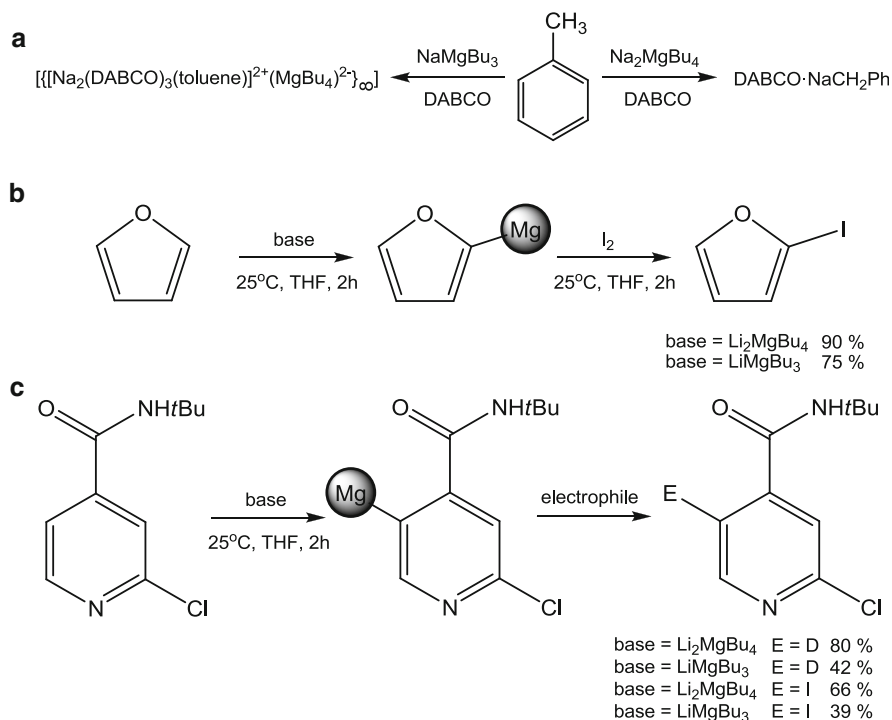
Fig. 30 Contrasting reactivity of higher order and lower order alkali-metal magnesiates

Similarly, Hoarau and Marsais successfully applied the lower order ate LiMgBu$_3$ for the regioselective *ortho*-deprotonation of (4′,4′-dimethyloxazolin-2-yl)benzene, with the reaction proceeding at synthetically desirable room temperature in THF [87].

3.6 Contrasting Reactivity of Higher Order and Lower Order Alkyl Magnesiates

The differing reactivity of these stoichiometrically distinct magnesiates was recognised by Mulvey who compared the reactivity of the sodium alkyl magnesiates NaMgBu$_3$ and Na$_2$MgBu$_4$ in the presence of the Lewis donor DABCO towards the deprotonative metallation of toluene (Fig. 30a) [88]. Interestingly the higher order magnesiate yielded a sodiated benzyl complex, while the lower order complex gave a DABCO- and toluene-solvated contact-ion pair in which no deprotonation to benzyl anions takes place.

Mongin also noted and quantified a reactivity difference between higher order Li$_2$MgBu$_4$ and lower order LiMgBu$_3$ in the regioselective deprotonation of furan,
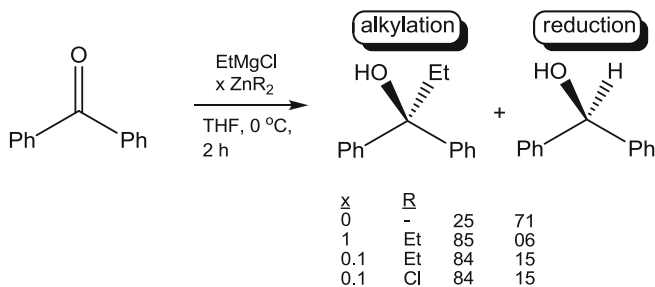
Fig. 31 Influence of a zinc reagent on reaction of a Grignard reagent with benzophenone

x	R		
0	-	25	71
1	Et	85	06
0.1	Et	84	15
0.1	Cl	84	15

while both bases deprotonated at the same site, the higher order magnesiate gave an improved yield under identical reaction conditions (Fig. 30b) [89]. Likewise, Marsais and co-workers saw a similar yield increase under identical conditions on moving from lower order to higher order magnesiate in the deprotonation of 2-chloro-*N*-*tert*-butylisonicotinamide (Fig. 30c) with the yield improving from 42 (39) to 80 (66) % upon electrophilic interception with D_2O (or I_2) [90].

Substituting homoleptic alkyl reagents by heteroleptic alkyl/amido reagents, Mongin reported the deprotonation of 4-chloropyridine at -10 °C in THF solution, evidenced via electrophilic trapping with iodine, using higher order $Li_2MgBu_3(TMP)$. Both homoleptic and heteroleptic lower order lithium magnesiates [namely $LiMgBu_3$ and $LiMgBu_2(TMP)$, respectively] failed to facilitate such a reaction under identical conditions [91].

3.7 Synthetic Applications Using Magnesium Zincates

A recently emerging form of heterometallic magnesium reagent in synthesis is the so called magnesium/zinc hybrid reagent, a name coined by Hevia. Not usually recognised as bimetallic reagents but more as magnesium and zinc compound mixtures, these tend to display lower reactivity than the alkali-metal/magnesium or alkali-metal/zinc species due to the absence of the highly reactive alkali-metal component, which can be credited with "boosting" the reactivity of the accompanying divalent metal through anionic (ate) activation. Nevertheless, Mg/Zn reagents have recently found use in a number of synthetic applications with a few of the highlights summarised below.

Ishihara studied the alkylation of ketones using a variety of Grignard reagents and additives [92, 93], finding that ethylation of benzophenone with EtMgCl was significantly enhanced by the presence of $ZnEt_2$ (Fig. 31) [94]. Indeed, the reactive bis-alkyl zinc reagent could be replaced by the salt $ZnCl_2$ with no diminishment of conversion. Only 10 mol% of the zinc additives were necessary for the improvement to take place, indicative of a catalytic process. Not only was the yield of the
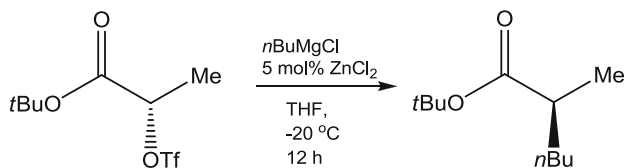
Fig. 32 Catalytic effect of $ZnCl_2$ on the cross-coupling reaction of a Grignard reagent with α-hydroxy ester triflates

desired tertiary alcohol product improved, but the amount of undesirable reduction product was inhibited.

Similar methodology has been applied to the alkylation of chlorosilanes to form new silicon–carbon bonds [95]. While these reactions proceed smoothly, when carried out with organolithium reagents low-temperature regimes are required; similarly the same reactions with less efficient homometallic organomagnesium reagents require heat and prolonged reaction times for comparable reactivity. As little as 1 mol% of $ZnCl_2$·TMEDA is sufficient to promote these reactions with, for example, the yield of product obtained from chlorodimethylphenylsilane and *para*-tolylmagnesium bromide in THF being improved from 13 to 67 or 77 % by adding $ZnCl_2$ or $ZnCl_2$·TMEDA. Studte and Breit noticed a significant effect on adding zinc additives in their cross-coupling studies of Grignard reagents with α-hydroxy ester triflates to yield enantiopure products [96]. In the absence of a second metallic co-reagent, problems such as nucleophilic addition of the chloride rather than the alkyl anion, homocoupling or reduction of the triflate functionality inhibited the purity and yield of the desired product (46 % yield, 62 % e.e.). However, in the presence of 5 mol% of $ZnCl_2$ a near quantitative yield of the desired ester product was obtained with complete inversion of configuration (Fig. 32). Using the chloro-Grignard reagent was found to be of high importance since *n*BuMgBr diminished the yield to only 11 % under identical conditions. Impressively, yields were continually greater than 90 % with e.e. values greater than 99 % when the reaction was extended to other alkyl Grignard reagents.

Shedding light on the structures involved in, and thereby increasing understanding of magnesium zincate hybrid induced reactions, Hevia crystallographically characterised the bimetallic product obtained from adding a sub-stoichiometric amount of $ZnCl_2$ to *t*BuMgCl in THF as the solvent-separated ion pair $[Mg_2Cl_3(THF)_6]^+$ $[Znt Bu_3]^-$ (Fig. 33) [97]. In synthesis, she found that this heterometallic tris-alkylzincate was active towards 3 molar equivalents of 4-iodotoluene via metal-halogen exchange to generate a tris-aryl zincate which is an effective precursor in Negishi cross-coupling reactions. Significantly, these structural studies revealed that though present in only sub-stoichiometric amounts, it is the zinc which is the "active" metal, although the magnesium clearly plays an important secondary role in the overall reaction since such reactivity could not be accessed by a dialkyl zinc or zinc halide reagent on its own.

Surprisingly, simply changing the Grignard reagent from *t*BuMgCl to EtMgCl and reacting it in a 3:1 ratio with $ZnCl_2$ gave a zinc-rich solvent-separated

Fig. 33 Molecular structure of the solvent-separated magnesium–zinc hybrid reagent $[Mg_2Cl_3(THF)_6]^+$ $[ZntBu_3]^-$ with hydrogen atoms omitted for clarity
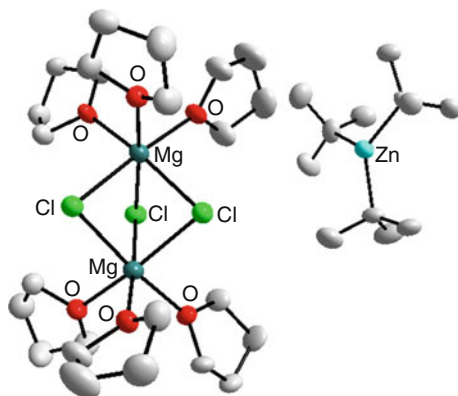
metathesis product formulated as $[Mg_2Cl_3(THF)_6]^+$ $[Zn_2Et_5]^-$ [98]. The product obtained upon reacting this heterometallic species with benzophenone was identified as homometallic $[Mg_2Cl_3(THF)_6]^+$ $[Mg_2(OC(Et)Ph_2)_2Cl_3(THF)]^-$ with Et_2Zn being co-produced and thus recycled, an important observation in the context of trying to rationalise the catalytic properties of the zinc component. The outcome of this reaction showcases the importance of the cooperative effect between the two metals since reduction of the ketone is observed using EtMgCl in the absence of $ZnCl_2$.

A more complicated trimetallic Mg/Zn/Li cooperativity has been implicated by Hevia and her team in their studies of magnesium/zinc hybrids with the sensitive fluorinated ketone trifluoroacetophenone [99]. They determined that their hybrid formulated as $[(THF)_2Mg(\mu\text{-}Cl)_3ZnEt]_2$ was a poor reagent for the alkylation of the ketone, yet the same hybrid in the presence of a stoichiometric amount of LiCl (initiating a Mg/Zn/Li tri-cooperativity) permitted the desired reaction to proceed in 74 % yield with concomitant diminishing of the amount of undesirable reduction products/recovered starting material (Fig. 34).

3.8 Heteroleptic Alkyl/Amido Alkali-Metal Magnesiates

Magnesium heterometallic bases containing a mixed organo-ligand set constitute another distinct class of magnesium reagent (mixed organo-ligand set in this context means ligands belonging to two distinct categories of ligand as opposed to those compounds, for example, $LiMgBu_2Me$ which although heteroleptic contain only one type of ligand, namely alkyl groups in this instance). The most studied species within this context are alkali-metal magnesiates containing a mixture of alkyl and secondary amide (R_2N) ligands. Because of the heteroleptic nature of these complexes, research in this area has seen considerable focus fall upon the constitution of the intermediate products, since a heteroleptic reagent clearly has more than one type of anion available for any given reaction. A clear understanding
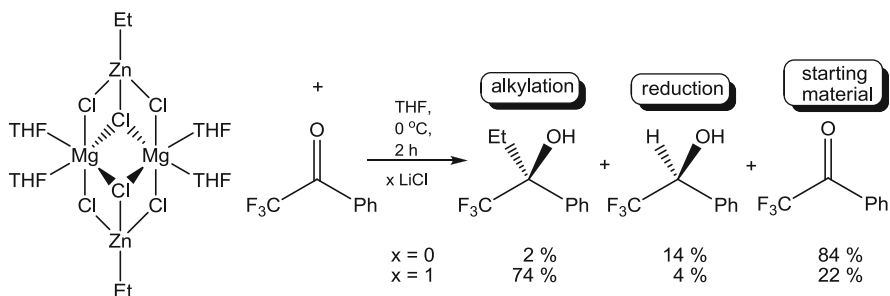
Fig. 34 Influence of LiCl on outcome of reaction between a MgZn hybrid reagent and trifluoroacetophenone
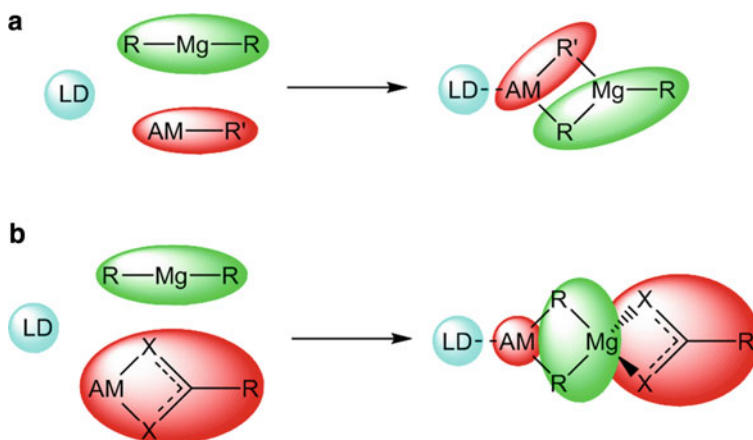
Fig. 35 Schematic examples of (**a**) co-complexation and (**b**) insertion routes to mixed-ligand alkali-metal magnesiates. Note that possible aggregation of the starting organometallics is not taken into account in this simplified depiction

of the intermediate products in any multi-step reaction can provide considerable insight into a number of facets including most obviously reactivity, selectivity and reaction mechanisms and can greatly aid the synthetic chemist in either the understanding of observed chemistry or the design of future work.

Mixed ligand-set alkali-metal magnesiates are typically prepared via a co-complexation route (Fig. 35a), whereby preexisting sigma bonds between metals and ligands remain intact, but the individual components come together via secondary bonding to produce the new framework. Also typically present on the alkali-metal is a co-ordinatively saturating neutral Lewis donor which prevents polymerisation, providing a discrete molecular species which is generally soluble in common organic solvents. These heterobimetallic complexes can effectively be considered as "hemi-Weiss motifs" (see Sect. 3.1) since there are no longer any anions bridging two magnesium centres or bridging one magnesium centre to two
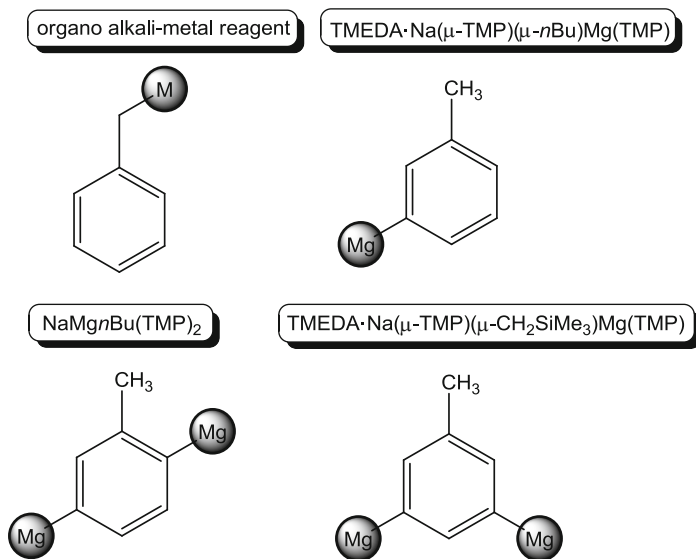
Fig. 36 Different deprotonation sites of toluene effected using the various metallic bases shown in the *boxes*

alkali-metal centres. When a bidentate anion is utilised rather than co-complexation occurring, insertion of the magnesium reagent into the alkali-metal anion bond can occur (Fig. 35b) [100].

The main use of magnesium heterometallic reagents such as these is in the selective deprotonative metallation reaction of organic substrates. The recurring theme, emphasised via the following representative examples, is that both metals must be present for the observed reactivity to occur (either component part on its own is typically unreactive or gives a different selectivity) and that it is the formally less reactive metal (in a conventional homometallic sense), magnesium, which carries out the metallation (although its reactivity has clearly been boosted by the presence of and the electronic input and redistribution caused by the reactive alkali-metal component).

Varying the individual components even slightly can have a profound influence on the resulting deprotonative metallation reaction. For example, the Lewis donor-free base mixture formulated as NaMgnBu(TMP)$_2$ will remarkably double deprotonate the aromatic substrates benzene or toluene at the 1,4 and 2,5 positions, respectively [101]. This reactivity can clearly be attributed to the groups 1 and 2 metals working in unison since these results cannot be replicated by either of the constituent parts of the base. Of particular note here is that toluene is prone to undergoing metallation at the methyl arm to give a benzyl anion (an example of thermodynamic acidity), which is energetically most favourable due to resonance stabilisation, but surprisingly treatment with this bimetallic base does not involve the methyl arm (Fig. 36). The reactivity of the base NaMgnBu(TMP)$_2$ is modified by the addition of TMEDA to the reactive co-complex, the result being only
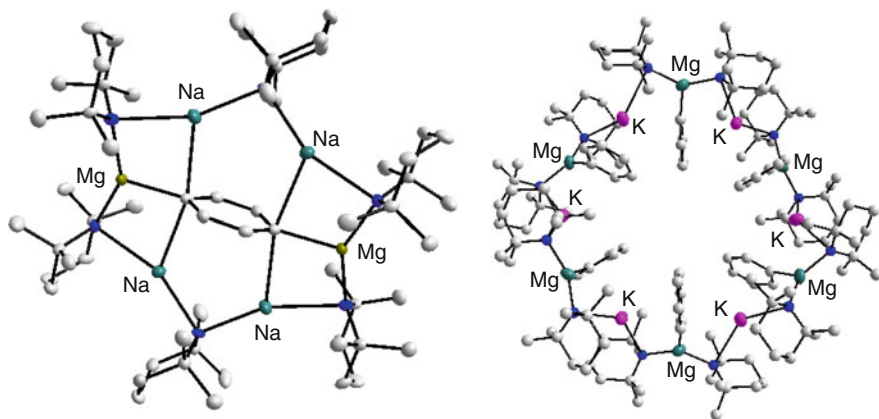
Fig. 37 Molecular structures of Na/Mg (*left*) and K/Mg (*right*) TMP inverse crowns with one $(C_6H_4)^{2-}$ and six $(C_6H_5)^-$ guest molecules, respectively

monodeprotonation of the arenes [102] (surprisingly at the *meta* position in the case of toluene). Changing the identity of the alkyl anion simply from *n*Bu to *t*Bu (whilst still in the presence of TMEDA) reverts the deprotonation of benzene back to 1,4-dideprotonation [103]. Finally, using the silyl-substituted neopentyl mimic CH_2SiMe_3 in place of a butyl group in $NaMg(CH_2SiMe_3)(TMP)_2$ results in dideprotonation of toluene but this time at the 3 and 5 positions (see Fig. 36) [104] The implication is that steric factors dictate this change of regioselectivity. What is clear from structural studies is that it is a magnesiation reaction that has taken place, with the Mg centres preferentially forming σ bonds with the aromatic carbon atoms and the sodium centres lying in a stabilising π-bound position.

These novel areneide and arenediide anions are typically found within a larger molecular framework, encapsulated by a "host" ring of metal cations and organic anions. The host ring itself carries a formal positive charge to balance the negative charge of the central deprotonated "guest" substrate and these species are referred to as "inverse crowns" to reflect the antithetical nature of their structural make-up with regard to a typical crown ether structure which contrastingly involves a central cationic species (e.g. a discrete Li^+ or Na^+ cation) encapsulated by a ring containing Lewis donating heteroatoms. Originally seen for heterometallic monovalent/divalent metal combinations, inverse crown chemistry has now been extended to include homometallic group 1 examples comprising solvent-separated ion pairs with the host ring a neutral entity which traps a halide anion [105].

While not taking a direct role in the metallation, the choice of alkali-metal is still of paramount importance as demonstrated on changing the bimetallic base from $NaMgBu(TMP)_2$ to $KMgBu(TMP)_2$. As previously mentioned, the former results in a 12-membered $(Na_4Mg_2N_6)$ inverse crown with a single arenediide encapsulated as the guest; however, the potassium congener only executes a single deprotonation of the same substrate, with the result being a 24-membered $(K_6Mg_6N_{12})$ inverse crown encapsulating six individual areneide molecules (Fig. 37) [106]. This represents the largest inverse crown known to date.

Fig. 38 Molecular structure of the tetrasodium-dimagnesium inverse crown $[Na_4Mg_4(NiPr_2)_8]^{4+}$ with $[(C_5H_3)_2Fe]^{4-}$ core. All carbon atoms of amide groups and all hydrogen atoms have been omitted for clarity
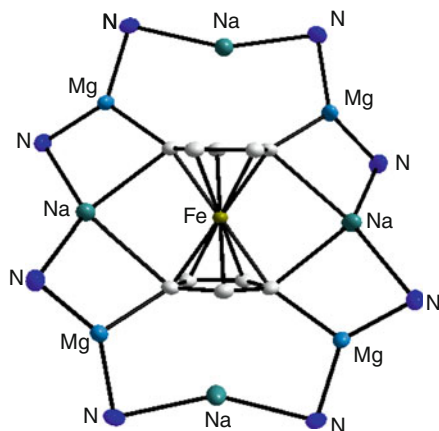
A particularly spectacular demonstration of the direct magnesiation of aromatic species via an alkali-metal magnesiate base is witnessed in the reaction of the tris (diisopropylamide) $NaMg(NiPr_2)_3$ with the series of group 8 parent metallocenes ferrocene [107], ruthenocene and osmocene [108]. These mixtures generate a 16-atom $(Na_4Mg_4N_8)$ inverse crown made up of metal-diisopropylamide-metal bridges carrying a formally 4+ charge and an unprecedented $[M(C_5H_3)_2]^{4-}$ tetra-anionic guest at its core (M = Fe, Ru, or Os—Fig. 38). This eyecatching outcome showcases the cooperative effect between the two metals since a metallocene cannot generally be metallated at more than two of its ten potential sites in a controlled manner, and certainly not with the homometallic constituents of the heterometallic base, $NaNiPr_2$ or $Mg(NiPr_2)_2$. Further, the products clearly display Mg–C σ-bonds, making this the first example of direct magnesiation of a metallocene, whether by a homometallic or heterometallic reagent.

The importance of the alkali-metal identity is illustrated once more by the reactivity of the homoleptic bimetallic amido bases $MMg(NiPr_2)_3$ (M = Li, Na) towards phenylacetylene [109]. The lighter alkali-metal congener will deprotonate 2 molar equivalents of substrate resulting in a linear dimeric, tetranuclear complex formulated as $[(TMEDA)LiMg(C≡CPh)_2(NiPr_2)]_2$, while the sodium derivative will deprotonate a single molar equivalent of alkyne to yield a product of formula $[NaMg(C≡CPh)(NiPr_2)_2]_2$ with an inverse crown motif.

As mentioned earlier, heteroleptic bases have the potential to react via any of their distinct anions making structural tracking an important facet for gaining a true understanding of the chemisty. This was clearly illustrated by Mulvey and co-workers who designed a heteroleptic potassium magnesiate, $PMDETA·K(μ-TMP)$ $(μ-CH_2SiMe_3)Mg(TMP)$, via the aforementioned co-complexation strategy [110]. Studied with the aromatic ether molecule anisole (PhOMe), this base was found to deprotonate this substrate on the aromatic ring, *ortho* to the lateral methoxy group in a regioselectivity conforming to the well-established principles of D*o*M chemistry. An interesting feature of this study was that two products were apparent, heterotrianionic $PMDETA·K(μ-MeOC_6H_4)(μ-CH_2SiMe_3)Mg(TMP)$ and
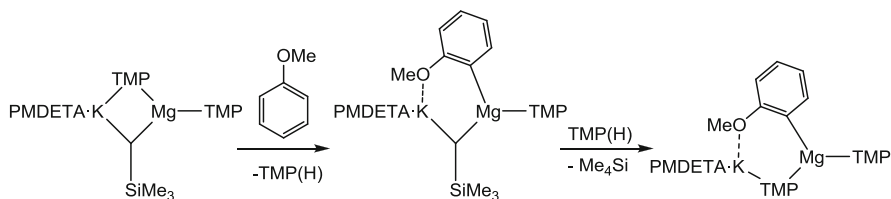
Fig. 39 Kinetic/thermodynamic products obtained from reaction of a heteroleptic potassium magnesiate with anisole

heterodianionic PMDETA·K(μ-TMP)(μ-MeOC$_6$H$_4$)Mg(TMP), that is, starting from the base one where TMP(H) has been lost (through amido deprotonation) and the other where SiMe$_4$ has been lost (through alkyl deprotonation). A time-dependent NMR spectroscopic study established that the former is the kinetic product, while the latter is the thermodynamic product. The TMP(H) amine which is extruded upon deprotonation of the substrate is not sufficiently volatile to be lost to the system, and being relatively acidic (pK_a = 37) it is then deprotonated by the Me$_3$SiCH$_2^-$ of the kinetic intermediate to give the final thermodynamic product (Fig. 39).

The TMEDA-solvated sodium derivative of this base [TMEDA·Na(μ-TMP) (μ-CH$_2$SiMe$_3$)Mg(TMP)] has also been used in one of the most spectacular demonstrations of the ability of heterometallic reagents to effect unusual deprotonations, namely in the "cleave-and-capture" of the cyclic ether THF [111]. While the deprotonation of THF is not uncommon with homometallic bases (in fact often seen as an unwanted side reaction when THF is employed as a solvent in organometallic chemistry), the proximity of the developed negative charge to the electron-rich oxygen atom typically results in a spontaneous ring opening of the anion into ethene and the enolate of acetaldehyde. However, by using the aggressive sodium magnesiate, the THF molecule is cleaved to an O^{2-} and a (butadienide)$^{2-}$ through the formal loss of four protons, with the two dianionic fragments being simultaneously captured within heterometallic frameworks, an oxo inverse crown for the former and a tetranuclear complex for the latter (Fig. 40).

While this magnesium-based reaction involves cleavage of the sensitive THF ring followed by capture of the parts, it should be noted that more "compassionAte" alkali-metal zinc [112] and alkali-metal aluminium reagents [113] α-deprotonate THF without opening the ring, with the resulting cyclic anion being captured. This clearly highlights the differing reactivity of these metals when used in conjunction with an alkali-metal and showcases the importance of carefully tailoring the bimetallic base.

Finally, in a remarkable new concept for a magnesiate system, Hevia and co-workers have recently reported an intriguing cascade reaction converting benzothiazole into a novel trianionic derivative with an N-C-C-C-N delocalised ligation centre. This conversion involves sequential deprotonation, C–C coupling, ring opening and nucleophilic addition steps (Fig. 41) [114]. This reaction was
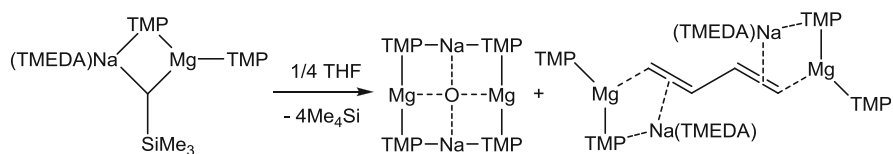
Fig. 40 Cleave and capture chemistry executed by a sodium magnesiate on the cyclic ether THF
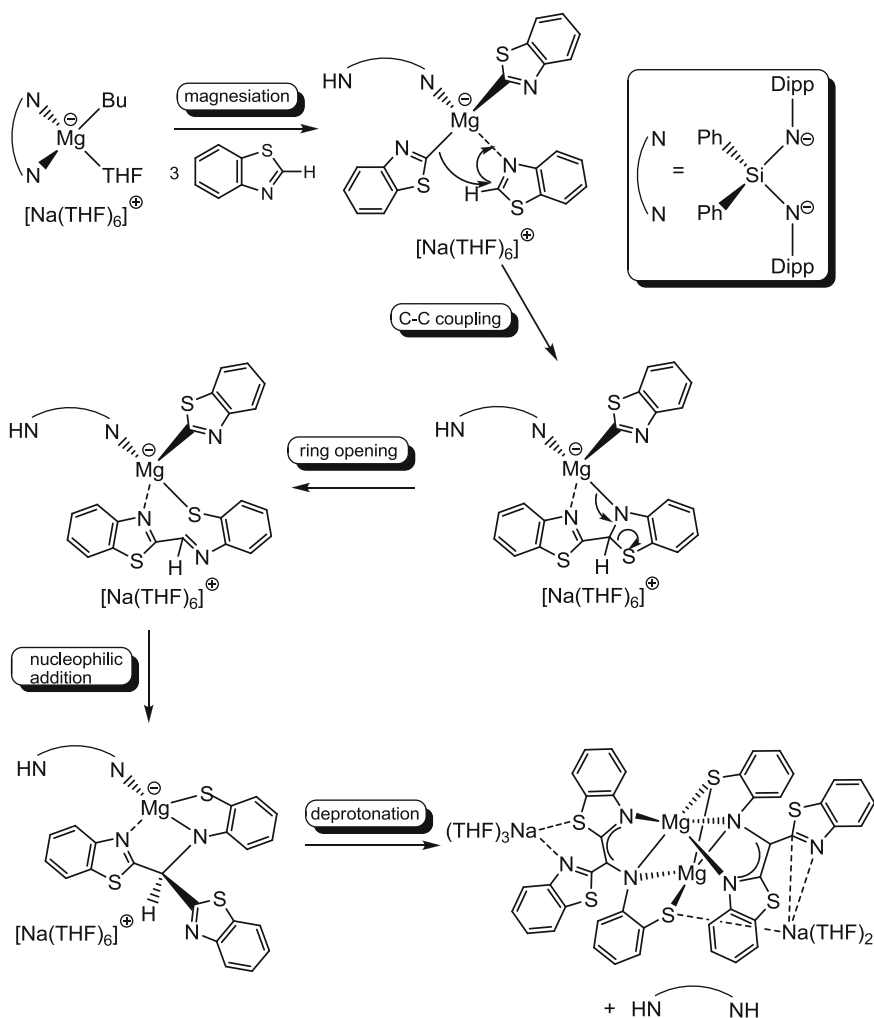
Fig. 41 Cascade reaction of a sodium magnesiate towards the important heterocycle benzothiazole

achieved by first converting the homoleptic sodium magnesiate NaMgBu$_3$ into the solvent-separated magnesiate [Na(THF)$_6$]$^+$ [BuMg(NR)$_2$SiPh$_2$·THF]$^-$ (R = 2,6-diisopropylphenyl) by deprotonation of the bis-amine (HNR)$_2$SiPh$_2$. This style of cascade reaction is normally more associated with redox-active transition or lanthanide metals, so its emergence here in magnesium chemistry could open up a promising new line of research.

4   Conclusion

Considering it was invented at the beginning of the twentieth century, organomagnesium reagent chemistry has retained its usefulness for a remarkably long time and amazingly in 2012 its usefulness is still growing. Every chemist from a young undergraduate to a career industrialist is familiar with the classical Grignard reagents. There have been numerous developments in this chemistry over the past 100 years, but arguably the past 10 or so years has seen the most significant subject-transforming advances. Previously organomagnesium reagents, known for their mild reactivity which made them excellent tools for nucleophilic addition reactions, had to defer to their more reactive organolithium rivals when faced with more challenging metal-halogen or metal-hydrogen exchange applications. With the advent of Turbo-Grignard reagents and Turbo-Hauser reagents, where classical organomagnesium reagents are activated by reactivity boosting salt (commonly LiCl) additives, new magnesium-halogen and magnesium-hydrogen methodologies have emerged that offer substantial benefits over established organolithium methods. Ate formulations made by combining organomagnesium compounds with other organometallic compounds (for example, most typically organolithiums or organosodiums) can also exhibit strikingly different chemistry in terms of both reactivity and regioselectivity compared to that of classical organomagnesium reagents. Clearly cooperative effects between the different components provide the key to the improved reactivity of these new types of multicomponent organomagnesium reagents. Further studies will be needed to gain a more complete understanding of how these cooperative effects operate and how we can best tune them for forthcoming synthetic campaigns. A grand challenge will be to transform these stoichiometric reagents into substoichiometric or better still catalytic reagents.

References

1. Grignard V (1901) Ann Chim 24:433
2. Seyferth D (2009) Organometallics 28:1598
3. Tidwell TT (2001) Angew Chem Int Ed 40:331
4. Schlenk W, Schlenk W Jr (1929) Chem Ber 62:920
5. Meunier L (1903) CR Hebd Seances Acad Sci 136:758
6. Hauser CR, Walker HG Jr (1947) J Am Chem Soc 69:295
7. Frostick FC Jr, Hauser CR (1949) J Am Chem Soc 71:1350
8. Hauser CR, Yost RS, Ringler BI (1949) J Org Chem 14:261
9. Olofson RA, Dougherty CM (1973) J Am Chem Soc 95:581
10. Lappert MF, Slade MJ, Singh A, Atwood JL, Rogers RD, Shakir R (1983) J Am Chem Soc 105:302
11. Eaton PE, Lee C-H, Xiong Y (1989) J Am Chem Soc 111:8018
12. Schlecker W, Huth A, Ottow E, Mulzer J (1995) J Org Chem 60:8414
13. Kondo Y, Yoshida A, Sakamoto T (1996) J Chem Soc Perkin Trans 1:2331
14. Shilai M, Kondo Y, Sakamoto T (2001) J Chem Soc Perkin Trans 1:442
15. Barr L, Kennedy AR, MacLellan JG, Moir JH, Mulvey RE, Rodger PJA (2000) Chem Commun: 1757
16. Kawachi A, Nagae S, Onoue Y, Harada O, Yamamoto Y (2011) Chem Eur J 17:8005
17. Whisler MC, MacNeil S, Snieckus V, Beak P (2004) Angew Chem Int Ed 43:2206
18. Gupta L, Hoepker AC, Singh KJ, Collum DB (2009) J Org Chem 74:2231
19. Ma Y, Hoepker AC, Gupta L, Faggin MF, Collum DB (2010) J Am Chem Soc 132:15610
20. Krasovskiy A, Knochel P (2004) Angew Chem Int Ed 43:3333
21. Baron O, Knochel P (2005) Angew Chem Int Ed 44:3133
22. Ren H, Krasovskiy A, Knochel P (2004) Org Lett 6:4215
23. Ren H, Krasovskiy A, Knochel P (2005) Chem Commun: 543
24. Krasovskiy A, Krasovskaya V, Knochel P (2006) Angew Chem Int Ed 45:2958
25. García-Álvarez P, Graham DV, Hevia E, Kennedy AR, Klett J, Mulvey RE, O'Hara CT, Weatherstone S (2008) Angew Chem Int Ed 47:8079
26. Armstrong DR, García-Álvarez P, Kennedy AR, Mulvey RE, Parkinson JA (2010) Angew Chem Int Ed 49:3185
27. Fraser RR, Mansour TS (1984) J Org Chem 49:3443
28. Wada A, Yamamoto J, Kanatomo S (1987) Heterocycles 26:585
29. Mosrin M, Boudet N, Knochel P (2008) Org Biomol Chem 6:3237
30. Lin W, Baron O, Knochel P (2006) Org Lett 8:5673
31. Jaric M, Haag BA, Unsinn A, Karaghiosoff K, Knochel P (2010) Angew Chem Int Ed 49:5451
32. Boudet N, Lachs JR, Knochel P (2007) Org Lett 9:5525
33. Mosrin M, Knochel P (2009) Chem Eur J 15:1468
34. Piller FM, Knochel P (2009) Org Lett 11:445
35. Kunz T, Knochel P (2011) Chem Eur J 17:866
36. Tanaka S, Tamba S, Tanaka D, Sugie A, Mori A (2011) J Am Chem Soc 133:16734
37. Tamba S, Mitsuda S, Tanaka F, Sugie A, Mori A (2012) Organometallics 31:2263
38. Verhelst T, Maes J, Liu Z, Sergeyev S, Maes BUW (2011) J Org Chem 76:6670
39. Bresser T, Knochel P (2011) Angew Chem Int Ed 50:1914
40. Hirone N, Sanjiki H, Tanaka R, Hata T, Urabe H (2010) Angew Chem Int Ed 49:7762
41. Wunderlich SH, Bresser T, Dunst C, Monzon G, Knochel P (2010) Synthesis 15:2670
42. Rohbogner CJ, Wunderlich SH, Clososki GC, Knochel P (2009) Eur J Org Chem: 1781
43. Piller FM, Bresser T, Fischer MKR, Knochel P (2010) J Org Chem 75:4365
44. Wunderlich SH, Kienle M, Knochel P (2009) Angew Chem Int Ed 48:7256
45. Wunderlich SH, Knochel P (2009) Angew Chem Int Ed 48:9717
46. Jeganmohan M, Knochel P (2010) Angew Chem Int Ed 49:8520

47. Metzger A, Bernhardt S, Manolikakes G, Knochel P (2010) Angew Chem Int Ed 49:4665
48. Wittig G, Meyer FJ, Lange G (1951) Justus Liebigs Ann Chem 571:167
49. Tochtermann W (1997) Liebigs Ann/Recueil: I–XXI
50. Tochtermann W (1966) Angew Chem Int Ed 5:351
51. Coates GE, Heslop JA (1968). J Chem Soc (A):514
52. Seitz LM, Brown TL (1966) J Am Chem Soc 88:4140
53. Hurd DT (1948) J Org Chem 13:711
54. Weiss E (1993) Angew Chem Int Ed Engl 32:1501
55. Kitagawa K, Inoue A, Shinokubo H, Oshima K (2000) Angew Chem Int Ed 39:2481
56. Inoue A, Kitagawa K, Shinokubo H, Oshima K (2001) J Org Chem 66:4333
57. Xu J, Jain N, Sui Z (2004) Tetrahedron Lett 45:6399
58. Dumouchel S, Mongin F, Trécourt F, Quéguiner G (2003) Tetrahedron Lett 44:2033
59. Dumouchel S, Mongin F, Trécourt F, Quéguiner G (2003) Tetrahedron Lett 44:3877
60. Dumouchel S, Mongin F, Trécourt F, Quéguiner G (2003) Tetrahedron 59:8629
61. Iida T, Wada T, Tomimoto K, Mase T (2001) Tetrahedron Lett 42:4841
62. Catel D, Chevallier F, Mongin F, Gros PC (2012) Eur J Org Chem: 53
63. Catel D, Payen O, Chevallier F, Mongin F, Gros PC (2012) Tetrahedron 68:4018
64. Kondo J, Inoue A, Shinokubo H, Oshima K (2001) Angew Chem Int Ed 40:2085
65. Inoue A, Kondo J, Shinokubo H, Oshima K (2002) Chem Eur J 8:1730
66. Thomas GL, Ladlow M, Spring DR (2004) Org Biomol Chem 2:1679
67. Sośnicki JG (2009) Synlett: 2508
68. Inoue A, Kitagawa K, Shinokubo H, Oshima K (2000) Tetrahedron 56:9601
69. Liu M, Kamienski C, Morton M, Fetters LJ (1986) J Macromol Sci Pure Appl Chem A 23:1387
70. Hsieh HL, Wang IW (1986) Macromolecules 19:299
71. Maréchal J-M, Carlotti S, Shcheglova L, Deffieux A (2004) Polymer 45:4641
72. Hsueh M-L, Ko B-T, Athar T, Lin C-C, Wu T-M, Hsu S-F (2006) Organometallics 25:4144
73. Honeyman GW, Kennedy AR, Mulvey RE, Sherrington DC (2004) Organometallics 23:1197
74. Hatano M, Matsumura T, Ishihara K (2005) Org Lett 7:573
75. Sośnicki JG (2005) Tetrahedron Lett 46:4295
76. Sośnicki JG (2007) Tetrahedron 63:11862
77. Sośnicki JG (2006) Tetrahedron Lett 47:6809
78. Sośnicki JG, Struk L (2009) Synlett: 1812
79. Fleming FF, Gudipati V, Steward OW (2002) Org Lett 4:659
80. Fleming FF, Gudipati V, Steward OW (2003) Tetrahedron 59:5585
81. Kikuchi M, Niikura S, Chiba N, Terauchi N, Asaoka M (2007) Chem Lett 36:736
82. Awad H, Mongin F, Trécourt F, Quéguiner G, Marsais F, Blanco F, Abarca B, Ballesteros R (2004) Tetrahedron Lett 45:6697
83. Bayh O, Awad H, Mongin F, Hoarau C, Trécourt F, Quéguiner G, Marsais F, Blanco F, Abarca B, Ballesteros R (2005) Tetrahedron 61:4779
84. Bayh O, Awad H, Mongin F, Hoarau C, Bischoff L, Trécourt F, Quéguiner G, Marsais F, Blanco F, Abarca B, Ballesteros R (2005) J Org Chem 70:5190
85. Bentabed-Ababsa G, Blanco F, Derdour A, Mongin F, Trécourt F, Quéguiner G, Ballesteros R, Abarca B (2009) J Org Chem 74:163
86. Conway B, Hevia E, Kennedy AR, Mulvey RE (2007) Chem Commun: 2864
87. Bellamy E, Bayh O, Hoarau C, Trécourt F, Quéguiner G, Marsais F (2010) Chem Commun 46:7043
88. Andrikopoulos PC, Armstrong DR, Hevia E, Kennedy AR, Mulvey RE, O'Hara CT (2005) Chem Commun: 1131
89. Mongin F, Bucher A, Bazureau JP, Bayh O, Awad H, Trécourt F (2005) Tetrahedron Lett 46:7989
90. Hawad H, Bayh O, Hoarau C, Trécourt F, Quéguiner G, Marsais F (2008) Tetrahedron 64:3236

91. Awad H, Mongin F, Trécourt F, Quéguiner G, Marsais F (2004) Tetrahedron Lett 45:7873
92. Hatano M, Ishihara K (2008) Synthesis: 1647
93. Hatano M, Suzuki S, Ishihara K (2010) Synlett: 321
94. Hatano M, Suzuki S, Ishihara K (2006) J Am Chem Soc 128:9998
95. Murakami K, Yorimitsu H, Oshima K (2009) J Org Chem 74:1415
96. Studte C, Breit B (2008) Angew Chem Int Ed 47:5451
97. Hevia E, Chua JZ, García-Álvarez P, Kennedy AR, McCall MD (2010) Proc Nat Acad Sci USA 107:5294
98. Armstrong DR, Clegg W, García-Álvarez P, McCall MD, Nuttall L, Kennedy AR, Russo L, Hevia E (2011) Chem Eur J 17:4470
99. Armstrong DR, Clegg W, García-Álvarez P, Kennedy AR, McCall MD, Russo L, Hevia E (2011) Chem Eur J 17:8333
100. Forret R, Kennedy AR, Klett J, Mulvey RE, Robertson SD (2009) Organometallics 29:1436
101. Armstrong DR, Kennedy AR, Mulvey RE, Rowlings RB (1999) Angew Chem Int Ed 38:131
102. Hevia E, Gallagher DJ, Kennedy AR, Mulvey RE, O'Hara CT, Talmard C (2004) Chem Commun: 2422
103. Armstrong DR, Clegg W, Dale SH, Graham DV, Hevia E, Hogg LM, Honeyman GW, Kennedy AR, Mulvey RE (2007) Chem Commun: 598
104. Andrikopoulos PC, Armstrong DR, Graham DV, Hevia E, Kennedy AR, Mulvey RE, O'Hara CT, Talmard C (2005) Angew Chem Int Ed 44:3459
105. Kennedy AR, Mulvey RE, O'Hara CT, Robertson GM, Robertson SD (2011) Angew Chem Int Ed 50:8375
106. Andrews PC, Kennedy AR, Mulvey RE, Raston CL, Roberts BA, Rowlings RB (2000) Angew Chem Int Ed 39:1960
107. Clegg W, Henderson KW, Kennedy AR, Mulvey RE, O'Hara CT, Rowlings RB, Tooke DM (2001) Angew Chem Int Ed 40:3902
108. Andrikopoulos PC, Armstrong DR, Clegg W, Gilfillan CJ, Hevia E, Kennedy AR, Mulvey RE, O'Hara CT, Parkinson JA, Tooke DM (2004) J Am Chem Soc 126:11612
109. García-Álvarez J, Graham DV, Hevia E, Kennedy AR, Mulvey RE (2008) Dalton Trans: 1481
110. Clegg W, Conway B, García-Álvarez P, Kennedy AR, Mulvey RE, Russo L, Sassmannshausen J, Tuttle T (2009) Chem Eur J 15:10702
111. Mulvey RE, Blair VL, Clegg W, Kennedy AR, Klett J, Russo L (2010) Nat Chem 2:588
112. Kennedy AR, Klett J, Mulvey RE, Wright DS (2009) Science 326:706
113. Crosbie E, García-Álvarez P, Kennedy AR, Klett J, Mulvey RE, Robertson SD (2010) Angew Chem Int Ed 49:9388
114. Blair VL, Clegg W, Kennedy AR, Livingstone Z, Russo L, Hevia E (2011) Angew Chem Int Ed 50:9857

Alkaline-Earth Metal Complexes in Homogeneous Polymerization Catalysis

Jean-François Carpentier and Yann Sarazin

Abstract This chapter describes the use of complexes of the alkaline-earth metals (magnesium, calcium, strontium, and barium) in homogeneous polymerization catalysis. The latest developments in the polymerization of monomers containing C=C unsaturations (ethylene, styrene, dienes, acrylates) and in the ring-opening polymerization (ROP) of cyclic esters [lactides (LA), ε-caprolactone, trimethylene carbonate] are covered. The mechanisms of chain growth polymerization of olefins and immortal ROP of cyclic esters, which is of particular relevance to these metals, are presented. In view of the current interest devoted to the organometallic chemistry of the larger alkaline-earth metals, the implementation of well-defined catalyst systems based on calcium, strontium, and barium for the polymerizations of styrene and lactide is highlighted.

Keywords Alkaline-earth complexes · Catalysis · Chain growth polymerization · Lactones · Polymerization · Styrene

Contents

J.-F. Carpentier (✉) and Y. Sarazin (✉)
Institut des Sciences Chimiques de Rennes, UMR 6226 CNRS–Université de Rennes 1, 263 avenue du Général Leclerc, 35042 Rennes Cedex, France
e-mail: jean-francois.carpentier@univ-rennes1.fr; yann.sarazin@univ-rennes1.fr

List of Abbreviations

Ae	Alkaline-earth
BD	Butadiene
BDI	β-Diketiminate
Bn	Benzyl
Bu	Butyl
CGP	Chain growth polymerization
CL	ε-Caprolactone
Cp	Cyclopentadienyl
Cp*	Pentamethylcyclopentadienyl
D,L-LA	*Racemic* lactide
equiv	Equivalent(s)
Et	Ethyl
Flu	Fluorenyl
GL	Glycolide
h	Hour(s)
Ind	Indenyl
IP	Isoprene
*i*Pr	*iso*-propyl
IR	Infrared
*i*ROP	Immortal ring-opening polymerization
LA	Lactide
L-LA	L-Lactide
Ln	Lanthanide
MALDI-ToF-MS	Matrix-assisted laser desorption ionization time-of-flight mass spectrometry
MAO	Methylaluminoxane
Me	Methyl
meso-LA	*meso* lactide
min	Minute(s)
MMA	Methyl methacrylate
M_n	Number-average molecular weight
M_w	Weight-average molecular weight
M_w/M_n	Polydispersity index
NMR	Nuclear magnetic resonance
Nu	Nucleophile

PBD	Poly(butadiene)
PCL	Poly(ε-caprolactone)
PE	Poly(ethylene)
PEO	Poly(ethylene oxide)
Ph	Phenyl
PIP	Poly(isoprene)
PLA	Poly(lactide)
PLLA	Poly(L-lactide)
P_m	Probability of *meso* linkages of consecutive monomer units
PMMA	Poly(methyl methacrylate)
Pr	Propyl
P_r	Probability of *racemic* linkages of consecutive monomer units
PS	Poly(styrene)
PTMC	Poly(trimethylene carbonate)
ROP	Ring-opening polymerization
rt	Room temperature
s	Second(s)
s	Secondary
SEC	Size exclusion chromatography
*t*Bu	*tert*-butyl
T_g	Glass transition temperature
THF	Tetrahydrofuran
T_m	Melting temperature
TMC	Trimethylene carbonate
TOF	Turnover frequency
TON	Turnover number
Tp	*Tris*(pyrazolyl)borate

1 Alkaline-Earth Metals and Polymerization Catalysis

The discovery of reliable access routes to synthetic polymers in the first part of the twentieth century had a bigger impact on our modern society than the introduction of other materials. Everyday commodity materials are routinely synthesized by polycondensation reactions (polyamides, polyterephthalates, etc.), ionic (polyacrylates, polyvinyl chloride, or acetate), or Ziegler–Natta (polyethylene, polypropylene, polystyrene, etc.) polymerizations.

Although heterogeneous catalyst systems are favored in the industry, research groups in academia have long endeavored the development of so-called "single-site" catalysts for homogeneous polymerization reactions. Indeed, as the physical, thermal, and mechanical properties of a polymer material are essentially governed by its macromolecular architecture, the development of well-defined polymerization catalysts that enable fine-tuning of the composition and architecture of the polymers is of obvious interest. In this context, single-site catalysts based on

transition metals have enjoyed tremendous success, even in industry, as demonstrated by the ubiquitous group 4 metallocenes. By contrast, alkaline-earth (Ae) metals seldom have been used, not least because of the difficulties encountered during the synthesis of stable and easy-to-handle complexes.

The considerable synthetic achievements of the last 10–15 years in the organometallic chemistry of the large Ae elements (calcium, strontium, and barium) have also concerned polymerization catalysis. New Ae-based catalyst systems for the polymerization of monomers with C=C unsaturations have been introduced, where the Ae species either is a chain transfer agent (CTA) acting as the surrogate of a catalytically active species in the chain growth polymerization (CGP) of ethylene, styrene, or conjugated dienes, or directly bears the growing polymer chain as in the simple anionic polymerization of styrene and dienes. Perhaps more significantly in view of the current issues related to the depletion of hydrocarbon sources, several efficient catalyst systems for the ring-opening polymerization (ROP) of cyclic monomers—partially derived from biomass—have been designed, and others are now disclosed on a regular basis. These systems, built not only around magnesium but also around the larger Ae elements, allow for very efficient ROP reactions. The latest achievements in these two areas of polymerization catalysis are reviewed in detail in the following sections.

2 Polymerization of Monomers with C=C Unsaturations

2.1 Introduction

Ae metal complexes have been involved in polymerization processes of C=C containing compounds to different extents and in different circumstances. In this chapter, C=C containing monomers include three main subclasses: (a) ethylene and related α-olefins, (b) styrene and conjugated dienes, and (c) what is often referred to as "polar" olefins, namely acrylates and methacrylates. For these three classes of monomers, Ae compounds have shown valuable, sometimes unique, abilities either as discrete compounds or in binary or even more complicated tertiary combinations with other main group or transition metal compounds. Another essential distinction to be highlighted is the actual role of the Ae compounds in these processes: they may be, as simply anticipated, the real active polymerization species, but they may be also involved in binary or tertiary combinations, as a "partner component", undergoing transmetallation reactions with another metallic species which is in charge of polymerization.

In contrast to the countless catalysts based on transition metals, polymerization of regular "unactivated" monomers such as ethylene and α-olefins via "coordination–insertion" onto Ae-alkyls remains undisclosed. On the other hand, and in line with their above-mentioned collaborative transmetallation action, Ae-alkyls can act in such olefin polymerizations as unique reversible transfer agents, leading to so-called CGP. The involvement of Ae-alkyl reagents (essentially

dialkylmagnesium derivatives) in this peculiar type of polymerization, which has enjoyed much popularity and witnessed significant progress over the past 2 decades [1–3], has also been demonstrated in the polymerization of styrene and conjugated dienes. Although Ae(Mg)-alkyls do not participate as the active polymerization species in these processes, they have enabled the preparation of unique Ae(Mg)-dipolymeryl compounds, which subsequently proved of great utility in macromolecular engineering. The first section of this chapter is therefore devoted to this type of polymerizations. The next sections address the use of discrete Ae-alkyl compounds or binary combinations involving an Ae compound as active catalysts or catalyst precursors for the polymerizations of styrene, conjugated dienes, and methacrylates.

2.2 Use of Dialkylmagnesiums as Reversible Transfer Agents in Chain Growth Polymerizations

2.2.1 General Considerations

Chain Growth Polymerization (hereafter abbreviated CGP, also referred to in the literature as Reversible Chain Transfer Polymerization or Coordinative Chain Transfer Polymerization) relies on the combination of a catalytically active transition metal complex and an excess of a comparatively inexpensive alkyl main group metal compound that acts as CTA [1–3]. To be highly effective, this process requires that transmetallation (i.e., chain transfer) between growing (Pol*) and dormant (Pol) polymer chains carried respectively by the transition and main group metals is reversible and fast compared to polymerization itself ($k_{transfer} \gg k_{prop}$). Under such conditions, the process no longer results in a simple organic polymer as for conventional polymerizations but in an organometallic compound carrying several polymer chains covalently bound to the metal center (Scheme 1). It is related to classical living polymerization, but in sharp contrast with this latter process in which the number of polymer chains generated by the metal center is strictly equal to 1, the number of polymer chains in CGP is related to the number of molecules of CTA initially introduced in the reaction medium (Scheme 1). Because the CTA is usually introduced in (large) excess in comparison to the catalytically active metal, the CGP process is truly catalytic: each transition metal center produces many polymer chains.

Although CGP is in no way limited to dialkylmagnesiums ($ZnEt_2$ and AlR_3 have also proved useful) [1–3], MgR_2 reagents have been particularly effective for a variety of polymerizations.

2.2.2 Chain Growth Polymerization of Ethylene

A seminal work along these principles is that of Mortreux and coworkers who first reported CGP of ethylene using a combination of otherwise inactive chlorolanthanidocene precursors $\{Cp^*\}_2LnCl_2Li(OEt_2)_2$ (Ln = Nd,

$$\left[\begin{array}{c} \text{Pol}_m \\ [\text{Nd}] \quad \quad \text{Mg}(\text{Pol}_p) \\ \text{Pol}_n \end{array} \right]$$

[Nd]-(Pol$_m$)* + Mg(Pol$_n$)(Pol$_p$) $\xrightleftharpoons[k_{\text{transfer}}]{\text{reversible transfer}}$ [Nd]-(Pol$_n$)* + Mg(Pol$_m$)(Pol$_p$)

propag. k_{prop}

propag. k_{prop}

monomer   monomer
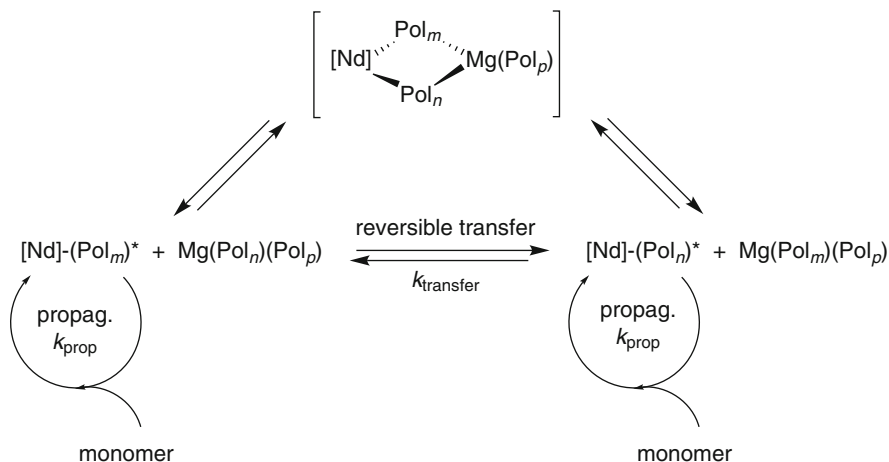
Scheme 1 Chain Growth Polymerization illustrated in the case of a neodymium complex ([Nd]; [Nd]-Pol stands for species carrying a growing polymer chain) associated with a dialkylmagnesium chain transfer agent. Reversible and fast CGP, achieved with $k_{\text{transfer}} \gg k_{\text{prop}}$, results in $m \approx n \approx p$

Sm; Cp* = C$_5$Me$_5$) with common dialkylmagnesium reagents (e.g., Mg(nBu)Et, Mg (n,sBu)$_2$, Mg(nBu)(n-octyl)...) [4–6]. These binary systems generate in situ alkyllanthanidocene species that are active for the polymerization of ethylene and that transfer growing polyethylenyl (PE) chains rapidly and reversibly into Mg(PE)$_2$. In further developments, the lanthanidocene pre-catalysts were substituted by simple homoleptic neodymium alkoxides, which also led to the formation of μ-alkyl-bridged Ln–Mg species [7–9]. With both systems, the resulting reaction was similar to an homologation of the MgR$_2$ co-reagent into Mg(PE)$_2$ species. The latter compounds are soluble in the reaction medium for PE segments with M_n up to ca. 1,400 g mol^{-1}. Provided these Mg(PE)$_2$ species remained soluble, the catalyst and polymerization activity were very stable; on the other hand, precipitation of Mg(PE)$_2$ species (above this critical M_n value) no longer allowed the stabilization of the catalytic species via a bimetallic Ln–Mg species (Scheme 1). Therefore, polymerizations typically show in a sudden burst in activity almost immediately followed by complete deactivation ([Ln]-alkyl species are extremely active but sensitive species). The size of the PE segments in the Mg(PE)$_2$ species could be readily manipulated by monitoring the ethylene consumption and/or adjusting the [Ln]/[Mg] ratio: the larger the Mg loading (up to 200 equiv could be used), the more PE chains, and the lower their size for a given ethylene consumption. Such a ready and efficacious access to Mg(PE)$_2$ species with tailored molecular weights proved particularly useful for the preparation of end-functionalized poly(ethylene)s. This was simply achieved by taking profit of the Mg–C nucleophilic or homolytic reactivity to install hydroxyl [4], carboxylic [4], iodo [10], thiol [11], thiocarbonyl [12], alkoxyamine etc., end groups via action of O$_2$ or ethylene oxide, CO$_2$, I$_2$, S$_8$, thiocarbonyl disulfides, alkoxyamine radicals [13], respectively, onto PE chains in Mg(PE)$_2$ species.

2.2.3 Chain Growth Polymerization of Styrene and Conjugated Dienes

The potential of this chemistry beyond the polymerization of ethylene was rapidly recognized and several examples of CGP of styrene, butadiene (BD) and isoprene (Ip) with binary Ln–Mg systems were reported. The combination of chloroneodymocene precursors $Cp*_2NdCl_2Li(OEt_2)_2$ or $[\{Me_2C(Cp)(Flu)\}NdCl]_2$ (Cp = cyclopentadienyl; Flu = fluorenyl) with excess dialkylmagnesium ($Mg(n,sBu)_2$, $Mg(allyl)_2$) afforded effective, although modestly active, catalytic systems for the oligomerization of styrene [14, 15]. This work was followed by similar efforts from the groups of Zinck and Duchateau who reported that homo- and heteroleptic rare-earth tetrahydroborates and chlorides could be associated to $Mg(nBu)(Et)$ to enable the CGP of isoprene [16] and styrene [17, 18] and their copolymerization. Achieving high regio- and stereospecificity in these polymerizations remained troublesome, and it is only recently that truly stereoselective CGP of styrene was documented. Combinations of the discrete neutral allyl *ansa*-lanthanidocenes $\{Me_2C(Cp)(Flu)\}Nd\{1,3-(SiMe_3)_2C_3H_3\}$ and *rac*-$\{Me_2C(Ind)_2\}Y\{1,3-(SiMe_3)_2C_3H_3\}$ (Ind = indenyl) with an excess of $Mg(nBu)_2$ constitute efficient CGP systems, yielding near-perfect syndio- and isospecific poly(styrene)s, respectively, with high activities and productivities [19]. By adjusting the amount of $Mg(nBu)_2$, up to 200 polymer chains can be generated *per* metal center, and good control of the molecular weight features enables the tailoring of low to medium molecular weight polymers. The same system proved effective also for the CGP of isoprene and isoprene-styrene, yet with the 1,4-*trans* specificity gradually decreasing in favor of the 3,4-polymer with increasing amounts of $Mg(nBu)_2$ [20].

Finally, it is noteworthy that, in contrast to $Mg(PE)_2$ species, the isolation and further manipulation of the $Mg(polystyryl)_2$ and $Mg(polydienyl)_2$ species generated in these Ln–Mg-mediated CGP processes remains to be demonstrated.

2.3 Polymerization of Styrenes and Conjugated Dienes with Discrete Ae Compounds or In situ Generated Catalysts

As mentioned above, the polymerization of styrenics and conjugated dienes such as BD and IP usually proceed via similar pathways involving metal-allyl type intermediates. Also, most often, catalyst systems that proved active for one type of monomers also display significant activity for the other type of monomers. These two classes of monomers will be therefore discussed together.

2.3.1 Early Works with In situ Generated Magnesium-based Systems

Mixed lanthanide/magnesium allyl complexes are readily prepared from the direct reaction of a Ln-halide precursor with an allyl Grignard reagent, and these
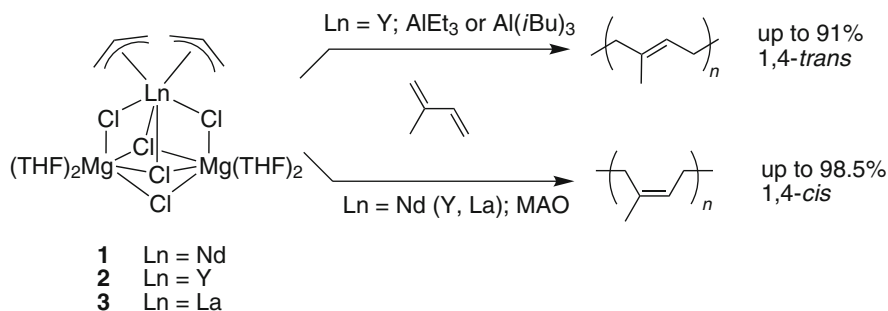
Scheme 2 Heterometallic Ln(allyl)$_2$Cl(MgCl$_2$)$_2$·(THF)$_4$ compounds for stereoselective polymerizations of isoprene [22]

derivatives proved to be valuable pre-catalysts for the stereospecific polymerization of 1,3-diene. For instance, the mixed Mg-samarocene compound {Me$_2$C(C$_5$H$_4$)$_2$} Sm(allyl)MgCl$_2$(Et$_2$O)$_2$LiCl(Et$_2$O) gives rise to 95 % *trans*-regular poly(isoprene) (PIP) with controlled molecular weights and relatively narrow polydispersity ($M_w/M_n \approx$ 1.5–1.8) [21].

Combinations of the even more readily available heterometallic Ln(allyl)$_2$Cl (MgCl$_2$)$_2$·(THF)$_4$ compounds (Scheme 2: Ln = Nd, **1**; Y, **2**; La, **3**) [23, 24] with alkylaluminum activators (methylaluminoxane (MAO), AlMe$_3$, AlEt$_3$, Al(iBu)$_3$; ca. 30 equiv vs. Ln) generate highly active catalysts for the polymerization of IP (average turnover frequencies up to ca. 5×10^4 mol$_{IP}$·(mol$_{Nd}$ h)$^{-1}$ at 20 °C; Scheme 2) [22]. The Nd–Mg precursor led to PIP in a controlled fashion with up to 98.5 % *cis* content, number-average molecular weights in reasonable agreement with calculated values and relatively narrow molecular weight distributions ($M_w/M_n \approx$ 1.2–1.7). The yttrium precursor **2** gave rise to much less active and less controlled systems, but enabled the formation of either 1,4-*cis*-enriched (75 %) or 1,4-*trans*-enriched (91 %) PIP, simply replacing the MAO activator by AlEt$_3$ or Al(iBu)$_3$, respectively. Although magnesium appeared to be necessary to achieve these performances, the exact nature of the active species generated in these systems was not elucidated.

Highly *trans*-stereospecific polymerization of BD and IP was achieved by using a binary catalytic combination made of a neodymium alkoxide, phenolate [25], or tetrahydroborate complex [26] with 1 equiv of a dialkylmagnesium. The combination {Cp'}Nd(BH$_4$)$_2$(THF)$_2$ (Cp' = C$_5$Me$_4$Pr; **4**)/MgBu$_2$ (1:1) proved particularly efficient, affording poly(butadiene) (PBD) and PIP with a 1,4-*trans* content higher than 95 % and relatively narrow molecular weight distributions ($M_w/M_n \approx$ 1.1–1.8) [26]. The dialkylmagnesium co-reagent is the key component to achieve *trans*-stereoselective polymerization (as opposed to alkyl-aluminums which give *cis*-stereoselective polymerization). Based on NMR experiments, the formation of a bimetallic Nd-(μ-BH$_4$)-Mg species (**5**) was proposed (Scheme 3).
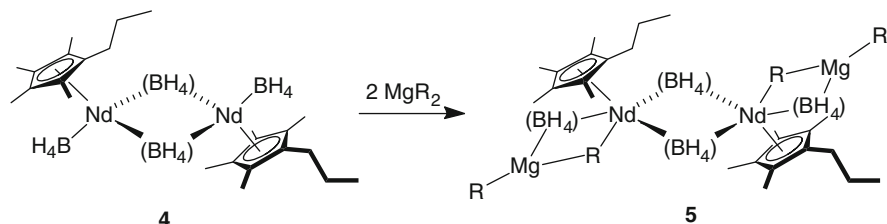
Scheme 3 Precursor and putative active borohydrido species involved in the polymerization of butadiene and isoprene [26]

2.3.2 Discrete Heavier Ae Compounds

The use of heavier Ae complexes for polymerization purposes can be traced back to the 1970s, with the use of dibenzylbarium. This compound was generated from a Ba mirror and $Hg(CH_2Ph)_2$ and converted to "dipolystyrylbarium" upon reaction with α-methylstyrene and then styrene [27]. Recent years have witnessed a strong revival of the synthetic chemistry of discrete heavier Ae complexes and some of these compounds have proved particularly effective for polymerization catalysis, especially for styrene.

Harder and coworkers reported the synthesis of a variety of homoleptic and heteroleptic benzyl barium complexes (Fig. 1) [28]. Among these, *bis*(1,1,3-triphenylpropyl)barium, $Ba(Ph_2CCH_2CH_2Ph)_2(THF)_2$ (**6**), was prepared from the insertion reaction of 1,1-diphenylethene (DPE) into each of the $Ba–CH_2Ph$ bonds in $Ba(CH_2Ph)_2(THF)_2$. This compound, which is particularly soluble also in nonpolar hydrocarbons, initiated the anionic polymerization of styrene to essentially atactic poly(styrene) (PS). The polymers had molecular weights in good agreement with values calculated from the monomer-to-initiator ratio and relatively narrow molecular weight distributions ($M_w/M_n \approx 1.2–1.4$). The heteroleptic complex (η^5,η^6-$C_5Me_4SiMe_2Ph)Ba(CPh_2CH_2CH_2Ph)$ (**7**) showed similar reactivity. Examination of the M_n values of PS produced from this initiator indicated that each triphenylpropyl group gives rise to one polymer chain, while the $C_5Me_4SiMe_2Ph$ chelate ligands remain unreactive.

The benzylcalcium complex [α,α-*bis*(trimethylsilyl)benzyl]$_2$calcium(THF)$_2$ (**8**) proved unreactive toward styrene (Fig. 2) [29]. This was ascribed to the kinetic as well as thermodynamic stabilization provided by the two trimethylsilyl groups attached to the carbanionic carbon. To obtain dibenzylcalcium compounds that are nucleophilic enough for the initiation of styrene polymerization, Harder and coworkers then replaced one of the TMS substituents by a hydrogen atom and compensated for the loss in stabilization by introducing intramolecular coordination via a dimethylamino group (**9**) (Fig. 2) [30]. The latter form of stabilization does not affect the nucleophilicity of the carbanionic center. In fact, the new compound **9** turned out to be an active initiator for the anionic polymerization of styrene, affording essentially atactic PS. The molecular weight distribution determined by size exclusion chromatography (SEC) showed a light tailing in the low molecular weight range which was ascribed to slow initiation compared to
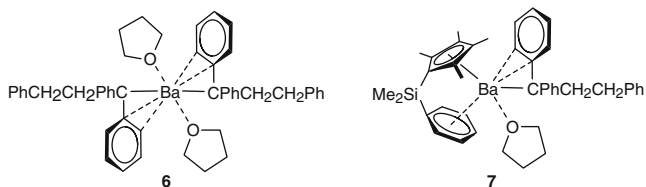
Fig. 1 Homoleptic and heteroleptic benzyl barium complexes (**6–7**) by Harder and coworkers [28]
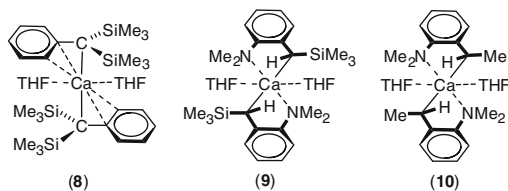
Fig. 2 Dibenzylcalcium compounds by Harder and coworkers [29, 30]
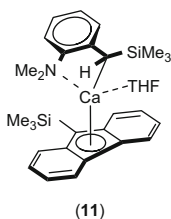
Fig. 3 Heteroleptic fluorenyl-benzylcalcium complex (**11**) by Harder and coworkers [31]

propagation. Yet, stepwise addition of styrene at different time intervals showed no significant chain termination, indicating a living behavior of the polymerization.

A significant step forward was accomplished with the heteroleptic fluorenyl-benzylcalcium complex **11** (Fig. 3), which was obtained by reaction of the homoleptic benzylcalcium compound **9** with 9-Me$_3$Si-fluorene. Compound **11** indeed allowed the syndioselective polymerization of styrene [31]. The PS obtained with the heteroleptic benzylcalcium initiator **11** under standard polymerization conditions (10 % of styrene in cyclohexane at 50 °C) was only slightly enriched in syndiotactic sequences. However, the syndiotacticity of the materials could be increased considerably by increasing the monomer concentration: in fact, polymerization in neat styrene yielded PS with 85 % *r*-diads and 76 % *rr*-triads.

Harder proposed a polymerization mechanism in which monomer insertion proceeds with a high degree of tacticity and where stereoerrors in the polymer chain are due to inversion of the chiral carbanionic chain end (Scheme 4) [31]. In such a mechanism, the ratio between the rates of monomer insertion and chain-end inversion determines the extent of stereoregularity of the PS. This accounted for the fact that an increase in the monomer concentration accelerated the insertion rate, while leaving the inversion rate largely unaffected, and resulted in higher
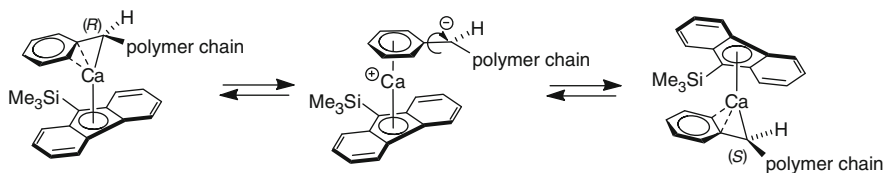
Scheme 4 Stereoerrors in PS arising from inversion of the chiral carbanionic chain end in styrene polymerizations mediated by heteroleptic fluorenyl-benzylcalcium complexes described by Harder and coworkers [31]
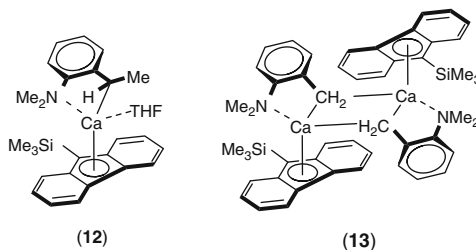
Fig. 4 Variations in fluorenyl-benzylcalcium complexes (**12–13**) by Harder and coworkers [32, 33]

syndiotacticity. On the other hand, an excess of THF (4 equiv vs. **11**) increased the rates of inversion of the chiral carbanionic chain ends, thus destroying the stereoregularity in the polymer chain [32].

Although a certain living character was evidenced, the PS obtained with the heteroleptic benzylcalcium complex **11** showed an even more extensive tailing in the low molecular weight part of the SEC trace than that obtained with the homoleptic **9**, evidencing more pronounced chain termination processes.

The α-methyl-benzylcalcium compound **12** (Fig. 4) is less stable and showed a higher reactivity and faster initiation of styrene polymerization than the analogue α-Me$_3$Si-benzylcalcium complex **11** [33]. This was evidenced by less tailing in the low molecular weight regions of the SEC trace. The unsubstituted aminobenzyl complex **13**, which exists as a methylene-bridged THF-free dimeric compound in the solid state and probably as well in benzene solution, is even more reactive towards styrene [32].The tacticity of the PS obtained with the initiators **11, 12**, and **13** was, as expected, comparable.

Harder and coworkers further prepared a series of complexes with bulky substituents like tBu-, Ph(Me)$_2$C-, Me(Ph)$_2$C-, and Me(4-tBu-C$_6$H$_4$)$_2$C- in the 2- and 7-positions of the fluorenyl ligand (complexes **14–18**, respectively) (Fig. 5) [34]. These complexes initiate styrene polymerization, and the syndiotacticity of the resulting polymers increases with the steric bulk of the substituents on the fluorenyl ligands; syndiotacticities up to 95 % r diads (i.e., 90 % rr triads) were thus obtained. However, the broad molecular weight distributions offered by these compounds precluded the synthesis of well-defined block copolymers.

Recently, Okuda and coworkers have prepared neutral [35] and monocationic [36] allyl complexes of calcium. Preliminary investigations into the polymerization of BD
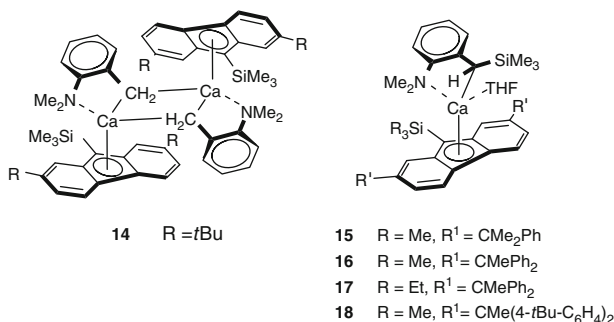
Fig. 5 Introduction of steric bulk in fluorenyl-benzylcalcium complexes (**14–18**) by Harder and coworkers [34]

in THF mediated by the *bis*(allyl)calcium Ca(η^3-C$_3$H$_5$)$_2$ (1 mol% vs. the monomer) resulted in quantitative conversion of the monomer, giving PBD with a low molecular weight of $M_w = 6,600$ g·mol^{-1} but a narrow molecular weight distribution $M_w/M_n = 1.15$. However, poor regioselectivity was achieved as the 1,2-PBD/1,4-PBD and 1,4-*cis*-PBD/1,4-*trans*-PBD ratios were 0.92 and 0.81, respectively. In contrast to *bis*(allyl)calcium, compounds that contain an allyl calcium monocation of the type [Ca(C$_3$H$_5$)]$^+$ were found to be inert towards BD. This observation was ascribed to the decreased nucleophilicity of the allyl calcium monocation and hints at an anionic mechanism of the BD polymerization initiated by Ca(η^3-C$_3$H$_5$)$_2$.

2.4 Polymerization of Methacrylate Esters with Discrete Ae Compounds or In situ Generated Catalysts

The isospecific polymerization of alkyl methacrylates with Grignard reagents at low temperatures in nonpolar solvents has been known for several decades. For example, the sterically bulky initiator *t*BuMgBr is particularly efficient for the polymerization of methyl methacrylate (MMA), affording highly isotactic (96–97 % of *mm* triads) poly(MMA) (PMMA) with almost 100 % initiation efficiency in toluene at −78 °C [37]. The polymerizations of other methacrylates such as ethyl and *n*-butyl methacrylates also afford highly isotactic poly(alkyl methacrylate)s but require the addition of 1–2 equiv of AlMe$_3$ vs. *t*BuMgBr, in order to obtain polymers with narrow molecular weight distributions.

Examples of polymerization of alkyl methacrylates with well-defined alkaline-earth compounds are much more seldom. Yet, a striking result was reported by Gibson and coworkers with the β-diketiminate (BDI) magnesium enolate complex **19** (Fig. 6), which turned out to be a highly efficient initiator for the living and syndioselective polymerization of MMA [38]. For example, the polymerization of 400 equiv of MMA proceeded at temperatures as low as −30 °C within 10 min, giving PMMA with very narrow molecular weight distribution ($M_w/M_n = 1.1$) and

Fig. 6 β-diketiminate magnesium enolate complex (**19**) by Gibson and coworkers [38] and related *bis*(pyridylamine) magnesium isopropyl complexes (**20**) by Carpentier and coworkers [39] for the polymerization of MMA
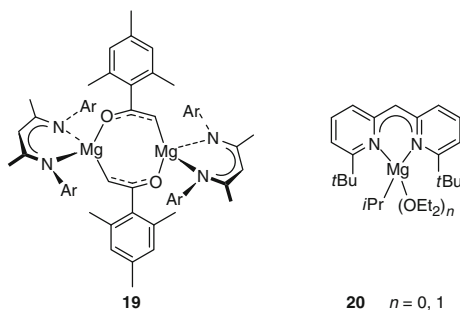
M_n values that matched the expected ones (based on the monomer-to-initiator ratio). In stark contrast to the highly isospecific MMA polymerization using *t*BuMgBr, the polymers formed were highly syndiotactic (*rr* triads up to 92 %) and showed accordingly high glass transition temperatures (T_g up to 135 °C). High levels of stereocontrol in these polymerizations were assumed to arise from a chain-end control mechanism thanks to the bulky BDI ligand.

Surprisingly enough, this preliminary report was never followed by systematic variations around this prototypal {BDI}Mg(enolato) compound. In a related work, Carpentier and coworkers showed that the sterically hindered isopropylmagnesium compound **20** (Fig. 6) stabilized by a monoanionic, symmetrically 2,2'-substituted bis (pyridyl)amine ligand is a moderately active catalyst for the polymerization of MMA (−78 °C, 1 mol% Mg vs. monomer in toluene; 65 % conversion in 3 h) [39]. The PMMA formed had a unimodal distribution ($M_w/M_n = 1.97$, $M_n = 27{,}000$ g mol^{-1}) and an isotactic-enriched microstructure (42 % *mm* and 43 % *mr* triads).

3 Ring-Opening Polymerization

First a brief introduction to the general aspects of the ROP of cyclic esters is presented. The use of heteroleptic discrete complexes of magnesium is discussed in an independent section, since it is more developed than that of complexes of the larger Ae metals. Recent breakthroughs with well-defined heteroleptic Ca–Ba complexes are then dealt with on their own. In the fourth section, unusual cases of discrete cationic complexes and neutral bimetallic species are covered. The perspectives offered by Ae-based ROP catalyst systems are briefly discussed in the last section.

3.1 Polymerization of Cyclic Esters and Carbonates: General Aspects

In the global context of sustainable development stigmatized by the depletion of the reserves of fossil fuel and the ever-increasing prices of oil-derived materials, linear

aliphatic poly(ester)s and poly(carbonate)s prepared by ROP of cyclic (di)esters
and carbonates are attracting growing attention as both commodity and specialty
materials. They are often biocompatible and biodegradable, and offer thermal,
physical, and mechanical properties which are complementary or comparable to
those of some oil-based polymers [40–45]. Monomers such as ε-caprolactone (CL)
or Glycolide (GL) have long been employed by organometallic and polymer
chemists, but more recently green monomers like lactide (LA) and trimethylene
carbonate (TMC) have emerged as particularly attractive raw materials since they
are derived from annually renewable resources (Fig. 7). Notably, LA is produced on
a scale of 150,000 metric tons p.a. by fermentation of sugars or starch [46, 47].

Because it possesses two stereogenic centers, the case of LA—the cyclic dimer
of lactic acid—particularly stands out. It is available in its enantiomerically pure
forms, L- and D-lactide (L-LA and D-LA) where the two chiral centers adopt,
respectively, the S and R configurations, or as a racemic mixture of these two
enantiomers (D,L-LA) and even as *meso* lactide (*meso*-LA) where the two optically
active centers adopt opposite configuration (Scheme 5). Depending on which type
of LA is polymerized, various microstructures can be envisaged for the resulting
poly(LA) (PLA). The tacticity of PLA chains is generally expressed as the proba-
bility of a *racemic* (P_r) or *meso* (P_m) enchainment between two consecutive
monomers. In the absence of epimerization, the ROP of D- and L-LA leads to the
formation of pure isotactic poly(D-LA) (PDLA) and poly(L-LA) (PLLA), respec-
tively ($P_m = 1.00$). The stereocontrolled ROP of *meso*-LA can produce
syndiotactic ($P_r = 1.00$) or heterotactic ($P_m = 1.00$) PLA chains, while atactic
PLA is obtained if no stereocontrol is exerted ($P_m = P_r = 0.50$). Finally, without
stereocontrol, the ROP of D,L-LA yields atactic PLA ($P_m = P_r = 0.50$), or
heterotactic ($P_r = 1.00$) and even isotactic ($P_m = 1.00$) PLA in the case of
stereocontrolled reactions; in this last case, various combinations (isotactic
homochiral, di- or multi-stereoblock) may arise depending on the ROP mechanism
and catalyst effectiveness (Scheme 5).

ROP reactions of cyclic esters/carbonates are promoted by a variety of catalyst
systems. Metal-based inorganic and organometallic systems belong to the most
effective ones, both in terms of reactivity (activity, productivity) and control over
the polymerization. In these systems, the metal is usually very oxophilic (metal
groups 1–4 and 12–14 of the Periodic table) and acts as a Lewis acidic center that
activates the cyclic ester via coordination of its carbonyl moiety. Such ROP catalyst
systems are based for the largest part on zinc, aluminum, and rare-earth metals; they
have been reviewed in length in the literature of the past decade, and the interested
reader may consult the relevant reviews to gain a more general view of catalyst
development in the field of ROP catalysis [44, 48–55]. However, it is only recently
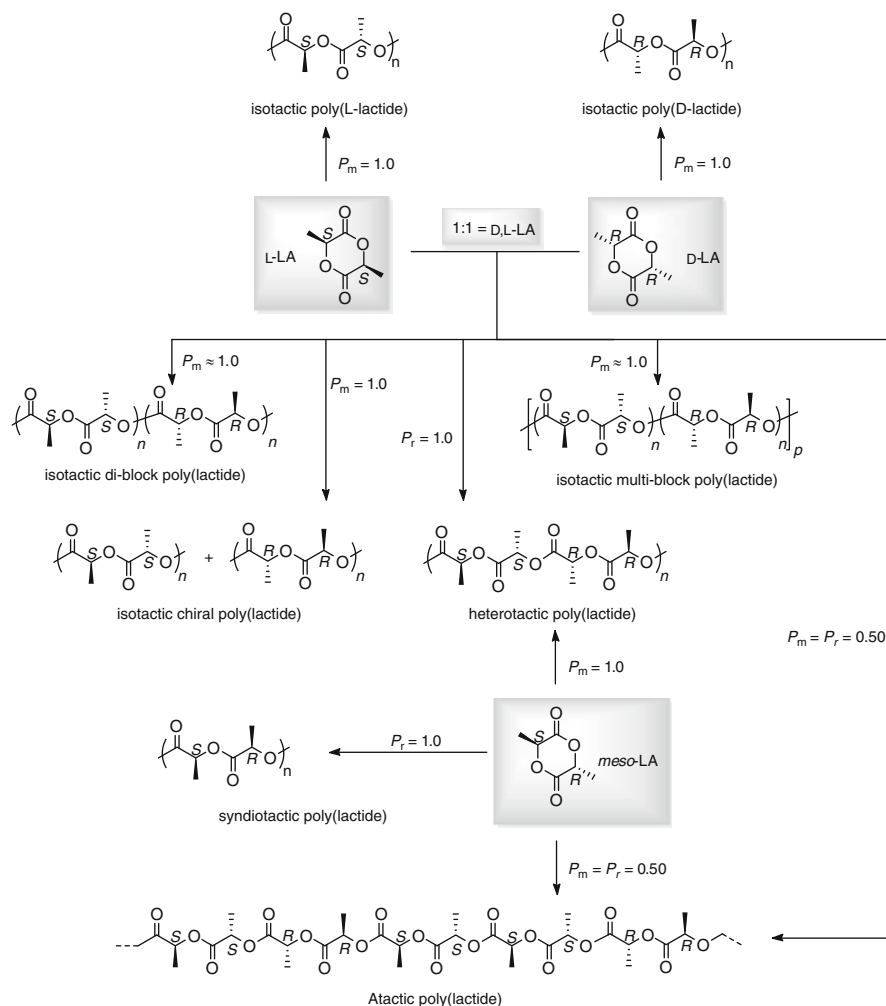
Scheme 5 Various isomers of LA and microstructures of PLA chains following ROP

that a variety of systems tailored around complexes of magnesium or the larger Ae metals (Ca, Sr, and Ba) have been disclosed, and in the following we shall focus exclusively on these innocuous elements.

Depending on the origin of the nucleophile which will open the monomer, two distinct mechanisms can be envisioned for the metal-mediated ROP of cyclic esters (Scheme 6). Upon coordination of the incoming monomer to the metal center, the electrophilicity at the carbonyl carbon atom is greatly enhanced. This eventually facilitates attack of either an *internal* nucleophilic moiety—that is, an anionic "active" ligand initially attached to the metal complex which accordingly operates via a so-called "coordination–insertion" mechanism—or an *external* (exogenous)
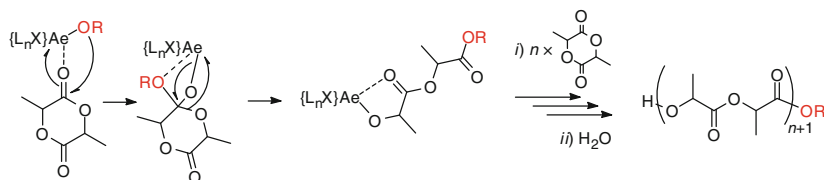
Scheme 6 "Coordination–insertion" and "activated monomer" mechanisms for the metal-mediated ROP of LA

nucleophile—typically a protic compound such as an alcohol or an amine—the global system then operating via a so-called "activated monomer" mechanism [55].

Note that a distinction must be made between the terms *initiator* and *catalyst*. In the "coordination–insertion" mechanism, the nucleophilic group is covalently bound to the Ae metal; its number is definite, and ranges from one to the valence of the metal at most. The metal complex is hence branded the name of *initiator* as it determines the number of polymer chains that shall be generated. In the majority of cases, a single nucleophilic group is attached to the metal center, and only one polymer chain can be generated *per* metal center: this grossly corresponds to a "*living*" polymerization. On the other hand, in the "activated monomer" mechanism or in a so-called "*immortal* ROP" (*i*ROP) with fast and reversible transfer between growing and dormant macromolecules, the number of polymer chains produced is preset by the number of added exogenous nucleophile equivalents. The latter can be in much larger excess with respect to the Ae metal complex, which therefore behaves as a true *catalyst* (Scheme 7).

Unless otherwise specified, all the systems in this section are generally considered to promote the living ROP of the relevant cyclic ester(s) or carbonate(s), that is, each metal center generates a single polymer chain, and all polymer chains are of equal length for a given initiator. Practical indicators for a living system include (a) a very narrow distribution of molecular weights for the resulting materials ($M_w/M_n < 1.10$), although slightly higher values (≈ 1.20–1.30) can be considered acceptable under particularly pushing experimental conditions (e.g., bulk monomer, high temperature, high monomer-to-initiator ratio), (b) a linear dependence of the polymer molecular weight on the monomer-to-metal ratio at a given monomer conversion, and (c) a linear increase of the polymer molecular weight with monomer conversion. The reader must however bear in mind that to fulfill the criteria for a perfectly living ROP, an initiating system must in essence feature (a) 100 %
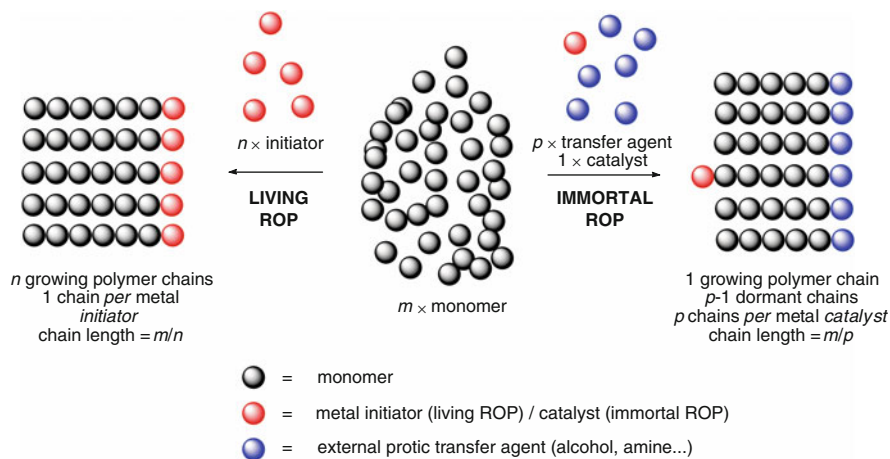
Scheme 7 Illustrative comparison of the living and immortal ROP processes

initiation efficiency, i.e., all metal centers initiate the formation of a macromolecule, (b) an initiation rate constant far greater than the propagation rate constant, and (c) the absence of termination and transfer reactions (e.g., elimination, transesterification).

3.2 Complexes of Magnesium

3.2.1 *Tris*(pyrazolyl) and *Tris*(indazolyl)Borate Ligands

The initial breakthrough came from Chisholm and coworkers who, in the first comprehensive study of well-defined initiators for the ROP of lactide, disclosed the structure and catalytic activity of magnesium-alkoxide complexes supported by bulky *tris*(pyrazolyl) (Tp) or *tris*(indazolyl)borate ligands (Fig. 8) [56, 57]. Complexes **21** and **22** proved highly effective for the ROP of both L- and *meso*-LA in dichloromethane at room temperature, converting up to 1,000 equiv of monomer within 1–3 h; these constituted at the time some of the most active initiators for the ROP of LA, second only to the ill-defined "Y[OCH₂CH₂NMe₂]₃" [58]. The reaction proceeded via acyl cleavage, with first-order dependence upon both monomer and initiator concentrations. The resulting polymers exhibited narrow molecular weight distributions ($M_w/M_n \approx 1.1$–1.3) up to 90 % conversion. The catalyst activity increased with the steric bulk of the ligand scaffold in these magnesium (and closely related zinc) systems. These initiators showed a preference (more pronounced in the case of the chiral **22** than with the achiral **21**) for the ROP of *meso*-LA above that of L-LA, as seen in the polymerization of 1:1 mixtures of the two diastereoisomers. Exclusively *meso*-LA was polymerized to slightly syndiotactic-enriched poly(*meso*-LA) when the polymerization of this mixture
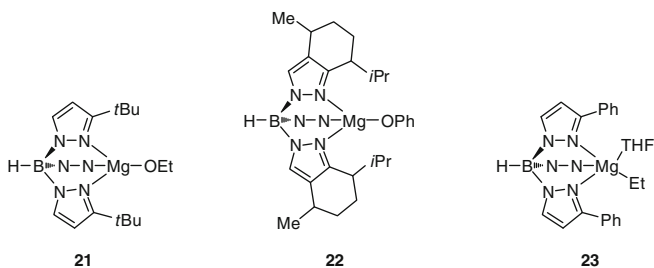
Fig. 8 *Tris*(pyrazolyl) and *tris*(indazolyl) heteroleptic Mg complexes by Chisholm and coworkers [56, 57]. Central substituents are abbreviated as N–N for clarity
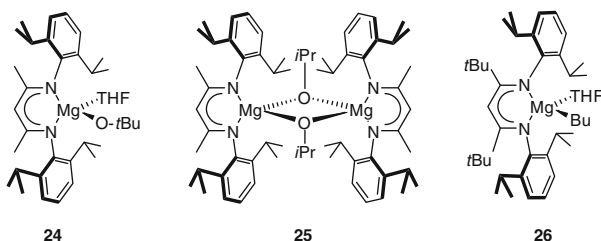
Fig. 9 Seminal BDI magnesium complexes (**24–25**) by Chisholm and coworkers [60, 61] and Coates and coworkers [62] and the sterically congested {BDI^{iPr4,*}}Mg(*n*Bu) (**26**) by Chisholm and coworkers [63]

was carried out at –40 °C with **22**, which hence showed enhanced diastereoselectivity but only limited stereoselectivity.

3.2.2 β-Diketiminate Ligands

The implementation of the very versatile family of BDI ligands for the design of ROP initiators has represented a milestone for researchers in this field. Initially introduced by Coates and coworkers for the synthesis of a truly remarkable range of Zn-based ROP catalysts [48–53, 59], the BDI ligands were further implemented by the groups of Chisholm [60, 61] and Coates [62] to the preparation of heteroleptic Ae-alkoxide complexes of low coordination numbers (Fig. 9).

Chisholm's monomeric {BDI^{iPr4}}Mg(O*t*Bu)(THF) (**24**) readily loses its coordinated THF molecule under polymerization conditions in CD$_2$Cl$_2$. It polymerizes 100 equiv of D,L- or L-LA in dichloromethane in 2 or 10 min, respectively, the former leading essentially to atactic PLA [60, 61]. Similarly, Coates' dimeric initiator [{BDI^{iPr4}}Mg(O*i*Pr)]$_2$ (**25**) converted quantitatively 100–500 equiv of D,L-LA to atactic PLA within 5 min at 20 °C; the addition of 1 equiv of *i*PrOH (vs. Mg) was required to obtain narrow molecular weight distributions ($M_w/M_n \approx$ 1.20–1.35) as otherwise the nature of the polymer chains is less controlled (M_w/M_n = 1.59) [62]. These two studies revealed that in dichloromethane, the Mg-based **24** and **25** were
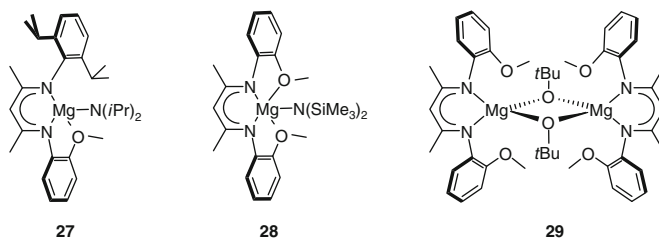
Fig. 10 Structure of the methoxy-containing BDI complexes by Gibson and coworkers (**27**) [64] and Chisholm and coworkers (**28–29**) [65]

much faster than their zinc congeners {BDI^{iPr4}}Zn(OtBu)(THF) and [{BDI^{iPr4}}Zn(OiPr)]$_2$; nevertheless, the latter initiators yielded highly heterotactic-enriched PLA while **24** and **25** invariably produced atactic PLA. Chisholm noticed a marked solvent effect [61]: the ROP of D,L-LA promoted by **24** in THF was slower than in dichloromethane owing to competitive coordination of the solvent, but it resulted in substantially heterotactic-enriched PLA; no explanation was given for the higher selectivity obtained in THF.

Subsequent attempts by Chisholm and coworkers to induce enhanced heteroselectivity in the ROP of D,L-LA by increasing the steric congestion around the Mg center with a sterically encumbered ligand backbone proved unsuccessful [63]. Using the initiator {BDI^{iPr4,*}}Mg(Bu)(THF) (**26**) in benzene at room temperature gave full conversion of D,L-LA to purely atactic PLA (Fig. 9).

In order to tame the extreme reactivity of the prototypal **24** and **25** and achieve better control of the ROP parameters (notably M_w/M_n), Gibson and coworkers prepared an asymmetric BDI ligand bearing an intramolecular chelating 2-MeO-phenyl substituent instead of the iPr groups on one of the aromatic rings [64]. The rationale was that the resulting Mg complex {BDI^{iPr2,OMe}}Mg(N(iPr)$_2$) (**27**) should be less active and less prone to transesterification reactions than **24** and **25**, owing to the presence of an extra coordinating side arm which should decrease the electrophilicity of the metal center (Fig. 10). The approach met no success, as **27** turned out to be as fast an initiator (>80 % conversion of 100 equiv of D,L-LA within 10 min in benzene-d_6 at room temperature) as **24** or **25** but without promoting the living or even controlled polymerization of the monomer ($M_w/M_n \approx$ 1.53–1.66; no linear relationship between M_n and conversion). The authors argued that these observations stemmed from the weakness of the interaction between the –OMe tether and the metal center in **27** (which consequently was not less electrophilic than in **24** or **25**), and the lower steric hindrance which resulted in higher rate of transesterification reactions. Poor initiation was also mentioned as a possible cause, perhaps because of the limited ability of amido groups to promote controlled ROP reactions as stated before by Chisholm and coworkers [61]

A similar strategy, albeit with a different aim, was instigated by Chisholm and coworkers who, following their early discoveries, prepared the less congested but more chelating ligand HC{C(Me)N–2,6–(OMe)$_2$C$_6$H$_3$}$^-$ ({BDI^{OMe2}}$^-$) with

Fig. 11 {Bamam}MgR(L)$_n$
complexes (**30**) by Chivers
and coworkers [66]

R = tBu, Mes, L = none
R = Me, Bu, L = Et$_2$O
R = Ph, iPr, L = THF
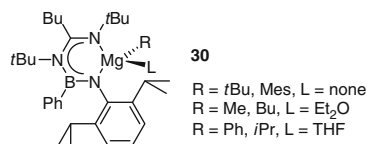
2-MeO-phenyl substituents instead of iPr groups on the aromatic rings [65]. The aim
was to achieve heteroselectivity in the ROP of D,L-LA in the way observed with **24** in
THF [61]. The methoxy groups in {BDI^{OMe2}}H could cancel the need for
coordinating solvent and maintain high polymerization rates. Both methoxy
groups were found to coordinate to the magnesium center in the monomeric
{BDI^{OMe2}}Mg(N(SiMe$_3$)$_2$) (**28**), but not in the dimeric [{BDI^{OMe2}}Mg(OtBu)]$_2$
(**29**) (Fig. 10). Complex **29** initiated the rapid ROP of 100 equiv of D,L-LA in dichlor-
omethane (91 % conversion in 20 min), but the control was poor ($M_{n,\ calculated}$
= 13,100 g·mol^{-1}, $M_{n,\ observed}$ = 96,500 g·mol^{-1}, M_w/M_n = 2.23). The poor control
was attributed to transesterification reactions with the hard, electrophilic magnesium,
and also to the dimeric nature of **29** resulting in a poor initiation rate. The authors also
stated that the order of reactivity decreased with the chelating ability of the ligand:
{BDI^{iPr4}}$^-$ (**24**) > {BDI^{iPr2,OMe}}$^-$ (**27**) > {BDI^{OMe2}}$^-$ (**29**). In dichloromethane,
29 afforded PLA chains with 50 % of [rmr] and [mrm] tetrads, whereas in THF this
value increased to 85 %. Hence, as previously observed with **24**, the use of THF as a
solvent was mandatory to achieve significant heteroselectivity with **29**, but at the
logical expense of catalyst activity (91 % conversion in 90 min in THF instead of
20 min in dichloromethane). The hemi-labile methoxy side arms were proposed to
play a discriminating role toward the incoming monomer, explaining the higher
degree of stereocontrol observed with **29** than with **24**.

Chivers and coworkers endeavored to introduce greater variety in the chemistry
of these N,N-chelating ligands with the elegant syntheses of {Bamam}MgR(L)$_n$
complexes (**30**) supported by the hybrid boroamidinate/amidinate ancillary ligand
(Fig. 11) [66]. The influence of the polar, electron-accepting tBu–N–B–Ph fragment
in the ligand backbone was examined. The complexes with small active groups
(R = Me, L = Et$_2$O; R = Ph, L = THF) displayed moderate activity in the ROP
of D,L-LA, achieving 61–100 % conversion of 200 equiv of monomer in 2–2.5 h
at room temperature in chloroform, but yielded only atactic or very mildly
heterotactic-biased PLA; the other complexes were either not active or not tested.
These initial results with this class of ligands were not followed up.

3.2.3 Hybrid and Heteroscorpionate Ligands

The family of heteroscorpionate ligands tailored around acetamidinate fragments
disclosed by Sánchez-Barba and coworkers constitutes another useful class of
nitrogen-containing ancillaries particularly suited to the synthesis of heteroleptic
Mg complexes. In a first study [67], they prepared {tbpamd}MgR (R = C$_3$H$_5$, **31**;

Fig. 12 Alkyl heteroscorpionate magnesium complexes {tbpamd}MgR (**31–33**) and {pbpamd}MgR (**34–36**) by Sánchez-Barba and coworkers [67]

| **31** | R = C$_3$H$_5$ | **34** | R = C$_3$H$_5$ |
| **32** | R = tBu | **35** | R = tBu |
| **33** | R = CH$_2$SiMe$_3$ | **36** | R = CH$_2$SiMe$_3$ |
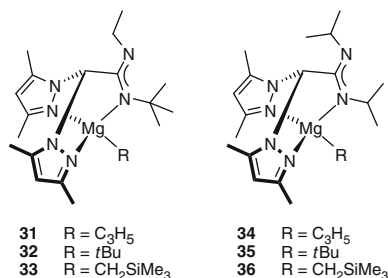
tBu, **32**; CH$_2$SiMe$_3$, **33**) and {pbpamd}MgR (R = C$_3$H$_5$, **34**; tBu, **35**; CH$_2$SiMe$_3$, **36**) complexes where the pyrazolyl chelating side arms contained Me substituents (Fig. 12). Complexes **31–36** displayed high activity in the ROP of CL. The polymerization of 500–5,000 equiv of CL readily took place between −60 and +20 °C, and near-complete conversion of the monomer in as little as 1–10 min to yield poly(CL) (PCL) with high molecular weights (18,000–161,000 g mol^{-1}) and fairly narrow molecular weight distributions ($M_w/M_n \approx 1.12$–1.45). The best results both in terms of catalyst activity and control were obtained with **33** and **36**. End-group analysis of the polymers generated with these two initiators showed the presence of the expected CH$_2$SiMe$_3$ termini, resulting from acyl cleavage after nucleophilic attack by this alkyl group. Complexes **33** and **36** also promoted the ROP of L- and D,L-LA, albeit with much lower reaction rates. Thus, only partial conversion of 100 equiv of monomer was achieved after 24–96 h at 70 °C or even in melted monomer (ca. 110–130 °C). The activity of **36** could be boosted by addition of 1 equiv of iPrOH to the initiator; the assumption was that the alkoxide complex {pbpamd}Mg(OiPr) was formed in situ, but no evidence was given to support this hypothesis. The reactions were highly controlled ($M_w/M_n \approx 1.05$–1.19 at 70 °C), but only low molecular weight P(L)LAs were obtained ($M_n \approx 3,100$–12,600 g mol^{-1}). No stereocontrol was operative with either **33** or **36**, as atactic PLA was systematically produced by polymerization of D,L-LA.

In a following study, Sánchez-Barba and coworkers greatly improved on their initial results. They reported the synthesis of {tbp*amd}MgR (R = Me, **37**; Et, **38**; CH$_2$SiMe$_3$, **39**; Bn, **40**; C$_3$H$_5$, **41**) and {pbp*amd}MgR (R = Me, **42**; Et, **43**; CH$_2$SiMe$_3$, **44**; Bn, **45**; C$_3$H$_5$, **46**), where the heteroscorpionate ligands carried bulky tBu substituents instead of simple Me groups [68] (Fig. 13). Complexes **37–41** were obtained as a mixture of isomers, depending on the nature of the N-alkyl fragment (N-Et vs. N-tBu) coordinating to the metal center; the distribution between the two structural isomers varied with the identity of the alkyl group on the metal center. These complexes were highly competent for the ROP of CL, converting in a controlled manner 500 equiv of monomer in toluene at 0–20 °C within 15 min ($M_n \approx 2,100$–53,500 g mol^{-1} and $M_w/M_n \approx 1.05$–1.19). Most remarkably, **44** only required 10 s to achieve complete conversion, yielding well-controlled PCL with $M_n = 53,500$ g·mol^{-1} and $M_w/M_n = 1.11$; **44** also afforded high molecular weight PCL by polymerizing 5,000 equiv of CL in 10 min ($M_n = 181,000$ g mol^{-1} and $M_w/M_n = 1.47$). In a marked amelioration of their early results [67], the authors

Fig. 13 Bulky
heteroscorpionate magnesium
complexes {tbp*amd}MgR
(**37–41**) and {pbp*amd}MgR
(**42–46**) by Sánchez-Barba
and coworkers [68]

37	R = Me	**42**	R = Me
38	R = Et	**43**	R = Et
39	R = CH$_2$SiMe$_3$	**44**	R = CH$_2$SiMe$_3$
40	R = Bn	**45**	R = Bn
41	R = C$_3$H$_5$	**46**	R = C$_3$H$_5$
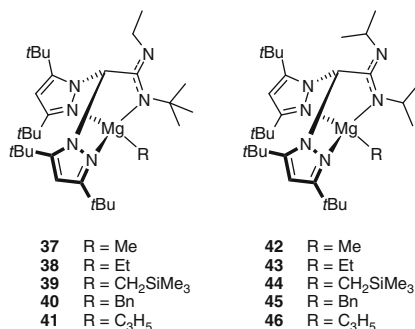
Fig. 14 Hybrid
cyclopentadienyl/scorpionate
magnesium complexes
{bpzcp}MgR (**47–52**) by
Sánchez-Barba and
coworkers [69]

47	R = Me
48	R = Et
49	R = nBu
50	R = tBu
51	R = CH$_2$SiMe$_3$
52	R = Bn
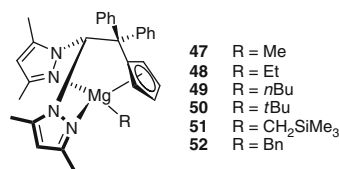
showed that **39** and **44** mediated very effectively the fast and living ROP of both L- and D,L-LA. Hence, 100–200 equiv of monomer were fully converted within 1–4 min at 20 °C in a controlled fashion. The agreement between calculated and observed molecular weights was excellent ($M_{n,obs} \approx M_{n,calc} \approx 5,000$–$50,300$ g mol^{-1}) and the polydispersity was narrow ($M_w/M_n \approx 1.01$–1.19). Besides, heterotactic-enriched PLA was obtained following the ROP of D,L-LA, with P_r values in the range 0.70–0.79. NMR analysis of the polymer end groups confirmed that initiation occurred by nucleophilic attack from Me$_3$SiCH$_2^-$ resulting in acyl cleavage. Kinetic investigations of the living ROP of D,L-LA catalyzed by **39** or **44** demonstrated that in both cases the reaction was first order in monomer and initiator concentrations.

In parallel, Sánchez-Barba and coworkers also reported a related family of hybrid scorpionate/cyclopentadienyl Mg species, {bpzcp}MgR (R = Me, **47**; Et, **48**; Bu, **49**; tBu, **50**; CH$_2$SiMe$_3$; **51**, Bn, **52**) (Fig. 14) [69]. These complexes were moderately competent for the ROP of cyclic esters, and their behavior was reminiscent of that of the non-bulky heteroscorpionate-supported initiators the authors had previously described [67]. The polymerization of 500 equiv of CL proceeded smoothly (0–20 °C, 1–10 min) with **51**, but was much more sluggish with the other complexes (2–48 h, 20–70 °C); the polydispersity was usually in the range 1.19–1.49. Complex **51**, the most efficient initiator in this series, also enabled the ROP of L–LA (200 equiv) in a controlled fashion at 90 °C in toluene (2.5 h) or at 65 °C in THF (5 h); the polydispersity of the resulting PLLAs was low ($M_w/M_n \approx 1.02$–1.15) and the molecular weight of the material was fully predictable on the basis of monomer-to-metal ratio ($M_{n,obs} \approx M_{n,calc} \approx 5,800$–$27,600$ g mol^{-1}). The ROP of D,L–LA was even slower (conversion <59 % after 8 h at 90 °C) but only returned atactic PLA.

Fig. 15 Complexes [{MICMP}$_2$Mg$_2$(THF)]$_2$ (**53**) and [{EDBP}$_2$Mg$_2$(L)$_2$] (**54**) by Lin and coworkers [71]
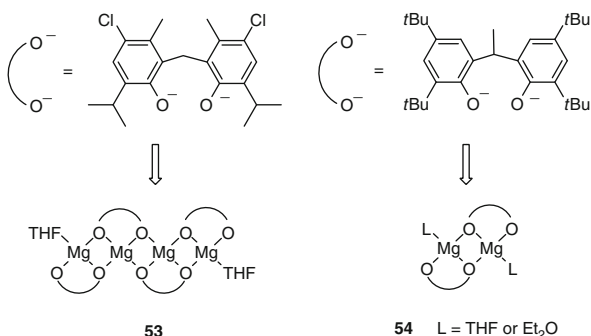
These comprehensive studies by Sánchez-Barba and coworkers [67–69] revealed that {L$_n$X}MgR alkyl complexes bearing (hetero/hybrid) scorpionate ligands provide large and highly efficient families of ROP initiators. Clearly, the best results were achieved with R = CH$_2$SiMe$_3$, which led to well-controlled and extremely fast ROP reactions. However, the influence of the alkyl nucleophilic group was not clearly rationalized by the authors, even if they stated that the trend of reactivity CH$_2$SiMe$_3$ ≫ tBu > Me might reflect the lability of the Mg–C bond [69].

3.2.4 Phenolate Ligands

Because they are readily amenable to steric and electronic modifications, monoanionic, multidentate phenolates constitute a very versatile family of ligands well suited to the preparation of stable Mg (as well as other divalent oxophilic metals) complexes. The interest in these ligands rose sharply following Fujita's discovery of "post-metallocene" catalysts supported by imino-phenolates for the Ziegler–Natta polymerization of olefins in the late 1990s [70]. Researchers in the field of ROP of cyclic monomers have since then endeavored to achieve similar success, in particular of late with phenolate ligands bearing various nitrogen-containing side arms.

Lin and coworkers disclosed in 2004 several multinuclear Mg phenolate complexes containing the bulky {MCIMP}$^-$ or {EBDP}$^-$ ligands, namely [{MICMP}$_2$Mg$_2$(THF)]$_2$ (**53**) and [{EDBP}$_2$Mg$_2$(L)$_2$] (**54**) (Fig. 15) [71]. Upon addition of BnOH, these complexes generated binary catalyst systems which polymerized CL (up to 5,000 equiv) and L-LA (up to 400 equiv). The tetranuclear **53** tolerated as high as 500 equiv of BnOH as an external CTA to achieve the near-complete iROP of 5,000 equiv of CL in toluene (56 °C) in 2 h while maintaining an excellent control over the ROP parameters ($M_w/M_n \approx$ 1.06–1.19). As expected, the ROP of L-LA with these systems was generally slower than that of CL, requiring more elevated temperature (83 °C) and several hours to polymerize 100–400 equiv of monomer in a controlled manner ($M_w/M_n \approx$ 1.04–1.21). In combination with a hydroxyl end-functionalized polystyrene, the dinuclear **54** enabled the formation of poly(styrene–b–L-LA) block copolymers.
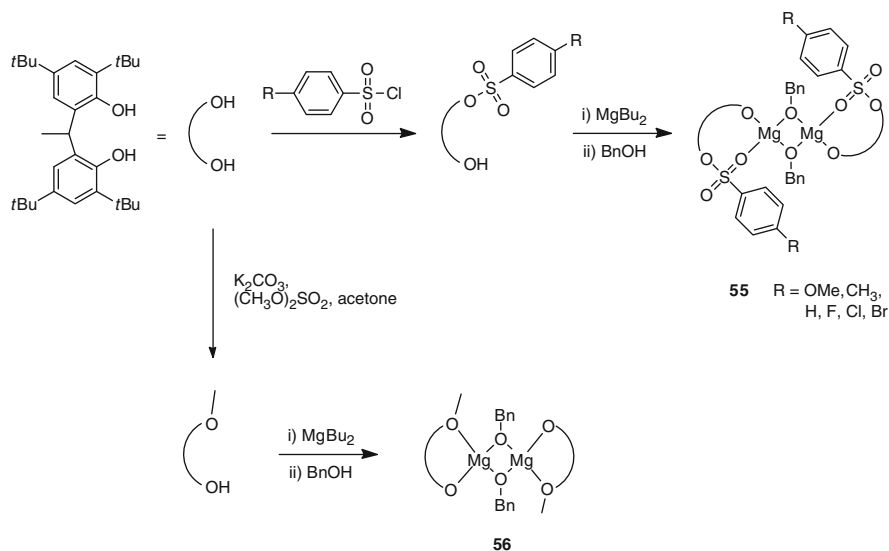
Fig. 16 Benzenesulfonate- (**55**) and methoxy-containing (**56**) alkoxide–Mg heteroleptic complexes {EDBP}MgR by Lin and coworkers [72, 73]

The implementation of benzenesulfonate moieties afforded initiators with markedly improved activity for the ROP of L-LA. Lin and coworkers developed a broad range of *n*-butyl- and especially alkoxide-Mg heteroleptic compounds featuring {EDBP^{sulf}}$^-$, the monosubstituted benzenesulfonate analogues of their {EDBP}$^{2-}$ ligands (Fig. 16) [72]. The series of Mg-alkoxide complexes [{EDBP^{sulf}}Mg(OBn)]$_2$ (**55**) constituted single-component initiators that were capable of polymerizing L-LA in THF or dichloromethane extremely rapidly; for instance, conversion of 1,000 equiv of monomer took place within 4 min at 0 °C in THF. End-group analysis by NMR spectroscopy showed the presence of the expected BnO–C(O) chain end in each macromolecule, the result of acyl cleavage by nucleophilic attack of the BnO$^-$ group onto the coordinated monomer. The distribution of molecular weights was very narrow ($M_w/M_n \approx 1.12$–1.23), which attested to the excellent control over the ROP parameters. Replacing the benzenesulfonate moiety by a Me group as in [{EDBP^{OMe}}Mg(OBn)]$_2$ (**56**) produced less effective initiators, as the catalyst activity towards the ROP of CL (200 equiv, 60 min, 25 °C) or L-LA (200 equiv, 15 min, 0 °C) diminished significantly in spite of a satisfactory control ($M_w/M_n \approx 1.08$ and 1.18, respectively) [73].

Inspired by these results, Ko and coworkers subsequently obtained the directly related homoleptic, discrete complexes supported by biphenol-derived benzenesulfonate monoanionic ligands bearing a CF$_3$ (**57**) or a OMe (**58**) substituent in *para* position of the sulfonate aromatic ring [74] (Fig. 17). The authors reported that in the presence of 2 equiv of BnOH, these complexes yielded potent binary catalyst systems for the ROP of CL (400 equiv, 25 °C) and TMC (200 equiv, 0–25 °C). The electron-withdrawing group in **57** allowed enhanced activity in comparison with **58**:
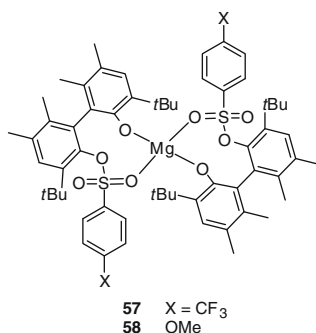
Fig. 17 Homoleptic sulfonated Mg–phenolate complexes **57** and **58** by Ko and coworkers [74]
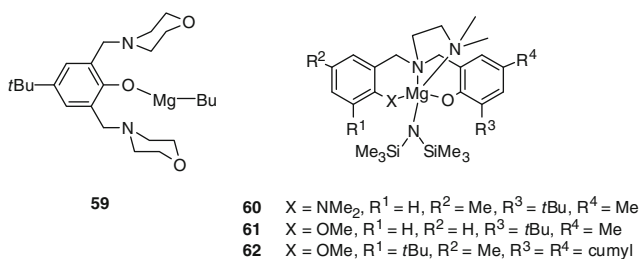
Fig. 18 Aminophenolate Mg complexes {LO}MgR by Carpentier and coworkers (**59**) [75] and Ma and coworkers (**60–62**) [76]

the latter required 15 min to convert 400 equiv of CL where the former only needed 5 min. While the ROP of CL was well controlled ($M_w/M_n \approx 1.06$–1.14), the larger molecular weight distributions obtained with poly(TMC)s ($M_w/M_n \approx 1.18$–1.74) are somewhat characteristic of this monomer [55].

Heteroleptic complexes {LO}MgNu (Nu = R, N(SiMe$_3$)$_2$) supported by ancillary aminophenolate ligands with the general designation {LO}$^-$ have yielded some of the most active catalyst systems for the ROP of cyclic esters known to date. Using the readily synthesized monoanionic, tridentate phenolate ligand {LO^{morph2}}$^-$, Carpentier and coworkers have prepared {LO^{morph2}}Mg(*n*Bu) (**59**) (Fig. 18), an extremely effective catalyst for the *i*ROP of L-LA [75]. The *i*ROP binary system **59**/*i*PrOH (up to 100 equiv of *i*PrOH vs. the metal) indeed achieved near-quantitative conversion of 5,000 equiv of monomer (toluene, 60 °C) within 1.5 h with very good control ($M_{n,calc} = 6,600$ g·mol^{-1}, $M_{n,obs} = 5,500$ g·mol^{-1}, $M_w/M_n = 1.18$), or even polymerized 1,000 equiv within 2 min ([L-LA]$_0$/[**59**]$_0$/[*i*PrOH]$_0$ = 1,000:1:10). End-group fidelity was demonstrated by a combination of NMR spectroscopy and MALDI-ToF-MS analyses, which both confirmed the presence of the expected *i*PrO–C(O)– and –CH(CH$_3$)OH termini. No structural information was available for **59**. Nonetheless, {LO^{morph2}}ZnEt, a zinc analogue of **59**, is dimeric in the molecular state: the metal centers are 4-coordinated, and each ligand forms a μ^2:κ^2,κ^1 chelate, with bridging O$_{phenolate}$ atoms and coordination of

Fig. 19 Homoleptic, monomer Mg{NO}$_2$ complexes Mg{tbpca}$_2$ (**63**) and Mg{S-tbpmpa}$_2$ (**64**) by Sobota and coworkers [79]
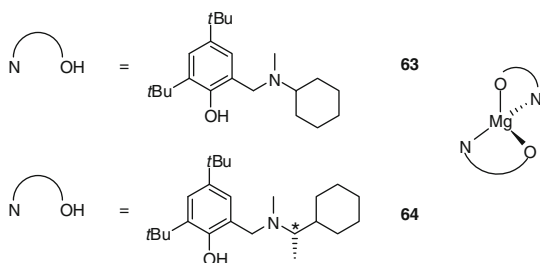
only one of its N atoms [75]. One can postulate that the main geometric patterns of **59** resemble those of {LO^{morph2}}ZnEt.

In a recent communication [76], Ma and coworkers recorded unprecedented success with asymmetric monoanionic tetradentate {NNNO}$^-$ and {ONNO}$^-$ ligands (Fig. 18) for the synthesis of rare stable heteroleptic amido complexes (**60–62**). Upon addition of iPrOH (1–2 equiv), {NNNO}Mg(N(SiMe$_3$)$_2$) (**60**) polymerized 5,000–10,000 equiv of D,L-LA in as little as 2–5 min under mild conditions (25 °C, [D,L-LA]$_0$ = 1.0 M in toluene), with corresponding TOF values of a staggering 100,000–135,000 mol$_{LA}$ (mol$_{Mg}$ h)$^{-1}$; this remains unequaled with any metal-based ROP initiator to date. Considering the high monomer loading and the amazing rate of the reaction, the match between theoretical ($M_{n,calc}$ = 32,600 g mol^{-1}) and observed ($M_{n,obs}$ = 22,300 g mol^{-1}) molecular weights was adequate, while the polydispersity was only slightly higher than desired (M_w/M_n = 1.54). Analysis performed on oligomers showed that they were all end-capped by the expected isopropoxy group. It was proposed that the catalyst was formed in situ by reaction of **60** and iPrOH and was of the type {NNNO}Mg (OiPr). The extreme activity displayed by this series of catalysts offers true potential. It is for instance possible to envisage that they could also be utilized successfully in the ROP of notoriously less reactive cyclic monomers such as morpholinediones, the cyclic dimers of α-hydroxy acids, and α-amino acids [49, 77, 78]. The stereocontrol was limited with these systems, as atactic or very slightly isotactic-enriched PLAs were obtained (P_m = 0.54–0.65). The slight isotactic bias observed in these PLAs is also promising, and higher isoselectivity in the ROP of D, L-LA could potentially be observed for the first time with Mg-based catalyst systems. Preliminary attempts by decreasing the temperature of the ROP reactions brought little improvement (P_m = 0.60 was obtained with **62** when the reaction was carried out at 25 °C, which only increased to P_m = 0.65 at −39 °C) [76], but structural modifications to the ligand scaffold could be considered.

Sobota and coworkers described the preparation of monomeric, homoleptic Mg complexes supported by bidentate aminophenolate ligands, Mg{tbpca}$_2$ (**63**) ({tbpca}H=N-(3,5-di-tert-butylbenzyl-2-hydroxy)-N-methylcyclohexanamine) and Mg{S-tbpmpa}$_2$ (**64**) ({S-tbpmpa}H=(S)-N-(3,5-di-tert-butylbenzyl-2-hydroxy)-N,α-dimethylbenzylamine), the latter one relying on the use of the enantiomerically pure proligand (Fig. 19) [79]. Although on their own these complexes were inactive toward L-LA, in the presence of 1 equiv of BnOH they afforded rapid and quantitative

Fig. 20 Imino-phenolate Mg complexes [{NNO}Mg(μ-OBn)]$_2$ (**65**) by Lin and coworkers [80]

65 R^1 = Me, Ph
R^2 = H, Cl, Br, OMe
R^3 = H, OMe
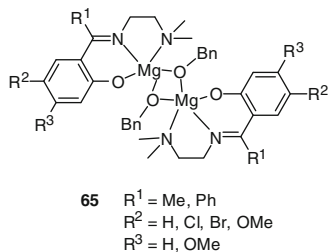
conversion of 50–100 equiv in 1–5 min at 25 °C; the molecular weights were reliably predictable, and the polydispersity of the resulting materials was very narrow ($M_w/M_n \approx 1.02$–1.10). Analysis of oligomers showed that initiation resulted from insertion of benzyloxy into the monomer. The implication was either that the binary system operated according to the activated monomer mechanism or that species of the type {tbpca}Mg(OBn) and {S-tbpmpa}Mg(OBn) were formed in situ prior to the start of the reaction which then followed the more traditional coordination-insertion mechanism [55]. Surprisingly, the authors did not report on the polymerization of D,L-LA with **64**, where the ligand possesses chiral centers.

NNO-tridentate Schiff-base ligands have also been employed, but with limited success. Lin and coworkers prepared a broad range of dimeric [{NNO}Mg(μ-OBn)]$_2$ complexes (**65**) supported by {NNO}$^-$ tridentate imino-phenolate ligands bearing Me or Ph substituents on the carbon atom of the imine group (Fig. 20) [80]. The activity of these initiators in the living ROP of L-LA was low, as they generally required up to 3.5 h to polymerize 50 equiv of monomer at 0 °C, yet in a controlled fashion ($M_w/M_n \approx 1.05$–1.10). The study showed that the catalytic activity in the family of initiators **65** increased by adding electron-donating groups in *para* position of the aromatic ring, while it dropped if electron-withdrawing groups were introduced instead (almost quantitative conversion of 100 equiv of L-LA could be observed when R^1 = Me, R^2 = OMe, and R^3 = H, whereas only ca. 25 % of 50 equiv were polymerized when R^1 = Me, R^2 = Cl or Br, and R^3 = H).

3.2.5 Miscellaneous Ligands

As the many research groups active in this field seek new ligand platforms for the optimization of the activity of (Mg) ROP catalysts, several well-defined Mg complexes which do not correspond to the categories previously discussed have been reported in the past 5 years. Although the various ligands considered are obviously not without interest, it must be noted that the complexes built around these scaffolds generally display inferior ability as ROP initiators/catalysts than those introduced in the above sections.

In 2007, Lin and coworkers reported the synthesis of dimeric complexes [{NNO}Mg(OBn)]$_2$ bearing tridentate {NNO}$^-$ amino-ketiminate ligands (**66**) (Fig. 21) [81]. They acted as potent initiators for the ROP of L-LA, converting 50–200 equiv within 8 min and affording polymers with fully predictable molecular weights
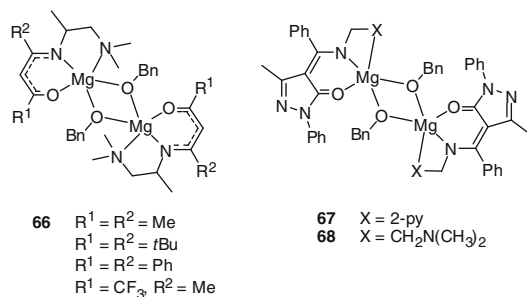
Fig. 21 Tridentate NNO-ketiminate benzyloxy Mg complexes (**66–68**) by Lin and coworkers [81, 82]
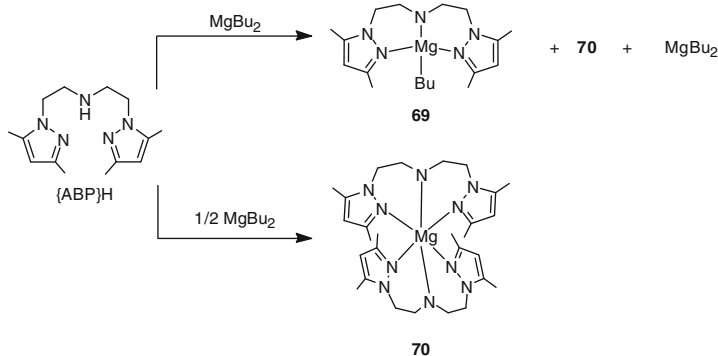
Scheme 8 Amido-*bis*(pyrazolyl) complexes (**69–70**) by Carpentier and coworkers [83]

($M_w/M_n \approx 1.07$–1.46). In a later work, Lin and coworkers elaborated further on these results, and reported two complexes where the more encumbered ligand {NNO^{py}}$^-$ and {NNO^{NMe2}}$^-$ (tailored around the use 4-benzoyl-3-methyl-2-pyrazolin-5-one) which presented substantial π-conjugation (Fig. 21) [82]. Whereas [{NNO^{py}}Mg(OBn)]$_2$ (**67**) was practically inactive towards LA, [{NNO^{amine}}Mg(OBn)]$_2$ (**68**) was capable of polymerizing both L- and D,L-LA in a living fashion in THF or dichloromethane. The rate of the reaction was lower than found previously with **66** since 1.6–4 h were necessary for **68** to polymerize 200 equiv of L-LA at 30 °C. More importantly, the ROP of D,L-LA in THF at 0 °C afforded heterotactic-enriched PLA (P_r up to 0.85).

Carpentier and coworkers attempted the preparation of a Mg-*n*-butyl complex bearing an amido-*bis*(pyrazolyl) tridentate ligand ({ABP}$^-$) [83], but found that desired heteroleptic complex {ABP}Mg(*n*Bu) (**69**) could not be isolated cleanly; instead, only mixtures of **69**, Mg(*n*Bu)$_2$, and the homoleptic Mg{ABP}$_2$ (**70**) were obtained (Scheme 8). Complex **70**, which could be independently and quantitatively synthesized, polymerized D,L-LA (100 equiv) in 10 min in THF at room temperature in a controlled manner ($M_{n,calc} = 7{,}200$ g·mol^{-1}, $M_{n,obs} = 10{,}000$ g·mol^{-1}, $M_w/M_n = 1.29$), but the
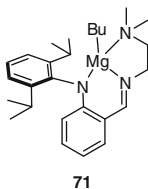
Fig. 22 Magnesium complex bearing an anilide-aldimine ligand, {NNN^{iPr2}}Mg(nBu) (**71**), by Ko and coworkers [82]

resulting PLA was atactic. NMR analysis on the polymers showed that initiation took place by ring-opening of the monomer by the {ABP}$^-$ amide.

In 2009, Ko and coworkers prepared {NNN^{iPr2}}Mg(nBu) (**71**), a monomeric complex supported by a very congested anilide-aldimine tridentate ligand (Fig. 22) [82]. The combination of **71** with BnOH (1–4 equiv) generated an effective catalyst system for the well-controlled iROP of CL and L-LA. The ROP of 100–400 equiv of CL was complete within 1 min at −30 °C, while the conversion of 400 equiv of L-LA was achieved at 30 °C in 20 min. All polymers displayed narrow molecular weight distributions (M_w/M_n < 1.20), and the agreement between calculated and observed molecular weights was excellent. In a way characteristic of iROP reactions, the molecular weight decreased linearly with increasing concentration in transfer agent; however, the authors did not attempt to capitalize on this feature as they did not use more than 4 equiv (vs. the metal) of BnOH.

3.3 Complexes of the Larger Alkaline-Earth Metals

3.3.1 ROP Studies with Ill-Defined Ca, Sr, and Ba Species

Early accounts of Ae (Ae = Ca, Sr, Ba) species for ROP reactions date back to the 1960s, when Ae hexammoniate (Ae[NH$_3$]$_6$), formed by reaction of elemental Ae and ammonia, were used as catalyst precursors for the Union Carbide epoxide polymerization processes [84, 85]. After early attempts [86], these heterogeneous compounds proved unable to promote truly efficiently the ROP of cyclic esters.

In 1996, Vert and coworkers employed a combination of CaH$_2$ and dihydroxy-telechelic poly(ethylene oxide) (PEO) to prepare PLA/PEO/PLA triblock copolymers by ROP of D,L-LA [87]. Such PEO macroinitiators were also utilized for the ROP of 3-(S)-isopropylmorpholine-2,5-dione or CL by Höcker and coworkers in 2001 [88] and Jing and coworkers [89] in 2004, respectively. They used CaH$_2$ and Ca[NH$_3$]$_6$ as metal sources to prepare triblock copolymers but, in all these studies, the focus was on the resulting materials rather than the catalyst system.

The solubility of all these Ae-based catalysts systems has been a long-standing issue. A few years ago, Jing and coworkers endeavored to prepare more soluble Ca and Sr initiators by reaction of Ae[NH$_3$]$_6$ and ethylene oxide or propylene oxide, and
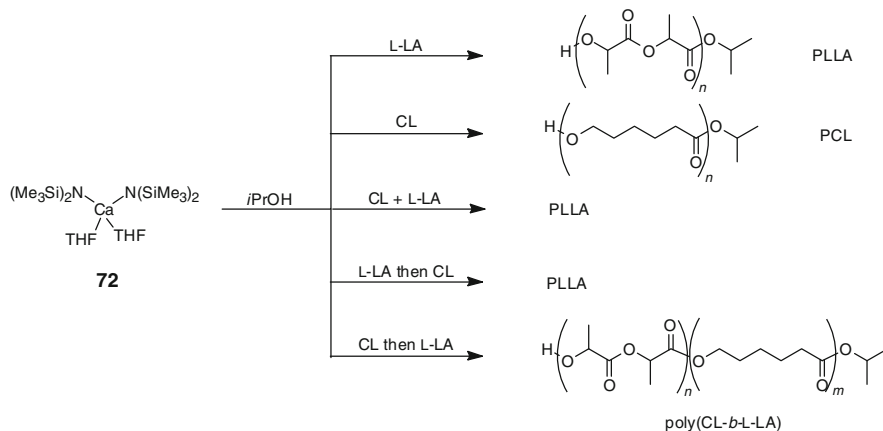
Scheme 9 Westerhausen and Feijen's synthesis of PCL and PLLA with discrete Ca-based systems [94]

proposed the general formula $(H_2N)Ae(OR)$ ($R = Et$, iPr), but the characterization of these species remained insufficient [90–92]. They initiated the ROP of CL (100–1,300 equiv, 40 °C, 2–6 h; $1.85 < M_w/M_n < 7.4$) and L-LA (60–340 equiv, 80 °C, 1–3 h; $1.57 < M_w/M_n < 2.26$) as well as the copolymerization of CL with 2-methyl-2-benzyloxycarbonyl-propylene carbonate; however, the evidence for the formation of block copolymers in this last case was not adequately supported. Finally, in 1999, Bero and coworkers used the somewhat more soluble calcium *bis* (acetylacetonate) to prepare copolymers of L-LA and GL by copolymerization of the neat monomers at 150–200 °C, but again no information regarding the catalyst system or the nature of the initiating group was given [93].

3.3.2 Homoleptic and Molecular Calcium Complexes

In the wake of Coates' and Chisholm's pioneering works with discrete complexes of the divalent zinc and magnesium [48–53], Westerhausen and Feijen jointly triggered the development of well-defined Ca-based initiators for the ROP of cyclic esters. In a first effort [94], they showed that the simple combination of $Ca(N(SiMe_3)_2)_2(THF)_2$ (**72**) and 2 equiv of alcohol (MeOH, iPrOH, or hydroxyl end-capped PEO) mediated the living ROP of L-LA and CL in THF (Scheme 9). These binary systems led to well-controlled and fast reactions, taking ca. 20–35 min and 10 min to quantitatively convert 100 equiv of L-LA ($M_w/M_n \approx 1.03$–1.05) or CL ($M_w/M_n \approx 1.24$–1.29), respectively, to give polyesters with predictable molecular weights. In the case of iPrOH, each polymer chain contained isopropoxy end groups, suggesting that initiation occurred via insertion of the monomer into the Ca–OiPr bond. Owing to the living nature of the **72**/ROH system, the sequential polymerization of CL and L-LA allowed for the controlled synthesis of poly(CL-*b*-L-LA) block copolymers, although
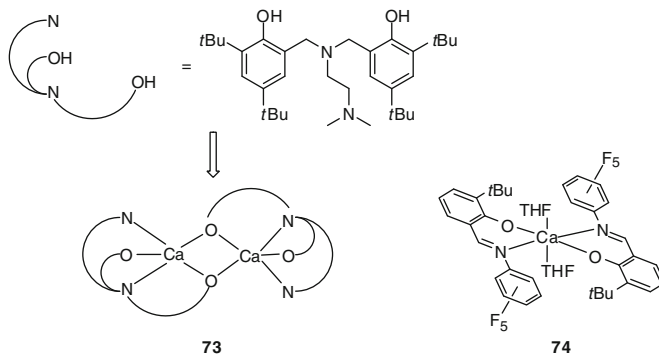
Fig. 23 Molecular Ca-based initiators (**73–74**) for the ROP of CL by Bochmann and coworkers [95]

the order of addition of the monomers was crucial: the reaction was successful if CL was polymerized first, but it proved impossible to grow a PCL block *after* a PLLA one; similarly, the attempted synthesis of random copolymers by simultaneous copolymerization of the two monomers was unsuccessful and only returned pure PLLA. These observations highlighted a markedly different behavior of the two monomers during homo- and copolymerization reactions.

Two examples of molecular calcium initiators supported by dianionic multidentate {ONNO}$^{2-}$ ligands were reported. In 2006, Bochmann and coworkers prepared the dimeric [{ONNO}Ca]$_2$ (**73**) (Fig. 23) [95]. They used it as a single-component initiator to promote the sluggish but *pseudo*-living ROP of CL, reaching half-conversion of 200 equiv of monomer after 12 h at 60 °C in toluene ($M_w/M_n \approx 1.1$–1.2); the nature of the mechanism was not discussed. The related Ca homoleptic complex {ON}$_2$Ca(THF)$_2$ (**74**) containing two imino-phenolate ligands {NO}$^-$ was inactive towards CL under the same conditions.

At the same time, Darensbourg and coworkers reported several {ONNO}Ca complexes supported by a variety of Schiff base derivatives (**75–77**), where the nature of the bridge and electronic and steric properties were tuned (Scheme 10) [96]. In combination with one equiv of additional anionic initiator (X$^-$ = Cl$^-$, Br$^-$, or N$_3$$^-$, coming from either Bu$_4N^+$·X$^-$ or (Ph$_3$P)$_2$N$^+$·X$^-$), **75–77** promoted the controlled ROP of TMC (275–700 equiv) in neat, melted monomer (86 °C; TOFs = 400–1,300 mol$_{TMC}$ (mol$_{Ca}$·h)$^{-1}$). The resulting poly(TMC)s (PTMCs) had controllable macromolecular features and polydispersities typical of the ROP of TMC ($M_w/M_n \approx 1.48$–1.76). The nature of the bridge had little impact, but clearly the presence of bulky and/or electron-donating groups on the aromatic ring was beneficial. The nature of the anion was of limited importance, even if slightly better results were obtained with X$^-$ = N$_3$$^-$ or Cl$^-$ (TOF = 1,123–1,286 mol$_{TMC}$ (mol$_{Ca}$·h)$^{-1}$) than with Br$^-$ (766 mol$_{TMC}$ (mol$_{Ca}$ h)$^{-1}$). Kinetic studies performed with **76**/Bu$_4$N$^+$ · Cl$^-$ demonstrated that the ROP reaction was first order in TMC, Bu$_4$N$^+$·Cl$^-$, and calcium complex.

Along these lines, Lin and coworkers used the 5-coordinated Ca{DAIP}$_2$ (**78**), prepared by reaction of 2-{[(2-(dimethylamino)ethyl)imino]methyl}phenol and

			TOF mol$_{TMC}$·(mol$_{Ca}$·h)$^{-1}$
75	phenylene bridge	R^1 = H, R^2 = H	416
		R^1 = H, R^2 = tBu	961
		R^1 = OMe, R^2 = tBu	1132
		R^1 = tBu, R^2 = tBu	1175
		R^1 = Cl, R^2 = Cl	756
76	ethylene bridge	R^1 = tBu, R^2 = tBu	1123
77	naphtylene bridge	R^1 = tBu, R^2 = tBu	1270
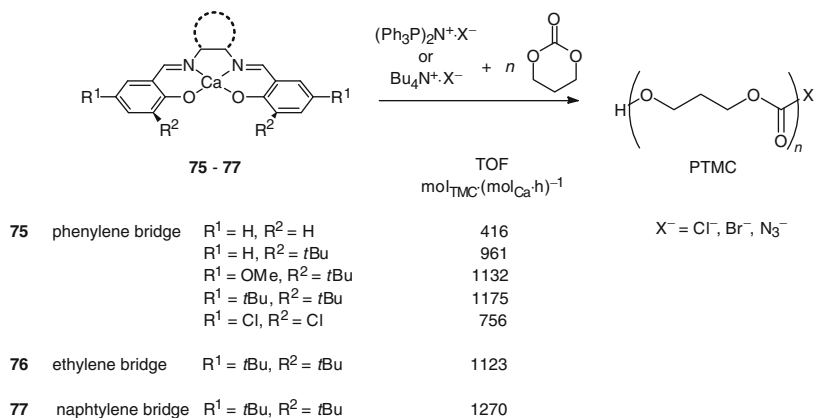
Scheme 10 Binary Ca{salen}/X$^-$ catalyst systems (**75–77**) for the ROP of TMC by Darensbourg and coworkers [96]
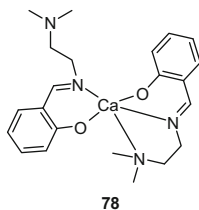
Fig. 24 Homoleptic Ca{DAIP}$_2$ complex (**78**) prepared by Lin and coworkers [97]
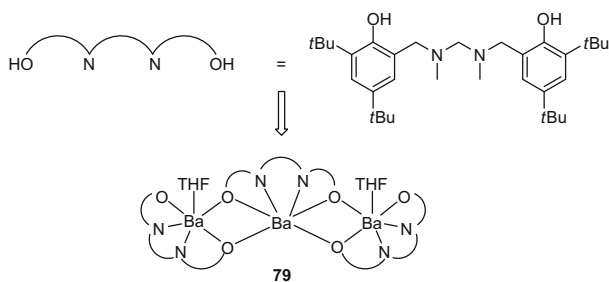
Fig. 25 Trinuclear [{ONNO}Ba]$_3$(THF)$_2$ barium complex (**79**) by Davidson and coworkers [98]

{Ca(OMe)$_2$}$_n$, in combination with 2 equiv of BnOH for the ROP of L-LA (Fig. 24) [97]. The polymerization of 100–250 equiv of monomer carried out at room temperature was well controlled ($M_w/M_n \approx 1.11$–1.28) but rather slow (40–60 min were necessary to reach full conversion).

Finally, Davidson and coworkers disclosed [{ONNO}Ba]$_3$(THF)$_2$ (**79**), an unusual trinuclear complex of barium containing three dianionic, tetradentate {ONNO}$^{2-}$ diamino-*bis*(phenolate) ligands (Fig. 25) [98]. Complex **79** promoted
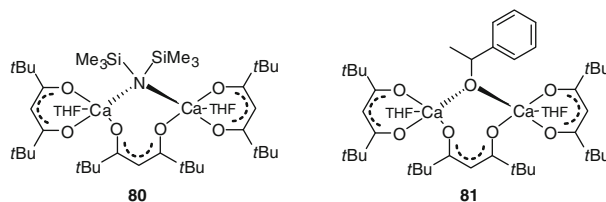
Fig. 26 Bimolecular complexes [(Ca(THF){tmhd})$_2${μ-tmhd}(μ-N(SiMe$_3$)$_2$)] (**80**) and [(Ca(THF){tmhd})$_2${μ-tmhd}(μ-OCH(Me)Ph)] (**81**) by Westerhausen and coworkers [99, 100]

the ROP of L-LA (900 equiv, melted monomer) or CL (300 equiv, toluene, rt), but the resulting polymers exhibited broad or bimodal molecular weight distributions, even in the presence of exogenous BnOH. The monomer was consumed with first-order dependence in its concentration. MALDI-ToF-MS and SEC analyses were consistent with the presence of at least two active sites.

3.3.3 Discrete Heteroleptic {L$_n$X}Ae(Nu) Complexes

Heteroleptic complexes of the type {L$_n$X}A(Nu), where {L$_n$X}$^-$ is a stabilizing ancillary ligand, Ae is a large alkaline-earth metal (Ca, Sr, Ba), and Nu$^-$ is a reactive nucleophile, represent the prototype of Ae-based ROP initiators. These species are soluble and well defined, readily characterized, and well suited to the study of ROP mechanisms because each of the component plays a specific role. Yet, until 2003, such species were not available for ROP studies, essentially because of their high lability in solution. Indeed, one of the still long-lasting challenges in this chemistry was the synthesis of complexes that are stable against Schlenk-type equilibria in solution.

The first hurdle was cleared in 2003 when Westerhausen and coworkers showed that the bimolecular complexes [(Ca(THF){tmhd})$_2${μ-tmhd}(μ-N(SiMe$_3$)$_2$)] (**80**) and [(Ca(THF){tmhd})$_2${μ-tmhd}(μ-OCH(Me)Ph)] (**81**) (Fig. 26) could polymerize the ROP of CL and L-LA in the presence of iPrOH [99, 100]. Complex **81** could also initiate the controlled ROP of these monomers even without additional alcohol. First-order kinetics in monomer concentration were determined. Up to 150 equiv of monomer were fully polymerized in THF at room temperature within 30 min (for CL) or 120 min (for L-LA) with **80**/iPrOH or **81** with generally adequate—although not perfect—control: $M_w/M_n = 1.67$ (resp. 1.13) for PCL and 1.26 (resp. 1.14) for PLLA with **80**/iPrOH (resp. **81**).

Roughly at the same time, Chisholm and coworkers obtained remarkable results with a new class of sterically encumbered Tp calcium complexes, {Tp^{tBu}}Ca(N(SiMe$_3$)$_2$) (**82**), {Tp^{tBu}}Ca(O-2,6-iPr$_2$-C$_6$H$_3$) (**83**), and {Tp^{iPr}}Ca(O-2,6-iPr$_2$-C$_6$H$_3$)(THF) (**84**) (Fig. 27) [101, 102]. All three complexes proved extremely active initiators in the ROP of D,L-LA, as the polymerization of 200 equiv of monomer reached over 90 % conversion in 1 min at room temperature in THF. The reactions were poorly controlled ($M_w/M_n = 1.74$, 1.68, and 1.61 with **82**, **83**, and **84**, respectively). Complexes **82** and **83** with the bulky ligand {Tp^{tBu}}$^-$ produced

Fig. 27 {HB(Tp^{tBu})$_3$}Ca–Nu (**82–84**) and {BDI^{iPr4}}M–N(SiMe$_3$)$_2$(THF)$_n$ (M = Zn, n = 0; M = Mg, n = 0; M = Ca, n = 1) (**85–87**) complexes by Chisholm and coworkers [101, 102]

Fig. 28 Heteroleptic, 4-coordinated {NNN}Ca–N(SiMe$_3$)$_2$ Ca complex (**88**) by Zou and coworkers [103]

highly heterotactic PLAs, with P_r > 90 %: these represented the first Ca-based initiators capable of stereocontrol in the ROP of D,L-LA. It was somewhat surprising that the slightly less congested **84** only yielded atactic PLA under the same conditions. The authors also presented a comparison of the respective ability of the {BDI^{iPr4}}$^-$ and {Tp^{tBu}}$^-$ ligands towards the stabilization of heteroleptic Ca complexes. They showed that while **84** (prepared by reaction of **82** and 2,6-iPr$_2$-C$_6$H$_3$OH) was perfectly stable in solution, the reaction of {BDI^{iPr4}}Ca(N(SiMe$_3$)$_2$) (THF) (**85**) with 2,6-iPr$_2$-C$_6$H$_3$OH only led to the isolation of the homoleptic {BDI^{iPr4}}$_2$Ca; the authors attributed this observation to a lack of steric protection around the metal center in **85**. In the same study, they also demonstrated that the reactivity of the complexes {BDI^{iPr4}}M(N(SiMe$_3$)$_2$)(THF)$_n$ (M = Zn, n = 0 (**86**); M = Mg, n = 0 (**87**); M = Ca, n = 1 (**85**)) towards D,L–LA decreased in the order Ca > Mg > Zn (Fig. 27); this was consistent with the degree of polarity of the M$^{\delta+}$–$^{\delta-}$N(SiMe$_3$)$_2$ bond which decreases from Ca to Zn.

Another example of {NNN}Ca(N(SiMe$_3$)$_2$) heteroleptic Ca complex (**88**) supported by a diamino-anilide ligand ({NNN}$^-$) was unveiled by Zou and coworkers in 2010 (Fig. 28) [103]. The idea was to employ a ligand much akin to the ubiquitous BDI ones such as {BDI^{iPr4}}$^-$ or {BDI^{iPr2,OMe}}$^-$ (see Sect. 3.2.2), but

Fig. 29 Structure of calcium complexes supported by tridentate Schiff base ligand (**89–94**) by Darensbourg and coworkers [104, 105]

89 $R^1 = R^2 = t$Bu   X = N(SiMe$_3$)$_2$
90 $R^1 = R^2 = t$Bu   X = OMe
91 $R^1 = t$Bu, $R^2 = $ H   X = N(SiMe$_3$)$_2$

92

93

94
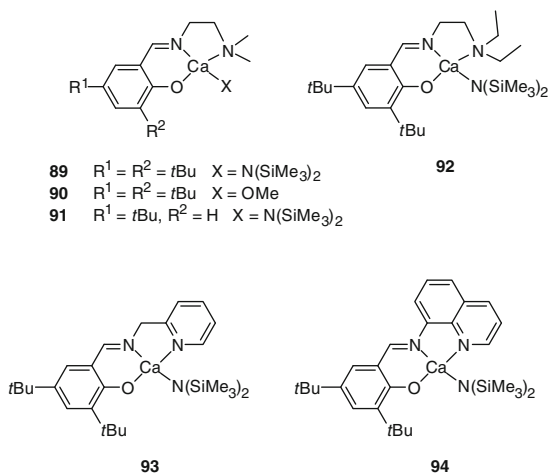
where the chelating side arm had greater flexibility and mobility. As a result, **88** represents a rare case of discrete, stable 4-coordinated heteroleptic Ca complex devoid of coordinated solvent. Its activity in the ROP of D,L-LA was, however, disappointing, as it could only partly convert 100 equiv of monomer in dichloromethane (30 min, conversion <90 %) or THF (2 h, conversion <66 %) at room temperature. Also, the control was limited ($M_w/M_n \approx 1.26$–1.34, $M_{n,calc} < M_{n,obs}$), and the resulting PLAs were essentially atactic.

As for magnesium, monoanionic imino- and especially amino-phenolate ligands have proved convenient in stabilizing heteroleptic calcium complexes. Building on their earlier success [96], Darensbourg and coworkers synthesized several {NNO}Ca(Nu)(THF) (Nu$^-$ = N(SiMe$_3$)$_2$$^-$, OMe$^-$) complexes (**89–94**) where the metal is stabilized by a tridentate Schiff base ligand {NNO}$^-$ (Fig. 29) [104, 105]. Unlike for their previous systems, which required a source of anions, these complexes were single-component initiators for the controlled ROP of L-LA (350 equiv of neat monomer, 110 °C, 15 min). The catalyst activity (TOF values in the range 227–1,124 mol$_{L-LA}$ (mol$_{Ca}$ h)$^{-1}$) increased slightly with the electron-donating capacity of the side arm but decreased with its steric bulk (**94** < **93** < **92** < **89**). The nature of the initiating group exerted limited influence (TOF = 1,124 and 826 mol$_{L-LA}$ (mol$_{Ca}$ h)$^{-1}$ for **89** and **90**, respectively). The polydispersity of the resulting PLLAs was systematically very narrow ($M_w/M_n \approx 1.02$–1.05). The polymerization of L-LA (350–700 equiv) using the most active initiator **89** in CDCl$_3$ at room temperature was first order in both monomer and initiator concentrations, with $k_p = 19.9$ L mol^{-1} s^{-1}, $\Delta H^{\neq} = 73.5 \pm 3.8$ kJ mol^{-1}, and $\Delta S^{\neq} = -42.5 \pm 12.6$ J (mol K)$^{-1}$. The polymerization was found to proceed faster in THF than in chloroform, presumably because the nucleophilicity of the N(SiMe$_3$)$_2$$^-$/OR$^-$ moiety (OR = growing polymer chain) increased upon coordination of THF to the metal center. The ROP of D,L-LA with **89** also took place, in either THF or chloroform; atactic to moderately heterotactic-enriched PLAs ($P_r = 0.52$–0.73) were obtained

Table 1 Rate constant dependence on the monomer feed ratio during the copolymerization of TMC and L-LA initiated by **89** in CDCl$_3$ at room temperature ([**89**]$_0$ = 20.7 mM) [104, 105]

L-LA/TMC feed ratio	k_{obs}(L-LA) (h^{-1})	$k_{obs,1}$(TMC) in the presence of L-LA (h^{-1})	$k_{obs,2}$(TMC) after full consumption of L-LA (h^{-1})
1:99	Not detected	0.2115	0.6450
5:95	0.3453	0.0620	0.5270
25:75	0.1971	0.0150	0.0158
50:50	0.1847	0.0113	0.0465
75:25	0.1722	0.0101	0.0360
995:5	0.1685	Not detected	0.0029
99:1	0.1540	Not detected	Not detected

depending on the solvent and the temperature of the reaction; steric crowding around the metal center favored the formation of heterotactic material. Complex **89** also polymerized TMC effectively at room temperature. Kinetic measurements gave k_p = 500 L·mol^{-1}·s^{-1} for this monomer, i.e., the ROP of TMC is faster than that of L-LA; accordingly, the activation energy for the ROP of TMC with **89** at 25 °C ($\Delta G^{\neq}$ = 78.2 kJ mol^{-1}) was substantially lower than found for L-LA ($\Delta G^{\neq}$ = 86.1 kJ mol^{-1}). During the copolymerization of L-LA and TMC, the rates of enchainment of the monomers were reversed, and L-LA was incorporated at least one order of magnitude faster than TMC; this corroborated the observations already made by Westerhausen and Feijen [94]. Thus, the preparation of PTMC-*b*-PLLA block copolymers was possible only by sequential polymerization where L-LA was added after complete consumption of TMC, whereas random copolymerization only yielded tapered copolymers where the contents of L-LA were initially very high and decreased gradually as the course of the reaction progressed. Detailed kinetic studies showed that during copolymerization reactions, the TMC/L-LA feed ratio influenced not only the overall rate of the reaction, but also the rates of consumption of each of the comonomers (Table 1). FTIR kinetic studies of the displacement of N$_3^-$ on the model {salen}Ca compound **76** demonstrated the better binding ability of L-LA in comparison with that of TMC, which the authors considered a reason for the enhanced rate of enchainment of the former monomer during copolymerization reactions.

Carpentier and coworkers prepared the amino-ether phenolate [{LO^{morph2}}Ca(N (SiMe$_3$)$_2$)]$_2$ (**95**), the calcium derivative of the Mg-based **59** [75]. **95** is dimeric is the solid state, and the ancillary ligands adopt an unusual μ^2:κ^3,κ^1 coordination mode (Fig. 30). The two metals are bridged by the O$_{phenolate}$ atoms, and in each ligand one of the morpholine side arms in boat conformation binds to a single metal center via both its N and O atoms, whereas the second one retains a more stable chair conformation and is entirely free of interaction with the metal centers. The binary catalyst system **75**/*i*PrOH displayed excellent activity in the controlled *i*ROP of *L*-LA at 60 °C. The polymerization of 500 equiv of monomer in the presence of 10 equiv of alcohol was complete within 1 min; the corresponding TOF value of
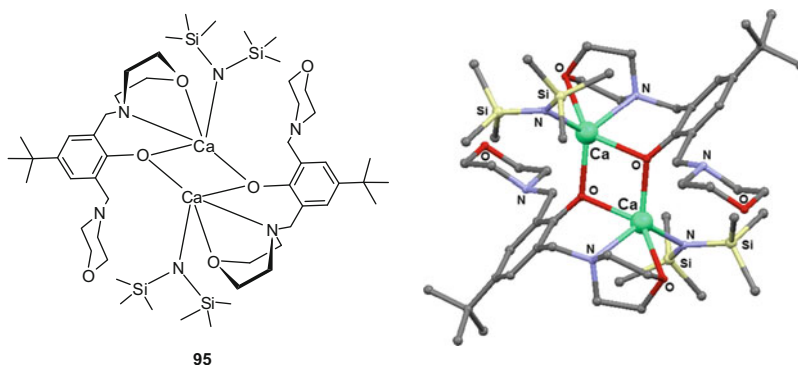
Fig. 30 Drawing and X-ray structure of [{LO^{morph2}}Ca(N(SiMe$_3$)$_2$)]$_2$ (**95**) by Carpentier and coworkers [75]
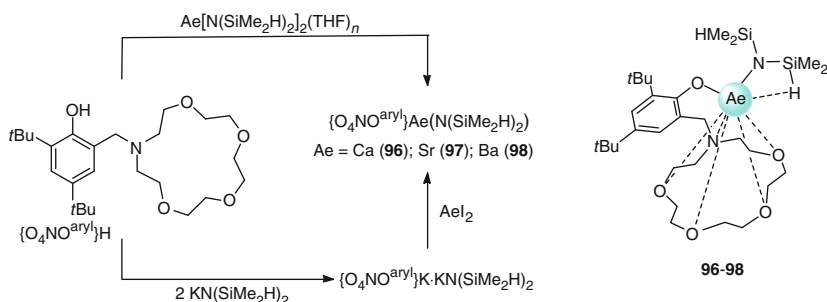
Scheme 11 Synthesis of {O$_4$NO^{aryl}}Ae(N(SiMe$_2$H)$_2$) complexes (**96–98**) by Carpentier and coworkers [106]

28,200 mol$_{L-LA}$ (mol$_{Ca}$·h)$^{-1}$ ranks amongst the highest reported to date, while the control was very good ($M_{n,calc}$ = 6,800 g·mol^{-1}, $M_{n,obs}$ = 6,500 g·mol^{-1}, M_w/M_n = 1.27). These high performances could be maintained for the ROP of up to 2,500 equiv of L-LA in the presence of 10–50 equiv of *i*PrOH.

In order to find a general access route to heteroleptic Ae complexes, Carpentier and coworkers have exploited advantageously the use of the N(SiMe$_2$H)$_2^-$ amido moiety. This particular amide helps stabilizing heteroleptic complexes against ligand scrambling thanks to the presence of internal β-agostic Ae···H–Si interactions [106]. The reaction of Ae[N(SiMe$_2$H)$_2$]$_2$(THF)$_n$ (Ae = Ca, n = 1; Sr, n = 2/3; Ba, n = 0) with the electron-rich amino-ether phenol proligand {O$_4$NO^{aryl}}H yielded the desired {O$_4$NO^{aryl}}Ae(N(SiMe$_2$H)$_2$) (Ae = Ca, **96**; Sr, **97**; Ba, **98**) which were stable in solution (Scheme 11). These complexes were also available in high yields by treatment of AeI$_2$ with the homobimetallic heteroleptic precursor {O$_4$NO^{aryl}}K·KN (SiMe$_2$H)$_2$. The presence of β-agostic Ae···H–Si interactions in **96–98** both in solution and in the solid state was proven experimentally by a combination of NMR, FTIR, and X-ray diffraction studies (Fig. 31); they were corroborated by

Fig. 31 X-ray structure of {O_4NO^{aryl}}Ba(N(SiMe$_2$H)$_2$) (**98**) by Carpentier and coworkers [106]. Hydrogen atoms (except those on the silicon atoms) are omitted for clarity
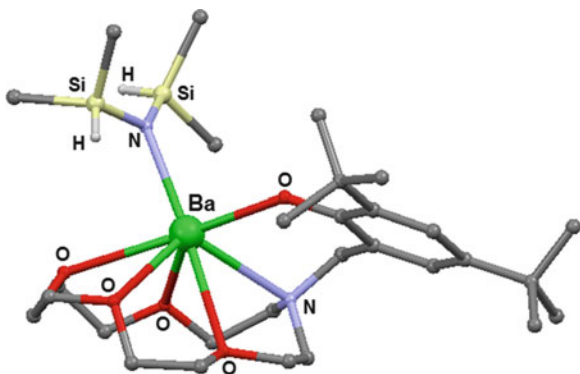
DFT calculations, which estimated the strength of the stabilization to ca. 12–20 kJ mol^{-1}. Upon combination with an alcohol (benzyl or propargyl alcohol, 2-propanol, 9-anthracenylmethanol) as a transfer agent, **96–98** yielded very active binary catalyst systems for the *i*ROP of L-LA in toluene of THF. Complete conversion of 1,000 equiv of monomer ([L-LA]$_0$:[Ae]$_0$: [ROH]$_0$ = 1,000:1:10) was achieved in less than 2 min at 30 °C with the Ca-based **96**, by far the least active catalyst in this series. The catalyst activity followed the order Ca (**96**) ≪ Sr (**97**) < Ba (**98**). As previously observed with the activity trend Zn < Mg < Ca [75, 101, 102], this may be the reflection of the increase of nucleophilicity of the Ae–Nu bond (Nu$^-$ = N(SiMe$_2$H)$_2^-$ or OR$^-$ where OR is the growing polymer chain), although a final conclusion on this issue is still pending.

In a following study [107], Carpentier and coworkers investigated more systematically the respective influence of the metal, ligand framework, and reactive nucleophilic group in {LO}Ae(Nu) heteroleptic charge-neutral complexes (Ae = Ca, Sr, Ba; Nu$^-$ = N(SiMe$_3$)$_2^-$, N(SiMe$_2$H)$_2^-$, HC≡CCH$_2$O$^-$) supported by various {LO}$^-$ amino-phenolate ligands. Hence, the strategy relying on intramolecular Ae···H–Si stabilization was further exploited to prepare the stable calcium complexes {$O_2N_2O^{aryl}$}Ca(N(SiMe$_2$H)$_2$) (**99**), {ONO^{aryl}}Ca(N(SiMe$_2$H)$_2$) (**100**), and {O_2NO^{aryl}}Ca(N(SiMe$_2$H)$_2$)(THF) (**101**) in good and reproducible yields. The alkoxide {O_2NO^{aryl}}Ca(OCH$_2$C≡CH) (**102**) was obtained cleanly by treatment of **101** with propargyl alcohol (Scheme 12). Complexes **96–102** mediated the *i*ROP of L-LA efficiently, converting up to 5,000 equiv of monomer at 0–30 °C in a controlled fashion. When performed with up to 100 equiv of exogenous 9-anthracenylmethanol or benzyl, isopropyl, or propargyl alcohols as a transfer agent, the activity of the catalyst increased again with the size of the metal (**96** < **97** < **98**). TOFs were high, typically in the range 2,000–27,000 mol$_{L-LA}$ (mol$_{metal}$·h)$^{-1}$. The control over the parameters remained satisfactory, with good match between calculated and observed molecular weight and narrow polydispersities ($M_w/M_n \approx 1.10$–1.20) for the resulting PLLAs. End-group fidelity was confirmed in all cases by a combination of NMR, FTIR, and UV-visible spectroscopies and MALDI-ToF MS analyses. For Ca-based complexes, enhanced electron-donating ability of the ancillary ligand favored catalyst activity (**96** > **101**
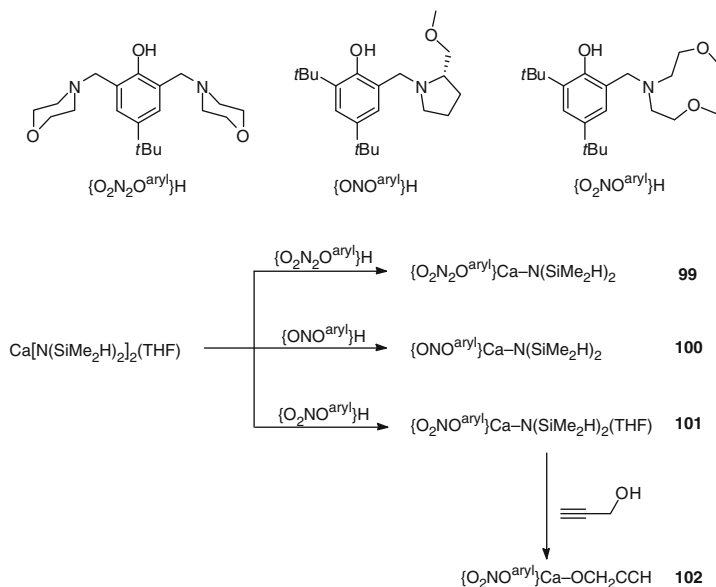
Scheme 12 Synthesis of $\{O_2N_2O^{aryl}\}Ca(N(SiMe_2H)_2)$ (**99**), $\{ONO^{aryl}\}Ca(N(SiMe_2H)_2)$ (**100**), $\{O_2NO^{aryl}\}Ca(N(SiMe_2H)_2)(THF)$ (**101**)**,** and $\{O_2NO^{aryl}\}Ca(OCH_2C\equiv CH)$ (**102**) by Carpentier and coworkers [107]

$> \mathbf{99} \approx \mathbf{100}$). Note than in **99** (dimeric in the solid state), the O atoms of the morpholine ring were not coordinated to the metal center, and the ligand was best described as a $\mu^2{:}\kappa^2,\kappa^2$ chelate. In *i*ROP reactions, the nature of the alcohol had little effect over the activity of the binary catalyst system **96**/ROH; in all cases, both the control and end-group fidelity were excellent. By contrast, in the *living* ROP of L-LA, the HC≡CCH$_2$O$^-$ initiating group, as in **102**, afforded a substantially better control of the ROP parameters than N(SiMe$_2$H)$_2$$^-$ or N(SiMe$_3$)$_2$$^-$, as in **101** or $\{O_2NO^{aryl}\}Ca(N(SiMe_3)_2)$, respectively.

3.4 Unusual Architectures: Cationic and Bimetallic Complexes

3.4.1 Discrete Cationic Complexes

Well-defined cationic complexes of the type $[\{L_nX\}Ae]^+{\cdot}[X]^-$ where the metal (Ae = Ca–Ba or even Mg) is stabilized by a bulky ligand ($\{L_nX\}^-$) and a weakly coordinating counterion (X$^-$) have attracted some interest very recently. They are thought to be key compounds for gaining a better insight into ROP processes. Moreover, it is considered plausible that the positive charge onto the metal center should result in strongly increased Lewis acidity and therefore highly active ROP catalysts. Thus, in order to achieve maximal efficiency, several research groups
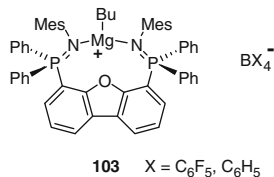
Fig. 32 Organomagnesium [{pidbf}Mg(nBu)]$^+$·[BX$_4$]$^-$ cationic complexes (**103**) (X = C$_6$H$_5$, C$_6$F$_5$) by Hayes and coworkers [111]

have tackled the challenging task of synthesizing cationic initiators devoid of coordinated solvent molecules.

The seminal work in this area was accomplished by Bochmann and coworkers in 2002–2005, who prepared several zinc and magnesium complexes of the type [(Et$_2$O)$_3$M(X)]$^+$·[B(C$_6$F$_5$)$_4$]$^-$ (M = Zn, X = Et, N(SiMe$_3$)$_2$; M = Mg, X = Bu, N(SiMe$_3$)$_2$) or [{DAD}Zn(X)]$^+$·[B(C$_6$F$_5$)$_4$]$^-$ (DAD = iPr$_2$C$_6$H$_3$-N=C(Me)-C (Me)=N-iPr$_2$C$_6$H$_3$; X = Me, Et, N(SiMe$_3$)$_2$) [108–110]. The magnesium complexes were inert towards cyclic esters, although they initiated the cationic polymerization of epoxides such as cyclohexene oxide (in toluene at 0 °C; productivity = 40–123 kg$_{polymer}$ (mol$_{Mg}$·h)$^{-1}$ in 30–45 min) or propylene oxide (9–28 % conversion of 20,000 equiv of monomer vs. Mg at room temperature after 24–120 h).

In 2010, Hayes and coworkers introduced the cationic solvent-free organomagnesium complexes [{pidbf}Mg(nBu)]$^+$·[BX$_4$]$^-$ (**103**) (X = C$_6$H$_5$, C$_6$F$_5$) supported by a *bis*(phosphinimine) ligand; the solvent-free complex was generated by treatment of Mg(nBu)$_2$ with the double Brönsted acid [{pidbf}HH]$^+$·[BX$_4$]$^-$ (Fig. 32) [111]. These complexes were active in the ROP of CL, yielding at room temperature near-quantitative conversion of ca. 100–500 equiv in 4 min. The control was limited ($M_{n,obs} < M_{n,calc}$; $M_w/M_n \approx 1.5$–1.6), which the authors assumed was the consequence of slow initiation with respect to propagation.

At the same time, Carpentier and coworkers designed synthetic routes to the complete families of well-defined, solvent-free cationic complexes [{O$_4$NO^{aryl}} M]$^+$·[H$_2$N{B(C$_6$F$_5$)$_3$}$_2$]$^-$ (M = Zn, **104**; Mg, **105**; Ca, **106**; Sr, **107**; Ba, **108**) and [{O$_4$NO^{alkF}}M]$^+$·[H$_2$N{B(C$_6$F$_5$)$_3$}$_2$]$^-$ (M = Zn, **109**; Mg, **110**; Ca, **111**; Sr, **112**; Ba, **113**), where {O$_4$NO^{aryl}}H and {O$_4$NO^{alkF}}H are electron-rich amino-ether phenol and fluorinated alcohols, respectively (Scheme 13) [112, 113]. While the ligand {O$_4$NO^{aryl}}H supporting **104–108** had already proved its worth in the synthesis of heteroleptic Ae complexes by the same group [106, 107], complexes **109–113** constituted the first examples of a whole family of Zn and Ae cationic complexes supported by an alkoxide ligand. The highly fluorinated tertiary alkoxide ligands {O$_4$NO^{alkF}}$^-$ with bulky, electron-withdrawing CF$_3$ groups in α position to the alkoxide are much weaker π-donors than conventional alkoxides; they are in many ways similar to the versatile phenolate ligands. The cationic complexes **104–113** were obtained by reaction of the amido precursors with the acids [{O$_4$NO^{aryl}} HH]$^+$·[H$_2$N{B(C$_6$F$_5$)$_3$}$_2$]$^-$ and [{O$_4$NO^{alkF}}HH]$^+$·[H$_2$N{B(C$_6$F$_5$)$_3$}$_2$]$^-$; in the case of the amino-ether phenolate ligand, complexes **106–108** could also be prepared by
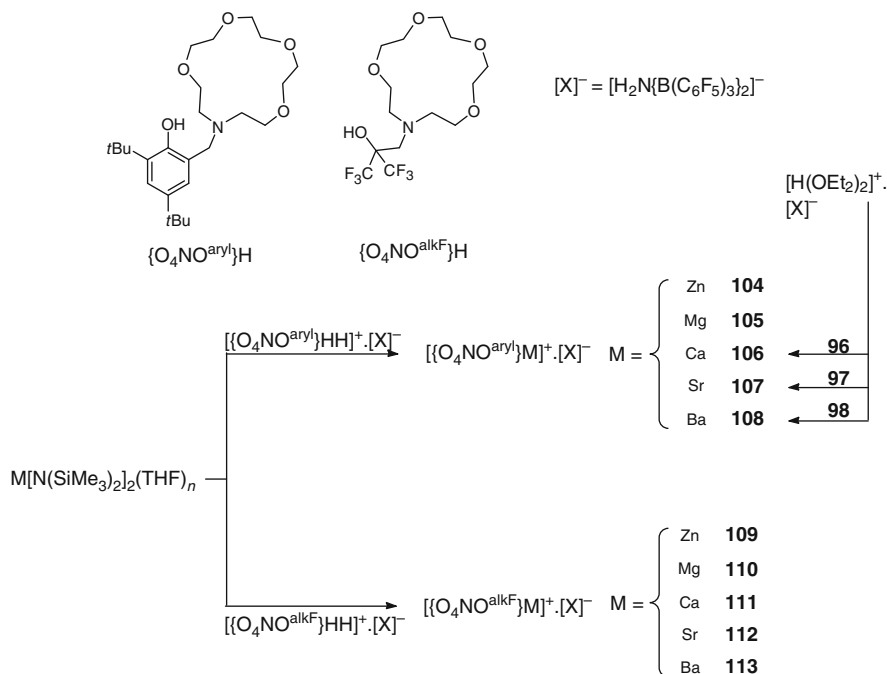
Scheme 13 Synthesis of well-defined cationic complexes $[\{O_4NO^{aryl}\}M]^+\cdot[H_2N\{B(C_6F_5)_3\}_2]^-$ (**104–108**) and $[\{O_4NO^{alkF}\}M]^+\cdot[H_2N\{B(C_6F_5)_3\}_2]^-$ (**109–113**) by Carpentier and coworkers [112, 113]

treatment of the corresponding homoleptic complexes **96–98** with Bochmann's acid, $[H(OEt_2)_2]^+\cdot[H_2N\{B(C_6F_5)_3\}_2]^-$ (Scheme 13). Close examination of the X-ray structures of **111–113**—where the large and extremely Lewis acidic Ae metal centers form bimetallic dications supported by two fluorine-containing ancillaries $\{O_4NO^{alkF}\}^-$—showed the presence of secondary Ae$\cdots$F–C *internal* interactions with the ligand (Fig. 33). These strong interactions (in the region of 25–40 kcal mol^{-1} according to DFT-optimized structures) certainly accounted for the stability of these otherwise highly electron-deficient and labile cationic species. In association with BnOH or *i*PrOH (5–50 equiv), the two families of cations were able to promote the slow (reaction times were typically 12–24 h to reach near-quantitative conversion) but very controlled *i*ROP of L-LA (1,000–3,000 equiv) in toluene. The zinc and magnesium cationic species were systematically far less efficient than Ca–Ba ones under identical conditions, and with both families the order of reactivity increased according to Mg < Zn < Ca < Sr $\approx$ Ba. In all cases, end-group fidelity and match between calculated and observed molecular weights were both excellent, and the polydispersity was very narrow ($M_w/M_n \approx 1.04$–1.20). Complexes **106–108** (effective already at 50–70 °C) were superior to **111–113** (only efficient at 80–100 °C) in terms of activity, possibly because the reactivity in the latter series was excessively diminished by the above-mentioned Ae$\cdots$F–C interactions. Kinetic
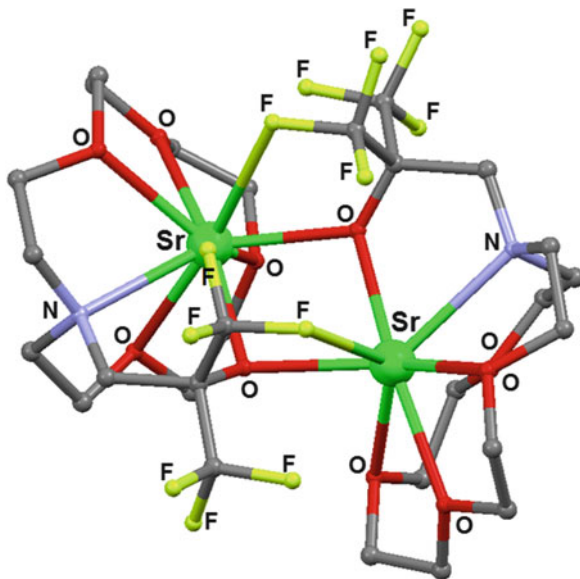
Fig. 33 Representation of one of the two independent and equivalent bimetallic cationic fragments [{O$_4$NO^{alkF}}Sr$^+$]$_2$ in **112**. The counterions H$_2$N{B(C$_6$F$_5$)$_3$}$_2$$^-$, solvent molecules, and hydrogen atoms are omitted for clarity

studies showed that the ROP of L-LA mediated by **112**/BnOH followed first-order kinetics in monomer, catalyst, and alcohol concentrations ($\Delta H^{\neq} = 61.8(5)$ kJ·mol^{-1} and $\Delta S^{\neq} = 31.8(2)$ J (K mol)$^{-1}$).

Sarazin and coworkers interrogated further the ability of the solvent-free barium cations **108** and **113** as *i*ROP catalysts [114]. In combination with 10–100 equiv of external nucleophile (benzyl alcohol, 1,3-propanediol, benzyl amine, or an hydroxyl-functionalized alkoxy-amine), the Ba cation **108** in particular proved effective for the *i*ROP of L-LA in the temperature range 0–30 °C. It converted up to 1,000–5,000 equiv. of monomer within 6 h (TOF up to 2,000 mol$_{L-LA}$ (mol$_{Ba}$·h)$^{-1}$) in a controlled fashion and with excellent end-group reliability, and yielded end-functionalized PLLAs suitable for further macromolecular engineering.

Mountford and coworkers also contributed to the development of Ca-based cationic species. In 2011, they reported the synthesis of the calcium complexes [Ca(BH$_4$)(THF)$_5$]$^+$·[BPh$_4$]$^-$ (**114**) and [(Tpm)Ca(BH$_4$)(THF)$_2$]$^+$·[BPh$_4$]$^-$ (**115**) (Fig 34) [115]. The simple initiator **114** polymerized quantitatively 200 equiv of CL at room temperature in 2 min or 50–300 equiv of D,L-LA at 70 °C in 3–5 h to give α,ω-dihydroxytelechelic polymers according to a ROP mechanism specific to metal tetrahydroborate species [116]. The reactions were controlled, giving polymers of predictable molecular weights and relatively narrow molecular weight distribution ($M_w/M_n \approx 1.4$). The more sterically shielded **115** proved more active and was capable of converting 250 equiv of D,L-LA in 2 h at room temperature with a comparable control ($M_w/M_n \approx 1.2$–1.4) to give PLAs with M_n up to
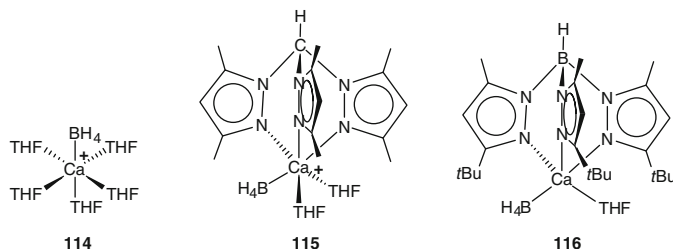
Fig. 34 Cationic (**114–115**) and corresponding neutral tetrahydroborate calcium complexes (**116**) by Mountford and coworkers [115]

35,000 g·mol^{-1}. Yet, both **114** and **115** only yielded essentially atactic PLA. The authors alleviated this issue by employing {Tp^{tBu,Me}}Ca(BH$_4$)(THF) (**116**), the highly congested *tris*(pyrazolyl)-supported analogue of **115** (Fig. 34). The ROP of D,L-LA at –20 °C initiated by **116** was both fast (conversion of 50–200 equiv of monomer was nearly complete within 5 min) and controlled; the resulting polymers were highly heterotactic, with P_r values in the range 0.88–0.90.

3.4.2 Bimetallic Complexes

In the aim of designing heteroleptic bimetallic complexes that could catalyze the copolymerization of CO$_2$ and epoxides, Harder and coworkers synthesized several dinucleating ligands that enabled the subsequent preparation of homobimetallic complexes. In their first contribution, *bis*(salicyladimine) ligands containing rigid bridges were employed to obtain the corresponding Mg or Ca (or even Zn) heteroleptic bimetallic species (Fig. 35) [117]. The magnesium complexes **117–119** supported by the ligands with the PARA, META, or PYR bridge, respectively, were stable. On the other hand, the calcium congeners **120** and **121** containing the PARA or Me$_4$PARA bridges, respectively, were not stable in solution, and readily led to mixtures of homoleptic or even polymeric Ca species; their use in polymerization could therefore not be assessed. Attempts to use the Mg complexes **117–119** dinuclear complexes for the ROP of epoxides (cyclohexene or propylene oxide) or the copolymerization of cyclohexene oxide with CO$_2$ were unsuccessful. More gratifyingly, they were active towards the ROP of D,L-LA, allowing partial conversion (22–86 %) of 50 equiv of monomer (vs. Mg) in 5 h at 20 °C in THF or dichloromethane or at 80 °C in toluene with limited control ($M_w/M_n \approx 1.42$–1.97, $M_{n,obs} > M_{n,calc}$); the resulting PLAs were all atactic. Complex **119** displayed the highest activity in non-coordinating solvents (conversion = 81 % in dichloromethane and 72 % in toluene) but was inferior to **117** and **118** when the reactions were performed in THF (**117**, 79 % conversion; **118**, 56 %; **119**, 35 %); this presumably translated the role of the heteroatom in the bridge of **119** during ROP reactions carried out in nonpolar medium.

This methodology was then extended by the same group to the design of dinucleating ligands comprising BDI moieties [118], or to the nitrogen–nitrogen-
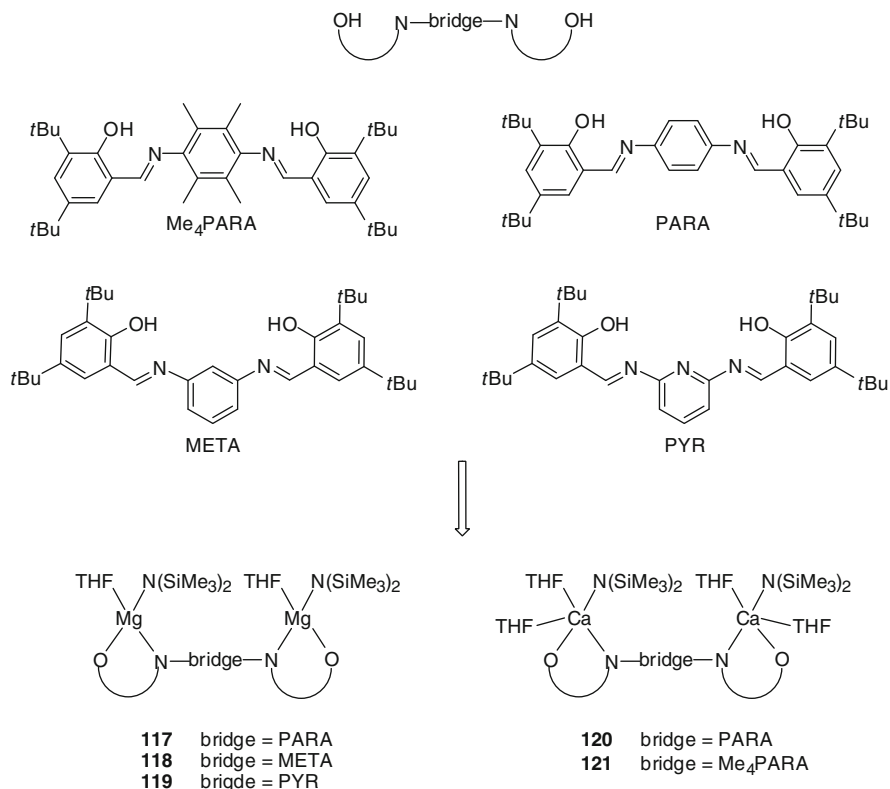
Fig. 35 Binuclear heteroleptic magnesium (**117–119**) and calcium (**120–121**) *bis*(salicylaldimine) complexes by Harder and coworkers [117]

coupled salicylaldimine analogues of those described previously [119]. The synthesis of several stable heteroleptic bimetallic complexes of magnesium and calcium (and zinc) was achieved but, disappointingly (and unlike the close zinc derivatives), they did not show activity in the (co)polymerization of epoxides nor towards the ROP of cyclic esters.

Several dinuclear magnesium complexes were successfully employed by Ding and coworkers for the copolymerization of cyclohexene oxide and CO_2 [120]. These pre-catalysts (**122**) were generated in situ by reaction of Mg(nBu)$_2$ with phenol-bridged bis(α,α-diarylprolinol) ligands (Scheme 14). In the presence of an alcohol co-catalyst (0.2–2 equiv vs. Mg), they competently produced perfectly alternating copolymers under mild conditions (P_{CO2} = 1 atm, T = 60 °C, 6 h), albeit with a high pre-catalyst loading (5 mol%). Medium molecular weight polycarbonates and reasonably narrow molecular weight distributions were obtained (M_n = 9,700–47,600 g·mol^{-1}, M_w/M_n = 1.5–2.0). The catalyst activity and chemoselectivity of the reaction were very sensitive to ligand substituents, as the presence of electron-withdrawing groups of the aromatic ring was found to influence
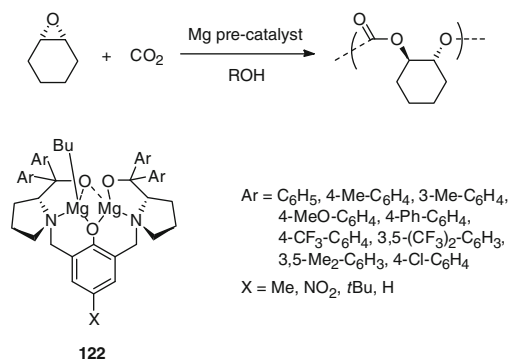
Scheme 14 Binuclear magnesium complexes supported by phenol-bridged bis(α,α-diarylprolinol) ligands for the copolymerization of cyclohexene oxide and CO_2 by Ding and coworkers [120]

negatively the course of the copolymerization. Zero- and first-order dependence upon CO_2 and cyclohexene oxide concentrations, respectively, was determined.

3.5 Perspectives

The discoveries of the past 10 years in the chemistry of the alkaline-earth elements applied to ROP catalysis have clearly shown that these metals bear true potential for future catalyst development. One of their great assets undeniably lies in their extreme reactivity; it is now possible to achieve the controlled polymerization of several thousands equiv of monomer with minute amounts of Ae-based well-defined complexes. This is of utmost importance as current ROP processes normally do not include (problematic) removal of the catalyst residues from the final polymers, but P(L) LA, PCL, PTMC, and their copolymers are typically used for packaging food and biomedical applications where the presence of toxic metal (and ligand) residues can be greatly troublesome. With this respect, the benign nature of the alkaline-earth metals gives them a comfortable edge over other metals traditionally used in ROP catalysis such as the more controversial tin or aluminum. An elegant illustration of the advantages of such innocuous initiators for the preparation of PLA-based nanoparticulate delivery vehicles was for instance reported by Cheng and coworkers in 2008 [121].

The search for increasingly efficient systems able to mediate the controlled *i*ROP of cyclic esters will surely be at the forefront of catalyst development in this area. Indeed, to date, only this methodology enables the production of hundreds of polymer chains *per* metal center in a controlled manner, thus making the metal complex a true catalyst towards the monomer *and* the number of polymer chains produced. Besides, if a polyfunctional exogenous transfer agent is judiciously selected, end-functionalized polyesters are generated and they can be used as building blocks towards higher, more sophisticated macromolecular architectures as illustrated for instance by Carpentier and coworkers [122, 123].

Synthetic organometallic and polymer chemists are now confronted to two daunting tasks which will imperatively have to be tackled in the coming years. The first and probably more challenging one will be to reduce the extreme sensitivity of Ae-based ROP catalysts towards impurities, a *sine qua non* if they are to be implemented for large-scale polymerizations. The second will consist in the tailoring of catalysts capable of achieving high levels of stereocontrol in the ROP of optically active monomers such as D,L-LA or the more reluctant β-butyrolactone. The intelligent and rational design of new ligand frameworks will be key to overcome these two issues.

References

1. Valente A, Mortreux A, Visseaux M, Zinck P (2013) Chem Rev (in press), DOI:10.1021/cr300289z
2. Kempe R (2007) Chem Eur J 13:2764
3. Sita LR (2009) Angew Chem Int Ed 48:2464
4. Pelletier JF, Mortreux A, Olonde X, Bujadoux K (1996) Angew Chem Int Ed Engl 35:1854
5. Chenal T, Olonde X, Pelletier JF, Bujadoux K, Mortreux A (2007) Polymer 48:1844
6. Bogaert S, Chenal T, Mortreux A, Carpentier JF (2002) J Mol Catal A 190:207
7. Gromada J, Chenal T, Mortreux A, Ziller JW, Leising F, Carpentier JF (2000) Chem Commun 2000:2183
8. Gromada J, Mortreux A, Chenal T, Ziller JW, Leising F, Carpentier JF (2002) Chem Eur J 8:3773
9. Gromada J, Mortreux A, Nowogrocki G, Leising F, Mathivet T, Carpentier JF (2004) Eur J Inorg Chem 2004:3247
10. Briquel R, Mazzolini J, Le Bris T, Boyron O, Boisson F, Delolme F, D'Agosto F, Boisson C, Spitz R (2008) Angew Chem Int Ed 47:1
11. Mazzolini J, Mokthari I, Briquel R, Boyron O, Delolme F, Monteil V, Bertin D, Gigmes D, D'Agosto F, Boisson C (2010) Macromolecules 43:7495
12. Godoy Lopez R, Boisson C, D'Agosto F, Spitz R, Boisson F, Gigmes D, Bertin D (2006) Macromol Rapid Comm 27:173
13. Godoy Lopez R, Boisson C, D'Agosto F, Spitz R, Boisson F, Gigmes D, Bertin D (2007) J Polym Sci A 45:2705
14. Bogaert S, Carpentier JF, Chenal T, Mortreux A, Ricart G (2000) Macromol Chem Phys 201:1813
15. Rodrigues AS, Kirillov E, Vuillemin B, Razavi A, Carpentier JF (2007) J Mol Catal A 273:87
16. Valente A, Zinck P, Mortreux A, Visseaux M (2009) Macromol Rapid Comm 30:528
17. Zinck P, Valente A, Mortreux A, Visseaux M (2007) Polymer 48:4609
18. Zinck P, Valente A, Bonnet F, Violante A, Mortreux A, Visseaux M, Ilinca S, Duchateau R, Roussel P (2010) J Polym Sci Polym Chem 48:802
19. Sarazin Y, de Frémont P, Annunziata L, Duc M, Carpentier JF (2011) Adv Synth Catal 353:1367
20. Annunziata L, Duc M, Carpentier JF (2011) Macromolecules 44:7158
21. Barbier-Baudry D, Bonnet F, Domenichini B, Dormond A, Visseaux M (2002) J Organomet Chem 647:167
22. Ajellal N, Furlan L, Thomas CM, Casagrande OL, Carpentier JF (2006) Macromol Rapid Comm 27:338
23. Wu W, Chen M, Zhou P (1991) Organometallics 10:98
24. Sánchez-Barba LF, Hughes DL, Humphrey SM, Bochmann M (2005) Organometallics 24:3792

25. Jenkins DK (1985) Polymer 26:147
26. Bonnet F, Visseaux M, Pereira A, Barbier-Baudry D (2005) Macromolecules 38:3162
27. De Groof B, Van Beylen M, Swarc M (1975) Macromolecules 8:396
28. Weeber A, Harder S, Brintzinger HH, Knoll K (2000) Organometallics 19:1325
29. Feil F, Harder S (2000) Organometallics 19:5010
30. Harder S, Feil F, Weeber A (2001) Organometallics 20:1044
31. Harder S, Feil F, Knoll K (2001) Angew Chem Int Ed 40:4261
32. Harder S, Feil F (2002) Organometallics 21:2268
33. Feil F, Müller C, Harder S (2003) J Organomet Chem 683:56
34. Piesik DFJ, Häbe K, Harder S (2007) Eur J Inorg Chem 2007:5652
35. Jochmann P, Dols TS, Spaniol TP, Perrin L, Maron L, Okuda J (2009) Angew Chem Int Ed 48:5715
36. Lichtenberg C, Jochmann P, Spaniol TP, Okuda J (2011) Angew Chem Int Ed 50:5753
37. Hatada K, Ute K, Tanaka K, Okamoto Y, Kitayama T (1986) Polymer J 18:1037
38. Dove AP, Gibson VC, Marshall EL, White AJP, Williams DJ (2002) Chem Commun 2002:1208
39. Zheng Z, Elmkaddem MK, Fischmeister C, Roisnel T, Thomas CM, Carpentier JF, Renaud JL (2008) New J Chem 32:2150
40. Uhrich EU, Cannizzaro SM, Langer RS, Shakesheff KM (1999) Chem Rev 99:3181
41. Drumright RE, Gruber PR, Henton DE (2000) Adv Mater 12:1841
42. Ikada Y, Tsuji H (2000) Macromol Rapid Comm 21:117
43. Albertsson AC, Varma IK (2003) Biomacromolecules 4:1466
44. Stanford MJ, Dove AP (2010) Chem Soc Rev 39:486
45. Becker JM, Pounder RJ, Dove AP (2010) Macromol Rapid Comm 31:1923
46. Zhou CH, Beltramini JN, Fana YX, Lu GQ (2008) Chem Soc Rev 37:527
47. Bozell JJ, Petersen GR (2010) Green Chem 12:539
48. O'Keefe BJ, Hillmyer MA, Tolman WB (2001) Dalton Trans: 2215
49. Okada M (2002) Prog Polym Sci 27:87
50. Dechy-Cabaret O, Martin-Vaca B, Bourissou D (2004) Chem Rev 104:6147
51. Wheaton CA, Hayes PG, Ireland BJ (2009) Dalton Trans: 4832
52. Thomas CM (2010) Chem Soc Rev 39:165
53. Carpentier JF (2010) Macromol Rapid Comm 31:1696
54. Sutar AK, Maharana T, Dutta S, Chen CT, Lin CC (2010) Chem Soc Rev 39:1724
55. Ajellal N, Carpentier JF, Guillaume C, Guillaume SM, Hélou M, Poirier V, Sarazin Y, Trifonov A (2010) Dalton Trans 39:8363
56. Chisholm MH, Eilerts NW (1996) Chem Commun 1996:853
57. Chisholm MH, Eilerts NW, Huffman JC, Iyer SS, Pacold M, Phomphrai K (2000) J Am Chem Soc 122:11845
58. McLain SJ, Ford TM, Drysdale NE, Jones N, McCord EF, Shreeve JL, Evans WJ (1994) Polym Prepr 35:534
59. Cheng M, Attygalle AB, Lobkovsky EB, Coates GW (1999) J Am Chem Soc 12:11583
60. Chisholm MH, Huffman JC, Phomphrai K (2001) J Chem Soc Dalton Trans: 222
61. Chisholm MH, Gallucci J, Phomphrai K (2002) Inorg Chem 41:2785
62. Chamberlain BM, Cheng M, Moore DR, Ovitt TM, Lobkovsky EB, Coates GW (2001) J Am Chem Soc 123:3229
63. Ayala CN, Chisholm MH, Gallucci JC, Krempner C (2009) Dalton Trans: 9237
64. Dove AP, Gibson VC, Marshall EL, White AJP, Williams DJ (2004) Dalton Trans: 570
65. Chisholm MH, Gallucci JC, Phomphrai K (2005) Inorg Chem 44:8004
66. Chivers T, Fedorchuk C, Parvez M (2005) Organometallics 24:580
67. Sánchez-Barba LF, Garcés A, Fajardo M, Alonso-Moreno C, Fernández-Baeza J, Otero A, Antiñolo A, Tejeda J, Lara-Sánchez A, López-Solera MI (2007) Organometallics 26:6403
68. Sánchez-Barba LF, Garcés A, Fernández-Baeza J, Otero A, Alonso-Moreno C, Lara-Sánchez A, Rodríguez AM (2011) Organometallics 30:2775

69. Garcés A, Sánchez-Barba LF, Alonso-Moreno C, Fajardo M, Fernández-Baeza J, Otero A, Lara-Sánchez A, Lopez-Solera I, Rodríguez AM (2010) Inorg Chem 49:2859
70. Makio H, Terao H, Iwashita A, Fujita T (2011) Chem Rev 111:2363
71. Shueh ML, Wang YS, Huang BH, Kuo CY, Lin CC (2004) Macromolecules 37:5155
72. Wu J, Chen YZ, Hung WC, Lin CC (2008) Organometallics 27:4970
73. Shen MY, Peng YL, Hung WC, Lin CC (2009) Dalton Trans: 9906
74. Chen PS, Liu YC, Lin CH, Ko BT (2010) J Polymer Sci Polymer Chem 48:3564
75. Poirier V, Roisnel T, Carpentier JF, Sarazin Y (2009) Dalton Trans: 9820
76. Wang L, Ma H (2010) Macromolecules 43:6535
77. Castro PM, Zhao G, Amgoune A, Thomas CM, Carpentier JF (2006) Chem Commun 2006:4509
78. Chisholm MH, Galucci J, Krempner C, Wiggenhorn C (2006) Dalton Trans 2006:846
79. Ejfler J, Krauzy-Dziedzic K, Szafert S, Jerzykiewicz LB, Sobota P (2010) Eur J Inorg Chem 2010:3602
80. Hung WC, Lin CC (2009) Inorg Chem 48:728
81. Tang HY, Chen HY, Huang JH, Lin CC (2007) Macromolecules 40:8855
82. Tsai YH, Lin CH, Lin CC, Ko BT (2009) J Polymer Sci Polymer Chem 47:4927
83. Lian B, Thomas CM, Casagrande OL, Roisnel T, Carpentier JF (2007) Polyhedron 26:3817
84. Hill FN, Fitzpatrick JT, Bailey FE (1961) US Patent 2969402
85. Hill, FN, Fitzpatrick, JT, Bailey, FE (1962) US Patent 3037943
86. Cox EF, Hostettler F (1962) US Patent 3021312
87. Li SM, Rashkov I, Espartero JL, Manolova N, Vert M (1996) Macromolecules 29:57
88. Feng Y, Klee D, Höcker H (2001) Macromol Chem Phys 202:3120
89. He C, Sun J, Deng C, Zhao T, Deng M, Chen X, Jing X (2004) Biomacromolecules 5:2042
90. Piao L, Deng M, Chen X, Jiang L, Jing X (2003) Polymer 44:2331
91. Tang Z, Chen X, Liang Q, Bian X, Yang L, Piao L, Jing X (2003) J Polymer Sci Polymer Chem 41:1934
92. Guan H, Xie Z, Tang Z, Xu X, Chen X, Jing X (2005) Polymer 46:2817
93. Dobrzyński P, Kasperczyk J, Bero M (1999) Macromolecules 32:4735
94. Zhong Z, Dijkstra PJ, Birg C, Westerhausen M, Feijen J (2001) Macromolecules 34:3863
95. Sarazin Y, Howard RH, Hughes DL, Humphrey SM, Bochmann M (2006) Dalton Trans: 340
96. Darensbourg DJ, Choi W, Ganguly P, Richers CP (2006) Macromolecules 39:4374
97. Chen HY, Tang HY, Lin CC (2007) Polymer 48:2257
98. Davidson MG, O'Hara CT, Jones MD, Keir CG, Mahon MF, Kociok-Köhn G (2007) Inorg Chem 46:7686
99. Westerhausen M, Schneiderbauer S, Kneifel AN, Söltl Y, Mayer P, Nöth H, Zhong Z, Dijkstra PJ, Feijen J (2003) Eur J Inorg Chem 2003:3432
100. Zhong Z, Schneiderbauer S, Dijkstra PJ, Westerhausen M, Feijen J (2003) Polymer Bull 51:175
101. Chisholm MH, Gallucci J, Phomphrai K (2003) Chem Commun 42003:8
102. Chisholm MH, Gallucci JC, Phomphrai K (2004) Inorg Chem 43:6717
103. Xu X, Chen Y, Zou G, Mac Z, Li G (2010) J Organomet Chem 695:1155
104. Darensbourg DJ, Choi W, Richers CP (2007) Macromolecules 40:3521
105. Darensbourg DJ, Choi W, Karroonnirun O, Bhuvanesh N (2008) Macromolecules 41:3493
106. Sarazin Y, Roşca D, Poirier V, Roisnel T, Silvestru A, Maron L, Carpentier JF (2010) Organometallics 29:6569
107. Liu B, Roisnel T, Guégan JP, Carpentier JF, Sarazin Y (2012) Chem Eur J 18:6289
108. Hannant MD, Schormann M, Bochmann M (2002) J Chem Soc Dalton Trans: 4071
109. Sarazin Y, Schormann M, Bochmann M (2004) Organometallics 23:3296
110. Hannant MD, Schormann M, Hughes DL, Bochmann M (2005) Inorg Chim Acta 358:1683
111. Ireland BJ, Wheaton CA, Hayes PG (2010) Organometallics 29:1079
112. Sarazin Y, Poirier V, Roisnel T, Carpentier JF (2010) Eur J Inorg Chem 2010:3423
113. Sarazin Y, Liu B, Roisnel T, Maron L, Carpentier JF (2011) J Am Chem Soc 133:9069

114. Liu B, Roisnel T, Sarazin Y (2012) Inorg Chim Acta 380:2
115. Cushion MG, Mountford P (2011) Chem Commun 47:2276
116. Barros N, Mountford P, Guillaume SG, Maron L (2008) Chem Eur J 14:5507
117. Range S, Piesik DFJ, Harder S (2008) Eur J Inorg Chem 2008:3442
118. Piesik DFJ, Range S, Harder S (2008) Organometallics 27:6178
119. Piesik DFJ, Stadler R, Range S, Harder S (2009) Eur J Inorg Chem 2009:3569
120. Xiao Y, Wang Z, Ding K (2006) Macromolecules 39:128
121. Tong R, Cheng J (2008) Angew Chem Int Ed 47:4830
122. Poirier V, Duc M, Carpentier JF, Sarazin Y (2010) ChemSusChem 3:579
123. Hélou M, Carpentier JF, Guillaume SM (2011) Green Chem 13:266

Homogeneous Catalysis with Organometallic Complexes of Group 2

Mark R. Crimmin and Michael S. Hill

Abstract This chapter provides details of the recent progress in heavier Group 2-catalyzed small molecule transformations mediated by well-defined heteroleptic and homoleptic complexes of the form LMX or MX_2, where L is a monoanionic ligand and X is a reactive σ-bonded substituent and M = Mg, Ca, Sr, and Ba. The intra- and intermolecular heterofunctionalization (hydroamination, hydrophosphination, hydrosilylation, hydroboration, hydrogenation, and hydroacetylation) of alkenes, alkynes, dienes, carbodiimides, isocyanates, pyridines, quinolines, and ketones is discussed, along with the dimerization of aldehydes, the trimerization of isocyanates, and the dehydrogenation of amine-boranes and the dehydrogenative coupling of amines with silanes. While studies in this field have focused largely on biocompatible and inexpensive catalysts of calcium and the heavier elements, the field has renewed interest in the chemistry of organomagnesium complexes.

Keywords Barium · Calcium · Catalysis · Dehydrocoupling · Dehydrogenation · Group 2 · Heavier Alkaline Earth · Heterofunctionalization · Hydroamination · Hydroboration · Hydrogenation · Hydrophosphination · Hydrosilylation · Magnesium · Strontium

Contents

M.R. Crimmin (✉)
Department of Chemistry, Imperial College London, South Kensington, London SW7 2AZ, UK
e-mail: m.crimmin@imperial.ac.uk

M.S. Hill
Department of Chemistry, University of Bath, Claverton Down, Bath BA2 7AY, UK
e-mail: msh27@bath.ac.uk

1 Background

1.1 An Analogy Between Organometallic Complexes of Group 2 and the 4f-Metals

With some remarkable exceptions, the organometallic compounds of group 2 are redox-inactive species that demonstrate a +2 oxidation state [1–6]. The M^{2+} cation achieves a noble gas configuration, while complexes of calcium, strontium and barium possess d^0 electron configurations. The ionic radii of the dications increase as the group is descended ($Mg^{2+} < Ca^{2+} < Sr^{2+} < Ba^{2+}$), whereas the Pauling electronegativity of the elements decreases as the group is descended (Mg > Ca > Sr > Ba) [7]. The result of these factors is that, while organometallic compounds of magnesium may show a degree of covalency in metal–ligand interactions, bonding in organometallic complexes of the heavier elements can be considered almost exclusively in terms of ionic and nondirectional interactions between the metal and auxiliary ligands. For example, in Me_2M the ionicity of the M–C bond, defined in terms of the natural charge on the metal per methyl group, has been calculated by ab initio methods using Hartree–Fock theory as Be–C, 74 %; Mg–C, 77 %; Ca–C, 87 %; Sr–C, 91 %; and Ba–C, 94 % [8].

Due to their ionic nature, parallels are often drawn between the chemistry of group 2 complexes and that of the trivalent and divalent organolanthanides. For example, in six-coordinate environments, Ca^{2+} and Yb^{2+} and Eu^{2+}/Sm^{2+} and Sr^{2+} have very similar ionic radii (Ca^{2+}, 1.00 Å; Yb^{2+}, 1.02 Å; Eu^{2+}, 1.22 Å; Sm^{2+}, 1.17 Å; Sr^{2+}, 1.18 Å) [7]. While the divalent lanthanides have a propensity to react via one-electron redox processes, the pioneering work of Marks showed that trivalent organolanthanide compounds of the form L_2MX^1, where L is a
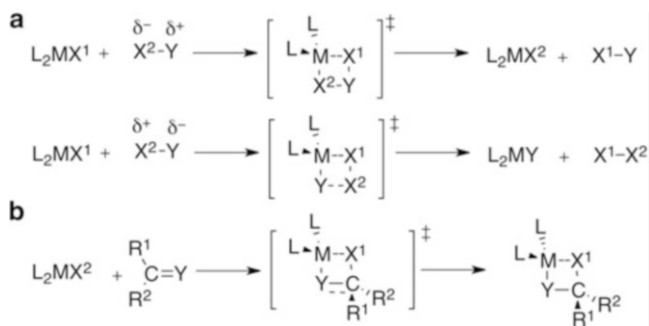
Scheme 1 Fundamental reactions of trivalent lanthanide organometallics. (**a**) σ-bond metathesis [2σ + 2σ] and (**b**) insertion of unsaturated substrates into M–X^2 σ-bonds [2σ + 2π]

monoanionic spectator ligand and X^1 is a monoanionic σ-bonded substituent, demonstrate two fundamental types of reactivity: (1) σ-bond metathesis and (2) the insertion of unsaturated carbon–carbon or carbon–heteroatom bonds into Ln–X^1 σ-bonds (Scheme 1) [9, 10].

By incorporating these two steps into cycles a number of catalytic reactions have been developed [9, 10]. Initial research centered upon the use of sterically demanding pentamethylcyclopentadienyl or *ansa*-bridged cyclopentadienyl ligands to stabilize low-coordinate, highly reactive, organolanthanide intermediates. Complexes of the form L$_2$MX^1 [L = η^5-C$_5$Me$_5$, L$_2$ = (η^5-C$_5$Me$_4$)$_2$SiMe$_2$, (η^5-C$_5$Me$_4$) SiMe$_2$(N^{t}Bu); X^1 = H, CH(SiMe$_3$)$_2$, N(SiMe$_3$)$_2$] were reported as catalysts for the hydroamination, hydrophosphination, hydrosilylation, hydrogenation, and hydroboration of unsaturated carbon–carbon bonds [9, 10].

In the past decade, the often-cited parallels in bonding between group 2 and trivalent lanthanide complexes have translated into parallels in reactivity. Group 2 complexes have been developed that act as homogeneous catalytic reagents using σ-bond metathesis and insertion reaction chemistries to construct catalytic cycles [11–14]. The following chapter details progress in this field, while related applications of group 2 complexes to the polymerization of activated alkenes [15–24], and the ring-opening polymerization of cyclic esters [25–31], along with the use of group 2 reagents in combination with chiral ligands for asymmetric carbon–carbon bond forming reactions [32–37], are covered in Chaps. 4 and 6, respectively. The coordination chemistry of heavier group 2 metals has been reviewed several times [38–50], while recent review articles have highlighted group 2 complexes in catalysis [11–14]. Throughout this chapter, and the literature, the terms "homoleptic" and "heteroleptic" are used to refer to complexes that contain either the same (i.e., L$_2$M or MX$_2$) or different monoanionic ligands (i.e., LMX) coordinated to the metal, respectively. As group 2 complexes are commonly isolated as solvates with additional charge neutral ligands such as THF coordinated to the metal center the term homoleptic is often misused, as it does not adhere to the strict IUPAC definition. Throughout this chapter, Ar is used as an abbreviation for 2,6-di-*iso*-propylphenyl.
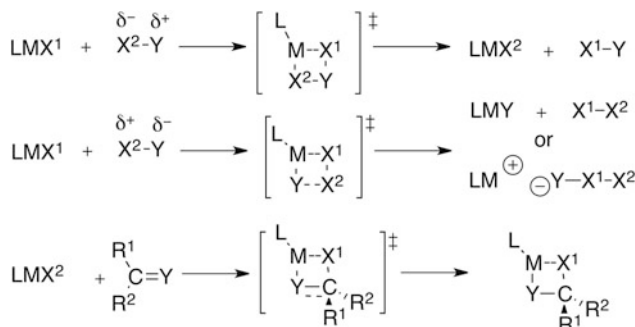
Scheme 2 Fundamental reactions of group 2 complexes relevant to catalysis

1.2 σ-Bond Metathesis and Insertion Reactivity at Group 2 Metal Centers

Insertion: The insertion of polarized unsaturated substrates into group 2 M–X^1 bonds has a long history. In early studies, Gilman and Coles showed that ill-defined group 2 complexes, proposed to contain metal–carbon σ-bonds, react with CO_2, benzonitrile and 1,1-diphenylethene [51–54]. Mingos and coworkers have demonstrated the insertion of carbonyl sulfide, carbon disulfide, and sulfur dioxide into group 2 metal–alkoxide bonds [55–60], while Harder and coworkers observed the insertion of 1,1-diphenylethene into the Ba–C bonds of [Ba(CH$_2$Ph)$_2$]$_n$ in THF solution, along with related reactions of Ca and Sr derivatives, during studies upon group 2 polymerization catalysts [24].

   σ-bond metathesis: Further to these observations, σ-bond metathesis has been frequently employed in stoichiometric heavier group 2 chemistry to synthesize new complexes. In cases were the substrate is an acid with a lower pK_a than that of the conjugate acid of the metal base, this reaction is also referred to as protonolysis, or more specifically transamination when a metal amide is employed (X = NR$_2$) [34–46]. Examples of σ-bond metathesis reactions of heavier group 2 organometallics with hydridic or non-protic substrates are more limited in scope and are highlighted in the sections of this chapter describing hydrosilylation and hydroboration catalysis. Importantly this reactivity may be, alternatively, considered as the formation and decomposition of a heavier alkaline-earth "ate" complex. An intermediate that can also potentially undergo charge separation to form a cation/anion pair.

1.3 Addressing the Schlenk Equilibrium

An underlying challenge in the development of catalytic reagents based upon the heavier alkaline earths is the propensity of LMX to undergo Schlenk-like solution redistribution reactions to L$_2$M and MX$_2$ (Scheme 3).

$$2 \text{ LMX} \rightleftharpoons \text{L}_2\text{M} + \text{MX}_2 \qquad M = Mg, Ca, Sr, Ba$$

Scheme 3 Schlenk equilibrium of group 2 complexes

Depending on the nature of X, the latter product is potentially polymeric and of low solubility in non-coordinating solvents, while the former product is potentially kinetically stabilized and unreactive. This solution redistribution reaction can result in the formation of a mixture from a potentially catalytically active species and may result in the loss of any ligand control over turnover- and stereo- or regio-determining steps in the catalytic cycle. This problem becomes increasingly important for the heavier alkaline-earth congeners; as the ionic radius increases and Lewis acidity decreases on descending the group and, for a given ancillary ligand set, the tendency toward solution redistribution, LMX to MX and L_2M, increases across the series M = Mg < Sr < Ca < Ba.

Sterically demanding ligand sets: In order to circumvent this problem, sterically demanding monoanionic ligand sets have been applied to the kinetic stabilization of group 2 complexes. Slowing the rate of the redistribution reaction allows subsequent study of the σ-bonded substituent in LMX. This approach was pioneered by Hanusa and coworkers who demonstrated that heteroleptic heavier group 2 complexes including halides [61–63], acetylides [64], amides [65], and a calcium borohydride [66] may be kinetically stabilized by bulky cyclopentadienyl ligands, allowing their synthesis and characterization in the solid state. Many of these compounds, however, are unstable in solution and undergo Schlenk-like equilibria; their application in catalysis remains unreported [61–66].

In contrast, the β-diketiminato-stabilized calcium amide [{(ArNCMe)$_2$CH}Ca {N(SiMe$_3$)$_2$}(THF)] and a tris(pyrazolylborate)-stabilized analogue were reported by Chisholm and coworkers as precatalysts for the ring-opening polymerization of *rac*-lactide to form heterotactic polylactide [25, 26], while substituted fluorenyl ligands have been reported by Harder and coworkers for the stereocontrolled polymerization of styrene to yield highly syndiotactic polystryene [23].

These papers demonstrated that controlled reactivity at an alkaline-earth center supported by a monoanionic spectator ligand was achievable, and paved the way for the application of heavier group 2 catalysts in organic synthesis. To date, the majority of group 2 precatalysts are heteroleptic complexes of the form LMX containing either κ^2-*N,N*-chelating ligands that form 4-,5-, or 6-membered rings upon coordination to the metal or tripodal face-capping κ^3-*N,N,N*-chelates or κ^3-*C, C,C*-chelates [L = β-diketiminato, triazenido, aminotropiniminato, bis(imidazolin-2-ylidene-1-yl)borato, tris(imidazolin-2-ylidene-1-yl)borato, and tris(oxazolino) borato]. The reactive σ-bonded substituent is typically an amide, hydride, or alkyl ligand with bis(trimethylsilyl)amide complexes being most prevalent due to their synthetic accessibility [X^1 = N(SiMe$_3$)$_2$, Me, CH(SiMe$_3$)$_2$, CH$_2$Ph, or H].

Agostic interactions: While factors that control the position of the Schlenk equilibrium are still not well understood, more recently Sazarin, Carpentier, and coworkers have reported Ca, Sr, and Ba complexes supported by rigid *N,N*-chelating ligands that are stable in C$_6$D$_6$ up to 60 °C with no evidence for Schlenk-like
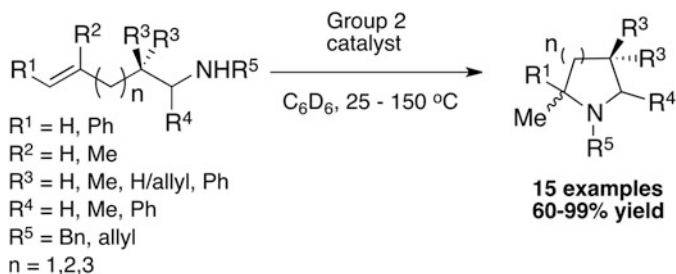
Scheme 4 Scope of the group 2-mediated hydroamination of aminoalkenes

redistribution. Additional stabilization at the metal is provided by the reactive σ-bonded substituent $-N(SiHMe_2)_2$ which protects the metal center via a series of metal–hydride anagostic interactions [67].

Grafting onto a surface: In an alternative approach, Harder, Gauvin, and coworkers have reported the grafting of group 2 organometallics MX^1_2 to nonporous Aerosil 380 following its activation by calcination at 700 °C. The resulting heterogeneous catalysts show activity in heterofunctionalization catalysis and are not susceptible to Schlenk-like redistribution under the conditions examined [68].

Homoleptic precatalysts: A number of amide and alkyl complexes of the form MX^1_2 $[X^1 = N(SiMe_3)_2, CH(SiMe_3)_2]$ have also been reported as precatalysts for heterofunctionalization of unsaturated substrates [69–71].

2 Heterofunctionalization of Unsaturated Substrates

2.1 Hydroamination of Alkenes, Carbodiimides, and Isocyanates (C–N bond formation)

2.1.1 Intramolecular Hydroamination/Cyclization of Aminoalkenes

Reaction Scope: A significant number of precatalysts based upon Mg, Ca, Sr, and Ba have been reported for the intramolecular hydroamination of aminoalkenes. Reactions proceed in high yield under mild conditions (25–80 °C, 0.25–132 h) allowing the synthesis of pyrrolidines, piperidines, and hexahydroazepines from the *n*-exo-trig ($n = 5, 6, 7$) cyclization of 1-amino-4-pentenes, 1-amino-5-hexenes, and 1-amino-6-heptenes, respectively (Scheme 4) [72–84]. The reaction scope is currently limited to the hydroamination cyclization of 1° and 2° aminoalkenes incorporating either the alkene at the terminal position or an internal alkene activated by conjugation to a phenyl group. A single example of the intramolecular hydroamination of an aminoalkyne has been reported [84].

As with $4f^n d^o$ catalysts and group 1 catalysts, reactions are dictated by substrate control and geminal disubstituted alkenes cyclize readily due a favorable Thorpe–Ingold effect while [85], consistent with Baldwin's guidelines for ring formation, the ease of the catalytic reactions increases with decreasing ring size (5 > 6 > 7-membered ring closures).

For 1-aminopent-4-enes possessing additional substitution that creates a prochiral center in the substrate, α-substitution gives rise to a highly diastereoselective reaction yielding predominantly *trans*-pyrrolidines, while β-substitution results in a nonselective C–N bond forming reaction resulting in approximately a 1:1 mixture of diastereomeric pyrrolidine products [72, 76]. It is noteworthy that 1-aminohex-5-ene substrates bearing α-substitution have not yet been reported in group 2 catalysis, and it is currently unknown whether the *cis*-selectivity observed in lanthanide systems will be retained [9, 10]. While related 1-amino-2,2-dialkylhex-6-ene substrates undergo clean intramolecular hydroamination with magnesium precatalysts, in the presence of [{(ArNCMe)$_2$CH}Ca{N(SiMe$_3$)$_2$}(THF)] alkene isomerization is observed as a minor pathway and 5–20 % of the corresponding *trans*-1-aminohex-2-enes are observed [76]. Related 2,5-bis{*N*-(2,6-di-*iso*-propylphenyl)iminomethyl}pyrrolyl calcium and strontium amide complexes yield *trans*-1-amino-2-methylpent-3-ene as the major reaction product at high temperatures during the attempted catalytic cyclization of 1-amino-2-methylpent-4-ene [80]. Group 2-catalyzed alkene isomerization in these systems is still not well understood.

Catalyst development has centered upon addressing the Schlenk equilibrium and approaches to this problem include kinetic stabilization of the metal center as outlined in Sect. 1.3. A series of homoleptic group 2 amides [M{N(SiMe$_3$)$_2$}$_2$(THF)$_n$] (n = 0, 2) and group 2 alkyls [M{CH(SiMe$_3$)$_2$}$_2$(THF)$_2$] have also been applied to intramolecular hydroamination catalysis [69, 82]. Despite precatalysts incorporating β-diketiminato [72, 76, 83], triazenido [73], aminotroponato, aminotroponiminato [77, 84, 86], bis(imidazolin-2-ylidene-1-yl) borato [75], tris(imidazolin-2-ylidene-1yl)borato [74], and bis(iminomethyl) pyrrolyl [80, 87] and dearomatized bis(imino)acenapthene [83] ligands being applied to intramolecular hydroamination catalysis (Fig. 1), to date a homologous series of catalysts Mg–Ba has not been reported for this reaction (see Sects. 2.1.2 and 2.2.1 for comparison). Furthermore, catalyst activities follow different trends depending upon the ligand set.

Although studies are consistent with calcium-based precatalysts demonstrating improved reaction kinetics over their magnesium counterparts, this trend is not extended neatly to strontium and barium. For example, [{(ArNCMe)$_2$CH}Ca{N(SiMe$_3$)$_2$}(THF)] and [{(ArNCMe)$_2$CH}MgMe(THF)] effect the hydroamination of (1-allylcyclohexyl)methylamine with TOFs of 54.5 and 17.0 h^{-1}, respectively, at 25 °C. Related triazenido complexes [{Ar$_2$N$_3$}M{N(SiMe$_3$)$_2$}(THF)$_n$] (M = Ca, n = 2; M = Sr, n = 3) effect the cyclization of 1-amino-2,2-diphenylpent-4-ene with TOF of 500 h^{-1} for Ca and 75 h^{-1} for Sr at 25 °C [72, 76]. Similar observations are made with the aminotropinimato catalysts [{(^{i}Pr)$_2$ATI}M{N(SiMe$_3$)$_2$}(THF)] (M = Ca, Sr), with the calcium complex displaying the highest activity for a given substrate [83], while bis(imidazolin-2-ylidene-1yl)borato
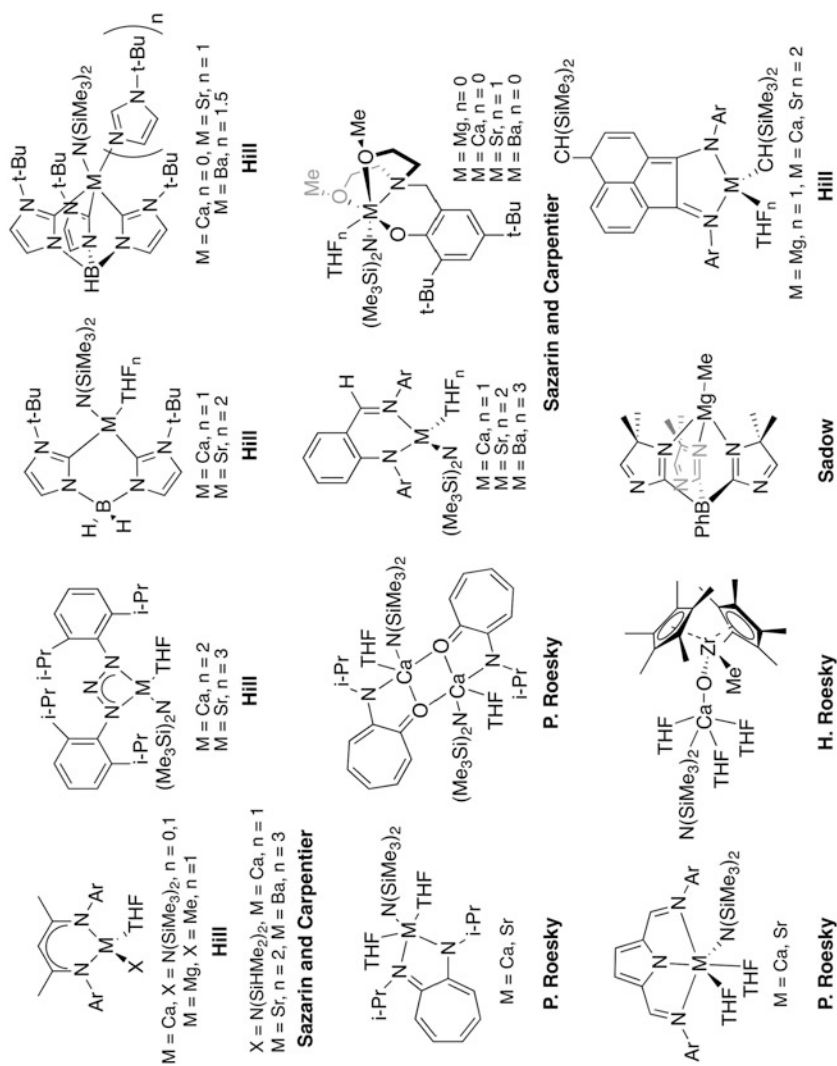
Fig. 1 Group 2 amides and alkyls as catalysts for hydroamination catalysis

Scheme 5 Scope of the group 2-mediated hydroamination of aminoalkenes with bimetallic catalysts
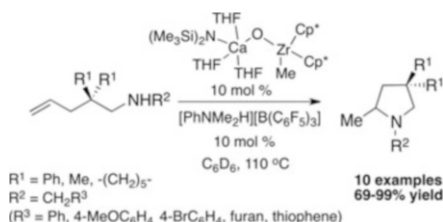
complexes $[\{H_2B(Im^tBu)_2\}M\{N(SiMe_3)_2\}(THF)_n]$ (M = Ca, $n = 1$; M = Sr, $n = 2$) displayed the opposite trend [84]. It is likely that these observations have an origin in loss of ligand control and a perturbation of catalyst nuclearity due to Schlenk equilibria.

While the activities of the catalyst systems outlined in Fig. 1 are broadly commensurate with one another, the tris(imidazolin-2-ylidene-1yl)borate complexes are of note as they are susceptible to B–N bond cleavage reactions and are thermally unstable above 50 °C [74]. In this regard it is also notable that deleterious Schlenk-like redistribution chemistry limits the catalyst lifetimes and in some of the magnesium catalysts proved *synthetically* advantageous for reactions conducted at elevated temperatures over long durations, despite their poorer reaction kinetics. For example, the cyclization of 1-amino-2,2-diphenylhept-6-ene to the corresponding hexahydroazepine proceeds selectively with 5 mol% of the magnesium catalyst $[\{(ArNCMe)_2CH\}MgMe(THF)]$ after 5.5 days at 80 °C while no reaction is observed at elevated temperatures with the calcium complex $[\{(ArNCMe)_2CH\}Ca\{N(SiMe_3)_2\}(THF)]$.

The reaction scope has been extended to incorporate a series of secondary amines by Roesky and coworkers employing the bimetallic group 4/group 2 complex $[Cp*_2ZrMe(\mu\text{-}O)Ca(THF)_3\{N(SiMe_3)_2\}]$ [79]. In the absence of any additive this latter precatalyst effects the cyclization of 1-aminopent-4-enes and 1-amino-hex-5-enes at 25 °C, while addition of a catalytic amount of $[PhNMe_2H][B(C_6F_5)_4]$ and conducting reactions at 110 °C allows the hydroamination of a series of N-substituted 1-amino-2,2-dialkylpent-4-enes (Scheme 5).

Reaction mechanism: Detailed mechanistic studies have been conducted on this reaction. While the stoichiometric protonolysis reaction of $[\{(ArNCMe)_2CH\}Mg^{n/s}Bu]_2$ with benzylamine, 2-methoxyethylamine, and pyrrolidine to yield the corresponding dimeric magnesium amides and methane proceeds rapidly and non-reversibly at room temperature [88], the reaction of $[\{(ArNCMe)_2CH\}Ca\{N(SiMe_3)_2\}(THF)]$ with benzylamine forms a quantifiable equilibrium between monomeric bis(trimethylsilyl)amide and dimeric benzylamide reaction products. A van't Hoff analysis of this equilbrium mixture allowed derivation of ΔG^o(298 K) as -2.7 kcal mol^{-1}, consistent with facile precatalyst activation via protonolysis with a primary amine [76, 87].

Further reactions of $[\{(ArNCMe)_2CH\}Ca\{N(SiMe_3)_2\}(THF)]$ with 2-methoxyethylamine and 2,6-di-*iso*-propylaniline demonstrated that the equilibrium could be effectively perturbed to the reaction products in the presence of chelating or more acidic substrates [89, 90]. A similar reaction of $[\{(ArNCMe)_2CH\}Sr\{N$

(SiMe$_3$)$_2$}(THF)] with 2-methoxyethylamine allowed the isolation of an additional reaction intermediate, the amine coordination complex, [{(ArNCMe)$_2$CH}Sr{N (SiMe$_3$)$_2$}{κ^2-NH$_2$CH$_2$CH$_2$OMe}], which was shown to be in equilibrium with 0.5 equiv. of the dimeric amide [{(ArNCMe)$_2$CH}Sr{NH$_2$CH$_2$CH$_2$OMe}]$_2$ and HN(SiMe$_3$)$_2$ [82].

These studies, along with a report by Harder and coworkers upon the addition of ammonia to [{(ArNCMe)$_2$CH}Ca{N(SiMe$_3$)$_2$}(THF)], have demonstrated that β-diketiminate group 2 primary amide complexes undergo facile external amine/ amide exchange along with intramolecular site exchange between amide and amine ligands [91]. Further mechanistic studies are consistent with the reaction proceeding via a rate-determining proton-assisted alkene insertion step with a rate law reminiscent of Michaelis–Menten kinetics. Thus, the cyclization of (1-allylcyclohexyl)methylamine with [{(ArNCMe)$_2$CH}MX^1(THF)] (M = Ca, Sr, X^1 = N(SiMe$_3$)$_2$; M = Mg, X^1 = Me) follows the empirical rate law $\nu = k'_{obs}$ [aminoalkene]^1[catalyst]^1. Experiments conducted on the magnesium system also demonstrate that the observed reaction rate is dependent upon the initial substrate concentration with high initial concentrations inhibiting catalytic turnover, suggesting that the observed rate constant k'_{obs} represents a series of elementary rate coefficients and equilibrium constants [76, 82]. Studies employing [M{N(SiMe$_3$)$_2$}$_2$(THF)$_2$] (M = Ca, Sr) as a precatalyst also demonstrate $\nu = k'_{obs}$ [aminoalkene]^1[catalyst]^1 with substrate inhibition at higher concentrations. KIEs of 4.5 (298 K) and 3.4 (318 K) for the calcium and strontium precatalysts, respectively, were calculated from comparison of k'_{obs} for the cyclization of (1-allylcyclohexyl) methylamine and d^2-(1-allylcyclohexyl)methylamine [82]. Catalytic cyclization of this substrate using [Cp*$_2$Zr(Me)O–Ca{N(SiMe$_3$)$_2$}(THF)$_3$] is again first order in substrate and first order in catalyst with a KIE of 2.42 (298 K) [79].

These observations have been interpreted in terms of a turnover-limiting transition state involving a six-membered metallocycle with alkene insertion into the M–N bond being assisted by a coordinated molecule of substrate. The coordinated amine transfers a proton to the newly forming M–C bond and results in N–H cleavage in the turnover-limiting step accounting for the large primary KIEs (Fig. 2). In addition, this mechanism obviates the inference of a long-lived, high-energy group 2 alkyl complex, a species that has limited precedent in the coordination chemistry of group 2. At higher substrate concentrations the metal center becomes coordinatively saturated and alkene coordination and insertion are inhibited. The coordinating solvent THF also acts as an inhibitor for this reaction and Hill and coworkers have proposed a rate law to account for the inhibition kinetics [76, 82].

Strong evidence for this model is provided by an elegant *substrate-catalyzed* single-turnover experiment presented by Sadow and coworkers [81]. The four-coordinate C_3-symmetric magnesium tris(oxazoline)borate alkyl complex [To^{M}MgMe] (To^M = tris(4,4-dimethyl-2-oxazolinyl)phenylborate) excludes additional ligands from the coordination sphere and is a competent precatalyst for the hydroamination of 1-aminopent-4-enes. In line with the expectations furnished by the aforementioned systems, the reaction of 1-amino-2,2-diphenylpent-4-ene follows the empirical rate law $\nu = k'_{obs}$[aminoalkene]^1[catalyst]^1, with a KIE of

Fig. 2 Proposed mechanism for the group 2-catalyzed hydroamination of aminoalkenes
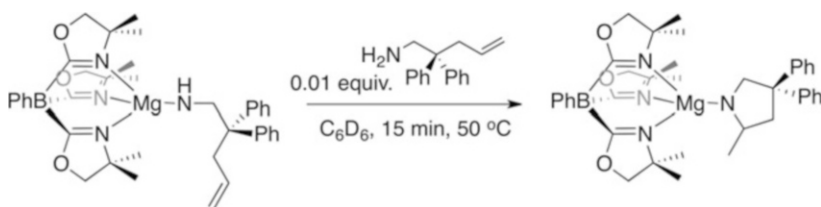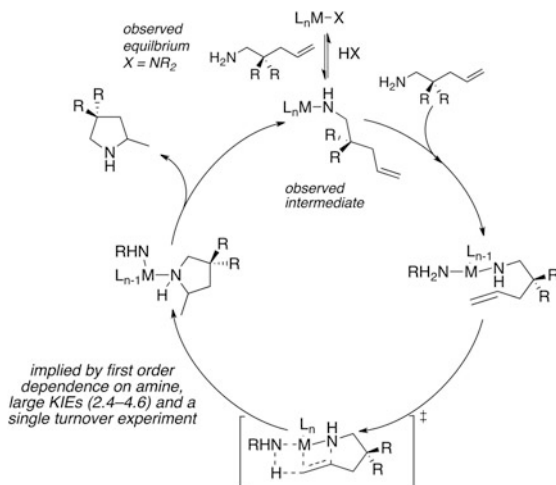
Scheme 6 Substrate-catalyzed intramolecular hydroamination of a magnesium amide complex

$k'^{(H)}_{obs}/k'^{(D)}_{obs}$ of 4.6 (323 K). Measuring initial rates at constant catalyst concentration and varying substrate concentration correlated the data to Michaelis–Menten kinetics and a rate law consistent with that proposed (subsequently) by Hill and coworkers which accounts for reversible amine binding and substrate inhibition [82]. Stoichiometric studies revealed that turnover did not occur in the absence of added substrate [81].

Thus, the reaction of 1-amino-2,2-pent-4-ene with [To^MMgMe] yielded the corresponding magnesium amide [To^MMgNHR] (R=CH_2C(Ph)_2CH_2CH=CH_2) which was not kinetically competent in a single-turnover experiment at temperatures up to 100 °C. Addition of 0.01 equiv. of 1-amino-2,2-pent-4-ene to this magnesium complex effected the cyclization under conditions reminiscent of the catalytic chemistry, yielding the magnesium-bound pyrrolidine. In combination with the KIE and derived rate law these data are consistent with a proton-assisted alkene insertion mechanism presented in Fig. 2 and provide direct experimental evidence for the turnover-limiting step involving an extra equivalent of amine (Scheme 6) [81].

DFT studies conducted by Tobisch on Sadow's magnesium trioxazoline catalyst disagree with these findings and suggest an alternative mechanistic pathway that accounts for the experimental data, namely reversible insertion of the alkene into

Scheme 7 Asymmetric intramolecular hydroamination of aminoalkenes
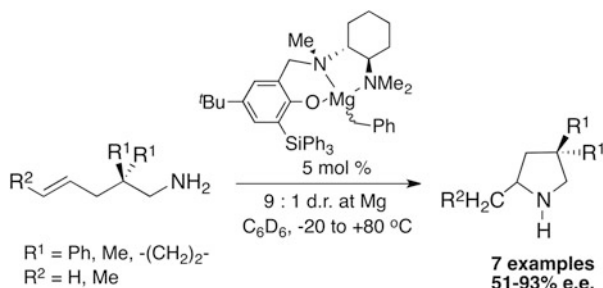
the M–N bond [92]. Calculations conducted with the Tao–Perdew–Staroverov–Scuseria (TPSS) functional and triple-ζ basis set imply that the highest transition state barrier for the proton-assisted insertion mechanism proposed by Sadow and coworkers is some 5.0 kcal mol^{-1} higher in energy than a more standard insertion mechanism that does not involve N–H bond cleavage [92]. These calculations suggest that alkene insertion is reversible with both the metal-bound pyrrolidine and the magnesium alkyl complex being >2.0 kcal mol^{-1} higher in energy than the observed magnesium amidoalkene resting state with a shallow energy barrier to conversion. Rate-determining protonolysis of the unstable magnesium alkyl complex explains the observed KIEs [92].

Activation parameters for the cyclization of (1-allylcyclohexyl)methylamine determined for the precatalysts [{(ArNCMe)$_2$CH}M{N(SiMe$_3$)$_2$}(THF)] (M = Ca, Sr) from Eyring analysis over the temperature range 298–313 K provide Gibbs free activation energies of 20.7 and 22.5 kcal mol^{-1} for calcium and strontium, respectively [82]. Similar experiments using [M{N(SiMe$_3$)$_2$}$_2$(THF)$_2$] (M = Ca, Sr) give values of 21.7 and 22.3 kcal mol^{-1} for calcium and strontium, respectively, [82]. These data are consistent with values recorded for lanthanide-based precatalysts [9, 10].

It is noteworthy that a series of catalysts follow alternative empirical rate laws and overgeneralization of the mechanism above should be avoided. For example, Hultszch and coworkers have shown that sterically crowded magnesium phenoxylate complexes [LMg^{i}Pr] (L = 4-*tert*-butyl-6-(triphenylsilyl)-2-{bis((3-(dimethylamino)propyl)amino)methyl}phenoxyl) demonstrate the empirical rate law $\nu = k'_{\text{obs}}$[aminoalkene]^0[catalyst]^1 while coordinatively unsaturated analogues of this catalyst exhibit a second-order dependence on substrate concentration [78]. Similarly, the unsolvated group 2 precatalysts [M{N(SiMe$_3$)$_2$}$_2$] (M = Ca, Sr) provide kinetic data for the cyclization of (1-allylcyclohexyl)methylamine at 298 K in C$_6$D$_6$ that are second order in catalyst [82].

Asymmetric catalysis: Although initial attempts to achieve the stereocontrolled intramolecular hydroamination of aminoalkenes using chiral calcium catalysts have met with limited success [69], a series of magnesium benzyl precatalysts supported by phenoxyamine ligands have been reported for the cyclization of substituted and non-substituted 1-aminopent-4-enes at 5 mol% catalyst loading with selectivities ranging from 51 to 94 % e.e. (Scheme 7) [93]. The work is based on not only an initial study employing achiral phenoxyamine ligands to effect the same reaction [78], but also the
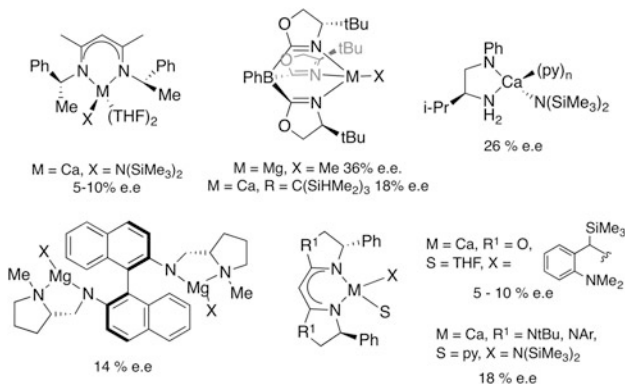
Fig. 3 Heavier group 2 precatalysts employed in asymmetric hydroamination catalysis (test substrates include 1-amino-2,2-diphenylpent-4-ene and (1-allylcyclohexyl)methylamine)

investigation of C_2-symmetric diamidonapththyl bimetallic complexes of magnesium and C_3-symmetric trisoxazoline borate complexes of magnesium for the asymmetric hydroamination of substituted aminoalkenes to pyrrolidines in 14 % and 36 % e.e., respectively (Fig. 3) [94, 95]. The highly efficient and selective C_1-symmetric phenoxyamine catalyst reported by Hultzsch and coworkers effect the hydroamination of the most reactive substrates at −20 °C allowing optimization of the enantioselectivity to previously unprecedented values [93].

Despite the chiral-at-metal precatalysts being obtained as a mixture of diastereomers from optically pure ligand precursors, the stereocenter at magnesium was shown to have no effect on the enantioselectivity of the reaction with both 9:1 and 5:1 mixtures of (R,R)-ligand-Mg^R and (R,R)-ligand-Mg^s giving (S)-methylpyrrolidines with the same selectivity [93]. The precatalysts are stable in solution up to 120 °C with no evidence of Schlenk equilibria under the catalytic reaction conditions. Kinetic studies demonstrated that the reaction follows the familiar empirical rate law $\nu = k'_{obs}[substrate]^1[catalyst]^1$ and displays a primary KIE of 3.6 (measured at 298 K by comparison of rate constants for the cyclization of (1-allylcyclohexyl) methylamine and d_2-(1-allylcyclohexyl)methylamine) [93]. The deuteration of the substrate has little effect on the enantioselectivity of the reaction. These findings have led Hultzsch and coworkers to suggest a concerted alkene/insertion protonolysis reaction consistent with that proposed by both Sadow and Hill [81, 82].

Calcium amide and alkyl precatalysts supported by a C_1-symmetric amide ligand derived from a chiral 1,2-diamine, C_2-symmetric (S)-Ph-pybox, β-diketiminate, or bisimidazoline ligand or a C_3-symmetric tris(oxazolinyl)borato ligand have been reported to effect the intramolecular hydroamination of (1-allylcyclohexyl) methylamine, 1-amino-2,2-diphenylpent-4-ene, and 1-amino-2,2-dimethylpent-4-ene providing non-racemic products in high yields but extremely low selectivities of 5–26 % e.e. (Fig. 3) [94–97]. The highest selectivity reported to date corresponds to an e.r. of 1.7:1. The low selectivities of these calcium precatalysts are in stark contrast to not only the magnesium systems which employ similar polydentate chelating ligands but also studies on C_2-symmetric PyBox calcium complexes for

asymmetric aldol and Michael addition reactions [33]. These results can be explained by facile Schlenk redistribution of the precatalysts and reaction intermediates producing achiral catalysts which may give rise to an achiral background reaction in hydroamination catalysis and improved ligand design is necessary in order to control the enantioselectivity-determining step with heavier group 2 precatalysts.

2.1.2 Intermolecular Hydroamination of Activated Alkenes

Reaction scope: The reaction of benzylamine, pyrrolidine, azetidine, aziridine, dibenzylamine, *tert*-butylamine, and piperidene with styrene, 4-methylstyrene, 4-methoxystyrene, and 4-chlorostyrene catalyzed by 5–10 mol% $[M\{N(SiMe_3)_2\}_2]_2$ or $[M\{CH(SiMe_3)_2\}_2(THF)_2]$ (M = Ca, Sr) was reported to proceed under mild solvent-free reaction conditions at 60 °C with the strontium alkyl catalyst displaying the highest reactivity for most substrate combinations [98, 99]. In all cases reactions proceed selectively to yield anti-Markovnikov products with styrenes bearing electron-rich substituents in the 4-position generally requiring more forcing reaction conditions. The hydroamination of more challenging substrates including α-methylstyrene and dihydronapthalene with primary and secondary amines requires higher catalyst loadings and reaction times of up to a week, but proceeds with these catalysts [98, 99].

While $[M\{N(SiMe_3)_2\}_2]$ (M = Mg, Ba) proved ineffectual for intermolecular hydroamination catalysis, non-racemic magnesium phenoxylate catalysts and three different homologous series of metal silazide precatalysts (M = Mg, Ca, Sr, and Ba) have also been reported for the hydroamination of styrenes with pyrrolidine, benzylamine, and *n*-hexylamine [67, 93]. Sarazin and coworkers demonstrated that the kinetically stabilized group 2 complexes bearing N,N'-chelating β-diketiminate and iminoamide ligands (Fig. 1) display exceptionally high activities for the hydroamination of styrenes with reaction rates increasing across the series Mg < Ca < Sr < Ba [67]. For example, the addition of pyrrolidine to styrene catalyzed by the barium complex $[\{ArN(o\text{-}C_6H_4)C(H)=NAr\}Ba\{N(SiMe_3)_2\}(THF)_3]$ was found to proceed at 60 °C with catalyst loadings as low as 0.1 or 0.5 mol% with TOFs ranging from 212 to 290 h^{-1}, values which are 1 or 2 orders of magnitude higher than existing lanthanide and transition metal catalysts [67].

Dienes, enynes, and alkynes are also reported to undergo intermolecular hydroamination. The barium catalyst $[\{ArN(o\text{-}C_6H_4)C(H)=NAr\}Ba\{N(SiMe_3)_2\}(THF)_3]$ results in selective 1,4-addition of pyrrolidine to isoprene, while homoleptic amide precatalsyts $[M\{N(SiMe_3)_2\}_2]$ (M = Ca, Sr) yield a mixture of 1,4-addition and 1,2-addition regisomers for the hydroamination of isoprene or myrcene with piperidene [67]. Attempts to effect the hydroamination of 1,3-cyclohexadiene with the homoleptic precatalysts led to an aromatization of the substrate with formation of benzene, while the addition of piperidene to but-3-en-1-ynylbenzene gave a selective reaction to yield the corresponding allene when conducted at 0 °C in toluene (Schemes 8 & 9) [98]. The hydroamination of myrcene with group 2 catalysts is of particular note as the synthesis of

a

R¹ = R³ = H, R² = Ph, 4-MeC$_6$H$_4$, 4-MeOC$_6$H$_4$, 4-ClC$_6$H$_4$, 4-BrC$_6$H$_4$
R¹ = Me, R² = Ph, R³ = H; R¹ = H, R² = R³ = o-(CH$_2$)$_2$C$_6$H$_4$
R⁴ = R⁵ = -CH$_2$-, -(CH$_2$)$_2$-, -(CH$_2$)$_3$-, -(CH$_2$)$_4$-, -(CH$_2$)$_5$-, -(CH$_2$)$_2$O(CH$_2$)$_2$-, CH$_2$Ph
R⁴ = H, R⁵ = ^{t}Bu, CH$_2$Ph, CH$_2$CH$_2$Ph
M = Ca, Sr

b

R¹ = Me, R² = H
R¹ = (CH$_2$)$_2$CH=CMe$_2$, R² = H
R³ = H, R⁴ = CH$_2$Ph
R³ = R⁴ = -(CH$_2$)$_5$-
M = Ca, Sr

1,2 : 1.4-addition = 1:9 to 0:100

3 examples 72-99% yield
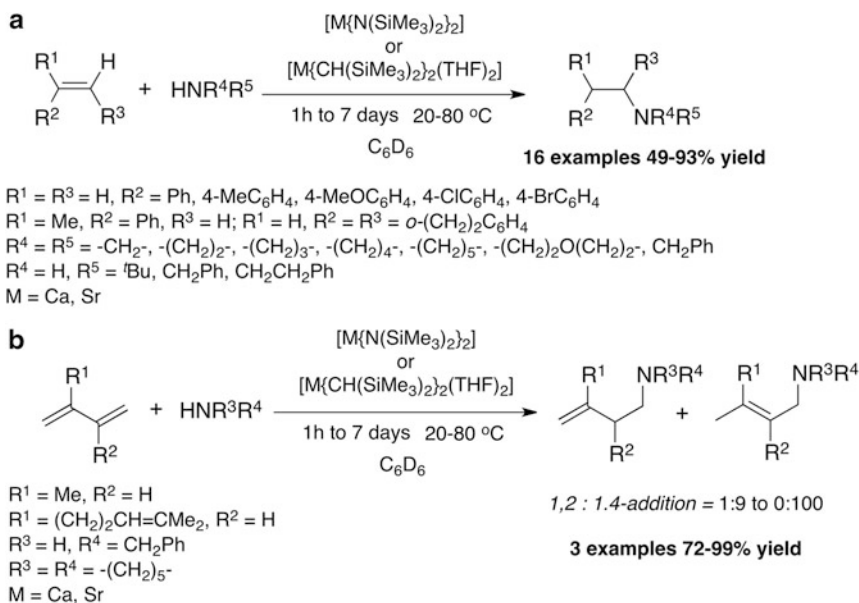
Scheme 8 Intermolecular hydroamination with group 2 precatalysts
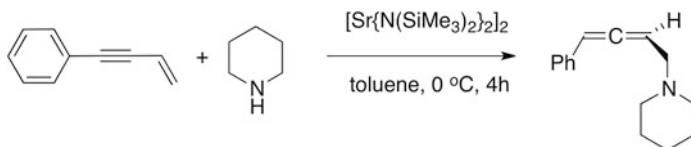
Scheme 9 Intermolecular hydroamination of an ene-yne with group 2 precatalysts

N,N-diethylgeranylamine, a precursor to (−)-menthol is achieved via the hydroamination of this substrate with lithium catalysts on an industrial scale [98]. A single example of intermolecular alkyne hydroamination also exists. Thus, piperidene undergoes addition to diphenylacetylene in the presence of 10 mol% [Sr{CH(SiMe$_3$)$_2$}$_2$(THF)$_2$] at 60 °C in C$_6$D$_6$ solution over a period of 17 h; a 10:1 mixture of *syn-* and *anti-*addition products are isolated consistent with an isomerization event occurring under the reaction conditions [98].

Reaction Mechanism: The preferential *anti*-Markovnikov or 2,1-addition to styrene can be attributed to the organization of the transition state to N–C bond formation. Factors that stabilize the developing anionic charge upon the atom adjacent to the metal center in the transition state to N–C bond formation will be expected to lower the activation energy of the insertion step [98, 99]. In the case of the 2,1-insertion of styrene into the Ca–N bond the phenyl group may stabilize the adjacent anionic center. In the case of a 1,2-insertion, no such stabilization exists. The product distribution for the hydroamination of dienes can be explained by invoking a metal allyl complex upon addition of M–NR$_2$ to the diene.

Consideration of its equilibration between η^3- and η^1-coordination modes along with the relative rates of protonolysis of the two η^1-coordination isomers indicates that off-cycle isomerization of the reaction products may also be occurring under the reaction conditions [98].

DFT calculations of the model reaction of ethylene with ammonia catalyzed by the model complexes [{HNC(Me)CHC(Me)NH}M(NH$_2$)] in the gas phase using B3LYP theory employing the LANL2DZ basis set were consistent with rate-determining alkene insertion within a catalytic cycle dominated by Coulomb interactions [99]. Alkene insertion into the M–N bond was reported to occur via a four-center transition state that is highly polarized; electron density equivalent to almost an entire electron is polarized onto the carbon adjacent to the metal and occurs with simultaneous depletion of electron density in the nitrogen-based lobe with electron density being directed to the newly forming carbon–nitrogen bond. Examination of the barrier heights of non-proton-assisted insertion (M = Mg, 21.0 kcal mol^{-1}; Ca, 16.7 kcal mol^{-1}; Sr, 15.5 kcal mol^{-1}; Ba, 18.6 kcal mol^{-1}) and protonolysis (M = Mg, 19.8 kcal mol^{-1}; Ca, 8.6 kcal mol^{-1}) suggest catalyst activity decreases across the series Mg < Ba < Ca < Sr. While these data conflict with more recent experimental observations suggesting a proton-assisted pathway, the relative barrier heights for alkene insertion into M–N bonds may be viewed as a result of a balance of the polarity of the M–N bond (i.e., the ability of the M–N bond to induce a dipole in the non-polarized alkene) and the polarizability of the M^{2+} cation [99].

Kinetic studies conducted upon the reaction of styrene with piperidene catalyzed by [Sr{N(SiMe$_3$)$_2$}$_2$] demonstrated that the reaction follows the empirically determined rate law $\nu = k'_{\text{obs}}[\text{amine}]^1[\text{alkene}]^1[\text{catalyst}]^2$ [98]. A similar second-order dependence on catalyst has been observed for related solvent-free homoleptic group 2 amides in intramolecular hydroamination catalysis (see Sect. 2.1.1) [82]. While monitoring the reaction rate as a function of initial amine concentration revealed that saturation occurs at higher amine concentrations, a large primary KIE was observed for this reaction taking values of 4.3(343 K) and 4.1(348 K) for calcium and 7.9(348 K) for strontium (Fig. 4). The latter value represents an extremely large primary KIE when compared to the maximum calculated value of 8.5 (for a N–H vibration at 3,100 cm^{-1}) [98].

Eyring analysis of kinetic reaction data upon the addition of piperidene to styrene catalyzed by [M{N(SiMe$_3$)$_2$}$_2$] (M = Ca, Sr) provided activation energies of $\Delta G^{\ddagger} = 24.2$ and 23.5 kcal mol^{-1} for calcium and strontium, respectively. Although these data are overestimated somewhat compared to those calculated on the model system, it was suggested that the strontium and calcium reagents provide the ideal balance of polarization and polarizability that allow facile insertion reactions with alkene substrates. Furthermore, the increased activity of the strontium catalyst was attributed to an influential entropic advantage, with the calcium catalyst providing data consistent with a much tighter and more ordered transition state in the insertion step than the strontium system ($\Delta S^{\ddagger} = -40.0(3.3)$ cal mol^{-1} K^{-1} and -22.0 (3.2) cal mol K^{-1} for calcium and strontium, respectively) [98].

Related studies on the highly active barium precatalyst [{ArN(o-C$_6$H$_4$)C(H)= NAr}Ba{N(SiMe$_3$)$_2$}(THF)$_3$] demonstrate an alternative rate law and, consistent

Fig. 4 Proposed mechanism of intermolecular hydroamination with group 2 precatalysts
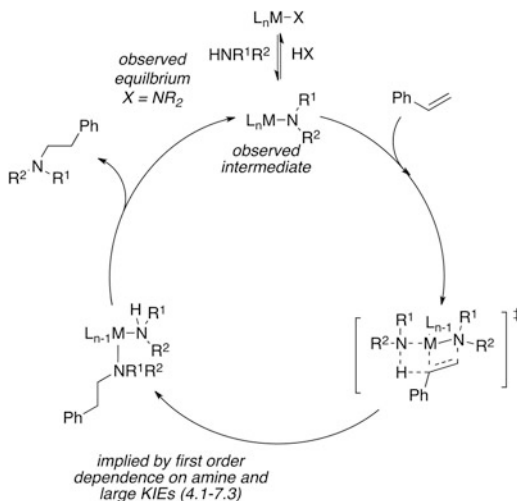
with the higher activity, a lower Gibbs free activation energy. Thus, the addition of pyrrolidine to styrene was found to follow the empirical rate law $\nu = k'_{obs}[\text{amine}]^1$ $[\text{alkene}]^1[\text{catalyst}]^1$ with KIEs determined as 6.8(313 K) and 7.3(333 K) and the activation parameters $\Delta H^{\ddagger}$, $\Delta S^{\ddagger}$, and $\Delta G^{\ddagger}$ of 18.3(0.8) kcal mol^{-1}, -13.1 (2.7) cal mol K^{-1}, and 22.4 kcal mol^{-1}, respectively [67]. As with the intramolecular hydroamination of aminoalkenes, these data have been rationalized in terms of a turnover-limiting proton-assisted alkene insertion step from a metal amide intermediate bearing additional amine ligands. The second order in catalyst behavior of reactions of homoleptic precatalyst [Sr{N(SiMe$_3$)$_2$}$_2$] is mitigated by the fact that these species are known to exist as dimers in the solid state.

2.1.3 Intermolecular Hydroamination of Carbodiimides

Reaction scope: The intermolecular hydroamination of carbodiimides with primary aryl amines has been reported to be catalyzed by [{ArNC(Me)}$_2$Ca{N(SiMe$_3$)$_2$} (THF)] or 2–4 mol% [M{N(SiMe$_3$)$_2$}$_2$(THF)$_2$] (M = Ca, Sr, Ba) [100]. The addition of the N–H bond of the amine across the carbodiimide occurs with a concurrent 1,3-proton shift, giving the guanidine products depicted in Scheme 10. While both electron-rich and electron-poor anilines, along with the sterically hindered nucleophile 2,6-di-*iso*-propylaniline may be employed, the reaction scope does not extend to aliphatic amines. Both alkyl-substituted and aryl-substituted carbodiimides have been employed as substrates with reactions proceeding in good isolated yields. While preliminary studies were conducted with a series of group 2 catalysts [M{N (SiMe$_3$)$_2$}$_2$(THF)$_2$], the ease of these preparations, in which the products typically crystallized from the reaction mixture, has limited the study of the reaction mechanism and the inexpensive calcium precatalyst [Ca{N(SiMe$_3$)$_2$}$_2$(THF)$_2$] has been widely employed without a detailed consideration of any metal effect on reactivity [100]. Hill and coworkers explored the limit of this catalysis and, by conducting the

2-4 mol%
[{(ArNCMe)$_2$CH}Ca{N(SiMe$_3$)$_2$}(THF)]
or
[M{N(SiMe$_3$)$_2$}$_2$(THF)$_2$]

ArNH$_2$ + R^{1}N=C=NR^2 $\xrightarrow{\hspace{3cm}}$

0.1 - 72h, 25 - 80 °C

n-hexane

Ar\
 \ N
  ‖
R^{1}HN   NHR^2

12 examples 37-81 % yield

Ar = 2-FC$_6$H$_4$, 4-MeC$_6$H$_4$, Ph, 2-MeOC$_6$H$_4$, 1-napthyl, 2,6-^{i}PrC$_6$H$_3$
R^1 = R^2 = ^{i}Pr, Cy, ^{t}Bu; R^1 = Et, R^2 = ^{t}Bu
M = Ca, Sr, Ba
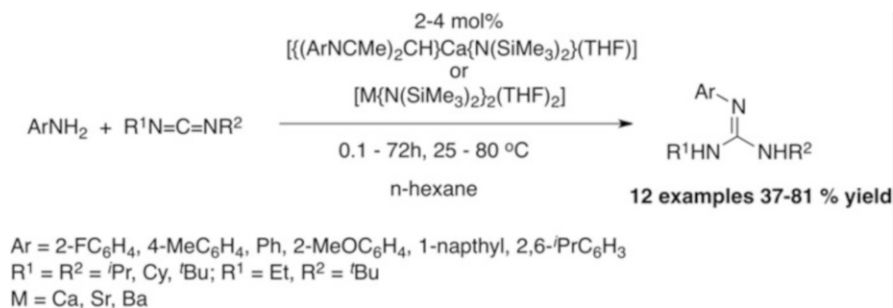
Scheme 10 Scope of the group 2-mediated hydroamination of carbodiimides

reaction of aniline with 1,3-dicyclohexyl carbodiimide in hexane on a 60 mmol scale, demonstrated that catalysis shutdown occurred below a 0.5 mol% loading of [Ca{N (SiMe$_3$)$_2$}$_2$(THF)$_2$]. In this instance the product was isolated in 86 % yield [100].

Reaction mechanism: The stoichiometric insertion of carbodiimides into the M–N bonds of group 2 amides has extensive precedent [101–103]. For example, five- and six-coordinate homoleptic guanidinate complexes of calcium and strontium of the form [M{(Me$_3$Si)$_2$NC{NR}$_2$}$_2$(Solv)$_n$] (Solv = THF, Et$_2$O; n = 1, 2; M = Ca, Sr; R = ^{i}Pr, Cy) have been isolated from insertion of the corresponding carbodiimide into the M–N bond of the silazide complexes [M{N(SiMe$_3$)$_2$}$_2$]$_2$ in either Et$_2$O or THF solution [101, 102], and a series of heteroleptic calcium complexes bearing both β-diketiminate and guanidinate ligands have been isolated from the reaction of [{(ArNCMe)$_2$CH}Ca{NR^{1}R^2}(THF)] (R^1 = H, R^2 = NHCH$_2$CH$_2$OMe, Ar; R^1 = R^2 = Ph) with 1,3-dialkylcarbodiimides [103]. Specific to the catalytic chemistry described above, reaction of [Ca{N (SiMe$_3$)$_2$}$_2$(THF)$_2$] with either 2 equiv. of aniline and 2 equiv. of 1,3-di-*iso*-propylcarbodiimide or 2 equiv. of [PhNC{NH^{i}Pr}$_2$] yielded a compound which gave identical spectroscopic data in benzene-d$_6$ solution to that formed from the addition of 4 equiv. of [PhNC{NH^{i}Pr}$_2$] to [Ca{N(SiMe$_3$)}$_2$]$_2$. The calcium complex [Ca{(PhNH)C{N^{i}Pr}$_2$}]$_2$ was isolated from the latter reaction; while site exchange between the terminal and bridging ligands ($\Delta G^{\ddagger}$ = 16.2 kcal mol^{-1}) was observed in d$_8$-toluene solution, the isolated intermediate proved catalytically competent for the catalytic hydroamination of 1,3-di-*iso*-propylcarbodiimide with aniline (Fig. 5) [100].

Based on this reactivity, the reaction has been proposed to proceed via the insertion of the carbodiimide into the M–N bond of a transient amide complex formed from σ-bond metathesis of the precatalyst with the aniline. Turnover occurs via a similar σ-bond metathesis of the guanidinate complex with a further equivalent of amine, a reaction that is most likely endothermic based upon pK_a considerations but occurs readily under catalytic conditions [100]. The potential for reversible insertion of the carbodiimide into M–N bonds has been probed by crossover experiments and studies on the current systems do not suggest a reversible insertion step (although this is likely to be a function of the stability of the metal-amide generated from carbodiimide extrusion). The molecularity or kinetic competence of
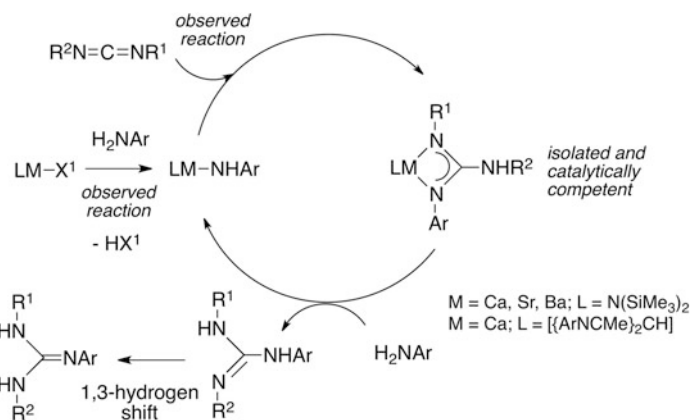
Fig. 5 Proposed mechanism of the group 2-mediated hydroamination of carbodiimides

heavier group 2 guanidinate complexes (M = Sr, Ba) in this chemistry has not been investigated and furthermore a κ^1-coordinated carbodiimide complex, presumably an intermediate in the insertion step, is unknown for alkaline-earth coordination chemistry [100].

2.1.4   Intermolecular Hydroamination of Isocyanates

Reaction scope: In related studies, the hydroamination of 2,6-di-*iso*-propylphenyl isocyanate and 1-adamantyl isocyanate with diphenylamine has been reported to be catalyzed by 5–6 mol% [{(ArNCMe)$_2$CH}Ca{N(SiMe$_3$)$_2$}(THF)] or [M{N (SiMe$_3$)$_2$}$_2$]$_2$ (M = Ca, Sr, and Ba) in benzene or toluene solution to give the corresponding ureas in 48–93 % isolated yield [104]. Although the aryl-substituted isocyanate was reported to undergo hydroamination at room temperature, the alkyl-substituted analogue required slightly more forcing conditions (60 °C). The reaction scope has not been expanded beyond these two substrate combinations. Despite the precedent for isocyanate polymerization [105], in situ NMR spectroscopic measurements demonstrate that under these conditions oligomerization or polymerization of the isocyanate was not observed (Scheme 11) [104].

   Reaction mechanism: In line with previous studies, Hill and coworkers demonstrated that the controlled insertion of 1-adamantyl isocyanate into the metal–nitrogen bond of [{ArNC(Me)CHC(Me)NAr}Ca(NPh$_2$)(THF)] occurs upon reaction in a 1:1 stoichiometry in hydrocarbon solution at room temperature [104]. The resulting ureido complex is catalytically competent for the hydroamination of 2,6-di-*iso*-propylphenyl isocyanate with diphenylamine. Kinetic data for reactions employing [M{N(SiMe$_3$)$_2$}$_2$]$_2$ as catalysts (M = Ca, Sr, Ba) are consistent with significant product inhibition. This effect has been ascribed to the urea binding the group 2 metal center and preventing substrate coordination and activation. A crossover experiment conducted in C$_6$D$_6$ between 1 equiv. of
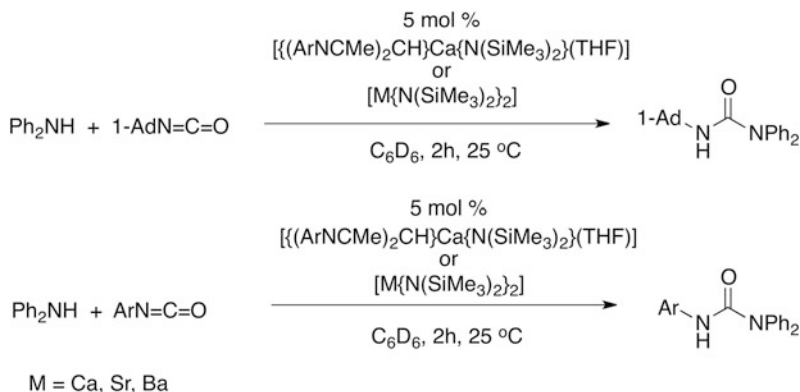
Scheme 11 Reaction scope of the group 2-mediated hydroamination of isocyanates
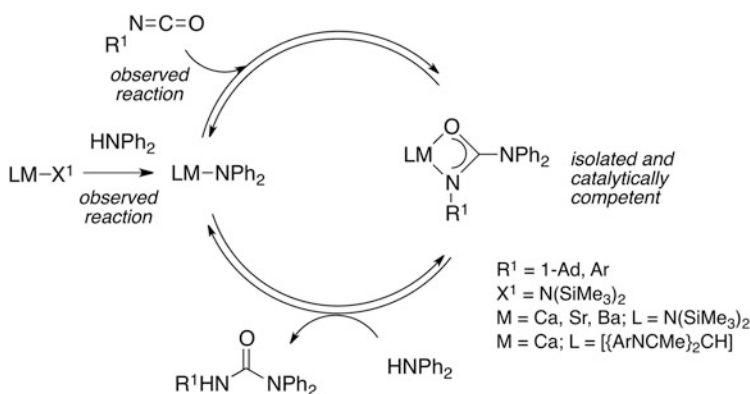
Fig. 6 Proposed mechanism of the group 2-mediated hydroamination of isocyanates

1-AdNHC(O)NPh$_2$ and 1 equiv. of 2,6-di-*iso*-propylphenyl isocyanate catalyzed by 5 mol% [Ca{N(SiMe$_3$)$_2$}$_2$]$_2$ demonstrated the reversibility in the insertion step. Thus, it was proposed that catalytic turnover occurs via reversible σ-bond metathesis and insertion reaction steps (Fig. 6) in a manner similar to that elucidated for the hydrophosphination of carbodiimides (see Sect. 2.2.2) [104].

2.2 Intermolecular Hydrophosphination (C–P Bond Formation)

2.2.1 Intermolecular Hydrophosphination of Activated Alkenes, Alkynes, and Diynes

In 2007, Hill and coworkers reported the intermolecular hydrophosphination of activated alkenes with diphenylphosphine catalyzed by [{(ArNCMe)$_2$CH}Ca {N(SiMe$_3$)$_2$}(THF)] [106]. Reactions were conducted in benzene solution and
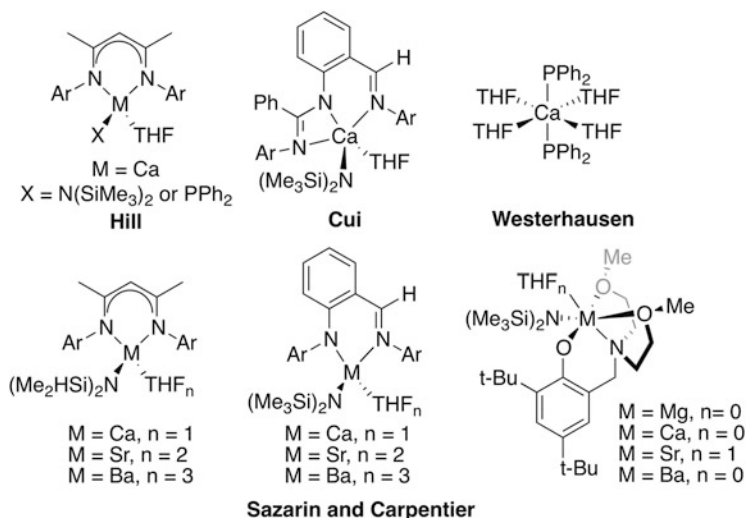
Fig. 7 Group 2 amide and phosphide complexes reported for the intermolecular hydrophosphination of alkenes, alkynes, dienes, and diynes

products isolated and characterized following oxidation to the phosphine oxides. It is noteworthy that lanthanide(III) complexes have only been reported for intramolecular hydrophosphination and the phosphine-terminated polymerization of alkenes [9, 10].

Reaction scope: The initial report included only a few examples of the catalytic hydrophosphination of activated alkenes and alkynes with diphenylphosphine at 25–80 °C in C_6D_6 solution with high catalyst loadings of the calcium precatalyst [{(ArNCMe)$_2$CH}Ca{N(SiMe$_3$)$_2$}(THF)] (10–20 mol%) [106]. Following this study, however, Westerhausen and coworkers reported [Ca(PPh$_3$)$_2$(THF)$_4$] as a precatalyst for the hydrophosphination of diphenylethyne and 1-phenylphenylprop-1-yne and the twofold functionalization of a series of 1,4-disubstituted butadiynes with HPPh$_2$ in THF solution at 25 °C [107, 108], while Cui and coworkers documented the hydrophosphination a wide range of substrates, including terminal and internal alkenes, terminal and internal alkynes, and dienes with HPPh$_2$ catalyzed by a calcium hexamethyldisilazide complex supported by a tridentate imino-amidinate ligand (Fig. 7) [109].

Although reports of catalysts incorporating magnesium, strontium, and barium for this transformation remain more limited, at 2 mol% loading three different homologous series of metal silazide precatalysts promote the addition of HPPh$_2$ (<96 % conversion) and HPCy$_2$ (<42 % conversion) to styrene at 60 °C in the absence of solvent [67]. In line with the expectations furnished by studying these species in intermolecular hydroamination, activities increase across the series Ba > Sr > Ca while TOFs reach 192 h^{-1} for the addition of diphenylphosphine to styrene with the barium analogue [{ArN(o-C$_6$H$_4$)C(H)=NAr}Ba{N(SiMe$_3$)$_2$} (THF)$_3$] (Fig. 7) [67]. In all reactions reported to date, the reaction scope is severely

a

R^1 = Ph, R^2 = R^3 = H
R^1 = 4-MeC$_6$H$_4$ R^2 = R^3 = H
R^1 = R^3 = Ph, R^2 = H
R^1 = Ph, R^2 = Me, R^3 = H

5 mol% **A**
or
10 mol% **B**

25-75 °C
C$_6$D$_6$
2-20 h

4 examples 72-99% yield

b

R^1 = R^2 = Me
R^1 = Me, R^2 = H
R^1 = (CH$_2$)$_2$CH=CMe$_2$, R^2 = H

2-5 mol% **A**
or
10 mol% **B**

25-60 °C
C$_6$D$_6$
1.5-24 h

For **A** *1,2 : 1,4-addition* = 1:9 to 0:100
For **B** *1,2 : 1,4-addition* = 8:2

3 examples 95-99% yield

c

R^1 = R^2 = Ph
R^1 = Ph, R^2 = H, Me, n-Bu
R^1 = 2-pyridyl, R^2 = H

5 mol% **A**
or
6 mol% **B**

25-75 °C
C$_6$D$_6$ or THF
2-38 h

For **A** *Z:E (anti:syn)* = 7:3 to 9:1
For **B** *Z:E (anti:syn)* = 1:9 to 0:100

6 examples 78-99% yield

Scheme 12 Reaction scope for the group 2-catalyzed hydrophosphination of (**a**) styrenes (**b**) dienes and (**c**) alkynes

limited with respect to the phosphine with most studies using only diphenylphosphine as a substrate.

Product selectivities differ between the different catalyst systems. In all cases, reactions are regioselective giving *anti*-Markovnikov or 2,1-addition of the phosphine to the least hindered end of the unsaturated system (Scheme 12a). For example, in the hydrophosphination of styrenes this selectivity can be attributed to the organization of the transition state to P–C bond formation. In the case of the 2,1-insertion of styrene into the Ca–P bond the phenyl group may stabilize the adjacent anionic center. In the case of a 1,2-insertion no such stabilization exists [106].

For dienes, precatalysts [{(ArNCMe)$_2$CH}Ca{N(SiMe$_3$)$_2$}(THF)] (**B**) and [{ArNC(Ph)N(*o*-C$_6$H$_4$)C(H)=NAr}Ca{N(SiMe$_3$)$_2$}(THF)] (**A**) demonstrate different selectivities, the latter complex being highly selective for 1,4-addition products, while the former complex is selective for 1,2-addition products [106, 109]. For alkynes the stereochemical outcome of hydrophosphination of the carbon–carbon triple bond must also be considered; whereas the precatalyst [{ArNC(Ph)N(*o*-C$_6$H$_4$)
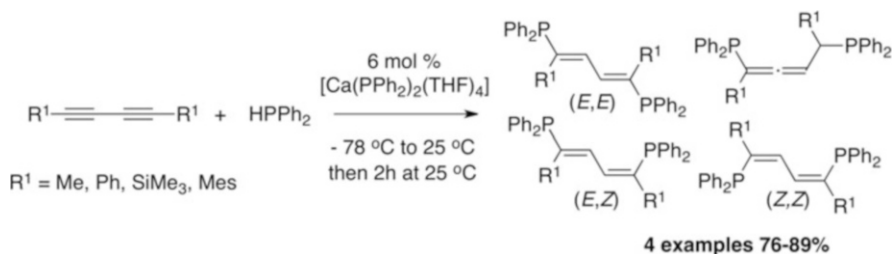
Scheme 13 Reaction scope for the group 2-catalyzed hydrophosphination of diynes major (1,4-addition) products only represented

C(H)=NAr}Ca{N(SiMe$_3$)$_2$}(THF)] (**A**) gives predominantly the (*E*)-vinylphosphines due to a formal *anti*-addition of diphenylphosphine to the alkyne, precatalyst [{(ArNCMe)$_2$CH}Ca{N(SiMe$_3$)$_2$}(THF)] (**B**) along with [Ca(PPh$_3$)$_2$(THF)$_4$] is reported to give high stereoelectivities for the *syn*-addition of diphenylphosphine to alkynes to give (*Z*)-vinylphosphines [106, 109].

Relative to the reactions presented in Scheme 12, the hydrophosphination of diynes with Ph$_2$PH catalyzed by 5 mol% [Ca(PPh$_3$)$_2$(THF)$_4$] proceeds with exceedingly low selectivties, despite the reaction being carried out at −78 °C. Westerhausen has examined a number of substituted 1,4-diynes under these conditions, and while reactions proceed in high yield and give predominantly twofold addition of the phosphine to the diyne producing 1,4-addition products, an unfavorable mixture of all possible stereoisomers is observed (Scheme 13). In the case of 1,4-di-*t*-butylbutadiyne an additional allene isomer was observed, while hydrophosphination of 1,4-diphenylbutadiyne yielded in addition to isomeric 1,4-addition products a 1,2-addition product (not represented in Scheme 13) [107, 108].

Reaction mechanism: Although kinetic studies have not been conducted on any of these catalyst systems, a number of stoichiometric studies are relevant to group 2 hydrophosphination catalysis. Westerhausen has studied the coordination chemistry of heavier group 2 phosphides extensively, and in contrast to monoaryl-phosphide complexes, which are known to readily form oligomeric or polymeric structures in non-coordinating solvents [110], diarylphosphides are monomeric in both solution and the solid state and soluble in coordinating solvents such as THF [110–113]. The two structural isomers *cis*-[Ca(PPh$_2$)$_2$(THF)$_4$] and *trans*-[Ca (PPh$_2$)$_2$(THF)$_4$] have both been structurally characterized and shown to undergo rapid equilibration in solution; a fast isomerization event is likely to have little or no importance to the solution catalytic activity [113].

In related studies, Hill and coworkers have isolated a heteroleptic calcium phosphide [{(ArNCMe)$_2$CH}Ca{PPh$_2$}(THF)] from the reaction of [{(ArNCMe)$_2$CH}Ca{N(SiMe$_3$)$_2$}(THF)] with HPPh$_2$ and demonstrated not only its catalytic competency in hydrophosphination catalysis but also its stereoselective reaction with diphenylacetylene and a single equivalent of HN(SiMe$_3$)$_2$ in C$_6$D$_6$ at 75 °C for 45 min to yield a 1:1 mixture of (*E*)-PhC(H)=C(PPh$_2$)Ph and the regenerated precatalyst in near quantitative yield [106]. This single-turnover experiment can be explained by considering the concerted insertion of the alkyne
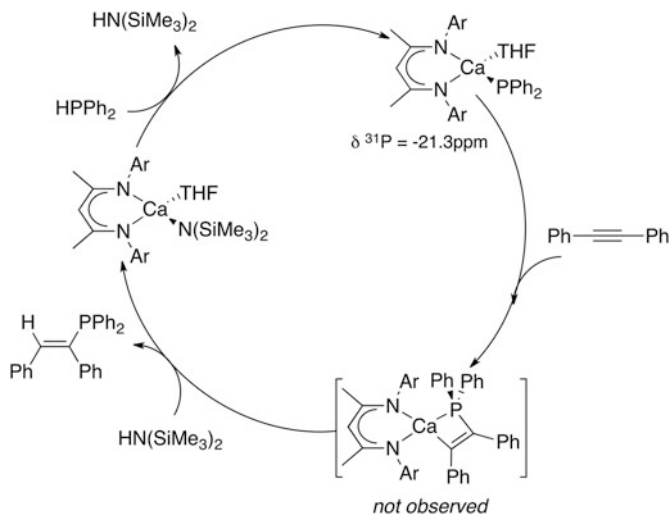
Fig. 8 Postulated catalytic cycle for hydrophospination of diphenylacetylene mediated by [{(ArNCMe)$_2$CH}Ca{N(SiMe$_3$)$_2$}(THF)]

into the Ca–P bond to generate a *putative* calcium vinyl intermediate which undergoes a subsequent σ-bond metathesis with hexamethyldisilazane to liberate the hydrophosphinated product and regenerate the calcium amide (Fig. 8) [106].

Studies to date suggest that σ-bond metathesis reactions of diphenylphosphine with calcium silazides are slow. Thus, the half-life of the reaction of [{(ArNCMe)$_2$CH}Ca{N(SiMe$_3$)$_2$}(THF)] with HPPh$_2$ (15 equiv.) is 200 min, while a competition experiment between the same group 2 complex and a 1:1 mixture of HNPh$_2$ and HPPh$_2$ yielded after 30 min at room temperature exclusive formation of the calcium diphenylamide in preference to phosphide, despite the fact that diphenylphosphine has a lower pKa than diphenylamine [106]. This disparity in the rate of the reaction with diphenylphosphine compared to diphenylamine was attributed to the fact that a coordination of the substrate to the metal is required for the σ-bond metathesis (protonolysis) step to occur and that the soft phosphine is a poorer ligand than the amine for the hard calcium center. In combination with the observation that organolanthanide catalysts mediate the phosphine-terminated polymerization of alkynes, the data contrast with those derived for hydroamination catalysis where the turnover-limiting step proceeds via a transition state involving proton-assisted alkene insertion (see Sect. 2.1), and raise the question of whether putative vinyl- and alkylcalcium species are true intermediates in the catalytic hydrophosphination of alkynes and alkenes or whether proton-assisted insertion occurs.

While the product distribution for the hydrophosphination of dienes can be explained by invoking a metal allyl complex upon addition of M–PR$_2$ to the diene system and consideration of its equilibration between η^3- and η^1-coordination modes along with the relative rates of protonolysis of the two η^1-coordination isomers, off-cycle isomerization of the reaction products may also be occurring

$$R^1N=C=NR^2 \quad + \quad HPAr_2 \xrightarrow[\substack{25\,°C \\ \text{hexane} \\ 0.25\text{-}28\ h}]{\substack{1.5 - 5\ \text{mol}\ \% \\ [\{(ArNCMe)_2CH\}Ca\{N(SiMe_3)_2\}(THF)] \\ \text{or} \\ [M\{N(SiMe_3)_2\}_2(THF)_2]}} \quad \substack{PAr_2 \\ R^1HN \diagdown NR^2}$$

Ar = Ph, 4-MeC$_6$H$_4$
R^1 = R^2 = i-Pr, Cy, p-tol
R^1 = Et, R^2 = t-Bu
M = Ca, Sr, Ba

5 examples 68-99% yield
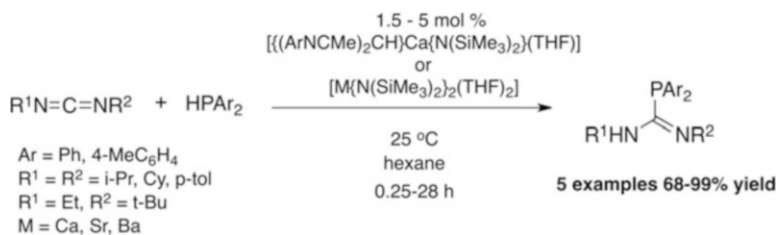
Scheme 14 Reaction scope for the group 2-catalyzed hydrophosphination of carbodiimides

under the reaction conditions. Although the *syn*-addition of phosphines to alkynes can be attributed to a concerted insertion of the unsaturated bond into the Ca–P σ-bond of an intermediate phosphide complex, *anti*-addition requires additional rationalization. This unusual selectivity may have its origin in (1) alkyne to allene isomerization of the substrate, (2) the isomerization of a vinylmetal intermediate, and (3) isomerization of a vinylradical intermediate derived from single-electron chemistry.

2.2.2 Intermolecular Hydrophosphination of Carbodiimides

The heteroleptic calcium silazide [{(ArNCMe)$_2$CH}Ca{N(SiMe$_3$)$_2$}(THF)] and the homoleptic complexes [Ca{N(SiMe$_3$)$_2$}$_2$]$_2$ and [M{N(SiMe$_3$)$_2$}$_2$(THF)$_2$] (M = Ca, Sr, Ba) have been applied to the hydrophosphination of carbodiimides [114].

Reaction scope: The hydrophosphination of a number of symmetric and unsymmetric carbodiimides with secondary arylphosphines was reported to proceed at room temperature using catalyst loadings as low as 1.5 mol% (Scheme 14). While [{(ArNCMe)$_2$CH}Ca{N(SiMe$_3$)$_2$}(THF)] was found to catalyze this reaction, the simpler homoleptic alkaline-earth amides proved more active with TOFs for the addition of diphenylphosphine to 1,3-di-*iso*-propylcarbodiimide exceeding 250 h^{-1} for the strontium-based precatalyst [Sr{N(SiMe$_3$)$_2$}$_2$(THF)$_2$]. Under these conditions the reaction scope could not be expanded to 1,3-di-*tert*-butylcarbodiimide or the less acidic phosphines such as dicyclohexylphosphine. Background reactions conducted in the absence of precatalysts reveal no reaction between Ph$_2$PH and 1,3-di-*iso*-propylcarbodiimide after 2 weeks at room temperature and upon heating to 140 °C [114].

Reaction mechanism: Based upon a series of stoichiometric reactions, and in contrast to the previously discussed hydrophosphination reactions (vide supra), it was postulated that unsaturated homoleptic heavier alkaline-earth phosphides are unlikely to be long-lived intermediates in the catalytic hydrophosphination of carbodiimides conducted in non-coordinating solvents. Rather, it was proposed that the phosphaguanidine product was acting as a ligand for the Lewis acidic metal center [114].

Westerhausen and coworkers have reported the stoichiometric insertion reactions of [Ca(PPh$_2$)$_2$(THF)$_4$] with 1,3-dicyclohexylcarbodiimide and 1,3-di-*iso*-propylcarbodiimide to yield homoleptic phosphaguanidinate complexes of
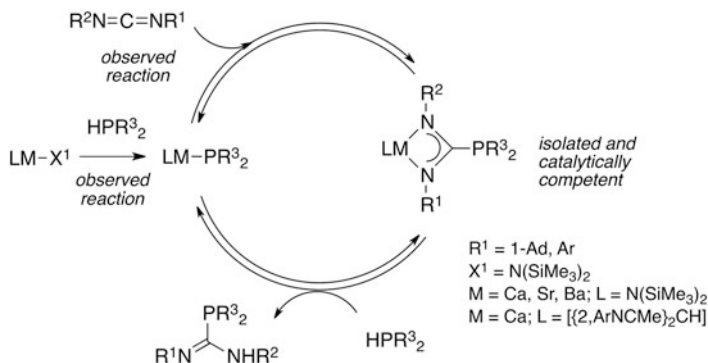
Fig. 9 Postulated catalytic cycle for group 2-mediated hydrophosphination of carbodiimides

calcium $[Ca\{Ph_2PC\{NR\}_2\}_2(THF)_2]$ ($R = Cy$, ^iPr) [115]. The phosphagua-nidinate ligands bind to the metal via κ^2-N,N-chelation and despite differing in the coordination geometry at calcium both derivatives are catalytically competent for the addition of diphenylphosphine to 1,3-di-*iso*-propyl- or 1,3-dicyclohexylcarbodiimide at 1–3 mol% catalyst loadings. These complexes may also be accessed by the reaction of the precatalysts with isolated samples of the phospha(III)guanidines, and strontium complexes $[Sr\{Ph_2PC\{NR\}_2\}_2(THF)_2]$ have also been synthesized and isolated in this manner [101, 114, 115].

Similar studies employing the heteroleptic precatalysts have allowed the isolation of a heteroleptic β-diketiminate/phospha(III)guanidinate complex from the insertion of 1,3-di-*iso*-propylcarbodiimide into the Ca–P bond of the phosphide $[\{(ArNCMe)_2CH\}Ca\{PPh_2\}(THF)]$ [114]. Although addition of diphenyl-phosphine to $[\{(ArNCMe)_2CH\}Ca\{Ph_2PC\{NCy\}_2\}(THF)]$ does not result in quantitive formation of the phosphide complex and liberation of the phospha(III) guanidine, catalytic turnover was observed upon addition of a mixture of diphenyl-phosphine and carbodiimide to $[\{(ArNCMe)_2CH\}Ca\{Ph_2PC\{NCy\}_2\}(THF)]$. These data suggest that the σ-bond metathesis (or protonolysis) reaction of the phosphaguanidinate complex with diphenylphosphine is thermodynamically uphill but kinetically feasible under catalytic conditions where this process is coupled to the insertion reaction step and the overall reaction is exothermic (Fig. 9). While these experiments suggested a degree of reversibility in the σ-bond metathesis step, the potential for reversibility in the insertion step was demonstrated by a crossover experiment. The reaction of 1 equiv. of $[Ph_2PC\{NHCy\}\{NCy\}]$ and 1 equiv. of 1,3-di-*iso*-propylcarbodiimide catalyzed by either 10 mol% $[\{(ArNCMe)_2CH\}Ca\{N(SiMe_3)_2\}(THF)]$ or 5 mol% $[Ca\{N(SiMe_3)_2\}_2]_2$ in C_6D_6 resulted in the formation of the crossover products $[Ph_2PC\{NH^iPr\}\{N^iPr\}]$ and 1,3-dicyclohexylcarbodiimide [114]. Thus, it is currently proposed that the reaction occurs via fast catalyst initiation with turnover proceeding via σ-bond metathesis and insertion reaction with both steps being reversible under the catalytic conditions (Fig. 9).
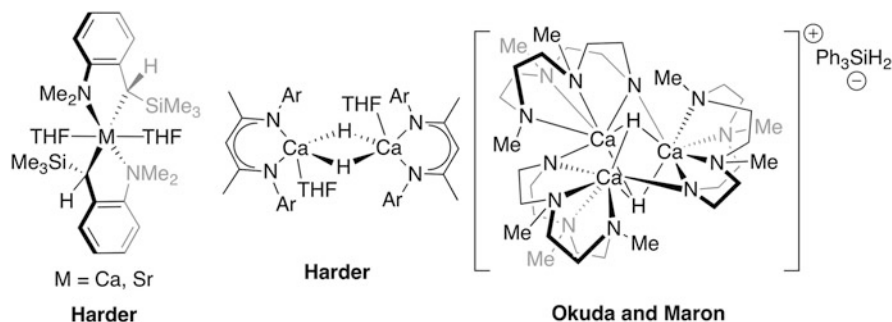
Fig. 10 Group 2 alkyl and hydride complexes reported as hydrosilylation and hydrogenation precatalysts

2.3 Hydrosilylation (C–Si Bond Formation)

2.3.1 Hydrosilylation of Activated Alkenes and Alkynes

Following the development of group 2 complexes for the controlled polymerization of styrene, in 2006 Harder and coworkers reported the hydrosilylation of a series of activated alkenes with Ph_nSiH_{4-n} ($n = 2$ or 3) catalyzed by [{$(Me_2N$-o-$C_6H_4)$ $CHSiMe_3$}$_2$M(THF)$_2$] (M = Ca, Sr) and isolated the first calcium-hydride complex [{$(ArNCMe)_2CH$}Ca{μ-H}(THF)]$_2$, a species relevant to the catalytic reaction [116, 117]. In related studies, Okuda and coworkers have isolated a cationic trinuclear calcium hydride cluster and demonstrated its competency for the hydrosilylation of styrene with phenylsilane (Fig. 10) [118].

   Reaction scope: For [{{2-$(Me_2N)C_6H_4$}$CHSiMe_3$}$_2$M(THF)$_2$], reactions proceeded with low catalyst loadings (0.5–10 mol%) under relatively mild conditions (50 °C, 0.5–16 h) with the strontium catalyst providing shorter reaction times than the calcium analogue [116]. The reaction scope is limited to activated alkenes including vinylarenes and dienes, and norbornene and allylbenzene were reported to not undergo hydrosilylation with group 2 precatalysts (Scheme 15). Despite the possibility that [{{2-$(Me_2N)C_6H_4$}$CHSiMe_3$}$_2$M(THF)$_2$] (M = Ca, Sr) may initiate the anionic polymerization of styrene, clean hydrosilylation reactivity was observed.

   The regiochemistry of the reaction proved solvent dependent for the hydrosilylation of diphenylethene, and while preparations in benzene gave products deriving from 2,1-insertion of the alkene into the M–H σ-bond, preparations in THF gave the opposite regioisomer proposed to derive from a similar 2,1-insertion into a M–Si σ-bond. Potassium hydride is also an active catalyst for the hydrosilylation of 1,1-diphenylethylene in hydrocarbon solvents with reactions proceeding with anti-Markovnikov addition of the silane to the alkene, but is inactive or shows polymerization of the alkene for other substrates [116].

   Despite the possible formation of CaH_2 upon catalyst initiation via reaction of [{{2-$(Me_2N)C_6H_4$}$CHSiMe_3$}$_2$M(THF)$_2$] (M = Ca, Sr) with $R_{4-n}SiH_n$
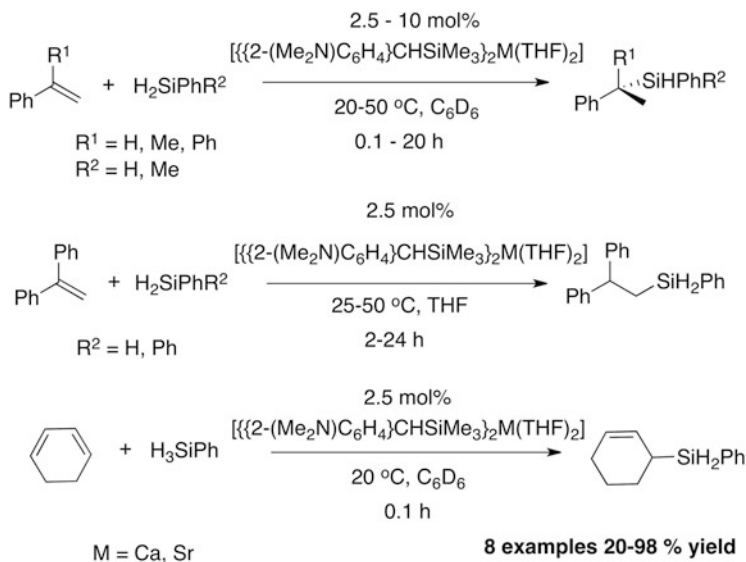
Scheme 15 Scope of group 2-catalyzed hydrosilylation of alkenes, alkynes and dienes

(*see below*), commercially available CaH_2 proved inactive for the hydrosilylation of alkenes under these reaction conditions [116]. Similarly, the cationic calcium hydride cluster depicted in Fig. 10 effects the hydrosilylation of 1,1-diphenylethylene with diphenylsilane in THF solution at 5 mol% loading in 18 h at 25 °C with anti-Markovnikov selectivity [118]. The grafting of calcium reagents onto silica supports, as means to control the deleterious solution equilibrium, has been achieved. The hydrosilylation catalysts, $[\{\{2\text{-}(Me_2N)C_6H_4\}CHSiMe_3\}_2Ca(THF)_2]$ and $[Ca\{N(SiMe_3)_2\}_2(THF)_2]$, have been reported to react with silica, to afford materials that proved catalytically active for the hydrosilylation of styrene, 1,3-cyclohexadiene, and 1,1-diphenylethylene with $PhSiH_3$ albeit with lower activities than those reported for homogeneous catalysis, particularly for the hydrosilylation of 1,1-diphenylethylene. While it is unclear whether the active catalyst is bound to the silica surface, the authors suggested that an observed sensitivity of the reaction to substrate size was an indication of a heterogeneous process [68].

   Reaction mechanism: While not directly observed for group 2 alkyl precatalysts, Harder and coworkers suggest that the catalyst resting state may be hydride-rich clusters of the general formulae $[\{\{2\text{-}(Me_2N)C_6H_4\}CHSiMe_3\}_{<1}MH_{>1}]_n$. In line with this hypothesis, the stoichiometric reaction of phenylsilane with $[\{(ArNCMe)_2CH\}Ca\{N(SiMe_3)_2\}(THF)]$ has been shown to yield the corresponding molecular calcium hydride complex $[\{(ArNCMe)_2CH\}Ca\{\mu\text{-}H\}(THF)]_2$ [117]. In addition, similar reactions of magnesium silazide and alkyl complexes bearing either binucleating β-diketiminate or *N*-heterocyclic carbene ligands with phenylsilane have allowed the isolation of hydride-rich molecular
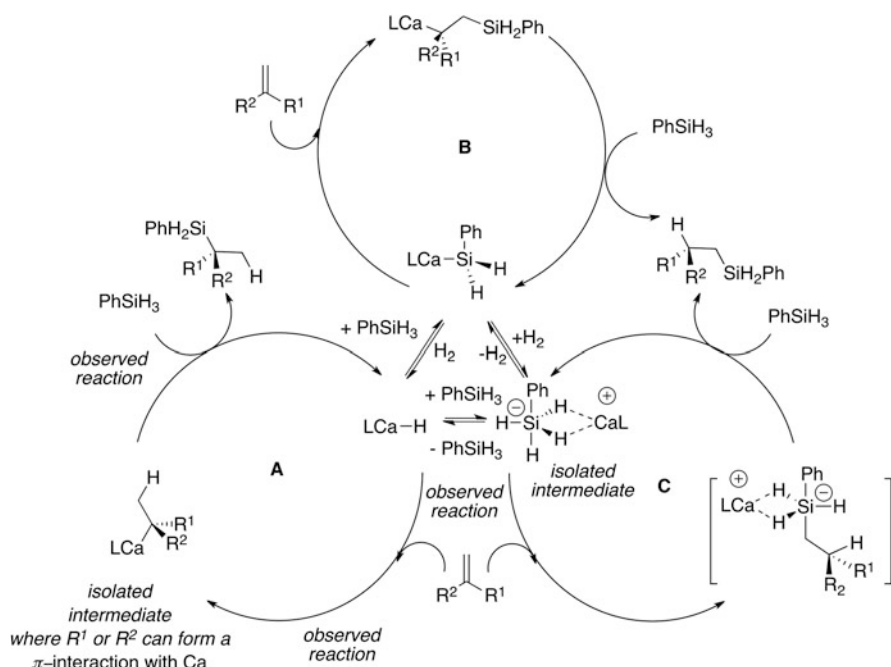
Fig. 11 Proposed divergent mechanism for group 2-catalyzed hydrosilylation

clusters containing Mg_8H_{10} and Mg_4H_6 fragments [119, 120]. The insertion of 1,1-diphenylethylene and myrcene (a diene) into the Ca–H bond of $[\{(ArNCMe)_2CH\}Ca\{\mu\text{-}H\}(THF)]_2$ yields the corresponding benzyl and allyl calcium complexes which have been isolated and crystallographically characterized [121]. Although these reactions provide direct evidence for the insertion step in hydrosilylation catalysis, it is of interest to note that neither of the products demonstrated η^1-coordination in the resulting metal-bound hydrocarbon ligand.

Based upon this evidence and the observed reaction products, Harder and coworkers have proposed two catalytic cycles, proceeding via either a metal hydride (Fig. 11, cycle **A**) or silanide intermediate (Fig. 11, cycle **B**) along with a silicate cycle which involves a charge-separated species (Fig. 11, cycle **C**) [116]. Furthermore, it has been suggested that more polar solvents favor the formation of charge-separated species of the form $[LM]^+[H_4SiPh]^-$ which in turn decompose to yield the metal silanide $[LM(SiPhH_2)]$ with liberation of H_2. Although this rationale neatly accounts for the observed solvent-dependent regiochemistry and the recent studies of Okuda and Maron provide evidence for the formation of charge-separated silicate complexes under condition relevant to catalysis [118], it remains a possibility that the two regioisomeric transition states of the σ-bond metathesis step between LMX^1 (X^1 = alkyl, M = Ca, Sr) and R_nSiH_{4-n} have similar activation energies which may be perturbed by solvent polarity.
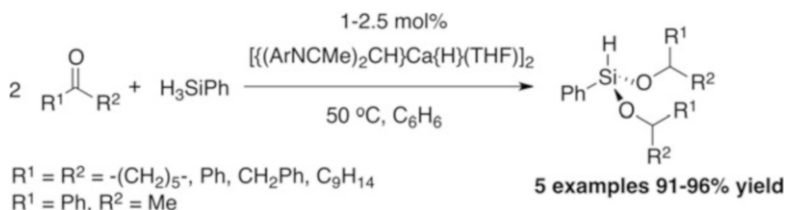
Scheme 16 Reaction scope of the calcium-catalyzed hydrosilylation of carbonyls

Asymmetric catalysis: Initial attempts to develop non-racemic catalysts for the enantioselective hydrosilylation of alkenes have not been successful with C_2-symmetric (*S*)-Ph-pybox and β-diketiminate calcium amide complexes catalyzing the addition of phenylsilane to styrene in the absence of solvent at 50 °C in, at best, 9 % e.e [69]. As with intramolecular hydroamination catalysis, these results have been explained in terms of the loss of ligand control due to facile ligand redistribution reactions under the catalytic reaction conditions.

2.3.2 Hydrosilylation of Carbonyls

The scope of group 2 hydrosilylation catalysis has been extended to incorporate ketones and the intermolecular hydrosilylation of cyclohexanone, benzophenone, adamantone, and acetophenone with phenylsilane catalyzed by $[\{(ArNCMe)_2CH\}Ca\{\mu\text{-}H\}(THF)]_2$ to afford the corresponding silyl ethers was reported in 2008 by Harder and coworkers (Scheme 16) [122]. Reactions proceed under mild conditions (50 °C, 0.2–34 h) and by-products originating from competitive carbonyl enolization reactions are only observed in low yield (<5 %). Irrespective of the initial silane:ketone ratio, the major reaction products are $[PhHSi(OCHR^1R^2)_2]$, derived from a 1:2 silane:ketone reaction stoichiometry. At low silane/ketone ratios, small amounts of the trialkoxy product could also be obtained. Similar observations have been made during the dehydrocoupling of amines with silanes (see Sect. 4.2) and increasing the electron-donating capacity of the substituents on the silicon increases the reactivity of the Si–H moiety and the rate of the second reduction reaction exceeds that of the first preventing the isolation of 1:1 adducts [122].

The precatalyst $[\{(ArNCMe)_2CH\}Ca\{\mu\text{-}H\}(THF)]_2$ has been shown to react with ketones to yield the corresponding dimeric β-diketiminato calcium alkoxide products derived from insertion of the ketone into the Ca–H bond. These latter species have been shown to be catalytically competent for the hydrosilylation of ketones. Stoichiometric preparations included reaction of $[\{(ArNCMe)_2CH\}Ca\{\mu\text{-}H\}(THF)]_2$ with benzophenone, acetophenone, cyclohexanone, 1,3-diphenylacetone, and 2-adamantone to yield the corresponding alkoxides in 9–73 % following crystallization from hydrocarbon solutions. Quenching the reaction mixtures with Me₃SiCl showed, in addition to the expected reduction products, moderate to significant
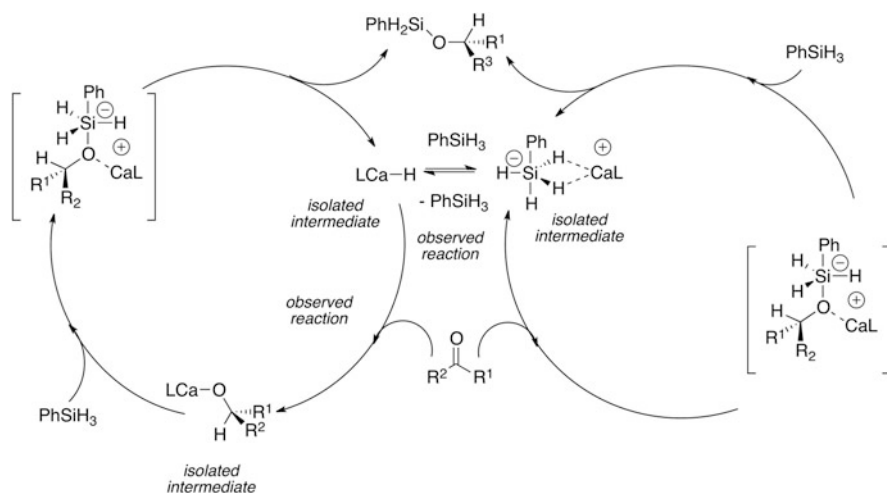
Fig. 12 Possible reaction mechanisms for the hydrosilylation of carbonyls

amounts of substrate enolization and aldol condensation products [121, 122]. Despite this observation, under the catalytic reaction conditions, these side reactions are apparently inhibited. Consistent with the studies upon the hydrosilylation of alkenes, two potential catalytic cycles are proposed, proceeding via either σ-bond metathesis steps with C–H bond formation from insertion of the carbonyl into a Ca–H bond and subsequent formation and decomposition of an intermediate calcium silicate (Fig. 12, cycle **A**) or generation of a calcium silicate with C–H bond formation via insertion of the carbonyl into an Si–H bond (Fig. 12, cycle **B**).

2.3.3 Attempted Hydrosilylation of Pyridines and Quinolines

Although $[\{(ArNCMe)_2CH\}Ca\{\mu\text{-}H\}(THF)]_2$ reacts with alternative substrates, including benzonitrile, cyclohexene oxide, 2-methylpropene oxide, 1,1,3,3-tetramethylbutyl isonitrile, and diphenylmethyl-*N*-phenylimine, via insertion of unsaturated carbon–nitrogen and carbon–oxygen bonds into the calcium–hydride bond of the organometallic reagent, the catalytic hydrosilylation (or hydrogenation) of these substrates with group 2 reagents has yet to be reported (Scheme 16b) [121].

In related studies, it has been shown that an analogous magnesium hydride complex, generated in situ from the reaction of $[\{(ArNCMe)_2CH\}Mg\{^nBu\}(Solv)]$ with $PhSiH_3$ (Solv = pyridine, substituted pyridine, quinoline), undergoes 1,2- or 1,4-addition to pyridine, substituted pyridines, and quinoline (Scheme 17) [123]. For example, the addition of $[\{(ArNCMe)_2CH\}Mg(n\text{-}Bu)(Py)]$ to pyridine at room temperature in toluene gave a mixture of 1,2- and 1,4-hydride addition products which could be converted to the thermodynamically more stable 1,4-addition product upon heating to 60 °C [124]. A related terminal magnesium
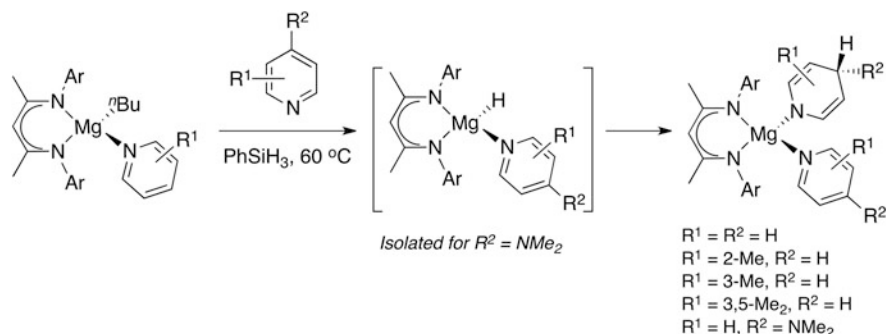
Scheme 17 Stoichiometric reactions of a magnesium hydride, generated in situ, with pyridines

hydride [{(ArNCMe)$_2$CH}Mg(H)(DMAP)] has been isolated by Jones and coworkers [125], while Hill and coworkers have shown that DMAP may be employed as a substrate in the dearomatization chemistry [124]. Blocking of the 4-position of the heterocycle for example in 4-methylpyridine results in selective 1,2-hydride addition.

The absence of a reaction between the magnesium alkyl complex and the heterocycles is noteworthy due to the precedent for the nucleophilic addition of calcium alkyls to pyridine and substituted pyridines. Catalytic dearomatization and hydrosilylation of these heterocycles employing magnesium hydrides and magnsium alkyls as precatalysts have yet to be reported. Under catalytic conditions the observed decomposition of the magnesium intermediates at elevated temperatures may be responsible for the lack of catalytic turnover.

2.4   Hydroboration of Activated Alkenes, Alkynes, Pyridines, and Carbonyls (C–B Bond Formation)

Reaction scope: Despite attempts to date to achieve a dearomatization and hydrosilylation of heteroaromatics with magnesium catalysts failing to achieve turnover, the hydroboration of pyridine and alkyl and aryl substituted pyridines along with quinoline and isoquinoline with pinacol-borane catalyzed by 5–10 mol% [{(ArNCMe)$_2$CH}Mg^{n}Bu] has been reported (Scheme 18) [126].

Reactions proceed under mild conditions (<80 °C), with control reactions in the absence of a catalyst giving no or very little dearomatization. While quinoline and isoquinoline undergo a selective 1,2-addition of HBpin at 5 mol% catalyst at 25 °C, the regiochemistry of the hydroboration of pyridines is controlled by the substitution of the heterocycle. Thus, pyridines substituted in the 4-position and 2/6-position yield predominantly 1,2- and 1,4-addition products, respectively, while those substituted in the 3-position give a near statistical mixture of regioisomeric reaction products [126].

1,2 versus 1,4-addition

$R^1=R^2=R^3=R^4=R^5=H$ and $R^1=Me$, $R^2=R^3=R^4=R^5=H$	1:9 to 0:100
$R^3=Me$, $R^1=R^2=R^4=R^5=H$ and $R^3=Ph$, $R^1=R^2=R^4=R^5=H$	100:0 to 8:2
$R^2=R^3=C_6H_4$, $R^1=R^4=R^5$ and $R^1=R^2=C_6H_4$, $R^3=R^4=R^5=H$	
$R^2=Me$, $R^1=R^3=R^4=R^5=H$ and $R^2=R^4=Me$, $R^1=R^3=R^5=H$	approx. 1:1
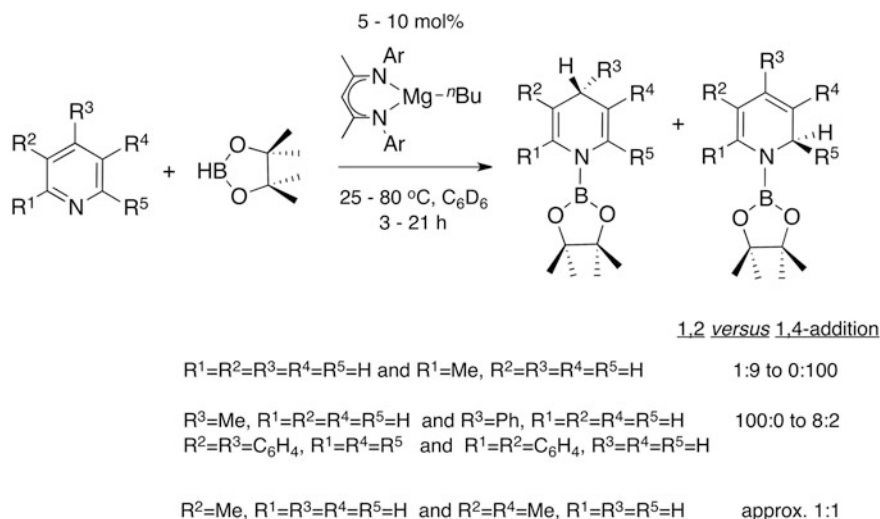
8 examples 51-99% yield

Scheme 18 Magnesium-catalyzed hydroboration/dearomatization of pyridines, quinoline and isoquinoline

When substrates bearing additional aldehyde, ketone, and nitrile functional groups were exposed to the reaction conditions, the selective hydroboration of the carbonyl or nitrile functional group could be achieved in the presence of a single equivalent of pinacol-borane at room temperature [127]. Only in the case of nitrile substituted pyridines could dearomatization be achieved by addition of a further equivalent of HBpin and extended heating. This observation was applied to a highly efficient hydroboration of aldehydes and ketones with 0.05–0.5 mol% [{(ArNCMe)$_2$CH}Mg(^{n}Bu)]. Reactions proceed at 25 °C and the scope includes aromatic and aliphatic aldehydes, aromatic ketones, aliphatic ketones, and diketones (Scheme 19). For example, benzil undergoes a stereoselective double hydroboration to selectively produce the (R,S)/(S,R) diastereomer in 72 % isolated yield after 2 h at 25 °C with 0.1 mol% of the precatalyst. The reaction tolerates alkene functional groups, with hex-5-en-2-one undergoing selective carbonyl reduction [127].

In related studies, Harder and coworkers have investigated the hydroboration of 1,1-diphenylethene with catechol-borane (HBcat) [128]. While the background reaction proceeds at 100 °C to yield the expected hydroboration product, in the presence of 2.5 mol% [{(ArNCMe)$_2$CH}Ca{μ-H}(THF)]$_2$ or [{{2-(Me$_2$N)C$_6$H$_4$}CHSiMe$_3$}$_2$Ca (THF)$_2$], [(Ph$_2$CHCH$_2$)$_3$B] is formed at 25–50 °C. Stoichiometric studies revealed that under the reaction conditions HBcat undergoes a metal-mediated decomposition to B$_2$(cat)$_3$, B(cat)$_2^-$, BH$_4^-$, B$_2$H$_7^-$, and BH$_3$•THF with the latter borane effecting the anti-Markovnikov hydroboration of the alkene at lower temperatures than HBcat itself. While the borates [{(ArNCMe)$_2$CH}Ca{BH$_4$}(THF)$_2$] and
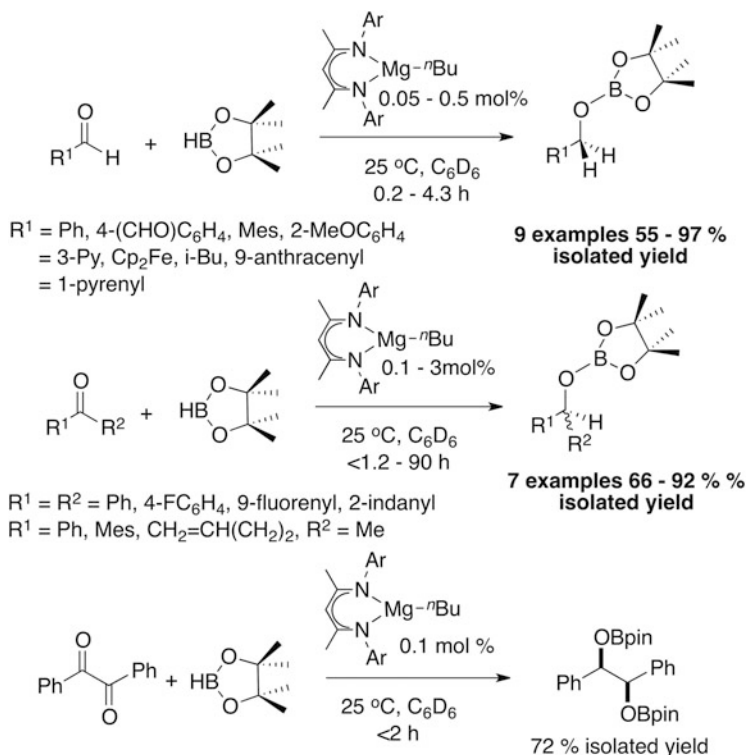
Scheme 19 Magnesium-catalyzed hydroboration of aldehydes and ketones

[{(ArNCMe)$_2$CH}Ca{H$_2$Bpin}] have been isolated and characterized, evidence for the hydroboration of 1,1-diphenylethylene with these complexes has not yet been observed [128].

Reaction mechanism: The stoichiometric reaction of the precatalyst [{(ArNCMe)$_2$CH}Mg^{n}Bu] with HBpin in d$_8$-toluene yields ^{n}BuBpin along with the known magnesium hydride [{(ArNCMe)$_2$CH}Mg(μ-H)]$_2$. Pulse-gradient spin-echo NMR studies suggest that the molecular hydride and borane exist in equilibrium with the corresponding magnesium borate [{(ArNCMe)$_2$CH}Mg(H^{n}BuBpin)] [124, 126]. An analogous calcium borate complex [{(ArNCMe)$_2$CH}Ca(H$_2$BR$_2$) (THF)] has been reported as the product of either (1) the reaction of β-diketiminate-stabilized calcium amides with 2 equiv. of the dialkylborane 9-BBN or (2) the addition of 9-BBN to [{(ArNCMe)$_2$CH}Ca(μ-H)(THF)]$_2$ [129]. Extensive precedent exists for the insertion of pyridines into Mg–H bonds (for details Sect. 2.3.3). Furthermore, although the stoichiometric reaction of [{(ArNCMe)$_2$CH}Mg(μ-H)]$_2$ with benzophenone proceeds via insertion of the carbonyl into the Mg–H bond, addition of a further 1 equiv. of benzophenone and 1 equiv. of HBpin to this product provides the magnesium borate complex represented in Fig. 13 [127].
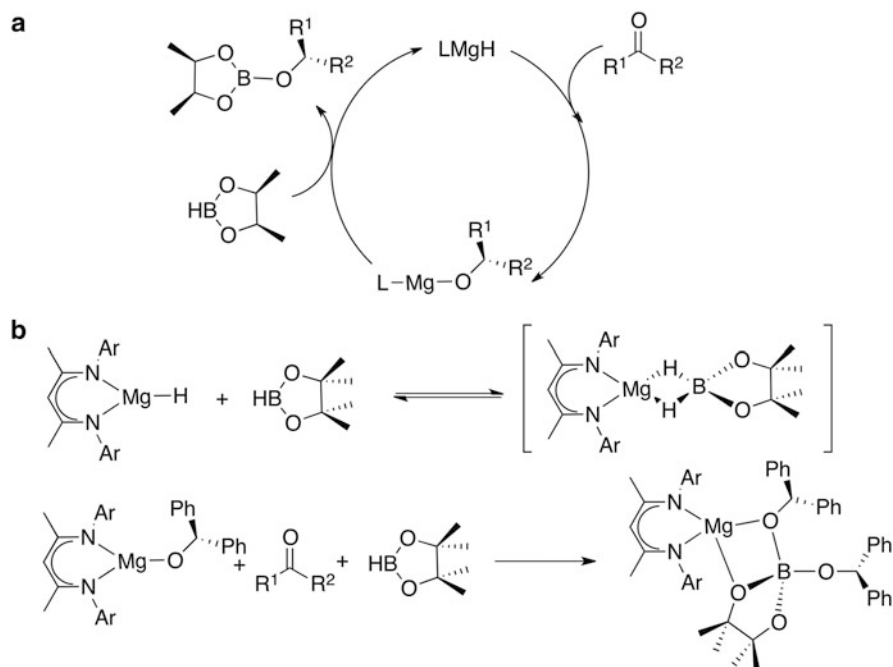
Fig. 13 (**a**) Simplified mechanism for the magnesium-catalyzed hydroboration of carbonyls (**b**) Borate formation during group 2-mediated hydroboration chemistry

While in combination these data are suggestive of a catalytic cycle involving σ-bond metathesis and insertion steps, the facile formation of borate complexes under the reaction conditions raises the question as to whether turnover occurs via discrete 3- or 4-coordinate magnesium species which equilibrate with a series of off-cycle borate complexes or whether the borate adducts themselves mediate C–H and Het–B bond formation. Similar complexities have been speculated upon in hydrosilylation catalysis with silicate formation and decomposition being invoked to explain the unusual solvent effects on regioselectivity (see Sect. 2.3.1). While the lower stability of silicates relative to borates should allow a more thorough study of the mechanism of hydroboration with group 2 catalysts, at the time of writing only a simplified mechanistic picture has been presented.

2.5 Hydrogenation of Activated Alkenes and Alkynes (C–H Bond Formation)

In 2008, Harder and coworkers reported the calcium-catalyzed hydrogenation of styrene, 1,1-diphenylethylene, 1,3-cyclohexadiene, α-methylstyrene, and 1-phenylcyclohexene (Scheme 20) [130]. Reactions were reported to proceed under mild conditions (20 °C,
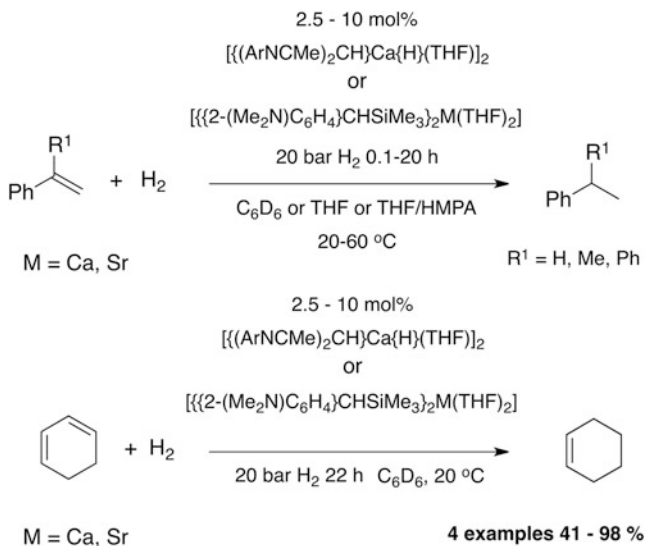
Scheme 20 Hydrogenation of alkenes with calcium and strontium alkyl and hydride catalysts

20 bar H_2), and while both $[\{(ArNCMe)_2CH\}Ca\{\mu\text{-}H\}(THF)]_2$ and $[\{\{2\text{-}(Me_2N)C_6H_4\}$ $CHSiMe_3\}_2M(THF)_2]$ (M = Ca, Sr) proved catalytically active, finely ground commercially available CaH_2 was an ineffective catalyst under these reaction conditions. More recently, Okuda demonstrated the hydrogenation of 1,1-diphenylethylene at 1 bar H_2 with 20 mol% of the cationic trinuclear calcium hydride represented in Fig. 10 in THF solution: The reaction took 13 days to reach completion [118].

The reaction scope of group 2-mediated hydrogenation is currently limited to activated alkenes and the product distribution has proved to be sensitive to solvent polarity. Although preparations in THF or a THF/HMPA mixture proceeded rapidly, in most instances the reaction products were accompanied by side products derived from the dimerization/polymerization of the alkene [130]. For example, although the attempted hydrogenation of styrene in THF/HMPA led to a calcium-mediated polymerization of this substrate, changing the solvent to benzene gave the hydrogenation product in 80 % yield.

Reaction mechanism: As discussed in Sect. 2.3.1, $[\{(ArNCMe)_2CH\}Ca(\mu\text{-}H)$ $(THF)]_2$ undergoes insertion reactions with 1,1-diphenylacetylene and myrcene (7-methyl-3-methylene-1,6-octadiene), a terpene that contains three double bonds [121]. Experimental evidence for the σ-bond metathesis step was provided by not only the reaction of the calcium complexes isolated from these latter reactions with H_2 but also an H/D exchange reaction. Treatment of the calcium deuteride $[\{(ArNCMe)_2CH\}Ca(\mu\text{-}D)(THF)]_2$ with 1 bar H_2 at 20 °C led to complete H/D exchange after 20 min at room temperature as evidenced by NMR spectroscopy. The reaction of H_2 with Ca–C bonds required slightly more forcing reactions conditions and, consistent with those reported for the catalytic reaction, could be achieved at 20 bar H_2 at 20 °C in either benzene or THF solution [130].
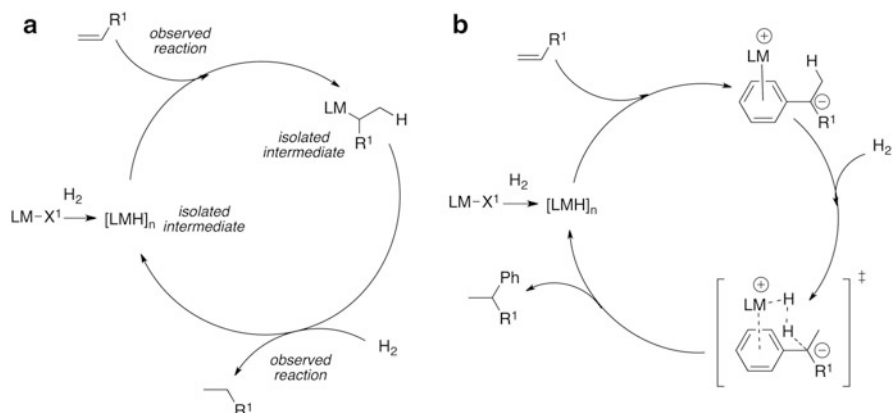
Fig. 14 Proposed mechanism of group 2-catalyzed hydrogenation of alkenes (**a**) lanthanide-mimetic mechanism and (**b**) frustrated Lewis acid/Lewis base mechanism

Although, based upon the reactivity of the observed reaction intermediates, it was suggested that alkene hydrogenation occurs via a lanthanide-mimetic catalytic cycle outlined in Fig. 14a involving σ-bond metathesis and insertion reaction steps, DFT studies suggest a related mechanism but invoke charge separation with formation of a contact-ion pair [131]. Calculations conducted with the B3LYP functional using a 6,311++G(d,p)/6,31G hybrid basis set (for the calcium cycle), imply that the reaction proceeds via (1) hydride transfer to the alkene with formation of a contact-ion pair with either η^3-coordination of an allyl ligand (diene insertion into M–H) or η^6-coordination of an aryl ring to the metal center (styrene insertion into M–H) and (2) heterolytic H_2 activation by this "frustrated" Lewis acid–Lewis base pair to liberate the product and regenerate the catalyst (Fig. 14b) [131].

While this hypothesis has a foundation in the observed solid-state structures of calcium alkyl complexes involved as intermediates in hydrogenation catalysis, it also explains the reaction scope and suggests that a similar mechanism is not feasbile for magnesium. Due to the involvement of charge separate species there are large variations in the data, depending on whether or not a solvent correction (polarization continuum model) is applied. For Mg, Ca, and Sr, hydride transfer (or alkene insertion) is the turnover-limiting step; when solvation effects (benzene) are taken into account the Gibbs activation energy barriers are calculated to be 34.3, 29.2, and 27.6 kcal mol^{-1}, respectively [131].

2.6 Hydroalkynylation of Alkynes and Carbodiimides (C–C Bond Formation)

While the bending of homoleptic heavier group 2 acetylides, i.e., deviations in the Ca–Cα–Cβ bond angle, in the solid state continues to promote interest in synthetic
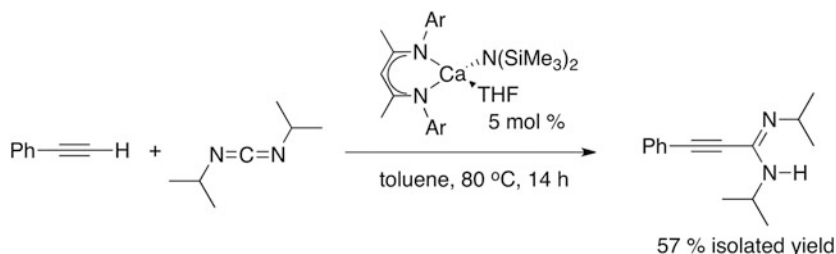
Scheme 21 Calcium-catalyzed hydroalkynation of 1,3-di-*iso*-propylcarbodiimide
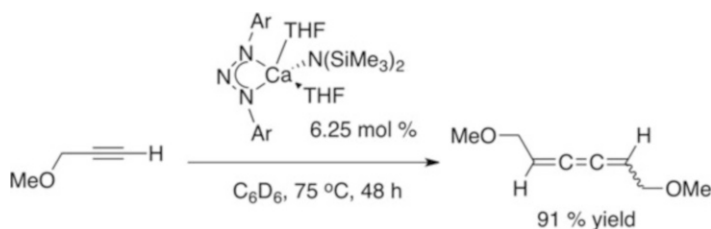
Scheme 22 Calcium-catalyzed hydroalkynation of 3-methoxypropyne

and structural investigations of these molecules [132–135], Hill and coworkers have reported the catalytic hydroalkynylation of carbodiimides and the dimerization of alkynes to form 1,2,3-hexatrienes [136, 137].

The low pK_a of terminal alkynes renders them susceptible to reactions with moderately strong bases such as group 2 hexamethyldisilazides. As part of a wider study into the synthetic chemistry of calcium acetylides, in 2008 the hydroalkylation of 1,3-di-*iso*-propylcarbodiimide with phenylacetylene to give [PhCC{N^{i}Pr}{NH^{i}Pr}] in 59 % isolated yield after 14 h at 80 °C catalyzed by 5 mol% [{(ArNCMe)$_2$CH}Ca{N(SiMe$_3$)$_2$}(THF)]$_2$ was reported (Scheme 21) [136]. While the substrate scope has not been expanded beyond this single example, the stoichiometric reation of [{(ArNCMe)$_2$CH}Ca{µ-CC(4-MeC$_6$H$_4$)}]$_2$, generated in situ, with 1,3-di-*iso*-propylcarbodiimide has been reported to yield the heteroleptic calcium amidinate/β-diketiminate complex from insertion of the carbodiimide into the M–C bond. This complex has, in turn, been shown to be unstable under the reaction conditions decomposing with formation of the protonated ligand [{(ArNCMe)$_2$CH}H], and homoleptic calcium propargyl amidinate complexes have been postulated as the true catalyst resting state [136].

During these studies the selective dimerization 3-methoxypropyne to a 1,2,3-hexatriene was observed as a side reaction (Scheme 22). Although initially limited to a stoichiometric synthesis, due to competing catalyst deactivation by formation of insoluble homoleptic calcium acetylides, the reaction was rendered catalytic using the triazenide supported precatalyst [{Ar$_2$N$_3$}Ca{N(SiMe$_3$)$_2$}(THF)$_2$] [137]. The reaction scope is currently limited to a single example. While the stereochemistry of the products has yet to be assigned the selective formation of

hexatrienes contrasts the product distribution found during the hydroalkynylation of alkynes with group 3 and rare-earth catalysts which typically produce a mixture of ene-yne isomers. Furthermore, the catalytic dimerization of alkynes to butatrienes presents a significant challenge as the butatriene skeleton has been calculated to be 17–18 kcal mol^{-1} less stable than the possible isomeric enyne forms [137].

Teuben and coworkers have shown that dimeric lanthanocene complexes bridged by alkynide ligands may exist in equilibium with the μ-(Z)-butatriene diyl bridged complex [138]. While similar equilibria have yet to been observed in group 2 chemistry it is notable that the calcium alkynide complexes of the general formula [{(ArNCMe)$_2$CH}Ca{μ-CC(R)}]$_2$ (R = CH$_2$OMe, ^{t}Bu, ^{n}Bu, Ph, 4-MeC$_6$H$_4$) have been shown to form asymmetric dimers, in the solid state and in benzene solution, in which the π-system of the alkyne coordinates to calcium to induce large deviations away from the symmetric 3c, 2-electron bonding picture [134, 137, 138]. In THF solution, data suggest that the monomeric complexes are formed and it is noteworthy that the dimerization of 3-methoxyprop-1-yne gave almost complete suppression of butatriene formation (ca. 10 % conversion) when conducted in THF.

3 Dimerization and Trimerization of Unsaturated Substrates

3.1 Dimerization of Aldehydes

The redox-neutral dimerization of aldehydes to form esters known as the Tischenko (or Tischtschenko) reaction may be catalyzed by group 2 hexamethyldisilazides [M{N(SiMe$_3$)$_2$}$_2$(THF)$_2$] (M = Ca, Sr, and Ba), bio-inspired magnesium thiolate complexes or with bicyclic guanidinate-stabilized magnesium amide complexes (Scheme 23) [139–142].

Reaction scope: The reaction scope with the heavier group 2 catalysts (M = Ca, Sr, Ba) includes electron-rich and electron-poor aromatic aldehydes along with non-enolizable and enolizable aliphatic aldehydes. A series of aromatic aldehydes may be dimerized with these catalysts and although heteroaromatic aldehydes are not reported the reaction may be conducted in both an inter- and intramolecular fashion and product yields decrease with the increasingly electron-rich aldehydes [139]. While magnesium catalysts supported by guanidinate and hexamethyldisilazide ligands are currently only known to catalyze aldehyde dimerization for three substrates (R = Ph, Me, CH$_2$CHMe$_2$) with TOFs ranging from 60 to 336 h^{-1} [140], magnesium thiolates generated in situ from a 1:1 mixture PhMgBr and RSH of have been reported for not only the dimerization of a series of aromatic and aliphatic aldehydes but also the crossed-Tischenko reaction of aromatic aldehydes with trifluorosubstituted ketones, albeit with lower activities than the guanidinate-stabilized complexes [141]. For the magnesium/thiolate systems, optimization of the separate reaction conditions revealed that benzylmercaptan and the
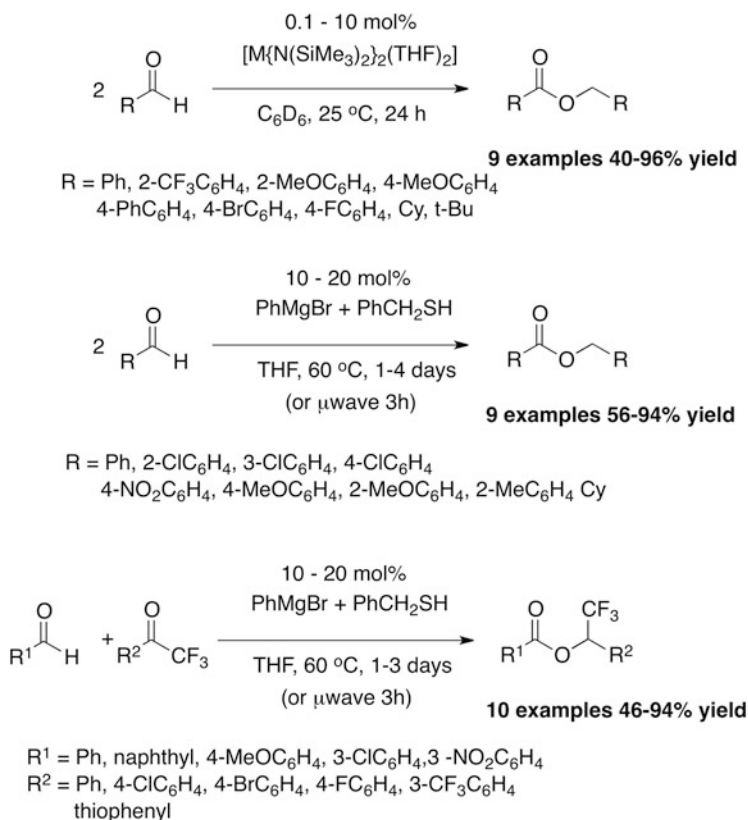
Scheme 23 Group 2-catalyzed dimerization of aldehydes

meta-substituted thiophenol *m*-CF$_3$C$_6$H$_4$SH provided the highest yields of ester products, with reactions proceeding with 10–20 mol% catalyst in THF at 65 °C. Nevertheless, preparations require long reaction times, 1–4 days, and a subsequent study demonstrated that increasing the substrate concentration and using microwave irridation the reaction times could be reduced to less than 3 h [142]. It is noteworthy that the very simple reagents NaH and LiBr/Et$_3$N also act as precatalysts for aldehyde dimerization under anhydrous and aqueous conditions, respectively [143, 144].

Reaction mechanism: Although thorough mechanistic studies have not been reported, the reaction is proposed to proceed via a calcium-alkoxide intermediate with hydride transfer occurring in a Meerwein–Ponndorf–Verley step (Fig. 15). An analogous mechanism has been estabilished in organoactinide chemistry [145], and a series experiments employing [Ca{N(SiMe$_3$)$_2$}$_2$(THF)$_2$] as a precatalyst implicate the alkoxide. Thus, employing 10 mol% of this latter compound as a precatalyst for the dimerization of benzaldehyde and quenching the reaction after 5 min revealed the formation of PhCH$_2$OH and PhC(O)N(SiMe$_3$)$_2$ as initial
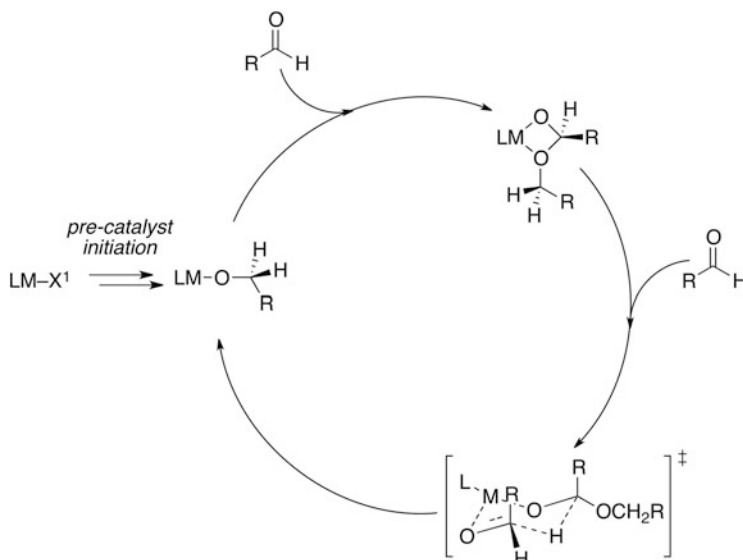
Fig. 15 Proposed mechanism of the group 2-catalyzed dimerization of aldehydes

by-products, furthermore a crossover experiment conducted between a 1:1 mixture of benzaldehyde and 4-bromobenzyl 4-bromobenzoate and 5 mol% [Ca{N (SiMe$_3$)$_2$}$_2$(THF)$_2$] gave in addition to benzaldehyde, benzylbenzoate, and 4-bromobenzyl 4-bromobenzoate the crossover product benzyl 4-bromobenzoate [139]. The possibility of hydride transfer via β-hydride elimination from the alkoxide intermediate and generation of a transient metal hydride intermediate cannot be discounted based upon the current experimental data.

3.2 Trimerization of Isocyanates

Despite the observation that phenyl- and 1-adamantylisocyanate may be used as substrates for hydroamination catalysis without polymerization or oligomerization of the unsaturated molecule (see Sect. 2.1.4), in the presence of catalytic quantities of a calcium "carbene" complex [{(ArN=PPh$_2$)$_2$C}Ca(THF)$_2$] phenyl- and cyclohexylisocyanate have been reported to undergo a selective cyclotrimerization to form the corresponding isocyanurate (Scheme 24) [106, 146]. Reactions proceed at low temperature and with phenylisocyanate requiring a lower catalyst loading and shorter reaction time to reach higher conversion than cyclohexylisocyanate.

The 2:1 reaction of cyclohexylisocyanate with the "carbene" precatalyst has been found to give a twofold addition product derived from an initial [2+2] addition of the Ca=C bond to the C=N bond. While this complex was characterized in the solid state and observed under the reaction conditions, it was found to decompose to

Scheme 24 Calcium-
catalyzed trimerization of
phenyl and
cyclohexylisocyanate

R = Cy, 5 mol %, 7d, 80 %
R = Ph, 1 mol %, 3h, 90%
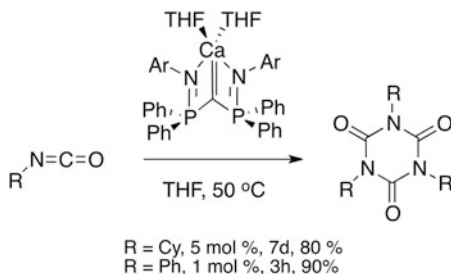
the mono-insertion product and CyN=C=O highlighting the potential for revers-
ibility in these reactions. A related mono-insertion product has been isolated
from the 2:1 reaction of CyN=C=O with the dimeric calcium "carbene"
complex [{(Me$_3$SiN=PPh$_2$)$_2$C}Ca]$_2$. While often referred to as metal "carbene"
complexes, consideration of simple valence bonding pictures in ionic complexes,
[{(Me$_3$SiN=PPh$_2$)$_2$C}Ca]$_2$ and [{(ArN=PPh$_2$)$_2$C}Ca(THF)$_2$], suggests that this
description does not satisfy the classical descriptions of Schrock alkylidenes or
Fischer carbenes and these complexes would be better represented as methandiide
resonance forms in which the "carbene" center formally bears a 2$^-$ charge. This
statement is supported by a series of DFT studies conducted by Harder and
coworkers in which the calculated atomic charge on the methandiide carbon by
natural population analysis varies between approximately -1.7 and -1.8
[106, 146].

4 Dehydrogenative Coupling of Acid and Base Partners

4.1 Amine-Borane Dehydrogenation

The dehydrogenation of amine–boranes is attracting increasing attention due to the
potential use of NH$_3$•BH$_3$, and related compounds as hydrogen storage materials.
The application of group 2 complexes in this field has two related focii, namely
(1) as use as catalysts for the dehydrogenation of ammonia–borane and
amine–boranes and (2) as model complexes to investigate the mechanism of
low-temperature hydrogen release from [M^1{NH$_2$BH$_3$}2] (M^1 = Mg, Ca) and the
related materials [M^2{NH$_2$BH$_3$}] (M^2 = Li, Na).

   Reaction scope: Although there have been extensive investigations into the
stoichiometric reactions of group 2 complexes with ammonia-borane [119,
147–153], secondary amine-boranes, and primary amine-boranes and their thermal
decomposition products, only a handful of catalytic reactions have been reported.
The reaction products depend on the substitution of the amine–borane. For
example, Harder and coworkers have reported that the sterically demanding
primary amine–borane ArNH$_2$•BH$_3$ (Ar = 2,6-di-*iso*-propylphenyl) reacts to

Scheme 25 Magnesium-catalyzed amine-borane dehydrocoupling

form a mixture of $HB(NHR)_2$, BH_3, and H_2 employing 2.5 mol% of a dialkyl magnesium catalyst, $[Mg^nBu_2]$ [155], Hill and coworkers have reported that dehydrocoupling of the secondary amine-borane $Me_2NH \cdot BH_3$ with 5 mol% $[Mg\{CH(SiMe_3)_2\}_2]$ at 60 °C yields a mixture of the four-membered dehydrocoupling product $[Me_2NBH_2]_2$ along with minor amounts of $HB(NMe_2)_2$ [151]. The sensitivity of the product distribution on the nature of the substrate is further underscored by the reaction of i-$Pr_2NH \cdot BH_3$ with 5 mol% $[Mg\{N(SiMe_3)_2\}_2]$ which gives the unsaturated product i-$Pr_2N=BH_2$ along with H_2 after 14 h at 25 °C (Scheme 25) [153]. Calcium complexes have not been reported in detail for amine-borane dehydrocoupling, while related yttrium and scandium complexes are known for this transformation [154].

Stoichiometric studies and proposed reaction mechanism: Group 2 amido-borane adducts can be synthesized by σ-bond metathesis (protonolysis) reactions. For example, $[\{(ArNCMe)_2CH\}M\{N(SiMe_3)_2\}(THF)]$ reacts with secondary amine-boranes $R_2NH \cdot BH_3$ to yield $[\{(ArNCMe)_2CH\}M\{NR_2BH_3\}]$ (M = Ca, R = Me; $R_2 = -(CH_2)_4-$; M = Sr, $R_2 = -(CH_2)_4-$) [151, 153], while similar reactions with primary amine-boranes $RNH_2 \cdot BH_3$ (R = H, Me, ^iPr, Ar) yield $[\{(ArNCMe)_2CH\}Ca\{NHRBH_3\}]$. The thermal decomposition of the derivatives where R = H and Ar has been studied [147, 148]. The molecular hydride $[\{(ArNCMe)_2CH\}Ca(\mu-H)(THF)]_2$ is also a viable synthetic entry point into calcium amido-borane complexes, and calcium ammine amido-borane adducts may be synthesized from $[\{(ArNCMe)_2CH\}Ca(NH_2)(NH_3)]$ [147, 148, 150]. For magnesium, a series of related complexes $[\{(ArNCMe)_2CH\}Mg\{NHRBH_3\}]$ has been isolated from the reactions of $RNH_2 \cdot BH_3$ with the magnesium amide $[\{(ArNCMe)_2CH\}Mg\{N(SiMe_3)_2\}]$ [155, 156].

In contrast, the homoleptic magnesium alkyls $[Mg^nBu_2]$ and $[Mg\{CH(SiMe_3)_2\}_2(THF)_2]$ react in a 4:1 stoichiometry with $R_2NH \cdot BH_3$ (R = Me; $R_2 = -(CH_2)_4-$) to yield the corresponding amido-boranes $[Mg\{NR_2BH_2NR_2BH_3\}_2(THF)]$ in which a B–N bond has formed [151]. The N–B–N–B moiety binds to magnesium to form a metallocycle via the terminal amido nitrogen and two hydrides of the terminal BH_3 unit and may be defined as a κ^3-coordinating ligand. The formation of the product has been rationalized in terms of an initial σ-bond metathesis event
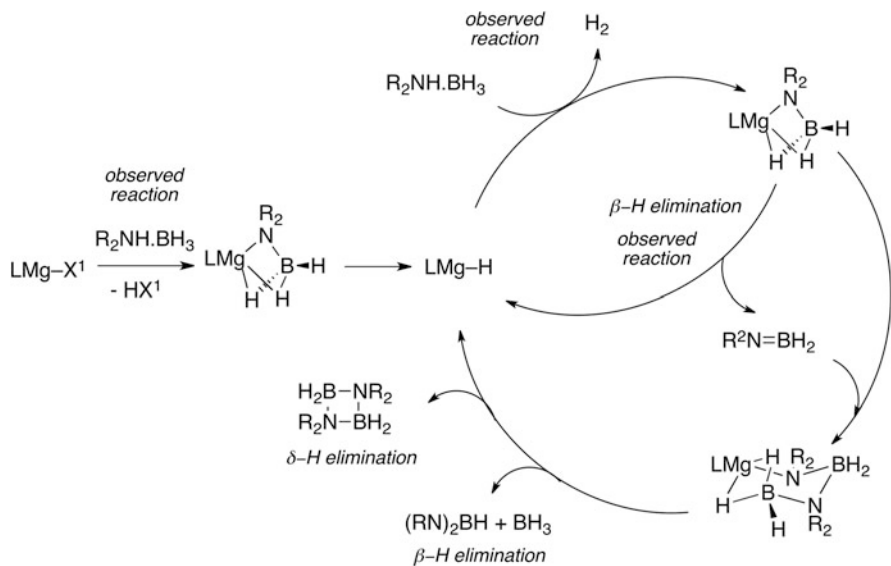
Fig. 16 Proposed mechanism of amine-borane dehydrogenation at group 2 centers

followed by insertion of $Me_2N=BH_2$ in to the M–N bond. The latter unsaturated, alkene analogue, has been observed under the catalytic reaction conditions and has been proposed to originate from β-hydride elimination of an intermediate amido-borane complex containing the $[R_2N–BH_3]^-$ anion. Heating of samples of $[\{(ArNCMe)_2CH\}MgNH\text{-}i\text{-}PrBH_3]$ yields $[\{(ArNCMe)_2CH\}Mg(\mu\text{-}H)]_2$ isolated as the THF adduct. While the by-product and $i\text{-}PrNH=BH_2$ was not isolated from this reaction a related stoichiometric reaction of $[Mg\{N(SiMe_3)_2\}_2]$ with $Me_2NH\bullet BH_3$ allows the in situ observation of $Me_2N=BH_2$. Increasing the steric hindrance of the alkyl groups on the secondary amine-borane to ^iPr prevents any further reaction of the unsaturated amido-borane and allows its isolation under catalytic conditions. The β-hydride elimination step is slower with increasing ionic radius and increasing electronegativity of the group 2 metal and follows the order Mg > Ca > Sr > Ba. Evidence for the insertion of $R_2N=BH_2$ into M–X bonds is provided by the thermal decomposition of $[Sr\{CH(SiMe_3)_2\}\{NR_2BH_3\}(THF)_2]_2$ (R = Me; $R_2 = -(CH_2)_4-$) to form $[R_2NBH\{CH(SiMe_3)_2\}]$ as the sole isolatable reaction product [152]. Thermolysis of $[Mg\{NMe_2BH_2NMe_2BH_3\}_2(THF)]$ yields $[Me_2NBH_2]_2$ along with $[MgH_2]_\infty$, presumed to form via a δ-hydride elimination step.

The overall mechanism is presented in Fig. 16 and is suggested to proceed via a metal hydride as the key intermediate with (1) reaction of the hydride with the amine-borane to form an amido borane, (2) β-hydride elimination from the amine-borane to form the unsaturated species $R_2N=BH_2$, (3) the insertion of $R_2N=BH_2$ into the M–N bond of the amido-borane complex, and (4) turnover from the corresponding metallocyclic species via either β- or δ-hydride elimination.

The product distribution depends on the substitution of the amine, and although kinetic studies have not been conducted, the proposed mechanism accounts for all reaction products and intermediates observed to date.

4.2 Amine and Silane Dehydrocoupling

Reaction scope: Based on the competency of a ytterbium(II) complex as a catalyst for the hydrophosphination of unsaturated substrates and the dehydrocoupling of acidic and hydridic reaction partners, Harder and coworkers reported the synthesis of the HMPA-stabilized calcium metallocycle $[\{\eta^2\text{-Ph}_2\text{CNPh}\}\text{Ca(HMPA)}_3]$ from the reduction of triphenylimine with calcium metal in a THF/HMPA solvent mixture [157]. This complex along with the dialkyl $[\{\{2\text{-(Me}_2\text{N)C}_6\text{H}_4\}\text{CHSiMe}_3\}_2\text{Ca(THF)}_2]$ was reported as a precatalyst for the dehydrocoupling with amines and triphenylsilane. The reaction scope includes the addition of non-hindered primary and secondary aliphatic amines and aniline to triphenylsilane and reactions proceed in THF at 20 °C in high conversions. For the addition of aniline to triphenylsilane the calcium dialkyl precatalyst proved catalytically competent only in the presence of HMPA (Scheme 26).

More recently, Sadow and coworkers extended this work to include C_3-symmetric magnesium alkyl precatalysts supported by tris(oxazoline)borato ligands, improving the reaction scope and mechanistic understanding of this reaction [158]. At 10 mol% catalyst loading, primary aliphatic amines and anilines are effective coupling partners for both primary and secondary silanes (Scheme 26). Under these conditions, multiple substitutions of the silane are observed, and while careful control of the reaction stoichiometry allows the selective dehydrocoupling of amine silane partners which may potentially undergo multiple condensations, the efficiency and selectivity of the reaction depends on the steric demands of both the amine and silane.

For example, n-PrNH$_2$, i-PrNH$_2$, and t-BuNH$_2$ react with phenylsilane to give condensation products derived from a 3:1, 2:1, and 1:1 reaction stoichiometry, respectively. Similar effects are observed for anilines and PhNH$_2$ undergoes dehydrocoupling with phenylsilane more readily than Ph$_2$NH. Hindered secondary amines do not react with phenylsilane nor do primary amines react with tertiary silanes even under more forcing conditions (3–5 days, 100–110 °C). Hydrazine and ammonia undergo a magnesium-catalyzed dehydrocoupling with tertiary silanes with the 1:1 reaction product being isolated in moderate yields (50−70 %). Reactions may be conducted in neat amine and it is noteworthy that the catalyst operates under conditions which would be expected to inhibit turnover due to coordinative saturation of the magnesium center with excess amine.

Reaction mechanism: Kinetic analysis of the magnesium-catalyzed reaction in combination with stoichiometric studies has elucidated a mechanism which proceeds via (1) catalyst initiation to form a magnesium amide catalyst, (2) turnover-limiting nucleophilic attack of the amide nitrogen on the silane to form an

a

R^1
N–H + HSiPh$_3$
R^2

3 - 10 mol %
[{Ph$_2$NCPh)Ca(HMPA)$_3$]
$\xrightarrow{\hspace{3cm}}$
THF, 20 °C, 0.5 - 24 h

R^1
N–SiPh$_3$ + H$_2$
R^2

4 examples 48-98 % conversion

R^1 = ^{n}pent, Ph, EtMe$_2$C, R^2 = H
R^1 = ^{n}Bu, R^2 = Me

b

R^1-NH$_2$ + HSiR^2(R^3)$_2$
$\xrightarrow[\text{C}_6\text{H}_6 \text{ or neat, 25 - 50 °C}]{\text{5 - 10 mol\%}}$

$\overset{\text{H}}{\overset{|}{\text{R}^1\text{-N}}}$—SiR^2(R^3)$_2$ + H$_2$

R^1 = ^{n}Pr, ^{i}Pr, ^{t}Bu, PhNH$_2$
R^2 = Ph, R^3 = H; R^2 = R^3 = Ph
R^2 = Ph, R^3 = Me

15 examples 43-99 % yield

R^1 = NH$_2$ or H
R^2 = R^3 = Et
R^2 = CH$_2$CH=CH$_2$, Bn, R^3 = Me

2 R^1-NH$_2$ + H$_2$SiR^{2}R^3
$\xrightarrow[\text{C}_6\text{H}_6, \text{ 25 - 50 °C}]{\text{5 - 10 mol\%}}$

$\overset{\text{NHR}^1}{\underset{\text{R}^2}{\text{R}^1\text{HN}-\overset{|}{\underset{|}{\text{Si}}}\cdots\text{R}^3}}$ + 2 H$_2$

R^1 = ^{n}Pr, ^{i}Pr, PhNH$_2$
R^2 = Ph, R^3 = H; R^2 = R^3 = Ph
R^2 = Ph, R^3 = Me

4 examples 99% yield

Scheme 26 (**a**) Calcium- and (**b**) magnesium-catalyzed amine-silane dehydrocoupling

intermediate silicate complex, and (3) decomposition of the silicate by β-hydride elimination with formation of the product and generation of a magnesium hydride that can go on to react with a further equivalent of amine regenerating the catalyst and liberating an equiv. of H$_2$ (Fig. 17).

Thus, at 335 K the reaction proceeds with an observed rate constant of k_{obs} = 0.060(4) M^{-1} s^{-1} and is first order in catalyst, first order in silane, and zeroth order in amine. Reaction of the precatalyst with a series of amines generated the corresponding magnesium amide complexes [To^{M}MgNHR] (To^M = tris(4,4-dimethyl-2-oxazolinyl)phenylborate; R = ^{i}Pr, ^{n}Pr, Ph, ^{t}Bu). Sadow and coworkers demonstrated that the reaction of [To^{M}MgNH^{t}Bu] with phenylmethylsilane proceeded with the same reaction order as the overall process, first order in the organometallic complex, and first order in silane. Furthermore, a linear regression analysis of the data allowed the second-order rate constant for the stoichiometric process to be correlated with the catalytic reaction k_{obs} = 0.04 M^{-1} s^{-1}. An Eyring analysis on the stoichiometric reaction gave data consistent with a highly organized transition state, $\Delta H^{\ddagger}$ = 5.9(2) kcal mol^{-1} and $\Delta S^{\ddagger}$ = −46.5(8) cal mol^{-1} K^{-1}. While the kinetic isotope effect of this reaction was calculated as k_H/k_D = 1.0(2)
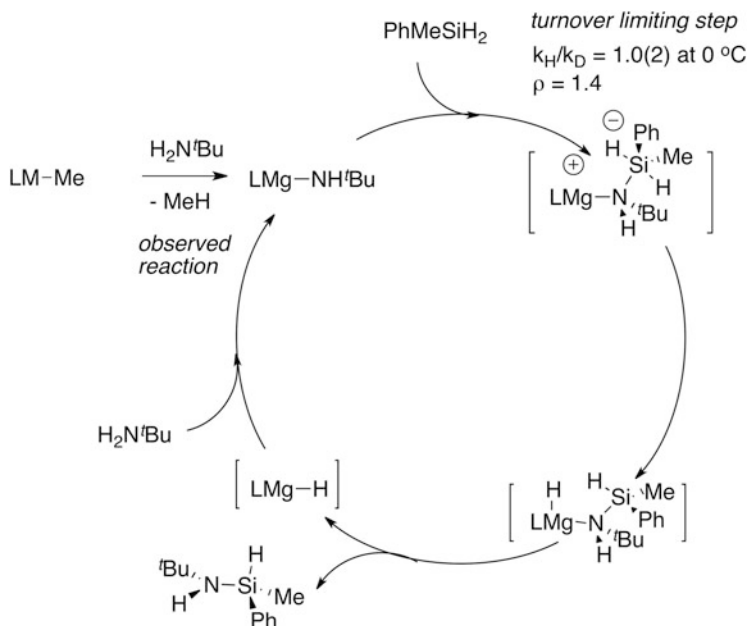
Fig. 17 Proposed mechanism of the magnesium-catalyzed dehydrocoupling of amines and silanes

at 0 °C and shown to be virtually temperature independent over a −20 to +80 °C range, the activation parameters calculated using PhMeSiD$_2$ as a substrate were identical to those derived from PhMeSiH$_2$. A Hammett analysis demonstrated that the reaction is accelerated by the addition of electron-withdrawing groups on the silane with $\rho = +1.4$. Sadow and coworkers argued that the magnitude of the ρ-factor in combination with the absence of a significant KIE did not satisfy the criteria for a β-H elimination step and could only be explained by the rate-determining addition of the magnesium amide to the silane [158].

5 Future Directions in Group 2 Catalysis

Recent years have seen a wealth of new reactivity for group 2 complexes including a series of heterofunctionalization and dehydrocoupling reactions that form new carbon–heteroatom bonds. While this trend is likely to continue, the use of s-block catalysts for the activation of inert C–H and C–F bonds is particularly attractive given the ability of group 3 and group 4 reagents to achieve transformations of these inert functional groups.

The importance of "ate"-complexes and charge separation in hydrosilylation, hydrogenation, and hydroboration catalysis is still unclear in determining catalytic turnover and the mechanisms of these reactions remain underexplored. While

factors that control the Schlenk equilibrium still remain poorly understood the discovery by Sarazin and Carpentier of kinetically stable group 2 catalysts that increase in catalytic activity for intermolecular hydroamination across the series $Mg < Ca < Sr < Ba$ is likely to spark additional interest in the catalytic chemistry of group 2.

References

1. Bonyhady SJ, Green SP, Jones C, Nembenna S, Stasch A (2009) Angew Chem Int Ed 48:2973
2. Green SP, Jones C, Stasch A (2007) Science 318:1754
3. Green SP, Jones C, Stasch A (2008) Angew Chem Int Ed 47:9079
4. Krieck S, Goerls H, Westerhausen M (2010) J Am Chem Soc 132:12492
5. Krieck S, Goerls H, Yu L, Reiher M, Westerhausen M (2009) J Am Chem Soc 131:2977
6. Velazquez A, Fernandez I, Frenking G, Merino G (2007) Organometallics 26:4731
7. Shannon RD (1976) Acta Cryst A32:751
8. Lambert C, Schleyer PV (1994) Angew Chem Int Ed 33:1129
9. Hong S, Marks TJ (2004) Acc Chem Res 37:673
10. Molander GA, Romero JAC (2002) Chem Rev 102:2161
11. Coles MP (2008) Curr Org Chem 12:1220
12. Smith JD (2009) Angew Chem Int Ed 48:6597
13. Barrett AGM, Crimmin MR, Hill MS, Procopiou PA (2010) Proc R Soc A 466:927
14. Harder S (2010) Chem Rev 110:3852
15. Feil F, Harder S (2000) Organometallics 19:5010
16. Feil F, Harder S (2001) Organometallics 20:4616
17. Feil F, Harder S (2003) Eur J Inorg Chem 2003:3401
18. Feil F, Muller C, Harder S (2003) J Organomet Chem 683:56
19. Harder S (2004) Angew Chem Int Ed 43:2714
20. Harder S, Feil F (2002) Organometallics 21:2268
21. Harder S, Feil F, Knoll K (2001) Angew Chem Int Ed 40:4261
22. Harder S, Feil F, Weeber A (2001) Organometallics 20:1044
23. Piesik DFJ, Habe K, Harder S (2007) Eur J Inorg Chem 2007:5652
24. Weeber A, Harder S, Brintzinger HH, Knoll K (2000) Organometallics 19:1325
25. Chisholm MH, Gallucci J, Phomphrai K (2003) Chem Commun 1:48
26. Chisholm MH, Gallucci JC, Phomphrai K (2004) Inorg Chem 43:6717
27. Sarazin Y, Howard RH, Hughes DL, Humphrey SM, Bochmann M (2006) Dalton Trans:340
28. Davidson MG, O'Hara CT, Jones MD, Keir CG, Mahon MF, Kociok-Kohn G (2007) Inorg Chem 46:7686
29. Westerhausen M, Schneiderbauer S, Kneifel AN, Soltl Y, Mayer P, Noth H, Zhong ZY, Dijkstra PJ, Feijen J (2003) Eur J Inorg Chem 2003:3432
30. Piao LH, Dai ZL, Deng MX, Chen XS, Jing XB (2003) Polymer 44:2025
31. Piao LH, Deng MX, Chen XS, Jiang LS, Jing XB (2003) Polymer 44:2331
32. Yamada YMA, Shibasaki M (1998) Tetrahedron Lett 39:5561
33. Saito S, Tsubogo T, Kobayashi S (2007) J Am Chem Soc 129:5364
34. Yamashita Y, Tsubogo T, Kobayashi S (2012) Chem Sci 3:967
35. Kumaraswamy G, Sastry MNV, Jena N (2001) Tetrahedron Lett 42:8515
36. Kumaraswamy G, Sastry MNV, Jena N, Kumar KR, Vairamani M (2003) Tetrahedron Asymmetry 14:3797
37. Suzuki T, Yamagiwa N, Matsuo Y, Sakamoto S, Yamaguchi K, Shibasaki M, Noyori R (2001) Tetrahedron Lett 42:4669

38. Torvisco A, O'Brien AY, Ruhlandt-Senge K (2011) Coord Chem Rev 255:1268
39. Buchanan WD, Allis DG, Ruhlandt-Senge K (2010) Chem Commun 46:4449
40. Hill MS (2011) Annu Rep Prog Chem Sect A 107:43
41. Alexander JS, Ruhlandt-Senge K (2002) Eur J Inorg Chem 2002:2761
42. Sarish SP, Nembenna S, Nagendran S, Roesky HW (2011) Acc Chem Res 44:157
43. Hanusa TP (1990) Polyhedron 9:1345
44. Hanusa TP (1993) Chem Rev 93:1023
45. Hanusa TP (2000) Coord Chem Rev 210:329
46. Hanusa TP (2002) Organometallics 21:2559
47. Westerhausen M (2001) Angew Chem Int Ed 40:2975
48. Westerhausen M, Gartner M, Fischer R, Langer J, Yu L, Reiher M (2007) Chem Eur J 13:6292
49. Westerhausen M (2008) Coord Chem Rev 252:1516
50. Westerhausen M (2009) Z Anorg Allg Chem 635:13
51. Coles MA, Hart FA (1971) J Organomet Chem 32:279
52. Gilman H, Meals RN, O'Donnell G, Woods L (1943) J Am Chem Soc 65:268
53. Gilman H, Haubein AH, O'donnell G, Woods LA (1945) J Am Chem Soc 67:922
54. Gilman H, Woods LA (1945) J Am Chem Soc 67:520
55. Arunasalam VC, Baxter I, Hursthouse MB, Malik KMA, Mingos DMP, Plakatouras JC (1994) J Chem Soc Chem Commun:2695
56. Arunasalam VC, Mingos DMP, Plakatouras JC, Baxter I, Hursthouse MB, Malik KMA (1995) Polyhedron 14:1105
57. Bezougli IK, Bashall A, McPartlin M, Mingos DMP (1997) J Chem Soc Dalton Trans:287
58. Arunasalam VC, Baxter I, Darr JA, Drake SR, Hursthouse MB, Malik KMA, Mingos DMP (1998) Polyhedron 17:641
59. Bezougli IK, Bashall A, McPartlin M, Mingos DMP (1998) J Chem Soc Dalton Trans:2665
60. Bezougli IK, Bashall A, McPartlin M, Mingos DMP (1998) J Chem Soc Dalton Trans:2671
61. Harvey MJ, Hanusa TP (2000) Organometallics 19:1556
62. McCormick MJ, Sockwell SC, Davies CEH, Hanusa TP, Huffman JC (1989) Organometallics 8:2044
63. Burkey DJ, Alexander EK, Hanusa TP (1994) Organometallics 13:2773
64. Burkey DJ, Hanusa TP (1996) Organometallics 15:4971
65. Sockwell SC, Hanusa TP, Huffman JC (1992) J Am Chem Soc 114:3393
66. Harvey MJ, Hanusa TP, Pink M (2000) Chem Commun 2000:489
67. Liu B, Roisnel T, Carpentier J-F, Sarazin Y (2012) Angew Chem Int Ed 51:4943
68. Gauvin RM, Buch F, Delevoye L, Harder S (2009) Chem Eur J 15:4382
69. Buch F, Harder S (2008) Z Naturforsch B 63:169
70. Westerhausen M (1991) Inorg Chem 30:96
71. Crimmin MR, Barrett AGM, Hill MS, MacDougall DJ, Mahon MF, Procopiou PA (2008) Chem Eur J 14:11292
72. Crimmin MR, Casely IJ, Hill MS (2005) J Am Chem Soc 127:2042
73. Barrett AGM, Crimmin MR, Hill MS, Hitchcock PB, Kociok-Kohn G, Procopiou PA (2008) Inorg Chem 47:7366
74. Arrowsmith M, Heath A, Hill MS, Hitchcock PB, Kociok-Kohn G (2009) Organometallics 28:4550
75. Arrowsmith M, Hill MS, Kociok-Kohn G (2009) Organometallics 28:1730
76. Crimmin MR, Arrowsmith M, Barrett AGM, Casely IJ, Hill MS, Procopiou PA (2009) J Am Chem Soc 131:9670
77. Datta S, Gamer MT, Roesky PW (2008) Organometallics 27:1207
78. Zhang X, Emge TJ, Hultzsch KC (2010) Organometallics 29:5871
79. Mukherjee A, Nembenna S, Sen TK, Sarish SP, Ghorai PK, Ott H, Stalke D, Mandal SK, Roesky HW (2011) Angew Chem Int Ed 50:3968
80. Jenter J, Koeppe R, Roesky PW (2011) Organometallics 30:1404

81. Dunne JF, Fulton DB, Ellern A, Sadow AD (2010) J Am Chem Soc 132:17680
82. Arrowsmith M, Crimmin MR, Barrett AGM, Hill MS, Kociok-Koehn G, Procopiou PA (2011) Organometallics 30:1493
83. Arrowsmith M, Hill MS, Kociok-Koehn G (2011) Organometallics 30:1291
84. Datta S, Roesky PW, Blechert S (2007) Organometallics 26:4392
85. Jung ME, Piizzi G (2005) Chem Rev 105:1735
86. Datta S, Gamer MT, Roesky PW (2008) Dalton Trans:2839
87. Arrowsmith M, Hill MS, Kociok-Kohn G (2010) Organometallics 29:4203
88. Barrett AGM, Casely IJ, Crimmin MR, Hill MS, Lachs JR, Mahon MF, Procopiou PA (2009) Inorg Chem 48:4445
89. Avent AG, Crimmin MR, Hill MS, Hitchcock PB (2004) Dalton Trans:3166
90. Avent AG, Crimmin MR, Hill MS, Hitchcock PB (2005) Dalton Trans:278
91. Ruspic C, Harder S (2007) Inorg Chem 46:10426
92. Tobisch S (2011) Chem Eur J 17:14974
93. Zhang X, Emge TJ, Hultzsch KC (2011) Angew Chem Int Ed 51:394
94. Horrillo-Martinez P, Hultzsch KC (2009) Tetrahedron Lett 50:2054
95. Neal SR, Ellern A, Sadow AD (2011) J Organomet Chem 696:228
96. Wixey JS, Ward BD (2011) Dalton Trans 40:7693
97. Wixey JS, Ward BD (2011) Chem Commun 47:5449
98. Brinkmann C, Barrett AGM, Hill MS, Procopiou PA (2012) J Am Chem Soc 134:2193
99. Barrett AGM, Brinkmann C, Crimmin MR, Hill MS, Hunt P, Procopiou PA (2009) J Am Chem Soc 131:12906
100. Lachs JR, Barrett AGM, Crimmin MR, Kociok-Kohn G, Hill MS, Mahon MF, Procopiou PA (2008) Eur J Inorg Chem 2008:4173
101. Barrett AGM, Crimmin MR, Hill MS, Hitchcock PB, Lomas SL, Mahon MF, Procopiou PA (2010) Dalton Trans 39:7393
102. Feil F, Harder S (2005) Eur J Inorg Chem 2005:4438
103. Barrett AGM, Crimmin MR, Hill MS, Hitchcock PB, Procopiou PA (2008) Dalton Trans:4474
104. Barrett AGM, Boorman TC, Crimmin MR, Hill MS, Kociok-Kohn G, Procopiou PA (2008) Chem Commun 2008:5206
105. Orzechowski L, Jansen G, Lutz M, Harder S (2009) Dalton Trans:2958
106. Crimmin MR, Barrett AGM, Hill MS, Hitchcock PB, Procopiou PA (2007) Organometallics 26:2953
107. Al-Shboul TMA, Goerls H, Westerhausen M (2008) Inorg Chem Commun 11:1419
108. Al-Shboul TMA, Palfi VK, Yu LA, Kretschmer R, Wimmer K, Fischer R, Gorls H, Reiher M, Westerhausen M (2011) J Organomet Chem 696:216
109. Hu HF, Cui CM (2012) Organometallics 31:1208
110. Gartner M, Gorls H, Westerhausen M (2007) Z Anorg Allg Chem 635:1568
111. Gartner M, Gorls H, Westerhausen M (2008) Inorg Chem 47:1397
112. Crimmin MR, Barrett AGM, Hill MS, Hitchcock PB, Procopiou PA (2007) Inorg Chem 46:10410
113. Langer J, Al-Shboul TMA, Younis FM, Gorls H, Westerhausen M (2011) Eur J Inorg Chem 2011:3002
114. Crimmin MR, Barrett AGM, Hill MS, Hitchcock PB, Procopiou PA (2008) Organometallics 27:497
115. Al-Shboul TMA, Volland G, Goerls H, Westerhausen M, Anorg Z (2009). Allg Chem:633
116. Buch F, Brettar H, Harder S (2006) Angew Chem Int Ed 45:2741
117. Harder S, Brettar J (2006) Angew Chem Int Ed 45:3474
118. Jochmann P, Davin JP, Spaniol TP, Maron L, Okuda J (2012) Angew Chem Int Ed 51:4452
119. Harder S, Spielmann J, Intemann J, Bandmann H (2011) Angew Chem Int Ed 50:4156
120. Arrowsmith M, Hill MS, MacDougall DJ, Mahon MF (2009) Angew Chem Int Ed 48:4013
121. Spielmann J, Harder S (2007) Chem Eur J 13:8928
122. Spielmann J, Harder S (2008) Eur J Inorg Chem 2008:1480

123. Hill MS, MacDougall DJ, Mahon MF (2010) Dalton Trans 39:11129
124. Hill MS, Kociok-Koehn G, MacDougall DJ, Mahon MF, Weetman C (2011) Dalton Trans 40:12500
125. Bonyhady SJ, Jones C, Nembenna S, Stasch A, Edwards AJ, McIntyre GJ (2010) Chem Eur J 16:938
126. Arrowsmith M, Hill MS, Hadlington T, Kociok-Kohn G, Weetman C (2011) Organometallics 30:5556
127. Arrowsmith M, Hadlington TJ, Hill MS, Kociok-Kohn G (2012) Chem Commun 48:4567
128. Harder S, Spielmann J (2012) J Organomet Chem 698:7
129. Barrett AGM, Crimmin MR, Hill MS, Hitchcock PB, Procopiou PA (2007) Organometallics 26:4076
130. Spielmann J, Buch F, Harder S (2008) Angew Chem Int Ed 47:9434
131. Zeng GX, Li SH (2010) Inorg Chem 49:3361
132. Green DC, Englich U, Ruhlandt-Senge K (1999) Angew Chem Int Ed 38:354
133. Burkey DJ, Hanusa TP (1996) Acta Cryst C52:2452
134. Avent AG, Crimmin MR, Hill MS, Hitchcock PB (2005) Organometallics 24:1184
135. Schumann H, Steffens A, Hummert M (2009) Z Anorg Allg Chem 635:1041
136. Barrett AGM, Crimmin MR, Hill MS, Hitchcock PB, Lomas SL, Mahon MF, Procopiou PA, Suntharalingam K (2008) Organometallics 27:6300
137. Barrett AGM, Crimmin MR, Hill MS, Hitchcock PB, Lomas SL, Procopiou PA, Suntharalingam K (2009) Chem Commun 2009:2299
138. Heeres HJ, Nijhoff J, Teuben JH, Rogers RD (1993) Organometallics 12:2609
139. Crimmin MR, Barrett AGM, Hill MS, Procopiou PA (2007) Org Lett 9:331
140. Day BM, Mansfield NE, Coles MP, Hitchcock PB (2011) Chem Commun 47:4995
141. Cronin L, Manoni F, O'Connor CJ, Connon SJ (2010) Angew Chem Int Ed 49:3045
142. O' Connor CJ, Manoni F, Curran SP, Connon SJ (2011) New J Chem 35:551
143. Mojtahedi MM, Akbarzadeh E, Sharifi R, Abaee MS (2007) Org Lett 9:2791
144. Werner T, Koch J (2010) Eur J Org Chem 2010:6904
145. Sharma M, Andrea T, Brookes NJ, Yates BF, Eisen MS (2011) J Am Chem Soc 133:1341
146. Harder S (2011) Coord Chem Rev 255:1252
147. Spielmann J, Jansen G, Bandmann H, Harder S (2008) Angew Chem Int Ed 47:6290
148. Spielmann J, Harder S (2009) J Am Chem Soc 131:5064
149. Spielmann J, Harder S (2011) Dalton Trans 40:8314
150. Harder S, Spielmann J, Tobey B (2012) Chem Eur J 18:1984
151. Liptrot DJ, Hill MS, Mahon MF, MacDougall DJ (2010) Chem Eur J 16:8508
152. Bellham P, Hill MS, Liptrot DJ, MacDougall DJ, Mahon MF (2011) Chem Commun 47:9060
153. Hill MS, Hodgson M, Liptrot DJ, Mahon MF (2011) Dalton Trans 40:7783
154. Hill MS, Kociok-Koehn G, Robinson TP (2010) Chem Commun 46:7587
155. Spielmann J, Bolte M, Harder S (2009) Chem Commun 2009:6934
156. Spielmann J, Piesik DFJ, Harder S (2010) Chem Eur J 16:8307
157. Buch F, Harder S (2007) Organometallics 26:5132
158. Dunne JF, Neal SR, Engelkemier J, Ellern A, Sadow AD (2011) J Am Chem Soc 133:16782

Chiral Ca-, Sr-, and Ba-Catalyzed Asymmetric Direct-Type Aldol, Michael, Mannich, and Related Reactions

Tetsu Tsubogo, Yasuhiro Yamashita, and Shū Kobayashi

Abstract Recent progress in asymmetric direct-type aldol, Michael, Mannich, and related reactions using chiral Ca, Sr, and Ba catalysts was summarized in this chapter. Ca, Sr, and Ba are very attractive, because they are abundant and ubiquitous elements found in nature, and form relatively safe and environmentally benign compounds compared with heavy transition metals. However, their use as catalysts in asymmetric synthesis has been limited compared with that of transition metal catalysts. Their strong Brønsted basicity and mild Lewis acidity are promising and attractive characteristics, and can influence their catalytic activity as well as their chiral modification capability in a positive manner. It was revealed that several catalytic asymmetric carbon–carbon bond-forming and related reactions proceeded smoothly in high enantioselectivites using the chiral Ca, Sr, and Ba catalysts.

Keywords Aldol reactions · Asymmetric reactions · Chiral catalyst · Mannich reactions · Michael reactions

Contents

T. Tsubogo, Y. Yamashita and S. Kobayashi (✉)
Department of Chemistry, School of Science, The University of Tokyo, Hongo,
Bunkyo-ku, Tokyo 113-0033, Japan
e-mail: shu_kobayashi@chem.s.u-tokyo.ac.jp

1 Introduction

Efficient synthesis of optically active compounds is one of the most important tasks in synthetic organic chemistry. The most promising methodology is catalytic asymmetric synthesis using chiral metal or nonmetal catalysts, which is an atom economic and wasteless technology. On the other hand, due to a recent stream toward green sustainable chemistry, environmentally friendly chemical methodologies are strongly preferred [1–4]. In this respect, the use of less harmful starting materials, catalysts, and solvents is desired. Among many useful metal species, alkaline-earth metals have long been recognized as belonging to less toxic and less harmful metals. However, besides the potential high utility of alkaline-earth metal species, their use in synthetic organic chemistry, especially in asymmetric synthesis as a chiral catalyst, has been quite limited for a long time. (Reviews of asymmetric reactions using alkaline-earth metal catalysts are: [5–9].)

Carbon–carbon (C–C) bond-forming reaction is an important method for preparation of the main skeleton of organic molecules. While several kinds of C–C bond-forming reactions have been developed and successfully applied to organic synthesis, development of reactions with less chemical waste is desired for the ideal chemical process from a viewpoint of green sustainable chemistry [1–4]. In Brønsted base-mediated reactions, use of a catalytic amount of base is preferred over the typical use of a stoichiometric amount of base to form nucleophilic carbanions [10]. In stereoselective aldol reactions, for example, catalytic "direct-type" aldol reactions using a base catalyst is of great interest. In the past few decades, catalytic "indirect-type" methods using pre-activated enol compounds in the presence of a catalytic (chiral) Lewis acid activator, such as in the Mukaiyama aldol process (for a general review of asymmetric aldol reactions, see [11, 12]), have been widely explored. However, while use of a stoichichiometric amount of base for preparation of pre-activated enol compounds is useful, catalytic "direct-type" aldol reactions using a base catalyst (for reviews of direct aldol reactions: [13]; for reviews of organocatalytic direct aldol reactions, also see [14, 15]), a simple proton transfer process, is more desirable from an atom economic point of view. According to this discussion, development of highly active and stereoselective Brønsted base catalysts is crucial in not only aldol reactions but also in other base-mediated carbon–carbon bond-forming reactions.

For designing effective chiral Brønsted base catalysts, its basicity and Lewis acidity are quite important to control reaction environments around the metal center. The Brønsted basicity is used for deprotonation of acidic protons, such as α-protons of carbonyl compounds, and the Lewis acidity is used for stereocontrol of the reactions. Since among group 2 metals beryllium (Be) and magnesium (Mg) show different behavior compared to other group 2 metals and are similar to group 12 metals such as zinc (Zn) and cadmium (Cd) [16], calcium (Ca), strontium (Sr), and barium (Ba) are of interest for this purpose. These alkaline-earth metal compounds are known to exhibit strong Brønsted basicity, which originates from the low electron negativity of the metal ions. Furthermore, they also exhibit a

Fig. 1 Strategy of chiral modification of alkaline-earth metals
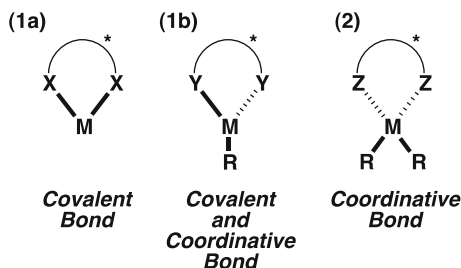
significant Lewis acidity, because they are located between the group 1 elements (i.e., the alkali metals, e.g., Na and K) and the group 3 elements (the rare earth metals, e.g., Sc, Y, and La) [16–19]. Since the orbitals of the alkaline-earth elements are similar to those of the lanthanoid elements, although the stable valences of the ions are different [20], the chemical properties of the compounds containing alkaline-earth metals are similar to those reported for the lanthanoid metals. These natures are important and promising for preparation of chiral alkaline-earth metal compounds [5–9]. Each alkaline-earth metal also possesses interesting properties for preparation of active catalysts. Calcium is less toxic toward humans; indeed, it is present in large amounts in mammalian bodies. Although the Brønsted basicity of calcium compounds with the less electronegative is weaker than that of barium and strontium compounds, their smaller ionic radius and smaller coordination number are beneficial to chiral modification using chiral ligands. Furthermore, calcium cations have the strongest Lewis acidity among these metals (Ca, Sr, Ba). Strontium and barium are also abundant elements in the earth's crust and usually their Brønsted basicities are higher than that of calcium compounds. Especially, barium has been recognized as a promising metal for application to highly stereoselective reactions including asymmetric reactions. However, chiral modification of strontium and barium is challenging, because these metals have larger ionic radii than calcium, and there are many coordination sites to be controlled. Recently, some promising strategies for modification of these metals as chiral catalysts have been reported [5–9].

For chiral modification of these metals, there are mainly two strategies which depend on their binding modes (Fig. 1): (1) a strategy using an anionic chiral ligand, and (2) a strategy that uses a neutral coordinative chiral ligand. In the former strategy, it is expected that a chiral moiety would be tightly introduced via rigid bonding. Type (1) catalyst can also be divided into two types: (1a) only polar covalent bonds are used; (1b) both polar covalent and coordinative bonds are used. The ligand skeleton employed most often for this purpose is a diol compound that can form two covalent bonds with Ca, Sr, and Ba ions (type 1a). Furthermore, methylene (CH_2)-tetheredbisoxazoline skeleton has also been successfully employed as a promising anionic ligand (type 1b). In the latter strategy (type 2), it has been revealed that significant Lewis acidity of the metals could make it possible to receive chiral neutral coordinative ligands, which could realize a flexible design of the ligands. Moreover, the basicity of the whole compound should be enhanced

by electron donation of the ligands to the metals, which should lead to an improvement of the Brønsted basicity of the catalysts. Although the latter strategy is promising, it has not been well explored yet. Based on these strategies, Ca, Sr, and Ba have been successufully modified with chiral ligands as chiral catalysts. In this section, we describe recent successful examples of Ca, Sr, and Ba complex-catalyzed direct-type asymmetric aldol, Michael, Mannich, and related reactions.

2 Asymmetric Aldol and Related Reactions

The aldol reaction is an important carbon–carbon bond-forming method for constructing β-hydroxy carbonyl compounds in which new stereogenic centers are created. Especially, regio- and stereoselective aldol reactions are the most useful for organic synthesis of complex molecular skeletons [11–15]. From a viewpoint of atom economy, an aldol reaction via direct formation of an enolate with a catalytic amount of base is highly desired, and high Brønsted basicity of the alkaline-earth metal compounds is suitable for this purpose. In recent researches on chiral alkaline-earth metal catalysis, direct-type asymmetric aldol and related reactions have been developed.

Shibasaki et al. first reported a chiral barium catalyst prepared from BINOL monomethyl ether and barium alkoxide, which was a good catalyst for asymmetric direct-type aldol reactions (Table 1) [21]. In the presence of a barium catalyst, several aliphatic aldehydes were tested, and the desired cross aldol products were obtained in good yields with moderate to good enantioselectivities. For the substrate $BnOC(CH_3)_2CHO$, the best enantioselectivity was observed (Table 1, entry 6). Although there is no definitive experimented proof, the barium catalyst was assumed to be monometallic and could be stored for several months under argon atmosphere.

Noyori and Shibasaki et al. also reported on a chiral calcium-diolate catalyst [22], which was prepared from bis[N,N-bis(trimethylsilyl)amide]calcium THF dicomplex $(Ca(HMDS)_2(thf)_2)$ and a chiral diol and worked well in asymmetric direct-type aldol reactions (Table 2). By adding KSCN to the chiral calcium catalyst, the enantioselectivity increased significantly (entry 1, 73 % ee to 89 % ee). Other bulky aldehydes showed good enantioselectivities, and the highest enantioselectivity was obtained for the substrate $BnOCH_2C(CH_3)_2CHO$ (entry 3). Unfortunately, a less bulky primary aldehyde (3-phenylpropionaldehyde) showed low enantioselectivity (entry 5). For the chiral intermediate, the formation of a highly aggregated chiral complex was suggested from a mass spectrometry analysis (CSI-MS). It was assumed that a ketone enolate was formed kinetically in the presence of a chiral hydrobenzoin–calcium complex, and retro-aldol process occurred in this reaction system to decrease enantioselectivity of the product.

Kobayashi et al. reported that a chiral barium complex prepared from a 3,3′-disilyl-substituted BINOL derivative was promising in asymmetric reactions [23]. By using the barium catalyst, direct-type aldol reactions of imides were investigated. Basically, a stereocontrolled direct-type aldol reaction between an

Table 1 The chiral barium complex-catalyzed aldol addition of ketones to aldehydes

Entry	R	Time (h)	Yield (%)	ee (%)
1	^tBu	48	77	67
2	$PhCH_2C(CH_3)_2$	39	77	56
3	^cHex	18	87	54
4	^iPr	24	91	50
5	$BnOCH_2C(CH_3)_2$	40	83	69
6	$BnOC(CH_3)_2$	20	99	70

Table 2 A chiral diol-calcium complex-catalyzed asymmetric aldol reaction

Entry	R	Ar	Time (h)	Yield (%)	ee (%)
1	^tBu	Ph	20	74(79)[a]	89(82)[a]
2	$PhCH_2C(CH_3)_2$	Ph	24	75	87
3	$BnOCH_2C(CH_3)_2$	Ph	24	76	91
4	^cHex	p-MeOC$_6$H$_4$	10	71	69
5	$PhCH_2CH_2$	Ph	14	13	15

[a] $Ca(HMDS)_2(thf)_2$ (1.0 mol%) was used. 3.0 M.

aldehyde and a nonactivated amide (imide) is one of the most difficult reactions, on account of the reversibility of the process. In these reactions, the use of modified imides (amide equivalents) is necessary because of the lower acidity of the α-proton. Therefore, N-Boc protected imides were adopted as nucleophiles to prevent any reversibility by an intramolecular Boc group transfer process to the aldol hydroxyl group. As a result, the desired aldol product was obtained in good yield with moderate enantioselectivity using the chiral barium catalyst (Scheme 1).

Ikegami et al. reported an asymmetric Morita–Baylis–Hillman reaction using a BINOL-calcium complex as a chiral Lewis acid and tributylphosphine as an achiral Lewis base (Scheme 2) [24]. It was found that an active calcium aryloxide catalyst could be prepared from $Ca(O^iPr)_2$ and (R)-BINOL in THF. The reaction of cyclopentenone with 3-phenylpropionaldehyde was tested in the presence of the calcium complex, and the desired Morita–Baylis–Hillman adduct was obtained in 62 % yield with 56 % ee.
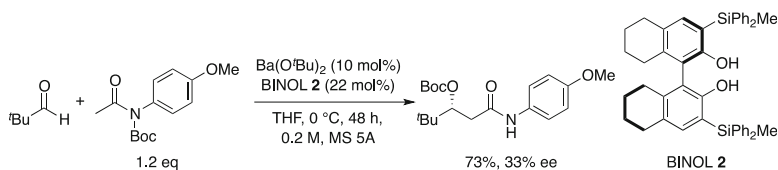
Scheme 1 The chiral H_8-BINOL-barium complex-catalyzed direct-type aldol reaction of an imide with an aldehyde
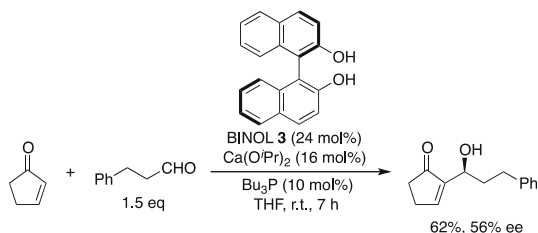
Scheme 2 The chiral calcium complex-catalyzed asymmetric Morita–Baylis–Hillman reaction

Table 3 Chiral BINOL-barium complex-catalyzed asymmetric aldol reactions of β,γ-unsaturated esters

Entry	R	BINOL	Temp. (°C)	Time (h)	α–(E)/γ	Yield (%)	ee (%)
1	Ph	3	0	24(55)[a]	>20/1(>20/1)[a]	85(84)[a]	99(99)[a]
2	4-MeC$_6$H$_4$	3	0	24	17/1	77	98
3	3-MeOC$_6$H$_4$	4	−20	42	15/1	81	99
4	3-BrC$_6$H$_4$	3	0	34	>20/1	78	96
5	2-thienyl	3	0	40	>20/1	80	98
6	3-thienyl	4	−20	34	>20/1	85	97
7	3-furyl	3	0	28	>20/1	82	98
8	(E)-PhCH=CH	4	−20	42	>20/1	63	99
9	^{i}Bu	4	0	48	>20/1	76	91
10	^{n}Pr	3	0	55	>20/1	53	87

[a] Ba(O^{i}Pr)$_2$ (5 mol%) was used.

BINOL **3**: X = H
BINOL **4**: X = OMe
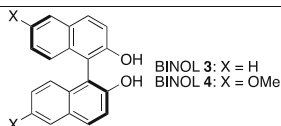
Shibasaki et al. also reported that similar Morita–Baylis–Hillman-type products were obtained via asymmetric aldol reaction of a β,γ-unsaturated ester with aldehydes using a chiral barium catalyst system (Table 3) [25]. The desired products formed in good yields with high enantioselectivities after isomerization. Several aromatic- and alphatic aldehydes were tested, and in all cases high α-(E) selectivities and high enantioselectivities were observed. Several aryl, heteroaryl, alkenyl, and alkyl aldehydes can be used as substrates in this reaction.

Table 4 Catalytic 1,4-addition reactions of malonates using a BINOL-calcium complex

Entry	R^1, R^2	R^3	Yield (%)	$[\alpha]_D^{25}$	ee (%)[a]
1	**1**	Me	90	+14	42
2	**2**	^iPr	84	+8	39
3	**4**	Me	75	+33	88
4	**4**	Et	76	+30	87
5	**5**	^iPr	55	+1	21
6	**3**	^iPr	60	+5	31

[a] Ee values were determined by optical rotation and comparison of values from known literature.
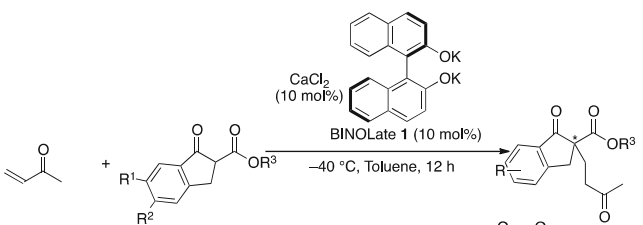
3 Asymmetric Michael and Related Reactions

The asymmetric 1,4-addition of nucleophiles to α,β-unsaturated carbonyl and related compounds is also an important and valuable method for preparation of highly functionalized alkyl chains. While chiral Brønsted base-catalyzed asymmetric transformation has been intensively explored (for reviews of asymmetric 1,4-addition reactions of 1,3-dicarbonyl compounds, see [26–33]; for reviews of asymmetric 1,4-addition reactions of glycine Schiff bases, see [34–37]; for reviews of asymmetric [3+2] cycloaddition reactions, see [38–41]), chiral alkaline-earth metal catalysts have been also successfully employed in this reaction.

Kumaraswamy et al. reported asymmetric 1,4-addition reactions using chiral calcium complexes prepared from calcium chloride and dipotassium salt of BINOL or H_8-BINOL (5,5′,6,6′,7,7′,8,8′-octahydro-1,1′-bi-2-naphthol) [42–45]. After optimization of the calcium salts and reaction conditions, the calcium catalyst was successfully applied to asymmetric 1,4-additions of malonates or β-ketoesters to α,β-unsaturated carbonyl compounds (Tables 4 and 5) [42, 44]. Among the α,β-unsaturated carbonyl compounds employed in the reactions with malonates, cyclopentenone was found to be a suitable substrate, and high enantioselectivities were obtained (Table 4, entries 3 and 4). In the cases of β-ketoesters, 2-oxocyclopentanecarboxylates are suitable for this reaction, and good yields and good enantioselectivities were observed (Table 5, entries 2, 7, and 8).
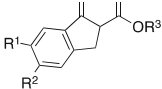
They also investigated asymmetric epoxidation reactions using the BINOL-calcium catalyst. Under optimum reaction conditions, α,β-unsaturated enones were oxidized using ^tBuOOH in moderate to good enantioselectivities [43, 45]. This is the first example of a Ca-catalyzed asymmetric epoxidation (Scheme 3).

Kobayashi et al. focused on chiral bisoxazoline (Box) ligands bearing methylene moieties with acidic hydrogen atoms as chiral ligands for preparation of chiral
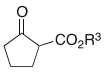
Table 5 Catalytic 1,4-addition reactions of β-ketoesters using a BINOL-calcium complex

Entry	R¹, R², R³	Yield (%)	$[\alpha]_D^{25}$	ee (%)ᵃ
1	**1**	93	55.5	72
2	**2**	91	46.2	68ᵇ
3	**3**	86	36.1	62
4	**4**	90	52.8	–
5	**5**	82	48.3	–
6	**6**	80	24.3	–
7	**7**	88	14.8	80
8	**8**	82	13.4	78
9	**9**	80	28.0	–
10	**10**	76	32.6	–
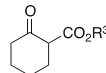
ᵃ Ee values were determined by optical rotation and comparison of values from known literature. ᵇ CCl₄.

1: R¹ = R² = H, R³ = Me
2: R¹ = R² = H, R³ = ⁱPr
3: R¹ = R² = H, R³ = ᵗBu
4: R¹ = H, R² = Cl, R³ = Me
5: R¹ = H, R² = Br, R³ = Me
6: R¹ = MeO, R² = H, R³ = Me
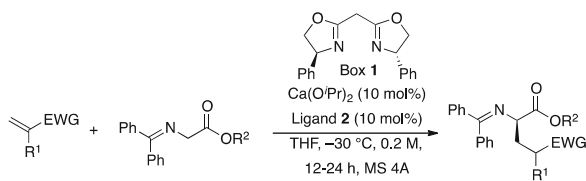
7: R³ = Me
8: R³ = Et

9: R³ = Me
10: R³ = Et
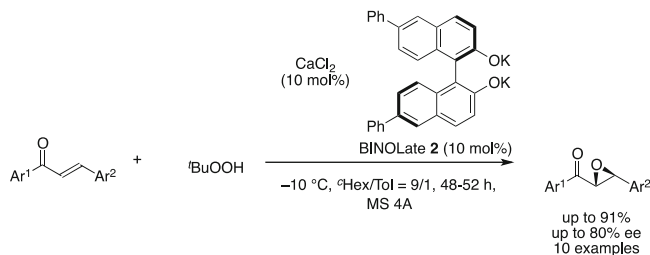
Scheme 3 Catalytic epoxidation reactions using a BINOL-calcium complex

calcium catalysts. Chiral Box ligands are often used in its neutral form to prepare chiral Lewis acid complexes. However, there have been few reports using single deprotonated Box ligands as chiral Brønsted base catalysts. It was found that chiral calcium complexes prepared from Box **1** and Ca(OⁱPr)₂ were effective in the asymmetric 1,4-addition reactions of glycine Schiff bases with α,β-unsaturated esters or amides [46–48]. They then screened several non- or α-substituted acrylic esters bearing alkyl, phenyl, and chloro groups. When acrylic esters were used, the desired 1,4-addition products were obtained in moderate to good yields with good to high enantioselectivities (Table 6, entries 1–4). For α-substituted acrylates, the reactions proceeded in good yields with good stereoselectivities (entries 6–11). The bulkier substituted groups are required for good diastereoselectivities (entries 10 and 11). Moreover, good enantioselectivities were observed in the case of

Table 6 Chiral Box-calcium complexes-catalyzed 1,4-addition reactions of glycine Schiff bases with α,β-unsaturated carbonyl compounds

Entry	R^1	EWG	R^2	Yield (%)	2,4-*syn/anti*	ee (%)
1	H	CO_2Me	^tBu	88		94
2	H	CO_2Me	Me	quant		83
3	H	CO_2Et	^tBu	56		95
4	H	$CO_2{}^tBu$	^tBu	74		92
5	H	$CO_2N(Me)OMe$	^tBu	46		87
6	Me	CO_2Me	^tBu	93	61/39	99/94
7	Et	CO_2Me	^tBu	quant	63/37	86/91
8	^iPr	CO_2Me	^tBu	81	55/45	92/80
9	^iBu	CO_2Me	^tBu	quant	67/33	90/86
10	Ph	CO_2Me	^tBu	quant	91/9	84
11	Cl	CO_2Me	^tBu	95	83/17	81
12	Me	$CO_2N(Me)OMe$	^tBu	83	91/9	85
13	H	SO_2Ph	^tBu	43		52

Weinreb amides (entries 5 and 12). Vinyl sulfone also worked; however, a moderate yield with a low enantioselectivity was observed (entry 13).

Kobayashi et al. have also investigated the synthesis of optically active 3-substituted glutamic acid derivatives [47, 48]. A problem that needs to be solved to realize the desired reactions with β-substituted α,β-unsaturated esters, such as methyl crotonate, is that chiral pyrrolidine derivatives via [3+2] cycloaddition were obtained exclusively (vide infra) and that the desired 1,4-addition adducts were not obtained. However, when a glycine derivative bearing *tert*-butylphenylmethylene group was used, the desired 1,4-adducts were obtained exclusively in high yields with excellent diastereoselectivities (usually as a single isomer) and excellent enantioselectivities (up to 99 % ee) (Table 7). β-Substituted α,β-unsaturated esters, such as methyl, ethyl, *n*-butyl, *i*-butyl, and $BnOCH_2$, were tested. In all cases, high diastereoselectivities were observed except for the $BnOCH_2$-substituted substrate, and the products were obtained in good to high yields with high enantioselectivities (entries 1–7). Weinreb amide substrates also worked well (entries 8–10). However, dimetyl amide substrates did not perform as good (entries 11 and 12). The obtained product could be easily converted to free 3-substituted glutamic acid by acid hydrolysis. This is the first report of highly diastereo- and enantioselective, catalytic asymmetric 1,4-addition reactions of a glycine Schiff base to form β-substituted glutamic acid esters. It was also reported that 1,4-addition reactions of cysteine derivatives proceeded to form α-substituted cysteine esters in good yields with high enantioselectivities [48].

As mentioned above, when β-substituted α,β-unsaturated esters, such as methyl crotonate, were adopted in these reactions, the [3+2] cycloaddition products were

Table 7 Synthesis of 3-substituted glutamic acid derivatives using a Box-calcium catalyst
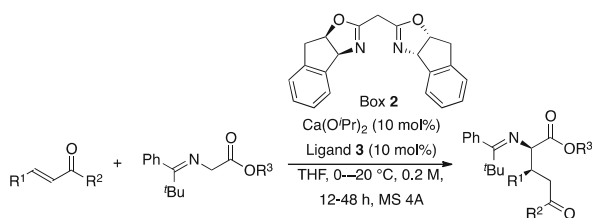
Entry	R^1	R^2	dr	Yield (%)	ee (%)
1	Me	OMe	>99/1	97(93)[a]	99(99)[a]
2	Me	OEt	>99/1	95	93
3	Et	OMe	>99/1	96	96
4	Et	OEt	>99/1	97	94
5	^{n}Bu	OMe	>99/1	73	91
6	^{i}Bu	OMe	>99/1	56	82
7	BnOCH$_2$	OEt	82/18	82	96
8	Me	N(Me)OMe	>99/1	94	98
9	Et	N(Me)OMe	>99/1	92	96
10	^{i}Bu	N(Me)OMe	>99/1	89	95
11	H	NMe$_2$		22	82
12	Me	NMe$_2$	88/12	2	51

[a] Catalyst (2 mol%) was used.

obtained in high yields with excellent diastereo- and enantioselectivities [46, 48]. This method was successfully applied in the synthesis of several chiral pyrrolidine derivatives, and excellent results, high yields, complete diastereoselectivities, and excellent enantioselectivities were obtained (Tables 8 and 9). When glycine Schiff base derivatives from benzophenone were used, the reactions proceeded smoothly in high yields with high enantioselectivities (Table 8, entries 1–10). In the case of glycine Schiff bases prepared from aromatic aldehydes, the [3+2] cycloaddition products were obtained in high yields with good to high enantioselectivities (Table 9, entries 1–10). In the case of glycine Schiff bases prepared from aliphatic aldehydes, low enantioselectivities were observed (entries 11 and 12). Moreover, it was found that these chiral calcium catalysts could be used to construct highly substituted contiguous chiral carbon centers (Table 10). Several amino acid derivatives containing α-alkyl and α-aliphatic oxygen-containing substrates were tested, and in almost all cases high enantioselectivities were observed.
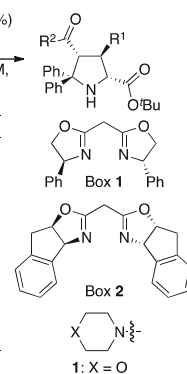
While calcium isopropoxide, Ca(O^{i}Pr)$_2$ has been employed successfully in the preparation of chiral catalysts, it was also found that calcium amide (e.g., Ca (HMDS)$_2$) worked well in these reactions as a catalyst. Calcium amides have a stronger Brønsted basicity and a higher solubility in many solvents compared with calcium alkoxides. Interestingly, it was reported that chiral calcium amide catalysts prepared from Ca(HMDS)$_2$ could be employed successfully in [3+2] cycloaddition reactions (Scheme 4) [48].

Kobayashi et al. also reported asymmetric Friedel–Crafts-type alkylation reactions of an indole with a chalcone (Scheme 5) [49]. A chiral calcium complex

Table 8 Box-calcium complex-catalyzed [3+2] cycloaddition reactions of glycine Schiff bases derived from benzophenone with α,β-unsaturated carbonyl compounds

Entry	R^1	R^2	Box	Time (h)	Yield (%)	ee (%)
1	MeO	Me	1	3	quant	>99
2	EtO	Me	1	3	98	98
3	^{t}BuO	Me	1	3	77	87
4	MeO	Et	2	24	quant	95
5	MeO	^{t}Bu	2	24	quant	99
6	MeO	^{n}Heptyl	2	48	97	>99
7	NMe$_2$	H	1	12	83	95
8	1	H	1	24	76	98
9	2	H	1	24	84	97
10	^{c}Hex$_2$N	H	1	24	93	91
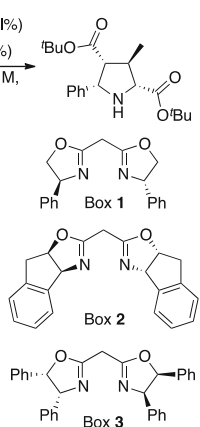
Table 9 Box-calcium complex-catalyzed [3+2] cycloaddition reactions of glycine Schiff bases derived from aldehydes with α,β-unsaturated carbonyl compounds

Entry	R	Box	Temp. (°C)	Yield (%)	ee (%)
1	Ph	1	10	86	86
2	p-ClC$_6$H$_4$	2	−20	92	82
3	p-BrC$_6$H$_4$	1	10	95	86
4	p-MeC$_6$H$_4$	3	−30	92	87[a]
5	m-MeC$_6$H$_4$	1	−20	quant	91
6	o-MeC$_6$H$_4$	2	10	86	78
7	3,5-Me$_2$C$_6$H$_3$	2	10	quant	94
8	2-Naphtyl	2	10	97	92
9	p-MeOC$_6$H$_4$	2	10	76	86
10	2-Furyl	3	−30	97	90[a]
11	^{t}Bu	1	−20	80	38
12	^{c}Hex	1	−20	97	29

[a] The absolute configuration of the product was reversed.

prepared from Ca(HMDS)$_2$ and the chiral TADDOL **1** showed better results than a calcium complex prepared from Ca(O^{i}Pr)$_2$ and TADDOL **1**. The strong basicity of Ca(HMDS)$_2$ may lead to the efficient deprotonation of the ligand to form a more active complex.

Masson and Zhu et al. applied a calcium phosphate catalyst in asymmetric amination reactions of enamides (Tables 11 and 12) [50]; for reviews of asymmetric amination reactions, see [51–58]. The amination products were easily converted to 2-hydrazinoketones and 1,2-diamines by hydrolysis or diastereoselective reduction.

Table 10 Box-calcium complex-catalyzed [3+2] cycloaddition reactions of amino acid Schiff bases derived from aldehydes with α,β-unsaturated carbonyl compounds
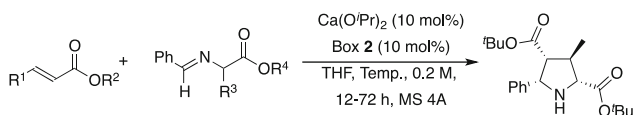
Entry	R^1	R^2	R^3	R^4	Temp. (°C)	Yield (%)	ee (%)
1	Me	Me	Me	Me	0	79	96
2	Me	Et	Me	Me	10	55	93
3	Et	Me	Me	Me	0	64	96
4^a	^{n}Bu	Me	Me	Me	0	81	98
5	Me	Me	Et	Me	−20	41	89
6^a	Me	Me	^{n}Bu	Me	−30	50	93
7^a	Me	Me	Bn	^{t}Bu	−30	98	85
8	Me	Me	^{t}BuOCH$_2$	^{t}Bu	10	80	97
9^a	^{i}Bu	Me	^{t}BuOCH$_2$	^{t}Bu	0	87	95

^{a} Catalyst (20 mol%) was used.
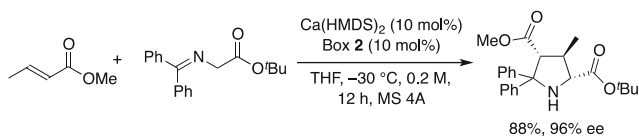
Scheme 4 Catalytic [3+2] cycloaddition reaction using a Box-calcium complex prepared from calcium amide and Box

TADDOL **1**: Ar = 2-Naphthyl
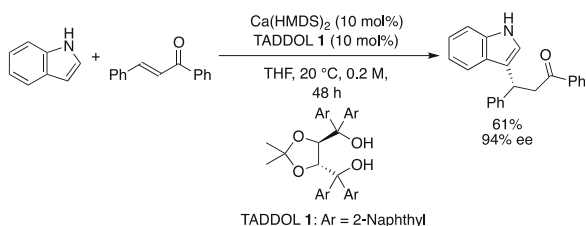
Scheme 5 Chiral Taddol-calcium complex-catalyzed Friedel–Crafts-type reaction

Several electron-donating and withdrawing aromatic enamides were tested, and the enantioselectivites of the desired 2-hydrazinoketones and 1,2-diamines were high.

Antilla et al. reported chiral calcium VAPOL phosphate-mediated asymmetric 1,4-addition reactions of 3-substituted oxindoles (Table 13) [59]; for reviews of asymmetric reactions of oxindole, see [60–63]. It was showed that VAPOL phosphate could be applied, and the desired products were obtained in excellent yields with high enantioselectivities. Four differently substituted oxindoles worked well in this reaction.

Table 11 Chiral calcium phosphate-catalyzed asymmetric amination reactions affording optically active α-hydrazinoketones

Entry	R^1	R^2	Yield (%)	ee (%)
1	3-Cl	Me	80	90
2	4-Cl	Me	97	85
3	3-F	Me	77	90
4	4-Br	Me	76	93
5	4-Me	Me	83	88
6	4-OMe	Me	73	91
7	4-CF$_3$	Me	75	93
8	H	Et	91	89[a]
9	H	^{n}Pr	94	94
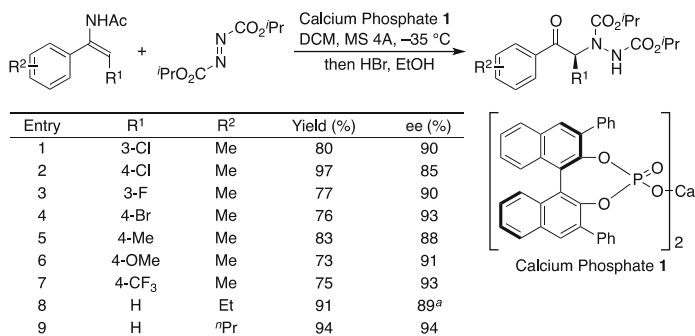
[a] 3,3'-Ph$_2$-BINOL-O$_2$P(O)OH (10 mol%) was used.

Table 12 Chiral calcium phosphate-catalyzed asymmetric amination reactions affording chiral 1,2-diamines

Entry	R^1	R^2	Yield (%)	ee (%)
1	H	Me	84	92
2	3-F	Me	88	88
3	3-CF$_3$	Me	84	93
4	H	^{n}Pr	99	96
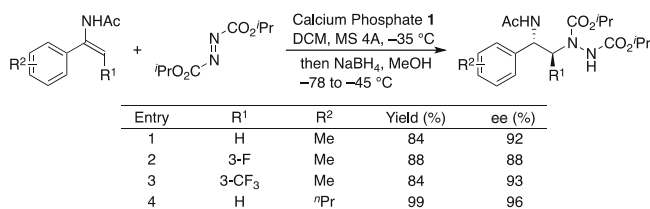
Table 13 Chiral calcium phosphate-catalyzed 1,4-addition reactions

Entry	R^1	R^2	Yield (%)	ee (%)
1	H	Ph	97	90
2	5-F	Ph	96	95
3	H	2-Naphthyl	95	95
4	H	p-MeC$_6$H$_4$	96	90
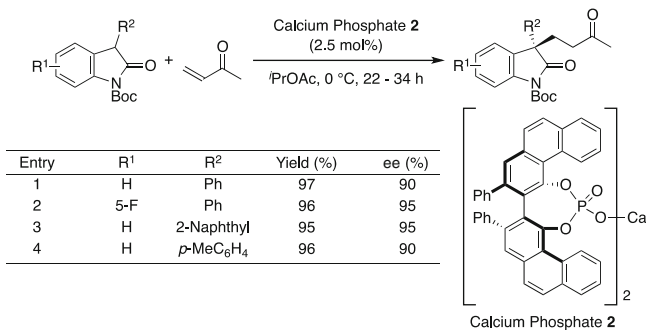
Table 14 Chiral Pybox-calcium complex-catalyzed 1,4-addition reactions of 1,3-dicarbonyl compounds with nitroalkenes

Entry	R^1	R^2	Yield (%)	ee (%)
1	Me	Ph	80(quant)	96(94)[a]
2	Et	Ph	95	92
3[b]	Me	p-MeOC$_6$H$_4$	95	93
4[b]	Me	p-MeC$_6$H$_4$	92	94
5[b]	Me	m-MeC$_6$H$_4$	quant	94
6[b]	Me	o-MeC$_6$H$_4$	97	65
7	Me	p-BrC$_6$H$_4$	93	93
8	Me	2-Furyl	96	94
9[c]	Me	^{c}Hex	73	87

[a] Catalyst (1.0 mol%) was used, 0.6 M, 18 days.
[b] 48 h. [c] 72 h.

Kobayashi et al. developed chiral calcium catalysts with neutral coordinative ligands [64–66] in asymmetric 1,4-addition reactions of 1,3-dicarbonyl compounds with nitroalkenes. As mentioned in the introduction, use of neutral coordinative ligands is valuable for designing asymmetric environments around metals and for increasing the catalyst activity. It was reported that asymmetric 1,4-addition reactions of 1,3-dicarbonyl compounds with nitroalkenes [64], which are one of the most important methods for the preparation of chiral γ-nitro carbonyl compounds, proceeded smoothly using a chiral calcium catalyst prepared from calcium alkoxide (Ca(OAr)$_2$) with $anti$-Ph$_2$-Pybox (Table 14). The desired products were obtained in excellent yields with high enantioselectivities. Aryl parts of the nitroalkene containing electron-donating and withdrawing groups were surveyed, and in all cases the products were obtained in high yields with high enantioselectivities (entries 1–9). Other 1,3-dicarbonyl compounds also worked well. It should be noted that neutral coordinative ligands significantly enhanced the reaction rate, as the reactions proceeded faster than those of ligand-free systems. This reaction is the first example of the use of a chiral coordinative alkaline-earth metal catalyst in catalytic asymmetric reactions.

The chiral calcium catalyst was applied to other asymmetric carbon–carbon bond-forming reactions successfully. The catalytic addition of malonate to α,β-unsaturated amides and the successive highly enantioselective protonation was achieved using the chiral Pybox-calcium catalyst system prepared from Pybox **2** and calcium ethoxide with aryloxide **1** (Table 15) for a review of asymmetric protonation reactions, see [65, 67–69]. The products were obtained in good yields with high enantioselectivities, and a broad substrate generality was also observed except for the phenyl subustituted substrate (entry 9). It should be noted that the smallest electrophile, i.e., a proton, could be controlled well using the chiral calcium complex.

Table 15 Catalytic 1,4-addition reaction and asymmetric protonation sequence using a chiral Pybox-calcium catalyst

Entry	R	Yield (%)	ee (%)
1	Me	90(88)[a]	95(92)[a]
2	Allyl	86	96
3[b]	Prenyl	85	93
4	cis-CH$_2$CH=CHCl	96	95
5[c]	Cinnamyl	85	94
6[d]	CH$_2$–C≡C–Ph	88	94
7	CH$_2$–C≡C–CH$_2$OBn	77	93
8	CH$_2$–C≡C–Bu	91	94
9[b,e]	Ph	72	48

[a] Catalyst (5 mol%) was used. [b] 0.06 M.
[c] CPME/THF = 2/1. [d] CPME/Tol = 4/1.
[e] Tol/DCM = 4/1.

Kobayashi et al. also applied the catalyst to asymmetric 1,4-addition reactions of azlactones with acrylates [66]. The active α-proton of the azlactone (5(4H)-oxazolone) skeleton showed a low pKa value compared to that of the alanine Schiff bases, because the anion formed is stabilized via enol formation and aromatization. After 1,4-addition reactions with acrylates, the 2-substituted glutamic acid derivatives formed could be obtained via hydrolysis using a weak acid. It was found that Pybox **3** prepared from alaninol derivatives was effective for this reaction. The desired products were obtained in good yields with good enantios-electivities. Several amino acid derivatives containing alkyl chains in the α-position were screened, and the leucine derivative (R = ^{i}Bu) showed the best enantio-selectivity in this reaction (Table 16, entry 8).

Not only calcium complexes but also strontium complexes were found to be effective in asymmetric 1,4-addition reactions. Kobayashi et al. firstly reported chiral strontium-catalyzed asymmetric 1,4-addition reactions of malonates with chalcones (Table 17) [70]. A chiral bissulfonamide derived from 1,2-diphenylethylenediamine was found to be effective, and the desired products were obtained in high yields with high enantioselectivities. Chalcone derivatives bearing electron-donating or withdrawing groups on the aromatic rings worked quite well in almost all cases. In the catalyst structure, it was revealed that both acidic hydrogen atoms on the nitrogens of the ligand were deprotonated to form a chiral strontium complex via bidentate bonding. The chiral strontium catalyst could also be prepared from strontium amide ([Sr(HMDS)$_2$]$_2$), and interestingly, the catalyst was found to be more active than that prepared from strontium alkoxide [71].

Shibasaki et al. reported asymmetric cyanation reactions of β,β-disubstituted α,β-unsaturated carbonyl compounds using a chiral strontium catalyst [72]; for selected examples of asymmetric cyanation reactions, see [73–80]. The catalytic

Table 16 Catalytic 1,4-addition reactions of azlactones with acrylates using a chiral Pybox-calcium catalyst

Entry	R^1	R^2	Pybox	Yield (%)	ee (%)
1	Me	Me	**3a**	78	81
2	Me	Et	**3a**	81	81
3	Me	^{t}Bu	**3b**	52	69
4	Me	Bn	**3b**	80	78
5	Et	Me	**3a**	77	71
6	^{n}Pr	Me	**3b**	92	76
7[a]	Bn	Me	**3b**	75	64
8	^{i}Bu	Me	**3b**	78	84

[a] 0.1 M.

Table 17 Catalytic asymmetric 1,4-addition reactions of α-substituted chalcone derivatives using a chiral strontium bissulfonamide catalyst

Entry	R^1	R^2	Yield (%)	ee (%)
1	o-ClC$_6$H$_4$	Ph	76	92
2	p-ClC$_6$H$_4$	Ph	93	97
3	p-FC$_6$H$_4$	Ph	92	98
4	p-MeOC$_6$H$_4$	Ph	80	>99
5	p-NO$_2$C$_6$H$_4$	Ph	98	96
6	m-NO$_2$C$_6$H$_4$	Ph	94	94
7	p-FC$_6$H$_4$	p-FC$_6$H$_4$	91	96
8	p-MeOC$_6$H$_4$	p-FC$_6$H$_4$	81	>99
9	3,4-(MeO)$_2$C$_6$H$_4$	p-FC$_6$H$_4$	61	96
10	p-ClC$_6$H$_4$	p-FC$_6$H$_4$	97	97
11	o-ClC$_6$H$_4$	p-FC$_6$H$_4$	80	93
12	p-FC$_6$H$_4$	p-MeC$_6$H$_4$	90	98
13	Ph	p-ClC$_6$H$_4$	98	99
14	Ph	p-FC$_6$H$_4$	92	99
15	Ph	p-MeOC$_6$H$_4$	85	99
16	2-Thienyl	2-Thienyl	73	97
17	5-Methylfuran-2-yl	Ph	71	96
18	Ph	1-Pyrrolyl	93	99
19	Ph	—CH=CHPh	97	86
20	—CH=CHPh	Ph	62	97

Table 18 Catalytic asymmetric cyanation reactions of β,β-disubstituted α,β-unsaturated ketones using a chiral strontium catalyst

Entry	R^1, R^2, R^3	Temp (°C)	Time (h)	Yield (%)	ee (%)
1	(E)-**1**	r.t.	16	100	97(R)
2	(Z)-**1**	r.t.	16	100	97(S)
3	(E)-**2**	r.t.	16	87	99(+)
4	(Z)-**2**	r.t.	16	77	99(−)
5	(E)-**3**	40	16	98	89(R)
6	(Z)-**3**	40	1	100	99(S)
7	(E)-**4**	40	2	79	99(−)
8	(Z)-**4**	40	2	84	99(+)
9	(E)-**5**	40	2	100	99(+)
10	(Z)-**5**	40	2	100	99(−)
11	**6**	50	16	74	99
12	**7**	50	16	100	99
13	(E)-**8**	50	16	70	89(−)
14	(Z)-**8**	50	2	80	98(+)
15	**9**	50	2	84ᵃ	99ᵇ

R^1, R^2, R^3 substrate legend:
1: R^1 = Ph, R^2 = ^{i}Pr, R^3 = Me
2: R^1 = Me, R^2 = Bu, R^3 = Me
3: R^1 = Me, R^2 = ^{i}Pr, R^3 = Me
4: R^1 = PhCH$_2$CH$_2$, R^2 = Bu, R^3 = Me
5: R^1 = ^{c}Hex, R^2 = Bu, R^3 = Me
6: R^1 = Me, R^2 = Ph, R^3 = Me
7: R^1 = Ph, R^2 = Ph, R^3 = Me
8: R^1 = Me, R^2 = Ph, R^3 = Et

ᵃ Yield of *cis* isomer. dr =20/1. ᵇ Ee of *cis* isomer.

Table 19 Catalytic asymmetric cyanation reactions of β,β-disubstituted α,β-unsaturated amides using a chiral strontium catalyst

Entry	R^1, R^2, R^3	x	Temp (°C)	Yield (%)	ee (%)
1	(E)-**10**	0.	40	100	98(−)
2	(Z)-**10**	2.5	40	73	95(+)
3	(E)-**12**	0.5	40	100	95(R)
4	(Z)-**12**	0.5	40	95	98(S)
5	(E)-**13**	10	50	92	96(+)
6	(Z)-**13**	2.5	50	100	99(−)

10: R^2 = Bu
11: R^2 = ^{i}Pr
12: R^2 = Ph

asymmetric 1,4-addition of cyanide to α,β-unsaturated carbonyl compounds is an important method for the preparation of optically active synthetic components. Furthermore, the cyanide group could be converted into several useful functional groups. It was found that a complex of strontium alkoxide and a tridentate ligand with dihydroxy groups worked well to afford the desired products with remarkable ee's up to 97 % (Tables 18 and 19). Many substrates such as β-substituted α,β-unsaturated ketones or amides were investigated, and in all cases the desired products were obtained in good yields with high enantioselectivities.

Kobayashi et al. investigated asymmetric Friedel–Crafts-type reactions of indoles with chalcone derivatives catalyzed by a chiral barium complex, and high

Table 20 Asymmetric Friedel–Crafts-type reactions of indole with chalcone derivatives using a chiral H_8-3,3′-SiPh$_3$-BINOL-barium catalyst

Entry	Ar^1	Ar^2	Yield (%)	ee (%)
1	Ph	Ph	86	95
2	p-ClC$_6$H$_4$	Ph	quant	93
3	o-ClC$_6$H$_4$	Ph	97	91
4	Ph	p-ClC$_6$H$_4$	92	93
5	p-FC$_6$H$_4$	Ph	89	96
6	p-MeOC$_6$H$_4$	Ph	68	95
7	Ph	p-MeOC$_6$H$_4$	80	95
8	p-MeC$_6$H$_4$	Ph	87	95
9	m-MeC$_6$H$_4$	Ph	81	85
10	o-MeC$_6$H$_4$	Ph	78	89
11	p-MeOC$_6$H$_4$	p-FC$_6$H$_4$	92	94

Table 21 Asymmetric Friedel–Crafts-type reactions of indole derivatives with chalcone using a chiral H_8-3,3′-SiPh$_3$-BINOL-barium catalyst

Entry	R	Yield (%)	ee (%)
1	H	86	95
2	5-Cl	90	85
3	5-MeO	96	93
4	4-MeO	67	96
5	5-Me	88	95
6[a]	2-Me	84	70

[a] BINOL **2** was used.

enantioselectivities were achieved using H_8-3,3′-SiPh$_3$-BINOL as ligand [49]. Several substituted chalcon derivatives bearing electron-donating or withdrawing groups on the benzene ring were tested (Table 20). In all cases, enantioselectivities of the desired produts were high. Several indole derivatives were also examined, and high enantioselectivities were obtained (Table 21). Up to now, while there have been many examples of asymmetric Friedel–Crafts-type reactions of indoles with chalcone derivatives, only Lewis acid catalysts or organocatalysts have been reported in this reaction (for reviews of asymmetric Friedel–Crafts-type reactions, see [81, 82]). In this report, chiral Brønsted base-catalyzed Friedel–Crafts-type reactions of indoles were described for the first time. In the proposed reaction mechanism, the acidic proton of indole was deprotonated by the barium complex to

Table 22 Chiral calcium phosphate-catalyzed asymmetric Mannich reactions

Entry	R^1, R^2	Ar	Yield (%)	ee (%)
1	**1**	Ph	>99	90
2	**2**	p-MeC$_6$H$_4$	>99	94
3	**2**	p-MeOC$_6$H$_4$	94	92
4	**2**	Ph	>99(>99)^a	94(98)^a
5	**2**	p-ClC$_6$H$_4$	90	90
6	**2**	p-BrC$_6$H$_4$	>99	91
7	**2**	1-Naphtyl	88	97
8	**2**	3-Thionyl	>99	96
9	**3**	Ph	94	95
10	**3**	p-MeOC$_6$H$_4$	81	91
11	**3**	p-BrC$_6$H$_4$	89	95

^{a} Calcium Phospate (0.5 mol%) was used.

form a chiral barium-indole species. In this reaction system, barium amide was found to be more effective than barium alkoxide because of its stronger Brønsted basicity and solubility in solvents.

4 Asymmetric Mannich and Related Reactions

The asymmetric Mannich reaction is a powerful tool for preparation of chiral β-aminocarbonyl compounds (for a review of asymmetric Mannich-type reactions for synthesis of α,β-diamino acids, see [83, 84]; for reviews of direct Mannich-type reactions: [85–89]). Up to now, several chiral catalysts have been developed, and high stereoselectivities have been achieved. In this Mannich reaction, chiral alkaline-earth metal complexes have also been successfully employed.

Ishihara et al. found that a chiral calcium phosphate worked well in asymmetric Mannich reactions [90, 91]. The chiral calcium phosphate prepared from calcium alkoxide and phosphoric acid bearing a chiral BINOL backbone was used in asymmetric Mannich reactions of 1,3-dicarbonyl compounds with N-Boc-imines. While α-substituted β-ketoesters showed moderate enantio- and diastereoselectivities, α-nonsubstituted β-ketothioesters and thiomalonates were good substrates for this reaction, and the Mannich products were obtained in high yields with high enantioselectivities (Table 22). Bulky thio esters (SPh or S(2,6-Xyl)) were necessary for good results. The ^{31}P NMR analysis of the catalyst in CD$_2$Cl$_2$ showed a broad peak at 0.05 ppm, which suggests an oligomeric structure. However, when imine (1

Table 23 Chiral calcium phosphate-catalyzed asymmetric Mannich reactions

Entry	Nu	R	Yield (%)	ee (%)
1	Ketoester **1**	$p\text{-MeC}_6\text{H}_4$	49	88
2	Ketoester **1**	$m\text{-ClC}_6\text{H}_4$	43	76
3	Ketoester **1**	$o\text{-BrC}_6\text{H}_4$	55	86
4	Ketoester **1**	Ph	43	52
5	Diketone **2**	$p\text{-MeC}_6\text{H}_4$	47	73
6	Diketone **2**	$o\text{-BrC}_6\text{H}_4$	49	83
7	Diketone **2**	$p\text{-CF}_3\text{C}_6\text{H}_4$	48	88
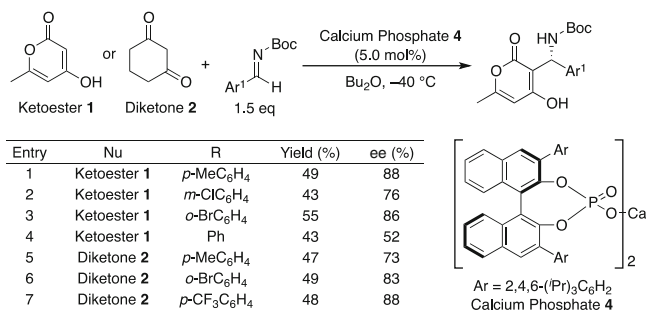
Table 24 Chiral calcium phosphate-catalyzed asymmetric phosphination of imines

Entry	R^1	Ar^1	Ar^2	Yield (%)	ee (%)
1	1	$p\text{-MeOC}_6\text{H}_4$	Ph	96	81
2	1	Ph	$p\text{-ClC}_6\text{H}_4$	77	79
3	2	Ph	Ph	95	90
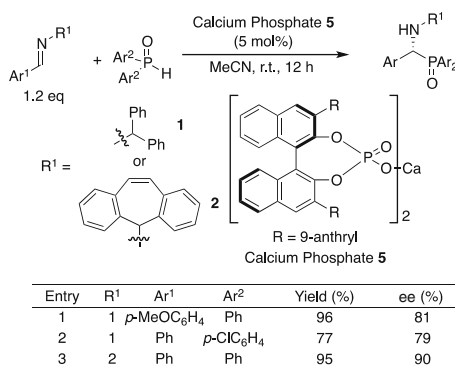
eq) and 1,3-dicarbonyl compound (1.1 eq) were added to the solution of catalyst (2.5 mol%), a new, sharp singlet was observed at 4.55 ppm at 1 min (just beginning) to 24 h, which suggests a monomeric structure of catalyst.

Rueping et al. reported asymmetric Mannich reactions of cyclic 1,3-diketones with *N*-Boc-amines using a chiral calcium phosphate bearing BINOL backbone (Table 23) [92]. Pyrone and 1,3-cyclohexadione were investigated as the carbonyl donors, and the Mannich products were obtained in high enantioselectivities. *N*-Boc-imines with electron-donating or withdrawing groups on the aromatic ring were also tested. The corresponding products were valuable intermediates in organic synthesis [93].

Antilla et al. also investigated chiral calcium BINOL phosphate catalysts [94]; for reviews of asymmetric phosphination reactions, see [95, 96]. This type of calcium catalyst was applied to asymmetric phosphination reactions (Table 24). Not only a chiral magnesium phosphate but also a chiral calcium phosphate was

Table 25 Chiral Pybox-calcium complex-catalyzed catalytic asymmetric Mannich reactions of malonates with *N*-Boc-imines
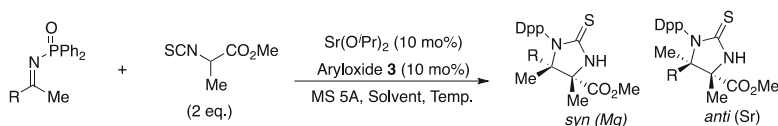
Entry	R¹	R²	Yield (%)	ee (%)
1	Ph	H	90	73
2	Ph	Me	84	62
3	Ph	Bn	95	16
4	*o*-MeC₆H₄	H	90	77
5	*m*-MeC₆H₄	H	93	71
6	*p*-MeOC₆H₄	H	75	66
7	*o*-MeOC₆H₄	H	92	56
8	*p*-FC₆H₄	H	91	72
9	*p*-ClC₆H₄	H	82	61
10	3,4-(OCH₂O)C₆H₃	H	92	67
11	1-naphthyl	H	73	66
12	2-Furyl	H	95	76
13	2-Thienyl	H	89	54
14	*c*Hex	H	80	5
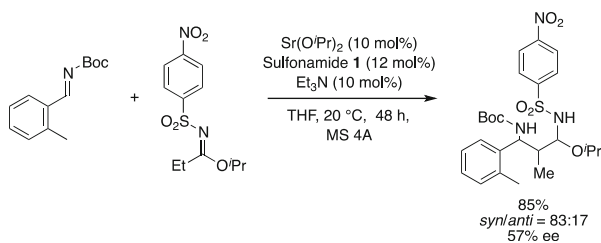
Scheme 6 A chiral strontium complex-catalyzed asymmetric Mannich reaction of sulfonylimidates

mainly employed in this reaction. In the calcium catalyst case, high enantioselectivities were obtained.

Kobayashi et al. have also applied their chiral coordinative calcium catalysts successfully to asymmetric addition of malonates to imines, and the desired products were obtained in high yields with moderate to good enantioselectivities (Table 25) [97]. Several aromatic *N*-Boc-imines bearing electron-withdrawing or donating groups were surveyed, and the enantioselectivities were around 70 % ees (entries 1–13). Unfortunately, an alkyl-substituted imine did not work well (entry 14).

Furthermore, Kobayashi et al. also revealed that chiral strontium catalysts could be applied to asymmetric Mannich reaction of a sulfonylimidate, which is an ester surrogate, with a *N*-Boc-imine [98, 99]. The desired product was obtained in good yield with moderate enantioselectivity in the presence of an additional tertiary amine (Scheme 6). This is the first example of a catalytic asymmetric Mannich-type reaction of sulfonylimidates.

Table 26 Catalytic asymmetric Mannich reactions of α-isothiocyanate esters with ketimines
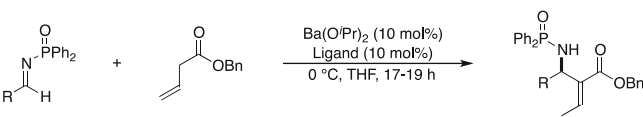
Entry	Cat	R	Solvent	Temp (°C)	Time (h)	Yield (%)	syn/anti	ee (%)
1	Sr	p-BrC$_6$H$_4$	A	r.t.	48	86	6/94	92
2	Sr	p-ClC$_6$H$_4$	A	r.t.	48	82	10/90	87
3	Sr	p-FC$_6$H$_4$	A	r.t.	48	71	6/94	90
4	Sr	p-CF$_3$C$_6$H$_4$	A	r.t.	48	85	11/89	92
5	Sr	p-MeC$_6$H$_4$	B	r.t.	20	97	6/94	95
6	Sr	p-MeC$_6$H$_4$	B	r.t.	24	99	8/92	93
7	Sr	p-MeOC$_6$H$_4$	B	r.t.	24	91	4/96	97
8	Sr	p-Me$_2$NC$_6$H$_4$	B	r.t.	69	45	4/96	97
9	Sr	1	B	−5	47	76	6/94	95
10	Sr	2-thienyl	B	0	48	70	13/87	90
11	Sr	3-thienyl	B	−5	48	74	12/88	92
12	Sr	2-furyl	B	−10	48	84	17/83	84
13	Mg	p-BrC$_6$H$_4$	A	−10	48	87	91/9	84
14	Mg	p-ClC$_6$H$_4$	A	−10	48	90	92/8	85
15	Mg	p-FC$_6$H$_4$	A	0	44	96	93/7	84
16	Mg	p-MeC$_6$H$_4$	C	−25	48	99	90/10	82
17	Mg	1	C	−5	17	96	92/8	81
18	Mg	2-Naphthyl	A	0	48	99	93/7	95
19	Mg	3-thienyl	C	−25	48	80	93/7	81
20	Mg	2-furyl	A	−5	48	70	93/7	80

A = CHCl$_3$ (0.2 M), B = CHCl$_3$/THF = 2/1 (0.17 M.), C = THF (0.2 M).
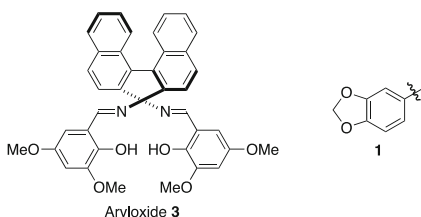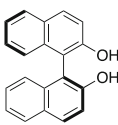
Aryloxide **3**

Shibasaki et al. reported asymmetric Mannich reactions of α-isothiocyanate esters with ketimines (Table 26) [100]. Monometallic salen catalysts containing Sr or Mg were found to be effective. While *anti* products were produced using the strontium complex, *syn* products were obtained using the magnesium complex. The diastereo- and enantioselectivities of the products were high in both cases. *N*-Dpp-imines derived from aromatic aldehydes electron-donating or withdrawing groups were surveyed.
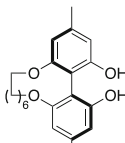
Shibasaki et al. also developed chiral barium catalysts prepared from barium alkoxide and optically active BINOL **3** or aryloxide **4** derivatives. These catalysts were applied to asymmetric Mannich reactions of β,γ-unsaturated esters (Table 27) [101]. In this reaction, the initially formed Mannich adducts isomerized to afford *aza*-Morita–Baylis–Hillman-type products in moderate to good yields with good enantioselectivities. For four substrate examples, ayloxide **4** ligand worked well (entries 2–4).

Table 27 Chiral barium aryloxides-catalyzed Mannich reactions of a β,γ-unsaturated ester

Entry	Ligand	R	Time (h)	Yield (%)	α/γ	ee (%)
1	BINOL **3**	Ph	19	58	>15/1	14
2	Aryloxide **4**	Ph	17	69	9/1	77
3	Aryloxide **4**	p-MeC$_6$H$_4$	19	78	>15/1	80
4	Aryloxide **4**	2-thienyl	17	73	>15/1	78

BINOL **3**   Aryloxide **4**
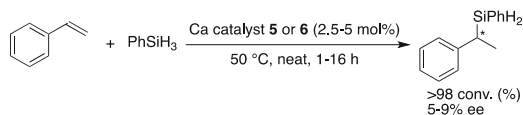
Scheme 7 A hydrosilylation reaction using a calcium catalyst
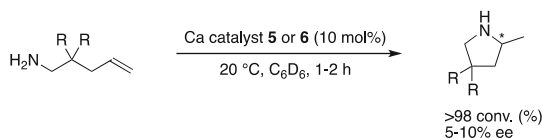
Scheme 8 Hydroamination reactions using a calcium catalyst

5 Other Asymmetric Reactions
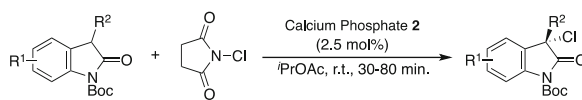
Chiral Ca, Sr, and Ba complexes have been developed in other important bond-forming reactions. Harder et al. investigated asymmetric hydroamination and hydrosilylation reactions (Schemes 7 and 8) using chiral calcium amide catalysts prepared from Ca(HMDS)$_2$(thf)$_2$ and a chiral diimine or Box ligand (**L**). The catalysts were characterized using single crystal X-ray diffraction [102]. It was revealed that a Schlenk equilibrium between heteroleptic ([Ca**L**(HMDS)]$_2$) and homoleptic (Ca**L**$_2$ + Ca(HMDS)$_2$(thf)$_2$) existed in solutions of these calcium amide complexes (Schemes 9 and 10). Using these chiral calcium amide catalysts, the intermolecular hydrosilylation of styrene using PhSiH$_3$ and the intramolecular hydroamination of aminoalkenes were investigated. In both reactions, the yields were high, but the enantioselectivities were
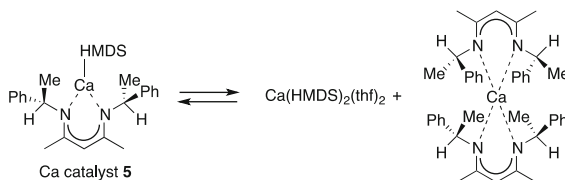
Scheme 9 Schlenk equilibrium of calcium catalyst **5**
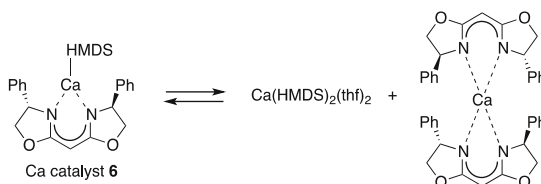
Scheme 10 Schlenk equilibrium of calcium catalyst **6**

Table 28 Chiral calcium phosphate-catalyzed asymmetric benzoylation reactions

Entry	R	Ar	Yield (%)	ee (%)
1	H	Ph	83	99.7
2	H	m-MeOC$_6$H$_4$	92	99
3	H	p-FC$_6$H$_4$	96	99
4	H	p-MeC$_6$H$_4$	78	99
5	H	p-MeOC$_6$H$_4$	87	99
6	H	o-MeOC$_6$H$_4$	63	91
7	H	2-Naphtyl	94	99
8	5-F	Ph	90	99
9	7-F	Ph	96	>99
10	7-F	p-FC$_6$H$_4$	90	99
11	H	3,5-(CF$_3$)$_2$C$_6$H$_3$	88	99
12	5-Me	Ph	92	99
13	5-MeO	Ph	96	99
14	H	2-Thionyl	60	97

not sufficient. From examination of the reactions using stoichiometric amounts of the chiral amide (Ca**L**(HMDS)) and the substrate, it was assumed that the true active species was mostly on the homoleptic side, which means that these reactions were catalyzed by achiral Ca(HMDS)$_2$ not by chiral Ca**L**(HMDS).

Antilla et al. reported chiral calcium-VAPOL phosphate-mediated asymmetric benzoyloxylations and chlorinations of 3-substituted oxindoles (Tables 28 and 29) [103]. It was shown that VAPOL phosphate could be applied to several reactions and that the desired products were obtained in excellent yields with high

Table 29 Chiral calcium phosphate-catalyzed asymmetric chlorination reactions

Entry	R^1	R^2	Yield (%)	ee (%)
1	H	Ph	99	94
2	H	p-MeC$_6$H$_4$	99	93
3	H	p-FC$_6$H$_4$	99	96
4	H	2-Naphtyl	99	>99
5	5-MeO	Ph	99	90
6	5-F	Ph	99	93
7	5-Me	Ph	99	87
8	7-F	Ph	99	97
9	5-Me	p-FC$_6$H$_4$	99	92
10	7-F	p-FC$_6$H$_4$	99	98
11	H	Me	>98	62
12	H^a	Ph	99	97

^{a} N-CO$_2$Me group was used instead of N-Boc.
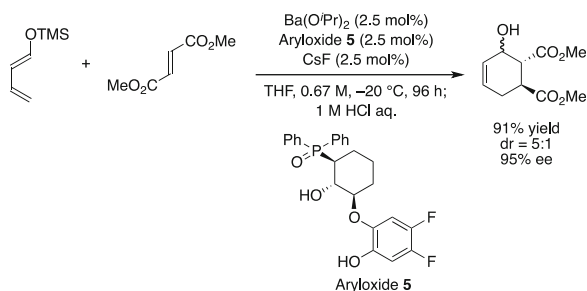
Scheme 11 A chiral barium complex-catalyzed asymmetric Diels–Alder-type reaction

enantioselectivities. Many 3-substituted oxindoles were examined, and in all cases the yields and enantioselectivities were high in both reactions.

Shibasaki et al. also developed a chiral barium-catalyzed asymmetric Diels–Alder reaction of a siloxydiene with fumarate for the synthesis of an optically active Tamiflu® precursor [104]; for a review of asymmetric Diels–Alder reactions, see [105]. Metal exchange from silicon to barium occurred via activation by CsF to form an activated chiral diene, which reacted with fumarate with high enantioselectivity (Scheme 11).

6 Conclusions

Recent progress in asymmetric direct-type aldol, Michael, Mannich, and related reactions using chiral Ca, Sr, and Ba catalysts was summarized in this chapter. Ca, Sr, and Ba are very attractive, because they are abundant and ubiquitous elements

found in nature, and form relatively safe and environmentally benign compounds compared with heavy transition metals. However, their use as catalysts in asymmetric synthesis has been limited compared with that of transition metal catalysts. Their strong Brønsted basicity and mild Lewis acidity are promising and attractive characteristics, and can influence their catalytic activity as well as their chiral modification capability in a positive manner. Further progress in chiral alkaline-earth metal chemistry is desired for the construction of useful and less toxic metal catalysts.

References

1. Anastas PT, Warner JC (1998) Green chemistry: theory and practice. Oxford University Press, New York, NY
2. Anastas PT, Kirchhoff MM (2002) Acc Chem Res 35:686
3. Trost BM (1995) Angew Chem Int Ed 34:259
4. Trost BM (1991) Science 254:1471
5. Kobayashi S, Yamashita Y (2011) Acc Chem Res 44:58
6. Kazmaier U (2009) Angew Chem Int Ed 48:5790
7. Harder S (2010) Chem Rev 110:3852
8. Yanagisawa A, Yoshida K (2011) Synlett 20:2929
9. Yamashita Y, Tsubogo T, Kobayashi S (2012) Chem Sci 3:967
10. Kobayashi S, Matsubara R (2009) Chem Eur J 15:10694
11. Geary LM, Hultin PG (2009) Tetrahed Asym 20:131
12. Kobayashi S, Manabe K, Ishitani H, Matsuo J, Kobayashi S, Manabe K, Ishitani H, Matsuo J (2002) In: Bellus D, Ley SV, Noyori R (eds) Silyl enol ethers. In science of synthesis, Houben–Weyl methods of molecular transformations, vol 4. Georg Thieme Verlag, Stuttgart, p 317
13. Mahrwald R (ed) (2004) Modern aldol reactions. Wiley-VCH, Weinheim
14. Notz W, Tanaka F, Barbas CF III (2004) Acc Chem Res 37:580
15. Mukherjee S, Yang JW, Hoffmann S, List B (2007) Chem Rev 107:5471
16. Riley RF (2009) McGraw-Hill concise encyclopedia of science and technology, 6th edn. McGraw-Hill, New York, NY
17. Cotton FA, Wilkinson G, Gaus PL (eds) (1995) Basic inorganic chemistry, 3rd edn. Wiley, New York, NY
18. Greenwood NN, Earnshaw A (1984) Chemistry of the elements. Pergamon, Oxford
19. Clarke FW (1924) The data of geochemistry, 5th edn. G.P.O, Washington, DC
20. Harder S (2004) Angew Chem Int Ed 43:2714
21. Yamada YM, Shibasaki M (1998) Tetrahedron Lett 39:5561
22. Suzuki T, Yamagiwa N, Matsuo Y, Sakamoto S, Yamaguchi K, Shibasaki M, Noyori R (2001) Tetrahedron Lett 42:4669
23. Saito S, Kobayashi S (2006) J Am Chem Soc 128:8704
24. Yamada YMA, Ikegami S (2000) Tetrahedron Lett 41:2165
25. Yamaguchi A, Matsunaga S, Shibasaki M (2009) J Am Chem Soc 131:10842
26. Jacobsen EN, Pfaltz A, Yamamoto H (eds) (1999) Comprehensive asymmetric catalysis, 1st edn. Springer, Berlin
27. Almaşi D, Alonso DA, Nájera C (2007) Tetrahed Asym 18:299
28. Tsogoeva SB (2007) Eur J Org Chem 11:1701
29. Hayashi T, Yamasaki K (2003) Chem Rev 103:2829
30. Christoffers J, Baro A (2003) Angew Chem Int Ed 42:1688
31. Berner OM, Tedeschi L, Enders D (2002) Eur J Org Chem 12:1877

32. Krause N, Hoffmann-Röder A (2001) Synthesis 2001:171
33. Sibi MP, Manyem S (2000) Tetrahedron 56:8033
34. Maruoka K, Ooi T (2003) Chem Rev 103:3013
35. O'Donnel MJ (2004) Acc Chem Res 37:506
36. Nájera C, Sansano JM (2007) Chem Rev 107:4584
37. Calaza MI, Cativiela C (2008) Eur J Org Chem 20:3427
38. Padwa A, Pearson WH (2002) Synthetic applications of 1,3-dipolar cycloaddition chemistry toward heterocycles and natural products. Wiley, New York, NY
39. Gothelf KV, Jørgensen KA (1998) Chem Rev 98:863
40. Coldham I, Hufton R (2005) Chem Rev 105:2765
41. Pandey G, Banerjee P, Gadre SR (2006) Chem Rev 106:4484
42. Kumaraswamy G, Sastry MNV, Jena N (2001) Tetrahedron Lett 42:8515
43. Kumaraswamy G, Sastry MNV, Jena N, Kumar KR, Vairamani M (2003) Tetrahed Asym 14:3797
44. Kumaraswamy G, Jena N, Sastry MNV, Padmaja M, Markondaiah B (2005) Adv Synth Catal 347:867
45. Kumaraswamy G, Jena N, Sastry MNV, Ramakrishna G (2005) ARKIVOC 53
46. Saito S, Tsubogo T, Kobayashi S (2007) J Am Chem Soc 129:5364
47. Kobayashi S, Tsubogo T, Saito S, Yamashita Y (2008) Org Lett 10:807
48. Tsubogo T, Saito S, Seki K, Yamashita Y, Kobayashi S (2008) J Am Chem Soc 130:13321
49. Tsubogo T, Kano Y, Yamashita Y, Kobayashi S (2010) Chem Asian J 5:1974
50. Drouet F, Lalli C, Liu H, Masson G, Zhu J (2011) Org Lett 13:94
51. Erdik E (2004) Tetrahedron 60:8747
52. Greck C, Drouillat B, Thomassigny C (2004) Eur J Org Chem 2004:1377
53. Marigo M, Jørgensen KA (2006) Chem Commun 2006:2001
54. Vilaivan T, Bhanthmnavin W (2010) Molecules 15:917
55. Evano G, Blanchard N, Toumi M (2008) Chem Rev 108:3054
56. Nugenta TC, El-Shazlya M (2010) Adv Synth Catal 352:753
57. Carbery DR (2008) Org Biomol Chem 6:3455
58. Matsubara R, Kobayashi S (2008) Acc Chem Res 41:292
59. Zheng W, Zhang Z, Kaplan MJ, Antilla JC (2011) J Am Chem Soc 133:3339
60. Zhou F, Liu Y-L, Zhou J (2010) Adv Synth Catal 352:1381
61. Trost BM, Brennan MK (2009) Synthesis 2009:3003
62. Lin H, Danishefsky SJ (2003) Angew Chem Int Ed 42:36
63. Marti C, Carreira EM (2003) Eur J Org Chem 2003:2209
64. Tsubogo T, Yamashita Y, Kobayashi S (2009) Angew Chem Int Ed 48:9117
65. Poisson T, Yamashita Y, Kobayashi S (2010) J Am Chem Soc 32:7890
66. Tsubogo T, Kano Y, Ikemoto K, Yamashita Y, Kobayashi S (2010) Tetrahed Asym 21:1221
67. Yanagisawa A, Yamamoto H (1999) In: Jacobsen EN, Pfaltz A, Yamamoto H (eds) Comprehensive asymmetric catalysis, vol III. Springer, Heidelberg, p 1295
68. Duhamel L, Duhamel P, Plaquevent J-C (2004) Tetrahed Asym 15:3653
69. Mohr JT, Hong AY, Stoltz BM (2009) Nat Chem 1:359
70. Agostinho M, Kobayashi S (2008) J Am Chem Soc 130:2430
71. Kobayashi S, Yamaguchi M, Agostinho M, Schneider U (2009) Chem Lett 38:299
72. Tanaka Y, Kanai M, Shibasaki M (2010) J Am Chem Soc 132:8862
73. Sammis GM, Jacobsen EN (2003) J Am Chem Soc 125:4442
74. Sammis GM, Danjo H, Jacobsen EN (2004) J Am Chem Soc 126:9928
75. Mazet C, Jacobsen EN (2008) Angew Chem Int Ed 47:1762
76. Mita T, Sasaki K, Kanai M, Shibasaki M (2005) J Am Chem Soc 127:514
77. Fujimori I, Mita T, Maki K, Shiro M, Sato A, Furusho S, Kanai M, Shibasaki M (2007) Tetrahedron 63:5820
78. Tanaka Y, Kanai M, Shibasaki M (2008) J Am Chem Soc 130:6072
79. Wang J, Li W, Liu Y, Chu Y, Lin L, Liu X, Feng X (2010) Org Lett 12:1280

80. Bernardi L, Fini F, Fochi M, Ricci A (2008) Synlett:1857
81. Bandini M, Eichholzer A (2009) Angew Chem Int Ed 48:9608
82. Bandini M, Umani-Ronchi A (eds) (2009) Catalytic asymmetric Friedel–Crafts alkylations. Wiley-VCH, Weinheim
83. Gómez Arrayás R, Carretero JC (2009) Chem Soc Rev 38:1940
84. Matsunaga S, Yoshino T (2011) Chem Rec 11:260
85. Kobayashi S, Mori Y, Fossey JS, Salter MM (2011) Chem Rev 111:2626
86. Kumagai N, Shibasaki M (2011) Angew Chem Int Ed 50:4760
87. Marques MMB (2006) Angew Chem Int Ed 45:348
88. Shibasaki M, Matsunaga S (2006) J Organomet Chem 691:2089
89. Córdova A (2004) Acc Chem Res 37:102
90. Hatano M, Moriyama K, Maki T, Ishihara K (2010) Angew Chem Int Ed 49:3823
91. Hatano M, Ishihara K (2010) Synthesis 22:3785
92. Rueping M, Bootwicha T, Sugiono E (2011) Synlett:323
93. Lou S, Dai P, Schaus SE (2007) J Org Chem 72:9998
94. Ingle GK, Liang Y, Mormino MG, Li G, Fronczek FR, Antilla JC (2011) Org Lett 13:2054
95. Merino P, Marques-Lopez E, Herrera RP (2008) Adv Synth Catal 350:1195
96. Ordońez M, Rojas-cabrera H, Cativiela C (2009) Tetrahedron 65:17
97. Poisson T, Tsubogo T, Yamashita Y, Kobayashi S (2010) J Org Chem 75:963
98. Nguyen HV, Matsubara R, Kobayashi S (2009) Angew Chem Int Ed 48:5927
99. Matsubara R, Florian B, Nguyen HV, Kobayashi S (2009) Bull Chem Soc Jpn 82:1083
100. Lu G, Yoshino T, Morimoto H, Matsunaga S, Shibasaki M (2011) Angew Chem Int Ed 50:4382
101. Yamaguchi A, Aoyama N, Matsunaga S, Shibasaki M (2007) Org Lett 9:338
102. Buch F, Harder S, Naturforsch Z (2008) Chem Sci J 63b:169
103. Zhang Z, Zheng W, Antilla JC (2011) Angew Chem Int Ed 50:1135
104. Yamatsugu K, Yin L, Kamijo S, Kimura Y, Kanai M, Shibasaki M (2009) Angew Chem Int Ed 48:1070
105. Corey EJ (2002) Angew Chem Int Ed 41:1650

Index